

Ecological Studies 247

Joseph Alfred Zinck · Otto Huber  
Pedro García Montero · Ernesto Medina  
*Editors*

# Psammic Peinobiomes

Nutrient-Limited Ecosystems of  
the Upper Orinoco and Rio Negro Basins



Springer

---

# **Ecological Studies**

## **Analysis and Synthesis**

**Volume 247**

### **Series Editors**

Josep G. Canadell, CSIRO Oceans and Atmosphere, Canberra, ACT, Australia

Sandra Díaz, National University of Córdoba, Córdoba, Argentina

Gerhard Heldmaier, University of Marburg, Marburg, Germany

Robert B. Jackson, Stanford University, Stanford, CA, USA

Delphis F. Levia, University of Delaware, Newark, DE, USA

Ernst-Detlef Schulze, Max Planck Institute for Biogeochemistry, Jena, Germany

Ulrich Sommer, GEOMAR | Helmholtz Centre for Ocean Research Kiel, Kiel, Germany

David A. Wardle, Nanyang Technological University, Singapore, Singapore

*Ecological Studies* is Springer's premier book series treating all aspects of ecology. These volumes, either authored or edited collections, appear several times each year. They are intended to analyze and synthesize our understanding of natural and managed ecosystems and their constituent organisms and resources at different scales from the biosphere to communities, populations, individual organisms and molecular interactions. Many volumes constitute case studies illustrating and synthesizing ecological principles for an intended audience of scientists, students, environmental managers and policy experts. Recent volumes address biodiversity, global change, landscape ecology, air pollution, ecosystem analysis, microbial ecology, ecophysiology and molecular ecology.

---

Joseph Alfred Zinck • Otto Huber •  
Pedro García Montero • Ernesto Medina  
Editors

# Psammic Peinobiomes

Nutrient-Limited Ecosystems of the  
Upper Orinoco and Rio Negro Basins

 Springer




*Editors*

Joseph Alfred Zinck  
Faculty of Geo-Information Science  
and Earth Observation  
University of Twente  
Enschede, Overijssel, The Netherlands

Otto Huber  
Museum of Nature South Tyrol  
Bolzano, Italy

Pedro García Montero  
Private Activity, Soil Survey and  
Environmental Planning  
Caracas, Venezuela

Ernesto Medina   
Instituto Venezolano de Investigaciones  
Científicas  
Centro de Ecología  
Caracas, Venezuela

ISSN 0070-8356

ISSN 2196-971X (electronic)

Ecological Studies

ISBN 978-3-031-20798-3

ISBN 978-3-031-20799-0 (eBook)

<https://doi.org/10.1007/978-3-031-20799-0>

© The Editor(s) (if applicable) and The Author(s), under exclusive license to Springer Nature Switzerland AG 2023

This work is subject to copyright. All rights are solely and exclusively licensed by the Publisher, whether the whole or part of the material is concerned, specifically the rights of translation, reprinting, reuse of illustrations, recitation, broadcasting, reproduction on microfilms or in any other physical way, and transmission or information storage and retrieval, electronic adaptation, computer software, or by similar or dissimilar methodology now known or hereafter developed.

The use of general descriptive names, registered names, trademarks, service marks, etc. in this publication does not imply, even in the absence of a specific statement, that such names are exempt from the relevant protective laws and regulations and therefore free for general use.

The publisher, the authors, and the editors are safe to assume that the advice and information in this book are believed to be true and accurate at the date of publication. Neither the publisher nor the authors or the editors give a warranty, expressed or implied, with respect to the material contained herein or for any errors or omissions that may have been made. The publisher remains neutral with regard to jurisdictional claims in published maps and institutional affiliations.

This Springer imprint is published by the registered company Springer Nature Switzerland AG  
The registered company address is: Gewerbestrasse 11, 6330 Cham, Switzerland

### *In Memoriam*

*We dedicate this book to the memory of Joseph Alfred Zinck Herzog (10-02-1938/ †19-06-2021), a great human being and outstanding researcher and professor who dedicated his professional life to the study and teaching of science, particularly Geography and Geopedology. Alfred leaves an immense scientific legacy for present and future generations distributed in hundreds of academic contributions as scientific papers and books, reflecting his wisdom and exceptional creativity. In the memory of his friends, disciples, and colleagues remains his warmth, humility, and his willingness to transmit his knowledge unconditionally. This book includes the synthesis of his long-term project focused on the landscape–soil–vegetation relationships in the Venezuelan Amazon region, a territory he loved and knew deeply.*



---

# Contents

<b>1</b>	<b>Introduction</b> . . . . .	<b>1</b>
	O. Huber, E. Medina, P. García Montero, and J. A. Zinck	
	References . . . . .	5
<b>2</b>	<b>White-Sand Ecosystems in the Amazon Region: Location, Distinctive Features, Ecology. A Review</b> . . . . .	<b>7</b>
	P. García Montero	
2.1	Introduction . . . . .	7
2.2	Identification: Naming and Geographic Distribution of the White-Sand Ecosystems . . . . .	9
2.3	Origin, Evolution, and Landscape Dynamics of the Amazon Region . . . . .	10
	2.3.1 Amazonian Landscape: Geodynamics and Evolution . . . . .	11
	2.3.2 Past Climate Change and Effects on Amazonian Vegetation . . . . .	13
	2.3.3 Expansion, Dissemination, and Diversification of the Vegetation in the Amazon Region . . . . .	14
2.4	The Contemporary Climate and Hydrological Environment . . . . .	15
	2.4.1 Climate Conditions . . . . .	15
	2.4.2 Hydrology . . . . .	16
2.5	Soilscape and Soil Characteristics . . . . .	17
	2.5.1 Parent Material Diversity . . . . .	17
	2.5.2 Soil-Landscape Relationships . . . . .	17
	2.5.3 Genesis of Bleached Soils . . . . .	18
	2.5.4 Morphological Soil Features . . . . .	18
	2.5.5 Soil Chemistry and Fertility . . . . .	21
	2.5.6 Soil Physical Features and Drainage Regime . . . . .	23
	2.5.7 Soil Classification . . . . .	23
2.6	Soil Biotic Communities in White-Sand Ecosystems: A Nutritional Alliance . . . . .	24
	2.6.1 The Functional Interaction Soil-Fungi . . . . .	24
	2.6.2 Other Soil Organisms Contributing Nutrient Supply . . . . .	25
2.7	Ecological Interactions in White-Sand Ecosystems . . . . .	26

2.7.1	The Causes of Heath Forests . . . . .	26
2.7.2	Ecophysiological Features and Nutritional Processes . . .	27
2.7.3	Nutrient Transfer Mechanisms . . . . .	27
2.7.4	Habitat Specialization . . . . .	28
2.7.5	Soil–Vegetation Relationships . . . . .	28
2.8	The Psammophilous Vegetation: General Features . . . . .	29
2.8.1	Common and Distinguishing Features of the White-Sand Ecosystems . . . . .	30
2.9	The White-Sand Ecosystem, a Peculiar Wildlife Habitat . . . . .	33
2.9.1	Origin and Dispersal of White-Sand Specialist Biota . . .	33
2.9.2	Faunal Diversity . . . . .	33
2.10	White-Sand Ecosystems: Vulnerability and Conservation Issues . . . . .	35
2.10.1	Anthropogenic Threats . . . . .	35
2.10.2	Natural Disturbances . . . . .	37
2.10.3	Conservation Concerns . . . . .	37
2.11	White-Sand Ecosystems Research: Covering Information Gaps . . . . .	38
2.12	Concluding Remarks . . . . .	40
	References . . . . .	42

## Part I Forest and Woodland Biomes

<b>3</b>	<b>The Forests of the Upper Rio Negro (North-Western Amazon) and Adjacent South-Western Orinoco Basins: A Phytosociological Classification . . . . .</b>	<b>55</b>
	H. Arellano-Peña, D. Cárdenas-López †, J. Stropp, N. Castaño-Arboleda, G. Romero-González, F. Castro-Lima, A. Lozano, M. C. Montilla, H. ter Steege, and G. A. Aymard-Corredor	
3.1	Introduction . . . . .	56
3.2	General Features of the Study Area . . . . .	57
3.3	Materials and Methods . . . . .	60
3.3.1	Tree Inventory Data . . . . .	60
3.3.2	Phytosociological Analysis . . . . .	62
3.4	Results . . . . .	64
3.4.1	Phytosociological Classification . . . . .	64
3.4.2	Vegetation and Environmental Conditions . . . . .	69
3.5	Discussion . . . . .	72
3.5.1	General Aspects . . . . .	72
3.5.2	Forest Structural Characteristics . . . . .	74
3.5.3	Plant Diversity . . . . .	76
3.6	Conclusions . . . . .	79
3.7	Forest Conservation Issues . . . . .	80

Appendix 3.1: Phytosociological Classification and Description of the New Alliances and Associations of the Forest Communities in the Rio Negro Region . . . . .	82
Appendix 3.2 Botanical Explorations in the Rio Negro Basin: A Review . . . . .	94
Introduction . . . . .	94
The Journeys . . . . .	94
References . . . . .	98
<b>4 Amazon Caatinga Complex: Sclerophyllous Vegetation on Nutrient-Poor White-Sand Soils . . . . .</b>	<b>111</b>
E. Medina and E. Cuevas	
4.1 Introduction . . . . .	111
4.2 Environment . . . . .	113
4.2.1 Caatinga Distribution and Climate . . . . .	113
4.2.2 Soil Characteristics and Flooding Regime . . . . .	114
4.3 Species Composition and Productivity . . . . .	115
4.3.1 Floristic Composition and Structural Variation . . . . .	115
4.3.2 Biomass and Nutrient Content . . . . .	116
4.3.3 Primary Productivity, Litter Production, and Nutrient Cycling . . . . .	122
4.4 Physiological Ecology . . . . .	123
4.4.1 Leaf Traits . . . . .	123
4.4.2 Water Relations . . . . .	125
4.4.3 Photosynthesis . . . . .	126
4.4.4 Leaf Lifespan . . . . .	128
4.4.5 Nutrient Limitations and Production of Fine Roots . . . . .	129
4.5 Mycorrhizal Associations in White-Sand Forests of the Río Negro Region . . . . .	130
4.6 Concluding Remarks . . . . .	130
References . . . . .	131
<b>Part II Meadow Biomes</b>	
<b>5 Multi-Temporal and Multi-Platform Satellite-Based Mapping of White Sand Ecosystems . . . . .</b>	<b>137</b>
H. F. del Valle, G. Metternicht, and J. A. Zinck	
5.1 Introduction . . . . .	137
5.2 Materials and Methods . . . . .	138
5.2.1 Study Area Characterization . . . . .	138
5.2.2 Remote Sensing Data Sources . . . . .	140
5.2.3 Methodology . . . . .	145
5.3 Results and Discussion . . . . .	151
5.3.1 Mapping Eco-Chorological Areas of the White Sands . . . . .	151
5.3.2 Land-cover Classification . . . . .	162

5.3.3	Change Detection . . . . .	167
5.4	Concluding Remarks . . . . .	171
	Appendix: Classified Land-Cover-Land-Use Cover Classes, Together with the Segmented and Classified High-Resolution Images, Per Study Area . . . . .	175
	References . . . . .	178
<b>6</b>	<b>Study Areas: Landscapes and Soils . . . . .</b>	<b>183</b>
	J. A. Zinck, H. F. del Valle, O. Huber, and P. García Montero	
6.1	Introduction . . . . .	183
6.2	Materials and Methods . . . . .	186
6.2.1	Digital Elevation Modelling and Terrain Analysis . . . . .	186
6.2.2	Field and Laboratory Data . . . . .	188
6.2.3	Landcover Products . . . . .	189
6.2.4	Estimation of the Total Area of White-Sand Ecosystem . . . . .	189
6.3	Sipapo Area . . . . .	190
6.3.1	Geographical Setting . . . . .	190
6.3.2	Terrain Features . . . . .	191
6.3.3	Relevant Features of the Sipapo Area . . . . .	200
6.4	Camani Area . . . . .	201
6.4.1	Geographic Setting . . . . .	201
6.4.2	Terrain Features . . . . .	201
6.4.3	Landscapes and Soils . . . . .	203
6.5	Ventuari Area . . . . .	203
6.5.1	Geographic Setting . . . . .	203
6.5.2	Terrain Features . . . . .	207
6.5.3	Relevant Features of the Ventuari Area . . . . .	209
6.6	Yapacana Area . . . . .	209
6.6.1	Geographic Setting . . . . .	209
6.6.2	Terrain Features . . . . .	210
6.6.3	Relevant Features of the Yapacana Area . . . . .	218
6.7	Atabapo Area . . . . .	219
6.7.1	Geographic Setting . . . . .	219
6.7.2	Terrain Features . . . . .	219
6.7.3	Relevant Features of the Atabapo Area . . . . .	226
6.8	Pasimoni Area . . . . .	226
6.8.1	Geographic Setting . . . . .	226
6.8.2	Terrain Features . . . . .	229
6.8.3	Geoforms and Soils . . . . .	231
6.8.4	Relevant Features of the Pasimoni Area . . . . .	231
6.9	Landcover Amazonas State . . . . .	233
6.10	Conclusions . . . . .	234
	References . . . . .	237

<b>7</b>	<b>Soil Properties, Formation, Distribution, and Classification . . . . .</b>	<b>239</b>
	J. A. Zinck and P. García Montero	
7.1	Introduction . . . . .	239
7.2	General Soil Characteristics . . . . .	240
7.2.1	Soil Taxa: Diversity, Similarity, Difference . . . . .	240
7.2.2	Soil Moisture and Drainage . . . . .	247
7.2.3	Biological Characteristics, Chemical Elements, and Nutrient Status . . . . .	250
7.2.4	A Special Feature: The Occurrence of Densic Layers (Densipan) . . . . .	255
7.3	Main Soil Types . . . . .	262
7.3.1	Typic Quartzipsamments . . . . .	263
7.3.2	Oxyaquic Quartzipsamments . . . . .	267
7.3.3	Udoxic Quartzipsamments . . . . .	269
7.3.4	Typic Udorthents . . . . .	274
7.3.5	Spodosols . . . . .	281
7.3.6	Other Soils Under Meadow Vegetation . . . . .	290
7.4	Conclusions . . . . .	291
	References . . . . .	292
<b>8</b>	<b>Origin and Sources of Sand: From Highlands to Lowlands . . . . .</b>	<b>295</b>
	J. A. Zinck and P. García Montero	
8.1	Introduction . . . . .	295
8.2	Sands of Multiple Origins . . . . .	296
8.3	Sand Sources at the Basin Periphery . . . . .	298
8.3.1	Highland Sand Sources . . . . .	299
8.3.2	Upland Sand Sources . . . . .	303
8.4	Lowland Sand Sources . . . . .	310
8.4.1	Subsurface Sand Generation Under Forest and Scrubland in Undulating Lowlands . . . . .	310
8.4.2	Subaerial Sand Generation . . . . .	314
8.4.3	Piedmont Sand: From Storing to Redistributing Allogenic Sand . . . . .	316
8.5	Conclusion . . . . .	320
	References . . . . .	321
<b>9</b>	<b>Sand Dynamics and Distribution in Meadow Environment: A Geo-Pedological Approach . . . . .</b>	<b>325</b>
	J. A. Zinck and P. García Montero	
9.1	Introduction: The Lowland Landscapes . . . . .	325
9.2	Sands in Alluvial Plains . . . . .	326
9.2.1	Floodplain Dynamics . . . . .	326
9.2.2	Riverine Features and Geoforms . . . . .	328
9.2.3	Alluvial Plain Sediments: Splay Mantles . . . . .	334
9.2.4	Alluvial Plain Sediments: Overflow Mantles . . . . .	340

---

9.2.5	Boundary Conditions . . . . .	344
9.2.6	Discussion . . . . .	350
9.3	Sands in Peneplains . . . . .	351
9.3.1	Annular Depositional Glacis . . . . .	355
9.3.2	Longitudinal Depositional Glacis . . . . .	358
9.3.3	Weathering Glacis . . . . .	362
9.3.4	Discussion . . . . .	366
9.4	Valley Sediments: River Levees and Terraces (Pasimoni and Siapa Valleys) . . . . .	373
9.4.1	Riverbank Overflow Levee . . . . .	373
9.4.2	Terrace Overflow Levee . . . . .	373
9.4.3	Terrace Overflow Mantle . . . . .	374
9.4.4	Discussion and Conclusion . . . . .	374
9.5	Wind-Blown Sand Deposits . . . . .	381
9.5.1	Dune-Like Mounds . . . . .	381
9.5.2	Eolian Blankets on Glacis . . . . .	384
9.5.3	Eolian Sheets in Drowned Depressions . . . . .	386
9.5.4	Discussion . . . . .	388
9.6	General Conclusion . . . . .	389
	References . . . . .	393
<b>10</b>	<b>Features and Trends of Meadow Landscape Evolution . . . . .</b>	<b>395</b>
	J. A. Zinck and P. García Montero	
10.1	Introduction . . . . .	395
10.2	Stratifications and Lithological Discontinuities in White-Sand Sediments and Soils: Signatures of Changes in the Meadow Environment . . . . .	396
10.2.1	Stratifications of Geogenic Origin . . . . .	396
10.2.2	Stratifications of Pedogenic Origin . . . . .	402
10.3	Contact Areas: Ecotone Dynamics . . . . .	403
10.3.1	Association Caatinga-Bana-Meadow on Sandy Alluvial Sediment . . . . .	405
10.3.2	Contact Bana-Meadow in Alluvial Plain . . . . .	405
10.3.3	Contact Caatinga-Meadow in Alluvial Plain: Woody Cover in Regression . . . . .	408
10.3.4	Contact Caatinga-Meadow on Peneplain Glacis: Woody Cover in Building . . . . .	413
10.4	Microrelief: Surface Features Caused by Erosion and Suffusion . . . . .	414
10.4.1	Microrelief in the Amazonian Lowlands . . . . .	414
10.4.2	Erosion Microrelief in the Meadow Environment and Contact Fringes . . . . .	416
10.4.3	Suffusion Microrelief in the Meadow Environment . . . . .	422



10.5	White Sands and Podzolization: Spodosols as Markers of Soil-Landscape Evolution . . . . .	426
10.5.1	Spodic Feature Related to Lateral Flow of Black Groundwater . . . . .	428
10.5.2	White Sands Covering Truncated Spodosols . . . . .	429
10.5.3	Bimodal Spodosol Developed in White Sand of Eolian Origin . . . . .	430
10.5.4	Podzolic Sand Mantle Modified by Fluvial Morphogenesis: Siapa and Pasimoni Valleys . . . . .	433
10.5.5	Spodosols and Meadow Landscape Evolution . . . . .	435
10.6	Concluding Remarks: Trends in Meadow Landscape Evolution . . . . .	438
	References . . . . .	442
<b>11</b>	<b>Plant Diversity and Endemism of the White-Sand Open Vegetation in the Lowlands of the Amazonas State, Venezuela . . . . .</b>	<b>445</b>
	J. R. Grande A., O. Huber, and R. Riina	
11.1	Introduction . . . . .	445
11.2	Botanical Exploration in the Study Area . . . . .	446
11.3	Main Vegetation Types Surveyed . . . . .	446
11.3.1	Amazon Caatinga (Rio Negro Caatinga) . . . . .	447
11.3.2	Palm Swamp (Morichal) . . . . .	447
11.3.3	Meadow (Herbazal) . . . . .	448
11.3.4	Shrubland (Scrub) . . . . .	448
11.4	Species Richness and Endemicity Patterns . . . . .	449
11.5	Ecological Determinants of Open White-Sand Vegetation . . . . .	458
11.6	Conservation of Amazonian White-Sand Areas . . . . .	458
	Appendix 11.1 . . . . .	459
	Appendix 11.2 . . . . .	476
	References . . . . .	515
<b>12</b>	<b>Ecophysiological Features of the Lowland meadow's Species within the Upper Rio Negro and Orinoco Basins . . . . .</b>	<b>519</b>
	E. Medina	
12.1	Introduction . . . . .	519
12.2	The Botanical Composition of Amazonian Meadows . . . . .	521
12.3	Physiological Traits Related to Nutrient Deficiency, Flooding Tolerance, and Drought . . . . .	521
12.3.1	Dicots Families . . . . .	521
12.3.2	Monocots Families . . . . .	523
12.3.3	Similarity of Species Composition among Study Areas . . . . .	525
12.4	Concluding Remarks . . . . .	525
	References . . . . .	527

---

**Part III Synthesis**

<b>13 Synthesis</b> . . . . .	533
J. A. Zinck, E. Medina, and P. García Montero	
13.1 Introduction . . . . .	533
13.2 Forested and Shrublands Peinobiomes . . . . .	534
13.3 The Meadow Environment . . . . .	535
13.3.1 Remote Sensing Analysis of Vegetation Cover . . . . .	535
13.3.2 The Soilscape: Soil Classes, Distribution, and Properties . . . . .	537
13.3.3 The Sandscape: Depositional Processes, Sand Distribution, Sediment Characteristics . . . . .	537
13.3.4 Trends in Meadow Landscape Evolution . . . . .	538
13.4 Diversity and Endemicity of White-Sand Vegetation . . . . .	539
13.5 Ecophysiological Features of Lowland Meadows Species within Upper Rio Negro and Orinoco River Basins . . . . .	540



O. Huber, E. Medina, P. García Montero, and J. A. Zinck

Toward the end of the nineteenth century, large territorial explorations and expansions took place in the South American Tropics. In countries like Brazil, Colombia, and Venezuela intensive programs of road building followed by the establishment of new settlements led to the creation of numerous development pools in large areas previously covered by dense tropical forests, populated mostly by indigenous tribes and nations.

Located in northern South America, the Venezuelan Amazonas state is the southernmost state of that country, covering a roughly rectangular territory of approximately 183.000 km<sup>2</sup> with a maximal North-South extent of approximately 600 km. Its wide and still mostly virgin land extends from the sources of the Orinoco river, located in the south-eastern corner of the Amazonas state, to 540 km westwards in Victorino on the Río Guainía along the Venezuelan-Colombian border. The eastern border of the state is formed by the Sierra Parima, a densely forested mid-elevation mountain range bordering on the Bolívar state.

Mountain ranges reaching elevations of up to 2000 m a.s.l. extend along the northern and the northeastern borders of the Amazonas state. In the center and along the southern border with Brazil, typically flat-topped, impressive Guayanan table

---

O. Huber  
Instituto Experimental Jardín Botánico Dr. Tobías Lasser, Universidad Central de Venezuela,  
Caracas, Venezuela

E. Medina (✉)  
Centro de Ecología, Instituto Venezolano de Investigaciones Científicas, Caracas, Venezuela  
Institute of Tropical Forestry, USDA Forest Service, San Juan, Puerto Rico

P. G. Montero  
Private Activity, Soil Survey and Environmental Planning, Caracas, Venezuela

J. A. Zinck  
Faculty of Geo-Information Science and Earth Observation (ITC), University of Twente, Enschede,  
The Netherlands

mountains with sheer upper walls, locally called *tepuis*, are present, but much less frequent and extensive than in the adjacent Bolívar state. The rest of the territory consists mainly of low hilllands alternating with extensive plains between 50 and 200 m a.s.l.

The political entity of this region has long been classified by the Venezuelan Government as a Federal Territory, due to its low population density centered in a few towns and settlements. Even after its legal conversion to the rank of state in 1985, Amazonas continues being the largest primitive natural region of Venezuela with the lowest population density (ca. 142,000 inhabitants) (0.77 inhab/Km<sup>2</sup>). Population consists of indigenous ethnic groups (piaroa, baniva, yekuana, a.o.) living in dispersed rustic villages, and a few settlements and towns of non-indigenous people, of which Puerto Ayacucho, located in the north-western corner of the state, is the largest with over 100,000 inhabitants.

The colonization of the southernmost Venezuelan territory has been very slow. Separated from the northern half of the country by the mighty Orinoco river, and to the west from adjacent Colombia by the middle Orinoco flowing to the north and the Río Negro flowing to the south, this land, for long inhabited almost exclusively by indigenous ethnic groups, has been left aside during the various colonization periods of Venezuela. Even today, very few roads have been built, concentrated mostly in the north-western sector around the state's capital Puerto Ayacucho. Alternative ways of travel and transport to the interior territory are either by river or by air.

Tall tropical forests cover nearly all lowlands and uplands with an astonishing diversity of forest types. Numerous small openings covered by herbaceous vegetation, nearly always associated with deep white-sand soils, are dispersed within the forested landscape. These non-forest spots are called campos, campinas, arenales, or meadows in Venezuela as well as in northern Brazil and south-eastern Colombia. Their origin and distribution as islands in a mainly forested landscape are still unclear.

The book focuses on a variety of vegetation types, including forests, scrublands, and herbaceous communities that live on white sands in the lowlands drained by rivers Orinoco and Rio Negro. These vegetation types have developed different kinds of strategies and mechanisms to overcome the limitations of the white-sand substrate, including very low nutrient content, very low water holding capacity, oscillating groundwater level, seasonal flooding, water shortage during the lower rainfall season, and dry spells during the rainy season. The severity of the limitations that affect the vegetation formations growing on white sands qualifies them as nutrient-limited biomes.

Biomes are distinct biological communities that have formed in response to shared environmental conditions. Water availability and temperature are the dominating factors determining terrestrial plant development and distribution. They allow the arrangement of vegetation on a global scale within zonobiomes, locally modified by differences in altitude (orobiomes), or by soil characteristics (pedobiomes) (Walter and Box 1976; Walter and Breckle 2004). Pedobiomes are ecological systems more dependent on soil than on climate, and they include psammobiomes (siliceous sandy soils) and lithobiomes (stony substrates with

shallow soils). Psammobiomes are frequently characterized by low plant nutrient availability and have been designated as peinobiomes (from the Greek “peína,” meaning hunger) (Mucina 2018).

White-sand soils under high rainfall regimes are usually characterized by (a) variability in water supply (excess after heavy rains and deficit after a few rainless days) and (b) very low levels of plant nutrients due to intensive leaching. Both traits derive from the low water and nutrient retention capacity of sandy soils.

White-sand soils of the Rio Negro basin are always associated with blackwaters draining from podzolized sands. The color of the water is due to the presence of humic acids remaining in solution because of low levels of earth-alkaline cations in the water.

The vegetation that thrives on Amazonian white sands ranges from dense tall caatinga forests to scrublands and non-graminaceous meadows (Huber 2006). Within the general pattern of low nutrient availability, nutrient reservoir is higher in forest soils than in meadow soils. The series from tall caatinga to herbaceous meadow probably represents a gradient in P availability.

Plants developing on white-sand soils have physiological and anatomical properties that allow them to grow and reproduce successfully under strong nutritional limitations, among which nutrient use efficiency in photosynthesis and growth, root fungi symbiotic associations (mycorrhiza), specialized root morphology, and leaf longevity, are probably the most important.

Forests and scrublands on white sands are sclerophyllous. The leaves are hard, rich in fiber, with thick cuticles and thick cell walls. These traits result in high values of leaf mass per area (LMA), and high ratios of total fiber to protein (Loveless 1961; Poorter et al. 2009). The degree of sclerophylly and leaf concentrations of N and P are similar to those of typical sclerophylls from other parts of the world with seasonal climate, except leaf size which is larger in the high rainfall areas of the upper Rio Negro (Medina et al. 1990).

Furthermore, many forest species on white sands are mostly mycorrhizal, vesicular-arbuscular mycorrhiza being particularly abundant, whereas ectomycorrhizal symbiosis appears to be restricted to a few families (Moyersoen 1993).

The herbaceous vegetation developing on extremely oligotrophic white-sand soils is dominated by monocot genera of Rapateaceae, Xyridaceae, Eriocaulaceae, Cyperaceae, and a few Poaceae species. Similar physiognomies develop on quartzitic sands at different altitudes within the Amazon basin such as the Araracuara sandstone (Duivenvoorden and van Cleef 1994), the “campos rupestres” of Minas Gerais, Brazil (Oliveira et al. 2015), and the Gran Sabana region in southern Venezuela (Huber 2006). These families belong to the monocot order Poales with mostly non-mycorrhizal species that have root anatomic and physiologic characteristics promoting efficiency of nutrient uptake such as carboxylate secreting cluster or dauciform roots and sand-binding roots (Brundrett 2009; Oliveira et al. 2015; Abrahão et al. 2019). It appears that under an extreme scarcity of soil, P mycorrhizal associations are not energetically viable (Lambers et al. 2010; Zemunik et al. 2018). Variations in the severity of nutrient deficiency, particularly P, from tall

caatinga to herbaceous meadow probably explain the decreasing occurrence of mycorrhizal associations along the gradient. Such studies are lacking for the herbaceous vegetation on white sands in the upper Rio Negro.

The book describes forest, scrub, and herbaceous vegetation types that match the concept of peinobiome. It comprises 13 chapters grouped in two parts dealing with forest-woodland biomes and herbaceous biomes, respectively.

Part I of the book starts in Chap. 2 with a large literature review of white-sand ecosystems, basically forest, in the Amazon region. A variety of subjects is documented, referring to the formation and evolution of the Amazon region, soils, vegetation, climate, hydrology, interactions between physical factors and biotic features, and calling attention on the vulnerability of the white-sand ecosystems to increasing threats caused by human activities. The forest biome is composed of two main wooded vegetation types, the terra-firme rainforest on medium to fine-textured soils and the sclerophyllous caatinga forest on nutrient-poor sandy soils. Chapter 3 provides a phytosociological classification of a vegetation gradient from terra-firme to caatinga to flooded forests. Chapter 4 analyzes specifically the caatinga complex, focusing on floristic composition, productivity, nutrient deficiencies and cycling, and ecophysiological interactions.

Part II of the book concerns herbaceous biomes. Herbaceous vegetation occurs as meadow patches within the forest matrix on white-sand soils. Meadows constitute a unique feature in the lowlands because of their scattered, island-like distribution and singular floristic composition, including a high number of endemic species. Meadow units were described from air (Chap. 5) and on the field (Chap. 6) in six eco-chorological study areas selected on the basis of criteria such as belonging to a major watershed, distinctive physiographic and drainage features, and previous botanical information. Synergistic integration of radar data shows in Chaps. 5 and 6 DTM relief variations, geomorphic landscape units, drainage network structure, and a variety of terrain surface features such as flooded areas, soil moisture variation, slope gradient, and bare sand patches, among others. The air-borne interpreted information is substantiated in Chap. 6 by field observation data to characterize landscape and soil relationships in the study areas. Meadow soils have peculiar characteristics such as white color, sandy texture, low nutrient content, low water holding capacity, variable groundwater regime, and seasonal flooding; these characteristics are described in Chap. 7 together with soil classification. The white sands on which meadow vegetation grows are mainly fluvial sediments; the issue of their origin and sources is analyzed in Chap. 8. Meadow vegetation occurs in two landscape types: peneplain and alluvial plain both covered by white-sand deposits and/or weathered residual materials. The processes controlling the distribution and reworking of white-sand sediments by shifting rivers are analyzed from a geo-pedological point of view in Chap. 9. Meadow landscape is a morphodynamic environment; its recent and current evolution is approached in Chap. 10 using criteria such as stratifications and lithological discontinuities, ecotone dynamics in contact areas between wooded and herbaceous formations, micro-relief caused by water erosion and suffusion, and the presence of truncated Spodosols. Meadow is a complex vegetation community with variations in flora composition, endemics,

vegetation types, and geographic distribution patterns; these features are described in Chap. 11. In Chap. 12 is presented a general approach related to the ecophysiological features of plants of the lowland meadows species in the upper Rio Negro and Orinoco basins, and finally Chap. 13 provides a synthesis of the main traits of forests and shrubland on white sands and the geo-pedological relationships between white sands environments and meadow vegetation in the Venezuelan Amazonas state.

---

## References

- Abrahão A, de Britto CP, Hans Lambers H, Andrade SAL, Christine A, Sawaya HF, Ryan MH, Oliveira RS (2019) Soil types select for plants with matching nutrient-acquisition and -use traits in hyperdiverse and severely nutrient impoverished Campos rupestres and cerrado in Central Brazil. *J Ecol* 107:1302–1316
- Brundrett MC (2009) Mycorrhizal associations and other means of nutrition of vascular plants: understanding the global diversity of host plants by resolving conflicting information and developing reliable means of diagnosis. *Plant Soil* 320:37–77
- Duivenvoorden JF, Cleef AM (1994) Amazonian savanna vegetation on the sandstone plateau near Araracuara, Colombia. *Phytocoenologia* 24:197–232
- Huber O (2006) Herbaceous ecosystems on the Guayana shield, a regional overview. *J Biogeogr* 33: 464–475
- Lambers H, Brundrett MC, Raven J, Hopper SD (2010) Plant mineral nutrition in ancient landscapes: high plant species diversity on infertile soils is linked to functional diversity for nutritional strategies. *Plant Soil* 334:11–31
- Loveless AR (1961) A nutritional interpretation of sclerophylly based on differences in the chemical composition of sclerophyllous and mesophytic leaves. *Ann Bot* 25:168–184
- Medina E, García V, Cuevas E (1990) Sclerophylly and oligotrophic environments: relationships between leaf structure, mineral nutrient content and drought resistance in tropical rain forests of the upper Río Negro region. *Biotropica* 22:51–64
- Moyersoén B (1993) Ectomicorrizas y micorrizas vesículo-arbusculares en caatinga Amazónica del Sur de Venezuela. *Scientia Guaianæ* 3, Caracas, Venezuela
- Mucina L (2018) Vegetation of Brazilian Campos rupestres on siliceous substrates and their global analogues. *Flora* 238:11–23
- Oliveira RS, Galvão HC, de Campos MCR, Eller CB, Pearse SJ, Lambers H (2015) Mineral nutrition of Campos rupestres plant species on contrasting nutrient-impooverished soil types. *New Phytol* 205:1183–1194
- Poorter H, Niinemets U, Poorter L, Wright IJ, Villar R (2009) Causes and consequences of variation in leaf mass per area (LMA): a meta-analysis. *New Phytol* 182:565–588
- Walter H, Box E (1976) Global classification of natural terrestrial ecosystems. *Vegetatio* 32:75–81
- Walter H, Breckle S (2004) *Ökologie der Erde* 3. Auflage Band 2. *Spezielle Ökologie der tropischen und subtropischen Zonen*. Elsevier Spektrum Verlag
- Zemunik G, Lambers H, Turner BL, Laliberté E, Oliveira RS (2018) High abundance of non-mycorrhizal plant species in severely phosphorus-impooverished Brazilian Campos rupestres. *Plant Soil* 424:255–271. <https://doi.org/10.1007/s11104-017-3503-7>



# White-Sand Ecosystems in the Amazon Region: Location, Distinctive Features, Ecology. A Review

# 2

P. García Montero

## 2.1 Introduction

The Amazon region is a mosaic of different types of ecosystems resulting from high environmental heterogeneity and landscape complexity, associated with the diversity of climate, geologic substratum, soils, and geomorphic surfaces (Fine and Bruna 2016; Fine et al. 2010; Guilherme et al. 2018), representing nearly 50% of the global tropical rainforest area (Hoorn and Wesselingh 2010). The area includes two main ecoregions, the Amazon basin that embraces river Amazon and its many tributaries, and the Guiana Shield (Fig. 2.1). Within the vast and megadiverse Amazon region, peculiar types of ecosystems growing on quartzose and dystrophic substrates are referred to as White-Sand Ecosystems (WSEs) or White-Sand Forests (WSFs). These white-sand areas are scattered across the Guiana and Brazilian Shields, as well as in the lowlands of the Amazon basin, and are especially common in the upper Rio Negro area of Colombia, Venezuela, Brazil, also in Guiana, Suriname, and around Iquitos in Peru.

White-sand ecosystems have particular characteristics that distinguish them from the so-called “terra-firme” forests, such as stunted, unbuttressed trees, pronounced sclerophylly, high tree density, and scarce large emergent trees, large lianas, and herbs (Anderson 1981; Medina et al. 1990; Huber 1995; Alvarez et al. 2013). They are examples of habitat specialization growing under climate conditions suitable for exuberant lowland tropical forests and non-flooded terra-firme forests. In contrast to this luxurious vegetation, white-sand vegetation is characterized by prominent endemism and low diversity (Anderson 1981). White-sand vegetation, also known as “tropical heath forests” (Keith et al. 2020), are widespread in South America and elsewhere (Anderson 1981; Gentry 1988; Mardegan et al. 2009; Córdoba 2014.

---

P. G. Montero (✉)

Private Activity, Soil Survey and Environmental Planning, Caracas, Venezuela



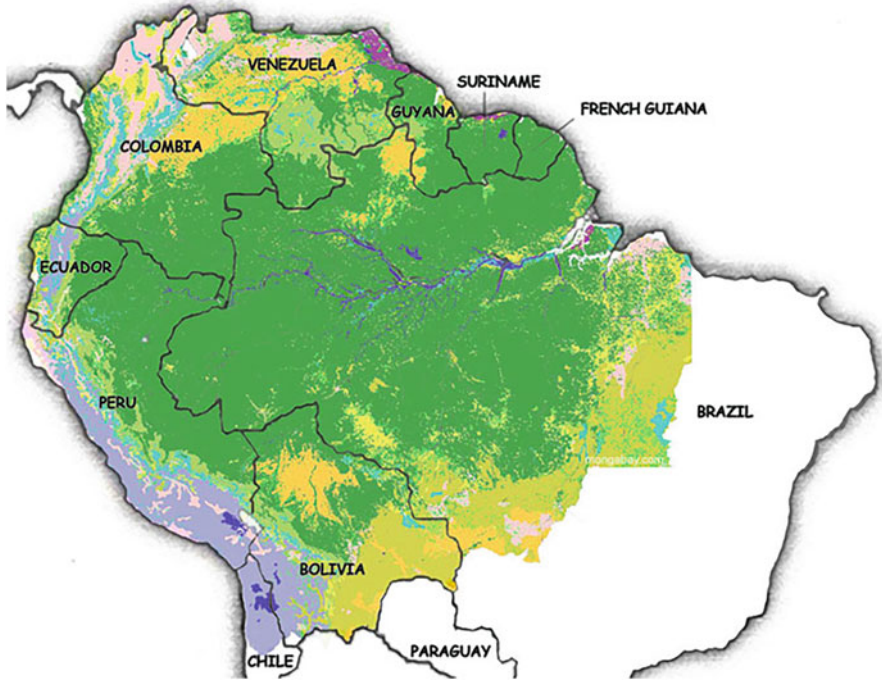


**Fig. 2.1** Amazon region with distinction of the countries that make it up. Source: Based on the Vegetation Map of Tropical South America, Eva et al. (1999). TREES Publications Series, European Commission, with modifications by Rhett A. Butler/Mongabay.com. <http://mongabay-images.s3.amazonaws.com/i/mongalogo24h.jpg>

Approximately, 335,000 km<sup>2</sup>, or about 5% of the Amazon ecoregions, are covered by WSE (Adeney et al. 2016).

Many authors have described white-sand vegetation in Brazil, Colombia, Guianas, Peru, Venezuela, and Southeast Asia. Pioneer studies in the Amazonia conducted by Lanjouw (1936), Ducke and Black (1954), Heyligers (1963), van Donselaar (1965, 1968), Sombroek (1966), Prance (1973), Herrera et al. (1978, 1981), Klinge et al. (1977), Klinge and Cuevas (2000), Klinge and Medina (1979), Soares (1979) and Huber (1995), have focused on the characterization of white-sand ecosystems. Since the 1980s, emphasis has shifted toward studying their origin and evolution, floristic composition, forest structure, soils, unique nutrient cycling, plant adaptations, ecophysiology, and biological diversity (Anderson 1981; Poels 1987; Medina et al. 1990; Matsumoto 1995; Duivenvoorden and Lips 1995; Luizao 1995; Coomes and Grubb 1996; Aymard et al. 1998, 2009; ter Steege et al. 2000; Luizao et al. 2007; Medina and Cuevas 2011; Huber and García, 2011; Zinck and Huber 2011; Damasco 2013; Damasco et al. 2012; Tanaka et al. 2013; Sobrado 2013; Guimarães and Bueno 2016; de Mendonça et al. 2017).

Even though in recent years, information and knowledge about the biophysical aspects of the WSE has increased, large areas of WSE remain unstudied or are underrepresented in the literature. In many parts of the vast and often inaccessible Amazon region, there is still information missing to decipher the interaction and variability of factors involved in the ecology of the WSE. New studies focus on topics such as soil metagenome, geophysical prospecting for mapping, carbon balance, ethnoecology, and phylogenesis with the aim of improving the knowledge of phytogeography, and the evolutionary and adaptive aspects of the WSE.

This chapter attempts to present a synthesis with prominence on the white-sand forests (WSFs) in the Amazon region (see also Chaps. 3 and 4). Herbaceous vegetation in the Venezuelan Amazon state (meadows) is the main emphasis of this book as it is developed in Chaps. 3, 6, 7, and 11. Previous syntheses of WSE in Amazonia have been elaborated by Anderson (1981) and more recently by Adeney et al. (2016). It is based on a literature review of a diversity of aspects associated with WSEs, resulting from studies and research conducted in several Amazonian countries to date.

---

## 2.2 Identification: Naming and Geographic Distribution of the White-Sand Ecosystems

The variety of terms used for similar vegetation throughout the Amazon reflects regional diversity, cultural perceptions of the environment, and real differences in species composition, soils, topography, hydrological regimes, fire frequency, and possible origin of the vegetation (Daly and Mitchell 2000).

Caatinga is a commonly used term to designate Amazonian white-sand forests. A distinction is made between tall caatinga (up to 20–30 m) or “caatinga alta” and low caatinga (<10 m) or “caatinga baixa” and “campina,” that cover about 64,000 km<sup>2</sup> in Brazil (Anderson 1981). Similar psammophilous vegetation has been described and identified in other areas of the Amazon region with vernacular names such as “campinas” and “campinaranas” in Brazil, and “bana” in Venezuela, “muri,” “white sand savannahs,” and “savanna forests” in Surinam and the Guianas (Lanjouw 1936; Heyligers 1963; van Donselaar 1965, 1968). White sand savannas refer to the vegetation growing on quartz-sand found in Suriname, British Guiana, and Brazil (Heyligers 1963; van Donselaar 1965, 1968). In the Paraíba and Pernambuco states, north-east Brazil, there are patches of savanna-like vegetation on white-sand soils called “Mussunungas” overlying sandy Spodosols surrounded by rainforest on low uplands (20–300 m a.s.l.) called “tabuleiros” (Matsumoto 1995; Saporetti-Junior et al. 2012; Gastauer et al. 2017). Other names for white-sand vegetation are “wallaba” forests, clump “wallaba,” “dakama” forests and “muri” in Guyana and Suriname, and “varillales” and “chamizales” (rods, poles, sticks) in Peru and Colombia.

White-sand areas are broadly scattered in the Amazon region and elsewhere. In Brazil, extensive areas of white-sand soils and related vegetation occur in the Rio

Negro basin, Serra do Cachimbo on the Pará-Mato Grosso boundary, Chapada dos Parecis in Rondônia, and along the Atlantic coast near the mouth of the Amazon and in Maranhão. Northern Brazil concentrates the largest territory under campinarana vegetation along the Rio Negro and Rio Branco basins (Matsumoto 1995; Guimarães and Bueno 2016; de Mendonça et al. 2017). In Colombia, patches of white-sand vegetation occur in the Inírida river basin, in parts of Vaupés, and in the Refugio savannahs or the Yari savannahs at the southern edge of La Macarena mountain range (Duivenvoorden and Lips 1995; Peñuela 2014; Córdoba 2014). In Guiana, a white-sand belt on low sandy hills supports a dense hardwood forest named “wallaba” (Daly and Mitchell 2000). The most conspicuous feature in the Zanderij area in Suriname is white sand covered with savannah vegetation (Poels 1987). In the Peruvian Amazon, white-sand forests with stick or rods species named “varillales” are found in the Nanay river basin south-west of Iquitos, at the locality of Jenaro Herrera in the Ucayali river basin, around Yurimaguas in the Morona river basin, and in the Yaguas-Cotuhé and Tapiche-Blanco interfluves (García-Villacorta et al. 2003, 2016; Vargas-Saboya et al. 2006; Honorio et al. 2008; Pitman et al. 2011, 2013, 2014, 2015). In Venezuela, caatinga forests and bana scrublands are found in the upper Río Negro basin (Klinge 1976; Klinge et al. 1977; Bongers et al. 1985; Gentry 1988; Huber 1995; Coomes and Grubb 1996; Coomes 1997; Aymard et al. 1998, 2009; Rojas and Tello 2006; Medina and Cuevas 2011), in the upper Orinoco river basin at localities close to La Esmeralda (Coomes and Grubb 1996; Coomes 1997), in the area San Carlos de Río Negro-Casiquiare river basin (Aymard et al. 2009); savanna and meadows growing on white sandy soils have been studied and in the Ventuari, Cuaio, Sipapo, and Atabapo rivers interfluves, in the Amazonas state (Huber and García 2011; Zinck and Huber 2011). Studies focused on the Venezuelan Amazonas state are dealt with in detail in Chaps. 3, 6, 7, and 11.

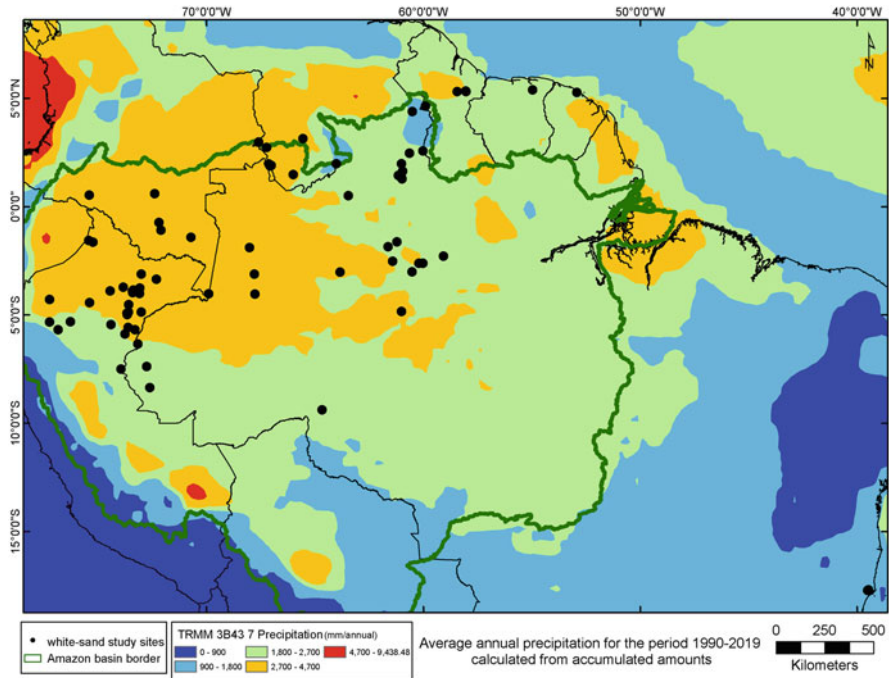
Patches of white-sand vegetation including sclerophyllous scrubland, open savannas, and shrub savannas have been reported in the Gran Sabana uplands (800–1500 m a.s.l.), in the upper and middle Caroni river basin, the principal tributary of river Orinoco (CVG Técnica Minera 1987; Berry et al. 1995; Edelca 2004).

Figure 2.2 reports locations in the Amazon region where studies and research on WSE have been conducted.

---

### 2.3 Origin, Evolution, and Landscape Dynamics of the Amazon Region

A comprehensive understanding of the processes that have contributed to the formation and evolution of the Amazon region, its landscapes, parent materials, climate, drainage systems, soils, and the environment where WSEs have originated and developed, is still the subject of discussion. To understand the contemporary state of the WSEs, their chorology and environment, it is necessary to review what past natural events have occurred in the Amazon territory and what factors allowed



**Fig. 2.2** Location of white-sand study sites included in this review, and average annual precipitation for the period 1990–2019, in the Amazonian region (rainfall data from [giovanni.gsfc.nasa.gov/giovanni/](http://giovanni.gsfc.nasa.gov/giovanni/)). Map produced by Lic. Grisel Velázquez, Centro de Ecología IVIC

the spreading and diversification of the vegetation types. Most of the species-rich Amazonian ecosystems are older than the geographic conditions in which they live today (Wesselingh and Salo 2006; Hoorn and Wesselingh 2010; Hoorn et al. 2010a, b).

### 2.3.1 Amazonian Landscape: Geodynamics and Evolution

Long periods of isolation and important geological events, in particular the Andean uplift and changes in the global climate are suggested to be mayor factors in determining vegetation evolution, expansion, speciation, specialization, and extinction leading to the contemporary patterns of biodiversity in the Amazonian ecosystems (Wesselingh and Salo 2006; Hoorn et al. 2010a, 2010b; Hoorn and Wesselingh 2010; Hoorn et al. 2010a, 2010b; Wesselingh et al. 2010; Albert et al. 2018). Variation of Amazonian geology from east to west in combination with differences in rainfall resulted in a gradient of soil fertility, which also contributed to the pattern of biodiversity (ter Steege et al. 2000).

The weathering of the shield bedrocks determined the composition (i.e., quartz, clay, and associations of stable, heavy minerals) and the bimodal grain size distribution, of the major sediment sources of the fluvial system (Hoorn 1993, 1994; Daly and Mitchell 2000). Many of the western Amazon white sands were placed during the Early Miocene (15–23 million years ago) by westward flowing rivers draining the Guiana and Brazilian Shields before the major fluvial systems changed direction by effect of the Andean cordillera uplift (Frasier et al. 2008; Hoorn 1993; Hoorn and Wesselingh 2010; Hoorn et al. 2010a, 2010b; Adeney et al. 2016).

Andean uplift controlled landscape evolution in Amazonia by affecting the regional climate and drainage patterns and during its progress triggered a rainfall increase along the eastern slope and created a vast flood of sediments into the Amazon basin. From the Early to Middle Miocene, the Andes cordillera became the major sediment source area. The landscape development and variability, the reversal of the northwestward-directed fluvial system into an eastward-directed fluvial-lacustrine system caused a major change in the palaeoenvironment of north-western Amazonia and soil heterogeneity, a factor creating and sustaining high diversity of the western Amazonian floras (Wesselingh and Salo 2006; Hoorn and Wesselingh 2010; Hoorn et al. 2010a, b; Wesselingh et al. 2010).

Most white sand substrata throughout the Amazon are ancient. The contemporary landscape, soilscape, drainage network, phytogeography, and species diversity are unquestionable signals of ancient processes that contributed to the evolution and current state of the Amazon basin, its terrain, and its biotic components (Honorio et al. 2019). Much of the present natural landscapes and biotic composition were formed during the Neogene. The combination of tectonic and climatic processes resulted in additional uplift, erosion, water and sediment source (Hoorn 1993, 1994; Daly and Mitchell 2000; Wesselingh and Salo 2006; Kroonenberg and de Roever 2010). Important Amazon river tributaries such as Rio Negro and Río Branco changed their flow courses as a response to isolated environmental changes largely associated with geo-climatic activity during the late glacial Pleistocene (Latrubesse et al. 1997; Latrubesse 2003; Latrubesse and Franzinelli 2005; Cremon et al. 2016). Modification of the river's flow direction caused considerable changes in sediment accretion and erosion, and variability in parent materials, geoforms, and soils.

Sandy substrata in Amazonia are derived from eolian activity and sediment accumulation in distributary alluvial systems during drier periods, leading to the spreading of open vegetation habitats surrounded by forest (Cordeiro et al. 2016; Rossetti et al. 2018, 2019) The largest areas of white sands in the Rio Negro watershed are most possibly ancient fluvial deposits from the Guiana Shield and the Roraima sandstone formation (Coomes and Grubb 1996; Coomes 1997; Dubroeuq and Volkoff 1998; Hoorn et al. 2010a, b).

### 2.3.2 Past Climate Change and Effects on Amazonian Vegetation

Climate conditions stimulated the formation of sandy substrata that encouraged the expansion of open psammophilous vegetation in northern Amazonia (Zular et al. 2019). The Amazon rainforest at the time of the last glaciation, during the late Pleistocene, suffered strong changes in its biotic composition and landscape. During the middle Pleniglacial (24,000 yr. BP), the Amazon basin was influenced by high precipitations at the Andes and a continuing change toward dry conditions in the lowlands; rivers were characterized by alluvial sedimentation, and eolian deposits extended over parts of the central and northern Amazonia. At the same time, the savanna vegetation reached maximum extension (Latrubesse 2000, 2003). In the context of more recent botanical, geological, and paleoecological advances, the refuge theory (Prance, 1973) has been strongly criticized due to the fact that it was defined in terms of endemic centers, and the Amazonia underwent deep biotic diversity and landscape modifications in times close to the last Glacial (Latrubesse 2000). Major landscape features in Amazonia were established by the initiation of the Quaternary; as a result, a significant portion of the current species richness is attributed to a combination of relatively constant wet and warm climates and a heterogeneous soil mantle (Wesselingh et al. 2010). Data suggest that the western Amazon lowland forest was not fragmented into refuges in glacial periods and was comparable to modern forests: The general decrease in temperature during the Quaternary glacial periods may have caused considerable extinctions in the lowlands, and changes in precipitation may have profoundly impacted the composition of vegetation communities (van der Hammen et al. 2000). Most of the Amazon lowlands remained under forest throughout the glacial cycles (Colinvaux et al. 1996, 2000).

A major change from more seasonal to more permanently wet conditions seems to have taken place in the western Amazonian basin around the Oligocene-Miocene boundary (Wesselingh and Salo 2006). Consequently, the wetter climate may have allowed the tropical rainforest to expand and retract to a mostly inland formation due to a decrease in precipitation at the Last Glacial Maximum (LGM) (Colinvaux et al. 1996). It has been suggested that from 66–34 Mya, the rainforest extended as far south as 45° (Wesselingh and Salo 2006; Hoorn et al. 2010a, 2010b; Wesselingh et al. 2010). It is now clear that the Amazon basin as a whole was not uniformly drier during Pleistocene glacial intervals. Past wet and dry intervals of the Quaternary occurred on millennial timescales, and the spatial trajectories of wet and dry regions also varied, both east-west and north-south. It has been hypothesized that alternately wet and dry conditions during the Quaternary brought about pulses of forest expansion and shrinkage (Baker and Fritz 2015; Baker et al. 2020).

During the Holocene, drought was strong in the east, whereas north-west and central Amazon was less affected causing minor floristic changes and allowing rainforest communities to prevail. Savannas expanded as a result of forest contraction in south-eastern Amazon (Olivares et al. 2015). Abrupt climate changes controlled the distribution of open vegetation environments in northern Amazon since the Last Glacial Maximum (Zular et al. 2019). The changes during the LGM were



only the latest expression of some 50 prior glacial stages that occurred over the past 2.6 million years. During the early-to-mid Holocene, around 9000–5000 years before the present, exceptional levels of precipitation, far wetter than contemporary ones, occurred in the eastern Amazon, while far drier than modern ones occurred in the western Amazon (Baker and Fritz 2015; Baker et al. 2020).

South-western Amazonia was a savanna environment during the last glacial times (Iriondo and Latrubesse 1994; D’Apolito et al. 2017). A dry season more pronounced and prolonged than the present one allowed rainforests to be replaced by savannas during different periods in the Late Pleistocene (Latrubesse and Ramonell, 1994; Latrubesse et al. 2007). Under glacial conditions, isolated areas of savanna-like vegetation expanded and so did sand accretions. There is no consensus on the chronology of the sand deposition, with estimates ranging from late Pleistocene to Holocene. Other authors suggest that the sand substrata are much older and were formed through weathering of ancient rocks (Zular et al. 2019).

### **2.3.3 Expansion, Dissemination, and Diversification of the Vegetation in the Amazon Region**

White-sand ecosystems have expanded and contracted over centuries, influencing the spatial arrangement of plants and animal life. River deposits and geological changes in the Pleistocene helped create unique life conditions in white-sand areas. Genetic isolation into separate populations is assumed to be a major factor in the evolution of species diversity in the psammophilous vegetation such as caatingas in the upper Rio Negro basin and campinas in the lower basin (Prance 1973).

The Quaternary was a time of dissemination and adaptations, but cannot longer be considered a time of diversification in the Amazon region (Wesselingh et al. 2010; Olivares et al. 2015). Thus, major diversifications are consistently placed in the pre-Pleistocene rather than the Quaternary (Haffer 2008). Strong relationships between plant species composition and soil properties suggest that floristic patterns may be determined by underlying geological variations (Tuomisto et al. 1995; ter Steege et al. 2000; Hoorn et al. 2010a, 2010b; Higgins et al. 2011). Soil and floristic patterns in Amazonia reflect a complex history of deposition–erosion cycles dating back to the Miocene and multifaceted geological processes and landscape evolution that have been decisive factors in neotropical diversification (Wesselingh and Salo 2006; Hoorn et al. 2010a, b; Albert et al. 2018; Rossetti et al. 2018, 2019).

In some areas, white sands are ancient, more than 100 million years old (Fine and Bruna 2016; Adeney et al. 2016). Contemporary white-sand areas in the Amazon region are assumed to be relict or ancestral areas of earlier, widespread habitats now covered by more recent sediments coming mainly from the Andean orogeny (Kubitzki 1990; Frasier et al. 2008). Climate-driven geomorphic processes that have affected the distribution of sandy deposits, may have created corridors for the dispersal of dry-adapted taxa (D’Apolito et al. 2017). Hence, the current biota is formed in part by the expansion and contraction of white-sand vegetation areas, the large-scale movement of sediments by rivers, and geologic subsidence during the

Pleistocene (Fine and Bruna 2016). Late Pleistocene-Holocene environmental disturbances caused by mega-fan sedimentary processes controlled the distribution of white-sand vegetation in some large areas of the Amazonian lowlands and may have also been an important factor in species diversification during this period (Rossetti et al. 2018, 2019). Capurucho et al. (2020) argue that the history of the WSE goes back millions of years; moreover, the variation and existing patterns of diversity of birds and plants specialized to the WSE were probably affected by abiotic conditions in very diverse ways relative to those in the high ground Terra Firme forests. WSEs present a distinctive assembly of species.

## 2.4 The Contemporary Climate and Hydrological Environment

### 2.4.1 Climate Conditions

The Amazon region is characterized by permanently high temperatures, low inter-annual thermic variation (less than 5 °C), high annual rainfall ranging from 1700 to 3000 mm or greater, and high relative humidity (70–90%) (Table 2.1). Some places have alternating dry and wet seasons, while other areas have rain most of the year (10–11 months), as in the case of the upper Rio Negro basin. The dry season goes from December to April, in the northern Amazon, and begins around mid-October in the southern part (Medina and Cuevas 1989; Stropp et al. 2011). Caatingas in the upper Rio Negro receive monthly rainfall exceeding 100 mm, while the forests located further south have a short period of drought (ter Steege et al. 2000; Stropp et al. 2011). The average temperature is 27.9 °C during the dry season and 25.8 °C during the rainy season.

According to data assembled in Table 2.1 climate in white-sand areas is relatively uniform with no significant differences in temperature (24–28 °C) and relative humidity (70–90%). Rainfall shows the greatest variability, ranging from 1300 to 4000 mm per year. Figure 2.2 illustrates the average annual precipitation in the Amazonian region for the period 1990–2019.

**Table 2.1** Climate data of some white-sand ecosystem areas in the Amazon region

Country	Range of climatic parameter			
	Temp °C	Rainfall mm	Rel. Hum. %	Evap/ETP mm
Brazil	26.0–33.0	1300–3.297	81.0–90.0	1437–1443
Colombia	25.7–26.4	2777–3340	85.0–87.0	1437–1443
Guiana	24.0–28.0	2280–2540	85.9	–
Peru	23.0–31.0	1375–3297	–	–
Surinam	25.8–26.1	2069–2200	–	–
Venezuela	17.8–26.7	1495–4000	75.0–85.0	1300–1600

Source: compiled from various authors



## 2.4.2 Hydrology

Ecosystems growing on white-sand soils are usually drained by blackwater rivers such as in the upper Rio Negro and Orinoco watersheds. The relative geomorphic position plays a determining role in the water relations of the sandy soil terrains. Soil saturation regime shows strong annual variations with topographic position (Klinge et al. 1977; Bongers et al. 1985). Bleached quartzose soils that support psammophilous vegetation are generally seasonally saturated by water. This environment was recognized as a relevant type of wetland in the Amazon basin (Junk et al. 2010). The magnitude of flooding has an effect on tree composition, structure, and diversity; however, for several authors, it is lower than the effect of soil texture and fertility (Damasco et al. 2012). In the Rio Negro basin, extensive plains are flooded due to poor internal soil drainage (e.g., Spodosols with hardened horizons, superficial rock beds), perched water table, and water infiltration from periodically flooded river margins. In floodplains, the structure of campinarana and igapó vegetation has been associated with flooding gradients or groundwater rise during wet seasons. Forests are replaced by open vegetation as flooding level increases or groundwater depth decreases (Vicentini 2004; Damasco et al. 2012).

White-sand forest soils in San Carlos de Rio Negro (Amazonas state, Venezuela) have an impermeable iron or humus pan. As a consequence, the water table can be near the surface or lateral drainage occurs quickly following heavy rainfalls. However, within a few days without rain, heath forest soils start to experience water stress and become dry (Klinge and Medina 1979; see Chaps. 6 and 7 in this book). Large forested zones are affected by deficient drainage and are periodically flooded such as the white-sand areas in the upper Rio Negro, Orinoco, and lower Amazon basins (Klinge 1976; Klinge et al. 1977; Bongers et al. 1985). Caatinga vegetation develops on waterlogged, root-mat-topped white-sandy soils at low-lying sites (Klinge et al. 1977; Anderson 1981; Medina et al. 1990; Klinge and Cuevas 2000; de Mendonça et al. 2014a, 2017; see Chaps. 4 and 7). Amazonian forests in blackwater floodplains (i.e., igapó) and on hydromorphic white-sand soils (campinarana) cover at least 500,000 km<sup>2</sup> of the Amazon basin (Targhetta et al. 2015).

Blackwater rivers drain large areas of bleached sandy soils (Spodosols, Quartzipsamments) into the center of the basin (Quesada et al. 2011). Their water is transparent, with low amounts of suspended matter but high amounts of dissolved organic acids (humic, fulvic) in various stages of polymerization that give the water a brownish-reddish color. The pH values are in the range of 4–5 and electrical conductivity is <20  $\mu\text{S cm}^{-1}$  (Junk et al. 2010). These rivers have an extremely low inorganic ion content, which is a consequence of the dystrophic conditions of the soils they drain, and the very efficient nutrient conservation mechanisms of the vegetation growing on them (Herrera et al. 1978). Concentrations of silica and aluminum are about 2.7 ppm and 300 ppb, respectively. Blackwater is near-distilled water quality in terms of nutrient content, resulting from the high capacity of forest to retain nutrients (Moran 1995).

## 2.5 Soilscape and Soil Characteristics

White-sand soils have formed and evolved from a diversity of parent materials and pedogenic processes. They result from in situ weathering of underlain bedrocks or the alteration of sediments transported by eolian, colluvial, and alluvial processes (Coomes and Grubb 1996; Coomes 1997; Dubroeuq and Volkoff 1998; Frasier et al. 2008; Carneiro et al. 2002; Schargel and Marvez 2009; Huber and García 2011; Quesada et al. 2011; Zinck and Huber 2011; see Chaps. 7 and 8 in this book).

### 2.5.1 Parent Material Diversity

Two large regional geological entities are the main primary sources of the sediments on which white-sand ecosystems are located, the Guiana-Brazilian Shields at the north-east and the Andean mountains at the north-west of the Amazon region.

Lithological units include crystalline Precambrian rocks (igneous-metamorphic rocks of the Guiana-Brazilian Shields), Precambrian, Palaeozoic and Mesozoic sandstones, Miocene sandstones and conglomerates, Tertiary and Quaternary quartz-rich sediments, Plio-Pleistocene sediments, late Pleistocene and Holocene quartzose sand sediments, Quaternary fluvial deposits (Dubroeuq and Volkoff 1998; Alvarez et al. 2013; Pitman et al. 2015; Myster 2017; Schargel and Marvez 2009). The largest white-sand areas in the Rio Negro basin are most likely ancient fluvial deposits originated from weathering and erosion of Precambrian shield rocks (Coomes and Grubb 1996; Coomes 1997; Dubroeuq and Volkoff 1998; Medina and Cuevas 2000; Frasier et al. 2008; Schargel and Marvez 2009; Quesada et al. 2011) and paleodune fields related to periods of drier climate during the Late Pleistocene-Holocene (Carneiro et al. 2002). In synthesis, three types of white-sand deposits can be distinguished in Amazonia: (1) white sands as residues from in situ weathering of acid, Si-rich hard bedrocks; (2) white sands redeposited by fluvial or eolian processes in well and poorly drained alluvial plains and in peneplains (terra-firme); and (3) white-sand materials resulting from podsolization (Anderson 1981; Duivenvoorden and Lips 1995). Chapter 7 in this book describes in detail the characteristics of white sand soils, their environment as well as their genesis.

### 2.5.2 Soil-Landscape Relationships

Amazon white-sand soils occur in diverse geomorphic conditions. On the Guiana Shield, in lowlands of western Amazon, and outside the Amazon basin, particularly in Brazil and Venezuela, it is common to find WSE on hilly uplands of granitic rocks and on lowland peneplains (pediplains), colluvial-alluvial fans, valley bottoms, and alluvial floodplains. Elevation ranges between 6 m and 190 m a.s.l., locally between 300 m and 2.000 m a.s.l. (Poels 1987; CVG Técnica Minera 1987; Berry et al. 1995; Matsumoto 1995; Duivenvoorden and Lips 1995; Dubroeuq and Volkoff 1998;

Aymard et al. 1998; Vriesendorp et al. 2006; Schargel and Marvez 2009; Quesada et al. 2011; Saporetti-Junior et al. 2012; de Mendonça et al. 2014a, 2017; Pitman et al. 2015; Gastauer et al. 2017; see Chaps. 6 and 7 in this book). Table 2.2 shows a summary of the most common Amazonian geofoms occupied by white sand ecosystems.

### 2.5.3 Genesis of Bleached Soils

Several hypotheses have been suggested to explain the genesis of the white-sand soils in the Amazon basin (see Chaps. 7 and 8 in this book) and beyond. White-sand soils are the outcome of deeply weathered sand mantles (Heyligers 1963). In some cases, they result from strong podsolization where repeated rising and falling of the water table causes the eluviation of organic matter and clay (van der Eyk 1957). Wet tropical climate and presence of quartz-rich materials with very low reserves of easily weatherable primary minerals favor podsolization in permeable sandy horizons, with migration of organometallic complexes and accumulation of Fe, Al, SiO<sub>2</sub>, and organic substances resulting in albic E horizons (Luizao 1995; Dubroeuq and Volkoff 1998; Nascimento et al. 2004; de Mendonça et al. 2014a). The leached material is deposited as hardpan or spodic horizon that may impede drainage and support perched water table (Poels 1987; Chauvel et al. 1987; Dubroeuq and Volkoff 1998; Schargel and Marvez 2009; Quesada et al. 2011).

In the Venezuelan upper Rio Negro, the quartz sands of savanna-like Spodosol areas are residues of the weathering of the crystalline basement (Schnütgen and Bremer 1985). The hillslope deposits and sandy sediments on which Spodosols have developed were probably formed during Quaternary dry periods (Sombroek, 1990; Dubroeuq and Volkoff, 1998). According to Horbe et al. (2004), Spodosols can develop as a consequence of vertical pedogenic processes, following the formation of white sands (see Chaps. 7 and 8 in this book).

### 2.5.4 Morphological Soil Features

Despite the relative soil homogeneity, morphological differences can be observed locally due to geomorphic position, water regime, and types of vegetation. Sandy layers are often topped by a mor humus horizon of variable thickness (Anderson 1981; Luizao et al. 2007; Nascimento et al. 2004; Dubroeuq and Volkoff 1998; Schargel and Marvez 2009; de Mendonça et al. 2014a). In Suriname, white-sand soils in savannas show a 1–2 m thick upper coarse layer. These white sands have thick bleached E horizons, often deeper than 2 m with clay content below 2%, and an underlying B horizon at 2–3 m depth as a dark brown to black hardpan, 15–30 cm thick, where organic matter has cemented the sand (Heyligers 1963; Poels 1987).

Soils of the Amazon caatinga and campina show under the litter layer an O horizon of incompletely decomposed organic matter, rich in fine roots, lying on the sandy, structureless mineral layers (Klinge et al. 1977). White-sand soils at San

**Table 2.2** Summary of the geopedologic environment characteristics of the white-sand soil per country

Country	Terrain characteristics				Drainage class
	Altitude m a.s.l.	Geology/Parent material	Geomorph	Soil class	
Brazil	30–200	Sandy sediments derived from granitic rocks; Tertiary and quaternary quartz-rich sediments (Pleistocene); tertiary sandstones; quaternary quartz-rich sediments; quartzose sand sediments derived crystalline Precambrian rocks of the Guiana shield; quartzose sand sediments, latest Pleistocene; reworked pre-Cambrian materials; Plio-Pleistocene and Holocene sediments derived from Precambrian rocks of the Guiana shield;	Tabuleiros; hills; alluvial terraces; alluvial plains; pediplains; inactive dunes; flat plateau; alluvial fans (Glacis); floodplains	Hydromorphic and sandy Spodosols; Tropaquents; Quartzipsamments (Aquodic, Spodic, Oxyaquic, Albic, Tropaquodic); Tropaquods, Haplorthods; Neossolos, Espodosolos	Well drained; well-poorly drained; moderate-poorly drained; poorly drained
Colombia	80–350	Sediments from sedimentary rocks (sandstones) of Precambrian; sediments from Palaeozoic and Mesozoic rock formations; Sandy tertiary sediments; sediments derived from Precambrian rocks of the Guiana shield; upper and lower tertiary; quartzose sand sediments	Plateau; sandstone plateaus; alluvial plain; high terraces; Tertiary sedimentary plains; peneplains; slightly hilly surfaces	Aquic Quartzipsamments; Psammaquents; Quartzipsamments; Tropaquod (Aeric, Arenic)	Well drained; well-poorly drained; poorly drained

(continued)

Table 2.2 (continued)

Country	Terrain characteristics				Soil class	Drainage class
	Altitude m a.s.l.	Geology/Parent material	Geoform	Geology/Parent material		
Guiana	120–130	Sedimentary rocks of the Miocene (sandstone, conglomerates)	Hilly landscape		Aquic Haploorthods and Udoxic Quartzipsammits	Well-imperfectly drained
Suriname	6–70	Sediments derived from metamorphosed igneous rocks (gneisses, schists, and conglomerates); sediments from tertiary to quaternary; Sandy Pleistocene- Holocene, derived from granites	Plateau; level and slightly undulating plains; level to undulating plains; footslope; swampy valley bottom		Podsolis; Tropaquods; Tropohumods; Typic and Aquic Quartzipsammits	Excessive- poorly drained; well-poorly drained
Venezuela	85–1587	Quaternary sandy sediments; sediments derived from Precambrian crystalline rocks of the Guiana shield; Holocene, sandy sediments; sediments from quaternary and sandstone rocks (Roraima group); quaternary sandy sediments, from sandstone rocks	Alluvial plain; peneplain; low hills and gently rolling plains; denudational and alluvial plains; surface, alluvial plains		Quartzipsammits; Troporthents, Tropaquods and Placaquods; Durorthods; Alaquods (Duric y Arenic) y Alorthods	Excessively drained; poorly drained; moderate-imperfectly drained; Imperfectly- poorly drained; moderate-poorly drained

Source: several authors

Carlos de Rio Negro (Venezuela) have an organic O horizon about 30 cm thick, followed by a bleached sandy horizon about 1 m thick and a Bh illuvial horizon of low permeability (Herrera et al. 1978; Medina and Cuevas 1989). In the Spodosols studied by Schargel and Marvez (2009) at the Venezuelan Amazonas state, the sandy layer is thicker than 75 cm and the spodic horizons are often located above and penetrate into altered rock layers or layers with higher clay content than the overlying layers; these very poorly drained Spodosols generally have high values of surface organic matter contents between 56.4 and 79.8 kg/m<sup>2</sup>, in the decomposed litter layers. In most of the analyzed leaf litter samples, only traces of calcium and magnesium were detected, and the authors conclude that these levels are due to the rapid extraction of nutrients from these layers, totally invaded by fine and very fine roots. They also observed that organic matter varies strongly in the A and B horizons, with the highest values observed in the A horizon in the profiles under Amazonian caatinga (1,2–11,5%) and in the Bh horizons (2,0–9,8%) (Schargel and Marvez 2009; see Chap. 7 in this book). The most common soil horizon arrangements include A-C, A-E-C, A-E-Bh, and A-E-Bh-C.

### 2.5.5 Soil Chemistry and Fertility

White-sand soils are among the most infertile tropical soils, being a very harsh stress substrate for plants due to lack of non-weatherable minerals, extreme nutrient scarcity, low organic matter content, and lack of buffering capacity because of shortage of sesquioxides. The extreme chemical poverty of the soil is the result of a long history of leaching and continued weathering after deposition of sediments that has determined a relatively homogeneous chemical substrate in most of the areas under white-sand vegetation (Poels 1987; Klinge 1976; Klinge et al. 1977; Cuevas and Medina 1986, 1988; Coomes and Grubb 1996; Medina and Cuevas 2011; Adeney et al. 2016; Keith et al. 2020; see Chaps. 7 and 8 in this book). The soil has low cationic exchange capacity, low concentration of elements such as sodium (Na), calcium (Ca), potassium (K), and magnesium (Mg) in the soil solution, very low base saturation, and very low nitrogen (N) content (Franco and Dezzeo 1994; Medina and Cuevas 2000). Available phosphorus (P) is extremely low. Soil reaction is very acid with pH values 3.3–5.6 and in many soils it is negatively related to organic matter content and CEC. Soil micronutrients levels (Zn, B, and Cu) are very low and iron (Fe) and aluminum (Al) concentrations in soil solution appear as mere traces (Duivenvoorden and Cleef 1994; Mardegan et al. 2009; Saporetto-Junior et al. 2012; Sobrado 2013). Coarse textures favor losses of nitrogen and other nutrients. In most soils, base saturation is less than 50% in both shallow and deep horizons (Schargel and Marvez 2009). These severe conditions, together or separately, restrict the production of heath forests and select only resistant species (Luizao 1995; Luizao et al. 2007; de Mendonça et al. 2014a). Forests located in the Rio Negro basin appear to be at the lower extreme of soil nutrient availability (Herrera et al. 1978; Medina and Cuevas 2000; Sobrado 2013). Table 2.3 displays a synthesis of some characteristics of the white sand soils for several countries of the Amazonian area.

**Table 2.3** Summary of some white-sand soils characteristics per country

Country	Soil properties										
	A horizon/Topsoil					E/C/Bh horizon					
	Org. layer cm	Total sand %	pH	OC %	CEC <sup>a</sup>	BS %	Total sand %	pH	OC %	CEC <sup>a</sup>	BS %
Brazil	0-10	63.0-98.0	3.4-5.3	0.15-32.0	0.35-88.2	1.0-33.3	63.0-99.2	4.0-5.4	0.07-5.3	0.7-16.4	0.0-73.5
Colombia	0	-	2.4-4.2	0.26-4.06	1.4-8.9	<6-<51	-	3.4-4.0	0.07-0.27	1.6-2.9	<20- <33
Guiana	5	91.8-94.1	4.6-4.7	1.1	2.2-2.3	6.9-10.9	88.7-96.8	4.4-5.6	0.33-1.24	0.7-7.8	0.57-8.6
Suriname	0-3	78.0-96.0	4.2-4.4	0.29-1.9	1.9-2.3	6.3-10.4	70-97	4.4-5.4	0.07-0.75	0.34-2.04	3.9-35.3
Venezuela	0-21	84.2-96.7	3.6-5.1	0.67-46.9	0.31-7.6	29.0-78.0	82.2-96.7	4.8-5.8	0.17-14.8	0.03-5.68	11.0-88.0

Source: compiled from various authors

<sup>a</sup>m-equiv 100 g<sup>-1</sup>; pH is estimated in water 1:5, 1:2.5, 1:1, 1:2 and KCl; OC% = %MO/1.724; BS% calculated from CECs

### 2.5.6 Soil Physical Features and Drainage Regime

Although WSEs are mostly in areas of poor drainage, they can be affected locally and seasonally by hydric stress. Low water-holding capacity of sandy deposits and structureless materials restrains water retention in the soil mantle. It is unlikely for WSE to have marked dry periods due to low topographic position; however, psammophilous vegetation can be affected by water stress a few days during drier periods. Most of the available water is stored in the humus O or A horizon. The relative geomorphic position plays a determining role in the water relations of sandy soils. Topographic changes control annual variations in the soil drainage (aeration or saturation) and flooding regime (Heyligers 1963; Klinge et al. 1977; Bongers et al. 1985; Medina and Cuevas 2000, 2011). Some soils remain saturated most of the year, especially after heavy rains, while others are only saturated in parts of the soil profile. Soil water regime influences vegetation changes, nutrient transport, and development of organic layer or exposed root mat (Franco and Dezzio 1994; Coomes and Grubb 1996; Coomes 1997; see Chap. 7 in this book). Some psammophilous forests can be temporarily exposed to waterlogging due to the presence of a hardpan at one meter or more below the soil surface, which impedes root penetration to deeper layers and exposes the forest to drought due to the sandy soil texture during the dry season (Luizao 1995; Duivenvoorden and Lips 1995; Medina and Cuevas 2011; Adeney et al. 2016). Soil data from various WSE study areas are reported in Table 2.3; it shows the relative spatial homogeneity of given soil attributes such as high sand content throughout the soil profiles, pH values, and the drastic decrease in organic carbon and nutrient contents below the topsoil (A and O horizons).

### 2.5.7 Soil Classification

Some soils show evidence of podsolization and podzol-like characteristics, although they do not meet all the criteria for this classification (de Mendonça et al. 2014a; see Chap. 7 in this book).

Soils of the WSE have been mostly classified as Spodosols and Entisols (Soil Survey Staff 1999). Main Spodosol taxa include Aquic Haplorthods, Tropaquods (Aeric and Arenic Tropaquods), Orthods (Durorthods) y Alquods (Duric and Arenic Alquods), Alorthods and Placaquods. Main Entisols taxa include Tropaquents, Spodic Quartzipsamments, Aquodic Quartzipsamments, Oxyaquic Quartzipsamments, Albic Quartzipsamments, Udoxic Quartzipsamments, Tropaquodic Quartzipsamments, Aquic Quartzipsamments, and Psammaquents (Klinge et al. 1977; Poels 1987; Medina et al. 1990; Duivenvoorden and Cleef 1994; Franco and Dezzio 1994; Duivenvoorden and Lips 1995; Luizao 1995; Soil Survey Staff 1999; Berroterán 2000; Luizao et al. 2007; Schargel and Marvez 2009; Cárdenas et al. 2007; Damasco et al. 2012; de Mendonça et al. 2014a, 2017). According to FAO soil classification, Albic Arenosols and Carbic Podzols are common soil taxa found in WSE of central Guyana (ter Steege et al. 1999).



Clear relationships between soil classes, drainage, geoforms, and vegetation physiognomy were found by de Mendonça et al. (2014a). They identified Typic Haplorthods in non-flooded pediplains under forest, Spodic Quartzipsamments also in non-flooded pediplains and inactive dunes under forest and grassy-woody vegetation, Aquodic Quartzipsamments in moderate to high flooding regime pediplains and fluvial plains with arboreal cover, and Oxyaquic Quartzipsamments in high flooding regime with grassy-woody vegetation. In line, Schargel and Marvez 2009 found a clear relationship between poorly drained Spodosols and the presence of Amazon Caatinga vegetation. A detailed classification from a large variety of WSE soils of the Amazonas state in Venezuela, associated with geomorphology and sand origin is given in Chaps. 7 and 8 in this book.

---

## 2.6 Soil Biotic Communities in White-Sand Ecosystems: A Nutritional Alliance

The soil biotic community has a protagonist role in integrating ecological and geochemical processes (Finlay, 2008). The soil microorganisms play a crucial role in the nourishing processes, thereby influencing element cycling, soil fertility, and soil development, as well as plant health and nutrition. Mycorrhizal fungi are considered one of the most important nutrient conservation mechanisms responsible for tight nutrient cycles of white-sand vegetation (Klinge 1976; Herrera et al. 1978, 1981; Jordan and Herrera 1981; Bongers et al. 1985; Medina et al. 1990; Luizao et al. 2007; Asghari and Cavagnaro 2011; Vasco-Palacios and Hernandez 2014).

### 2.6.1 The Functional Interaction Soil-Fungi

The fungal community structure is strongly linked with plants, both in terms of species composition and species richness (Peay et al. 2013).

Mycorrhizal fungi infect most plants in the majority of ecosystems (Francis and Read 1994; Asghari and Cavagnaro 2011). Large differences in plant and fungus species diversity, nutrient status, and litter input have been noted between the two types of mycorrhizal forests: i.e., (1) arbuscular mycorrhizal forest patches and (2) ectomycorrhizal forest stands (Francis and Read 1994; Vasco-Palacios and Hernandez). Endomycorrhizal or vesiculo-arbuscular mycorrhiza (VAM) roots are the dominant type of mycorrhiza in all rainforest types (Moyersoen 1993). Mycorrhizal plants may obtain nutrient supply through arbuscular mycorrhizae fungi of up to 80% nitrogen and 90% phosphorus (Marinho et al. 2018).

Major contributions of mycorrhizal associations consist in improved uptake of mineral nutrients from poor soils, especially phosphorus and microelements (zinc, copper, boron, and molybdenum), due to the extension of the nutrient-absorbing organ of host plants by the external mycelium; increased water absorption, protection against pathogens, and mitigation of abiotic stresses such as soil acidification, aluminum, heavy metals, salinity, drought and pollution, improving survival,

increasing drought resistance of young plants, release of nutrients from mineral particles or rock surfaces through weathering, soil aggregate stability, effects on carbon cycling, influence on ecological processes such as plant succession, on the ability of invasive species to colonize new habitats, on the response of plant communities to habitat fragmentation and perturbations, and on productivity of plant communities (Francis and Read 1994; Onguene 2000; Cardoso and Kuyper 2006; Finlay 2008; Roy et al. 2016, 2017; Hijri and Bâ 2018; Vasco-Palacios 2016; Vasco-Palacios et al. 2018; Montesinos-Navarro et al. 2018).

Most of the roots of Amazonian psammophilous forest communities form mycorrhizal symbiosis. The dominant trees of the campinarana-type forests are obligatorily ectotrophically mycorrhizal (Singer and Araujo 1979). White-sand forests in the lower Rio Negro basin host a high diversity and heterogeneity of ectomycorrhizal communities. From a total of 1006 unique ectomycorrhizal specimens, 137 specimens and 64 species have been described in white-sand forests, mainly in the Brazilian state of Amazonas (Roy et al. 2016). In Venezuelan caatinga, most of the dominant tree species are vesiculo-arbuscular mycorrhizae (VAM), but a few ectomycorrhizal tree species appear locally codominant in the same area. The presence of vesicular-arbuscular mycorrhizae in 42 woody species of the caatinga forest around San Carlos de Río Negro in southern Venezuela is considered as an adaptive mechanism to extreme soil conditions (Moyersoen 1993; Moyersoen et al. 2001). See Chaps. 4 and 12 in this book for further analysis of these relationships/associations.

## 2.6.2 Other Soil Organisms Contributing Nutrient Supply

### 2.6.2.1 Termites

Termites are important in tropical terrestrial ecosystems due to their role in fragmenting organic material and thus in energy and nutrient flows; their population parameters are positively associated with forest productivity, biomass, stature, and soil fertility. Termitaria cycle a great proportion of nitrogen (12.8%), phosphorus (8.5%), and potassium (7.3%), concentrating actively nutrients and subsequently recycling them (Salick et al. 1983). Termites play a minor role in the forests of the Rio Negro basin because less than 5% of the annual litter and treefall is cycled through their population (Salick et al. 1983). Termite population in white-sand soils decreases during dry periods due to diminished litter provision and soil moisture (Adis et al. 1989a, 1989b; Araújo et al. 2015). About 58,000 arthropods per m<sup>2</sup> soil were extracted in a dryland forest on white-sand soil (campinarana) during the dry season near Manaus, Brazil, while the population in the rainy season ascended to 74,000 individuals per m<sup>2</sup>. During the dry season, about 63% of the termites lived in the top 3–5 cm, 21% underneath at 3.5–7 cm depth, and only 16% at 7–14 cm depth. Decreasing abundance was significantly correlated with lower soil temperature and lower soil humidity at greater soil depth (Adis et al. 1989a, 1989b; Ribeiro et al. 2008). Brazilian white-sand forests have few species of ants and termites, and no earthworms (Alvarez 2002).

### 2.6.2.2 Rhizobacteria and Myrmecophillia

Many trees and other plant species living in nutrient-depleted heath forests have developed unusual ways to get nutrients (see Chap. 12 in this book). Some tree species use rhizobia as nitrogen-fixing bacteria in their root nodules (Proctor 1999).

Other plants, for instance, *Drosera ssp.* and *Utricularia ssp.*, are carnivorous and attain nutrients by trapping and digesting insects (Proctor 1999). The myrmecophytes of Amazonas example Tocosca (Melastomataceae) and many epiphytes also capture nutrients in this way. Minatel et al. (2020) reported two new species of *Utricularia* (Lentibulariaceae), collected in an area of white-sand vegetation in the eastern Amazon Basin recognized as Campos do Ariramba in Brazil seemingly. The role of the residing ants seems to vary through ant species and/or plant species; inhabiting ants protect the plants from potential herbivores and the degree of protection can vary either through environments or ant species; additionally, some ants may play a role in plant-plant competition for light and nutrients (Michelangeli 2010).

---

## 2.7 Ecological Interactions in White-Sand Ecosystems

Many studies have been conducted to understand the causes that have led to their origin and performance. Distribution range of plant species is related to physical variables of ecosystems that limit plant growth and each plant species response to extreme physical factors.

### 2.7.1 The Causes of Heath Forests

The origin of WSE remains uncertain, and it is unclear which factor, or set of factors acting together, are more relevant (Mardegan et al. 2009; Keith et al. 2020). Several factors or causes seem to be related to explain the origin of the white-sand vegetation, among them: coarseness of the sand, intense leaching (de Mendonça et al. 2014a, b), free drainage, low capacity to retain water, and drought stress (Klinge et al. 1977; Franco and Dezzeo 1994), waterlogging (Herrera et al. 1978; Bongers et al. 1985; Kubitzki 1990; Franco and Dezzeo 1994; Klinge and Cuevas 2000; Keith et al. 2020), low nutrient content (1978; Anderson 1981; Coomes 1997; Medina and Cuevas 2011; Sobrado 2013), soil acidity (Luizao 1995), impermeable subsurface layers or ortstein (iron or humus pan), presence of phenolic compounds, intense human disturbance (Klinge, et al. 1977; Poels 1987; Herrera et al. 1978; Anderson 1981; Bongers et al. 1985; Medina and Cuevas 2000; Herrera 2000; Luizao et al. 2007; Mardegan et al. 2009; Medina and Cuevas 2011; Damasco et al. 2012). It is emphasized that soil flooding is a severe abiotic constraint on the growth of woody plants and limits plant diversity to stress-tolerant species.

## 2.7.2 Ecophysiological Features and Nutritional Processes

Singular and complex ecophysiological features and processes are typical of white-sand ecosystems (see Chaps. 4 and 12 in this book).

Despite having low rates of litter inputs and flux of N from litter-fall to soil, WSEs are highly efficient in circulating available N from litter (Medina and Cuevas 2000; Mardegan et al. 2009). The density of fine roots in the upper soil layers or in the root mat above the mineral soil is an influential factor for the conservation and efficiency of the nutrient-catching process and improving respiration (Medina et al. 1990; Medina and Cuevas 2000). Local distribution of species may be prepared by their abilities to maintain a balance of micronutrients collected through roots under critically low levels of available Zn, B, and Cu, whereas excluding potentially deleterious ions of Mn, Fe, and Al (Sobrado 2013).

Leaves are characterized by a high degree of sclerophylly and low foliar nitrogen and phosphorus contents, which can result in low decomposition rates and, in turn, slow nutrient release, low photosynthetic efficiency, low leaf concentrations of N and P, and longevity (Klinge et al. 1977; Cuevas and Medina 1986, 1988; Medina et al. 1990; Medina and Cuevas 2000, 2011; Keith et al. 2020). Overheating of leaves is prevented by most species through pronounced leaf surface inclination, lowering water demand for transpiration during dry days (Medina et al. 1990). High leaf hardness is an advantage by reducing herbivory and increasing drought tolerance (Peñuela 2014). Smoother canopies and smaller tree crowns can reduce transpiration, because it lowers the mass-flow delivery to the root surface of potentially toxic hydrogen ions and possibly phenolic compounds that strongly inhibit ion uptake by roots. Tree species growing in white-sand soils allocate more of their resources in herbivore defense and consequently have less to assign in growth (Fine et al. 2004).

## 2.7.3 Nutrient Transfer Mechanisms

White-sand forests have well-developed structural and physiological mechanisms for efficient re-cycling of the nutrients stored in their biomass so that losses are minimal. Mechanisms include sclerophylly and growth rates, slow decomposition rates, low nutrient demands, root mat development in close contact with decomposing litter with a relatively high nutrient retention capacity, degree of mycorrhizal infection which allows transfer of certain elements of the decomposing leaf litter to the roots by hyphal bridges of mycorrhizal fungi, nutrient re-translocation before leaf abscission, nutrient conservation in plant components by means of herbivory reduction through accumulation of secondary metabolic chemicals in leaves and roots, physiological adaptation of trees to calcium-deficient and aluminum-rich acid soils, flooding conditions and resistance against low oxygen environment, arrangement of fallen leaves on the forest floor that reduces the residence time of water on them and decreases nutrient extraction through leaching, and the multilayered structure of the forest which functions as a filter extracting

nutrients from through-fall water, where epiphytic organisms (bacteria, algae, lichens, and bryophytes) play an important role with some of them being able to fix nitrogen from the air (Herrera et al. 1978, 1981; Cuevas and Medina 1986, 1988; Medina and Cuevas 2000; Herrera 2000). The poorer the ecosystem, the greater the development of the fine root layer, and the greater the presence of toxic substances which inhibit the predation of leaves (Moran 1995). In white-sand savannas, low N level can be inferred from the low species number of Leguminosae in the herbaceous layer (Duivenvoorden and Cleef 1994).

#### 2.7.4 Habitat Specialization

White-sand forests have been referred to as a classic case study of habitat specialization and a source of high endemism in both animal and plant communities of Amazonian forests (Fine et al. 2006; Fine and Baraloto 2016; Keith et al. 2020). The flora is disseminated as habitat-islands across the Amazon and Guiana Shield regions; it has many local and regional endemics, building an important contribution to overall neotropical plant diversity (Guevara et al. 2016; García-Villacorta et al. 2016).

The growth-defense strategy may result from long-term habitat specialization. Herbivores accentuate habitat differences and thereby increase the potential for soil heterogeneity to produce habitat specialists; thus, this interaction between herbivory and resource heterogeneity promotes divergent selection in plant growth and defense strategies that increase the potential for ecological speciation. Species growing in white-sand forests develop by allocating relatively more resources to defense than species growing in terra-firme forests (Fine et al. 2004, 2006; Fine and Baraloto 2016), determining habitat specialization of plants (Stropp et al. 2011, 2014). Sequences of extreme flood and drought have led to the selection of plants with highly specialized adaptations to these conditions, in the form of unusually high root biomass and leaves that are either leathery or spiny (Moran 1995). About 23% of plant species in western Amazonia white-sand forests are white-sand specialists (Fine and Bruna 2016). Many species have morpho-physiological characters that allow for survival in white-sand soils but very few possess the set of traits that allow them to become dominant (Fine et al. 2004, 2006, 2010).

#### 2.7.5 Soil–Vegetation Relationships

The fluctuation between high water saturation and water shortage in nutrient-poor sandy soils may explain the low stature of the bana-type vegetation in the upper Rio Negro basin (Franco and Dezzio 1994; Coomes 1997) and patterns of decreasing species richness, and aboveground wood biomass in the campinarana-type vegetation (Targhetta et al. 2015). Jimenez et al. (2020) found a high correlation between mortality rates and rainfall in the non-flooded white-sand forests in the Colombia Amazon and concluded that their leaf area index (LAI) did not reflect the differences

in net primary productivity (NPP) components and their response to rainfall. Under drought events, the white sand forests responded asynchronously allocating carbon to fine root production. Specific soil characteristics such as their propensity to waterlogging were important factors in determining the degree of belowground NPP (Jimenez et al. 2020).

Organic matter content and cation exchange capacity (CEC) are the main distinguishing variables for the separation of campinarana types. The more open oligotrophic vegetation with reduced tree height in the campinaranas reflects low fertility, very sandy texture, and soil hydromorphy (Alder and van Kuijk 2009). In other white-sand forests, less tree diversity and low basal area are positively related to soil texture and fertility (Damasco et al. 2012). Soil moisture and soil phosphate availability are among the many soil properties that might differentially influence tree seedling growth on white-sand podzolic soils of the Guiana Shield (Baraloto et al. 2006).

The effect of soil on WSE floristic composition has been recognized as higher than that of other environmental variables examined (Damasco et al. 2012; Daly et al. 2016). Species richness increases along the gradient from grassland to woodland as well as fine sand percentage rises, and soil water holding capacity content increases (Saporetti-Junior et al. 2012). The sum of bases in the exchange complex is the soil variable that has been directly related to species floristic composition. Changes in species composition of white-sand vegetation can be associated with small variations in soil parameters, although these variations do not necessarily influence the richness and other structural parameters (Demarchi et al. 2018). Studies carried out in the Amazonas state by Aymard et al. (2009) reported the presence of caatinga forests, clustered as black-water forests, in the Rio Negro and Casiquiare river interfluves and found that flooding had an important influence on the floristic composition of the forests studied. They concluded that species richness (alpha diversity) is higher on well-drained “terra-firme” forests; meanwhile, in inundated forests on sandy Spodosols, dominant species were present in high densities and restricted to this forest type. The contents of sand and clay, the poorly drained soils, the length of the drought period, and the geomorphological position explain about 70% of the variability.

---

## 2.8 The Psammophilous Vegetation: General Features

Vegetation growing on white sand is very specialized and its remarkable physiognomy, with a diversity of unusual characteristics, suggests physiological strain distinctive from the “terra-firme forests” (Soares 1979; Anderson 1981; Klinge and Cuevas 2000; Medina and Cuevas 2000; Daly and Mitchell 2000; García-Villacorta et al. 2003, 2006, 2016; Damasco et al. 2012; Adeney et al. 2016; Guilherme et al. 2018; Keith et al. 2020).

### 2.8.1 Common and Distinguishing Features of the White-Sand Ecosystems

In this section are summarized the most important features of white-sand forests (WSF) growing in the Amazonian environment. Herbaceous vegetation like meadows and white sand savannas are not included in this synthesis; they are analyzed with detail in Chaps. 7 and 11.

WSF ecosystems are a remarkable example of habitat specialization and a source of high endemism in both animal and plant communities of Amazonian forests, representing a stressful environment. A set of distinctive characteristics synthesizes the distinguishing features of these peculiar ecosystems (Klinge et al. 1977; Soares 1979; Klinge and Medina 1979; Anderson 1981; Duivenvoorden and Lips 1995; Medina and Cuevas 2000; Vriesendorp et al. 2006; Frasier et al. 2008; Stropp et al. 2011; Damasco 2013; Keith et al. 2020).

- WSEs have less vegetation cover, less wood volume, and a partially open canopy. Some woody plants (caatinga baixa or low caatinga, bana) are mostly small and scrubby, with a very distinct floristic composition (Bongers et al. 1985; Medina et al. 1990; Alvarez 2002; Vicentini 2016; Sobrado 2013; Mardegan et al. 2009; Medina and Cuevas 2011; Damasco et al. 2012; Adeney et al. 2016; Guilherme et al. 2018).
- WSEs have a high density of trees, scarcity of large emergent trees, large lianas, and herbs, and absence of a marked buttressing of the trunks. Vines are uncommon in contrast to epiphytes. Large gaps are never seen (Anderson 1981; Alvarez 2002; Keith et al. 2020).
- The occurrence of epiphytic species is very common in these ecosystems, mainly the Orchidaceae, for instance, in campinaranas environments (Quaresma et al. 2017; Klein and Piedade 2019).
- Vegetation varies along a gradient from high caatinga or campinarama to low caatinga or bana. The herbaceous cover and the proportion of roots in the total biomass increase with increasing oligotrophy (Klinge et al. 1977; Soares 1979; Klinge and Medina 1979; Medina and Cuevas 2000).
- Tree and shrub leaves have small (microphyll) to larger leaves (mesophyll to macrophyll); they are hard, leathery, and sclerophyllous, with xeromorphic appearance and high longevity. They have developed anti-herbivore defenses through coriaceous texture and the presence of secondary compounds, especially phenolics and tannins. Leaves tend to be steeply inclined and have a heavy waxy cuticle that is probably an adaptation to minimize leaching of nutrients by rain. Leaf area index is smaller than that of terra-firme forests, probably to diminish the effect of drought stress (Sobrado and Medina 1980; Anderson 1981; Medina and Cuevas 1989; Medina et al. 1990; Alvarez 2002; Mardegan et al. 2009; Medina and Cuevas 2011; Sobrado 2013; Keith et al. 2020).
- A major proportion of nutrients is tied up in the organic matter, so that decomposition constitutes a critical pathway for the maintenance of ecosystem production.



- Psammophilous plants develop a thick root mat that efficiently traps decomposing nutrients from the often very thick layer of accumulated leaf litter (Vriesendorp et al. 2006; Schargel and Marvez 2009). Fine roots are abundant in the litter layer but do not penetrate into the underlying sand. About 86% of the roots are found in the A and O horizons and 70% are considered extremely fine.
- Plants in WSE have unusual trophic strategies such as “ant-plants” that host ant colonies inside themselves, plants with nitrogen-fixing root nodules, insectivorous plants, associations and symbiosis with organisms such as mycorrhizae, termites, and arthropods (Salick et al. 1983; Adis et al. 1989a, 1989b; Moyersoen et al. 2001; Roy et al. 2016, 2017; Vasco-Palacios et al. 2018; Minatel et al. 2020).
- Values referring to tree height, tree density, and basal area vary from country to country. The stunted facies named campina or low caatinga (also bana) is a 3–12 m high scrub, and the taller facies referring to campinarana or tall caatinga is 10–25 m high (Klinge and Medina 1979; Anderson 1981; Coomes 1997; Barbosa and Ferreira 2004). The canopy of the rods or varillales in the Peruvian Amazon varies between 10 m and 22 m high, with emerging trees of up to 26 m (Rojas and Tello 2006; Honorio et al. 2008; Zarate et al. 2013; Alvarez et al. 2013; Pitman et al. 2013, 2014, 2015, 2016; Myster 2017; Honorio et al. 2019). The chamizales are 3–12 m high (García-Villacorta et al. 2003; Vriesendorp et al. 2006; Honorio et al. 2008; Fine et al. 2010; Pitman et al. 2015). The density of individuals varies between 518 and 880 trees per ha and the basal area ranks between 19.7 and 32.0 m<sup>2</sup> per ha (Dezzeo et al. 2000; Vargas-Saboya et al. 2006).
- Total biomass measured in plots of high caatinga is about 820 tons/ha, while it is only 20 tons/ha in plots of low caatinga or open bana (Bongers et al. 1985). Biomass in caatinga is twice that of bana (i.e., 28 kg/m<sup>2</sup> vs. 10–17 kg/m<sup>2</sup>) (Moran 1995). The total biomass and that of animals are also much smaller in WSE than those of most tropical forests (Adeney et al. 2016).
- White-sand forests are less complex in floristics than terra-firme forests (Vriesendorp et al. 2006; Myster 2017). Low plant diversity in WSE is not necessarily due to low soil nutrient status but is, at least partly, caused by their small extent and fragmented distribution, which influence large-scale and long-term evolutionary processes (ter Steege et al. 2000; Stropp et al. 2011).
- WSEs have a proclivity for species dominance, in contrast to other Amazonian forests where dominance is rare (Moran 1995; García-Villacorta et al. 2003, 2006, 2016); local dominance by a few species that account for more than half of all individuals is a common phenomenon in these forests (Boubli 2002; Fine et al. 2004, 2006, 2010; Stropp et al. 2011; Demarchi et al. 2018). As stated by Aymard et al. (2009), in the Venezuelan Amazon caatinga forests on sandy Spodosols, the species *Micrandra sprucei* (Euphorbiaceae) and *Eperua leucantha* (Caesalpinaceae) represented 41.2% of the individuals measured.
- Higher similarity of campinaranas, for instance, is associated with monodominant species which have a continental distribution, Brazil (de Mendonça et al. 2017; Saporetto-Junior et al. 2012). Likewise, caatinga at Pico da Neblina (Brazil) is recognized as one of the least diverse forests, associated with high dominance of



*Eperua leucantha*, *Micrandra sprucei*, and *Hevea* cf. *brasiliensis*, which together account for 66% of all sampled trees (Boubli 2002).

- Leguminosae is one the most abundant family in half of the Amazon forest regions and forest types. They are especially in forests on white-sand podzols in the Guianas. Leguminosae and Bombacaceae are very common families in forests on white-sand podzols of the Guiana Shield (ter Steege et al. 2000). Studies in WSE of the Peruvian Amazon, middle Colombian Amazon, and Guiana Shield have reported 531 tree species out of the 1.583 fully identified species (Peñuela 2014). A total of 33 families, 65 genera, and 52 species were recorded in plots on varillales and shambles in the Peruvian Amazon (García-Villacorta et al. 2003). A total of 114 species have been classified as endemics and specialists to white sands; they are extremely dominant, accounting for more than 83% of the total number of stems surveyed in white-sand forest plots in the Peruvian Amazon (Fine et al. 2010; Zarate et al. 2013). According to Flores et al. (2020), latest evidence suggests that monodominance is probably a consequence of metacommunity dynamics in harsh isolated ecosystems, such as white-sand forests. Another usually accepted mechanism is the symbiosis between dominant trees and ectomycorrhizal fungi, which improves nutrient uptake and defence against pathogens, and gives a competitive benefit to the host tree.
- According to Draper et al. (2019), Boubli (2002) in Amazonian forests a small number of dominant species account for the majority of individuals, whereas the large majority of species are locally and regionally extremely scarce; dominant species contribute little to local species richness (alpha diversity). According to Damasco et al. (2021), metapopulations of a hyperdominant taxon may be interpreted as much more resilient to future global changes than relatively rare lineages within a species complex.
- Geographic proximity may help explain some part of the observed phyto-geographic affinities of white-sand floras. It has been suggested that a majority of the species diversity found in white-sand forests in the Amazon basin can be attributed to plants from other habitats (Peñuela 2014; García-Villacorta et al. 2016). By contrast, a majority of the species (54.5%) in the white-sand forests of the Brazilian Amazon is restricted to it (García-Villacorta et al. 2016). Of the total western Amazon white-sand specialist species, 88% occur in floras within the Guiana Shield region, whereas 12% are endemic to the western Amazon. In effect, the Caquetá moist forests, Guiana highland moist forests, and Negro-Branco moist forests share the highest proportions of western Amazon white-sand specialists (García-Villacorta et al. 2016). The Amazon areas in Brazil, Colombia, and Venezuela are geographically adjacent and were found to have close links to western Amazon white-sand forests.

## 2.9 The White-Sand Ecosystem, a Peculiar Wildlife Habitat

White-sand forests are far from uniform and they have outstanding value as wildlife refuge. Some endemic, rare, or specialist fauna species are restricted to white-sand habitats. Although zoologists have much less studied WSE than botanists, the existence of some species of birds, mammals, and butterflies restricted to these habitats has been recognized. WSEs have reduced abundance of fauna individuals and reduced species richness (Alvarez 2002). In the last decade, ornithologists have described many new bird species from white-sand ecosystems, an unequivocal demonstration of their biotic peculiarity. Low number of species, high individual dominance, and elevated level of endemism characterize, for instance, bird communities in the Amazon region (Borges 2006; Borges et al. 2016a, b; Alvarez 2002; Alvarez and Whitney 2003; Alvarez et al. 2013).

### 2.9.1 Origin and Dispersal of White-Sand Specialist Biota

Ornithological studies have been among the most prolific in the Amazon region. Many white-sand forest (WSF) specialist bird species are common in the Guiana Shield in Brazil, Colombia, Peru, and Venezuela. A relatively ancient avifauna of Guianan heritage, through some millions of years of soil fragmentation, is the source of white-sand avian community. The contribution of floristics and vegetation structure to habitat specialization and diversity in birds is one of the factors contributing strongly to the high regional species richness in the neotropics. Bird communities of white-sand forests are more similar to each other than they are to terra-firme or flooded forest communities (Alvarez et al. 2013). Vegetation growing on white-sand “islands” or mini-refuges within the surrounding terra-firme forest offers a range of food resources capable of attracting seasonal migrants from other open biomes. This explains the comparatively large number of migratory species in small patches of white-sand vegetation (Borges et al. 2016a, b; Guilherme and Borges 2011; Guilherme et al. 2018).

### 2.9.2 Faunal Diversity

Some white-sand specialist species are restricted to particular white-sand forest types. As a result, recognizing the plant community helps locate the forest faunal specialist species (Shany et al. 2007).

WSEs harbor a unique avifauna with a smaller number of species and lower species richness than terra-firme and seasonally flooded forests (Alvarez et al. 2013; Borges et al. 2014; Díaz-Alván et al. 2017; Kvarnäck and Bosque 2017). Despite its low diversity, the avifauna of white-sand vegetation has a distinctive species composition and makes a significant contribution to Amazonian beta diversity. There have been reported 544 bird species in white-sand vegetation, with most of them (58%) being sporadically found in this habitat. At least 235 bird species were

recorded in Amazonian savannas and white-sand caatinga (Nascimento et al. 2004; Borges 2006; Damasco et al. 2012; Alvarez et al. 2013; Borges et al. 2014, 2016a, b; Díaz-Alván et al. 2017).

In the Peruvian WSF, 177 bird species have been reported. About 73% of the white-sand forest avifauna community was found to be rare and only 15% of bird species were found to be common (García-Villacorta et al. 2006). A number of 114 bird species was registered in an isolated enclave of campina-campinarama in the western extreme of the Brazilian state of Acre (Guilherme and Borges 2011). A collection of 313 bird species has been reported from several white-sand sites in the southern Amazonas state in Venezuela, and the total number of species recorded is quite high when compared to those of other studies on white-sand vegetation (bana/campina and caatinga/campinarama) in the Brazilian and Peruvian Amazon basin. Bird communities in lowland white-sand vegetation of southern Venezuela include 22 habitat specialists that can be considered as indicators of white-sand vegetation (Kvarnäck and Bosque 2017). Some 35–37 bird species closely associated with vegetation on sandy soils are rarely or never found in other forest types (Borges et al. 2016a, b). Bird assemblages in white-sand vegetation are species-poor but distinct (Borges 2006; Alvarez et al. 2013; Borges et al. 2016a, b; Kvarnäck and Bosque 2017).

In the Peruvian Amazon, 74 species of amphibians and 35 species of reptiles (18 lizards, 13 snakes, 2 caimans, and 2 turtles) have been registered in the vast white-sand archipelago of the Matsés region. WSE in Tapiche and Blanco watersheds, in the Peruvian Amazon, represent some of the most diverse herpetological communities in the world. In an area of white-sand forest with varillales, 36 amphibians and 13 reptiles have been registered. These patterns of diversity suggest degrees of endemism at local and regional levels (Pitman et al. 2013, 2014, 2015, 2016).

As with plants, animal diversity is lower in the campinarana forest than in the surrounding terra-firme forest. A collection of 153 mammals has been reported from white-sand forests. Mammals that have a restricted distribution include various primates such as white-faced sakis (*Pithecia pithecia*), black uakari monkeys (*Cacajao melanocephalus*), black spider monkeys (*Ateles paniscus*), tamarins (*Saguinus inustus*), bats (*Diclidurus isabellus*, *Lonchorhina marinkellei*, *Micronycteris pusilla*, *Scleronycteris ega*, *Vampyressa brocki*), and rodents such as Brazilian squirrels (*Sciurus gilvularis*), rats (*Akodon urichi*), porcupines (*Coendou melanurus*), and spiny rats (*Proechimys semispinosus*). Larger and widespread mammals include peccaries (*Tayassu tajacu* and *Tayassu pecari*), tapir (*Tapirus terrestris*), jaguars (*Panthera onca*), and deer (*Mazama americana*) (Borges et al. 2016a, b). In the Río Curaray region, Peruvian Amazon, 304 groups of 13 primate species have been reported. Woolly monkeys (*Lagothrix poeppigii*) were the most frequently observed. This region harbors a very high diversity of primates, comparable to other sites in Amazonia and worldwide. The lowest number of primates was found in the varillal vegetation, which may be explained by the low floristic diversity and probably productivity of white-sand forests. The Río Napo region is also recognized as one of the most species-rich areas of the world (Fine

et al. 2010; de Oñate-Calvín et al. 2013; Aquino et al. 2014). Despite the fact that WSE are less biodiverse, the existence of specialist, endemic and rare species is an evident reason to protect and formulate conservation policies for these singular and fragile ecosystems.

---

## 2.10 White-Sand Ecosystems: Vulnerability and Conservation Issues

White-sand vegetation is a fragile ecosystem with very low resilience. Currently, they are threatened and poorly represented within the protected area system created in the Amazon region. It is important to study and protect these forests not only because they are biologically unique and harbor a rich community of rare and range-restricted species, but also because once they are disturbed, they may require hundreds or thousands of years to recover. According to Herrera et al. (1981), WSEs are able to prosper even on poor soils thanks to nutrient recycling mechanisms; however, they stop functioning when the forest is disturbed and the nutrients are irreversibly lost. Anthropogenic and natural disturbances threats are affecting the survival and ecological functioning of WSE, affecting their biodiversity and the environmental services they provide.

### 2.10.1 Anthropogenic Threats

In the Amazon region, many people and particularly indigenous communities depend on shifting agriculture associated with fire practice and the use of forest products for wood and firewood. Nowadays, surface mining creates increasing and locally irreversible impacts on the territory and the ecosystems.

White-sand soils are for the most part inappropriate for agriculture, but people who live within WSE have no economic alternatives. Agriculture and extraction of wood for timber, charcoal, and firewood are practiced unsustainably and unproductively in habitats that are extremely slow in recovering. While many white-sand forests are protected by geographic isolation, others are being exploited near major urban centers, such as Iquitos in Peru, Manaus and Belem in Brazil, and some localities in Guiana, Suriname, and Colombia (Daly et al. 2016). In Brazil, one of the main human-driven disturbances of white-sand vegetation is sand extraction for construction, threatening WSV patches close to large cities such as Belem and Manaus, with mining activity resulting in the destruction of vegetation, soils, and biota (Alvarez et al. 2013; Borges et al. 2016a, b; Guilherme et al. 2018).

Demarchi et al. (2019) consider that overexploitation is one of the main causes of biodiversity loss and local extinction. In the Brazilian Amazon, the intensive use of high-value timber of “terra-firme” is stimulating an apparently current increase in the exploitation of white-sand species, usually non-exploited because of their relatively low commercial value. Campinaranas forests are currently experiencing several anthropic pressures. A replacement process with abundant species from

campinarana, such as *Aldina heterophylla* (macucu), is currently happening (Demarchi et al. 2019), because it is one of the few species that reach comparable basal area to species from terra-firme forests.

In the Venezuelan Amazonia, white-sand areas have been so far less affected by deforestation due to: (1) very low population density (less than 1 inhabitant per km<sup>2</sup>) and limited accessibility; (2) the presence of national parks, natural monuments, and a biosphere reserve that protect a large proportion of the state territory; and (3) nutrient-poor white-sand soils that are mostly inadequate for agriculture, limited to small-scale pineapple and manioc cultivation around human settlements. Currently, the most threatening activity is illegal mining for gold, diamond, and more recently coltan. Open mining as a consequence of the “Orinoco Mining Arch” project has had devastating effects and will probably exacerbate destructive consequences of mining in the Venezuelan Amazonian region (Kvarnäck and Bosque 2017).

Numerous endemic species may face extinction due to widespread burning and deforestation of white-sand vegetation. Repeated fires result in the effective detention of succession; subsequent illegal mining for sand and minerals eliminates any possibility of vegetation reestablishment (Anderson 1981). Mining practice results in complete suppression of vegetation with drastic effects on biota. Populations of bird specialists in small and isolated patches may experience local extinction at higher rates than populations in larger and more connected patches. Some bird species have low population density and their local maintenance depends on colonization from nearby patches; therefore, maintaining connectivity among isolated patches should be a priority for bird conservation (Alvarez and Whitney 2003; Alvarez et al. 2013). Roads have consistently been implicated as drivers of ongoing Amazon deforestation and may act as corridors to facilitate species invasions and forest fragmentation. It is crucial to determine how ecological succession alters avian communities following deforestation and whether established roads lead to a constant influx of new species (Rutt et al. 2019). Birds specialized in living in white-sand forests disappear after the site is disturbed (Vriesendorp et al. 2006). In Brazil and in other amazonian countries, roads have consistently been considered as drivers of ongoing Amazon deforestation (including forest fragments), affecting the forest bird community and acting as corridors to facilitate species invasions, both directly as invasion strips and indirectly by promoting land-use changes (Rutt et al. 2019). Some animals, especially the obligate white-sand specialists, may be affected by minor forest disturbances such as those caused by selective timber extraction (Alvarez 2002; Alvarez et al. 2013). Legal and illegal logging, and oil and gas exploration and production represent a long-term threat to herpetofauna due to habitat fragmentation and soil disturbances associated with the construction of roads and platforms, affecting places where amphibians and reptiles reproduce (Pitman et al. 2013, 2015). Seven of the white-sand vegetation indicator species (20% of this avifauna) are in an IUCN-threatened category. Isolated distribution, small area occupied, and fragility to human-driven disturbances make WSE one of the most threatened vegetation types in the Amazon basin (Borges et al. 2016a, b).

### 2.10.2 Natural Disturbances

Expected climate change can be seen as a natural menace affecting significantly various regions of the Amazon. The probability of a decline in the dry season rainfall is about 50% in the south-east Amazon, 30% in Guyana and the eastern region, and 10% in the central and western regions (USAID, 2018). This means that low resilience and fragile ecosystems like the Amazonian white-sand ecosystems could be serious. In a dryer climate scenario, herbivory rates may decrease which would favor growth in leaf area, but would most likely affect growth in height of white-sand vegetation seedlings (Peñuela 2014). In the future, drought may cause extensive savannization, particularly in the east. In terms of ecosystem functioning, droughts will reduce root growth and standing biomass, and may shift the Amazonian forest from being CO<sub>2</sub> sinks to become CO<sub>2</sub> sources. Predicted responses of the Amazon forests to drier rainfall regimes show significant biomass loss (Fine et al. 2006; Jiménez et al. 2014; Adeney et al. 2016; Longo et al. 2018).

In the opinion of Flores and Holmgren (2021), climate change is increasing the frequency and severity of wildfires, exposing tropical forests to the risk of shifting into an open vegetation state. If recurrent fires continue, topsoil erosion intensifies, transforming clay-rich soils into white sand soils that may favor savanna tree species. They conclude that white-sand savannas may expand through seasonally flooded ecosystems at the core of the Amazon, facilitated by wildfires. Their results indicate that the magnitude and severity of these disturbances will facilitate the spread of white-sand savannas across the core of the Amazon basin (Flores and Holmgren 2021).

### 2.10.3 Conservation Concerns

Despite an increase in studies of these ecosystems in recent years, many aspects remain largely unknown scientifically (Adeney et al. 2016; Fine and Bruna 2016; Guilherme et al. 2018). Fragility and low resilience, sparse distribution, and small population sizes of some specialized species of plants and animals (i.e., birds) make the WSE one of the most threatened vegetation types in the Amazon region. Preservation of Amazonian white-sand forests depends on prompt actions to reduce greenhouse gas emissions, diminish deforestation rates, reforest and preserve forest areas, and maintain corridors connecting them in the lowland environments (Olivares et al. 2015). Survival from the point of view of biodiversity, wildlife habitat, hydrology, and carbon sequestration or C-sink, depends directly on decreasing deforestation rates (Dias e Sarmiento and Costa Franca 2018).

White-sand ecosystems are inadequately protected (Gaworecki 2016). Due to their island-like distribution patterns and resultant complex metapopulation dynamics, endemism, extremely slow recovery after disturbance, and important contributions to basin-wide diversity patterns and ecosystem services, WSEs should be given special consideration in conservation efforts to ensure their persistence in Amazonia (Adeney et al. 2016; Kvarnäck and Bosque 2017). Conservation will

require the maintenance of regional dispersal processes that connect the archipelagos of habitat islands and other ecologically similar oligotrophic habitats across the Amazon and the Guiana Shield (García-Villacorta et al. 2016).

Despite well-intentioned attempts to protect WSE in the Amazonian region by legal figures such as Reserves, National Parks, Natural Monuments, these have not been so effective. WSEs are inadequately protected and, where accessible, are regularly mined for sand, gold and diamond, logged with poor timber extraction practices, burned and cleared for agriculture (Adeney et al. 2016; Guilherme et al. 2018; Dias e Sarmiento and Costa Franca 2018).

WSE should be the object of clear environmental policies with the purpose of generating initiatives to intensify and improve their inventories, integrated characterization and cartography, as well as the accomplishment of interdisciplinary studies and research programs aimed at clarifying their origin, their complex ecological relationships, and their conservation and protection, especially in areas close to high resource-demanding locations.

---

## 2.11 White-Sand Ecosystems Research: Covering Information Gaps

Resulting from this review, some general study and research topics are proposed with the objective of increasing the information and improving the knowledge about Amazonian white-sand ecosystems. WSEs in many parts of the Amazon region remain understudied, and there is little amalgamation of the interaction of factors across different areas (Adeney et al. 2016; Guimarães and Bueno 2016). Consequently, multidisciplinary long-time research programs must be conceptualized and planned in order to reduce the lack of information about these singular ecosystems and to support national conservation policies and environmental management plans for these habitats. These studies and research could be oriented toward the following topics.

- Detailed and integrated inventories of WSE
  - Continue WSE detailed inventories, integrated characterization, update cartography, and use of advanced technology in high-resolution remote sensing tools. Characterization and inventory of small WSE patches (Borges et al. 2016a, b; Rossetti et al. 2018). Deforestation rates in Amazonia are likely to increase in the next few years and yet one-third of the total number of tree species are likely still undescribed or undiscovered (Damasco et al. 2021).
  - Integration of geopedological and biological data to reduce uncertainty on the existence of many areas of white-sand vegetation in the amazon region
- Distribution, structure, and functioning of broadleaf meadows in natural white sand areas with and without anthropogenic disturbance
  - Experimental analysis of physiological mechanisms of nutrient uptake and conservation in different white sand habitats, with emphasis on dominant families and genera



- Field study of reproductive systems, germination, and establishment under natural conditions
- Nutrient inventory and cycling, organic matter production, and biotic interactions in selected WSE sites throughout the Amazon lowlands
- It is relevant to the creation of WSE corridors to evaluate ecological connectivity and successional processes in the Amazonian region.
- Climate change impacts
  - Assessment of expected climate change impact on the Amazonian region, including among others white sand biodiversity, endemism, successional processes, soils, organic matter production and accumulation and water resources.
  - Monitoring of the phenological, physiological, and ecological responses of white sand vegetation in order to evaluate for instance increase in temperature, increased evapotranspiration and a reduction in soil water storage, decreased precipitation during dry months, potential increase in flooding in some areas, more variable climate, higher rate of organic matter decomposition and more extreme events (Olivares et al. 2015; USAID 2018).
  - To study the effects of the changing environment on increasing population of invasive species that may out-compete native, endemic, and specialist species, leading to a decline in white sand species diversity (USAID 2018).
  - Studies of the oligotrophic ecosystems in the Amazon region with emphasis on climate change impacts and responses, and their contribution to global carbon cycles (Targhetta et al. 2015), and studies on white-sand vegetation C-cycling, driving factors, accumulation, decomposition, and loss rates among different WSE ecosystems.
  - Comparative studies of key factors should address the relationships and interactions between soils, hydrology, and fire regimes with vegetation structure and stature, and plant, animal, and fungal communities in sites that show characteristics thought to be representative of WSE (Adeney et al. 2016; de Mendonça et al. 2014b).
- Soil microorganism, plant communities, and nutrient cycling
  - Studies that provide accurate information and general understanding of the functional characteristics of the soil microbiota in extreme environments like the WSE. More investigation is necessary in order to improve the knowledge about the interactions between plants and the soils below them, and with soil microorganisms, and how would be these interactions under a scenery of climate change.
  - Studies related to fungal communities and species grouped by soil types to correlate species composition in WSE and evaluate the role of soil biotic community in structuring plant communities and facilitating nutrient cycling
  - Studies on biotic communities other than fungi that are closely associated with WSE, including certain species that appear to be white-sand specialists (Adeney et al. 2016)



- Studies on white-sand vegetation N-cycling and P-cycling in order to comprehend the adaptations and strategies of WSE to respond to limited nutrient conditions (Mardegan et al. 2009)
- Impact of water deficit and intense flooding events on mycorrhizal species and population and their effects on nutrient cycling
- Conservation and management of WSE
  - To formulate a coherent strategic research program of conservation requirements and priorities, and establish an effective management plan for the WSE under protected areas in the context of the Amazon region
  - Promotion of sustainable development projects or alternative sources of legal income generation for local people in order to discourage individuals to explore illegal activities such as gold mining and coca production, threatening the biological and cultural diversity in some of the WSE areas (Peñuela 2014)
  - Studies related to the impact assessment of deforestation, fire, and diversity of land use on white-sand ecosystems (flora, fauna, microclimate, and soils)
  - To implement long-term fauna studies to generate data, necessary to determine how ecological succession alters avian and other species communities following deforestation and whether established roads lead to a constant influx of new species and provide a non-static picture in this continual process (Rutt et al. 2019)
  - It is necessary to identify and monitor relevant timber species in both terra-firme and white-sand forests, and to increase the participation of the local community in the development of logging management practices (Demarchi et al. 2019).
  - Studies to evaluate the impact of removing individuals and species from white sand communities, and its consequences for human populations, who depend on the extraction of forest resources (Demarchi et al. 2019); and also to know the effects on fauna habitat and successional processes
  - To promote the use of non-timber species in white sand forests (non-wood products), especially for nutrition and medicinal purposes. The trade of non-timber forest products represents an important sustainable source of income for many families in the Amazon (Demarchi et al. 2019).
  - To establish species requires management guidelines, considering that the impacts of logging activities may vary depending on the species exploited (Demarchi et al. 2019).

---

## 2.12 Concluding Remarks

White-sand ecosystems represent about 335,000 km<sup>2</sup> of lowland forests in the whole Amazon basin. They are a clear example of habitat specialization and represent the most extensive heath forests in the world along with other types of vegetation such as

shrublands, meadows, and grasslands on oligotrophic sandy soils, commonly found in the Amazon region and across the Guiana and Brazilian Shields.

Long-term landscape evolution and climate change have been identified as important drivers of expansion, speciation, and extinction, determining the current patterns of biodiversity in Amazonian ecosystems. Various important past events have strongly contributed to the contemporary pattern of biodiversity in the Amazon region, including (1) a long period of isolation, (2) the Andean uplift, and (3) changes in the global climate. Most white-sand substrata throughout the Amazon are ancient. In some areas of tropical South America, white sands are more than 100 million years old (Fine and Bruna 2016); however, the recent history of the present habitats is quite dynamic.

The largest areas of white-sand soils in the Rio Negro basin are possibly ancient fluvial deposits from the Guiana Shield and the Roraima sandstone formation. Most recent sand deposits range from late Pleistocene to Holocene and were formed through the weathering of ancient rocks in uplands and highlands.

Abrupt climate changes have controlled the distribution of open vegetation environments in northern Amazonia since the Last Glacial Maximum. Present-day white-sand areas are supposed to be relict areas of earlier, widespread habitats now covered by more recent sediments mainly from the Andean orogeny. These ancient, nutrient-poor areas may be ancestral regions of neotropical plant diversity.

The Guiana Shield with Precambrian bedrocks in the north-east of the Amazon region and the north-western Andean mountains are the two large regional geological entities, the erosion of which provides sediments that constitute parent materials of the white-sand ecosystems. White-sand soils derive from a variety of parent materials, including Precambrian igneous-metamorphic and siliceous sedimentary (sandstones) rocks, and Quaternary eolian, alluvial, and colluvial sediments.

White-sand soils share characteristics of extreme nutrient scarcity, low organic matter content, and high acidity. These characteristics explain why even the most developed forests on white-sand soils have much lower basal areas, aboveground biomass, and primary productivity than terra-firme forests. WSEs are a stressful environment and are considered as an example of habitat specialization and a source of high endemism in both animal and plant communities, with rare species that are absent in other Amazonian forest types, low plant species diversity, and a wide range of vegetation types from herbaceous savannas to closed-canopy forests. White-sand forests are less complex in floristics than terra-firme forests. Low plant diversity in WSE is, at least partly, caused by their small extent and fragmented distribution, which influence large-scale and long-term evolutionary processes. They have a tendency for species dominance, in contrast to other Amazonian forests where dominance is rare. Local dominance by a few species that account for more than half of all individuals is a common phenomenon in these forests.

They embody habitats of low resilience and high adaptation to extreme environmental conditions such as extreme soil acidity, inhibition of nitrifying bacteria, water stress due to flooding, permanent or temporary soil saturation associated with spodic horizon depth, and seasonal fluctuation of the water table. WSEs host a flora and

fauna clearly distinguishable and specialized, with a low diversity and reduced animal life.

White-sand forests are distinctive and fragile habitats that are especially vulnerable to anthropogenic disturbances. They are unsatisfactorily protected and, where accessible, are regularly mined for sand and other minerals (gold, diamond), logged for timber and firewood, burned and cleared for agriculture, and used for road construction. White-sand vegetation should be given special protection that takes into account its fragmented distribution pattern, endemism, presence of species that have undergone long-term adaptation to live in nutrient-poor environments, extremely slow recovery after disturbance, importance to biodiversity and ecosystems across the entire Amazon basin, and intrinsic value and attractiveness of its nature.

Research suggests that parts of the Amazon region may be susceptible to biome shifts, biodiversity loss, and depletion of carbon stores because of climate changes and variability. Rainfall predictions for the region indicate stronger and longer dry seasons, particularly in southern and eastern Amazonia, which would affect the fragile and low resilient WSE. In the future, drought may produce forest contractions causing extensive savannization, particularly in the east. In terms of ecosystem functioning, droughts will reduce root growth and standing biomass, and may shift the Amazonian forest from being CO<sub>2</sub> sinks to become CO<sub>2</sub> sources. There is still information missing to decipher the interactions and variability of factors involved in the ecology of the psammophilous vegetation across the Amazon region. In this regard, multidisciplinary long-time research programs must be planned in order to reduce the lack of information and to support conservation and environmental management plans for these habitats.

---

## References

- Adeney M, Christensen NL, Vicentini A, Cohn-Haft M (2016) White-sand ecosystems in Amazonia. *J. Biotropica* 48(1):7–23. Review. <https://doi.org/10.1111/btp.12293>
- Adis J, Ribeiro EF, de Moraes JW, Cavalcante ETS (1989a) Vertical distribution and abundance of arthropods from white sand soil of a neotropical Campinarana forest during the dry season. *J Stud Neotrop Fauna Environ* 24:201–211
- Adis J, de Moraes JW, Ribeiro EF, Ribeiro JC (1989b) Vertical distribution and abundance of arthropods from white sand soil of a neotropical Campinarana forest during the rainy season. *J Stud Neotrop Fauna Environ* 24:193–200
- Albert JS, Val P, Hoorn C (2018) The changing course of the Amazon River in the Neogene: center stage for neotropical diversification. *Neotropical Ichthyol* 16(3):e180033
- Alder D, van Kuijk M (2009) A baseline assessment of forest carbon in Guyana. Prepared for Guyana Forestry Commission
- Alvarez AJ (2002) Characteristic avifauna of white-sand forests in northern Peruvian Amazonia. Master's Theses, Louisiana State University. [https://digitalcommons.lsu.edu/gradschool\\_theses/2776](https://digitalcommons.lsu.edu/gradschool_theses/2776)
- Alvarez AJ, Whitney BM (2003) New distributional records of birds from white-sand forests of the northern Peruvian Amazon, with implications for biogeography of northern South America. *Condor* 105:552–566

- Alvarez AJ, Metz M, Fine PVA (2013) Habitat specialization by birds in western Amazonian white-sand forests. *Biotropica* 45(3):365–372
- Anderson AB (1981) White-sand vegetation of Brazilian Amazonia. *Biotropica* 13(3):199–210. <http://www.jstor.org/stable/2388125>
- Aquino R, López L, García G, Heymann EW (2014) Diversity, abundance and habitats of the primates in the Río Curaray basin. *Peruvian Amazonia Primate Conservation* 28:1–8
- Araújo VFP, Silva MP, Vasconcellos A (2015) Soil-sampled termites in two contrasting ecosystems within the semiarid domain in North-Eastern Brazil: abundance, biomass, and seasonal influences. *Sociobiology* 62(1):70–75
- Asghari HRA, Cavagnaro TR (2011) Arbuscular mycorrhizas enhance plant interception of leached nutrients. *Funct Plant Biol* 38:219–226
- Aymard G, Berry P, Schargel R (1998) Estudio de la composición florística y los suelos en bosques altos del área Maroa-Yavita, Amazonia Venezolana. *Revista UNELLEZ de Ciencia y Tecnología* 16(2):115–130
- Aymard G A, Schargel R, Berry P, Stergios B (2009) Estudio de los suelos y vegetación (estructura, composición florística y diversidad) en bosques macrotérmicos no-inundables, Estado Amazonas, Venezuela (Aprox. 01° 30'-- 05° 55' N; 66° 00'-- 67° 50' O). En *BioLlania* pp 6-251, Edición Especial No. 9. Editores Gerardo A. Aymard y Richard Schargel. Guanare, Venezuela
- Baker PA, Fritz SC (2015) Nature and causes of quaternary climate variation of tropical South America. *Quat Sci Rev* 124:31–47
- Baker PA, Fritz SC, Battisti DS, Dick CW, Vargas OM, Asner GP, Martin RE, Wheatley A, Prates I (2020) Beyond refugia: new insights on quaternary climate variation and the evolution of biotic diversity in tropical South America. In: Rull V, Carnaval AC (eds) *Neotropical diversification: patterns and processes*. Springer, Berlin, pp 51–70
- Baraloto C, Bonal D, Goldberg DE (2006) Differential seedling growth response to soil resource availability among nine neotropical tree species. *J Trop Ecol* 22:487–497
- Barbosa RI, Ferreira CAC (2004) Densidade básica da madeira de um ecossistema de “campina” em Roraima. *Amazônia Brasileira Acta Amazonica* 34(4):587–591
- Beroterán JL (2000) Tropical rainforests of Kwakwani-Guyana. Part 1 pedosphere. Sediments and vegetation structure. *Acta Biol Venez* 20(3):17–33
- Berry PE, Huber O, Holst BK (1995) Floristic analysis and phytogeography. In: Berry PE, Holst BK, Yatskievych K (eds) *Flora of the Venezuelan Guayana*, vol 1. Vegetation. Missouri Botanical Garden/Timber Press, St. Louis/Pórtland, OR, pp 97–160
- Bongers F, Engelen D, Klinge H (1985) Phytomass structure of natural plant communities on spodosols in southern Venezuela: the bana woodland. *Plant Ecol* 63(1):13–34
- Borges SH (2006) Rarity of birds in the Jaú National Park, Brazilian Amazon. *Anim Biodivers Conserv* 29(2):179–189
- Borges SH, Whittaker A, Machado de Almeida A (2014) Bird diversity in the Serra do Aracá region, northwestern Brazilian Amazon: preliminary checklist with considerations on biogeography and conservation. *Fortschr Zool* 31(4):343–360. <https://doi.org/10.1590/S1984-46702014000400006>
- Borges SH, Cornelius C, Moreira M, Ribas CC, Conh-Haft M, Capurucho JM, Vargas C, Almeida R (2016a) Bird communities in Amazonian white-sand vegetation patches: effects of landscape configuration and biogeographic context. *Biotropica* 48(1):121–131. Special issue: Neotropical White-Sand Forests
- Borges SH, Cornelius C, Ribas CC, Almeida R, Guilherme E, Aleixo A, Dantas S, Santos MPD, Moreira M (2016b) What is the avifauna of Amazonian white-sand vegetation? *Bird Conserv Intern* 26:192–204. <https://onlinelibrary.wiley.com/doi/abs/10.1111/btp.12296>
- Boubli JP (2002) Lowland floristic assessment of Pico da Neblina National Park, Brazil. *Plant Ecol* 160:149–167. <https://doi.org/10.1023/A:101583281120>
- Capurucho JMG, Borges SH, Cornelius C, Vicentini A, Prata EMB, Costa FM, Campos P, Sawakuchi AO, Rodrigues F, Zular A, Aleixo A, Bates JM, Ribas CC (2020) Patterns and

- processes of diversification in Amazonian white sand ecosystems: insights from birds and plants. In: Rull V, Carnaval A (eds) *Neotropical diversification: patterns and processes*. Fascinating Life Sciences. Springer, Cham, pp 245–270. [https://doi.org/10.1007/978-3-030-31167-4\\_11](https://doi.org/10.1007/978-3-030-31167-4_11)
- Cárdenas LD, Barreto SJS, Murcia GUG, Salazar CC, Méndez QO (2007) Caracterización y tipificación forestal de ecosistemas en el municipio de Inírida y el corregimiento de Cacahual (departamento del Guainía): una zonificación forestal para la ordenación de los recursos. Instituto Amazónico de Investigaciones Científicas -Sinchi-, Corporación para el Desarrollo Sostenible del Norte y el Oriente Amazónico, CDA, Bogotá, Colombia
- Cardoso IM, Kuyper TW (2006) Mycorrhizas and tropical soil fertility. *Agric Ecosyst Environ* 116: 72–84
- Carneiro AF, Schwartz D, Tatumi SH, Rosique T (2002) Amazonian paleodunes provide evidence for drier climate phases during the Late Pleistocene–Holocene. *Quat Res* 58(2):205–209. <https://doi.org/10.1006/qres.2002.2345>
- Chauvel A, Lucas Y, Boulet R (1987) On the genesis of the soil mantle of the region of Manaus, Central Amazonia, Brazil. In: multi-author review. The dynamics of the amazonian terra firme forest. *Experientia*, vol 43, pp 234–241
- Colinvaux PA, De Oliveira PE, Moreno JE, Miller MC, Bush MB (1996) A long pollen record from lowland Amazonia: forest and cooling in glacial times. *Science* 274:85–88. <https://doi.org/10.1126/science.274.5284.85>
- Colinvaux PA, De Oliveira PE, Bush MB (2000) Amazonian and neotropical plant communities on glacial time-scales: the failure of the aridity and refuge hypotheses. *Quat Sci Rev* 19:141–169
- Coomes DA (1997) Nutrient status of Amazonian caatinga forests in a seasonally dry area: nutrient fluxes in litter fall and analyses of soils. *Can J For Res* 27:831–839
- Coomes DA, Grubb PJ (1996) Amazonian caatinga and related communities at la Esmeralda, Venezuela: forest structure, physiognomy and floristics, and control by soil factors. *Vegetatio* 122:167–191
- Cordeiro CLO, Rossetti DF, Gribel R, Tuomisto H, Zani H, Ferreira CAC, Coelho L (2016) Impact of sedimentary processes on white-sand vegetation in an Amazonian megafan. *J Tropical Ecol* 32:498–509. <http://www.cambridge.org/core.INPE>
- Córdoba SMP (2014) Análisis de la riqueza vegetal y patrones fitogeográficos para la región del Escudo Guayanés Colombiano. Tesis de Doctorado, Universidad Nacional de Colombia, Bogotá, Colombia
- Cremon EH, Rossetti DF, Sawakuchi AO, Lisboa CMC (2016) The role of tectonics and climate in the late quaternary evolution of a northern Amazonian river. *Geomorphology* 271:22–39
- Cuevas E, Medina E (1986) Nutrient dynamics within Amazonian forest ecosystems. I. Nutrient flux in fine litter fall and efficiency of nutrient utilization. *Oecologia* 68:466–472
- Cuevas E, Medina E (1988) Nutrient dynamics within Amazonian forest ecosystems. II. Root growth, organic matter decomposition and nutrient release. *Oecologia* 76:222–235
- CVG Técnica Minera (1987) Informe de vegetación. Hoja NB 2012. Gerencia de Proyectos Especiales. Proyecto Inventario de los Recursos Naturales de la Región Guayana. Ciudad Bolívar, Venezuela
- D'Apolito C, Latrubesse EM, Absy ML (2017) Results confirm a relatively dry setting during the last glacial (MIS 3 and LGM) in Carajás, Amazonia: a comment on Guimarães et al. *The Holocene* 28(2):1–2
- Daly DC, Mitchell JD (2000) Lowland vegetation of tropical South America. An overview. In: Lentz D (ed) *Imperfect balance: landscape transformations in the pre-Columbian Americas*. Columbia University Press, New York, pp 391–454
- Daly DC, Silveira M, Medeiros H, Castro W, Obermuller FA (2016) The white-sand vegetation of acre, Brazil. *Biotropica* 48(1):81–89
- Damasco G (2013) Understanding the origin and the landscape dynamics of white-sand vegetation in Amazonia. Tinker research reports. Center for Latin American Studies, University of California, Berkeley

- Damasco G, Vicentini A, Castilho CV, Pimentel TP, Nascimento EM (2012) Disentangling the role of edaphic variability, flooding regime and topography of Amazonian white-sand vegetation. *J Veg Sci* 24(2):384–394. <https://doi.org/10.1111/j.1654-1103.2012.01464.x>
- Damasco G, Baraloto C, Vicentini A, Daly DC, Baldwin BG, Fine PVA (2021) Revisiting the hyperdominance of neotropical tree species under a taxonomic, functional and evolutionary perspective. *Scientific Reports* 11:9585. <https://doi.org/10.1038/s41598-021-88417-y>
- de Mendonça FBA, Bello SFN, Reynaud SCE, Fernandes FEI, do Vale Júnior JF, de MJG F (2014a) Podzolized soils and paleoenvironmental implications of white-sand vegetation (Campinarana) in the Viruá National Park, Brazil. *Geoderma Reg* 2- 3:9–20
- de Mendonça FBA, Fernandes FEI, Reynaud SCE, de Carvalho AF, do Vale JF, Resende CG (2014b) Use of geophysical methods for the study of sandy soils under Campinarana at the National Park of Viruá, Roraima state, Brazilian Amazonia. *J Soils Sediments* 14(3):525–537
- de Mendonça FBA, Fernandes FEI, Schaefer CEGR, de Mendonça JGF, Vasconcelos BNF (2017) Soil-vegetation relationships and community structure in a “terra-firme”-white sand vegetation gradient in Viruá National Park, northern Amazon. *Brazil An Acad Bras Cienc* 89(2): 1269–1293
- de Oñate-Calvín R, San Miguel-Ayaz A, Orensanz-García J, Salazar-Vega AA, Roig-Gómez S (2013) Amazonian white-sand forest: a black future? *Bois et Forêts des Tropiques* 315(1):63–72
- Demarchi LO, Scudeller VV, Carvalho ML (2018) Floristic composition, structure and soil-vegetation relations in three white-sand soil patches in Central Amazonia. *Acta Amazónica* 48(1):46–56
- Demarchi LO, Scudeller VV, Moura LC, Lopes A, Piedade MT (2019) Logging impact on Amazonian white-sand forests: perspectives from a sustainable development reserve. *Acta Amazon* 49:316–323
- Dezzeo N, Maquirino P, Berry PE, Aymard G (2000) Principales tipos de bosques en el área de San Carlos de Río Negro, Venezuela. *Scientia Guaianae* 11:15–36
- Dias e Sarmiento C, Costa Franca MG (2018) Neotropical forests from their emergence to the future scenario of climatic changes. Published by Intech, pp 59–81. <https://doi.org/10.5772/intechopen.72608>
- Díaz-Alván J, Socolar JB, Álvarez AJ (2017) The avifauna of the río Tigre basin, northern Perú. *Ornitología Neotropical* 28:11–21
- Draper FC, Asner GP, Coronado H, Baker TR, Garcia-Villacorta R, Pitman NCA, Fine PVA, Phillips OL, Zarate GR, Amasifuén GCA, Arévalo FM, Vásquez MR, Brienen RJW, Monteagudo-Mendoza A, Torres MLA, Valderrama SE, Roucoux KH, Arevalo FRR, Mesones AI, Del Aguila PJ, Tagle CX, Llampazo GF, Corrales MM, Huaymacari JR, Baraloto C (2019) Dominant tree species drive beta diversity patterns in western Amazonia. *Ecology* 00(00): e02636. <https://doi.org/10.1002/ecy.2636>
- Dubroeuq D, Volkoff B (1998) From Oxisols to spodosols and histosols: evolution of the soil mantles in the Rio Negro basin (Amazonia). *Catena* 32:245–280
- Ducke A, Black GA (1954) Notas sobre a fitogeografia da Amazônia brasileira. *Boletim Técnico* 29:1–62. IAN, Belém, PA
- Duivenvoorden JF, Cleef AM (1994) Amazonian savanna vegetation on the sandstone plateau near Araracuara, Colombia. *Phytocoenologia* 24:197–232
- Duivenvoorden JF, Lips JM (1995) A land-ecological study of soils, vegetation, and plant diversity in Colombian Amazonia. The Tropenbos foundation, III. Tropenbos series 12, Wageningen, The Netherland
- EDELCA (2004) Estudio plan maestro de la Cuenca del río Caroní. Volumen 1. Diagnóstico y caracterización de la cuenca. Tomo 6. Aspectos bióticos. Capítulo 3. Formaciones vegetales. Gerencia de Gestión Ambiental, Caracas, Venezuela
- Fine PVA, Baraloto C (2016) Habitat endemism in white-sand forests: insights into the mechanisms of lineage diversification and community assembly of the neotropical flora. *Biotropica* 48(1): 24–33. <https://doi.org/10.1111/btp.12301>

- Fine PVA, Bruna EM (2016) Neotropical white-sand forests: origins, ecology and conservation of a unique rain forest environment. *Biotropica* 48(1):5–6
- Fine PVA, Mesones I, Coley PD (2004) Herbivores promote habitat specialization by trees in Amazonian forests. *Science* 305:663–665
- Fine PVA, Miller ZJ, Mesones I, Irazuzta S, Appel HM, Stevens MH, Saaksjarvi I, Schultz JC, Coley PD (2006) The growth-defense trade-off and habitat specialization by plants in Amazonian forests. *Ecology, Supplement* 87(7):150–162
- Fine PVA, García-Villacorta R, Pitman NCA, Mesones I, Kembel SW (2010) A floristic study of the white-sand forests of Peru. *Ann Missouri Bot Gard* 97(3):283–305
- Finlay RD (2008) Ecological aspects of mycorrhizal symbiosis: with special emphasis on the functional diversity of interactions involving the extraradical mycelium. *J Exp Bot* 59(5): 1115–1126. Special issue review paper. <https://doi.org/10.1093/jxb/ern059>
- Flores BM, Holmgren M (2021) White-sand savannas expand at the core of the Amazon after forest wildfires. *Ecosystems*. <https://doi.org/10.1007/s10021-021-00607-x>
- Flores BM, Oliveira RS, Rowland L, Quesada CA, Lambers H (2020) Editorial special issue: plant-soil interactions in the Amazon rainforest. *Plant Soil* 450:1–9. <https://doi.org/10.1007/s11104-020-04544-x>
- Francis R, Read DJ (1994) The contributions of mycorrhizal fungi to the determination of plant community structure. *Plant Soil* 159(1):11–25
- Franco W, Dezzeo N (1994) Soils and soil water regime in the terra firme-caatinga forest complex near San Carlos de río Negro, state of Amazonas. *Venezuela Interciencia* 19(6):305–316
- Frasier CL, Albert VA, Struwe L (2008) Amazonian lowland, white sand areas as ancestral regions for south American biodiversity: biogeographic and phylogenetic patterns in *Potalia* (Angiospermae: Gentianaceae). *Organisms, Diversity & Evolution* 8:44–57
- García-Villacorta R, Reátegui MA, Olórtégui ZM (2003) Clasificación de bosques sobre arena blanca de la zona Reservada Allpahuayo-Mishana (ZRAM), Amazonía Peruana. *Folia Amaz* 14:11–28
- García-Villacorta R, Meza VKM, Díaz-Alván J, Sánchez W, Gallardo G, Rojas G (2006) Assessment of the avifauna and flora of the white-sand forests in upper Peruvian Amazonia. Final Report Varillal, 58 p [www.conservationleadershipprogramme.org](http://www.conservationleadershipprogramme.org)
- García-Villacorta R, Dexter K, Pennington RT (2016) Amazonian white-sand forests show strong floristic links with surrounding oligotrophic habitats and the Guiana shield. *Biotropica* 48(1): 47–57. <https://doi.org/10.1111/btp.12302>
- Gastauer M, Saporetti-Junior AW, Valladares F, Meira-Neto JAA (2017) Phylogenetic community structure reveals differences in plant community assembly of an oligotrophic white-sand ecosystem from the Brazilian Atlantic Forest. *Acta Botanica Brasílica* 31(4):531–538
- Gaworecki M (2016) South America's white-sand forests: poorly known and under threat. *Biotropica* 48(1):5–6. <https://doi.org/10.1111/btp.12305>
- Gentry AH (1988) Tree species richness of upper Amazonian forests. *Proc Natl Acad Sci* 85:156–159
- Guevara JE, Damasco G, Baraloto C, Fine PVA, Peñuela MC, Castilho C, Vincentini A, Cardenas D, Wittmann F, Targhetta N, Phillips O, Stropp J, Amaral I, Maas P, Monteagudo A, Jimenez EM, Thomas R, Brienen R, Duque A, Magnusson W, Ferreira C, Honorio E, de Almeida MF, Arevalo FR, Engel J, Petronelli P, Vasquez R, ter Steege H (2016) Low phylogenetic beta diversity and geographic neo-endemism in Amazonian white-sand forests. *Biotropica* 48(1):34–46. <https://doi.org/10.1111/btp.12298>
- Guilherme E, Borges SH (2011) Ornithological records from a campina/campinarana enclave on the upper Juruá River, acre, Brazil. *The Wilson Journal of Ornithology* 123(1):24–32. <https://doi.org/10.1676/10-036.1>
- Guilherme E, Lemes ME, Souza SG (2018) Avifauna of a white-sand vegetation enclave in north-West Rondônia, Brazil: relevant records, body mass and morphometrics. *Bull Br Ornithol Club* 138(4):286–306



- Guimarães FS, Bueno TG (2016) As campinas e campinaranas amazônicas. The Amazonian campinas and campinaranas. *Cuaderno de Geografía* 26(45):113–133
- Haffer J (2008) Hypotheses to explain the origin of species in Amazonia. *Braz J Biol* 68(4 Suppl):917–947
- Herrera R (2000) Algunos aportes del proyecto amazonas al conocimiento sobre los suelos del Rio Negro y a la biogeoquímica de la region. *Scientae Guaianae* 11:7–13. Caracas, Venezuela
- Herrera R, Jordan C, Klinge H, Medina E (1978) Amazon ecosystems. Their structure and functioning with a particular emphasis on nutrients. *Interciencia* 3:223–232
- Herrera R, Jordan CF, Medina E, Klinge H (1981) How human activities disturb the nutrient cycles of a tropical rainforest in Amazonia. *Ambio* 10(2/3):109–114
- Heyligers PC (1963) Vegetation and soil of a white-sand savanna in Suriname. *Verhand Kon Ned Akad Wetensch* 54(3):1–148
- Higgins MA, Ruokolainen K, Tuomisto H, Llerena N, Cardenas G, Phillips OL, Vásquez R, Matti R (2011) Geological control of floristic composition in Amazonian forests. *J Biogeogr* 38: 2136–2149
- Hijri M, Bâ A (eds) (2018) Mycorrhiza in tropical and neotropical ecosystems. *Frontiers Media. Frontiers in Plant Science*, Lausanne. <https://doi.org/10.3389/978-2-88945-544-7>
- Honorio EN, Pennington TR, Freitas A, Nebel G, Baker TR (2008) Analysis of the floristic composition of the forests of Jenaro Herrera, Loreto. *Peru Rev Peru Biol* 15(1):53–60
- Honorio EN, Dexter KG, Hart ML, Phillips OL, Pennington RT (2019) Comparative phylogeography of five widespread tree species: insights into the history of western Amazonia. *Ecol Evol* 00:1–13
- Horn C (1993) Marine incursions and the influence of Andean tectonics on the Miocene depositional history of northwestern Amazonia: results of a palynostratigraphic study. *Palaeogeogr Palaeoclimatol Palaeoecol* 105(3–4):267–309
- Horn C (1994) Fluvial palaeoenvironments in the intracratonic Amazonas Basin (early Miocene–early middle Miocene, Colombia). *Palaeogeogr Palaeoclimatol Palaeoecol* 109:1–54
- Horn C, Wesselingh FP (2010) Introduction: Amazonia, landscape and species evolution. In: Horn C, Wesselingh FP (eds) *Amazonia, landscape and species evolution: a look into the past*, 1st edn. Blackwell Publishing, Oxford, pp 1–6
- Horn C, Wesselingh FP, Hovikoski J, Guerrero J (2010a) The development of the Amazonian mega-wetland (Miocene; Brazil, Colombia, Peru, Bolivia). In: Horn C, Wesselingh FP (eds) *Amazonia, landscape and species evolution: a look into the past*, 1st edn. Blackwell Publishing, Oxford, pp 123–142
- Horn C, Wesselingh FP, ter Steege H, Bermudez MA, Mora A, Sevink J, Sanmartín I, Sanchez-Meseguer A, Anderson CL, Figueiredo JP, Jaramillo C, Riff D, Negri R, Hooghiemstra H, Lundberg J, Stadler T, Särkinen T, Antonelli A (2010b) Amazonia through time: Andean uplift, climate change, landscape evolution, and biodiversity. *Science* 330:927–931
- Horbe AMC, Horbe MA, Kenitiro S (2004) Tropical spodosols in northeastern Amazonas state. *Brazil Geoderma* 119(1–2):55–68
- Huber O (1995) Vegetation. In: Berry PE, Holst BK, Yatskiyevych K (eds) *Flora of the Venezuelan Guayana*. Missouri Botanical Garden, St. Louis & Timber Press, Oregon, pp 97–160
- Huber O, García P (2011) The Venezuelan Guayana region and the study areas: geo-ecological characteristics. In: Zinck JA, Huber O (eds) *Peatlands of the Western Guayana highlands, Venezuela*, Chap. 3. Springer, Heidelberg. [https://doi.org/10.1007/978-3-642-20138-7\\_3](https://doi.org/10.1007/978-3-642-20138-7_3)
- Iriondo M, Latrubesse M (1994) A probable scenario for a dry climate in Central Amazonia during the late quaternary. *Quat Int* 21:121–128
- Jiménez EM, Peñuela-Mora MC, Sierra CA (2014) Edaphic controls on ecosystem-level carbon allocation in two contrasting Amazon forests. *J Geophys Res Biogeo* 119(9):1820–1830. <https://doi.org/10.1002/2014jg002653>
- Jimenez EM, Peñuela-Mora MC, Moreno F, Sierra CA (2020) Spatial and temporal variation of forest net primary productivity components on contrasting soils in northwestern Amazon. *Ecosphere* 11(8):e03233. <https://doi.org/10.1002/ecs2.3233>



- Jordan CF, Herrera R (1981) Tropical rain forests: are nutrients really critical? *Am Nat* 117(2): 167–180. <http://www.jstor.org/stable/2460498>
- Junk WJ, Wittmann MTF, Schöngart J (2010) Amazonian floodplain forests: ecophysiology, biodiversity and sustainable management. *Ecological studies* 210. Springer, Dordrecht
- Keith DA, Young RT, Etter A (2020) Tropical heath forests. In: Keith DA, Ferrer-Paris JR, Nicholson E, Kingsford RT (eds) *The IUCN global ecosystem typology 2.0: descriptive profiles for biomes and ecosystem functional groups*. IUCN, Gland, Switzerland
- Klein VP, Piedade FMT (2019) Orchidaceae occurring in white-sand ecosystems of the Uatumã sustainable development reserve in Central Amazon. *Phytotaxa* 419(2):113–148. <https://www.mapress.com/j/pt/>
- Klinge H (1976) Studies on the ecology of Amazon caatinga. Fresh phytomass composition of tree vegetation in Amazon caatinga near San Carlos de Río Negro. *Acta Cient Venez* 28:270–276
- Klinge H, Cuevas E (2000) Bana: una comunidad leñosa sobre arenas blancas en el alto Río Negro, Venezuela. *Scientia Guaianae* 11:37–49
- Klinge H, Medina E (1979) Río Negro caatingas and Campinas, Amazonas states of Venezuela and Brazil. In: Specht RL (ed) *Ecosystems of the world 9A, heathlands and related shrublands, descriptive studies*. Elsevier Scientific Publications, Amsterdam, Oxford, New York, pp 483–488
- Klinge H, Medina E, Herrera R (1977) Studies on the ecology of Amazon caatinga forest in southern Venezuela. I General features *Acta Cient Venezolana* 28:270–276
- Kroonenberg SB, de Roever EWF (2010) Geological evolution of the Amazonian craton. In: Hoom C, Wesselingh FP (eds) *Amazonia, landscape and species evolution: a look into the past*, 1st edn. Blackwell Publishing, Chichester, pp 9–28
- Kubitzki K (1990) The psammophilous flora of northern South America. *Memories of the New York Botanical Garden* 64:248–253
- Kvarnäck JF, Bosque C (2017) An inventory of the birds of white-sand vegetation of the Guainía-Río Negro basin, southern Amazonas state, Venezuela. *BioLlania ed esp* 15:533–560. <https://www.researchgate.net/publication/330369903>
- Lanjouw J (1936) Studies on the vegetation of Surinam savannas and swamps. *Ned Kruidk Arch* 46:823–851
- Latrubesse EM (2000) The Late Pleistocene in Amazonia: a palaeoclimatic approach. In: Smolka P, Volkheimer W (eds) *Southern hemisphere paleo and Neoclimates*. Springer-Verlag, New York, pp 209–222
- Latrubesse EM (2003) The late-quaternary palaeohydrology of large south American fluvial systems. In: Gregory KJ, Benito G (eds) *Palaeohydrology: understanding global change*. John Wiley & Sons, Chichester, pp 193–212
- Latrubesse EM, Franzinelli TE (2005) The late quaternary evolution of the Negro River, Amazon, Brazil: implications for Island and floodplain formation in large anabranching tropical systems. *Geomorphology* 70:372–397
- Latrubesse EM, Ramonell CG (1994) A climatic model for southwestern Amazonia in last glacial times. *Quat Int* 21:163–169
- Latrubesse EM, Bocquentin J, Santos JCR, Ramonell CG (1997) Paleoenvironmental model for the late Cenozoic of southwestern Amazonia: paleontology and geology. *Acta Amazon* 27(2): 103–118
- Latrubesse EM, da Silva Silane AF, Cozzuol M, Absy ML (2007) Late Miocene continental sedimentation in southwestern Amazonia and its regional significance: biotic and geological evidence. *J S Am Earth Sci* 23:61–80
- Longo M, Knox RG, Levine NM, Alves LF, Bonal D, Camargo PB, Fitzjarrald DR, Haye MN, Restrepo-Coupe N, Saleska SR, da Silva R, Stark SC, Tapajós RP, Wiedemann KT, Zhang K, Wofsy SC, Moorcroft PR (2018) Ecosystem heterogeneity and diversity mitigate Amazon forest resilience to frequent extreme droughts. *New Phytol* 219(3):914–931. <https://doi.org/10.1111/nph.15185>. Hal-01896160

- Luizao FJ (1995) Ecological studies in contrasting forest types in Central Amazonia. Doctor thesis, University of Stirling, Scotland, UK
- Luizao FJ, Luizao RC, Proctor J (2007) Soil acidity and nutrient deficiency in central Amazonian heath forest soils. *Plant Ecol* 192:209–224
- Mardegan SF, Bielefeld NG, Higuchi N, Moreira MZ, Martinelli LA (2009) Nitrogen availability patterns in white-sand vegetations of central Brazilian Amazon. *Trees* 23:479–488
- Marinho F, da Silva IR, Oehl F, Maia LC (2018) Checklist of arbuscular mycorrhizal fungi in tropical forests. *Sydowia* 70:107–127
- Matsumoto E (1995) White sand soils in Northeast Brazil. United Nations University. In: Nishizawa T, Uitto J (eds) *The fragile tropics of Latin America: sustainable Management of Changing Environments*. United Nations University Press, Tokyo, pp. 263–294. [archive.unu.edu > unupress > unupbooks University](http://archive.unu.edu/unupress/unupbooks/University)
- Medina E, Cuevas E (1989) Patterns of nutrient accumulation and release in Amazonian forests of the upper Río Negro basin. In: Proctor J (ed) *Mineral nutrients in tropical forest and savanna ecosystems*. Blackwell scientific publications, special publication number 9 of the British Ecological Society, Oxford, pp 217–240
- Medina E, Cuevas E (2000) Eficiencia de utilización de nutrientes por plantas leñosas: eco-fisiología de bosques de San Carlos de Río Negro. *Scientia Guianae* 11:51–70
- Medina E, Cuevas E (2011) Complejo caatinga amazónica: bosques pluviales esclerófilos sobre arenas blancas. *BioLlania ed esp* 10:241–249. UNELLEZ, Guanare, Venezuela
- Medina E, García V, Cuevas E (1990) Sclerophylly and oligotrophic environments: relationships between leaf structure, mineral nutrient content, and drought resistance in tropical rain forests of the upper Rio Negro region. *Biotropica* 22:51–64
- Michelangeli FA (2010) Neotropical Myrmecophilous Melastomataceae: An Annotated List and Key. *Proceedings of the California Academy of Sciences*. Series 4, 61(9), 409–449, Appendix
- Minatel GP, Gomes RB, Fleischmann AS, Zappi DC, Baleeiro PC, Oliveira AC (2020) Hidden biodiversity of Amazonian white-sand ecosystems: two distinctive new species of utricularia (Lentibulariaceae) from Pará, Brazil Paulo. *PhytoKeys* 169:75–98. <https://doi.org/10.3897/phytokeys.169.57626>
- Montesinos-Navarro A, Valiente-Banuet A, Verdú M (2018) Processes underlying the effect of mycorrhizal symbiosis on plant-plant interactions. *Fungal Ecol* 30:1–9
- Moran EF (1995) Rich and poor ecosystems of Amazonia: an approach to management. In: Nishizawa T, Uitto J (eds) *The fragile tropics of Latin America: sustainable management of changing environments*. United Nations University Press, Tokyo, pp 46–65
- Moyersoen, B (1993) Ectomicorrizas y micorrizas vesículo-arbusculares en Caatinga Amazónica del sur de Venezuela. *Scientae Guianae Vol 3*, Caracas, Venezuela
- Moyersoen B, Becker P, Alexander IJ (2001) Are ectomycorrhizas more abundant than arbuscular mycorrhizas in tropical heath forests? *New Phytol* 150:591–599. [www.newphytologist.com](http://www.newphytologist.com)
- Myster RW (2017) Case study: Sabalillo. In: Myster RW (ed) *Forest reserve: forest structure, function, and dynamics in Western Amazonia*. John Wiley & Sons Ltd, Oxford, pp 2–19
- Nascimento NR, Bueno GT, Fritsch E, Herbillon AJ, Allard T, Melfi AJ, Astolfo R, Boucher H, Li Y (2004) Podzolization as a deferralitization process: a study of an Acrisol-podzol sequence derived from Palaeozoic sandstones in the northern upper Amazon basin. *Eur J Soil Sci* 55: 523–538
- Olivares I, Svenning JC, van Bodegom PM, Balslev H (2015) Effects of warming and drought on the vegetation and plant diversity in the Amazon Basin. *Bot Rev* 81:42–69. <https://doi.org/10.1007/s12229-014-9149-8>
- Onguene NA (2000) Diversity and dynamics of mycorrhizal associations in tropical rain forests with different disturbance regimes in South Cameroon. *Tropenbos Cameroon Series* 3:134
- Peay KG, Baraloto C, Fine PV (2013) Strong coupling of plant and fungal community structure across western Amazonian rainforests. *ISME J* 2013:1–10
- Peñuela MC (2014) Understanding Colombian amazonian white sand forests. Doctor thesis Utrecht University and National University of Colombia, Bogotá, Colombia

- Pitman N, Vriesendorp C, Moskovits DK, von May R, Alvira D, Wachter T, Stotz DF, del Campo A (eds) (2011) Perú: yaguas-Cotuhé. Rapid biological and social inventories report 23. The Field Museum, Chicago, p 377
- Pitman N, Gagliardi UGG, Jenkins C (2013) La biodiversidad de Loreto, Perú. El conocimiento actual de la diversidad de plantas y vertebrados terrestres. Center for International Environmental Law (CIEL), p 39 <http://www.tropicos.org/Project/PEC>
- Pitman N, Vriesendorp C, Alvira D, Markel JA, Johnston M, Inzunza RE, Lancha PA, Sarmiento VG, Alvarez-Loayza P, Homan J, Wachter T, del Campo A, Stotz DF, Heilpern S (eds) (2014) Peru: Cordillera Escalera-Loreto. Rapid Biological and Social Inventories Report 26. The Field Museum, Chicago, p 544
- Pitman N, Vriesendorp C, Chávez RL, Wachter T, Alvira RD, del Campo A, Gagliardi-Urrutia G, Rivera GD, Trevejo L, González RD, Heilpern S (eds) (2015) Perú: Tapiche-Blanco. Rapid biological and social inventories report 27. The Field Museum, Chicago, p 508
- Pitman N, Bravo A, Claramunt S, Vriesendorp C, Alvira RD, Ravikumar A, del Campo A, Stotz DF, Wachter T, Heilpern S, Rodríguez GB, Sáenz RAR, Smith RC (eds) (2016) Perú: Medio Putumayo-Algodón. Rapid Biological and Social Inventories Report 28. The Field Museum, Chicago, p 522
- Poels, RLH (1987) Soils, water and nutrients in a forest ecosystem in Suriname. Doctoral Thesis, Agricultural University Wageningen
- Prance GT (1973) Phytogeographic support for the theory of Pleistocene forest refuges in the Amazon Basin based on evidence from distribution patterns in Caryocaraceae, Chrysobalanaceae, Dichapetalaceae and Lecythidaceae. *Acta Amaz* [Online] 3(3):5–26. <https://doi.org/10.1590/1809-43921973033005>. issn: 0044-5967
- Proctor J (1999) Heath forests and acid soils. *Bot J Scotl* 51:1–14. <https://doi.org/10.1080/03746609908684920>
- Quaresma AC, Piedade MTF, Oliveira FY, Wittmann F, ter Steege H (2017) Composition, diversity and structure of vascular epiphytes in two contrasting central Amazonian floodplain ecosystems. *Acta Botanica Brasilica* 31(4):686–697. <https://doi.org/10.1590/0102-33062017abb0156>
- Quesada CA, Lloyd J, Anderson LO, Fyllas NM, Schwarz M, Czimczik CI (2011) Soils of Amazonia with particular reference to the RAINFOR sites. *Biogeosciences* 8:1415–1440
- Ribeiro JC, Amorim MA, Apo-linano FB, Bandeira AG, Cavalcante ETS, Guerrero JCH, Leite SS, Machado LC, Ribeiro de A MO, Rocha RA, Schwamborn R, da Silva BM, Adis J, de Moraes JW, Ribeiro EF, Ribeiro JC (2008) Vertical distribution and abundance of arthropods from white sand soil of a Neotropical Campinarana forest during the rainy season. Results obtained during the post-graduate course “Entomological Field Ecology” of INPA/Univ. Amazonas, pp 193–200. <https://doi.org/10.1080/01650528909360791>
- Rojas TR, Tello ER (2006) Natural regeneration abundance and stock of forest species in varillal forest, of the CIEFOR, Iquitos-Peru. Universidad Nacional de la Amazonia Peruana
- Rossetti DF, Gribel R, Toledo PM, Tatum SH, Yee M, Tudela DRG, Munita CS, de Souza CL (2018) Unfolding long-term Late Pleistocene–Holocene disturbances of forest communities in the southwestern Amazonian lowlands. *Ecosphere* 9(10):1–32
- Rossetti DF, Moullet GM, Tuomisto H, Gribel R, Toledo PM, Valeriano MM, Ruokolainen K, Cohen MCL, Cordeiro CLO, Rennó CD, Coelho LS, Ferreira CAC (2019) White sand vegetation in an Amazonian lowland under the perspective of a young geological history. *An Acad Bras Cienc* 91(4):1–21. <https://doi.org/10.1590/0001-3765201920181337>
- Roy M, Schimann H, Braga-Neto R, Da Silva RA, Duque J, Frame D, Wartchow F, Neves MA (2016) Diversity and distribution of ectomycorrhizal fungi from Amazonian lowland white-sand forests in Brazil and French Guiana. *Biotropica* 48(1):90–100
- Roy M, Vasco-Palacios A, Geml J, Buyck B, Delgat L, Giachini A, Grebenc T, Harrower E, Kuhar F, Magnago A, Rinaldi AC, Schimann H, Selosse MA, Sulzbacher MA, Wartchow F, Neves MA (2017) The (re)discovery of ectomycorrhizal symbioses in neotropical ecosystems sketched in Florianópolis. *New Phytol* 214:920–923

- Rutt CL, Jirinec V, Cohn-Haft M, Laurance WF, Stouffer PC (2019) Avian ecological succession in the Amazon: a long-term case study following experimental deforestation. Faculty Publications 2. [https://digitalcommons.lsu.edu/agrn\\_r\\_pubs/2](https://digitalcommons.lsu.edu/agrn_r_pubs/2)
- Salick J, Herrera R, Jordan CF (1983) Termitaria: nutrient patchiness in nutrient-deficient rain forests. *Biotropica* 15(1):1–7
- Saporetto-Junior AW, Reynaud SCEG, de Souza AL, Pereira SM, Dunn ADS, Alves M-NJA (2012) Influence of soil physical properties on plants of the Mussununga ecosystem, Brazil. *Folia Geobot* 47:29–39
- Schargel R, Marvez P (2009) Suelos. In: Aymard GA, Schargel R (eds) Estudio de los suelos y la vegetación (estructura, composición florística y diversidad) en bosques macrotérmicos no-inundables, Estado Amazonas, Venezuela. *BioLlania edic esp* 9:99–125, UNELLEZ, Guanare, Venezuela
- Schnütgen A, Bremer H (1985) Die Entstehung von Decksanden im oberen Rio Negro-Gebiet. *Z. Geomorph. N.F. Suppl.-Bd.* 56:55–67
- Shany N, Alván JD, Alvarez AJ (2007) Finding white-sand forest specialists in Allpahuayo-Mishana reserve, Peru. *Neotropical Birding* 2:60–68. <https://doi.org/10.25226/bboc.v138i4.2018.a2>
- Singer R, Araujo IJS (1979) Litter decomposition and ectomycorrhiza in Amazonian forests. A comparison of litter decomposing and ectomycorrhizal basidiomycetes in latosol-terra-firme rain forest and white podzol campinarana. *Acta Amazon* 9(1):25–41
- Soares BPI (1979) Subdivisão fitogeográfica, tipos de vegetação, conservação e inventário florístico da floresta Amazônica. *Supl Acta Amazônica* 9(4):53–80
- Sobrado MA (2013) Soil and leaf micronutrient composition in contrasting habitats in podzolized sands of the Amazon region. *Am J Plant Sci* 4:1918–1923
- Sobrado MA, Medina E (1980) General morphology, anatomical structure, and nutrient content of sclerophyllous leaves of the “bana” vegetation of Amazonas. *Oecologia* 45:341–345
- Soil Survey Staff (1999) Soil taxonomy: a basic system of soil classification for making and interpreting soil surveys sec ed USDA Agriculture Handbook 436
- Sombroek W (1966) Amazon soils. A reconnaissance of the soils of the Brazilian Amazon region. Centre for Agricultural Publication and Documentation, Wageningen, 292p. (Agricultural Research Reports, 672)
- Sombroek W (1990) Amazon landforms and soil diversity in relation to biological diversity. Workshop Proceedings Manaus, Brazil
- Stropp J, van der Sleen P, Apóstolo AP, Lopes da SA, ter Steege H (2011) Tree communities of white-sand and terra-firme forests of the upper Rio Negro. *Acta Amazon* 41(4):521–544
- Stropp J, van der Sleen P, Quesada CA, ter Steege H (2014) Herbivory and habitat association of tree seedlings in lowland evergreen rainforest on white-sand and terra-firme in the upper Rio Negro. *Plant Ecology & Diversity* 7(1–2):255–265. <https://doi.org/10.1080/17550874.2013.773103>
- Tanaka S, Nakamoto K, Sakurai K, Limin SH (2013) Characteristics of the contrasting soils on Kahayan River banks in Central Kalimantan. *Indonesia Tropics* 22(3):99–112
- Targhetta N, Kesselmeier J, Wittmann F (2015) Effects of the hydroedaphic gradient on tree species composition and aboveground wood biomass of oligotrophic forest ecosystems in the Central Amazon basin. *Folia Geobot* 50(3):185–205
- ter Steege H, Lilwah R, Ek R, van der Hout P, Thomas R, van Essen J, Jetten V (1999) Composition and diversity of the rain forest in Central Guyana. *Tropenbos Guyana Reports* 99- 2:51
- ter Steege H, Sabatier D, Castellanos H, van Andel T, Duivenvoorden J, de Oliveira AA, Ek R, Lilwah R, Maas P, Scott M (2000) An analysis of the floristic composition and diversity of Amazonian forests including those of the Guiana shield. *J Trop Ecol* 16:801–828
- Tuomisto H, Ruokolainen K, Kalliola R, Linna A, Danjoy W, Rodriguez Z (1995) Dissecting Amazonian biodiversity. *Science* 269(5220):63–66
- USAID (2018) Climate risk profile Amazon basin: climate risk profile. Climate integration support facility blanket purchase agreement AID-OAA-E-17-0008, p 9

- Eyk JJ van der (1957) Reconnaissance soil survey in northern Surinam. PhD Thesis, Wageningen
- van der Hammen T, Hooghiemstra H, de Vries H (2000) Neogene and quaternary history of vegetation, climate, and plant diversity in Amazonia. *Quat Sci Rev* 19:725–742
- van Donselaar J (1965) An ecological and phytogeographic study of northern Surinam savannas. *Wentia* 14:1–163
- van Donselaar J (1968) Phytogeographic notes on the savanna flora of southern Surinam (South America). *Acta Bot Neerl* 17(5):393–404
- Vargas-Saboya V, Panduro-Rengifo D, Falcón-Cometivos J (2006) Estudio de la estructura bisimétrica del estrato superior de un bosque varillal húmedo en Loreto. *Ciencia Amazónica* 3(1):19–23. <https://doi.org/10.22386/ca.v3i1.48>
- Vasco-Palacios AM (2016) Ectomycorrhizal fungi in Amazonian tropical forests in Colombia. PhD Thesis Utrecht University. Editorial Panamericana, Bogotá, Colombia, p 201
- Vasco-Palacios A, Hernandez J (2014) Biodiversity of ectomycorrhizal (ECM) fungi associated with tropical lowlands forests in Colombia, Amazonia. Fundación Biodiversa, Colombia. [www.fundacionbiodiversa.org/bi](http://www.fundacionbiodiversa.org/bi)
- Vasco-Palacios AM, Hernandez J, Peñuela-Mora MC, Franco-Molano AE, Boekhout T (2018) Ectomycorrhizal fungi diversity in a white sand forest in western Amazonia. *Fungal Ecol* 31:9–18
- Vicentini A (2004) A vegetação ao longo de um gradiente edáfico no Parque Nacional do Jaú. In: Borges SH, Iwanaga S, Durigan CC, Pinheiro MR (eds) *Janelas para a biodiversidade no Parque Nacional do Jaú: uma estratégia para o estudo da biodiversidade na Amazônia*. Fundação Vitória Amazônica (FVA), WWF, IBAMA, Manaus, pp 117–143
- Vicentini A (2016) The evolutionary history of *Pagamea* (Rubiaceae), a white-sand specialist lineage in tropical South America. *Biotropica* 48:58–69
- Vriesendorp C, Pitman N, Rojas MJI, Pawlak BA, Rivera CL, Calixto ML, Vela CM, Fasabi RP (eds) (2006) Perú: Matsés. Rapid Biological Inventories Report 16. The Field Museum, p 336. <https://doi.org/10.4236/ajps.2013.410235>
- Wesselingh FP, Salo JA (2006) A Miocene perspective on the evolution of the Amazonian biota. *Scr Geol* 133:439–458. <https://doi.org/10.7717/peerj.5644>
- Wesselingh FP, Hoorn C, Kroonenberg SB, Antonelli A, Lundberg JG, Vonhof HB, Hooghiemstra H (2010) On the origin of Amazonian landscapes and biodiversity: a synthesis. In: Hoorn C, Wesselingh FP (eds) *Amazonia, landscape and species evolution: a look into the past*, 1st edn. Blackwell Publishing, pp 420–427
- Zarate R, Mori TJ, Maco JT (2013) Estructura y composición florística de las comunidades vegetales del ámbito de la carretera Iquitos-Nauta. Loreto-Perú *Folia Amazónica* 22(1–2):77–89
- Zinck JA, Huber O (eds) (2011) Peatlands of the western Guayana highlands, Venezuela. Properties and paleogeographic significance of peats. Appendix: site and profile characteristics. *Ecological Studies* 217. Springer, Heidelberg
- Zular A, Sawakuchi AO, Chiessi CM, de Mendonça HF, Cruz FW, Melo DJA, Ribas CC, Hartmann GA, Fonseca GPC, Amaral SEA (2019) The role of abrupt climate change in the formation of an open vegetation enclave in northern Amazonia during the late quaternary. *Glob Planet Chang* 172:140–149. <https://doi.org/10.1111/btp.12301>

---

## **Part I**

# **Forest and Woodland Biomes**



# The Forests of the Upper Rio Negro (North-Western Amazon) and Adjacent South-Western Orinoco Basins: A Phytosociological Classification

H. Arellano-Peña, D. Cárdenas-López †, J. Stropp, N. Castaño-Arboleda, G. Romero-González, F. Castro-Lima, A. Lozano, M. C. Montilla, H. ter Steege, and G. A. Aymard-Corredor

*“Sábado víspera de la Santísima Trinidad (3 de junio de 1542). . . .vimos una boca de otro río grande á la mano siniestra, que entraba en el que nosotros navegávamos, el agua del cual era negra como tinta, y por esto le pusimos nombre del Río Negro, el cual corría tanto y con tanta ferocidad que en más de veinte leguas hacia raya en la otra abu, sin resolver la una con la otra” (Fr. Gaspar de Carvajal. Relación del viaje de Francisco de Orellana al río Amazonas—1541–1542).*

*“On some black-water rivers, such as the Pacimoni, the Atabapo, and the Rio Negro in some parts of its course, the breadth of inundated land is entirely clad with bushes and small trees of very equable height, on the skirts of which the Virgin Forest rises abruptly to a height more than twice as great. This is called by the natives ‘caatinga-gapo.’ Besides these differences of aspect, the natives will tell you there are other more intrinsic ones.” (Notes of botanist on the Amazon and Andes, Richard Spruce, 1908)*

**Supplementary Information** The online version contains supplementary material available at [https://doi.org/10.1007/978-3-031-20799-0\\_3](https://doi.org/10.1007/978-3-031-20799-0_3).

H. Arellano-Peña (✉)

Nuevo Estándar Biotropical NEBIOT SAS, Bogotá, Colombia

Compensation International Progress S.A., Greenlife, Bogotá, DC, Colombia

e-mail: [harellano@nebiot.org](mailto:harellano@nebiot.org)

D. Cárdenas-López † · N. Castaño-Arboleda

Herbario Amazónico Colombiano, Instituto SINCHI, Bogotá, DC, Colombia

### 3.1 Introduction

The entire Amazon watershed (*sensu lato*: 8, one million km<sup>2</sup>) includes 22 main tributaries, covering Bolivia, Brazil, Colombia, Ecuador, Peru, and Venezuela (including Amazon *sensu stricto*, Guayana Shield *pro parte*, Andean foothills and Gurupí basin; *sensu ter* Steege et al. 2013; Antonelli et al. 2018). These regions are home to a great diversity of ecosystems and to nearly 40% of the world's tropical vegetation, with more than 50,000 plant species (Prance 2001; Morley 2011). The number of tree species inside the Amazon basin has been the subject of continuous debate during the last two decades (Hubbell et al. 2008; *ter* Steege et al. 2016, 2019a). Based on a comprehensive database of 1946 forest plots with up-to-date taxonomy, the most recent estimate is that over 15,000 tree species are expected to occur in Amazonia (*ter* Steege et al. 2020). In the exceptionally diverse Amazonian forests, between 1.4% (227 ssp.) and 4.03% (654 ssp.) of the tree species are extremely common and make up 50% of all trees over 10 cm DBH. This subset of disproportionately common trees has been dubbed the hyperdominants (*ter* Steege et al. 2013; Draper et al. 2021). The increase of hyperdominants is the result of a larger set of plots: for the first time, 1240 small 0.1 ha plots (that included all individuals with a minimum DBH cut-off of 2.5 cm) were assembled in a study that examined tree dominance across forest strata, from the understory to the tallest canopy, and emergent layers as well (Draper et al. 2021). These authors also found that although species belonging to a range of phylogenetically dispersed lineages have become hyperdominant in small size classes, hyperdominants in large size classes are restricted to a few lineages. In addition, some of the hyperdominants that dominate large forest areas are tree, treelet, and palm species with some evidence of domestication, especially in locations near archeological sites (Levis et al. 2017;

---

J. Stropp

Department of Biogeography and Global Change, Museo Nacional de Ciencias Naturales (MNCN-CSIC), Madrid, Spain

G. Romero-González

Orchid Herbarium of Oakes Ames, Harvard University Herbaria, Cambridge, MA, U.S.A

F. Castro-Lima

Investigador Independiente, Villavicencio, Meta, Colombia

A. Lozano · M. C. Montilla

Compensation International Progress S.A., Greenlife, Bogotá, DC, Colombia

H. *ter* Steege

Naturalis Biodiversity Center, Leiden, RA, The Netherlands

Quantitative Biodiversity Dynamics, Dept. of Biology, Utrecht University, Utrecht, The Netherlands

G. A. Aymard-Corredor

UNELLEZ-Guanare, Programa de Ciencias del Agro y el Mar, Herbario Universitario (PORT), Mesa de Cavacas, Venezuela

Compensation International Progress S.A., Greenlife, Bogotá, DC, Colombia



Montoya et al. 2020). Moreover, the distribution range of only a few Amazonian tree species extends across the entire Amazon basin, while most tree species have restricted geographic coverage (Kristiansen et al. 2009).

A similar imbalance is observed in species-to-genus ratios: over half of all Amazonian tree species belong to genera with 100 or more species, while the majority of genera have ten or fewer species (Gentry 1993; Dexter and Chave 2016; ter Steege et al. 2019a).

Currently, there is a relatively good understanding of the structure and floristic composition of the forests in the Amazon basin, mainly the forests located in the western sector of the basin and in the Andes foothills (for reviews, see Pitman et al. 2008; Tuomisto et al. 2016, 2019; Alvez-Valles et al. 2018; Silva-Souza and Souza 2020).

Among the main rivers of the Amazon watersheds, the Rio Negro is remarkable: it is the second largest tributary of the Amazon river and the largest blackwater river in the world (Latrubesse and Stevaux 2015; Marengo et al. 2016). Its basin, together with the Amazon delta represents the wettest section of Amazonia (Espinoza et al. 2009; Nascimento et al. 2019). Rio Negro is the name that the Guainía river takes at its confluence with the Casiquiare channel. The botanical exploration of the Rio Negro basin was summarized in Huber and Wurdack (1984), Huber (1995a), Aymard et al. (2016), ter Steege et al. (2016), and in Appendix 3.2.

Here we present a phytosociological analysis of the forests in the upper Rio Negro (north-western Amazon) and adjacent south-western Orinoco basins, including terra-firme forests growing on clay soils, Amazonian white-sand forests, and flooded areas that occur along black, white, and clear-water rivers. This phytosociological classification provides vegetation information organized in hierarchical units to analyze and explain the floristic composition, vegetation structure, and diversity of the forests, as well as their relationship with environmental conditions, hitherto not presented in more conventional studies.

---

## 3.2 General Features of the Study Area

The study focuses on the Rio Negro (northern/north-western Amazon basin) and part of the adjacent south-western Orinoco basins. This region comprises the south-west of the Amazonas state of Venezuela, the south-east of the Guainía and Vaupés departments of Colombia, and the Roraima and north-west portion of the Amazonas states of Brazil. The Rio Negro basin has an area of ca. 750,652 km<sup>2</sup> and a combined river length of ca 1600 km (Arellano-Peña et al. 2019). The two largest freshwater archipelagoes (Mariuá and Anavilhanas, with ca. 1200 and 400 islands, respectively), which also include the largest flooded igapó forest systems in the world with a highly diverse fauna (Latrubesse and Stevaux 2015), are located in the middle and lower portions of this river. Furthermore, in its upper course, the Rio Negro has the longest set of river rapids of the Amazon basin (ca. 16 km long, in São Gabriel de Cachoeira, Amazonas state, Brazil). This river originates in the headwaters of the Guianía river in Colombia, flows southward into north-western Brazil, and turns eastward north of the municipality of São Gabriel da Cachoeira, where it receives the

waters of the Xié, Isana, and Vaupés rivers. It then continues in an east-south-east direction until it flows into the Solimões river, near Manaus (Brazil), together forming the main body of the Amazon river.

The geographic boundaries of the Rio Negro basin are defined in the north by the drainage divide that separates its watershed from the Guaviare, upper Atabapo, and Orinoco rivers; in the west by the upper watersheds of the Guainía and Vaupés rivers; to the south by the junction of the Japurá river with the Solimões river; and in the east by the southern foothills of the Guayana Shield drained primarily by the Rio Branco. The Serranía de la Neblina (Cerro de La Neblina: 2992 m and Pico de Neblina 3014 m), which divides Brazil from southern Venezuela, located in the Rio Negro basin, is part of the Guayana Shield highlands known as Tepuis (Huber 1987). The Serranía de la Neblina is formed by ancient rocks of the Serra dos Surucucus formation (1046 m) (Santos et al. 2003) and is rich in endemic species and unique habitats (Riina et al. 2019). The basin also holds other important ancient highlands such as: Serra da Aracá (ca. 2000 m), Serra de Curicuriari (1400 m, also known as Serra da Bela Adormecida), Serra do Pirapucu (2134 m), Pico Rondon (1189 m) in the Brazilian state of Amazonas; Serra do Apiaú (1222), Serra da Lua (532 m), and Serra do Tepequém (595 m) in Roraima state (Brazil); the Serranía de Naquén (ca. 900 m) which divides Brazil from southern Colombia and the Kanuku Mountains (1067 m) in southwestern Guyana; the Aracamuni and Avispa massifs (with a maximum elevation ca. 1600 m) in Southern Venezuela; and Pico Tamacuari (2349 m) in Sierra Curupira and Sierra Tapirapecó along the Brazilian-Venezuelan border (Huber 1995b).

The average annual rainfall in the Rio Negro basin varies between 3000 and 4095 mm (Espinoza et al. 2009), with the highest values in the upper stretch ( $\geq 3600$  mm) and 0–2 months with less than 100 mm precipitation. Mean annual temperature fluctuates between 26 and 32 °C.

The upper Rio Negro and part of the adjacent south-western Orinoco region have a dense fluvial network, composed of numerous rivers the waters of which flow into the Amazon and Orinoco rivers (Goulding et al. 1988). The system is connected with the Orinoco basin through the Casiquiare channel (Fig. 3.1). The latter establishes a permanent water connection between the drainage basins of the Amazon and Orinoco (Stokes et al. 2018). The Rio Negro watershed is characterized predominantly by blackwater tributaries that originate from habitats encompassing large areas covered by white-sand soils, formed from the erosion of Precambrian Guayana Shield rocks (Klinge 1965, 1967; Junk et al. 2011). However, the Rio Branco is the exception, as it is the largest white water tributary of the Rio Negro basin. In contrast, the Orinoco basin distinguishes itself by having primarily clear and white water tributaries that drain Tertiary sediments of the Andes and the strongly weathered soils on the Guayana Shield (Ríos-Villamizar et al. 2020). The middle Orinoco river basin does have a few minor black water tributaries, such as the Atabapo, Inírida (vía the Guaviare), Ucata, and Sipapo rivers, among others, and a major one in its lower course, the Caroní river.

The basins show considerable variation in floristic composition and forest structure along local and regional environmental gradients. According to previous



**Fig. 3.1** Junction of the Casiquiare channel with river Guianá, Colombia and Venezuela borders; photograph by Gerardo A Aymard C

studies, such variation is strongly correlated with geomorphology, soils, geology, drainage, and climate (Rodrigues 1961; Takeuchi 1961, 1962a, 1962b, 1962c; Klinge et al. 1977; Anderson 1981; Klinge and Herrera 1983; Salamanca 1983; Medina et al. 1990; Ballesteros 1995; Schargel et al. 2000; Córdoba and Etter 2001; Boubli 2002; Rudas et al. 2002; Aymard et al. 2009; Stropp et al. 2011; Pombo de Souza 2012). The region also comprises a large, low-altitude peneplain of ca 165,000 km<sup>2</sup>, where hydromorphic Spodosols and Quartzipsamments are very frequent (Dubroeuq and Volkoff 1998; Schargel et al. 2000; Schargel and Marvez 2009). The peneplain landscape comprises a mosaic of unique vegetation types, particularly sclerophyllous forests on oligotrophic and acid soils, known as “caatinga Amazónica” (Colombia, Venezuela), “caatinga Amazónica baja,” “bosques de arena blanca” (Colombia), “campinarana forestada,” “campina alta” (Brazil), “varillales” (Colombia, Perú), “tastaboa” in Tucano, “parabcoha” in Desano (Ballesteros 1995), and “hamáliani” in Baniwa languages (Abraão et al. 2009).

The peneplain landscape also harbors small to extensive areas of savannas, shrubby savannas, and scrublands growing on white sands (Huber 1995c; Lleras 1997), locally called “caatinga gapó” by the natives of the upper Rio Negro (Spruce 1908), “sabanas de arena blanca,” “banas” (Klinge and Medina 1979), or low campinas, and further south “campina de solo arenoso” (Anderson 1981), “campinarana arbustiva” (Lisbôa 1975) or “campinarana graminea lenhosa” (Pombo de Souza 2012). A similar type of vegetation also occurs as far south as the Peruvian Amazon in the Jenaro Herrera district and the Allpahuayo-Mishana Reserve near Iquitos, where these plant communities are known as “varillales” and “chamizales” (Fine et al. 2010), as “varillales” in Leticia, Amazonas department in Colombia (Peñuela 2014), “muri bush” in Guyana (Richards 1952), and also in southern Brazil (Acre and Rondônia states), where they are known as “Chapada de Parecis” (Prance 2001).

**Table 3.1** Characteristic tree species per locations

Location	Characteristics tree species
Taracuí, Amazonas (Brazil); Rodrigues (1961)	<i>Hevea rigidifolia</i> , <i>Micrandra sprucei</i> , <i>Pagamea coriacea</i> , <i>Caraipa</i> sp.
Ilha das Flores, Amazonas (Brazil); Rodrigues (1961)	<i>Eperua leucantha</i> , <i>Micrandra sprucei</i> , <i>Catostemma sclerophyllum</i> , <i>Hevea nitida</i>
Iucabí river, Amazonas (Brazil); Takeuchi (1962a)	<i>Eperua leucantha</i> , <i>E. purpurea</i> , <i>E. rubiginosa</i> , <i>Aldina discolor</i>
Timbó de Betania, Vaupés (Colombia); Ballesteros (1995)	<i>Aspidosperma fendleri</i> , <i>Calophyllum lucidum</i> , <i>Aldina latifolia</i> , <i>Clusia spathulifolia</i>
La Esmeralda, upper Orinoco river, Amazonas, (Venezuela); Coomes and Grubb (1996)	<i>Eperua obtusata</i> , <i>Micrandra siphonioides</i> , <i>Caraipa longipedicellata</i> , <i>Macrolobium gracile</i> , <i>Byrsonima wurdackii</i>
Base of Pica da Neblina National Park; Amazonas (Brazil); Boubli (2002)	<i>Micrandra sprucei</i> , <i>Eperua leucantha</i> , <i>Hevea</i> cf. <i>brasiliensis</i> , <i>Caraipa</i> sp.
San Carlos de Río Negro, Amazonas (Venezuela); Klinge and Medina (1979); Dezzeo et al. (2000); Aymard et al. (2009). Eastern sector of Guianá department (Colombia); Cárdenas-López et al. (2007)	<i>Micrandra sprucei</i> , <i>Eperua leucantha</i> , <i>Micropholis maguirei</i> , <i>Caraipa densifolia</i>
Along road Maroa-Yavita, Amazonas (Venezuela); Aymard et al. (2009)	<i>Eperua leucantha</i> , <i>Micrandra sprucei</i> , <i>Couma catinae</i> , <i>Xylopia benthamii</i>
Middle Içana river, Amazonas (Brazil); Stropp (2011)	<i>Inga</i> sp., <i>Micrandra sprucei</i> , <i>Aldina heterophylla</i> , <i>Eperua purpurea</i> , <i>E. leucantha</i>
São Gabriel da Cachoeira, Amazonas (Brazil); Stropp (2011)	<i>Eperua leucantha</i> , <i>E. purpurea</i> , <i>Aldina heterophylla</i> , <i>Inga</i> sp.
Middle Cuy(i)arí river, Guainía (Aymard et al. 2016)	<i>Micrandra sprucei</i> , <i>Hevea rigidifolia</i> , <i>Caraipa longipedicellata</i> , <i>Iryanthera juruensis</i>

The Rio Negro white-sand caatinga forests or campinaranas are not uniform in terms of floristic composition. Different white-sand forest types have been described and are summarized in Table 3.1. In addition, these white-sand forests are established through an ecological and floristic transition between terra-firme forests commonly found on peneplain red-yellow clay soils, and flooded forest communities on alluvial plains called igapó and varzea (Prance 1980; Kubitzki 1989; Aymard et al. 2009; Wittmann et al. 2017; Luize et al. 2018). Chapters 5 and 6 in this book complement the results of the present chapter, as they describe the pattern of forest cover distribution within the Amazonas state in Venezuela.

### 3.3 Materials and Methods

#### 3.3.1 Tree Inventory Data

The inventory data used in this study include all Angiosperm treelets and trees with diameter at breast height (DBH)  $\geq 2.5$  cm. The dataset contains 1368 species identified in inventory samples that were established across 226 localities

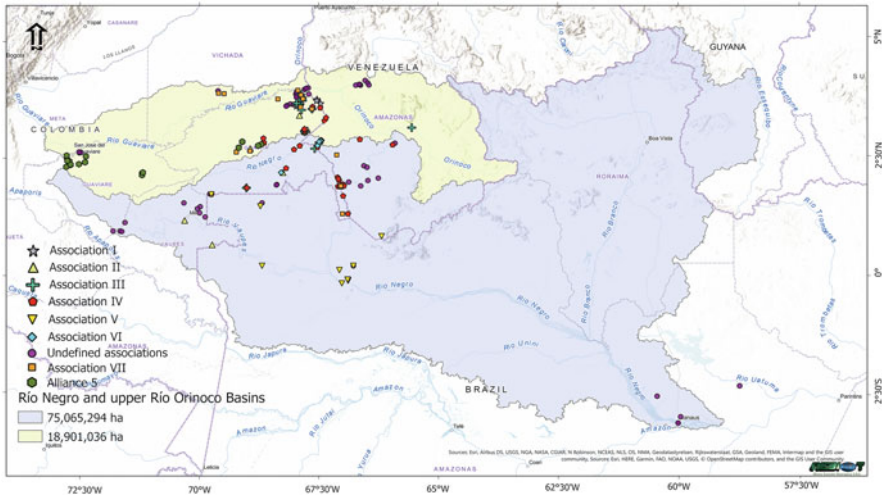


**Fig. 3.2** Location of the study plots in the Rio Negro basin of Brazil, Colombia, Guyana and Venezuela (blue area) and the Orinoco basin of Colombia and Venezuela (light green area). A high-resolution image is found in the following link: [https://1drv.ms/f/s!AsgLjs\\_JMencgZsGYB0klyDnwkiIg](https://1drv.ms/f/s!AsgLjs_JMencgZsGYB0klyDnwkiIg)

(Appendices 3.1, 3.2, and Fig. 3.2; this information is available at the following link: [https://1drv.ms/f/s!AsgLjs\\_JMencgZsGYB0klyDnwkiIg](https://1drv.ms/f/s!AsgLjs_JMencgZsGYB0klyDnwkiIg)

The subset of 1368 species was selected from a database that includes 49,116 individuals and 2877 species and morphospecies; 1509 taxa were eliminated due to either too low representation in the region or difficulties in obtaining a good taxonomical resolution.

In Colombia, plots were located in Guainía (127), Guaviare (20), Vaupés (7), Amazonas (4), and Vichada (3) departments. In Venezuela, plots were concentrated in the Amazonas state (42) and, in Brazil, plots were located in the state of Amazonas (23) along the banks of the Rio Negro.

The tree identification names and taxonomic nomenclature were standardized and updated, using a dynamic list of Amazonian tree species (ter Steege et al. 2019 onward: <http://atdn.myspecies.info/node/2466>).

All maps were based on the reflectance data of a LANDSAT 5, 7, and 8 mosaic (58 tiles), and produced using a combination of supervised interpretation techniques. The final composition was built with algorithms from the software packages Octave (version 5.2.0; <https://www.gnu.org/software/octave/>) and Grass (version 7.8.2; <https://grass.osgeo.org/>). Using satellite mosaic classification and an artificial neural network, vegetation reflectance in areas without available plots was matched with the reflectance of plant communities already detected and identified in this study. Areas with unidentified vegetation types resulted from the lack of both plots and correlation with a known reflectance signal (Fig. 3.5).

Variation in floristic composition and forest structure across physical variables such as geomorphology, soils, geology, drainage, and climate were interpreted in the framework of previous studies including Schargel et al. (2000), Schargel and Marvez (2009), Quesada et al. (2011), IGAC (2014, 2018), and Zinck (Chaps. 6 and 7 this book).

### 3.3.2 Phytosociological Analysis

Information on species and field data was stored and managed using Microsoft Excel. The aboveground biomass for all species was calculated using a raw field and estimated data set with the Chave et al. (2005) allometric formula. Artificial neuronal networks (ANN) were employed to find some missing values of DBH (diameter at breast height), tree height, and wood density. Based on 11,100 complete tuple records (DBH, height, wood density; in a matrix  $m \times n$  a tuple refers to a set of data in a complete row  $m_i$ ), a new matrix was constructed incorporating 39,211 new records (no tuples). The ANN outcomes showed a good fit for the missing values related to the known and raw field data behavior (Haykin 2009; Arellano-Peña and Rangel-Ch. 2015). According to the correlation coefficients (R), the R training describes the behavior between the existing variables within two matrices. The main matrix (X) has several columns that hold integer type data, where every number represents the classification of different taxa levels, besides some known vegetation variables (double type data) such as height and wood density.

In contrast, the second matrix (Y) has the known values of the dependent variables such as DBH. It is essential to emphasize the possibility of setting different configurations. As a consequence of the learning process with ANN, the training phase registered R values between 0.812 and 0.994. The R validation aims to compare some known and observed results within the model with some predicted results. The R values fluctuated between 0.792 and 0.994. The R test value proves the behavior of the predicted variables, their fit to the model with values between 0.805 and 0.994, and the whole process with R between 0.808 and 0.994; these results validate the ability of the model to estimate missing values (Fig. 3.3).

The plot data were analyzed using two-way indicator species analysis (TWINSPAN) (Hill 1979). The latter was carried out using PC-ORD Multivariate Analysis of Ecological Data for Windows, version 7.0 (McCune and Mefford 2016). TWINSPAN reveals clusters or groupings of plots similar in terms of species composition. Such clusters can indicate associations of tree communities or sub-communities.

The resulting TWINSPAN was interpreted in terms of syntaxonomical classification of the vegetation, based on floristic affinities, according to the Zürich-Montpellier approach (Braun-Blanquet 1979; Westhoff and van der Maarel 1973). TWINSPAN classifies species and samples in a way that approaches the results of a Braun-Blanquet vegetation table. This was used to build a key to the classification of the samples by identifying one to several species, which were particularly diagnostic of each division in the classification. The pseudo-species



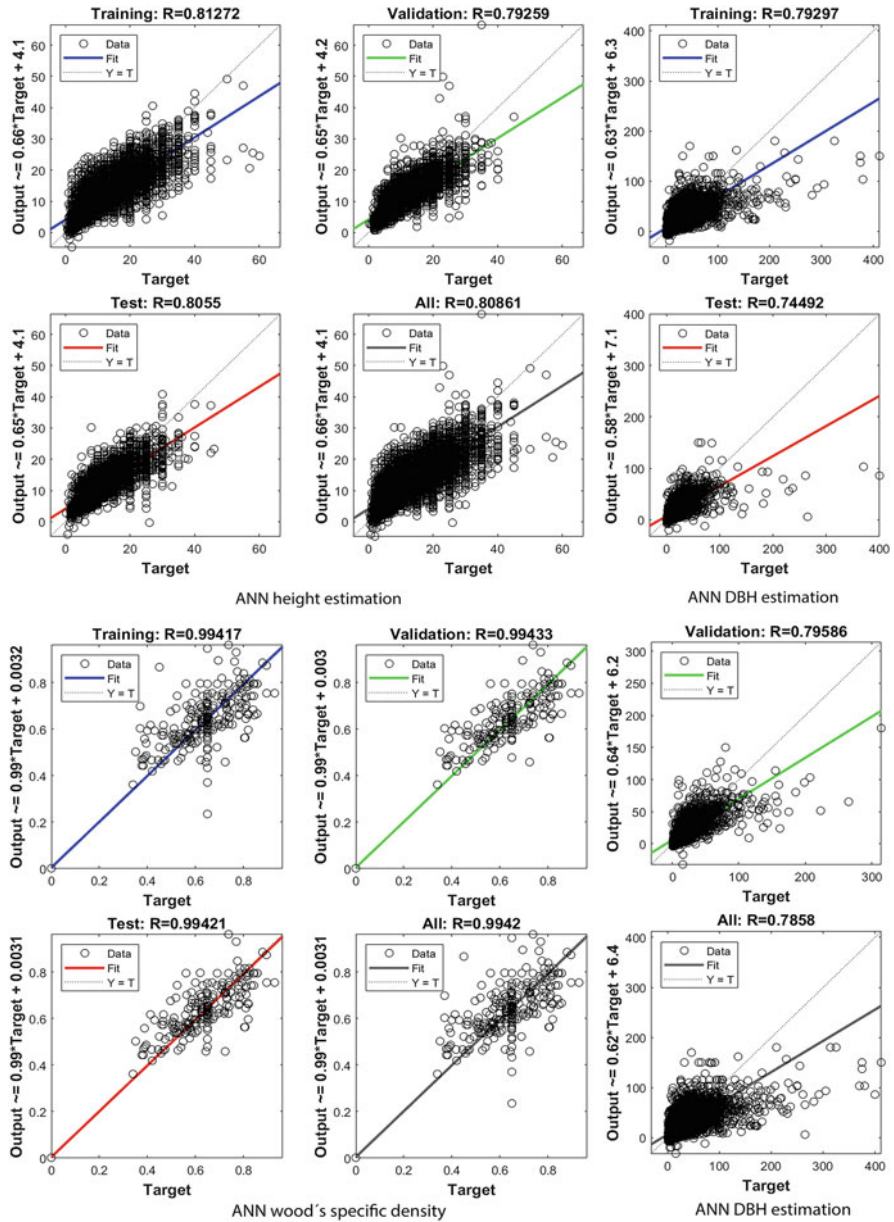


**Fig. 3.3** Estimation of missing values of DBH, height, and wood density using artificial neuronal network (ANN)

analysis cuts were carried out in TWINSPLAN with five levels or intervals. Five plots were chosen as the minimum group size for division, and five species as the maximum number of indicators per division.

### 3.4 Results

TWINSPLAN produced five levels and established 21 indicator species. These species classify the samples and plots under a unique class (two main orders, with five alliances, seven associations, and a larger group integrated by several indeterminate associations) (Figs. 3.4 and 3.5). The results of this phytosociological classification divided the forests into three main pedobiomes that occur in the study area. These pedobiomes reflect three forest types associated with different substrates and floristic and structure differences: the Amazonian caatinga (campinarana) on well-drained sandy soils on slightly higher peneplain surfaces, the tall terra-firme forests on deep well-drained clay soils, and forests in alluvial plains on soils with water-logging at different depths. Soil features (e.g., drainage, very low water retention capacity, and nutrient availability in lesser degree), and types of water are the factors that split the forests into three main pedobiomes in the study area. The influence of these factors is reflected in the floristic and structure differences among Amazonian caatinga, terra-firme forests, and forests in alluvial plains.

#### 3.4.1 Phytosociological Classification

The procedure defined the phytosociological class *Eperuo leucanthae*—*Eperuetea purpureae* from which the first division level distinguished two orders.

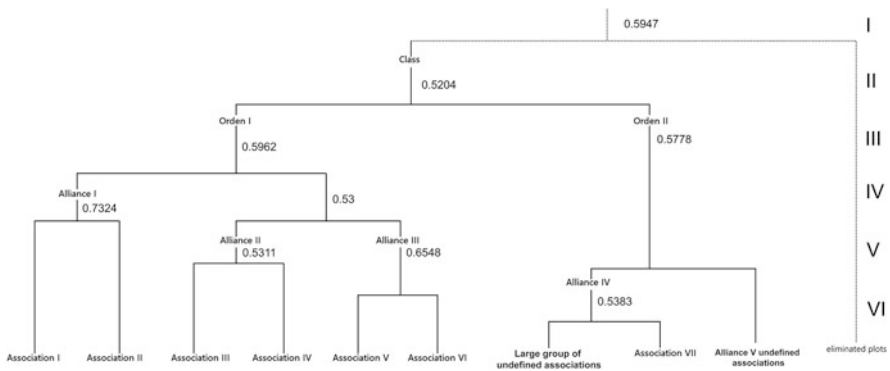
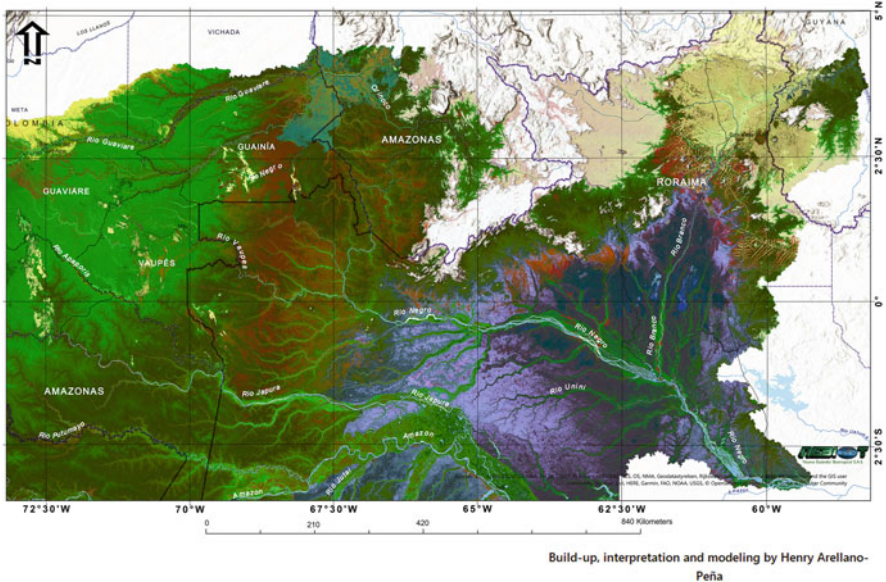


**Fig. 3.4** Dendrogram showing TWINSPLAN classification of species (eigenvalues numbers in normal text)





LEGEND  
UPPER RÍO NEGRO AND RÍO ORINOCO BASINS PHYTOSOCIOLOGICAL GROUPS

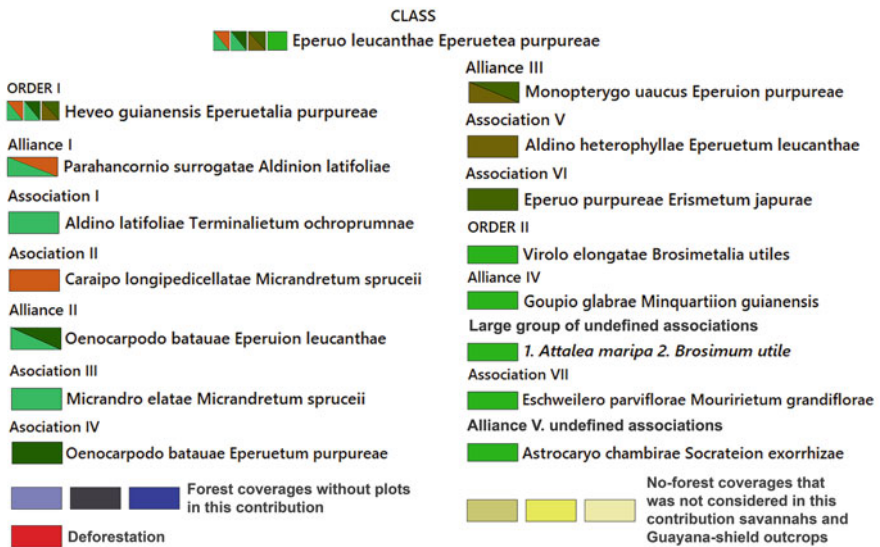


**Fig. 3.5** Map of the study region showing the phytosociological groups in the upper Rio Negro and Orinoco basins. A high-resolution imagen is found in the following link: [https://1drv.ms/f/s!AsgLjs\\_JMencgZsGYB0kItyDnwkiIg](https://1drv.ms/f/s!AsgLjs_JMencgZsGYB0kItyDnwkiIg)

### 3.4.1.1 Order I

The first order (Parahancornio surrogatae-Aldinion latifoliae) is composed of communities strongly associated with blackwater drainage (i.e., tall caatinga (campinarana) forest and *Micrandra spruceana*, *Monopteryx uauacu*, and *Erisma japura* forests), with the following indicator species: *Hevea guianensis*, *Eperua purpurea*, *Mucua duckei*, *Monopteryx uauacu*, *Oenocarpus batatua*, *Pouteria cuspidata*, *Caraipa longipedicellata*, *Calophyllum brasiliense*, *Iryanthera elliptica*, and *Aldina kunhardtiana*. This order was separated at the second level by alliance II with the indicator species *Parahancornia surrogata* and *Aldina latifolia*. At the third level, alliance I was split into association I (*Aldina latifolia*, *Terminalia ochroprumna*, *Swartzia sericea*, *Pachira nitida*) and association II (*Caraipa longipedicellata*, *Micrandra sprucei*, *Compsonera debilis*, *Cyrilla recemiflora*).

Association I also includes the flooded forest communities on blackwater floodplains, called igapó (Figs. 3.6 and 3.7) by Ducke (1954), Prance (1980), and Kubitzki (1989). In the Rio Negro region, about 119,000 km<sup>2</sup> of the basin are covered by igapó with forest coverage >85% (Householder et al. 2021). The same authors are in agreement with the general hypothesis that the flood duration gradient is a major environmental driver of compositional turnover in floodplain forests, even among distant sites. This implies that species ecological distributions along the flood duration gradient are predictable and unlikely to be geographically distinctive between sites (Householder et al. 2021). The igapó in the Rio Negro also contains unique large areas made up of medium high trees with small dark leaves, very different from the exuberant Amazonian vegetation, even from the igapó forests. These communities are known as “boyaes” or “selvas de boya” in Colombia and Venezuela (Vareschi 1963) and “formações do Molongó” in Brazil (Ducke 1938). “Boyaes” are abundant in flooded areas of the northern Rio Negro basin in Colombia and Venezuela, and extend south to the river Urubú in Brazil (Ducke 1944). In general, they are made up of numerous small trees with extremely light wood (mainly at the base of the trunks), adapted to the blackwater habitats (Mägdefrau and Wutz 1961; Berry and Wiedenhoef 2004). The unique ecological



**Fig. 3.6** Rio Negro basin: igapó forest; upper Cuy(i)ari river, Guianía department, Colombia; photograph by Jorge L. Contreras, ©Ciprogress Greenlife



**Fig. 3.7** Rio Negro basin: igapó forest; (a) “Caño Emeri,” San Miguel river basin, sector “Pajara,” Amazonas state, Venezuela; photograph by Gustavo A. Romero-González; (b) upper Guianía river, Guianía department, Colombia; photograph by Adela Lozano, ©Ciprogress Greenlife

characteristics of the “boyaes” make their flora predominantly endemic (e.g., *Anaxagorea inundata*, *Malouetia molongo*, *Micrandra inundata*, *Pouteria pimichinensis*), and well adapted to the extreme conditions of annual flooding (Fig. 3.8). These communities are dominated by taxa from Annonaceae, Apocynaceae, Malvaceae, and Euphorbiaceae (Aymard et al. 1989). This kind of vegetation represents unique and large riparian communities in the north-western Amazon basin and part of the Orinoquia (Romero-G et al. 2019). Nonetheless, recent studies and reviews of the vegetation associated with the rivers of both basins make





**Fig. 3.8** Boyales dominated by *Molongum laxum* (Benth.) Pichon (Apocynaceae) in floodplain of the Atabapo river, Venezuela; photograph by Gustavo A. Romero-González

no mention of “boyales” or “formações do Molongó” (Wittmann et al. 2017; Luize et al. 2018; Householder et al. 2021).

The third level also recognized alliance II (*Clathrotropis glaucophylla*, *Eperua leucantha*, *Micrandra sprucei*, *Oenocarpus bataua*) and association III (*Macrobium limbatum*, *Micrandra elata*, *M. sprucei*, and *Mucua duckei*). The fourth level produced alliance III (*Eperua leucantha*, *E. purpurea*, *Hevea guianensis*, *Monopteryx uauco*, *Virola michelii*) and association IV (*Eperua purpurea*, *Oenocarpus bataua*). The fifth level divided the rest of alliance III in associations V (*Aldina heterophylla*, *E. leucantha*) and VI (*Eperua purpurea*, *Erismia japura*). Association VI harbors the forests dominated by *E. purpurea*, a soil generalist species (Aymard et al. 2009), known as “aceitón” in Colombia, “copaibarama” in Brazil, “yevaro” in Venezuela, and “waapa” in Kuripako language (A. Calero-Cayopare, pers. com).

### 3.4.1.2 Order II

The second order (Goupio glabrae—Minquartiion guianensis) corresponds to forests associated with white and clear waters, growing mostly on clay soils. This syntaxon is named after the exclusive species *Goupia glabra* and *Minquartia guianensis* as the dominant species on disturbed forests. The Goupio glabrae—Minquartiion guianensis holds two alliances and two associations: an undefined *Attalea maripa*—*Brosimum utile* association, and the Eschweilero parviflorae—Mourietum grandiflorae association. Forests dominated by palms are represented by the undefined alliance of *Astrocaryo chambirae*—Socrateion exorrhizae.



**Fig. 3.9** (a) “Sasafrás” forest, a community that extends from the alluvial plains to terra-firme forests on terraces drained by clear waters; (b) forest dominated by *Mespilodaphne cymbarum* (Kunth) Trofimov (Lauraceae), a valuable timber known as “Sasafrás del Orinoco”; Guaviare river, Guainía department, Colombia; photographs by Francisco Castro-Lima

The second level of this order separated alliances IV (*Goupia glabra*, *Miquartia guianensis*, *Mouriri grandiflora*) and V (*Astrocaryum chambira*, *Calycophyllum megistocaulum*, *Euterpe precatória*, *Inga tessmannii*, *Pseudolmedia laevis*, *Psychotria remota*, *Socratea exorrhiza*), the latter being a complex group without defined forest associations in alluvial plains mixed with palm communities. The third level showed two different divisions, the association VII (*Clathrotropis brachypetala*, *Erismia laurifolium*, *Eschweilera parviflora*, *Mouriri grandiflora*, *Pouteria baehiana*, *Protium divaricatum*, *Virola elongata*, *Zamia ulei*), and another branch including a larger group without clear associations. The last cluster was characterized by the following indicator species: *Attalea maripa*, *Brosimum utile*, *Eschweilera parviflora*, *Euterpe precatória*, *Goupia glabra*, *Mayaba elengans*, *Mespilodaphne cymbarum*, and *Virola elongata*. These communities extend from the alluvial plains to terra-firme forests on terraces such as the “sasafrás” forests, a community dominated by *Mespilodaphne cymbarum* (Fig. 3.9).

### 3.4.2 Vegetation and Environmental Conditions

Soil and water types were related to the clustering of species dominance data into two orders. The first one comprises three alliances and six associations, mainly dominated by the high caatinga (campinarana) because of the abundance of *Caraipa longipedicellata*, *Eperua leucantha*, *Micrandra sprucei*, and *Mucoa duckei* growing on very poorly drained Spodosols (Figs. 3.10 and 3.11). Other communities, such as tall and medium forests on somewhat poorly drained Entisols on terraces, appeared in this order (i.e., *Monopteryx uauco* and *Erismia japura* forests). These communities were separated from the high caatinga because their floristic composition shows that



**Fig. 3.10** Rio Negro basin: high caatinga on very poorly drained Spodosols; “Caño Vitina,” lower Atabapo river, Guanía department, Colombia; photograph by Francisco Castro-Lima

they share species well distributed over moderately and poorly drained Entisols, Inceptisols, Oxisols, and Ultisols. The tall and medium forests also contained taxa that were common in areas with Spodosols. The variety of habitats strongly suggests that the above-mentioned species are not white-sand specialists, as it has been proposed (García-Villacorta et al. 2016). Examples of taxa with a wide habitat preference and frequent in forests that grow on white sands in the upper Rio Negro are: *Aldina kunhardtiana*, *Dendropanax neblinae*, *Eperua leucantha*, *E. purpurea*, *Erismia micranthum*, *Hebepetalum humiriifolium*, *Helianthostylis steyermarkii*, *Pentamerista neotropica*, *Sloanea floribunda*, and *Tetrameranthus duckei*, all considered soil generalists by Aymard et al. (2009). Plant communities of the upper Rio Negro basin found on white sands and terra-firme forests growing on clay soils may have a common evolutionary history (Aymard et al. 2016).

The second order includes the communities associated with white and clear waters, growing on clayey soils. Under this physical condition, communities tolerate considerable differences in drainage, because in poorly drained soils root mats develop below the litter layer. These communities are composed of an array of medium to tall forests mixed with palm communities, with three to four vertical layers at heights of 25–35 m, 15–25 m, 7–12 m, and 3–7 m. The top layer included emergent trees reaching heights of 35–45 m, such as *Erismia laurifolium* and *Goupia glabra*, giving the canopy of this forest type a very irregular aspect. The vertical discontinuities are further accentuated by the frequent occurrence of gaps caused by tree falls. The third and fourth layers are not always easily distinguished because of



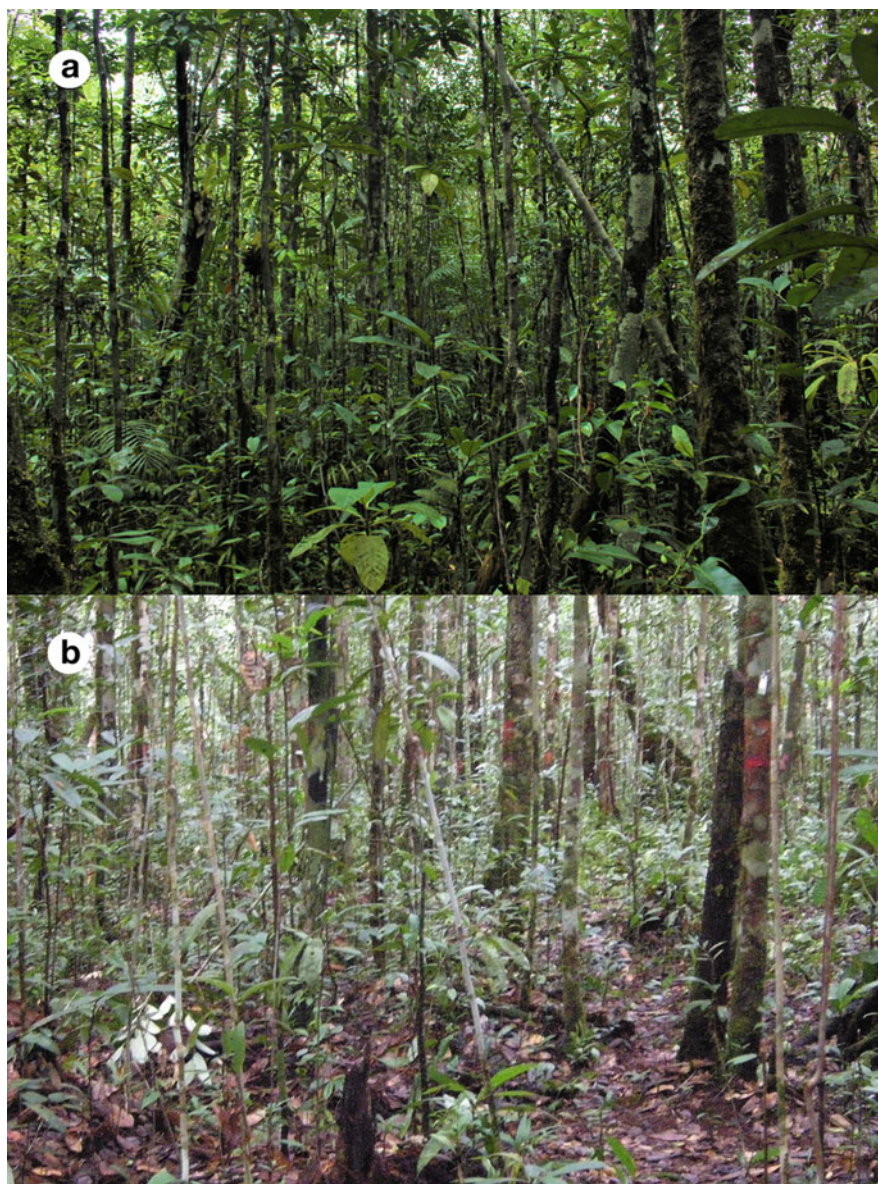


**Fig. 3.11** Rio Negro basin: high caatinga on very poorly drained Spodosols; (a) “Campo Alegre,” upper Cuy(i)ari river, Guanía department, Colombia; photograph by Francisco Castro-Lima, ©Ciprogress Greenlife; (b) San Carlos de Río Negro, Amazonas state, Venezuela; photograph by Gerardo A. Aymard C

the high density of species such as *Anaxagorea brachycarpa*, *Clathrotropis glaucophylla*, *Heterostemon conjugatus*, *Iryanthera paradoxa*, *Matisia ochrocalyx*, *Pseudosenefeldera inclinata*, *Sagotia heterocalyx*, and *Zygia claviflora*. Dense colonies of palm species such as *Astrocaryum chambira*, *Bactris corosilla*, *Euterpe precatoria*, *Iriartella setigera*, and *Socratea exorrhiza*, as well as the giant caulescent herb *Phenakospermum guyannense* (considered an indicator of disturbed forest) were present in the third layer. The phytosociological classification and description of the new alliances and associations of the forest communities of the Rio Negro region are outlined in Appendices 3.1, 3.3, and Figs. 3.4 and 3.5.

---

## 3.5 Discussion

### 3.5.1 General Aspects

The study shows that a relatively low number (226) of small to medium-sized transects and plots (mostly 0.1 ha transects) may be sufficient to set up a robust phytosociological analysis of vast regions (Figs. 3.4 and 3.5). This approach allows comparing local variations in forest structure and floristic composition by soil topography across areas with different environmental conditions. An important issue in evaluating the results is the degree to which site diversity (alpha diversity) is being measured vs. locally varying habitat diversity (beta diversity). Local diversity can be affected by the shape of the plot, with increasingly narrow rectangular plots generally showing higher diversity values than broader or square plots (Condit et al. 1996). Large plots ( $\geq 1$  ha) have provided useful data to characterize forest structure and composition, and if properly tagged, protected, and monitored, they can provide long-term data on the growth, mortality, regeneration, dynamics of forest trees, and climate change (ForestPlots.net 2021). However, given the costs and labor they require to sample and maintain, such plots are relatively few and spatially scattered. A lower-cost and faster alternative, especially when permanent plots are not required or are not feasible to maintain, is 0.1 ha transects (Gentry 1982). With similar effort necessary to set up one-ha plots, many smaller plots can be established, yielding valuable information about variability in forest sites at a local scale (Gentry 1988a, 1988b; Clinebell et al. 1995; Aymard et al. 2009). Often, a lower diameter cut-off (usually 2.5 cm DBH) is used in small plots, which yields individual stem numbers of the same magnitude as those obtained from hectare plots sampled at  $\geq 10$  cm DBH. Gentry (1988a, b; Draper et al. 2021) used 980 transects of 0.1 ha, combining efficient ecological sampling with high-quality botanical identifications to describe large-scale patterns of alpha diversity and floristics, and then create highly distributed measurements of the world's forests (for a review, see Phillips and Miller 2002; ForestPlots.net et al. 2021).

The phytosociological study presented here shows that the order level was most useful to characterize the alliances and their communities. At this level, the eigenvalues were as high as 0.5. High values determine a significant dispersion of the data in the analysis that allows displaying the species along environmental



variables (ter Braak, 1987). The analysis with TWINSpan generated end-groups of five blocks that represent vegetation units in five alliances and nine associations that form the dendrogram (Fig. 3.4).

Variations in floristic composition could be related to the particular drainage and water-holding capacity of soils where these forest types grow. For example, there are species that tend to occur on deep well-drained terra-firme soils (e.g., *Allantoma lineata*, *Caryocar pallidum*, *Erismia japura*, *Eschweilera micrantha*, *Guarea trunciflora*, *Manilkara huberi*, *Mezilaurus itauba*, *Minuartia guianensis*, *Pseudosenefeldera inclinata*, *Scleronema micranthum*), or on very poorly drained Spodosols in lowlands (e.g., *Aspidosperma verruculosum*, *Caraipa longipedicellata*, *Compsonera debilis*, *Couma catinae*, *Hevea rigidifolia*, *Mabea arenicola*, *Micrandra sprucei*, *Micropholis maguirei*, *Myrcia neoforsteri*, *Neocouma ternstroemiacea*). In addition, a considerable amount of taxa appear only in riparian, swamp, and seasonally black water-flooded forests on alluvial plains growing on soils with water-logging at different depths (e.g., *Eschweilera tenuifolia*, *Guatteria heteropetala*, *Handroanthus barbatus*, *Leopoldinia piassaba*, *Lissocarpa benthamii*, *Molongum laxum*, *Mouriri acutiflora*, *Myrcia argentigemma*, *Parahancornia negroensis*, *Spongiospermum riparium*); individual species respond differently to the flood duration gradient (Householder et al. 2021).

This point is illustrated by Sabatier et al. (1997), who in French Guiana observed substantial changes in forest communities in the transition of soils with deep vertical drainage to superficial lateral drainage. At large scale, however, the forest structure and dynamics have been noted to vary across the Amazon basin in an east-west gradient in a pattern that coincides with variations in soil fertility, topography, and geology (Pitman et al. 2008; Quesada et al. 2011, 2012).

Therefore, large-scale variations in forest biomass could not be explained by any of the soil or climate properties analyzed here. A recent study using one-ha forest inventory plots in Costa Rica showed that, while plant species richness was controlled by climate and soil water availability, vegetation carbon storage was strongly related to wood density and soil phosphorus availability (Hofhansl et al. 2020). These results also suggest that local heterogeneity in resource availability and plant functional composition should be considered to improve projections of tropical forest ecosystem functioning under future climate scenarios.

Oligotrophic soils (either Spodosols or clay soils) throughout the Rio Negro basin (Herrera 1985; Dubroeuq and Volkoff 1998; Schargel and Marvez 2009; Quesada et al. 2011; IGAC 2014) influence in minor degree differences in forest types in this region (Schargel and Marvez 2009; Stropp et al. 2014). Moreover, several studies showed that soils, drainage, moisture retention, and water types (i.e., black, clear, and white waters) are the principal factors that separate terra-firme, caatinga, and alluvial plain forests in the study area (Medina et al. 1990; Franco and Dezzeo 1994; Coomes and Grubb 1996; Schargel et al. 2000; Stropp et al. 2011).

Besides, human intervention by way of shifting cultivation and the enrichment of the original forests with introduced, useful species, on the better-drained soils, cannot be discarded as a cause for creating floristic differences (Levis et al. 2017; Montoya et al. 2020). Total rainfall does not need to decrease drastically to favor

vegetation change on these nutrient-poor soils, most of which have low water retention capacity. An increase in the length and severity of the dry season would be sufficient. It was observed that the geographical distribution of many non-generalist species is related to average annual rainfall and the duration of the dry season. For example, *Aldina kunhardtiana*, *Caraipa longipedicellata*, *Chrysophyllum sanguilentum*, *Eperua purpurea*, *E. leucantha*, *Helianthostylis steyermarkii*, *Inga neblinensis*, *Leptobalanus cardiophyllus*, *Macrobium limbatum*, *Mezilaurus itauba*, *Monopteryx uauacu*, *Ouratea clarkii*, *Protium carolense*, *P. crassipetalum*, *Roucheria punctata*, *Swartzia benthamiana*, and *Tachigali odoratissima* represent taxa that belong to a larger group of species that is only found in areas within the basin with precipitations between 3000 and 3600 mm and 0–2 months with less than 180 mm precipitation, suggesting that the distribution pattern of many species is also directly related to annual precipitation patterns and the duration of the dry season. These climatic parameters, in conjunction with the gradient in soil fertility, are considered by ter Steege et al. (2003, 2006, 2010) as the two main variables that predict values of alpha diversity and stem density in Amazonian forests. In their proposed model, they found that the most diverse forests are located just south of the equatorial line (areas with 0–1 month with precipitation <100 mm); while the less diverse ones were found on the Guayana Shield and in the Amazon area of Bolivia (areas having 5–7 months with precipitation <100 mm). A comparison of this pattern with data provided by Aymard et al. (2009) shows that the duration of the dry season (DSL) was more useful in determining species distributions than predicting alpha diversity values, because the upper Rio Negro and part of the adjacent south-western Orinoco region, with higher rainfall and few months of little rain, also has low alpha diversity. This finding contradicts the assumption that predicts that high elevation and extremes of substrate-related factors underpin the floristic segregation of environmentally “marginal” vegetation types and “terra-firme” forests, rather than climatic factors, which in these case are relatively unimportant (Oliveira-Filho et al. 2021).

### 3.5.2 Forest Structural Characteristics

The upper Rio Negro (north-western Amazon) and adjacent south-western Orinoco basins, where forest structure varies across different soil types and local topography, holds a top layer that includes emergent trees reaching heights of 35–45 m, and a medium to short dynamic tree stratum like most northwestern Amazon forests (Quesada et al. 2012). According to Draper et al. (2021), smaller-statured species may be exposed to different biotic and abiotic filters across large spatial scales, and these variables develop greater local specialization associated with distinct functional characteristics.

Canopy and mean tree height decreased from soils with moderate to poor drainage to very poorly drained Spodosols. Very low moisture retention, due to shallow soil depth or coarse sandy saprolite, also determined a tree height decrease in the somewhat poorly drained Entisols (Schargel and Marvez 2009) together with an

increase in high values of stems (Uhl and Murphy 1981; Aymard et al. 2009; Stropp et al. 2011).

In the San Carlos de Río Negro area, Klinge and Medina (1979) and Bongers et al. (1985) found that the reduction in height of the caatinga (campinarana) community was related to a reduction in depth of the aerated soil layer above the water table. This forest community dominated by *Micrandra sprucei* and *Eperua purpurea* is similar to those of caatingas nearby Manaus (Takeuchi 1962a, 1962b). Moreover, the tallest layer of this forest is 15–25 m high, and dense colonies of *Mauritia carana* and *Euterpe catinga* also occurred in this layer (Aymard et al. 2009).

The frequency of tall trees (DBH > 80 cm, over 45 m high) is low in the upper Rio Negro basin compared with the adjacent south-western Orinoco basin. The most frequent trees which reached over 45 m high were: *Allantoma lineata*, *Brosimum utile*, *Caryocar* spp., *Eperua purpurea*, *Ecclinusa ramiflora*, *Erisma bicolor*, *E. japura*, *Eschweilera* spp., *Goupia glabra*, *Mespilodaphe cymbarum*, *Micrandra spruceana*, *Micropholis brochidodroma*, *Minuartia guianensis*, *Monopteryx uauçu*, *Parahancornia negroensis*, *Pouteria* spp., *Swartzia floribunda*, *Terminalia* (*Buchenavia*) spp., and *Vochysia* ssp. By contrast, all forest types had a larger number of medium and smaller trees located in the second and third strata that defined the forest structure.

With the minimum DBH cut-off of 2.5 cm used in this study, the number of stems sampled varied from 101 to 1017 per plot, whereas one-hectare plots with a minimum DBH of 10 cm often have around 500 stems (Valencia et al. 2005). The high density of individuals with lower average diameter in very nutrient-poor soils is due to increased tree longevity in the lower strata and understory levels, very slow growth, presence of sclerophyllous leaves with low nutrient content, and high levels of phenols and tannins that inhibit herbivory (Janzen 1974). Cuevas and Medina (1986, 1991), Medina et al. (1990), and Sanford and Cuevas (1996) observed in the upper Rio Negro region that plant individuals on soils with the lowest fertility invest more resources in the development of fine roots to penetrate the soil and obtain nutrients, than in photosynthetic tissues (discussed in Chap. 4). This reduction in photosynthetic tissue reduces the population of herbivores and eventually produces a positive result by developing plants with better defense mechanisms, representing an evolutionary response of species that grow on very nutrient-poor soils (Fine et al. 2006). However, Stropp et al. (2014) provide no evidence that an interaction between herbivory and soil nutrient availability drives habitat association of tree species in white-sand and terra-firme forests of the upper Rio Negro. Nutrient conservation depends on the structure of plant communities; forests on nutrient-poor soils, located in the upper Rio Negro in front of the Guayana Shield, have high wood density values, defense mechanisms, and more efficient nutrient conservation (Vitousek and Sanford 1986; Medina et al. 1990) than Amazonian forests located on more fertile soils on the foothills of the Andean Cordillera (Pitman et al. 2008), and in well-drained upland forests in north-western Amazonia (Duivenvoorden et al. 2005; Cano and Stevenson 2009).

The forests located in the south-western Orinoco basin have four vertical layers (35–45 m, 15–25 m, 7–12 m, and 3–7 m). The top layer included more emergent trees than in the Rio Negro basin, reaching heights of 45 m, giving the canopy of this forest a very irregular aspect. The second layer (15–25 m) is quite heterogeneous, and the third and fourth layers are not always easy to distinguish because of the high density of species such as *Clathrotropis brachypetala*, *Matayba elegans*, *Mouriri grandiflora*, *Pseudolmedia laevis*, and *Virola elongata*. These communities harbor numerous colonies of palms, of which stand out *Euterpe precatoria*, *Iriartella setigera*, *Socratea exorrhiza*, *Oenocarpus bataua* as well as the Strelitziaceae *Phenakospermum guyannense*. Palms perhaps represent the most characteristic physiognomic element of the terra-firme and riverine forests of the Amazon and Orinoco basins (for a review, see Alvez-Valles et al. 2018). In the tall forests studied here, seedlings of *Oenocarpus bataua* were abundant everywhere, and *Astrocaryum gynacanthum* and *Bactris corosilla* often formed a layer 3–6 m high with their long, divided leaves. Other small to medium-stature species, such as *Astrocaryum chambira* (“palma cumare”) with long spines along its trunks, were scattered in the forest. Individuals of *Oenocarpus bataua* were the tallest palms (to ca 30 m), and sometimes appeared as canopy emergent. The distribution of palm species in lowland forests is usually correlated with gradients from well to poorly drained soils (Alvez-Valles et al. 2018). In the study area, *Mauritia carana*, for example, occurs on poorly drained sites between the caatinga forest and white sand savannas, and *Leopoldinia piassaba* is generally associated with poorly drained Spodosols and low water retention soils (Vareschi 1963; Kubitzki 1991).

North-western Amazonian forests appear to be comparatively poor in climbers (Putz and Mooney 1991). The so-called “matas de cipós” (liana forests), found in other Amazonian regions especially between the Xingu and Tocantins rivers (Prance 1989) do not occur in the upper Rio Negro area (Putz 1983). In this study, lianas were represented by only 143 species (10.45%), mainly in terra-firme forests on moderately to poorly drained soils.

### 3.5.3 Plant Diversity

The upper Río Negro region is reportedly not a region rich in local tree diversity when compared to other Amazonian ecosystems (Uhl and Murphy 1981; Dezzio et al. 2000; Boubli 2002; Cárdenas-López et al. 2007; Aymard et al. 2009; Stropp et al. 2011; Pombo de Souza 2012). The same pattern has been observed in other places with white-sand ecosystems in the basin (Capurucho et al. 2020). A study in a forest dominated by *Eperua purpurea* in San Carlos de Rio Negro (Venezuela) identified 183 species, detected by combining the results of a 0.10 ha transect and a 1-ha plot (Aymard et al. 2009). In this area, the highest number of species occurred in terra-firme forests because these are the largest communities, the terra-firme occupies 70–80% of Amazonia (ter Steege et al. 2003, 2019b).

Similarly, in the upper Rio Negro basin, terra-firme forests located in the upper Isana region are plant communities with high species diversity, recording between

108 and 162 species in three plots of  $40 \times 40$  m ( $1600 \text{ m}^2$ ) with  $\text{DBH} \geq 5$  cm (Arellano-Peña et al. 2019). In areas on podzolic soils and with high rainfall within the upper Rio Negro basin, the fewest species occur in sectors with drainage limitations, dominance of ectomycorrhiza in the topsoil layer, and lower nutrient retention capacity (Kubitzki 1990; Moyersoen 1993). This relationship is coherent with the high local species endemism reported by Steyermark (1982) and Kubitzki (1989) in the Rio Negro basin, including *Duguetia aberrans*, *D. sancticaroli*, *Besleria yatuana*, *Chamaecrista ipanorensis*, *Eschweilera rionegrense*, *Mezilaurus caatingae*, *Pseudephedranthus fragans*, and *Vochysia steyermarkiana*. These forests consist of relatively few species (oligarchic) mixed with taxa represented by just one or a few individuals known as rare species (ter Steege et al. 2019b). The latter contribute enormously to regional diversity, have very low values of abundance in the oligarchic forests, and are usually the most difficult to identify at the level of species (Aymard et al. 2009).

The low diversity of species in the region is perhaps partially explained by factors related to the history and evolution of Neotropical forests, such as climatic events that the biota of the lowlands of northern South America lived through from Tertiary to Quaternary (Hooghiemstra et al. 2002, 2006; Hooen et al. 2010, 2017; Wesselingh et al. 2010), including variations in precipitation patterns during the last glacial advance (Last Glacial Maximum, LGM) approximately 18,000 years ago (van der Hammen and Absy 1994; Ruiz-Pessenda et al. 2009). These events caused changes in forest vegetation in some sectors of the Amazon basin, which was replaced by savannas (Ruiz-Pessenda et al. 2009), shrubs or other characteristic communities of dry environments (Häggi et al. 2017). In other areas like the region that currently corresponds to the Rio Negro basin, vegetation may have been constantly subjected to changes through longer dry periods, with overall less rainfall, and higher sediment flow than in the western Amazon (Hooghiemstra et al. 2006), where forest cover was persistent (Bush et al. 2004). By responding to these changes in climate and significant landscape transformations, biomes expanded or contracted, becoming either connected or disjointed (Colinvaux et al. 2000; Pennington et al. 2004; Baker et al. 2020).

These environmental factors have produced significant alterations of the forest due to fires during the Holocene, a fact that is supported by the numerous samples of charcoal found in the region of San Carlos de Río Negro (Venezuela) and Lake Acarabixi (Brazil) dating from the Holocene (Saldarriaga and West 1986; Rodríguez-Zorro et al. 2018). Continuous changes in vegetation perhaps did not allow maintaining a previous flora or the formation of a flora as rich in species as that of western Amazonia (Stropp et al. 2009, 2011). Bush et al. (2004) and Cordeiro et al. (2011) conducted palynological and geochemical studies in the “Lagoa da Pata,” in the upper Rio Negro (Amazonas state, Brazil), that revealed significant changes in the environmental history of this portion of the Amazon basin during the late Quaternary. The authors found pollen from elements of Andean regions such as *Alnus*, *Hedyosmum*, *Myrsine*, *Podocarpus*, and *Weinmannia*, mixed with lowland genera (e.g., *Cedrela*). The sediment core (113.6 cm deep) indicated that the

elements of the mountainous regions were very abundant between 45,000 and 12,000 yr. calBP.

Subsequently, in the range of 12,000 yr. calBP to the present, the pollen of the Andean genera disappeared completely from the sample studied (even *Cedrela*). Furthermore, the geochemical study from “Lagoa da Pata” matched perfectly with the results forwarded by Bush et al. (2004). This outcome revealed three hydrological and climatic regimes from 50,000 to 10,000 yr. calBP, characterized by a relatively wet climate (from 50,000 to 26,300 yr. calBP), a decrease in productivity (from 26,300 to 15,300 yr. calBP) that indicated a dry phase, and an increase in lacustrine productivity from approximately 15,300 to 10,000 yr. calBP (Cordeiro et al. 2011). In addition, two recent studies in the upper Rio Negro region (Lake Acarabixi) revealed that between 9000 and 4000 yr. calBP took place in the warmest and driest period of the last 100,000 years which coincided with changes in evaporation and precipitation that caused lake levels to drop over most of tropical South America (Rodríguez-Zorro et al. 2018; Nascimento et al. 2019). Furthermore, highland taxa such as *Hedyosmum* and *Myrsine* were found at that time together with igapó forest species like *Astrocaryum*, *Eschweilera*, *Macrobium*, *Myrtaceae*, and *Swartzia*. During the late Holocene (1600 to 650 yr. calBP), no drastic changes in vegetation were observed, but the presence of pioneer species like *Vismia* and *Cecropia*, along with the evidence of fires, pointed to human disturbance. Currently, with the exception of *Podocarpus* (*P. tepuinensis*), *Gordonia* (*G. spathulata*), *Cyathea* (*C. macrosora*), two species of *Otoba* (*O. glycyarpa*, *O. parviflora*) and few species of *Ilex* (e.g., *I. casiquiarensis*, *I. davidsei*, and *I. spruceana*), none of the highland genera mentioned in the palynological study have been registered in the present-day flora of this region. Nowadays, *Podocarpus* is an almost exclusive genus of montane zones; nonetheless, *P. tepuinensis* was found in the watershed of the upper Rio Negro (Berry and Aymard 1997). The presence of these five genera in the lowlands indicates the remnants of a relict flora that existed in the region between 45,000 and 12,000 yr. calBP and was different in species than the current one. Therefore, other species may have disappeared, leading to very distinctive forests than we see now (Bush et al. 2004).

The occurrence of highlands taxa found in the study area, partially agree with the Oliveira-Filho et al. (2021) assumption that the lack of these taxa in lowland Amazonia is likely driven by temperature, an important environmental factor driving floristic differentiation between montane and terra firme forests in the Amazon basin.

All this evidence points out that perhaps the forest did not fragment, but suffered significant variations in floristic composition due to drastic changes in temperature and precipitation, which effected diversity during the late Quaternary.

Because of its important number of taxa and their endemic elements, Huber (1994) placed the upper Rio Negro basin in the Guayana phytogeographical region, rather than as part of the Amazonian phytogeographical region, where it has traditionally been placed by phytogeographers. Nevertheless, a recent study aimed to regionalize the Amazon tree flora identified the upper Rio Negro as a main subregion through 161 indicator taxa (Silva-Souza and Souza 2020).

At local scale, the diversity in the upper Rio Negro and south-western Orinoco basins is low, partially explained by factors related to the history, area and evolution of Neotropical forests. This condition is related to climatic events that affected the biota of the lowlands of northern South America from Tertiary to Quaternary. It is documented that a more seasonal dry-wet climate caused marginal forest retraction and, together with temperature decrease, rearranged forest composition to some extent. This is observed in pollen records across Amazonia, depicting the presence of taxa at glacial times in localities where they do not live presently (D'Apollito et al. 2017).

Most of the taxa recorded in this study show a wide distribution throughout much of the Amazon basin, while some of the dominant species are restricted to the upper Rio Negro area, such as *Eperua purpurea*, *E. leucantha*, *Erismia japura*, and *Micrandra sprucei* (Clark et al. 2000). However, sampling artifacts certainly contribute to distort species distributions in the Amazon basin due to the strong tendency for collection density to be high in very few localities (Nelson et al. 1990; Schulman et al. 2007), such as close to main towns (e.g., Barcelos, San Carlos de Rio Negro, São Gabriel de Cachoeira), and lower in more distant rural areas (Hopkins 2019). Furthermore, a recent study showed that ca 300,000 km<sup>2</sup> of the Brazilian Amazon had been deforested by 2017, without having a single tree specimen recorded (Stropp et al. 2020).

---

### 3.6 Conclusions

This study provides new information on the floristic composition, structure, and diversity of the vegetation using a phytosociological classification. The analysis with TWISNPAN shows that the order level was the most useful variable to characterize vegetation. At this level, the classification developed notable resolution represented by five alliances and nine associations (Fig. 3.4). However, significant compositional differences may arise from chance alone, even among sites with identical environmental conditions, because small forest inventories yield a diverse pool of regional taxa (Gentry 1982; Ricklefs 1987).

Soil features (e.g., drainage, very low water retention capacity, and nutrient availability in lesser degree), and types of waters are the factors that split the forests in three main pedobiomes in the study area. The influence of these factors is reflected in the floristic and structure differences among Amazonian caatinga on well-drained sandy soils on slightly higher penepain surfaces, tall terra-firme forests on deep well-drained clay soils, and forests in alluvial plains on soils with water-logging at different depths.



Although the Rio Negro basin harbors the largest blackwater river in the world, it is still one of the least studied regions of the Amazon (Hopkins 2019; Stropp et al. 2020). Lleras (1997) pointed out that the entire basin (ca 750,652 km<sup>2</sup>), at a regional level, holds an exceptionally high species diversity (over 15,000), with several genera (e.g., *Asteranthos*—Scytopetalaceae, *Hylaea*—Apocynaceae, *Neblinaea*—Asteraceae, *Neblinantha*—Gentianaceae, *Neblinantha*—Melastomataceae, *Pyrrohiza*—Haemodoraceae) and a significant number of species only known to occur in the Rio Negro basin and its tributaries.

The predominantly descriptive nature of this phytosociological study is justified considering the state of baseline knowledge on the northern and north-western Amazonian ecosystems, particularly concerning spatial components of soil, types of draining water, and forest variation. Nonetheless, our results support the hypothesis predicting that distinct forest categories are associated with soil and climate conditions. Moreover, our study detected a dominance of important tree species. In addition, we found that sites with similar vegetation types (i.e., tall caatinga forest) show high affinity (in terms of structure but not in floristical composition, see Table 3.1) between them regardless of their separation along a geographic gradient. This affinity was also pointed out by Oliveira-Filho et al. (2021) in the entire Amazon basin, at least in reference to forest structure.

---

### 3.7 Forest Conservation Issues

Despite the relatively low number of one-ha plots and transects (226) analyzed here, it was possible to report differences in species composition and structure of the forests, and their relationships with environmental conditions such as soil characteristics and drainage across the upper Rio Negro region. Some of the differences between the forest characteristics observed in this study may be easily detectable on satellite images (Tuomisto et al. 2019). Rapid diversity assessments in small plots and transects preceded by general physiographic surveys based on remote sensing would be an efficient tool to estimate the overall level of the vascular plant diversity and its variability over large regions, or else in separate physiographic subdivisions, such as floodplains, swamps, or well-drained areas. Such information would offer basic reference material to evaluate the desirability for conservation and protection of certain rainforest areas and to help interpret the effects of human intervention and fragmentation of forests upon local and regional levels of vascular plant diversity. Moreover, a larger number of smaller inventory sites, such as those established during rapid diversity assessments, is likely to capture more diverse and heterogeneous tropical forest habitats than a smaller set of larger transects (Clinebell et al. 1995).



One alternative approach to improve data collection, at least in the Rio Negro region, involves local inhabitants in academic research collaborations. While the deforestation rate inside indigenous territories and protected natural areas remains well below the rates outside, unsustainable forest clearing is on the rise across the Amazon basin (Walker et al. 2020). Indigenous rights are violated by changes in current legislation that threaten to weaken indigenous peoples' constitutionally-guaranteed territorial rights. Regarding the Rio Negro indigenous territories, a total of 387 requests for mining concessions were pending in Brazil already in 2016 (Almeida et al. 2016) and 75 in Colombia by 2020 (ANLA 2020). The most severe threat may be in Venezuela, where the government overlooked illegal mining and deforestation. All these actions put at risk the forests of the indigenous people of the region, even though the Brazilian, Colombian, and Venezuelan constitutions recognize that indigenous people have rights to their traditional territories. Large protected areas of the Amazon basin north of the Equator are located in the Rio Negro region (Lleras 1997). These include the "Alto Orinoco-Casiquiare" Biosphere Reserve (82,662 km<sup>2</sup>, in Venezuela), a bi-national Park that features "Parque Nacional Serranía de la Neblina" (13,600 km<sup>2</sup>) in Venezuela, and "Parque Nacional del Pico de la Neblina" (22,200 km<sup>2</sup>) in adjacent Brazil, as well as "Monumento Natural Piedra del Cocuy" (0.15 km<sup>2</sup>) in Venezuela, a place close to which the frontiers of three countries merge. Lleras (1997) recommended giving high priority for the conservation of the large area along the Colombian-Venezuelan border (Rio Negro, Atabapo, and Vichada river basins), which would extend south to merge with existing conservation units in Brazil. Therefore, more conservation strategies and public policies are needed to respect the indigenous peoples' rights, and at the same time, understand their ancestral role in accomplishing Amazonian forest sustainability for centuries.

**Acknowledgments** We gratefully acknowledge the support provided by indigenous communities with particular reference to the Baniwa and Kuripako nations, who have contributed directly and indirectly to build and collect information and scientific field material used in this contribution. The first and last authors also thank Germán Bernal-Gutiérrez, a CEO of –Greenlife– for providing logistic and economic support to set up 12 permanent plots located in faraway and unexplored botanical places in the upper Guainía river basin, Guainía department, Colombia, which made this undertaking possible. Finally, we thank Ernesto Medina and Alfred Zinck for their comments on earlier versions of this text.

### Appendix 3.1: Phytosociological Classification and Description of the New Alliances and Associations of the Forest Communities in the Rio Negro Region

Phytosociological classification	Physiognomy and composition	Syntaxonomy	Ecology and distribution
<p><b>ORDEN I</b></p> <p><b>1. Parahancornio surrogatae Aldinion latifoliae all. Nov.</b> (Figs. 3.5 and 3.6)</p> <p><b>Typus:</b> Aldino latifolia - Terminalietum ochroprumnae (this study; Appendix 3.1 (this information is available in the following link: <a href="https://1drv.ms/f/s!AsgLjs_JMencgZsGYB0klyDnwkilg">https://1drv.ms/f/s!AsgLjs_JMencgZsGYB0klyDnwkilg</a>).</p> <p>Lowlands forests of the <i>Parahancornia surrogata</i> - <i>Aldina latifolia</i> alliance</p> <p>Cover area: 81,621.43 km<sup>2</sup> (Figs. 3.5 and 3.6)</p>	<p>The forest communities of this alliance are of medium to high stature (25–35 m tall), characterized by the presence of trees of:</p> <p>Apocynaceae, Euphorbiaceae, Lauraceae, Fabaceae, Malvaceae, Moraceae, Myristicaceae, and Sapotaceae</p>	<p>This alliance is defined on the basis of 24 samples that included 279 species, 166 genera in 62 families. This syntaxon is named with the elective species <i>Parahancornia surrogata</i> and the dominant legume species <i>Aldina latifolia</i>. Within the elective species are: <i>Calophyllum brasiliense</i>, <i>Glandonia williamsii</i>, <i>Caraipo longipedicellata</i>, <i>Sloanea laurifolia</i>, <i>Hevea nitida</i>, <i>Mollia speciosa</i>, <i>Pachira nitida</i> and <i>Licania mollis</i>. Other species can be found in Appendix 1. This alliance includes two new associations: Aldino latifoliae - Terminalietum ochroprumnae and Caraipo longipedicellatae - Micrandretum spruceii</p>	<p>The <i>Parahancornia surrogata</i> - <i>Aldina latifolia</i> alliance is found on slightly elevated positions in depressions, and on a sandy, somewhat poorly drained Entisols and spodosols. It is exposed to water-logging and also more susceptible to short droughts than other poorly or very poorly drained sandy soils, due to the shallow depth to the coarse sandy saprolite. This alliance is compound by forests on white sands, “terra firme,” and seasonally flooded forests with or without palm dominance.</p>
<p><b>1.1 Aldino latifoliae - Terminalietum ochroprumnae assoc. nov.</b> (Figs. 3.5 and 3.6).</p> <p><b>Typus:</b> Plot no. CC_130, TWINSPAN ID 69. Coordinates datum WGS84 LAT 3.6877,</p>	<p>The forests of <i>terminalia ochroprumna</i> and <i>Pachira nitida</i> are medium to high in stature and density, composed by trees with a DBH average greater than 10 cm. In this association, the</p>	<p>This association is defined on the basis of 7 samples that included 90 species, 61 genera in 27 families. The name of this syntaxon was based on the elective species, the legume</p>	<p>This vegetation community consists of low caatingas on white sand and seasonally flooded forests in black water. The forest of the association Aldino latifoliae Terminalietum</p>

(continued)

Phytosociological classification	Physiognomy and composition	Syntaxonomy	Ecology and distribution
<p>LON -67.4550. Altitude 89 m. Colombia. (Appendix 2; this information is available in the following link: <a href="https://1drv.ms/f/s!AsgLjs_JMencgZsGYB0KltyDnwkilg">https://1drv.ms/f/s!AsgLjs_JMencgZsGYB0KltyDnwkilg</a>) <b>Forests of <i>terminalia ochroprumna</i> and <i>Aldina latifolia</i></b> Cover area: 11,703.52 km<sup>2</sup> (Figs. 3.5 and 3.6)</p>	<p>following species registered the largest height: <i>Vochysia catingae</i> (26.1 m), <i>Parkia discolor</i> (25.7 m), <i>terminalia ochroprumna</i> (21.3 m), <i>Elaeoluma crispa</i> (18 m), and <i>Aldina latifolia</i> (16 m). The species with the highest physiognomic expression (relativized units) are: <i>Aldina latifolia</i> (5.7%), <i>Calophyllum brasiliense</i> (5.6%), <i>Hevea guianensis</i> (5.1%), <i>Pachira nitida</i> (4.9%), <i>Humiriastrum excelsum</i> (3.3%), <i>Leptabalanus wurdackii</i> (3.1%), <i>Elaeoluma crispa</i> (2.9%) and <i>Mollia lepidota</i> (2.8%).</p>	<p><i>Aldina latifolia</i> and <i>terminalia ochroprumna</i>, the most dominant and exclusive species. In this association, <i>Elaeoluma crispa</i> was registered as exclusive species as well. Within the elective species are: <i>Pachira nitida</i>, <i>Macrolobium multijugum</i>, <i>Mollia lepidota</i>, <i>Peltogyne paniculata</i>, <i>Swartzia sericea</i>, <i>Tachigali paniculata</i>, <i>Humiriastrum excelsum</i>, and <i>Leptobalanus apetalus</i>. Other species can be found in the Appendix 3.1.</p>	<p>ochroprumnae was determined based on seven (7) samples located in Colombia (i.g., along the Atabapo river in the border with Venezuela). Detailed information about these localities are found in Appendix 3.2.</p>
<p><b>1.2. Caraipo longipedicellatae -Micrandretum spruceii assoc. nov.</b> (Figs. 3.5 and 3.6) <b>Typus:</b> Plot CC_153, TWINSPAN ID 92. Coordinates datum WGS84 LAT 3.0986, LON -67.7889. Altitude 110 m. Colombia. (Appendix 3.1) <b>Forests of <i>Caraipa longipedicellata</i> and <i>Micrandra sprucei</i></b> Cover area: 69,917.91 km<sup>2</sup> (Figs. 3.5 and 3.6)</p>	<p>The forests of <i>Caraipa longipedicellata</i> and <i>Micrandra sprucei</i> exhibit medium statures and densities. These are composed of trees with a DBH average greater than 10 cm. In some areas there are some emergent trees of up to 35 m. The highest heights were recorded to <i>Parahancornia negroensis</i> (35 m), <i>P. surrogata</i> (28 m), <i>Discophora guianensis</i> (26.5 m), <i>Caraipa llanorum</i></p>	<p>This association is defined on the basis of 17 samples that included 222 species, 145 genera and 60 families. This syntaxon is named with the elective species <i>Caraipa longipedicellata</i> and the dominant species <i>Micrandra sprucei</i>; <i>Humiria crassifolia</i> and <i>Cyrilla racemiflora</i> were recorded as exclusive species. <i>Micrandra sprucei</i>, <i>Compsonera debilis</i>, and <i>Caraipa longipedicellata</i> are</p>	<p>This association includes caatingas on white sands, “terra firme” forests, and seasonally flooded forests in black water with or without palms dominance over poorly drained sandy soils. A substrate that tolerate considerable differences in drainage classes, probably by the root mat develops in the litter layer. The forest of the association Caraipo longipedicellatae Micrandretum</p>

(continued)

Phytosociological classification	Physiognomy and composition	Syntaxonomy	Ecology and distribution
	<p>(21.5 m), and <i>Micrandra sprucei</i> (20 m). Some of the species that present a high physiognomic expression in this syntaxon are: <i>Micrandra sprucei</i> (18.7%), <i>Aspidosperma verruculosum</i> (8.9%), <i>Henriquezia nitida</i> (6.6%), <i>Caraipa longipedicellata</i> (5.4%), <i>Parahancornia surrogata</i> (3.2%), <i>Pradosia schomburgkiana</i> (1.8%), <i>Chrysophyllum amazonicum</i> (1.8%), and <i>Doliocarpus novogranatensis</i> (1.5%).</p>	<p>among the elective species</p>	<p><i>sprucei</i> was described based on 17 samples located in Colombia (e.g., Atabapo and Guasacavi rivers, near of Inirida, Mirití, Mitú towns, and the “Serranía de Naquén”) and Venezuela (e.g., along San Carlos de Río Negro-Solano road). Detailed information about these localities is found in Appendix 3.2.</p>
<p><b>2. Oenocarpodo batauae - Eperuion leucanthae all. Nov.</b> (Figs. 3.5 and 3.6)  <b>Typus:</b> <i>Micrandro elatae</i> - <i>Micrandretum sprucei</i> (this study; Appendix 3.1)  <b>Lowlands forests of the Oenocarpus bataua and Eperua leucantha</b>  Cover area: 38,073.06 km<sup>2</sup> (Figs. 3.5 and 3.6)</p>	<p>The forest communities of this alliance are forests of medium to high stature, reaching to 40 m height. These are characterized by the presence of trees of Apocynaceae, Arecaceae, Lauraceae, Fabaceae, Malvaceae, Moraceae, and Myristicaceae.</p>	<p>This alliance is defined on the basis of 61 samples that included 852 species, 323 genera in 87 families. <i>Oenocarpus bataua</i> (as the elective species) and <i>Eperua leucantha</i> (as the dominant) were chosen to coined the name of this syntaxon. The exclusive species are: <i>Erisma micranthum</i>, <i>Retiniphyllum concolor</i>, and <i>Hevea rigidifolia</i>. <i>Eperua leucantha</i>, <i>Clathrotropis glaucophylla</i>, <i>Macrolobium limbatum</i>, and</p>	<p>This alliance contains low and high Caatingas on white sands, “terra firme” forests and seasonally flooded forests in black water with or without palms dominance. The <i>Oenocarpus bataua</i>—<i>Eperua leucantha</i> alliance is located on elevated positions in depressions, very poorly drained sandy Spodosols on plains, with similar characteristics to the Spodosols located in the San Carlos de Rio Negro (Herrera 1979, 1985; Schargel and Marvez 2009).</p>

(continued)

Phytosociological classification	Physiognomy and composition	Syntaxonomy	Ecology and distribution
		<p><i>Micrandra sprucei</i> were registered as elective species. This alliance comprises two new upper Rio Negro typical associations such as the Amazonian caatinga, and the “Yévaro” forests (<i>Micrandrum elatum</i> - <i>Micrandrum spruceae</i> and <i>Oenocarpo batauae</i> <i>Eperuetum purpureae</i>).</p>	
<p><b>2.1. <i>Micrandro elatae</i> - <i>Micrandretum sprucei</i> assoc. nov.</b> (Figs. 3.5 and 3.6)  <b>Typus:</b> Plot CC_154, TWINSPAN ID 93. Coordinates datum WGS84 LAT 3.0833, LON -67.7833. Altitude 108 m. Colombia. (Appendix 1)  <b>Forests of <i>Micrandra elata</i> and <i>Micrandra sprucei</i></b>  Cover area: 21,835.99 km<sup>2</sup> (Figs. 3.5 and 3.6)</p>	<p>The forests of <i>Micrandra elata</i> and <i>M. sprucei</i> are of medium stature (28 and 25 m) and high density composed of trees with a DBH greater than 10 cm. <i>Calophyllum brasiliense</i> (30 m), <i>Hevea benthamiana</i> (30 m), <i>H. guianensis</i> (30 m), and <i>Sloanea floribunda</i> (30 m) recorded the highest heights in this formation. The species with the biggest dominance expression (relativized units) are: <i>Micrandra sprucei</i> (25.4%), <i>M. elata</i> (6.9%), <i>Caraipa longipedicellata</i> (4.1%), <i>Hevea benthamiana</i> (3.1%), <i>Eperua leucantha</i> (3.0%), <i>E. obtusata</i> (2.8%), <i>Hevea pauciflora</i> (2.7%), <i>Micrandra sprucei</i></p>	<p>This association is defined on the basis of 18 samples that included 255 species, 136 genera in 52 families. This syntaxon was named used <i>Micrandra elata</i> (the elective species) and <i>Micrandra sprucei</i> as the dominant. <i>Chrysophyllum bombycinum</i> and <i>Hevea benthamiana</i> were recorded as exclusive species. Among the elective species are: <i>Micrandra sprucei</i>, <i>M. elata</i>, <i>Macrolobium limbatum</i>, <i>Ficus guianensis</i>, <i>Caraipa longipedicellata</i>, and <i>Mucoa duckei</i>.</p>	<p>This kind of vegetation is composed of low and high caatingas on white sands, “terra firme” forests and seasonally flooded forests over black and white water with or without palms dominance. The forest of the association <i>Micrandrum elatum</i>-<i>Micrandrum spruceanum</i> can be found on areas in upper Rio Negro over poorly drained sandy soils. This community tolerates considerable differences in drainage classes. This association was determined based on 18 samples located in Colombia (e.g., near Inírida, Almidón/La Ceiba area, Chorro Bocón at Inírida river, Campo Alegre at Cuari river) and Venezuela (e.g., La</p>

(continued)

Phytosociological classification	Physiognomy and composition	Syntaxonomy	Ecology and distribution
	(2.7%), and <i>Macrolobium limbatum</i> (2.1%).		Esmeralda, upper Orinoco river, along Maroa-Yavita road). Detailed information on these localities is found in Appendix 3.2.
<p><b>2.2. Oenocarpodo batauae - Eperuetum purpureae assoc. nov.</b> (Figs. 3.5 and 3.6)</p> <p><b>Typus:</b> Plot CC_115, TWINSPAN ID 54. Coordinates datum WGS84 LAT 3.3822, LON -67.3386. Altitude 101 m. Colombia. (Appendix 3.1)</p> <p><b>Forests of <i>Oenocarpus bataua</i> and <i>Eperua purpurea</i></b></p> <p>Cover area: 16,237.07 km<sup>2</sup> (Figs. 3.5 and 3.6)</p>	<p>The forests of <i>Oenocarpus bataua</i> and <i>Eperua purpurea</i> are medium to tall stature and high density. These are composed of trees with a DBH average diameter greater than 10 cm. The canopy of the forest is composed of trees of between 20 and 40 m with a dense cover and great number of palms. In this association, the following species registered the highest heights: <i>Eperua purpurea</i> (46 m), <i>Erismia japura</i> (40 m), <i>Eschweilera tessmannii</i> (40 m), <i>Monopteryx uauacu</i> (40 m), <i>Pseudoxandra leiophylla</i> (37 m), <i>Vochysia grandis</i> (37 m), and <i>Oenocarpus bataua</i> (25 m). The species with the most physiognomic expression are <i>Eperua purpurea</i> (10.3%), <i>Micrandra sprucei</i> (6.3%), <i>Swartzia parvifolia</i> (4.4%), <i>Eperua leucantha</i> (3.6%), <i>Leopoldinia piassaba</i> (3.2%), <i>Monopteryx</i></p>	<p>This association is defined on the basis of 44 samples that included 761 species, 297 genera in 82 families. The elective species <i>Oenocarpus bataua</i> and the dominant species <i>Eperua purpurea</i>, were chosen to coined the name of this syntaxon. Within the elective species are: <i>Brosimum utile</i>, <i>Minuartia guianensis</i>, <i>Virola elongata</i>, <i>Pseudolmedia laevigata</i>, <i>Clathrotropis glaucophylla</i>, <i>Iryanthera crassifolia</i>, <i>Erismia splendens</i>, <i>Ocotea aciphylla</i>, <i>Roucheria Columbiana</i>, and <i>Leopoldinia piassaba</i>.</p>	<p>This association harbors the low and high caatingas on white sands, “terra firme” forests and seasonally flooded forests over mixed water with palms dominance. The forest of the association Oenocarpodo batauae Eperuetum purpureae can be found on areas in the upper Río Negro over poorly drained sandy soils. This type of vegetation was described based on samples located in Colombia (e.g., along Atabapo river, Nabuquén at Inírida river, upper Isana river) and Venezuela (Casiquiare channel, near San Carlos de Río Negro). Detailed information on these localities is found in Appendices 3.2, 3.3 and 3.4.</p>

(continued)

Phytosociological classification	Physiognomy and composition	Syntaxonomy	Ecology and distribution
	<p><i>uaucu</i> (3.1%), <i>Erismia japura</i> (3.0%), <i>Oenocarpus bataua</i> (2.4%), and <i>Aldina kunhardtiana</i> (2.0%).</p>		
<p><b>3. Monopterygo uaucus - Eperuion purpureae all. Nov.</b> (Figs. 3.5 and 3.6)  <b>Typus:</b> Aldino heterophyllae Eperuetum leucanthae (this study; Appendix 3.1)  <b>Lowlands forests of Monopteryx uaucu and Eperua purpurea</b>            Cover area: 120,675.10 km<sup>2</sup> (Figs. 3.5 and 3.6)</p>	<p>The communities of this alliance are composed of forests of medium to high stature (up to 30–45 m tall), characterized by the presence of emergent trees. According to the abundance, frequency and basal area values, the most important families are Apocynaceae, Arecaceae, Lauraceae, Fabaceae, Malvaceae, Moraceae, and Myristicaceae.</p>	<p>This alliance is defined on the basis of 27 samples, that included 919 species, corresponding to 314 genera in 78 families. <i>Monopteryx uaucu</i> as the elective species, and <i>Eperua purpurea</i> as the dominant were chosen to coined the name of this syntaxon. Within the elective species are: <i>Eperua leucantha</i>, <i>Hevea guianensis</i>, <i>Micrandra sprucei</i>, <i>M. spruceana</i>, <i>Brosimum guianense</i>, <i>Erismia japura</i>, <i>Eschweilera pedicellata</i>, <i>Monopteryx uaucu</i>, <i>Iryanthera laevis</i>, <i>Zygia claviflora</i>, <i>Micropholis guyanensis</i>, and <i>Abarema jupunba</i>. Other species can be shown in Appendix 3.1.</p>	<p>This kind of vegetation assembles low and high Caatingas on white sands and “terra firme” forests. The <i>Monopteryx uaucu</i>—<i>Eperua purpurea</i> alliance hold forests with four vertical layers. This forest was located on a poorly drained sandy Entisol in depression, on a moderately drained Ultisol on a hill, and a poorly drained Inceptisol on a foot-slope of a low hill. Both the Ultisol and the Inceptisol have sandy loam, and sandy clay loam textures below the sandy surface horizon (Schargel and Marvez 2009).</p>
<p><b>3.1. Aldino heterophyllae Eperuetum leucanthae assoc. nov.</b> (Figs. 3.5 and 3.6)  <b>Typus:</b> Plot S_6, TWINSPAN ID 218. Coordinates datum WGS84 LAT – 0.1007, LON –66.8804. Brazil.</p>	<p>The forests of <i>Aldina heterophylla</i> and <i>Eperua leucantha</i> are of medium stature and high density. These are composed of trees with a DBH average greater than 10 cm. In some areas there are some emergent trees of up to 46 m; the highest</p>	<p>This association is defined on the basis of 19 samples that included 716 species, 262 genera in 70 families. This syntaxon is named used <i>Aldina heterophylla</i> (the exclusive species) and <i>Eperua leucantha</i> (the</p>	<p>This kind of vegetation harbors low caatingas on white sands and “terra firme” forests. The forest of the association Aldino heterophyllae - Eperuetum leucanthae can be found on areas in the upper Rio Negro</p>

(continued)

Phytosociological classification	Physiognomy and composition	Syntaxonomy	Ecology and distribution
<p>(Appendix 3.1)  <b>Forests of <i>Aldina heterophylla</i> and <i>Eperua leucantha</i></b>            Cover area: 9358.28 km<sup>2</sup>            (Figs. 3.5 and 3.6)</p>	<p>heights were recorded to <i>Scleronema micranthum</i> (46.4 m), <i>Brosimum utile</i> (35 m), <i>Erismalaurifolium</i> (35 m), <i>protium alvarezianum</i> (35 m), <i>Swartzia tomentifera</i> (34.4 m), <i>Eperua purpurea</i> (30 m), <i>E. leucantha</i> (30 m), and <i>Aldina heterophylla</i> (28.1 m). Several species presented higher physiognomic expression in this syntaxon (relativized units) such as: <i>Eperua leucantha</i> (13.1%), <i>E. purpurea</i> (9.4%), <i>Monopteryx uauacu</i> (7.3%), <i>Aldina heterophylla</i> (4.7%), <i>Clathrotropis macrocarpa</i> (3.6%), <i>Micrandra spruceana</i> (3.0%), <i>Scleronema micranthum</i> (2.2%), <i>Swartzia polyphylla</i> (1.6%), and <i>Swartzia tomentifera</i> (1.3%).</p>	<p>dominant species). In this vegetation pattern, <i>Chamaecrista adiantifolia</i>, <i>Sloanea obtusifolia</i>, <i>Himatanthus obovatus</i>, <i>Pradosia schomburkiana</i>, and <i>Vitex sprucei</i> were identified as exclusive species. Within the elective species are: <i>Swartzia tomentifera</i>, <i>Trattinnickia glaziovii</i>, <i>Ocotea rhynchophylla</i>, <i>Sandwithia guyanensis</i>, <i>Brosimum rubescens</i>, <i>Pouteria cuspidata</i>, <i>Bocageopsis pleiosperma</i>, <i>Virola calophylla</i>, <i>Erismacalcaratum</i>, <i>Micrandra spruceana</i>, <i>Hevea guianensis</i>, <i>Chimarrhis duckeana</i>, <i>Couma guianensis</i>, and <i>Cyrillopsis paraensis</i>.</p>	<p>growing on poorly drained sandy soils; it tolerates considerable differences in drainage class. This association was determined based on 19 samples located in Brazil (e.g., São Gabriel da Cachoeira, middle Içana river, Pico da Neblina National Park), Colombia (e.g., Punta de Tigre, upper Isana river) and Venezuela (i.g. Mawarinuma river at the base of “Sierra de la Neblina”) as well. Detailed information on these localities is found in Appendix 3.2.</p>
<p><b>3.2. Eperuo purpureae - Erismetum japurae assoc. nov.</b> (Figs. 3.5 and 3.6)  <b>Typus:</b> Plot P6, TWINSPAN ID 191. Coordinates datum WGS84 LAT 2.2071, LON -68.2781. Colombia. (Appendix 3.1)  <b>Forests of <i>Eperua purpurea</i> and <i>Erismajapura</i></b></p>	<p>The forests of <i>Eperua purpurea</i> and <i>Erismajapura</i> have a medium to tall stature, high density and great number of palms. The trees have a DBH average greater than 10 cm. In this association the following species have the highest heights: <i>Pouteria ucuqui</i> (45 m), <i>Eschweilera collina</i></p>	<p>This association is defined on the basis of 8 samples, that included 332 species, 169 genera in 55 families. <i>Eperua purpurea</i> (as elective species) and <i>Erismajapura</i> (as the dominant) were chosen to name this taxon. Within the elective species are: <i>Protium crassipetalum</i>,</p>	<p>This association assembles the “terra firme” forests and the tall catings. The forest of the association Eperuo purpureae Erismetum japurae can be found on areas in the upper Rio Negro growing on poorly drained sandy and clay soils; it tolerates considerable differences in</p>

(continued)



Phytosociological classification	Physiognomy and composition	Syntaxonomy	Ecology and distribution
Cover area: 111.316.82 km <sup>2</sup> (Figs. 3.5 and 3.6)	(44 m), <i>Brosimum utile</i> (40 m), <i>Micropholis brochidodroma</i> (40 m), <i>Swartzia floribunda</i> (40 m), <i>Allantoma lineata</i> (35 m), <i>Ecclinusa ramiflora</i> (35 m), and <i>Goupia glabra</i> (35 m). The species with most physiognomic expression (relativized units) are: <i>Erisma japura</i> (18.3%), <i>Eperua purpurea</i> (13.9%), <i>Goupia glabra</i> (3.3%), <i>Heterostemon conjugatus</i> (2.9%), <i>Ecclinusa ramiflora</i> (2.9%), <i>Swartzia pinnata</i> (2.5%), <i>Sandwithia heterocalyx</i> (2.5%), <i>Pseudosenefeldera inclinata</i> (2.1%), <i>Hevea guianensis</i> (2.1%), and <i>Eschweilera pedicellata</i> (2.0%).	<i>Aldina kunhardtiana</i> , <i>Heterostemon conjugatus</i> , <i>Swartzia pinnata</i> , <i>Clathrotropis glaucophylla</i> , <i>Oenocarpus bacaba</i> , <i>Ecclinusa bullata</i> , <i>Helianthostylis steyermarkii</i> , and <i>Pouteria guianensis</i> . Other species can be shown in the Appendix 3.1.	drainage classes. This kind of vegetation was described based on eight (8) samples located in Colombia (e.g., mouth of Naquén river, Puerto Colombia - Guainía) and Venezuela (e.g., Maroa-Yavita road). Detailed information on these localities is found in Appendix 3.2.
<b>ORDER II</b> <b>1. Goupia glabrae - Minquartiion guianensis all. Nov.</b> (Figs. 3.5 and 3.6) <b>Typus:</b> Eschweilero parviflorae - Mouririetum grandiflorae (this study; Appendix 1) <b>Lowlands forests of the Eschweilera parviflora and Mouriri grandiflora</b> Cover area: 333,950.47 km <sup>2</sup> (Figs. 3.5 and 3.6)	The forest communities of this alliance are medium to high in stature, up to 45 m tall. These communities are characterized by the presence of trees of Arecaceae, Burseraceae, Lauraceae, Lecythidaceae, Fabaceae, Melastomataceae, Moraceae, Myristicaceae, Olacaceae,	This alliance is defined on the basis of 95 samples that included 1983 species, 532 genera in 120 families. This syntaxon is named with the exclusive species <i>Goupia glabra</i> and the dominant species <i>Minquartia guianensis</i> . In this vegetation alliance others exclusive species were: <i>Abuta grandifolia</i> ,	This alliance is compound by “terra firme” forests, forests with palm dominance and seasonally flooded forests in white and clear waters with or without palm dominance. The <i>Eschweileia parviflora</i> — <i>Mouriri grandiflora</i> order is located on in the transition between alluvial plains and the hills (“lomeríos”)

(continued)

Phytosociological classification	Physiognomy and composition	Syntaxonomy	Ecology and distribution
	Rubiaceae, Sapindaceae, and Sapotaceae.	<p><i>Cynometra marginata</i>, <i>Mabea nitida</i>, <i>Clarisia racemosa</i>, <i>Oenocarpus minor</i>, and <i>Richeria grandis</i>. The elective species are: <i>Dendrobangia boliviana</i>, <i>Siparuna guianensis</i>, <i>Mouriri grandiflora</i>, <i>Virola elongata</i>, <i>Heterostemon mimosoides</i>, <i>Trichilia micrantha</i>, and <i>Xylopia nervosa</i>. This alliance includes two associations: An undefined named compound by <i>Attalea Maripa</i> and <i>Brosimum utile</i>, and the Eschweilero parviflorae - Mouririetum grandiflorae.</p>	over Ultisol and poorly drained Entisol.
<p><b>1.1 Attalea Maripa - Brosimum utile</b> (Figs. 3.5 and 3.6). Representative plot no. P2, TWINSPAN ID 187. Coordinates datum WGS84 LAT 1.7449, LON -69.7660. Altitude 193 m. Colombia, Venezuela and Brazil (Appendix 3.1)  <b>Forests of Attalea Maripa and Brosimum utile</b>  Cover area: 267,160.37 km<sup>2</sup> (Figs. 3.5 and 3.6)</p>	<p>The forests of <i>Attalea Maripa</i> and <i>Mespilodaphe cymbarum</i> are communities of medium to high stature and density, mainly composed by trees with a DBH average greater than 15 cm. This analysis was outline such as an undefined association. The canopy of the forest is composed of trees with heights between 20 and 40 m. <i>Brosimum utile</i>, <i>Euterpe precatória</i>, <i>Matayba elegans</i>, <i>Eschweilera parviflora</i>, and</p>	<p>This kind of vegetation was defined on the basis of 68 samples, that included 1905 species, 516 genera in 117 families. This group of undefined associations registered <i>Attalea Maripa</i> as the elective species, and <i>Brosimum utile</i> as the dominant. As exclusive species were registered: <i>Brosimum utile</i>, <i>Zygia cataractae</i>, <i>Maprounea guianensis</i>, <i>Mouriri acutiflora</i>, <i>Garcinia madruno</i>, <i>Piper arboreum</i>, <i>protium</i></p>	<p>This vegetation is represented by “terra firme” forests, flooded forests with palm dominance, and seasonally flooded forests with or without palm dominance. The forest of <i>Attalea Maripa</i> and <i>Brosimum utile</i> assembles 68 samples located in Brazil (e.g., near Manaus city, Uatuma river, Pico da Neblina National Park), Colombia (i.g. Cumaribo-Vichada, Mitú, middle Caquetá river, “El Retiro” (“La</p>

(continued)

Phytosociological classification	Physiognomy and composition	Syntaxonomy	Ecology and distribution
	<p><i>Virola elongata</i> being the most abundant species. Some of the highest heights were recorded in <i>Minquartia guianensis</i> (58 m), <i>Aldina latifolia</i> (40 m), <i>Brosimum utile</i> (40 m), <i>Caryocar glabrum</i> (40 m), <i>Eschweilera parviflora</i> (40 m), <i>Mespilodaphe cymbarum</i> (40 m), <i>Vochysia assua</i> (40 m), <i>V. grandis</i> (40 m), and <i>Attalea Maripa</i> (20 m). To this syntaxon the species with the biggest dominance expression are <i>Eschweilera parviflora</i> (3.0%), <i>Attalea Maripa</i> (1.9%), <i>Goupia glabra</i> (1.7%), <i>Allantoma lineata</i> (1.6%), <i>Swartzia tomentifera</i> (1.5%), <i>Euterpe precatorea</i> (1.4%), <i>Minquartia guianensis</i> (1.3%), <i>Chaetocarpus schomburgkianus</i> (1.3%), and <i>Brosimum utile</i> (1.2%).</p>	<p><i>laxiflorum</i>, <i>Zygia inaequalis</i>, and <i>Homalolepis cedron</i>. Other exclusive species can be shown in the Appendix 3.1. Among the elective species are: <i>Gustavia augusta</i>, <i>Myrcia fallax</i>, <i>protium stevensonii</i>, <i>Inga acrocephala</i>, <i>Macrosamanea amplissima</i>, <i>Maquira calophylla</i>, <i>Duguetia quitarensis</i>, and <i>Gustavia acuminata</i>. Other species can be shown in Appendix 1.</p>	<p>Lindosa”), Infrida river, near mouth of “caño Bocón,” Guaviare river, upper Isana river) and Venezuela (e.g., along Casiquiare river, middle and lower Ventuari river). Detailed information on these localities is found in Appendix 3.2.</p>
<p><b>1.2 Eschweilero parviflorae - Mouririetum grandiflorae assoc. nov.</b> (Figs. 3.5 and 3.6). <b>Typus:</b> Plot CC_173, TWINSPAN ID 112. Coordinates datum WGS84 LAT 3.7917, LON -67.8197. Altitude 108 m.</p>	<p>The forests of <i>Eschweilera parviflora</i> and <i>Erisma laurifolium</i> are communities of medium to high stature and density, mainly composed of trees with a DBH average greater than 15 cm. <i>Protium divaricatum</i>,</p>	<p>This association is defined on the basis of 28 samples that included 373 species, 176 genera and 60 families. This syntaxon is named with the exclusive species <i>Eschweilera parviflora</i> and the dominant species <i>Mouriri grandiflora</i>.</p>	<p>This association is compound by “terra firme” forests and seasonally flooded forests with or without palms dominance. The forest of the association Eschweilero parviflorae Mouririetum</p>

(continued)

Phytosociological classification	Physiognomy and composition	Syntaxonomy	Ecology and distribution
<p>Colombia. (Appendix 3.1). <b>Forests of <i>Eschweilera parviflora</i> and <i>Erismia laurifolium</i></b> Cover area: 66,790.09 km<sup>2</sup> (Figs. 3.5 and 3.6)</p>	<p><i>Eschweilera parviflora</i>, <i>Brosimum utile</i>, <i>Pouteria baehniiana</i>, <i>Mouriri grandiflora</i>, <i>Clathrotropis brachypetala</i>, and <i>Virola elongata</i> being the most abundant species. In this association following species registered the highest heights <i>Clathrotropis glaucophylla</i> (35 m), <i>Eperua purpurea</i> (35 m), <i>Erismia laurifolium</i> (35 m) <i>Goupia glabra</i> (35 m), <i>Vochysia splendens</i> (33 m), <i>Caryocar glabrum</i> (32 m), <i>Qualea ingens</i> (32 m), <i>Eschweilera parviflora</i> (30 m), and <i>Mouriri grandiflora</i> (30 m). Some of the species that present a high physiognomic expression in this syntaxon (relativized units) are: <i>Eperua purpurea</i> (5.2%), <i>Caryocar glabrum</i> (4.2%), <i>Mouriri nigra</i> (3.4%), <i>Goupia glabra</i> (2.9%), <i>Leopoldinia piassaba</i> (2.7%), <i>Leptobalanus apetalus</i> (2.6%), <i>Eschweilera parviflora</i> (2.6%), <i>protium divaricatum</i> (2.4%), <i>Virola elongata</i> (2.2%), and <i>Mouriri grandiflora</i> (1.8%).</p>	<p>In this vegetation pattern <i>Pouteria baehniiana</i> was registered as exclusive species. Within the elective species are: <i>Clathrotropis brachypetala</i>, <i>Mouriri grandiflora</i>, <i>Eschweilera parviflora</i>, <i>Virola elongata</i>, <i>protium divaricatum</i>, <i>Erismia laurifolium</i>, and <i>Aptandra tubicina</i>. Other species can be shown in the Appendix 1.</p>	<p><i>grandiflorae</i> was determined based on 28 samples located in Colombia (e.g., Guaviare river at mouth Inírida river, near Inírida, Nukak reservation). Detailed information on these localities is found in Appendix 3.2.</p>

(continued)

Phytosociological classification	Physiognomy and composition	Syntaxonomy	Ecology and distribution
<p><b>2. <i>Astrocarium chambirae</i> - <i>Socratea</i> <i>exorrhizae</i> all. Nov.</b> (Figs. 3.5 and 3.6). Representative plot. GB_8, TWINSPAN ID 172. Coordinates datum WGS84 LAT 2.4232, LON -72.3699. Colombia. (Appendix 3.1)</p> <p><b>Lowlands forests of the <i>Astrocarium chambira</i> and <i>Socratea exorrhiza</i></b> without indefinite associations</p> <p>Cover area: 6958.74 km<sup>2</sup> (Figs. 3.5 and 3.6)</p>	<p>The forest communities of this alliance are medium to high stature, up to 25–30 m tall, characterized by the high presence of palms and trees of Burseraceae, Lauraceae, Lecythidaceae, Fabaceae, Melastomataceae, Moraceae, Myristicaceae, Rubiaceae, Sapindaceae, and Sapotaceae. Some of the highest heights were recorded in <i>Vochysia splendens</i> (26.5 m), <i>Virola marleneae</i> (22.4 m), <i>Clathrotropis macrocarpa</i> (21.4 m), <i>Socratea exorrhiza</i> (13.9 m), and <i>Astrocarium chambira</i> (9.3 m). The species with most physiognomic expression are <i>Erythroxylum macrophyllum</i> (6.8%), <i>Psychotria remota</i> (6.0%), <i>Palicourea raveniana</i> (6.0%), <i>Sorocea muriculata</i> (4.8%), <i>Theobroma subincanum</i> (2.5%), <i>Socratea exorrhiza</i> (2.3%), <i>Astrocarium chambira</i> (2.1%), <i>Miconia punctata</i> (2.0%), <i>Pseudolmedia laevis</i> (1.8%), and <i>Clathrotropis macrocarpa</i> (1.8%).</p>	<p>This alliance is defined on the basis of 16 samples that included 102 species, 79 genera and 39 families.</p> <p><i>Astrocarium chambira</i> (as the elective species) and <i>Socratea exorrhiza</i> (as the dominant) were chosen to name this syntaxon. As exclusive species were registered: <i>Inga tessmannii</i>, <i>Psychotria remota</i> and <i>Jacaratia spinosa</i>. The elective species are: <i>Calycophyllum megistocaulum</i>, <i>Astrocarium chambira</i>, <i>Pseudolmedia laevis</i>, <i>Euterpe precatatoria</i>, and <i>Socratea exorrhiza</i>.</p>	<p>This alliance is composed of “terra firme” forests with palms dominance, located in the transitions between the alluvial plains and the terraces over Entisol and Ultisol soils. This kind of vegetation was described based on 16 samples located in Colombia (e.g., San José del Guaviare. Nabuquén creek, Puinawai natural reserve). Detailed information on these localities is found in Appendix 3.2.</p>

## Appendix 3.2 Botanical Explorations in the Rio Negro Basin: A Review

### Introduction

The record of human occupation in the upper Rio Negro basin, based on ceramic shards, dates back to between 3750 (Sanford et al. 1985) and 3570 (Neves 1998) years B.P. Other data, based on soil charcoal samples, dates human occupation to between 640 and 250 years B.P. for the top 20 cm soil layers, and between 6260 and 530 years B.P. for the lower 20–90 cm soil layers (Saldarriaga and West 1986). It is interesting that the dates reported by these authors correspond with dry episodes in the Amazon basin and surrounding areas (van der Hammen 1972; Bush and McMichael 2016). The authors suggest that dry and humid periods alternated from 6000 to 400 B.P. The age estimated from charcoal and shards confirms that the region has been subjected to fires during extreme dry periods, and indicates periods of human disturbance (e.g., shifting cultivation) for the last 3750 years.

It is well known that the region comprising the upper Río Negro and Orinoco basins was traveled, explored, and inhabited for several millennia by ancestral groups such as the Makú-Puinave, the Arawak, and the Tucano (Zucchi 2006). Migrations or movements of these ancestral groups came from the Central Amazon region to the Rio Negro basin approximately 4500–3500 B.P. (Meggers 1979), perhaps escaping the devastating droughts or Mega-Niño events that took place in Central Amazonia during this time (Meggers 1994; van der Hammen 2006; Olivares et al. 2015). No doubt, the Río Negro basin was relatively well explored by the earliest inhabitants of the region, who were able to classify vegetation types and its most important plant species before Europeans arrived (Abraão et al. 2009). Also, Pre-Columbian populations categorized Amazonian rivers by the color of their water, and they knew that water color was related with fish richness or soil fertility (Junk et al. 2011).

### The Journeys

#### Fifteenth to Nineteenth Centuries

The first Iberian journeys down the Amazon river, from the Andes to the Atlantic Ocean, were undertaken by two groups of Spaniards, one commanded by Francisco de Orellana (1541–1542) and later by Pedro de Ursúa (1560–1561) accompanied by, among others, the infamous Lope de Aguirre. Chronicles of these travels, written by Fray G. de Carvajal in the case of Orellana's saga (Carvajal 1848), and by several witnesses and second-hand accounts in the case of Ursúa and Aguirre's (e.g., Vazquez 1881), spoke of large areas of forest along the Amazon river and numerous, well-populated native villages. During Orellana's journey a mighty black water river was sighted flowing from "El Poniente," and was called "Río Negro" (Carvajal 1848).

After the two Iberian voyages down the Amazon river, the interest in knowing the Amazon basin in greater detail took a remarkable impact at the cartographic level, especially by the French, Portuguese, and Jesuits and Franciscans priests (Cintra 2012a). The first accurate map of the Amazon River was drawn by French cartographers, including one by Count of Blaise François Pagan (1655) and several by Nicolas Sanson (1656, 1657, 1680, 1698, and 1699), drawn and engraved during the golden age of French cartography (Cortêsão 1965). Pagan's map, *Magni Amazoni Fluvii* (Pagan 1655), is considered the most remarkable of all the charts, not just of the Amazonas river, but of the whole of Amazon basin (Cortêsão 1965; Cintra 2011). It was based mainly on the account of Father Cristóbal de Acuña, who descended the river with Pedro Teixeira in 1639, and determined some latitudes and estimated distance in leagues between consecutive locations. This chart was the first established canvas of the meridians and parallels that scientifically situated the Amazon and took full advantage of the geographic data supplied by the discoverers. Nicolas Sanson (the royal cartographer of France) published his first Amazonas map in 1656. He improved his first map with several versions published in 1657, 1680, 1698, and 1699. The maps of the Amazon River traced by Sanson present precise geographic coordinates considering its time, shows a well-determined prime meridian, and also employs a creative methodology to deduce longitudes from latitudes and distances that had been covered (Cintra and de Oliveira 2014). After Pagan's and Sanson's maps, the Jesuit priest Samuel Fritz drew a map of the Amazon in 1691 and later had one engraved in 1707. Much simplified versions of Fritz' map were first published in 1717 (engraved in French), 1726 (in German), 1755 (in Spanish), and in 1819 (a second version in French), accompanying an extract of his description of the "Maragnon." Of the map engraved in 1707, apparently, only a few copies circulated are fewer are extant; the other four maps were published in "*Lettres Édifiantes et Curieuses*" (in Fritz 1717 and 1819, for the first and second versions in French, respectively), in *Der Neüer Welt-Bott* (Fritz 1726, in German), and "*Cartas edificantes, y Curiosas*" (Fritz 1755), journals then little read outside religious circles. It is evident that the scientific cartography of Amazonas begins with the map of Count of Pagan (for a review see: Cintra 2011, 2012b; Cintra and Freitas 2011; Cintra and Furtado 2011; Cintra and de Oliveira 2014).

Some years later, researchers started collecting plants and studying the vegetation of the Amazon river. Charles de La Condamine, who navigated this river in 1743, wrote the first biological report (de La Condamine 1745). European scientists considered his expedition the beginning of the great era of Amazonian travel (ter Steege et al. 2016). La Condamine remarked on numerous plant products such as curare, the arrow poison, derived from *Strychnos* spp. (Loganiaceae); he also documented for the first time the quinine tree, *Cinchona officinalis* L. (Rubiaceae) and the rubber tree, *Hevea* spp. (Euphorbiaceae). However, the first known large collection of Amazon plants was made by Alexandre Rodrigues Ferreira (1756–1815) during his voyage of 1783–1792 (Wurdack 1971). He explored the Amazon river and its main tributaries, including the Rio Negro and Rio Branco between 1785 and 1786, where his itinerary notably included the Isana and Vaupés rivers (Pereira da Silva 2008). His group collected and drew numerous plants and



**Fig. 3.12** *Asteranthos brasiliensis* Desf. Lecythidaceae. Predominantly occupies a geographical range from Eastern Colombia and stretches to incorporate Southern Venezuela and Northern Brazil, with a specific concentration in the Upper Río Negro region. This species is classified as arboreal and grows best primarily in hydric or moisture-rich environments—image captured by H. ter Steege

animals during this expedition. *Asteranthos brasiliensis* Desf. (Scytopetalaceae), with showy yellow, fused petals, and an actinomorphic androecium, is an endemic genus of the Río Negro basin, and perhaps one of the most extraordinary plants they documented (see Fig. 3.12 on the text of Chap. 3).

Later, “caño” Pimichín and the rivers Guanía and upper reaches of the Río Negro were explored by the famous naturalists F. H. A. von Humboldt and A. J. A. Bonpland (in April 1800), gathering the first biological collections of that section of the Río Negro basin. They were followed by C. F. P. von Martius and J. B. von Spix (1819–1820), A. Plée (1821), L. Reidel (1828), J. B. Natterer (1830–1832), R. H. Schomburgk (1839; 1855), P. J. Ayres (1842–1844), A. R. Wallace (1850–1851), and R. Spruce (1850–1854), at a time when scientists in Europe were fascinated by the tremendous diversity of fishes, insects, mammals and plants being discovered, and before modern scientific research on ecology and evolutionary biology.

Richard Spruce (1817–1893) was remarkable among all personalities above mentioned. He was a pioneer botanical explorer of the north-west Amazon and the northern Andes in the middle of the last century. He collected ca 7000 botanical specimens and made numerous important botanical discoveries. This British botanist, who opened up the Río Negro region to science between 1850 and 1854, must be counted amongst the greatest naturalists ever to have engaged in collecting and studies anywhere in unexplored Neotropical territories (Schultes 1983). As a result of his meticulous observation and insatiable curiosity, a basis for our understanding of great areas of the Amazon was early and most firmly laid. Not only did Spruce



advance taxonomy and floristics, but he was also a notable bryologist and made many important observations in ethnology, ethnobotany, linguistics, and geology (Spruce 1908).

### Nineteenth to twentieth Centuries

The Portuguese and later Brazilians started an ambitious plan of exploration in the Rio Negro during the nineteenth century, shortly after the consolidation of Amazonas province in 1850. Several explorers visited the watersheds of main affluents (for a review see: Tenreiro-Aranha 1906). After this period, the exploration of the Rio Negro basin and its most important rivers continued with the work of, among others, G. Wallis (1863–1864), J. W. H. Traill (1874), J. Barbosa Rodrigues (1884–1885), P. H. W. Taubert (1896), E. H. G. Ule (1901–1902), É. Bommechaux (1903), G. A. E. Hübner (1903–1907, 1914), C. T. Koch-Grünberg (1903–1905), J. Huber (1904), H. Schmidt and L. Weiss (1907–1908), W. A. Ducke (1910–1932, 1933–1936, 1941–1942), J. G. Kuhlmann (1918), and D. E. Melin (1924). Also, it is important to point out that large sections of the Rio Negro and some of its tributaries, as well as the Casiquiare and the upper Orinoco, were extensively explored in the first quarter of the twentieth century by H. A. Rice and P. P. von Bauer. Their emphasis was geographical exploration; unfortunately, little biological material was collected, but important cartographical material resulted from their travels (Rice 1910, 1914, 1918, 1921, 1928; von Bauer 1919).

To this list of explorers, we should also mention the many plant collectors who worked on behalf of commercial horticultural houses in Europe and the United States who, although remaining largely anonymous, were behind the discovery and introduction of many plant species, particularly orchids, bromeliads, and other ornamental plants.

After the Treaty of Bogotá between Colombia and Brazil was signed in 1907, the Brazilian government started another program of exploration in the Rio Negro basin in 1927–1929, under the charge of Marshall Boaberges Lopes de Sousa. The botanist on this expedition, F. von Luetzelburg made significant botanical collections and annotations of types of vegetation of the upper Rio Negro (Lopes de Sousa 1955, 1959); he also visited the Casiquiare channel (Huber and Wurdack 1984). *Attalea luetzelburgii* (Burret) Wess. Boer (Arecaceae), a palm with subterranean stems represents a notable species among the numerous plants collected during his expedition.

The exploration of the Río Negro basin continued with the field work of G. H. H. Tate (1928–1929), E. G. Holt, W. Gehriger and E. R. Blake (1930–1931), B. A. Krukoff (1936), J. Cuatrecasas (1939), R. de Lemos Fróes (1941–1952), Ll. Williams (1942), J. A. Steyermark (1944; 1970), P. H. Allen (1943–1945), F. Cardona-Puig (1946), R. E. Schultes and F. López (1947–1948), J. Murça Pires (1947–1952), G. A. Black (1947–1950), B. Maguire et al. (1950–1966), J. J. Wurdack et al. (1951–1959), H. García-Barriga (1951), R. Romero-Castañeda (1952), A. Fernández-Pérez (1953), W. A. Rodrigues (1954–1968), V. Vareschi and K. Mägdefrau (1958–1962), L. A. Garay (1960), G. Eiten (1963), J. Ewel (1964), N. T. da Silva and U. Brazão (1966), E. Medina (1968), L. Ruiz-Terán and J. Bautista (1968), M. Fariñas et al. (1969), J. A.

Steyermark, C. Brewer-Carias and G. C. K. Dunsterville (1970), P. Maas (1971), B. Manara (1971), and G. T. Prance (1971). As shown here, numerous botanists, anthropologists, and ecologists have visited the Rio Negro basin to study the flora, vegetation, ethnography, and inhabitants in the last two hundred years. In the last five decades, fieldwork was carried out primarily by botanists, ecologists, and naturalists from the three countries that share the Rio Negro basin. Multiple studies have been done, too numerous to cite them all here.

Besides this remarkable amount of fieldwork, thousands of plant collections from Amazonia (including some from the Rio Negro) were products of the 8 expeditions to the Amazon basin conducted by B. A. Krukoff in 1923–1950 (Landrum 1986), and the 25 expeditions sponsored by the bi-national plant collecting program “Projeto Flora Amazônica” (Prance et al. 1984).

In addition, thousands of botanical specimens were collected in Brazil during the execution of the “Biological Dynamics of Forest Fragments Project (BDFFP)” set up near Manaus, and resulting from the field work conducted by “Instituto Amazônico de Investigaciones Científicas SINCHI” for nearly three decades in the Colombian Amazon. Likewise, in Venezuela, many botanical collections and publications resulted from: the interdisciplinary and multi-national project conducted by the “Instituto Nacional de Investigaciones Científicas (IVIC),” perhaps the most detailed study of Amazon caatinga and terra-firme forests ever conducted in the Upper Rio Negro (Medina 2000); the “Proyecto inventario de los recursos naturales de la región Guayana-PIRNRG-” (Zinck 1986); and the expeditions to “Serranía de la Neblina” (Brewer-Carías 1988). Finally, we must cite the collections generated by “Proyecto inventario de los recursos naturales de la región Guayana-PIRNRG-”, conducted by “CVG-Tecmin” (Corporación Venezolana de Guayana-Técnica Minera, C.A.) and other national and international institutions, a major effort to inventory the natural resources of the Venezuelan Guayana. As part of this project, a multidisciplinary team studied the upper Rio Negro and Orinoco basins in 1990–1992, which gathered large sets of plant specimens, ecological data (Aymard 2001), as well as soils and rocks samples. This field work resulted in the discovery of numerous new plant species and the gathering of data for a chorological report for this region (Aymard, [in preparation](#)).

---

## References

- Abraão MB, Shepard GH Jr, Nelson BW, Baniwa JC, Andrello G, Yu DW (2009) Baniwa vegetation classification in the white-sand Campinarana habitat of the Northwest Amazon. In: Johnson LM, Hunn E (eds) *Landscape ethnoecology: concepts of biotic and physical space*. Berghahn Books, New York and Oxford, pp 83–115
- Almeida A, Futada S, Klein T (2016) Protected areas and indigenous lands in the Amazon region are affected by more than 17,500 mining processes. <https://www.socioambiental.org/en/node/5044>
- Alvez-Valles CM, Balslev H, Garcia-Villacorta R, Carvalho FA, Menini Neto L (2018) Palm species richness, latitudinal gradients, sampling effort, and deforestation in the Amazon region. *Acta Bot Bras* 32(4):527–539

- Anderson AB (1981) White-sand vegetation of Brazilian Amazonia. *Biotropica* 13(3):199–210
- ANLA (2020) Autoridad Nacional de Licencias Ambientales, Minambiente, Bogotá, Colombia. <http://www.anla.gov.co/>. (Accessed 05 October 2020)
- Antonelli A, Zizka A, Antunes Carvalho F, Scharn R, Bacon CD, Silvestro C, Condamine FL (2018) Amazonia is the primary source of neotropical biodiversity. *Proc Nat Acad Sci (USA)* 115:6034–6039
- Arellano-Peña H, Rangel-Ch JO (2015) A solution to the high bias in estimates of carbon held in tropical forest above-ground biomass. arXiv:1508.03667v1 [q-bio.QM]
- Arellano-Peña H, Bernal-Gutiérrez G, Calero-Cayopare A, Castro-L F, Lozano A, Bernal-Linares DS, Méndez-R C, Aymard G (2019) The first botanical exploration to the upper Cuiarí (Cuyarí) and Isana rivers, upper Río Negro basin, Guainía department. *Colombia Harvard Papers in Botany* 24(2):83–102
- Aymard G (2001) Estructura y composición florística en bosques de tierra firme del alto Río Orinoco, sector La Esmeralda. Estado Amazonas Venezuela *Acta Botánica Venezuelica* 23(2):123–156
- Aymard, G (in preparation) “Proyecto Inventario de los Recursos Naturales de la Guayana Venezolana” (PIRNRG): Nine years of botanical expeditions (1985–1994). *Boletín de Historia de las Geociencias en Venezuela*
- Aymard G, Stergios B, Cuello N (1989) Informe sobre la vegetación del Interfluvio Orinoco-Atabapo, sector “Los Pozos” (03°10' N; 67°17' O). Departamento Atabapo. Territorio Federal Amazonas, Venezuela. *Boletín Técnico (Programa de R. N. R. UNELLEZ-Guanare, Venezuela)* 15:170–219
- Aymard G, Schargel R, Berry PE, Stergios B (2009) Estudio de los suelos y la vegetación (estructura, composición florística y diversidad) en bosques macrotérmicos no-inundables, estado Amazonas Venezuela (aprox. 01° 30' - 05° 55' N; 66° 00' - 67° 50' O). *Biollania ed esp* 9:6–251
- Aymard G, Arellano-Peña H, Minorta-C V, Castro-Lima F (2016) First report of Rhabdodendraceae for the vascular flora of Colombia and the upper Río Negro basin, with comments on phytogeography, habitats, and distribution of *Rhabdodendron amazonicum*. *Harv Pap Bot* 21:5–21
- Baker PA, Fritz SC, Battisti DS, Dick CW, Vargas OM, Asner GP, Martin RE, Wheatley A, Prates I (2020) Beyond refugia: new insights on quaternary climate variation and the evolution of biotic diversity in tropical South America. In: Rull V, Carnaval A (eds) *Neotropical diversification*. Springer, Berlin, pp 51–70
- Ballesteros MM (1995) Estructura, biomasa e inventario de nutrientes de la Caatinga baja Amazónica y su comparación con el bosque de tierra firme (Departamento del Vaupés, Colombia), Tesis MSc Universidad de los Andes, Facultad de Ciencias, Postgrado de Ecología Tropical. Mérida, Venezuela
- Berry P, Aymard G (1997) “A historic Portage” revisited. *Biollania ed esp* 6:263–273
- Berry P, Wiedenhoef AC (2004) *Micrandra inundata* (Euphorbiaceae), a new species with unusual wood anatomy from black-water river banks in southern Venezuela. *Syst Bot* 29:125–133
- Bongers F, Engelen D, Klinge H (1985) Phytomass structure of natural plant communities on sodosols in southern Venezuela: the bana woodland. *Vegetatio* 63(1):13–34
- Boubli JP (2002) Lowland floristic assessment of Pico da Neblina National Park, Brazil. *Plant Ecol* 160:149–167
- Braun-Blanquet J (1979) *Plant sociology, the study of plant communities*. Transl by Fueller GD and Conard HS. Mc Graw-Hill, New York
- Brewer-Carías C (1988) Cerro de la Neblina: Resultados de la Expedición 1986-1987. In: *Fundación para el Desarrollo de las Ciencias Físicas, Matemáticas y Naturales, Caracas, Venezuela*
- Bush MB, McMichael CN (2016) Holocene variability of an Amazonian hyperdominant. *J Ecol* 104(5):1370–1378

- Bush MB, de Oliveira BPE, Colinvaux PA, Miller MC, Moreno JE (2004) Amazonian paleoecological histories: one hill, three watersheds. *Paleogeography, Palaeoclimatology, Palaeoecology* 214:359–393
- Cano A, Stevenson PR (2009) Diversidad y composición florística de tres tipos de bosque en la estación biológica Caparú, Vaupés. *Revista Colombia Forestal* 12:63–80
- Capurucho JMG, Borges SH, Cornelius C, Prata EMB, Costa FM, Campos P, Sawakuchi AO, Rodrigues Zular A, Aleixo A, Bates JM, Ribas CC (2020) Patterns and processes of diversification in Amazonian white sand ecosystems: insights from birds and plants. In: Rull V, Carnaval A (eds) *Neotropical diversification: patterns and processes*. Fascinating Life Sciences, Springer, Cham, pp 245–270
- Cárdenas-López D, Barreto Silva JS, Arias García JC, Murcia García UG, Salazar Cardona CA, Méndez Quevedo O (2007) Caracterización y tipificación forestal de ecosistemas en el municipio de Inírida y el corregimiento de Cacahual (Guainía); una zonificación forestal para la ordenación de los recursos. Sinchi y Corporación para el Desarrollo Sostenible del norte y el oriente Amazónico, Bogotá, 252 p
- Carvajal de Fr. G. (1848) Descubrimiento del río de las Amazonas según la relación hasta ahora inédita del viaje de Francisco de Orellana. (Edited by J. T. Medina.) Imp. E. Rasco, Sevilla, España
- Chave J, Andalo C, Brown S, Cairns MA, Chambers JQ, Eamus D, Fölster H, Fromard F, Higuchi N, Kira T, Lescure JP, Nelson BW, Ogawa H, Puig H, Riéra B, Yamakura T (2005) Tree allometry and improved estimation of carbon stocks and balance in tropical forests. *Oecologia* 145:87–99
- Cintra JP (2011) Magni Amazoni Fluvii: o mapa do Conde de Pagan. *Anais do 1º Simpósio Brasileiro de Cartografia Histórica*. Belo Horizonte, Brasil 1:1–20
- Cintra JP (2012a) O mapa das cortes e as fronteiras do Brasil. *Boletim Ciências Geodésicas*, sec Artigos (Curitiba) 8(3):421–445
- Cintra JP (2012b) Cartography and historical maps: techniques, applications and peculiarities. *Revista Brasileira de Cartografia* (Rio de Janeiro) 64(6):901–918
- Cintra JP, de Oliveira RH (2014) Nicolas Sanson and his map: the course of the Amazon River. *Acta Amazon* 44(3):353–366
- Cintra JP, Freitas JC (2011) Sailing down the Amazon River: La Condamine's map. *Surv Rev* 43: 550–566
- Cintra JP, Furtado JF (2011) A Carte de l'Amérique Méridionale de Bourguignon D'Anville: eixo perspectivo de uma cartografia amazônica comparada. *Revista Brasileira de História* 31:273–316
- Clark H, Liesner R, Berry P, Fernández A, Aymard G, Maquirino P (2000) Catálogo anotado de la flora del área de San Carlos de Río Negro, Venezuela. *Scientia Guaianae* 11:101–316
- Clinebell RR, Phillips OL, Gentry AH, Stark N, Zuurhig H (1995) Prediction of neotropical tree and liana species richness from soil and climatic data. *Biodivers Conserv* 4:56–90
- Colinvaux PA, de Oliveira PE, Bush MB (2000) Amazonian and neotropical plant communities on glacial time-scales: the failure of the aridity and refuge hypotheses. *Quat Sci Rev* 19:141–169
- Condit R, Hubbell SP, Lafrankie JV, Sukumar R, Manokaran N, Foster BR, Ashton PS (1996) Species-area and species-individual relationships for tropical trees: a comparison of three 50-ha plots. *J Ecol* 84(4):549–562
- Coomes DA, Grubb PJ (1996) Amazonian caatinga and related communities at La Esmeralda, Venezuela: forest structure, physiognomy and floristics, and control by soils factors. *Vegetatio* 122:167–191
- Cordeiro RC, Turcq BJ, Sifeddine A, Lacerda LD, Silva Filho EV, Gueiros BB, Cunha YPP, Santelli RE, Pádua EO, Pachinelam SR (2011) Biogeochemical indicators of environmental changes from 50 ka to 10 ka. *Palaeogeogr Palaeoclimatol Palaeoecol* 299:426–436
- Córdoba MP, Etter A (2001) Flora Puinawai. In: Etter A, Baptsite LG, Córdoba M, Muñoz Y, Repizzo A, Romero M, Álvarez M, Escobar F, Fernández F, Mendoza H, Rojas A (eds) *Puinawai y Nukak*. Caracterización ecológica de dos reservas nacionales naturales de la

- Amazonia Colombiana. Pontificia Universidad Javeriana, Colciencias, Inst A von Humboldt y Fundación FES, Bogotá, Colombia, pp 102–107
- Cortesão J (1965) História do Brasil nos velhos mapas. Tomos 1 e 2. Ministério das Relações Exteriores, Instituto Rio Branco, Rio de Janeiro, Brasil
- Cuevas E, Medina E (1986) Nutrient dynamics within Amazonian forest ecosystems I. nutrient flux in fine litter fall and efficiency of nutrient utilization. *Oecologia* 68:466–472
- Cuevas E, Medina E (1991) Phosphorus/nitrogen interactions in adjacent Amazon forests with contrasting soils and water availability. In: Tiessen H, López-Hernández D, Salcedo TH (eds) Regional workshop 3: south and Central America. Saskatchewan Institute of Pedology, pp 84–94
- D'Apolito C, Absy ML, Latrubesse EM (2017) The movement of pre-adapted cool taxa in north-Central Amazonia during the last glacial. *Quat Sci Rev* 169:1–12
- de La Condamine CM (1745) Relation Abrégée d'un Voyage fait dans l'Intérieur de l'Amérique Méridionale, Depuis la Côtes de la Mer du Sud, jusqu'aux Côtes du Brésil & de la Guyane, en Descendant la Riviere des Amazones. Veuve Pissot, Paris, France
- Dexter K, Chave J (2016) Evolutionary patterns of range size, abundance and species richness in Amazonian angiosperm trees. *PeerJ* 4:e2402. <https://doi.org/10.7717/peerj.2402>
- Dezzeb N, Maquirino P, Berry PE, Aymard G (2000) Principales tipos de bosques en el área de San Carlos de Río Negro, Venezuela. *Scientia Guaianae* 11:15–36
- Draper F, Costa FRC, Arellano G, Phillips OL, Duque A, Macía MJ, ter Steege H, Asner GP, Aymard G et al (2021) Amazon tree dominance across forest strata. *Nature Ecol Evol*. <https://doi.org/10.1038/s41559-021-01418-y>
- Dubroeuq D, Volkoff B (1998) From Oxisols to spodosols and histosols: evolution of the soil mantles in the Rio Negro basin (Amazonia). *Catena* 32:245–280
- Ducke A (1938) A Flora do Curicuriari, afluente do Rio Negro, observada em viagens com a comissão demarcadora das fronteiras do setor Oeste. In: Anais da Primeira Reuniao Sul-Americana de Botanica 3 (1):389-398. Rio de Janeiro
- Ducke A (1944) Flora do Rio Urubú (observações realizadas durante as viagens da comissão que escolheria as terras para a colônia agrícola nacional do Amazonas). Boletim Ministerio da Agricultura, Servico Florestal do Brasil, Rio de Janeiro
- Ducke A (1954) Notas sobre a fitogeografia Amazônia Brasileira. Boletim técnico do Instituto Agrônômico do Norte 29:1–62
- Duivenvoorden JF, Cavelier J, García A, Grandez C, Macía M, Romero-Saltos H, Sánchez M, Valencia R (2005) Density and diversity of plants in relation to soil nutrient reserves in well-drained upland forests in NW Amazonia. *Biologiske Skrifter* 55:25–35
- Espinoza JC, Ronchail J, Guyot JL, Cochonneau G, Naziano F, Lavado W, de Oliveira E, Pombosa R, Vauchel P (2009) Spatio-temporal rainfall variability in the Amazon basin countries (Brazil, Peru, Bolivia, Colombia, and Ecuador). *Int J Climatol* 29(11):1574–1594
- Fine PV, Miller ZJ, Mesones I, Irazuzta S, Appel HM, Stevens MH, Sääksjärvi I, Schultz JC, Coley PD (2006) The growth-defense trade-off and habitat specialization by plants in Amazonian forests. *Ecology* 87(7):S150–S162
- Fine PV, García-Villacorta R, Pitman NCA, Mesones I, Kembel SW (2010) A floristic study of the white-sand forests of Peru. *Ann Mo Bot Gard* 97:283–305
- ForestPlots.net, Blundo C, Carilla J, Grau R, Malizia A, Malizia L, Osinaga-Acosta O et al (554 co-authors) (2021) Taking the pulse of Earth's tropical forests using networks of highly distributed plots. *Biol Conserv*. <https://doi.org/10.1016/j.biocon.2020.108849>
- Franco W, Dezzeb N (1994) Soils and water regime in the terra firme-caatinga forest complex near San Carlos de Río Negro, state of Amazonas, Venezuela. *Interciencia* 19(6):305–316
- Fritz S (1717) Description abrégée du Maragnon, et des missions établies aux environs de ce grand fleuve, tirée d'un mémoire espagnole du père Samuel Fritz, missionnaire de la Compagnie de Jésus. Lettres Édifiantes et Curieuses, Écrites des Missions Etrangères, par Quelques Missionnaires de la Compagnie de Jesus 12:212–231

- Fritz S (1726) Beschreibung des Fluß Maragnon und deren Missionen. Der Neuer Welt-Bott 5(111):59–61
- Fritz S (1755) Descripción abreviada del río Marañón, y de las misiones establecidas en sus contornos—Sacada de una memoria española del padre Samuël Fritz, Misionero de la Compañía de Jesus. *Cartas edificantes, y Curiosas, Escritas de las Misiones Estrangeras, por Algunos Misioneros de la Compañía de Jesus* [Traducidas del idioma francés por el padre Diego Davin, de la Compañía de Jesus] 8:42-50
- Fritz S (1819) Description abrégée du Maragnon, et des missions établies aux environs de ce grand fleuve, tirée d'un mémoire espagnole du père Samuel Fritz, missionnaire de la Compagnie de Jésus. *Lettres édifiantes et curieuses, écrites des Missions Étrangères* Nouvelle Édition. Mémoires d'Amérique [Lyon] 5:172–180
- García-Villacorta R, Dexter KG, Pennington T (2016) Amazonian white-sand forests show strong floristic links with surrounding oligotrophic habitats and the Guiana shield. *Biotropica* 48:47–57
- Gentry AH (1982) Neotropical floristic diversity: phytogeographical connections between central and South America: Pleistocene climatic fluctuations or an accident of the Andean orogeny? *Ann Mo Bot Gard* 69:557–593
- Gentry AH (1988a) Tree species richness of upper Amazonian forests. *Proceedings of the National Academy of Sciences USA* 85:156–159
- Gentry AH (1988b) Changes in plant community diversity and floristic composition on environmental and geographical gradients. *Ann Mo Bot Gard* 75:1–34
- Gentry AH (1993) Diversity and floristic composition of lowland forest in Africa and South America. In: Goldblatt P (ed) *Biological relationships between Africa and South America*. Yale University Press, New Haven, pp 500–547
- Goulding M, Leal Carvalho M, Ferreira EG (1988) Rio Negro, rich life in poor water (Amazonian diversity and foodchain ecology as seen through fish communities). SPB Academic Publishing, The Netherlands
- Häggi C, Chiessi CM, Merkel U, Mulitza S, Prange M, Schulz M, Schefuß E (2017) Response of the Amazon rainforest to late Pleistocene climate variability. *Earth Planet Sci Lett* 479:50–59
- Haykin S (2009) *Neural networks and learning machines*, 3rd edn. Pearson Prentice Hall, Upper Saddle River, New Jersey, USA
- Herrera R (1979) Nutrient distribution and cycling in an Amazon Caatinga rainforest on Spodosols in southern Venezuela. PhD. thesis. University of Reading
- Herrera R (1985) Nutrient cycling in Amazonian forests. In: Prance GT, Lovejoy TE (eds) *Key environments: Amazonia*. Pergamon Press, Oxford, pp 95–105
- Hill MO (1979) TWINSPAN—a Fortran program for arranging multivariate data in an ordered two-way table of classification of individuals and attributes. Cornell University, Ithaca, NY
- Hofhansl F, Chacón-Madrigal E, Fuchslueger L, Jenking D, Morera-Beita A, Plutzer C, Silla F, Andersen KM, Buchs DM, Dullinger S, Fiedler K, Franklin O, Hietz P, Huber W, Quesada CA, Rammig A, Schrodter F, Vincent AG, Weissenhofer A, Wanek W (2020) Climatic and edaphic controls over tropical forest diversity and vegetation carbon storage. *Sci Rep* 10:5066. <https://doi.org/10.1038/s41598-020-61868-5>
- Hooghiemstra HT, van der Hammen T, Cleef AM (2002) Paleoecología de la flora boscosa. In: Guariguata MR, Kattan GH (eds) *Ecología y conservación de bosques Neotropicales*. Editorial Libro Universitario Regional, Costa Rica, pp 43–58
- Hooghiemstra HT, Wijninga VM, Cleef AM (2006) The paleobotanical record of Colombia; implications for biogeography and biodiversity. *Annals of Missouri Botanical Garden* 93: 297–325
- Hoorn C, Wesselingh FP, ter Steege H, Bermudez MA, Mora A, Sevink J, Sanmartín I, Sánchez-M A, Anderson CL, Figueiredo JP, Jaramillo C, Riff D, Negri RF, Hooghiemstra HT, Lundberg J, Stadler T, Särkinen T, Antonelli A (2010) Amazonia through time: Andean uplift, climate change, landscape evolution, and biodiversity. *Science* 330:927–931
- Hoorn C, Bogotá-A GR, Romero-Báez M, Lammertsma E, Flantua SGA, Dantas EL, Dino R, do Carmo DA, Chemale F Jr (2017) The Amazon at sea: onset and stages of the Amazon river from

- a marine record, with special reference to Neogene plant turnover in the drainage basin. *Glob Planet Chang* 153:51–65
- Hopkins MJG (2019) Are we close to knowing the plant diversity of the Amazon? *An Acad Bras Cienc* 91(3):1–7. <https://doi.org/10.1590/0001-3765201920190396>
- Householder JE, Schöngart J, Piedade MTF, Junk WJ, ter Steege H, Montero JC, de Assis RL, de Aguiar DPP, Pombo MM, Quaresma AC, Demarchi LO, Parolin P, Lopes A, Feitoza GV, Durgante FM, Albuquerque BW, Chu A, Enßlin D, Fabian T, Fettweiß K, Hirsch M, Hombach M, Hubbuch A, Hutter B, Jäger T, Kober-Moritz R, Lindner MKR, Maier F, Nowak J, Petridis Z, Schierling L, Snjaric E, Egger G, Schneider E, Damm C, Wittmann F (2021) Modeling the ecological responses of tree species to the flood pulse of the Amazon Negro River floodplains. *Front Ecol Evol* 9:628606. <https://doi.org/10.3389/fevo.2021.628606>
- Hubbell SP, He F, Condit R, Borda-de Agua L, Kellner J, ter Steege H (2008) How many tree species are there in the Amazon and how many of them will go extinct? *Proc Nat Acad Sci USA* 105:11498–11504
- Huber O (1987) Consideraciones sobre el concepto de Pantepui. *Pantepui* 2:2–10
- Huber O (1994) Recent advances in the phytogeography of the Guayana region, South America. *Mémoires de la Société de Biogéographie* 4:53–63
- Huber O (1995a) History of botanical exploration. In: Berry PE, Holst B, Yatskievych K (eds) *Flora of Venezuelan Guayana*, vol I. Timber Press, Portland, Oregon, pp 63–95
- Huber O (1995b) Geographical and physical features. In: Berry PE, Holst B, Yatskievych K (eds) *Flora of Venezuelan Guayana*, vol I. Timber Press, Portland, Oregon, pp 1–62
- Huber O (1995c) Vegetation. In: Berry PE, Holst B, Yatskievych K (eds) *Flora of Venezuelan Guayana*, vol I. Timber Press, Portland, Oregon, pp 97–192
- Huber O, Wurdack JJ (1984) History of botanical exploration in Territorio Federal Amazonas, Venezuela. *Smithson Contrib Bot* 56:1–86
- IGAC (2014) Departamento del Guainía: Estudio general de suelos y zonificación de la tierra, escala 1:100.000/Instituto Geográfico Agustín Codazzi. Subdirección de Agrología. Imprenta Nacional de Colombia, Bogotá
- IGAC (2018) Estudio general de suelos y zonificación de tierras departamento de Vichada, escala 1:100.000/Instituto Geográfico Agustín Codazzi. Subdirección de Agrología. Imprenta Nacional de Colombia, Bogotá
- Janzen DH (1974) Tropical Blackwater rivers, animals and mass fruiting by the Dipterocarpaceae. *Biotropica* 6:69–103
- Junk WJ, Piedade MTF, Schöngart J, Cohn-Haft M, Adeney JM, Wittmann FA (2011) Classification of major naturally-occurring Amazonian lowland wetlands. *Wetlands* 31:623–640
- Klinge H (1965) Podzol soils in the Amazon basin. *J Soil Sci* 16(1):96–103
- Klinge H (1967) Podzol soils: a source of Blackwater rivers in Amazonia. *Atas do Simpósio sobre a Biota Amazônica* 3:117–125
- Klinge H, Herrera R (1983) Phytomass structure of natural plant communities on spodosols in southern Venezuela: the tall Amazon caatinga forest. *Plant Ecol* 53:65–84
- Klinge H, Medina E (1979) Rio Negro caatingas and Campinas, Amazonas states of Venezuela and Brazil. In: Specht RL (ed) *Heathlands and related shrublands*. Elsevier Scientific Publications, New York, pp 483–488
- Klinge H, Medina E, Herrera R (1977) Studies on the ecology of Amazon caatinga forest in southern Venezuela. Part 1: general features. *Acta Científica Venezolana* 28:270–276
- Kristiansen T, Svenning JC, Grandez C, Salo J, Balslev H (2009) Commonness of Amazonian palm (Arecaceae) species: cross-scale links and potential determinants. *Acta Oecol* 35(4):554–562
- Kubitzki K (1989) The ecogeographical differentiation of Amazonian inundation forests. *Plant Syst Evol* 162:285–304
- Kubitzki K (1990) The psammophilous flora of northern South America. *Mem N Y Bot Gard* 64:248–253
- Kubitzki K (1991) Dispersal and distribution in *Leopoldinia* (Palmae). *Nord J Bot* 11:429–432

- Landrum LR (1986) The life and botanical accomplishments of Boris Alexander Krukoff. *Adv Econ Bot* 2:1–96
- Latrubesse EM, Stevaux JC (2015) The Anavilhanas and Mariuá archipelagos: fluvial wonders from the Negro River, Amazon Basin. In: Carvalho-Viera B, Rodrigues-Salgado AA, Cordeiro-Santos L (eds) *Landscapes and landforms of Brazil*. World geomorphological landscapes series. Springer, Dordrecht, Heidelberg, New York, London, pp 157–170
- Levis C, Costa FRC, Bongers F, Peña-Claros M, Clement CR, Junqueira AB, Neves EG, Tamanaha EK, Figueiredo FOG, ter Steege H et al. (2017) Persistent effects of pre-Columbian plant domestication on Amazonian forest composition. *Science* 355(6328):925–931
- Lisbôa PL (1975) Estudos da vegetação das Campinas Amazonica - II. Observações gerais e revisão bibliográfica sobre as campinas amazônicas de areia branca. *Acta Amazon* 5:211–223
- Lleras E (1997) Upper Rio Negro region (Brazil, Colombia, Venezuela). In: Davies SD, Heywood VH, Herrera-MacBryde O, Villa-Lobos J, Hamilton AC (eds) *Centres of plant biodiversity. Volumen 3: The Americas*. World Wildlife Fund for Nature & The World Conservation Union, Cambridge, UK, pp 333–337
- Lopes de Sousa B (1955) Índios e explorações geográficas. Publicação no. 110. Conselho Nacional de Proteção aos Índios, Ministério da Agricultura, Rio de Janeiro, Brasil
- Lopes de Sousa B (1959) Do Rio Negro ao Orenoco (A Terra-O Homen). Publica no. 111. Conselho Nacional de Proteção aos Índios, Ministério da Agricultura, Rio de Janeiro, Brasil
- Luize BG, Lima Magalhães JÂL, Queiroz H, Lopes MA, Venticinque EM, de Moraes Novo EML, Silva TSF (2018) The tree species pool of Amazonian wetland forests: which species can assemble in periodically waterlogged habitats? *PLoSOne* 13(5):1–13
- Mägdefrau K, Wutz A (1961) Leichthölzer und Tonnenstämme in Schwarzwassergebieten und Dornbuschwäldern des tropischen Südamerika. *Forstwissenschaftliches Centralblatt* 80:17–28
- Marengo JA, Williams RE, Alves LM, Soares WR, Rodriguez DA (2016) Extreme seasonal climate variations in the Amazon basin: droughts and floods. In: Nagy L, Forsberg BR, Artaxo P (eds) *Interactions between biosphere, atmosphere and human land use in the Amazon basin*. Ecological studies 227. Springer, Heidelberg, Berlin, pp 54–76
- McCune B, Mefford MJ (2016) PC-ORD multivariate analysis of ecological data, Version 7.0. Wild Blueberry Media, Corvallis, Oregon, USA
- Medina E (2000) El Proyecto Amazonas del Instituto Venezolano de Investigaciones Científicas: Origen y desarrollo. *Scientia Guaianae* 11:1–6
- Medina E, Garcia V, Cuevas E (1990) Sclerophylly and oligotrophic environments: relationships between leaf structure, mineral nutrient content, and drought resistance in tropical rain forests of the upper Río Negro region. *Biotropica* 22:51–64
- Meggers BJ (1979) Climatic oscillation as a factor in the prehistory of Amazonia. *Am Antiq* 44(2): 252–266
- Meggers BJ (1994) Archeological evidence for the impact of mega-Niño events on Amazonia during the past two millennia. *Climate Change* 28:321–338
- Montoya E, Lombardo U, Levis C, Aymard G, Mayle FE (2020) Human contribution to Amazonian diversity: pre-Columbian legacy to current plant communities. In: Rull V, Carnaval A (eds) *Neotropical diversification*. Springer, Berlin, pp 495–520
- Morley RJ (2011) Cretaceous and tertiary climate change and the past distribution of megathermal rainforests. In: Bush MB, Flenley JR, Gosling WD (eds) *Tropical rainforest responses to climatic change*, 2nd edn. Springer-Verlag, Berlin-Heidelberg, pp 1–34
- Moyersoen B (1993) Ectomicorizas y micorizas vesículo-arbusculares en caatinga Amazónica del sur de Venezuela. *Scientia Guianae* 3:1–83
- Nascimento MN, Renato-C GSM, Turcq CB, Moreira LS, Bush MB (2019) Vegetation response to climatic changes in western Amazonia over the last 7,600 years. *J Biogeogr* 46(11):2389–2406
- Nelson WB, Ferreira CAC, da Silva MF, Kawasaki ML (1990) Endemism centres, refugia and botanical collection density in Brazilian Amazonia. *Nature* 345:714–716
- Neves EG (1998) Paths in dark waters: archaeology as indigenous history in the upper Rio Negro basin, Northwest Amazon. PhD thesis, Indiana University, USA



- Olivares I, Svenning JC, van Bodegom PM, Balslev H (2015) Effects of warming and drought on the vegetation and plant diversity in the Amazon Basin. *Bot Rev* 81(1):1–28
- Oliveira-Filho AT, Dexter KG, Pennington RT, Simon MF, Bueno ML, Neves DM (2021) On the floristic identity of Amazonian vegetation types. *Biotropica*. <https://doi.org/10.1111/btp.12932>
- Pagan BF (1655) *Relation Historique et Géographique de la Grande Rivière des Amazones dans l'Amérique*. Gardin Bensogne, Paris, France
- Pennington RT, Lavin L, Prado DE, Pendry CA, Pell SK, Butterworth CA (2004) Historical climatic change and speciation: neotropical seasonally dry forest plants shows pattern of both tertiary and quaternary diversifications. *Philos Trans Royal Soc B London* 359:515–538
- Peñuela MC (2014) Understanding Colombian Amazonian white sand forests. PhD Thesis, Utrecht University, The Netherlands
- Pereira da Silva J (2008) Carta e inventario enviados per A. Rodrigues-Ferreira desde Barcelos el 17 de abril de 1786. In: Monteiro Soares JP Ferrão C (ed) *Viagem ao Brasil de Alexander Rodrigues Ferreira volume 3. [Correspondência 1a parte (1779–1788); “Transcrição, Establecimiento do Texto e Notas” de J. Pereira da Silva]* Kapa Editorial, Petrópolis, Brasil, pp 80–86
- Phillips O, Miller JS (2002) Global patterns of plant diversity: Alwyn H Gentry's forest 980 transect data set *Monographs Systematic Botany* 89:1–319. Missouri Botanical Press
- Pitman NC, Mogollón H, Dávila N, Ríos M, García-Villacorta R, Guevara JE, Baker T, Monteagudo A, Phillips O, Vásquez-Martínez R, Ahuite M, Aulestia M, Cárdenas-López D, Cerón C, Loizeau PA, Neill D, Nuñez P, Palacios W, Spichiger R, Valderrama R (2008) Tree community change across 700 km of lowland Amazonian forest from the Andean foothills to Brazil. *Biotropica* 40:525–535
- Pombo de Souza MM (2012) *Estrutura e composicao das comunidades de arvores na bacia do alto rio Negro*. Master's Thesis, Instituto Nacional de Pesquisas da Amazônia-INPA, Manaus, Brasil
- Prance GT (1980) A terminologia dos tipos de florestas amazonicas sujeitas a inundação. *Acta Amazon* 10:495–504
- Prance GT (1989) American tropical forests. In: Lieth H, Werger MJA (eds) *Tropical rain Forest ecosystems, ecosystems of the world 14B*. Elsevier, Amsterdam, The Nerderlands, pp 99–132
- Prance GT (2001) Amazon ecosystems. In: Asher-Levin S (ed) *Encyclopedia of biodiversity, A-C, vol 1*. Academic Press, New York, pp 145–157
- Prance GT, Nelson BW, Freitas da Silva M, Daly DC (1984) Projeto Flora Amazônica: eight years of binational botanical expeditions. *Acta Amazonica* 14(Supl. 1/2):5–29
- Putz FE (1983) Liana biomass and leaf area of a “terra firme” forest in the Rio Negro basin, Venezuela. *Biotropica* 15:185–189
- Putz FE, Mooney HA (1991) *The biology of vines*. Cambridge University Press, Cambridge
- Quesada CA, Lloyd J, Anderson LO, Fyllas NM, Schwarz M, Czimczik CI (2011) Soils of Amazonia with particular reference to the RAINFOR sites. *Biogeosciences* 8:1415–1440
- Quesada CA, Phillips OL, Schwarz M, Czimczik CI, Baker TR, Patino S, Fyllas NM, Hodnett MG, Herrera R, Almeida S, Alvarez-Dávila E, Arneth A, Arroyo L, Chao KJ, Dezzeo N, Erwin T, di Fiore A, Higuchi N, Honorio Coronado E, Jimenez EM, Killeen T, Torres-Lezama A, Lloyd G, Lopez-González G, Luizão FJ, Malhi Y, Monteagudo A, Neill DA, Nuñez Vargas P, Paiva R, Peacock J, Peñuela MC, Peña Cruz A, Pitman N, Priante Filho N, Prieto A, Ramírez H, Rudas A, Salomão R, AJB S, Schmerler J, Silva N, Silveira M, Vásquez R, Vieira I, Terborgh J, Lloyd J (2012) Basin-wide variations in Amazon forest structure and function are mediated by both soils and climate. *Biogeosciences* 9:2203–2246
- Rice HA (1910) The river Uaupés. *Geogr J* 35(6):682–700
- Rice HA (1914) Further explorations in the North-Western Amazon Valley. *Geogr J* 44(2):137–168
- Rice HA (1918) Notes on the Rio Negro (Amazons). *Geogr J* 52(4):205–218. [“The journey. . . was made during the first three months of 1917”]
- Rice HA (1921) The Río Negro, the Casiquiare Canal, and the upper Orinoco, September 1919–April 1920. *Geogr J* 63(5):321–244
- Rice HA (1928) The Rio Branco, Uraricuera, and Parima. *Geogr J* 71(2):113–143

- Richards PW (1952) *The tropical rain forest*. Cambridge University Press, Cambridge
- Ricklefs RE (1987) Community diversity: relative roles of local and regional processes. *Science* 235:167–171
- Riina R, Berry PE, Huber O, Michelangeli FA (2019) Pantepui plant diversity and biogeography. In: Rull V, Vegas-Villarrúbia T, Huber O, Señaris J (eds) *Biodiversity of Pantepui: the pristine “lost world” of the neotropical Guiana highlands*. Academic Press, Cambridge, pp 121–147
- Ríos-Villamizar EA, Adeney JM, Junk WJ, Piedade MTF (2020) Physicochemical features of Amazonian water typologies for water resources management. *IOP Conf Series: Earth and Environmental Science* 427:012003. <https://doi.org/10.1088/1755-1315/427/1/012003>
- Rodrigues WA (1961) Aspectos fitosociológicos das caatingas do rio Negro. *Boletim do Museu Paraense Emílio Goeldi (Botânica)* 15:3–41
- Rodriguez-Zorro PA, Turcq B, Cordeiro RC, Moreira LS, Costa RL, McMichael CH, Behling H (2018) Forest stability during the early and late Holocene in the igapó floodplains of the Rio Negro, northwestern Brazil. *Quat Res* 89(1):75–89
- Romero-G GA, Gómez-D CA, González-Ñañez AG (2019) Las cuatro “Yavitas”. *Boletín de historia de las Geociencias en Venezuela* 131:1–133
- Rudas A, Prieto A, Rangel JO (2002) Principales tipos de vegetación de La Ceiba (Guainía), Guayana Colombiana. *Caldasia* 24:243–365
- Ruiz-Pessenda LC, de Oliveira PE, Mofatto M, Brito de Medeiros V, Francischetti- García RJ, Aravena R, Bendassoli JA, Zuniga-Leite A, Saad AR, Etchebehere ML (2009) The evolution of a tropical rainforest/grassland mosaic in southeastern Brazil since 28,000 14C yr BP based on carbon isotopes and pollen records. *Quat Res* 71:437–452
- Sabatier D, Grimaldi M, Prévost MF, Guillaume J, Gedron M, Desso M, Curmi P (1997) The influence of soil cover organization on the floristic and structural heterogeneity of a Guianan rain forest. *Plant Ecol* 131:81–108
- Salamanca S (1983) La vegetación de la Orinoquia-Amazonia: fisiografía y formaciones vegetales. *Colombia Geográfica* 10:5–31
- Saldarriaga JG, West DC (1986) Holocene fires in the northern Amazon basin. *Quat Res* 26:358–366
- Sanford RL, Cuevas E (1996) Root growth and rhizosphere interactions in tropical forests. In: Mulkey SS, Chazdon RL, Smith AP (eds) *Tropical forest plant ecophysiology*. Chapman & Hall, USA, pp 268–300
- Sanford RL, Saldarriaga JG, Clark KE, Uhl C, Herrera R (1985) Amazon rain-forest fires. *Science* 227:53–55
- Santos JOS, Potter PE, Reis NJ, Hartmann LA, Fletcher IR, McNaughton NJ (2003) Age, source, and regional stratigraphy of the Roraima supergroup and Roraima-like outliers in northern South America based on U-pb geochronology. *Geol Soc Am Bull* 115(3):331–348
- Schargel R, Marvez P (2009) Suelos. En: Aymard G (ed) *Estudio de los suelos y la vegetación (estructura, composición florística y diversidad) en bosques macrotérmicos no-inundables, estado Amazonas Venezuela (aprox. 01° 30' - 05° 55' N; 66° 00' -- 67° 50' O)*. *Biollania ed esp* 9:99–108
- Schargel R, Aymard A, Berry P (2000) Características y factores formadores de Spodosoles en el sector Maroa-Yavita, Amazonía Venezolana. *Revista UNELLEZ de Ciencia y Tecnología* 18(1):85–96
- Schultes RE (1983) Richard Spruce: an early ethnobotanist and explorer of the Northwest Amazon and northern Andes. *J Ethnobiol* 3(2):139–147
- Schulman L, Toivonen T, Ruokolainen K (2007) Analysing botanical effort in Amazonia and correcting for it in species range estimation. *J Biogeogr* 34:1388–1399
- Silva-Souza KJP, Souza AF (2020) Woody plant subregions of the Amazon forest. *J Ecol* 108(6): 2321–2335. <https://doi.org/10.1111/1365-2745.13406>
- Spruce R (1908) Notes of botanist on the Amazon and Andes (being records of travel on the Amazon and its tributaries, the Trombetas, Rio Negro, Uaupés, Casiquiare, Pacimoni, Huallaga

- and Pastasa; as also to the cataracts of the Orinoco along the eastern side of the Andes of Peru and Ecuador, and the shores of the Pacific, during the years 1849–1864). Volume edited by AR Wallace. The Macmillan Company, London
- Steyermark JA (1982) Relationships of some Venezuelan forest refuges with lowland tropical floras. In: Prance DT (ed) *Biological diversification in the tropics*. Columbia University Press, New York, pp 182–220
- Stokes MF, Goldberg SL, Perron JT (2018) Ongoing river capture in the Amazon. *Geophys Res Lett* 45:5545–5552
- Stropp J, ter Steege H, Malhi Y, ATDN and RAINFOR (2009) Disentangling regional and local tree diversity in the Amazon. *Ecography* 32:46–54
- Stropp J, van der Sleen P, Assunção PA, Lopes da Silva A, ter Steege H (2011) Tree communities of white-sand and terra-firme forests of the upper Rio Negro. *Acta Amazon* 41:521–544
- Stropp J, van der Sleen P, Quesada CA, ter Steege H (2014) Herbivory and habitat association of tree seedlings in lowland evergreen rainforest on white-sand and terra-firme in the upper Rio Negro. *Plant Ecol Diversity* 7(1–2):255–265
- Stropp J, Umbelino B, Correia BRA, Campos-Silva JV, Ladle RJ, Malhado ACM (2020) The ghosts of forests past and future: deforestation and botanical sampling in the Brazilian Amazon. *Ecography* 43:1–11
- Takeuchi M (1961) The structure of the Amazonian vegetation. III Campina forest in the Río Negro region. *J Fac Sci, University of Tokyo (Sect Bot 3)* 8(2):27–35
- Takeuchi M (1962a) The structure of the Amazonian vegetation. IV High Campina forest in the upper Rio Negro. *J Fac Sci, University of Tokyo (Sect Bot 3)* 8(5):279–288
- Takeuchi M (1962b) The structure of the Amazonian vegetation V. Tropical rain forest near Uaupés. *J Fac Sci: University of Tokyo (Sect Bot 3)* 8(6):289–296
- Takeuchi M (1962c) The structure of the Amazonian vegetation. VI igapo. *J Fac Sci, University of Tokyo (Sect Bot 3)* 8(7):297–304
- Tenreiro-Aranha B de F (1906) As explorações e os exploradores do Rio Uaupés. *Arquivo do Amazonas, año I, I (2):23–54 (23 de octubre), Manaus, Brasil*
- Ter Braak CJE (1987) The analysis of vegetation-environment relationships by canonical correspondence analysis. *Vegetatio* 69:69–77
- ter Steege H, Pitman NC, Sabatier D, Castellanos H, van der Hout P, Daly DC, Silveira M, Phillips O, Vasquez R, van Andel T, Duivenvoorden J, de Oliveira AA, Ek R, Lilah R, Thomas R, van Essen J, Baider C, Maas P, Mori S, Terborgh J, Nuñez P, Mogollón H, Morawetz W (2003) A spatial model of tree  $\alpha$ -diversity and tree density for the Amazon. *Biodivers Conserv* 12:2255–2277
- ter Steege H, Pitman NC, Phillips O, Chave J, Sabatier D, Duque A, Molino DF, Prévost MF, Spichiger R, Castellanos H, von Hildebrand P, Vasquez R (2006) Continental-scale patterns of canopy tree composition and function across Amazonia. *Nature* 443(28):444–447
- ter Steege H, ATDN (Amazon Tree Diversity Network: collective author) and RAINFOR (The Amazon Forest Inventory Network: collective author) (2010) Contribution of current and historical processes to patterns of tree diversity and composition of the Amazon. In: Hoorn C, Wesseling FP (eds) *Amazonia landscape and species evolution: a look into the past*. Wiley-Blackwell Publishing Ltd, pp 347–359
- ter Steege H, Pitman NC, Sabatier D, Baraloto C, Salomão RP, Guevara JE, Phillips OL, Castilho CV, Magnusson WE, Molino JF, Monteagudo A, Núñez P, Montero JC, Feldpausch et al (2013) Hyper-dominance in the Amazonian tree flora. *Science* 342:325–335
- ter Steege H, Vaessen RW, Cárdenas-López D, Sabatier D, Antonelli A, Mota de Oliveira S, Pitman NCA, Jørgensen PM, Salomão RP (2016) The discovery of the Amazonian tree flora with an updated checklist of all known tree taxa. *Sci Rep* 6:29549. <https://doi.org/10.1038/srep29549>
- ter Steege H, Mota de Oliveira S, Pitman NCA, Sabatier D, Antonelli A, Guevara Andino JE, Aymard G, Salomão RP (2019a) Towards a dynamic list of Amazonian tree species. *Sci Rep* 9: 3501. <https://doi.org/10.1038/s41598-019-40101-y>

- ter Steege H, Henkel TW, Marimon BS, Pitman NCA, Phillips O, Aymard G, Salomão AR et al (2019b) Rarity of monodominance in hyperdiverse Amazonian forests. *Sci Rep* 9:13822. <https://doi.org/10.1038/s41598-019-50323-9>
- ter Steege H, Prado HPI, Lima RF, Pos E, de Souza CL, de Andrade Lima Filho D, Salomão RP, Phillips OL, Aymard G et al (2020) Biased-corrected richness estimates for the Amazonian tree flora. *Sci Rep* 10:10130. <https://doi.org/10.1038/s41598-020-66686-3>
- Tuomisto H, Moulatlet GM, Balslev H, Emilio T, Figueiredo FOG, Pedersen D, Ruokolainen K (2016) A compositional turnover zone of biogeographical magnitude within lowland Amazonia. *J Biogeogr* 43:2400–2411
- Tuomisto H, Van Doninck J, Ruokolainen K, Moulatlet GM, FOG F, Sirén A, Zuquim G (2019) Discovering floristic and geoeological gradients across Amazonia. *J Biogeogr* 46(8): 1734–1748
- Uhl C, Murphy P (1981) A comparison of productivities and energy values between slash and burn agriculture and secondary succession in the upper Rio Negro region of the Amazon Basin. *Agro-Ecosystems* 7(1):63–83
- Valencia R, Foster R, Villa G, Condit R, Svenning JC, Hernández C, Romeleroux R, Losos E, Magaard E, Balslev H (2005) Trees species distributions and local habitat variation in the Amazon: a large forest plot in eastern Ecuador. *J Ecol* 92:214–229
- van der Hammen T (1972) Changes in vegetation and climate in the Amazon basin and Sur-rounding areas during the Pleistocene. *Geologie Mijnbouw* 51:641–643
- van der Hammen T (2006) Bases para una prehistoria ecológica amazónica y el caso Chiribiquete. In: Morcote-Ríos G, Mora-Camargo S, Franky-Calvo C (eds) *Pueblos y paisajes antiguos de la selva amazónica*. Universidad Nacional de Colombia, Facultad de Ciencias, Bogotá, Taraxacum, Smithsonian Institution, Washington DC, pp 29–48
- van der Hammen T, Absy ML (1994) Amazonia during the last glacial. *Palaeogeogr Palaeoclimatol Palaeoecol* 109:247–261
- Vareschi V (1963) La bifurcación del Orinoco. Observaciones hidrográficas y ecológicas de la expedición conmemorativa de Humboldt del año 1958. *Acta Cient Venez* 14(4):98–103
- Vazquez F (1881) Relación de lo que Sucedió en la Jornada de Omagua y Dorado hecha por el Gobernador Pedro de Orsúa [“Advertencia Preliminar” de Feliciano Ramírez de Arellano, Marqués de la Fuensanta del Valle]. Sociedad de Bibliófilos Españoles, Madrid
- Vitousek PM, Sanford RL (1986) Nutrient cycling in moist tropical forest. *Annu Rev Ecol Syst* 17: 137–167
- von Bauer PP (1919) NW-Amazonien: Ein Beitrag zur Geographie Äquatorial-Amerikas. Rudolf M, Rohrer, Brünn
- Walker WS, Gorelika SR, Baccinia A, Aragon-Osejo JL, Josse C, Meyerd C, Macedo MN, Augusto C, Rios S, Katan T, Almeida de Souza A, Cuellar S, Llanos A, Zager I, Díaz Mirabal G, Solvika KK, Farina MK, Moutinho P, Schwartzmand S (2020) The role of forest conversion, degradation, and disturbance in the carbon dynamics of Amazon indigenous territories and protected areas. *Proc Nat Acad Sci USA* 117(6):3015–3025
- Wesselingh FP, Hoorn C, Kroonenberg SB, Antonelli A, Lundberg JG, Vonhof HB, Hooghiemstra H (2010) On the origin of Amazonian landscapes and biodiversity: a synthesis. In: Hoorn C, Wesselingh F (eds) *Amazonia, landscape and species evolution*. Wiley-Blackwell, Oxford, pp 421–432
- Westhoff V, van der Maarel E (1973) The Braun-Blanquet approach. In: Whittaker RH (ed) *Handbook of vegetation science*, vol 5. Junk, The Hague, pp 617–726
- Wittmann F, Marques MC, Júnior GD, Budke JC, Piedade MTF, Wittmann de Oliveira A, Montero JC, de Assis RL, Targhetta N, Parolin P, Junk WJ, Householder JE (2017) The Brazilian freshwater wetcape: changes in tree community diversity and composition on climatic and geographic gradients. *PLoS One* 12(4):1–18
- Wurdack JJ (1971) The Melastomataceae collections of A. Rodrigues Ferreira *Taxon* 20:595–596
- Zinck A (1986) El inventario de los recursos naturales de la Guayana en marcha. *Pantepui* 1:2–16

Zucchi A (2006) Ríos de aguas blancas y negras, asentamientos, organización social y patrones migratorios de grupos Arawacos del alto negro venezolano. In: Morcote-Ríos G, Mora-Camargo S, Franky-Calvo C (eds) *Pueblos y paisajes antiguos de la selva amazónica*. Universidad Nacional de Colombia. Facultad de Ciencias, Bogotá, Taraxacum, Smithsonian Institution, Washington DC, pp 157–170



# Amazon Caatinga Complex: Sclerophyllous Vegetation on Nutrient-Poor White-Sand Soils

# 4

E. Medina and E. Cuevas

## 4.1 Introduction

Sclerophyllous forests and shrublands of variable stem density and structure, locally known as Caatingas, occur on white-sand soils in the upper Río Negro basin (Klinge and Medina 1979; Anderson 1981). The Amazon caatinga appears to be restricted to the equatorial zone, approximately from 3°S to 5°N. This vegetation type is distributed over the Amazonas state in southern Venezuela, the departments of Vichada, Guainía, and Vaupés in Colombia, lowlands in Guyana, Suriname, and French Guiana, and the states of Amazonas and Pará in northern Brazil.

Amazon caatinga vegetation was first described by Spruce (1908) in the upper Río Negro basin, distinguishing two different types: a 20–30 m tall “caatinga alta” and a 10 m tall or lower “caatinga baixa.” Floristically and ecologically related is the “Campina” forest in the lower Río Negro (Takeuchi 1961, 1962; Anderson et al. 1975; Anderson 1981). The name of Amazon caatinga has been adopted to distinguish it from the dry caatinga vegetation of the Brazilian north-eastern region (Hueck 1966; Klinge and Medina 1979).

Earlier literature on Amazon caatinga was reviewed by Klinge and Medina (1979) and Anderson (1981). During the last few decades, numerous vegetation studies in the Amazon basin have produced a wealth of information related to the structural and functional properties of caatinga in Venezuela (Dezzeo et al. 2000; Aymard et al. 2009), Colombia (Peñuela-Mora 2014), and Brazil (Nardoto et al. 2008; Stropp et al. 2011; Daly et al. 2016). An attempt to define a phytosociological

---

E. Medina (✉)

Centro de Ecología, Instituto Venezolano de Investigaciones Científicas, Caracas, Venezuela

Department of Biology, University of Puerto Rico, Río Piedras, Puerto Rico

Institute of Tropical Forestry, USDA Forest Service, San Juan, Puerto Rico

E. Cuevas

Department of Biology, University of Puerto Rico, Río Piedras, Puerto Rico

classification of forests within the upper Orinoco and Rio Negro basins is described in Chap. 3.

Adeney et al. (2016) generated a vegetation map of the whole Amazon basin based on an extensive review of forest structure and species composition studies. The map shows that white-sand forests occupy nearly 340,000 km<sup>2</sup>. The largest continuous patches are located in the north-western Amazonas state of Brazil, the Amazonas state of Venezuela, and the Vaupés and Amazonas departments in Colombia.

The Amazon caatinga is a vegetation complex characterized by (a) sandy soils with low nutrient status and low water holding capacity, (b) recurrent flooding during heavy rainy days due to shallow groundwater table, (c) dominant sclerophyllous species, and (d) an association of species tolerant to pulses of short-term hypoxia during flooding, and water stress after dry days because of low soil water holding capacity.

The Amazon caatinga is associated with black water rivers in the Río Negro basin (Rodríguez 1961; Anderson 1981) and the occurrence of podzols (Klinge 1965). The color of the water is due to the presence of dissolved humic acids that remain in solution due to the scarcity of divalent cations (Sioli and Klinge 1961). The upper Río Negro waters are very acidic (pH 3.7–3.9) and have conductivity values that do not correspond with the measured amount of metal cations (Vegas-Villarrubia et al. 1988).

Characteristic species of the tall Amazon caatinga within the genera *Micrandra* (Euphorbiaceae) and *Eperua* (Fabaceae) are markedly sclerophyllous. These species are restricted to flood-prone, poorly drained, white-sand soils with a thick organic top layer (Barthés 1991; Klinge and Medina 1979).

Topographic variations and intergradation with terra-firme forests located on relatively higher grounds determine strong variations in the frequency of flooding and supply of leached nutrients from surrounding terra-firme sites. This is the reason for the observed strong structural development gradient from tall caatinga to low caatinga.

The latter includes lower and scrubby vegetation forms described as campina or bana (Anderson et al. 1975; Bongers et al. 1985). In our opinion, this gradient constitutes a floristic, functional, and ecological continuum. We combine structural and functional data of the whole gradient from tall caatinga to low caatinga (differentiated here as tall bana, low bana, and open bana following denominations by Bongers et al. 1985) for a better depiction of the Amazonian caatinga forests. The present contribution focuses on the ecophysiological aspects of the caatinga vegetation on white sands. The discussion of ecophysiological features of the herbaceous vegetation in white-sand ecosystems of the upper Rio Negro basin is included in Chap. 11.

## 4.2 Environment

### 4.2.1 Caatinga Distribution and Climate

Amazon caatinga forests in the Amazonas state of Venezuela are located south of the 5° parallel, in areas with annual rainfall above 2500 mm on strongly leached white sands. Area covered amounts to 37,000 km<sup>2</sup> of tall caatinga and 14,000 km<sup>2</sup> of low and open caatinga (Adeney et al. 2016). Floristic and structural features of Amazon caatinga forests have been described in three areas of the Amazonas state of Venezuela, including San Carlos de Río Negro in the upper Río Negro basin (01° 56'N, 67°03'W) (Klinge et al. 1977; Klinge and Medina 1979; Klinge and Herrera 1983; Bongers et al. 1985; Dezzeo et al. 2000; Klinge and Cuevas 2000; Aymard et al. 2009), La Esmeralda in the upper Orinoco basin (3°10'N, 65°33'W) (Coomes and Grubb 1996), and the area between Maroa and Yavita, about 100 km northeast from San Carlos (Aymard et al. 2009). In the area of San Carlos de Río Negro, the caatinga forests are found on white sands, frequently podzolized, on geomorphic positions where it receives the leachates from surrounding hilly lateritic areas (Medina and Cuevas 1989).

More recent studies in the neighboring areas of Brazil and Colombia describe ecosystems similar in floristic composition, structure, and ecological behavior, including the Parque Nacional Pico Neblina (0°24'N, 66°18'W) (Boublil 2002), the Estación Biológica El Zafire, Reserva Biológica del Río Calderón (4°0' 20.9" S, 69°53'55.2" W) (Jiménez et al. 2009), and along the upper Río Negro between 0 and 1.5°N (Stropp et al. 2011).

In the upper Río Negro, the climatic regime is characterized by monthly rainfall above 100 mm around the equator, while further south the annual rainfall shows a short dry period (Medina and Cuevas 1989; Stropp et al. 2011) (Fig. 4.1). The annual distribution of rainfall is clearly seasonal. Northern Amazon caatinga locations receive the largest rain volumes between May and July, the peak values ranging from 300 to 500 mm per month. The localities south of the equator receive larger volumes between February and April.

Mean monthly rainfall near or above 100 mm and average temperatures above 25 °C confirm a very humid climate, but water surplus is frequently counteracted by the low water holding capacity of the sandy soils. Besides, seasonality is accentuated by the number of dry days per month, defined as rainless days or days when rainfall does not compensate evaporation measured in a meteorological tank (tank A). At the San Carlos site, the number of dry days per month varies from a maximum of 20 during the dry season to eight or less during the rainy season (Medina and Cuevas 1989).

The number of dry days per month is ecologically significant due to the low water holding capacity of the sandy soils. Thus, the period between November and February is relatively dry, and this is reflected in the phenological behavior of the vegetation. In San Carlos de Río Negro, tree species flower mainly between November and March (Clark et al. 2000).



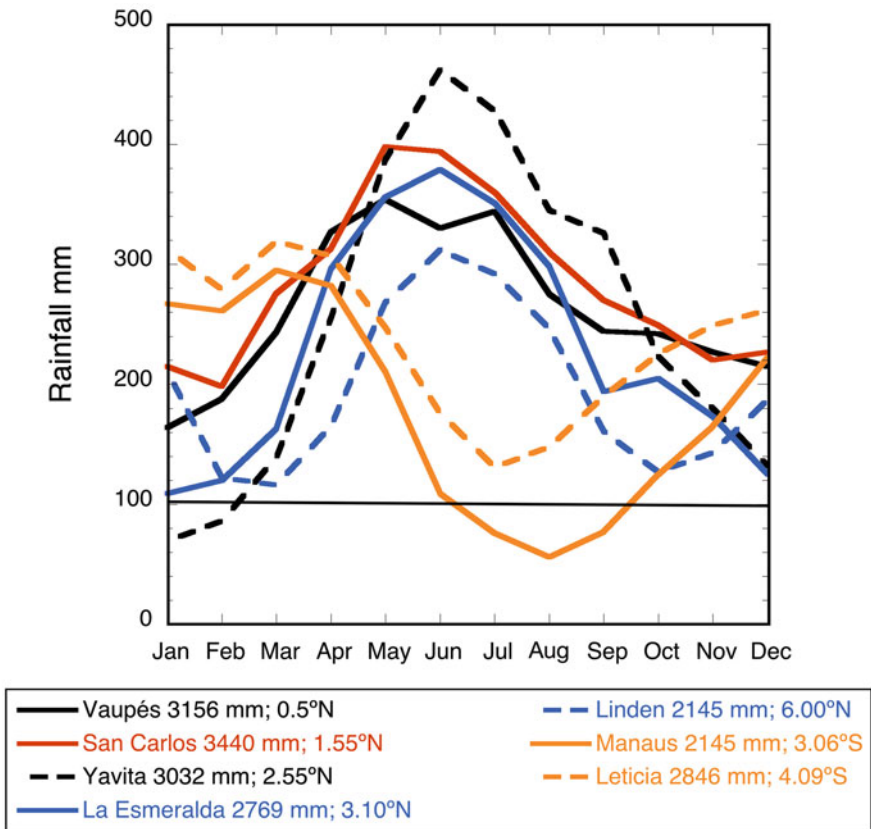


**Fig. 4.1** Monthly rainfall patterns at localities in the central and northern Amazon basin mentioned in the text. Data source: from the European Centre for Medium-Range Weather Forecasts (1999–2019) through [Climate-Data.org](https://climate-data.org) (Attribution-NonCommercial 4.0 International (CC BY-NC 4.0))

### 4.2.2 Soil Characteristics and Flooding Regime

Soils of the tall caatinga have loamy sand to sandy textures in the A horizon and high organic matter content in the A and Bh horizons (Schargel et al. 2001; Aymard et al. 2009). The B horizon is well developed below 1 m depth (Klinge et al. 1977; Franco and Dezzeo 1994). Bongers et al. (1985) and Coomes and Grubb (1996) did not report the presence of this horizon in their study sites.

Amazon caatinga soils are nutrient-poor, particularly in nitrogen (N), but high rainfall and sandy textures allow free soil solution flow transporting cations leached from lateritic soils located at higher geomorphic terrains surrounding caatinga forests (Tiessen et al. 1994).

Topographic position plays a critical role in water relations of sandy soils. Klinge et al. (1977) and Bongers et al. (1985) showed that small variations in relative soil

elevation determine strong variations in the water saturation regime. Franco and Dezzeo (1994) measured the level of soil saturation during 15 months in forests near San Carlos de Río Negro and showed that tall caatinga soils remained saturated most of the year, particularly after strong rain events, whereas low caatinga soils remained saturated at 75 cm depth around 85% of the year, but only 31% of the year at 20 cm depth.

Aymard et al. (2009) reported that low caatingas were more vulnerable to short rainless periods on soils resting on bedrock at 120 cm depth. Dry days cause a rapid reduction in water availability in such relatively shallow sandy soils. Soil water saturation reduces N availability because of decreased microbial activity but increases P availability by reductive dissolution of Fe ( $\text{PO}_4$ ) (Cuevas and Medina 1990).

---

### 4.3 Species Composition and Productivity

#### 4.3.1 Floristic Composition and Structural Variation

The floristic composition of the caatinga forests in Venezuela has been documented by Clark et al. (2000) and Dezzeo et al. (2000) in San Carlos de Río Negro, Coomes and Grubb (1996) in La Esmeralda, and Aymard et al. (2009) in San Carlos de Río Negro and the forests between the towns of Maroa and Yavita in the upper Guainía river (Río Negro basin).

Caatinga forests have several genera in common, but despite physiognomic similarities, they may be separated by the presence of marker species (Table 4.1). The tall caatingas share the genera *Micrandra*, *Eperua*, and *Caraipa*, but with different species. Similarly, banas share characteristic genera such as *Pachira* and *Clusia*. However, *Catostemma sancarlosianum*, *Compsonera sprucei*, and *Pradosia schomburgkiana* are distinctive species of the low and open banas in San Carlos, while *Byrsonima wurdackii* appears only in La Esmeralda.

Species dominance is pronounced in most reported caatinga forests. In the San Carlos tall caatinga, four species are responsible for 63% of the community importance value ( $\text{IVI} = \sum [\text{relative density} + \text{frequency} + \text{relative dominance}]$ ) in a 0.6 ha plot containing 39 species with  $\geq 10$  cm dbh (Dezzeo et al. 2000). Total basal area in the same plot amounted to  $31.3 \text{ m}^2 \text{ ha}^{-1}$  with *Micrandra sprucei*, *Eperua leucantha*, *Micropholis maguirei*, and *Caraipa densifolia* as dominant species (Fig. 4.2a). Structural analyses of caatinga plots reported by Klinge and Herrera (1983) (1.3 ha plot) and Aymard et al. (2009) ( $3 \times 0.1$  ha plots) confirm the dominance of the first two species.

In a species-rich tall caatinga forest in Yavita with 79 species and 530 individuals in 0.1 ha, the 10 most important species conform 55% of the total IVI and account for 61% of the individuals (Fig. 4.2b).

In a study of white-sand forests conducted near San Gabriel da Cachoeira ( $0.1^\circ\text{S}$ ), in the upper Río Negro basin, about 200 km south of San Carlos, Stropp et al. (2011) surveyed three 1-ha plots of forests similar to those described above. The plots had between 547 and 642 trees per ha, and up to 102 species per ha (Fig. 4.2c). *Eperua*

**Table 4.1** Characteristic tree species in caatinga forest at San Carlos de Río Negro and La Esmeralda

San Carlos	La Esmeralda
<b>Tall caatinga</b>	
White sands, thick surficial humus layer, extended flooding Trees 20 m, $\leq 30$ cm dbh <i>Micrandra sprucei</i> <i>Eperua leucantha</i> <i>Micropholis maguirei</i> <i>Caraipa densifolia</i> <i>Pradosia schomburgkiana</i>	White sands, thick surficial humus layer, seasonal flooding Trees 18–23 m, $\leq 30$ cm dbh <i>Pachira amazonica</i> <i>Caraipa longipedicellata</i> <i>Iryanthera elliptica</i> <i>Micrandra siphonoides</i> <i>Eperua obtusata</i>
<b>Low caatinga</b>	
White sands, surficial ground water level, quick depth increase during dry days	White sands, thick superficial humus layer Ground water level near the surface during humid months
Small trees and shrubs 3–8 m, trees $\leq 20$ cm dbh	
<i>Aspidosperma verruculosum</i> <i>Pradosia schomburgkiana</i> <i>Catostemma sancarlosianum</i> <i>Pachira sordida</i> <i>Mouriri uncitheca</i> <i>Clusia</i>	<i>Pachira amazonica</i> <i>Byrsonima wurdackii</i> <i>Caraipa longipedicellata</i> <i>Iryanthera elliptica</i> <i>Eperua obtusata</i> <i>Clusia spathulifolia</i>

Source: data from Klinge et al. (1977), Bongers et al. (1985), Sobrado and Medina (1980), Coomes and Grubb (1996)

*leucantha* dominated with a number of individuals accounting for between 26% and 44% of the total.

The study by Boubli (2002) in a caatinga located on the piedmont of Pico de la Neblina about 140 km south-east of San Carlos showed similar composition. The five species with highest importance value were *Eperua leucantha*, *Hevea cf. brasiliensis*, *Micrandra sprucei*, *Eschweilera* sp., and *Micrandra spruceana*.

### 4.3.2 Biomass and Nutrient Content

Biomass studies in San Carlos de Río Negro by Klinge and Herrera (1983) and Bongers et al. (1985) documented the sequence of Amazon caatinga physiognomy, showing the range of variation from tall forests to open woody scrub on white sands. A Google Earth image from the surroundings of the Bongers et al.'s (1985) study site shows the contrast between dark green tall forests (terra-firme and tall Amazon caatinga) and lighter green areas of decreasing vegetation density including varieties of low caatinga (Fig. 4.3a). The vegetation map of Bongers et al. (1985) shows various levels of caatinga with differences up to 4.5 m between the reference elevation of the tall caatinga and that of the open bana (Fig. 4.3b). We included the original denominations of tall bana, low bana, and open bana as designations of

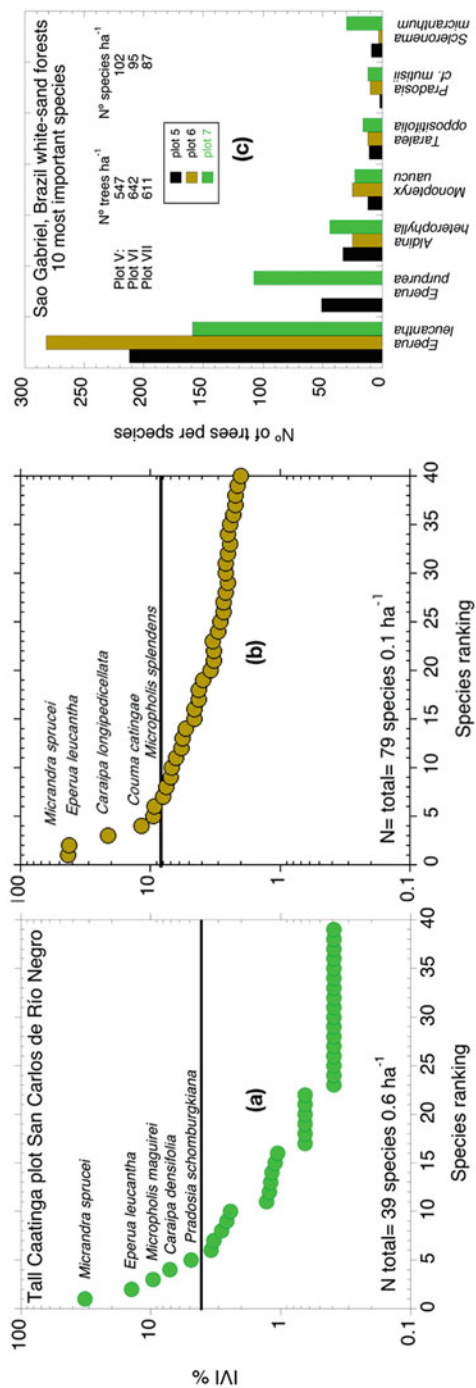


**Fig. 4.2** Species dominance at several Amazon caatinga sites in the upper Rio Negro basin expressed as % of importance value index and the number of trees per species; (a) tall caatinga near San Carlos de Rio Negro (data from Dezzzo et al. 2000); only the five dominant species are named; (b) species-rich tall caatinga along the Maroa-Yavita road (data from Aymard et al. 2009) 120 km north of San Carlos; (c) forest plots on white sands near São Gabriel da Cachoeira, Brazil, 200 km south of San Carlos (data from Stropp et al. 2011)

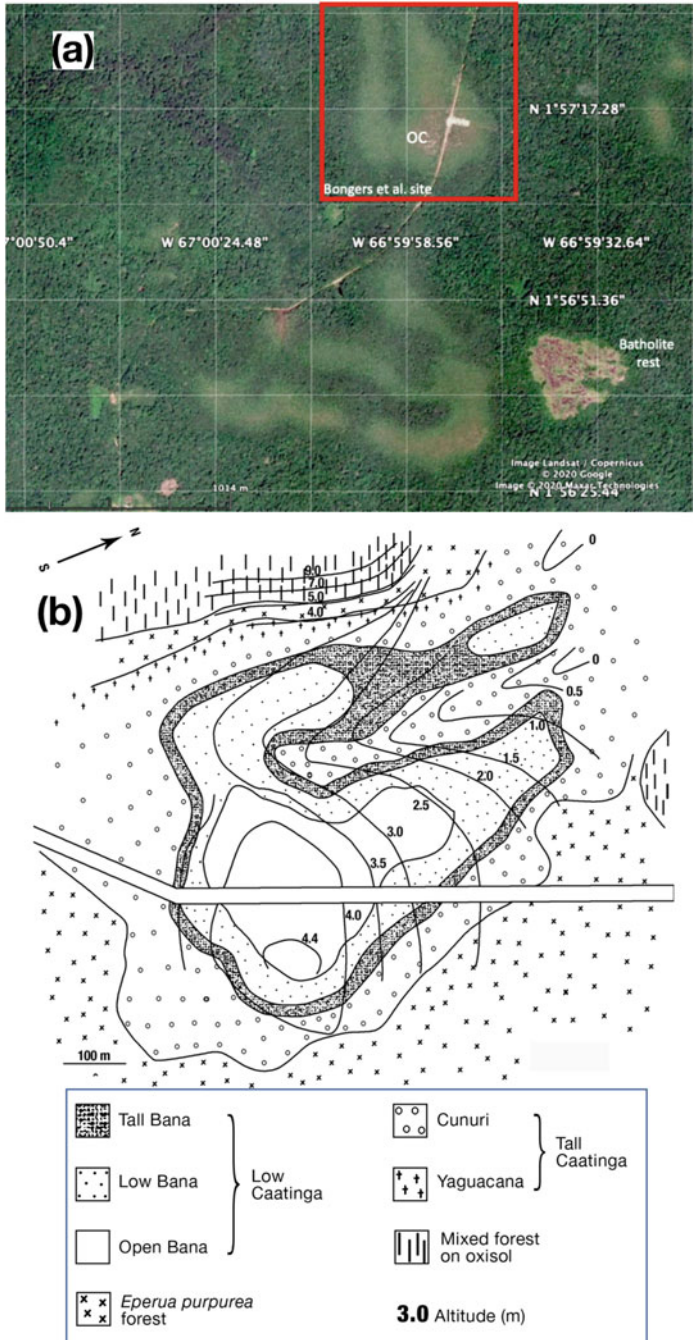


**Fig. 4.3** (a) Image from Google Earth showing the location of the Bongers et al. (1985) site surrounded by tall forests and different forms of Amazon caatinga; areas with lighter color correspond to the less dense Amazon caatinga; remnant of a batholite outcropping in the area

low caatinga of varying density. In the map mentioned above, the location of terra-firme and *Eperua purpurea* forests can be clearly separated from the different forms of Amazon caatinga: “cunuri” corresponding to a facies dominated by *Micrandra sprucei* and “yaguacana” corresponding to a facies dominated by *Eperua leucantha*.

Together, the results of Klinge and Herrera (1983) and Bongers et al. (1985) show that total biomass amounted to about 850 Mg ha<sup>-1</sup> in some tall caatinga plots but only 20 Mg ha<sup>-1</sup> in open bana plots. In Fig. 4.4a, the biomass axes are depicted on a log scale to better appreciate the low biomass values. The figure shows that as the total biomass increases, the aboveground portion grows faster than that of the belowground organs. The point where there is an equal proportion of above- and belowground organs is about 200 Mg ha<sup>-1</sup>, and that is the biomass delimiting tall from low caatinga plots. The proportion of belowground to aboveground biomass changes significantly with the total biomass. The percentage of roots decreased rapidly from about 90% in the open low caatinga to 30% in taller forests with total biomass amounting to 300 Mg ha<sup>-1</sup> or more (Fig. 4.4b). This tendency can be considered an indicator of the constraints to plant growth in the Amazon caatinga. The constraints can be summarized as (a) nutrient limitation, most probably due to low availability of N and P, (b) recurrent flooding in the tall caatinga, estimated from high frequency of zero soil water tension between 20 and 75 cm depth (Franco and Dezseo 1994), and (c) recurrent water stress, especially in the case of low and open caatingas, associated with the low water holding capacity of white sands and their relative geomorphic positions favoring water drainage.

The basal area (BA) of the caatinga forests is well correlated with aboveground biomass, covering a range of 2–75 m<sup>2</sup> ha<sup>-1</sup> from 6 to 600 Mg ha<sup>-1</sup>. Moreover, the aboveground biomass allows estimating with confidence the leaf area index (LAI) (Fig. 4.5). Most plots measured by Klinge and Herrera (1983) had LAI values between 3 and 6. The two plots with largest aboveground biomass figures showed LAI values reaching 9 and above, which are relatively high for tropical forests (Asner et al. 2003; Clark et al. 2008).

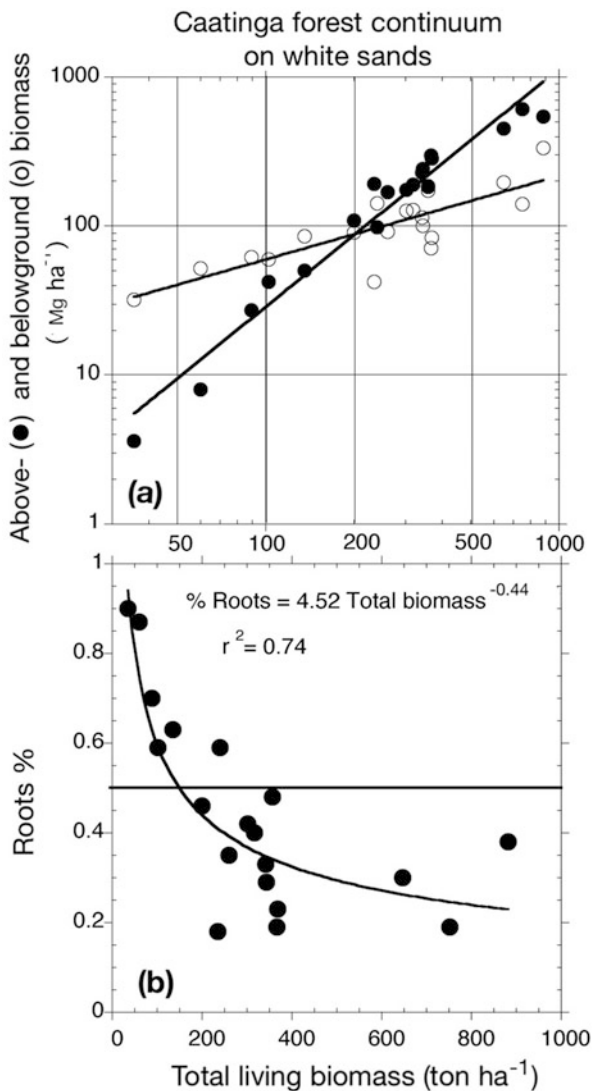
Table 4.2 summarizes the physiognomic sequence of the Amazon caatinga as measured in San Carlos de Río Negro. Average height, basal area, and LAI decrease from tall caatinga to low open caatinga, whereas stem density increases markedly in the opposite direction. Total biomass decreases markedly in the transition from closed low caatinga to sparse and open low caatinga, whereas root biomass increases from 33% to 88%. A significant differentiation between the selected subtypes is the range of specific leaf area (SLA), a parameter that estimates the amount of leaf area per unit dry matter invested in leaf construction. Leaves of the low caatinga are thicker and probably denser. Lower SLA values are also associated with lower photosynthetic capacity, but also with higher drought tolerance.



**Fig. 4.3** (continued) between San Carlos and Solano, probably the rock type from which sandy soils originated; **(b)** map depicting the extension of the low caatinga types sampled for biomass and chemical analysis



**Fig. 4.4** (a) Linear relationship between fractions of above- and belowground biomass and total biomass in the continuum of Amazon caatinga at San Carlos de Río Negro; (b) root fraction from total biomass (data from Klinge and Herrera 1983, and Bongers et al. 1985)



Inventories of main nutrients ( $\text{kg ha}^{-1}$ ) measured in a caatinga gradient in San Carlos de Río Negro show in each vegetation type larger mass of N and smaller mass of P (Fig. 4.6). The cation amounts followed the sequence  $\text{K} > \text{Ca} > \text{Mg}$ , except in the low bana where Ca was higher than K. Despite the smaller total biomass in tall bana compared to tall caatinga, the inventories of cations were higher in the former, indicating higher concentration of those cations in the biomass of tall bana trees.

Lira-Martins et al. (2019) assessed the leaf nutrient concentrations of trees in Amazonian forests growing on soils of low nutrient status ( $\sum \text{ex Ca} + \text{K} + \text{Mg} < 20 \text{ mmol kg}^{-1}$ ) from Bolivia, Perú, and Ecuador. The survey did



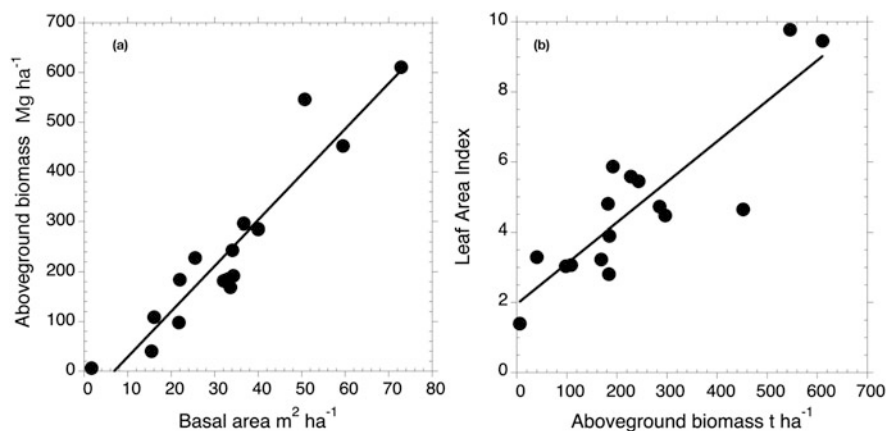


**Fig. 4.5** Relationships between basal area and aerial biomass (a) and to leaf area index (b) in 16 plots of Amazon caatinga in San Carlos de Rio Negro (data from Klinge and Herrera 1983, and Bongers et al. 1985)

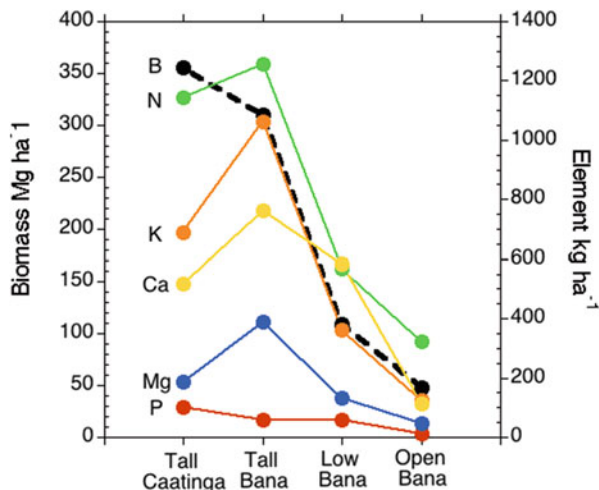
**Table 4.2** Gradation of structural characteristics and biomass distribution in Amazon caatinga as measured in topographic sequences at San Carlos de Rio Negro

	Tall Caatinga	Tall Bana	Low Bana	Open Bana
Maximum height (m)	20.9	18.3	6.3	1.7
Tree density (n/100 m <sup>-2</sup> )	114	260	280	600
Basal Area (m <sup>2</sup> ha <sup>-1</sup> ) DBH ≥ 1 cm	36.9	32.1	15.5	1.7
Leaf size (Raunkiaer)	m <sub>e</sub> m <sub>a</sub>	m <sub>e</sub>	n <sub>o</sub>	n <sub>o</sub>
Specific Leaf area range (cm <sup>2</sup> g <sup>-1</sup> )	20–160	31–84	30–138	27–41
Leaf Area Index	5.1	4.8	3.3	1.4
Biomass trees >1 cm DBH				
Aboveground biomass (kg m <sup>-2</sup> )	27.2	18.2	4	0.6
Belowground biomass	13.2	12.8	6.9	4.2
Total biomass	40.4	31	10.9	4.8
% Underground	33	40	64	88
Root/shoot ratio	0.5	0.7	1.8	7

Source: data from Klinge and Herrera (1983) (13 plots 10 × 10 m) and Bongers et al. (1985) (7 plots 5 × 5 m); Raunkiaer leaf sizes: m<sub>a</sub> macrophyll (180–1640 cm<sup>2</sup>), m<sub>e</sub> mesophyll (45–180 cm<sup>2</sup>), n<sub>o</sub> notophyll (20–45 cm<sup>2</sup>)

not include white-sand soils. Comparing the average leaf element concentrations (values in mg g<sup>-1</sup>) of this survey with the leaf analyses conducted in the tall caatinga of San Carlos de Río Negro, we find that concentrations of N, P, K, and Ca of white sands trees are 45–60% lower (N 22.4 vs 10.1, P 1.0 vs 0.6, K 9.4 vs 5.7, and Ca 5.2 vs 2.4), whereas Mg averages were nearly identical (2.3 vs 2.4).

**Fig. 4.6** Biomass (B) and nutrient inventories (N, P, K, Ca, Mg) along the topographic gradient



### 4.3.3 Primary Productivity, Litter Production, and Nutrient Cycling

There are few studies on the net primary productivity (NPP) of Amazonian forests on white sands. The studies of Aragão et al. (2009) and Jiménez et al. (2009) in the Forest Reservation of Río Calderón (ZAR-01), near Leticia in Colombia, are among the most comprehensive. The authors estimated an NPP of  $9.3 \pm 1.3 \text{ Mg C ha}^{-1} \text{ yr}^{-1}$ , corresponding to about  $18.6 \text{ Mg organic matter ha}^{-1} \text{ yr}^{-1}$  ( $0.5 \text{ g C per g organic matter}$ ), 54% of which corresponded to aboveground biomass. Litter fall was considered as an estimator of canopy productivity and amounted to  $2.7 \pm 0.1 \text{ Mg C ha}^{-1} \text{ yr}^{-1}$  ( $5.4 \text{ Mg organic matter ha}^{-1} \text{ yr}^{-1}$ ). This amount corresponded to 52% of aboveground NPP and to 29% of total NPP. These proportions are well in agreement with previous estimations of forest productivity based on litter fall (Bray and Gorham 1964; Clark et al. 2001; Mahli et al. 2011). We estimated NPP in white-sand forests in San Carlos de Río Negro and La Esmeralda using the production of fine litter (leaves, small branches, and flower matter), considering that the fine litter production makes up to 50% of aboveground NPP and 30% of total NPP (Table 4.3).

In San Carlos, the concentration of N and P in litter was higher and that of K lower in the tall caatinga as compared to the low caatinga. In La Esmeralda, plot litter production and concentrations of N, P, K, and Mg were essentially similar in tall and low caatingas (Coomes 1997). However, there was a much higher concentration of Ca in the low caatinga (Table 4.3). Tall caatinga plots showed in units of  $\text{mol ha}^{-1} \text{ yr}^{-1}$  that N is the element cycling in higher amounts (1990–2400), followed by Ca (700–780), Mg (300–514), K (205–230), and P (26–65).

The figures on nutrient concentration and nutrient return in litter confirm previous assessments indicating that caatinga forests are comparatively poorer in N and P, but richer in Ca and Mg than forests on other soil types (Cuevas and Medina 1986).

**Table 4.3** Nutrient flux in leaf litter fall in Amazon tall caatinga and low caatinga forests at San Carlos de Río Negro and La Esmeralda

	San Carlos		La Esmeralda	
	Tall	Low	Tall	Low
Litter fall ( $\text{mg ha}^{-1} \text{ yr.}^{-1}$ )				
Leaf	4.0	2.1	4.3	4.2
Total	5.4	2.4	6.7	5.2
Net primary productivity (estimation: total litter fall x 3.3)				
	18	8	22	17
Nutrient concentration in leaf litter ( $\text{mg g}^{-1}$ )				
Nitrogen	7.0	5.8	7.5	7.0
Phosphorus	0.5	0.2	0.2	0.2
Potassium	2.1	4.7	2.0	2.3
Calcium	7.7	7.4	6.2	15.5
Magnesium	3.1	2.5	1.7	2.0
Nutrient flux in leaf litter ( $\text{kg ha}^{-1} \text{ yr.}^{-1}$ )				
N	27.9	12.1	33.0	29.0
P	2.0	0.4	0.8	1.0
K	8.0	9.9	9.1	10.0
Ca	31.4	15.2	28.0	69.0
Mg	12.5	5.1	7.3	8.3

## 4.4 Physiological Ecology

### 4.4.1 Leaf Traits

Caatinga vegetation is remarkably sclerophyllous. Mature leaves are hard, coriaceous, and even brittle in some cases, due to the abundance of sclerenchyma in their tissues. These characteristics have been documented anatomically (Sobrado and Medina 1980; Medina et al. 1990; Sobrado 2009a) and correlated with several sclerophylly indexes such as toughness (measured with special penetrometers), area/mass ratios, and total fiber to protein ratios. Leaves of sclerophyllous plants have also remarkable low concentrations of N and P on a mass basis, explained by the thickness of cell walls and the abundance of fibrous components. Comparison of average values of leaf mass/area and N and P concentrations with global data bases highlights the strong sclerophyllous character of the caatinga woody species (Poorter et al. 2009; Tian et al. 2018 (Table 4.4).

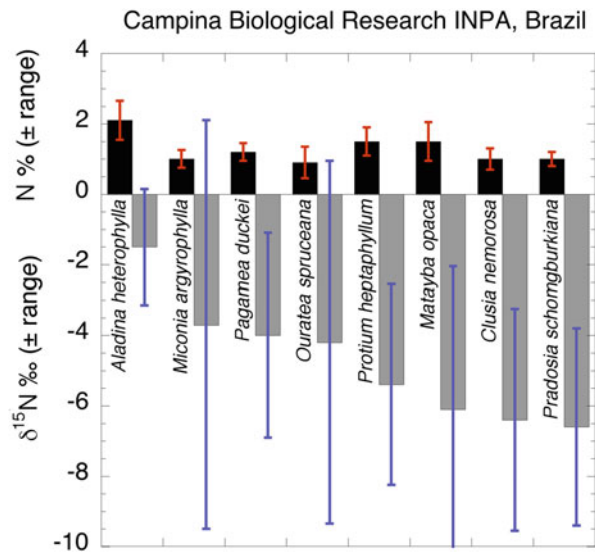
Another remarkable trait of leaves from caatinga forests is their strongly negative  $\delta^{15}\text{N}$  values as shown first by Sobrado (2008) and Nardoto et al. (2008) and confirmed by Mardegan et al. (2009) and Sobrado (2010). These negative leaf values have been repeatedly found despite the consistently positive soil values (Fig. 4.7). Soil  $\delta^{15}\text{N}$  values in *campina* and *campinarana* sites near Manaus increase smoothly from 3.5‰ near the soil surface to around 8‰ at 45 cm depth. In forests on Oxisols

**Table 4.4** Comparison of Leaf Mass/Area (LMA) ratios, and leaf concentrations of N and P between white-sand woody species and global data sets

	<i>n</i>	LMA g m <sup>-2</sup>	N	P	N/P	Ref
			mg g <sup>-1</sup>			
Tropical evergreen Broadleaved plants	1679		17.0	0.78	21.9	(1)
Tropical rain forest	680	73				(2)
Tropical deciduous forest	320	83				
Woodland	350	129				
Shrubland	690	168				
Open caatinga	18	239	8.6	0.51	18	(3)
Open caatinga	14	227	7.4	0.49	16	(4)
Tall caatinga	6	152	11.6	0.73	16	(4)

Source: data from (1) Tian et al. (2018); (2) Poorter et al. (2009); (3) Sobrado and Medina (1980); (4) Medina et al. (1990)

**Fig. 4.7** Nitrogen concentrations and  $\delta^{15}\text{N}$  values of mature leaves of woody species from white-sand vegetation in Brazil (data from Mardegan et al. 2009)



in the Amazon basin,  $\delta^{15}\text{N}$  values of both soils and plant leaves are mostly positive and decrease consistently with rainfall (Nardoto et al. 2008; Sobrado 2010).

The negative  $\delta^{15}\text{N}$  values have been explained mainly as resulting from the widespread occurrence of mycorrhizal symbiosis in white-sand forests, and the extreme N deficiency in white-sand soils compared to Oxisols under forest (Sobrado 2008, 2010; Mardegan et al. 2009). Indeed, in a comprehensive review on the global patterns of foliar N isotopes, Craine et al. (2009) found that  $\delta^{15}\text{N}$  decreased with local rainfall and mycorrhizal associations and increased with higher leaf N and lower P concentrations. However, it is necessary to reassess local conditions such as the actual N availability, the role of P deficiency, and the recurrent flooding.

Nitrogen availability at the root level plays a relevant role in N fractionations. Craine et al. (2015) define availability as the soil supply relative to plant demand for N and, in opposition to the report of Craine et al. (2009), state that if N concentration is low, the discrimination during uptake by the roots is greatly reduced, while significant fractionation takes place only when soil N is high. If low P and hypoxia reduce N demand by the plant, it may result in strong N fractionation. This has been shown in P-limited ecosystems such as bog plants (Clarkson et al. 2005; Medina et al. 2008) and mangroves growing on peat (McKee et al. 2002; Medina et al. 2010).

#### 4.4.2 Water Relations

Sclerophyllous leaf anatomy has been frequently related to water-stress-tolerant plants, particularly in shrubs and trees from Mediterranean climates (Logullo and Salleo 1988). A comparison of sclerophyllous leaf traits between species from tall and low caatingas and Mediterranean climate sclerophyllous species (Cape Town, South Africa; Palo Alto, California; and Perth, Australia) showed a high degree of similarity between sclerophyllous indexes and concentrations of N and P, the major difference being the much larger leaf size of white-sand vegetation sclerophylls (Medina et al. 1990). This fact is explained by higher water availability throughout the year in Amazonian vegetation.

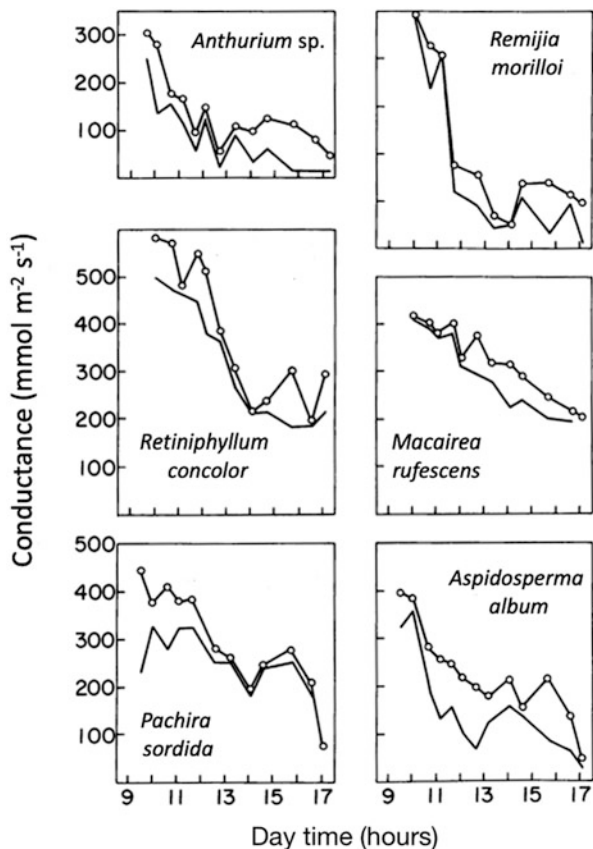
The study of water relations in Amazon caatinga plants, particularly from low caatinga, shows that sclerophylls are highly sensitive to air humidity. Stomates close progressively during rainless days shortly before noon and do not recover in the afternoon (Fig. 4.8). Therefore, leaf water potential seldom decreases below  $-1.5$  MPa (Medina et al. 1990).

Comprehensive water relations studies by Sobrado (2009b, 2012), including species from tall and low caatingas, showed that during rainy days minimum leaf water potentials were similar for all species approaching  $-1$  MPa at noon time (Fig. 4.9). During rainless days however, low caatinga species reached values below  $-1.5$  MPa, whereas two tall caatinga species never reached that level. Notably, the water potential at turgor loss point ( $\approx$  osmotic potential of the vacuolar sap) was much lower for open caatinga species (from  $-1.9$  to  $-2$  MPa) than for tall caatinga species ( $-1.1$  to  $-1.4$  MPa).

These studies support the concept of peinomorphosis (Walter and Breckle 2004), suggesting that sclerophyllous species are more competitive in nutrient-poor environments, particularly poor in P (Beadle, 1962). The oligotrophic character of white-sand soils was suggested as an explanation for the sclerophyllous character of the Amazon caatinga in the upper R o Negro vegetation by Ferri (1960, 1961).

Stomatal sensitivity to leaf-air water vapor deficit leads to considerable limitation of transpiration, and it can result in leaf overheating during rainless, sunny days, especially because the large leaf sizes are associated with high boundary layer resistances. This effect is counteracted by the pronounced leaf inclination that is dominant in Amazon caatinga species, thus reducing radiation load at noon and

**Fig. 4.8** Decrease in leaf conductance during the daytime shown by species of an open bana; each figure includes measurements on two separate leaves (data from Medina et al. 1990)



allowing maintaining leaf temperatures below harmful levels despite low stomatal conductance (Medina et al. 1978).

#### 4.4.3 Photosynthesis

Sclerophyllous plants tend to have relatively low maximum rates of photosynthesis ( $A_{max}$ ). Medina and Cuevas (2000) showed that the photosynthetic rate of a set of species from open caatinga decreased significantly from 10–12  $\mu\text{mol m}^{-2} \text{s}^{-1}$  during the morning down to around 5  $\mu\text{mol m}^{-2} \text{s}^{-1}$  in the afternoon as a result of decreased stomatal conductance as discussed above (Fig. 4.10). Sobrado (2009b) reported  $A_{max}$  values for low caatinga species in San Carlos de Río Negro ranging from 4.3  $\mu\text{mol m}^{-2} \text{s}^{-1}$  in *Catostemma sancarlosianum* to 6.6  $\mu\text{mol m}^{-2} \text{s}^{-1}$  in *Remijia morilloi*. The values of  $\delta^{13}\text{C}$  of several species of the low caatinga averaged -30.3‰, indicating that the sporadic water stress during rainless days is not reflected in the natural abundance of  $^{13}\text{C}$  in leaf tissues (Sobrado 2008).

**Fig. 4.9** Minimum water potential during rainy and rainless days and the water potential at zero turgor in leaves of tree species from tall caatinga and low bana in San Carlos de Río Negro (data from Sobrado 2009a, 2012)

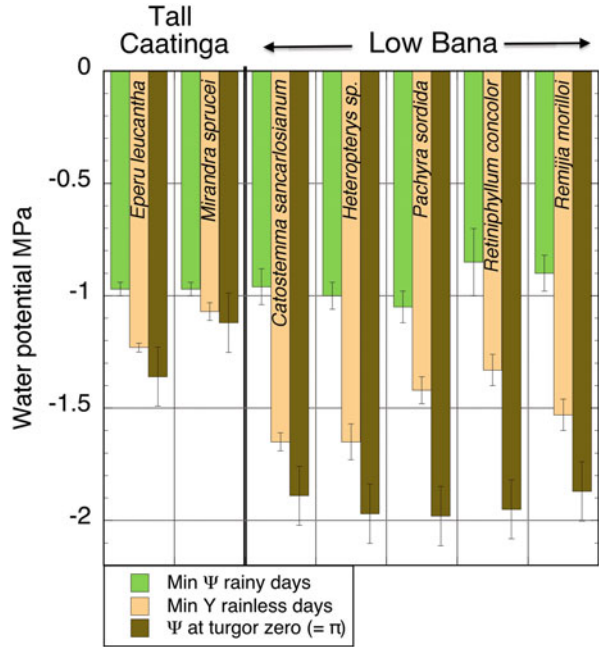
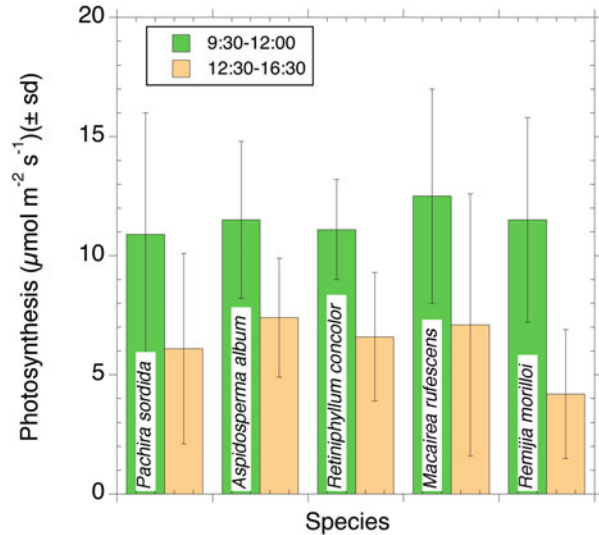


**Fig. 4.10** Average rates of photosynthesis during morning and afternoon of low bana species (measured with an ADC portable infrared gas analyzer, under natural light, environmental CO<sub>2</sub>, and humidity) (data from Medina and Cuevas 2000)



In a study of the nitrogen–photosynthesis relationships and leaf longevity in forests close to San Carlos, Reich et al. (1991, 1994) report that species with median leaf lifespan of 12 or more months have Amax rates of 5–8  $\mu\text{mol m}^{-2} \text{s}^{-1}$ .



#### 4.4.4 Leaf Lifespan

One of the most relevant physiological aspects related to sclerophylly is the leaf lifespan or leaf duration. In nutrient-poor environments, leaf construction costs are high (Sobrado 2009a), and the increase in leaf lifespan has an adaptive value because it increases the productive period of the photosynthetic area. Long-lived leaves on the other hand require defense traits to prevent or reduce herbivore attacks.

In a multiannual demographic study in the forests near San Carlos de Río Negro, Reich et al. (2004) showed that the median leaf lifespan of primary species of Amazon caatinga lasts well beyond one year. Leaf lifespans of canopy leaves are 2–3 years in tall caatinga and 1–3 years in low caatingas (Fig. 4.11). Shade leaves of tall caatinga lasted more than 3 years in all species measured. In the same study, Reich et al. (1991) measured leaf N, specific leaf area, and photosynthesis of species differing in mean lifespans at their peak “physiological” age (i.e., young, fully

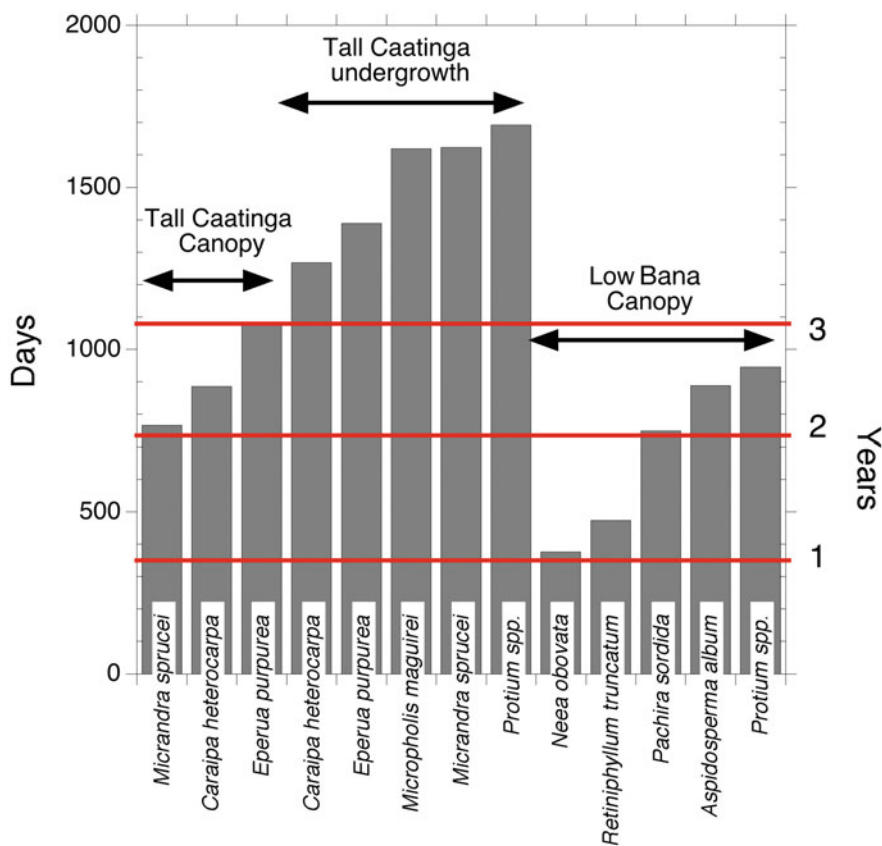


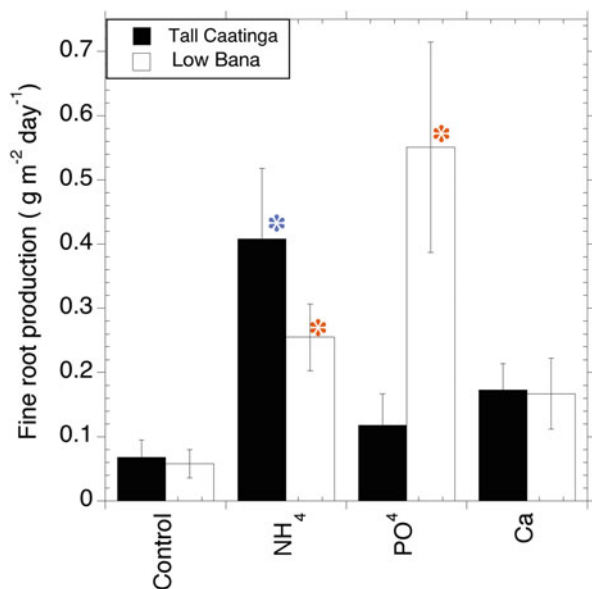
**Fig. 4.11** Median lifespan of canopy and shade leaves in tall and open bana plots in San Carlos de Río Negro (data from Reich et al. 2004)

expanded leaves). The analysis showed that species with leaf lifespan beyond 12 months have specific leaf areas below  $100 \text{ cm}^2 \text{ g}^{-1}$ , optimum photosynthetic rates around or below  $50 \text{ nmol CO}_2 \text{ g}^{-1} \text{ s}^{-1}$ , and photosynthetic N use efficiency of around  $50 \text{ } \mu\text{mol CO}_2 \text{ mol}^{-1} \text{ N s}^{-1}$ . However, out of 10 species,  $A_{\text{mass}}$  was not correlated to specific leaf in 5 species, and the slope of  $A_{\text{mass}}$  vs  $N_{\text{mass}}$  was not significant in 4, revealing that the relationships between gas exchange, leaf biochemistry, and anatomy in sclerophyllous species are not yet fully understood. In particular, it would be necessary to clearly specify how nitrogen is allocated between photosynthetic proteins, pigments, and herbivore deterring compounds.

#### 4.4.5 Nutrient Limitations and Production of Fine Roots

Nutrient limitations in the rainforests in the area of San Carlos de Río Negro have been assessed through measurements of nutrient use efficiency (Cuevas and Medina 1986) and through measurements of the fine root growth response to additions of specific nutrients (N, P, and Ca) (Cuevas and Medina 1988). A summary of these experiments in tall and low caatingas showed that fine root growth in tall caatinga is enhanced by N addition in the form of  $\text{NH}_4^+$ , whereas in low caatinga enhancement was induced by increasing N supply, and more markedly by the addition of P (Fig. 4.12). The same type of experiments showed that terra-firme forests are not constrained by N but are responsive to both P and Ca additions.

**Fig. 4.12** Growth of fine roots into vermiculite-filled cylinders tucked 10 cm into the soils; cylinders saturated with  $\text{NH}_4\text{Cl}$ ,  $\text{K}_2\text{PO}_4$ , and  $\text{CaCl}_2$  solutions, respectively; the stars indicate significant difference with the control within each forest type ( $p = 0.1$ , Kruskal–Wallis non-parametric analysis of variance) (blue tall caatinga; red low caatinga) (data from Cuevas and Medina 1988)



## 4.5 Mycorrhizal Associations in White-Sand Forests of the Río Negro Region

The extremely low nutrient status suggested that special mechanisms for nutrient acquisition and conservation should be operating in forests on white-sand soils. It was hypothesized that trees in nutrient-poor soils were strongly dependent on mycorrhizal associations for nutrient collection and uptake. The “direct nutrient cycling” hypothesis of Went and Stark (1968) inspired several studies in Amazonian forests (Herrera et al. 1978). Singer and Araujo (1979) observed that forests on white sands accumulate slowly decomposing organic matter and showed that several characteristic species of forests on white sands were obligatory ectotrophic mycorrhizae. The authors suggested that this is a general trend in forests on white sands under wet climates. Studies on mycorrhizal associations in other Amazonian forest sites confirmed the occurrence of ectomycorrhizal species dominating in patches within low caatinga vegetation, but ectotrophic species were restricted to a relatively small number of genera, belonging mostly to Fabaceae, Nyctaginaceae, and Polygonaceae (Moyersoen 1993). Endomycorrhizae, however, were abundant in all caatinga sites, including species that had both mycorrhiza types on the same tree. A study carried out outside the Amazon basin to test the hypothesis that forests on white sands are dominated by ectomycorrhizal species concluded that most species developed VA mycorrhizae, while ectomycorrhizae were present only in Dipterocarpaceae and Fagaceae species and one Myrtaceae species (Moyersoen et al. 2001).

Ectomycorrhizal fungus species have been surveyed recently in plots of white-sand forests in western Amazon (Colombia) where species of Fabaceae belonging to the genera *Dycimbe* and *Aldina* are common. Both genera are well-known hosts of ectomycorrhizal fungi (Vasco-Palacios et al. 2018). The authors report that white-sand forests support a high ectomycorrhizal fungal diversity. The authors report that white-sand forests support a high ectomycorrhizal fungal diversity. Besides, they emphasize that several of those species form symbiotic associations with other species of Fabaceae and Dipterocarpaceae from forests in distant locations. Functional aspects of mycorrhizal symbiosis in nutrient-poor white-sand soils remain to be investigated. Little is known about the differential efficiency of nutrient uptake, the energy cost for the plant, and why should ectomycorrhizal associations be more common in white sands than in other soil types.

---

## 4.6 Concluding Remarks

Ecological research in Amazon basin forests has significantly increased in the last 30 years, as a result of strong growth of academic institutions in countries having territories within the basin, and also the development of comprehensive cooperative international projects. The field studies have allowed the understanding of the ecological adaptation to low soil nutrient availability and the evolution of sclerophylly as an integration of biological mechanisms increasing nutrient use

efficiency. Future developments along this line depend on the possibility of conducting experimental studies on the physiology and genetics of white-sands specialists. The phylogenetic guidelines for these studies are being established on sound taxonomic and biogeographic basis (Fine and Baraloto 2016; Capurucho et al. 2020).

The study of Amazon basin forests has been strongly supported by the use of a variety of satellites to measure forest optical properties, effects of land use, road construction, and agroforestry developments, and the use of flying laboratories measuring gas exchange, rain chemistry, and particulates input (Nagy et al. 2016).

## References

- Adeney JM, Christensen NL, Vicentini A, Cohn-Haft M (2016) White-sand ecosystems in Amazonia. *Biotropica* 48:7–23
- Anderson AB (1981) White-sand vegetation of Brazilian Amazonia. *Biotropica* 13:199–210
- Anderson AB, Prance GT, de Albuquerque BWP (1975) Estudos sobre a vegetação das Campinas Amazonicas – III. A vegetação lenhosa da Campina da Reserva Biológica INPA- SUFRAMA (Manaus - Caracará, km 62). *Acta Amazon* 5(3):225–246
- Aragão LEOC, Mahli Y, Metcalf DB, Silva-Espejo JE, Jiménez E, Navarrete D, Almeida S, Costa ACL, Salinas N, Phillips OL, Anderson LO, Alvarez E, Baker TR, Goncalvez PH, Huamán-Ovalle J, Mamani-Solórzano M, Meir M, Monteagudo A, Patiño S, Peñuela MC, Prieto A, Quesada CA, Rozas-Dávila A, Rudas A, Silva JA Jr, Vásquez R (2009) Above- and below-ground net primary productivity across ten Amazonian forests on contrasting soils. *Biogeosciences* 6:2759–2778
- Asner GP, Scurlock JMO, Hicke JA (2003) Global synthesis of leaf area index observations: implications for ecological and remote sensing studies. *Global Ecology & Biogeography* 12: 191–205
- Aymard GA, Schargel R, Berry P, Stergios B (2009) Estudio de los suelos y la vegetación (estructura, composición florística y diversidad) en bosques macrotérmicos no-inundables, estado Amazonas Venezuela (aprox. 01°30'– 05°55' N; 66°00'– 67°50' O). *BioLlania edic esp* 9:6–251, UNELLEZ, Guanare, Venezuela
- Barthés B (1991) Influence des caractères pédologiques sur la répartition spatiale de deux-espèces du genre *Eperua* (Caesalpinaceae) en forêt guyanaise. *Rev Ecol (Terre Vie)* 46:303–320
- Beadle NCW (1962) Soil phosphate and the delimitation of plant communities in eastern Australia. *II Ecology* 43:282–288
- Bongers F, Engelen D, Klinge H (1985) Phytomass structure of natural plant communities on spodosols in southern Venezuela: the Bana woodland. *Vegetatio* 63:13–34
- Boublí JP (2002) Lowland floristic assessment of Pico da Neblina National Park, Brazil. *Plant Ecol* 160:149–167
- Bray R, Gorham E (1964) Litter production in forests of the world. *Adv Ecol Res* 2:101–157
- Capurucho JMG, Borges SH, Cornelius C, Vicentini A, Prata EMB, Costa FM, Campos P, Sawakuchi AO, Rodrigues F, Zular A, Aleixo A, Bates JM, Ribas CC (2020) Patterns and processes of diversification in Amazonian white-sand ecosystems: insights from birds and plants. In: Rull V, Carnaval AC (eds) *Neotropical diversification: patterns and processes*. Springer, Cham, pp 245–270. <https://doi.org/10.1007/978-3-030-31167>
- Clark H, Liesner R, Berry PE, Fernández A, Aymard G, Maquirino P (2000) Catálogo anotado de la flora del área de San Carlos de Río Negro, Venezuela. *Scientia Guianae* 11:101–316
- Clark DA, Brown S, Kicklighter DW, Chambers JQ, Thomlinson JR, Ni J, Holland EA (2001) Net primary production in tropical forests: an evaluation and synthesis of existing field data. *Ecol Appl* 11(2):371–384

- Clark DB, Olivas PC, Oberbauer SF, Clark DA, Ryan MG (2008) First direct landscape-scale measurement of tropical rain forest leaf area index, a key driver of global primary productivity. *Ecol Lett* 11:163–172
- Clarkson BR, Schipper LA, Moyersoen B, Silvester WB (2005) Foliar  $^{15}\text{N}$  natural abundance indicates phosphorus limitation of bog species. *Oecologia* 144:550–557
- Coomes DA (1997) Nutrient status of Amazonian caatinga forests in a seasonally dry area: nutrient fluxes in litter fall and analyses of soils. *Can J For Res* 27:831–839
- Coomes DA, Grubb PJ (1996) Amazonian caatinga and related communities at La Esmeralda, Venezuela: forest structure, physiognomy and floristics, and control by soil factors. *Plant Ecol* 122:167–191
- Craine JM, Elmore AJ, Aidar MPM, Bustamante M, Dawson TE, Hobbie EA, Kahmen A, Mack MC, McLauchlan KK, Michelsen A, Nardoto GB, Pardo LH, Peñuelas J, Reich PB, Schuur EAG, Stock WD, Templer PH, Virginia RA, Welker JM, Wright IJ (2009) Global patterns of foliar nitrogen isotopes and their relationships with climate, mycorrhizal fungi, foliar nutrient concentrations, and nitrogen availability. *New Phytol* 183:980–992
- Craine JM, Brookshire NJ, Cramer MD, Hasselquist NJ, Koba K, Marin-Spiotta E, Wang L (2015) Ecological interpretations of nitrogen isotope ratios of terrestrial plants and soils. *Plant Soil* 396: 1–26
- Cuevas E, Medina E (1986) Nutrient dynamics within Amazonian forest ecosystems. I. Nutrient flux in fine litter fall and efficiency of nutrient utilization. *Oecologia (Berlin)* 68:466–472
- Cuevas E, Medina E (1988) Nutrient dynamics within Amazonian forest ecosystems. II. Fine root growth, nutrient availability and leaf litter decomposition. *Oecologia (Berlin)* 76:222–235
- Cuevas E, Medina E (1990) Phosphorus/nitrogen interactions in adjacent Amazon forests with contrasting soil and water availability. In: Tiessen H, López-Hernández D, Salcedo IH (eds) Phosphorus cycles in terrestrial and aquatic ecosystems. SCOPE-UNEP regional workshop 3: south and Central America. Saskatchewan Institute of Pedology, Saskatoon, Canada, pp 83–94
- Daly DC, Silveira M, Medeiros H, Castro W, Obermüller FA (2016) The white-sand vegetation of acre. *Brazil Biotropica* 48(1):81–89
- Dezzeo N, Maquirino P, Berry PE, Aymard G (2000) Principales tipos de bosque en el área de San Carlos de Río Negro, Venezuela. *Scientia Guaianae* 11:15–36
- Ferri MG (1960) Contribution to the knowledge of the ecology of the “Río Negro caatinga” (Amazon). *Bulletin Research Council Israel* 8:195–208
- Ferri MG (1961) Problems of water relations of some Brazilian vegetation types, with special consideration of the concepts of xeromorphy and xerophytism. *Arid Zone Research* 16:191–197. UNESCO, Paris
- Fine PVA, Baraloto C (2016) Habitat endemism in white-sand forests: insights into the mechanisms of lineage diversification and community assembly of the neotropical Flora. *Biotropica* 48:24–33
- Franco W, Dezzeo N (1994) Soils and soil water regime in the terra-firme - caatinga forest complex near San Carlos de Río Negro, state of Amazonas, Venezuela. *Interciencia* 19:305–316
- Herrera R, Jordan CF, Klinge H, Medina E (1978) Amazon ecosystems. Their structure and function with particular emphasis on nutrients. *Interciencia* 3:223–232
- Hueck K (1966) *Die Wälder Südamerikas*. Fischer, Stuttgart, Ökologie, Zusammensetzung und wirtschaftliche Bedeutung
- Jiménez EM, Moreno FH, Peñuela MC, Patiño S, Lloyd J (2009) Fine root dynamics for forests on contrasting soils in the Colombian Amazon. *Biogeosciences* 6:2809–28279
- Klinge H (1965) Podzol soils in the Amazon basin. *J Soil Sci* 16:95–103
- Klinge H, Cuevas E (2000) Bana: una comunidad leñosa sobre arenas blancas en el Alto Río Negro, Venezuela. *Scientia Guaianae* 11:37–49
- Klinge H, Herrera R (1983) Phytomass structure of natural plant communities on spodosols in southern Venezuela: the tall Amazon caatinga forest. *Vegetatio* 53:65–84
- Klinge H, Medina E (1979) Río Negro caatingas and Campinas, Amazonas states of Venezuela and Brazil. In: Specht RL (ed) *Ecosystems of the world 9A, heathlands and related shrublands*,

- descriptive studies. Elsevier Scientific Publications, Amsterdam-Oxford-New York, pp 483–488
- Klinge H, Medina E, Herrera R (1977) Studies on the ecology of the Amazon caatinga. 1. General features. *Acta Científica Venezolana* 28:270–276
- Lira-Martins D, Humphreys-Williams E, Strekopytov S, Ishida FY, Quesada CA, Lloyd J (2019) Tropical tree branch-leaf nutrient scaling relationships vary with sampling location. *Front Plant Sci.* <https://doi.org/10.3389/fpls.2019.00877>
- Logullo MA, Salleo S (1988) Different strategies of drought resistance in three Mediterranean sclerophyllous trees growing in the same environmental conditions. *New Phytol* 108:267–276
- Malhi Y, Dougherty C, Galbraith D (2011) The allocation of ecosystem net primary productivity in tropical forests. *Phil Trans R Soc B* 366:3225–3245
- Mardegan SF, Nardoto GB, Higuchi N, Moreira MZ, Martinelli LA (2009) Nitrogen availability patterns in white-sand vegetations of central Brazilian Amazon. *Trees* 23:479–488
- McKee KL, Feller IC, Popp M, Wanek W (2002) Mangrove isotopic ( $\delta^{15}\text{N}$  and  $\delta^{13}\text{C}$ ) fractionation across a nitrogen vs phosphorus limitation gradient. *Ecology* 83:1065–1075
- Medina E, Cuevas E (1989) Patterns of nutrient accumulation and release in Amazonian forests of the upper Río Negro basin. In: Proctor J (ed) *Mineral nutrients in tropical forest and savanna ecosystems*. Blackwell Scientific Publications, Oxford, pp 217–240
- Medina E, Cuevas E (2000) Eficiencia de utilización de nutrientes por plantas leñosas: Eco-fisiología de bosques de San Carlos de Río Negro, Venezuela. *Scientia Guaianae* 11: 51–70
- Medina E, Sobrado M, Herrera R (1978) Significance of leaf orientation for leaf temperature in an Amazonian sclerophyll vegetation. *Radiat Environ Biophys* 15:131–140
- Medina E, García V, Cuevas E (1990) Sclerophylly and oligotrophic environments: relationships between leaf structure, mineral nutrient content and drought resistance in tropical rain forests of the upper Río Negro region. *Biotropica* 22:51–64
- Medina E, Francisco M, Quilice A (2008) Isotopic signatures and nutrient relations of plants inhabiting brackish wetlands in the northeastern coastal plain of Venezuela. *Wetlands Ecol Manag* 16:51–64
- Medina E, Cuevas E, Lugo AE (2010) Nutrient relations of dwarf *Rhizophora mangle* L. mangroves on peat in eastern Puerto Rico. *Plant Ecol* 207:13–24
- Moyersoen B (1993) Ectomicorrizas and micorrizas vesículo-arbusculares en Caatinga Amazónica del Sur de Venezuela. *Scientia Guaianae* 3:83
- Moyersoen B, Becker P, Alexander IJ (2001) Are ectomycorrhizas more abundant than arbuscular mycorrhizas in tropical heath forests? *New Phytol* 150(3):591–599
- Nagy L, Forsberg BR, Artaxo P (eds) (2016) *Interactions between biosphere, atmosphere and human land use in the Amazon*. Springer ecological studies 227. Springer, Heidelberg
- Nardoto GB, Ometto JPHB, Ehleringer J, Higuchi N, Bustamante MMC, Martinelli LA (2008) Understanding the influences of spatial patterns on N availability within the Brazilian Amazon forest. *Ecosystems* 11:1234–1246
- Peñuela Mora MC (2014) *Understanding Colombian Amazonian white-sand forests*. Utrecht University, 167 p. isbn: 978-90-393-6196-2
- Poorter H, Niinemets Ü, Poorter L, Wright IJ, Villar R (2009) Causes and consequences of variation in leaf mass per area (LMA): a meta-analysis. *New Phytol* 182:565–588
- Reich PB, Uhl C, Walters MB, Ellsworth DS (1991) Leaf lifespan as a determinant of leaf structure and function among 23 Amazonian tree species. *Oecologia* 86:16–24
- Reich PB, Walters MB, Ellsworth DS, Uhl C (1994) Photosynthesis-nitrogen relations in Amazonian tree species I. Patterns among species and communities *Oecologia* 97:62–72
- Reich PB, Uhl C, Walters MB, Prugh L, Ellsworth DS (2004) Leaf demography and phenology in Amazonian rain forest: a census of 40 000 leaves of 23 tree species. *Ecol Monogr* 74:3–23
- Rodríguez WA (1961) Aspectos fitosociológicos das catingas do Río Negro. *Boletim Museu Paraense Emilio Goeldi* 15:41

- Schargel R, Marvez P, Aymard G, Stergios B, Berry P (2001) Características de los suelos alrededor de San Carlos de Río Negro, Estado Amazonas, Venezuela. *BioLlania edc esp* 7:234–264, UNELLEZ, Guanare, Venezuela
- Singer R, Araujo IJS (1979) Litter decomposition and ectomycorrhiza in Amazonian forests 1. A comparison of litter decomposing and ectomycorrhizal basidiomycetes in latosol terra-firme rain forest and white podzol campinarana. *Acta Amazon* 9(1):25–41
- Sioli H, Klinge H (1961) Über Gewässer und Boden des brasilianischen Amazonasgebietes. *Erde* 92(3):205–219
- Sobrado MA (2008) Leaf characteristics and diurnal variation of chlorophyll fluorescence in leaves of the ‘Bana’ vegetation of the Amazon region. *Photosynthetica* 46(2):202–207
- Sobrado MA (2009a) Cost-benefit relationships in sclerophyllous leaves of the ‘Bana’ vegetation in the Amazon region. *Trees* 23:429–437
- Sobrado MA (2009b) Leaf tissue water relations and hydraulic properties of sclerophyllous vegetation on white-sands of the upper Río Negro in the Amazon region. *J Trop Ecology* 25: 271–280
- Sobrado MA (2010) Leaf characteristics, wood anatomy and hydraulic properties in tree species from contrasting habitats within upper Río Negro forests in the Amazon region. *J Trop Ecology* 26:215–226
- Sobrado MA (2012) Leaf tissue water relations in tree species from contrasting habitats within the upper Rio Negro forests of the Amazon region. *J Trop Ecol* 28:519–522
- Sobrado M, Medina E (1980) General morphology, anatomical structure and nutrient content of sclerophyllous leaves of the “Bana” vegetation of Amazonas. *Oecologia (Berlin)* 45:341–345
- Spruce R (1908) Notes of a botanist on the Amazon and the Andes. Macmillan, London
- Stropp J, Van der Sleen P, Assunção PA, da Silva A, Ter Steege H (2011) Tree communities of white-sand and terra-firme forests of the upper Río Negro. *Acta Amazon* 41(4):521–544
- Takeuchi M (1961) The structure of the Amazonian vegetation. III. Campina forest in the Río Negro region. *J Fac Sci Univ Tokyo, Section III, Bot* 8:27–35
- Takeuchi M (1962) The structure of the Amazonian vegetation. IV. High campina forest in the upper Río Negro. *J Fac Sci Univ Tokyo, Section III, Bot* 8:279–288
- Tian D, Yan Z, Niklas KJ, Han W, Kattge J, Reich PB, Luo Y, Chen Y, Tang Z, Hu H, Wright IJ, Schmid B, Fang J (2018) Global leaf nitrogen and phosphorus stoichiometry and their scaling exponent. *Natl Sci Rev* 5:728–739. <https://doi.org/10.1093/nsr/nwx142>
- Tiessen H, Chacon P, Cuevas E (1994) Phosphorus and nitrogen status in soils and vegetation along a toposequence of dystrophic rainforests on the upper Río Negro. *Oecologia* 99:145–150
- Vasco-Palacios AM, Hernández J, Peñuela-Mora MC, Franco-Molano AE, Boekhout T (2018) Ectomycorrhizal fungi diversity in a white-sand forest in western Amazonia. *Fungal Ecol* 31:9–18
- Vegas-Villarrubia T, Paolini J, Herrera R (1988) A physico-chemical survey of Blackwater rivers from the Orinoco and the Amazon basins in Venezuela. *Arch Hydrobiol* 111:491–506
- Walter H, Breckle S (2004) *Ökologie der Erde. Band 2. Spezielle Ökologie der tropischen und subtropischen Zonen. 3. Auflage.* Elsevier
- Went FW, Stark N (1968) Mycorrhiza *BioScience* 18:1035–1039



---

## Part II

### Meadow Biomes



# Multi-Temporal and Multi-Platform Satellite-Based Mapping of White Sand Ecosystems

# 5

H. F. del Valle, G. Metternicht, and J. A. Zinck

## 5.1 Introduction

The origin of the distribution of the white-sand ecosystems within the extent of the Amazonian lowlands remains unknown (Adeney et al. 2016). A thorough understanding of how these landscapes have emerged is still lacking, and it is the subject of debate (Damasco et al. 2012; Cordeiro et al. 2016; Rossetti et al. 2019). Additionally, detailed cartography of these ecosystems is much needed for sustainable land management, monitoring of disturbances, biodiversity assessment, and understanding habitat distribution as well as the carbon cycle and energy budget estimations.

The Amazonas state (Venezuela) is a complex mosaic landscape of forest and non-forest areas, where satellite-based land-cover (LC) and land-use change (LUC) mapping to identify and characterize the white-sand cover remains difficult, mainly due to the high cloud coverage of these tropical regions. Over the last few decades, algorithm refinements of the growing base of optical and radar archives have led to progressively improved research-quality products, ideally suited for studies of biophysical parameters in complex ecosystems such as the white sands of the Amazon basin (e.g., Friedl et al. 2010; Channan et al. 2014; Reiche et al. 2016; Jesus and Kuplich 2020). More to the point, the Japan Aerospace Agency (JAXA) released a global 25-m resolution mosaic using Advanced Land Observing Satellites

---

H. F. del Valle (✉)

Centro Regional de Geomática (CeReGeo), Facultad de Ciencia y Tecnología (FCyT), Universidad Autónoma de Entre Ríos (UADER), Oro Verde, Argentina  
e-mail: [delvalle.hector@uader.edu.ar](mailto:delvalle.hector@uader.edu.ar)

G. Metternicht

Earth and Sustainability Science Research Centre (ESSRC), University of New South Wales, Sydney, Australia

J. A. Zinck

Faculty of Geo-Information Science and Earth Observation (ITC), University of Twente, Enschede, The Netherlands

(ALOS 1 and 2), carrying the Phased Array Type L-band Synthetic Aperture Radar (PALSAR 1 and 2) and the Japanese Earth Resources Satellite (JERS-1) Synthetic Aperture Radar (SAR) images (L-band), and a global forest/non-forest map (Shimada et al. 2010) to increase the usage of SAR products for environmental monitoring and security. On the other hand, the European Spatial Agency (ESA) launched the Sentinel-1 (C-band) in 2014. As in the case of the optical Sentinel-2 products, Sentinel-1 data are open access in the Copernicus platform, covering the entire Earth.

Research over the last decade has reported enhanced effectiveness and accuracy of LC-LUC mapping of tropical regions using SAR products (Joshi et al. 2016; Reiche et al. 2016; Rosenqvist 2016; Pereira et al. 2018). It is known that the sensitivity of the microwave range (particularly at longer wavelengths) to soil moisture and open water surfaces facilitates identifying inundated areas (including small ponds and wetlands) much more effectively than when sensors cover the visible range of the electromagnetic spectrum, enabling to capture landscape features and phenomena that may be missed otherwise. SAR signals at different wavelengths are also sensitive to changes in structures and roughness of surface features, and therefore, prior research using multi-wavelength SAR data has demonstrated it can enhance LC classification performance (Li et al. 2012; Furtado et al. 2015; Hagensieker and Waske 2018).

The synergistic use of optical and radar data is already a well-known alternative in the literature. Another option to improve the accuracy of LC-LUC mapping is the inclusion of spectral indices of vegetation, soil, and water, among others, as part of the classification workflow (Akar and GÜngör 2015; Deus 2016). In this perspective, this study investigates the synergetic use of Global PALSAR-2 and Sentinel-1 products to carry out LC-LUC mapping based on an Expectation-Maximization (EM) classification approach. Additionally, it is posited that the integration of spectral vegetation indices and radar datasets could enhance the selection of data training and improve class statistics in the classification, thereby increasing the effectiveness of the classification algorithm. To this end, a Landsat-derived Normalized Difference Vegetation Index (NDVI) was input in the EM classification to help select the most accurate dataset and processing technique for mapping white-sand LC-LUC at a regional scale, with a focus on identification of flooded vegetation, as this is one of the distinctive characteristics of the white-sand ecosystem. Considering the dramatic impacts of extreme El Niño-Southern Oscillation (ENSO), special attention was also paid to remote sensing data in 2015–2016 and 2018.

---

## 5.2 Materials and Methods

### 5.2.1 Study Area Characterization

The study region encompasses the lowlands lying between the upper Orinoco and Rio Negro river basins to the west and the borders of the Guyana highlands to the east, between 5°N and 2°N (Fig. 5.1). The region has an equatorial climate, with a

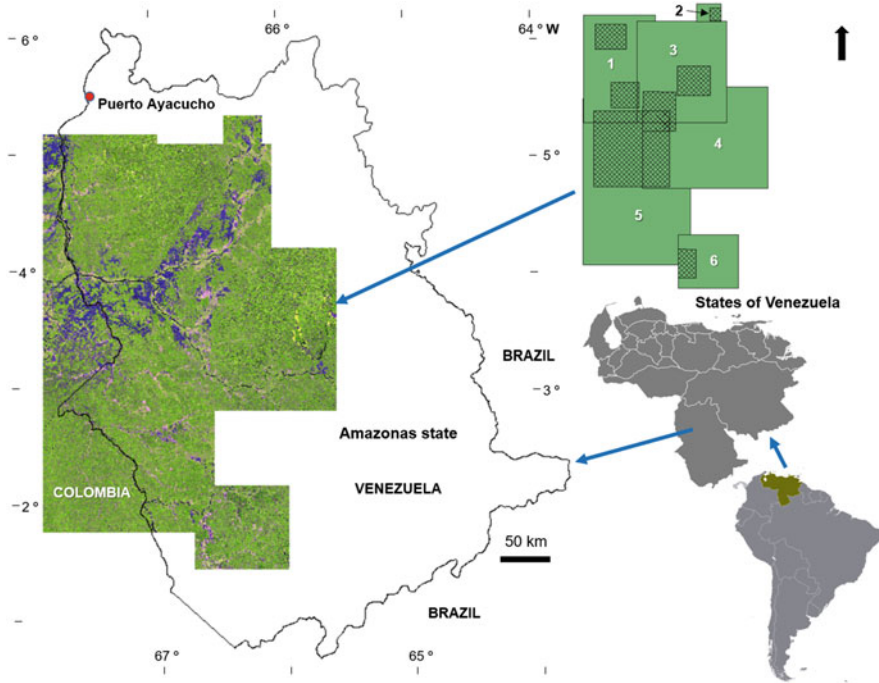


**Fig. 5.1** ALOS PALSAR-1 mosaic (JAXA) using data from 2007, shown as false-color composite of  $L_{HH}$  (red),  $L_{HV}$  (green), and  $L_{HH}/L_{HV}$  (blue). The changes in the intensity of each color are related to various surface conditions. Areas of interest: (1) Sipapo, (2) Camani, (3) Ventuari, (4) Yapacana, (5) Atabapo, and (6) Pasimoni; crosshatched areas are training areas (test sites)

mean annual temperature of 26 °C and mean annual precipitation of 3500 mm. On average more than 200 mm falls in all months of the year. Precipitation is lowest from October to March, though rainless periods longer than 10 days are rare (MARNR-ORSTOM 1986). Mostly, slash-and-burn activities take place from November to February.

Factors controlling the presence of white-sand ecosystems in the study region are flooding, soil type, wildfire, and nutrient scarcity (Adeney 2009). Also, white-sand soils are not necessarily present in all vegetation communities called “white-sand vegetation.” Six eco-chorological areas were distinguished in the study region as a whole and delineated based on variations in meadow vegetation patterns and floristic composition. These six areas are labeled after the name of the main river draining each area, or a relevant relief feature, including from north to south: Sipapo (18,754 sq. km), Camani (1056 sq. km), Ventuari (22,071 sq. km), Yapacana (30,883 sq. km), Atabapo (43,523 sq. km), and Pasimoni (7798 sq. km). The study areas are described in Chap. 6 of this book. The total surface where the six areas are embedded comprises 124,085 sq. km, centered at 3°25′3″N and 66°42′27″W.

Meteorological records of rainfall estimation from remotely sensed information using artificial neural networks (Arvor et al. 2017; Nguyen et al. 2019) were

consulted to assess the potential impact of precipitation on radar backscatter (<https://chrsdata.eng.uci.edu/>).

Long-term climatic records for the season of image acquisition (June to November) in the Amazonas state/study region show that it rained 1304–1525 mm during 2015 against 1715–2014 mm in 2016 (Table 5.1). Instead of the drought affecting the entire Amazon region, as in other years of El Niño-Southern Oscillation (ENSO), there was a marked distinction between drought in the east and above-average rainfall in the west. A similar pattern occurred during a weaker ENSO in 2009–2010 (WonMoo et al. 2011).

Figure 5.2 shows the rainfall deficit in the eastern part of Amazonas state in 2015–2016, as well as the rainfall contrast between north and south of the state with a limit corresponding to the east-west course of the Orinoco (La Esmeralda, Tamatama, San Fernando de Atabapo). In 2015, it rained significantly more toward the NW of Amazonas state.

## 5.2.2 Remote Sensing Data Sources

### 5.2.2.1 Global PALSAR-2 Dataset

The Japanese observation satellite ALOS-2 carries the Phased Array Type L-band Synthetic Aperture Radar (PALSAR-2) instrument built on the lineage of ALOS-1 PALSAR-1 and the Japanese Earth Resources Satellite-1 (JERS-1). The PALSAR-2 instrument operates at 1.2 GHz (L-band, corresponding to a radar wavelength of about 23.5 cm).

Free and open-access PALSAR-2 backscatter mosaics were available through the Japan Aerospace Exploration Agency (JAXA) at [https://www.eorc.jaxa.jp/ALOS/en/palsar\\_fnf/fnf\\_index.htm](https://www.eorc.jaxa.jp/ALOS/en/palsar_fnf/fnf_index.htm).

The JAXA global mosaic datasets are analysis-ready data (ARD), meaning that they have been subject to full geometric and radiometric corrections and organized into a form, with corresponding metadata, which should allow immediate analysis with a minimum of additional user effort.

Tiles were selected for the year 2015 or 2016 (according to the absence of data gaps) with dual-polarization  $L_{HH}$  and  $L_{HV}$  (Fine Beam Dual mode), local incidence angle of  $34.3^\circ$ , ascending orbit, and right-looking. Backscatter mosaic products are distributed as  $1^\circ \times 1^\circ$  tiles, at a resolution of 0.8 arcsec ( $\sim 25$  m) ground resolution. A total of 23–24 scenes per tile and year were collected. The backscatter of the images is given as gamma naught ( $\gamma^0$ ), and all data are orthorectified and slope corrected by JAXA (2018) before distribution as digital number (DN) values, along with ancillary files such as date, local incidence angle, and masking required during preprocessing (Shimada et al. 2014).

### 5.2.2.2 Sentinel-1 Dataset

The Sentinel-1 instrument operates at 5.405 GHz (C-band, corresponding to a radar wavelength of about 5.6 cm) and supports four exclusive imaging modes providing different resolution and coverage: Interferometric Wide Swath (IW), Extra Wide

**Table 5.1** Rainfall statistics of the Amazonas state and the study region (rows in italics)

Rainfall statistics	2015 mm												2016 mm											
	Jun	Jul	Aug	Sep	Oct	Nov	Total	Year	Jun	Jul	Aug	Sep	Oct	Nov	Total	Year								
<i>Max</i>	378	330	373	336	512	404	2333	3385	524	418	398	378	604	591	2913	4731								
	349	330	373	335	512	404	2303	3385	524	418	398	378	604	591	2913	4731								
<i>Min</i>	32	28	33	10	46	54	203	513	44	68	60	84	103	74	433	1002								
	129	122	149	94	184	187	865	1685	207	154	180	149	225	184	1099	2510								
<i>Mean</i>	207	177	199	155	316	250	1304	2246	288	257	240	229	367	334	1715	3067								
	240	226	255	194	330	280	1525	2705	351	325	290	255	406	387	2014	3599								
<i>Median</i>	215	196	214	159	327	261	1372	2325	296	281	236	226	373	333	1745	3160								
	234	226	252	192	331	279	1514	2743	337	328	294	255	406	396	2016	3502								

Source: PERSIANN (Precipitation Estimation from Remotely Sensed Information using Artificial Neural Networks) system developed by the Center for Hydrometeorology and Remote Sensing (CHRS) at the University of California, Irvine (UCI). Resolution:  $0.25^\circ \times 0.25^\circ$  pixel. <https://chrsdata.eng.uci.edu/>

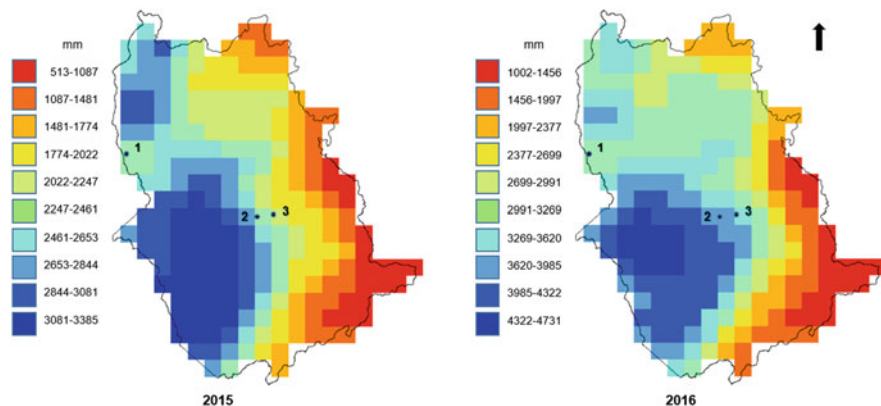


**Fig. 5.2** Mean annual rainfall ranges (2015 and 2016) in the Amazon state measured using the Precipitation Estimation from Remotely Sensed Information using Artificial Neural Networks (PERSIANN) data. (1) San Fernando, (2) Tamatama, (3) La Esmeralda

Swath (EW), StripMap (SM), and Wave (WV). However, as IW is the main mode of operation over the landmasses, special attention was paid to the IW-SLC (Single Look Complex) products in this study. Their spatial resolution is typically in the order of  $\sim 3 \times 20$  m in slant range and azimuth.

A total of twelve IW-SLC polarization ( $C_{VV}$  and  $C_{VH}$ ) images from the Sentinel-1 satellite were acquired for different dates (June–July 2015–2016, September 2016, and November 2015), in ascending mode at an off-nadir angle of  $34^\circ$ – $39^\circ$ . Data were accessed via the Copernicus Open Access Hub (<https://scihub.copernicus.eu>).

Although the Synthetic Aperture Radar (SAR) images cover the rainy season, there was no rainfall (validated against meteorological observations) at the time of image selection and capture of Sentinel-1 for this study. Some cartographic units mapped in the radar images as flooded could be free of surface water during the short period of less rainfall (January to March).

### 5.2.2.3 Landsat Mosaics

For the estimation of the Normalized Difference Vegetation Index (NDVI), we used two Landsat mosaics, one referring to the Amazonian biome (Van doninck and Tuomisto 2018; Tuomisto et al. 2019), and the other derived from Global Forest Change (Hansen et al. 2013).

The Amazonia mosaic was compiled using all Landsat Thematic Mapper (TM)/ Enhanced Thematic Mapper Plus (ETM+) images with less than 60% cloud cover acquired during July, August, and September of the years 2000–2009 (<https://etsin.fairdata.fi/dataset/1b32feb8-e297-4113-b91f-c58fff275039/data>). The composite images from 6-bands: blue, green, red, near infrared (NIR), short-wave infrared 1 (SWIR1), and short-wave infrared 2 (SWIR2) were subdivided into tiles of 2.5 degrees. The composite images were based on more than 16,000 sufficiently cloud-free acquisitions from the 10 years. Filenames indicate the coordinates at the



lower-left corner of each tile. Filenames with extension “D” indicate the date of the observation of each pixel selected in the composite image; filenames with extension “N” indicate the number of cloud-free observations during the compositing period for each pixel.

The other Landsat mosaic assessed was from Global Forest Change (Hansen et al. 2013) using the platform of Google Earth Engine (<https://explorer.earthengine.google.com/>). Reference composite imagery is based on observations from a set of quality assessed growing season observations in four spectral bands, specifically Red, NIR, SWIR1, and SWIR2. The asset ID UMD/hansen/global\_forest\_change\_2018\_v1\_6 was applied. Special attention was paid to the reference multispectral imagery Landsat-8 Operational Land Imager (OLI) from the last available year, typically 2018 (improved version). If no cloud-free observations were available for this year, the imagery was taken from the closest year with cloud-free data, within the range of 2010–2015.

The Google Earth Engine (GEE) public data catalog also includes a variety of standard Earth science raster datasets. We imported some datasets (U.S. Geological Survey Landsat 7/8 and Moderate Resolution Imaging Spectroradiometer (MODIS) collections) into our script environment and loaded our raster and vector data for private use. Landsat and MODIS yield similar estimates of the start of greenness ( $r^2 = 0.60$ ), although Fisher and Mustard (2007) found that a high degree of spatial phenological variability within coarser-scale MODIS pixels may be the cause of the remaining uncertainty.

Coarser resolution (i.e., 250 m) NDVI from the Moderate Resolution Imaging Spectroradiometer (MOD13Q1 V6) were also integrated to account for surface variations in NDVI occurring among the Landsat acquisitions (2000-02-18 to 2018-12-31). Visual inspection of the date from Landsat and MODIS data showed a high degree of correlation. The MODIS NDVI product is computed from atmospherically corrected bi-directional surface reflectance that has been masked for water, clouds, heavy aerosols, and cloud shadows. Using the same product (MOD13Q1 V6) for the Amazonas state, Olivero et al. (2016) characterized land classes using patterns of greenness temporal change and topo-hydrological information and proposed 12 land-cover types, grouped into five main landscape units: (1) water bodies; (2) open lands/forest edges; (3) evergreen forests; (4) submontane semi-deciduous forests; and (5) cloud forests.

#### 5.2.2.4 Google Earth and Bing Images

Google Earth images were evaluated as a tool to visualize different meadow and white-sand covers. The images give excellent visual information on vegetation distribution in such a way that landforms, vegetation, and disturbances are easily recognized.

High-resolution imagery subsets mainly from Bing maps like Worldview ([www.digitalglobe.com](http://www.digitalglobe.com)) and GeoEye ([www.geoeye.com](http://www.geoeye.com)) were used for testing polygon representation of vegetation objects in different types of white-sand cover.

### 5.2.2.5 Forest Canopy Height

A 30-m spatial resolution global forest canopy height (FCH) map was recently developed by Potapov et al. (2020) through the integration of the Global Ecosystem Dynamics Investigation (GEDI)-Laser Imaging Detection and Ranging (LiDAR) forest structure measurements and Landsat analysis-ready data time-series (Landsat ARD). Access to data available only for 2019 was obtained through GEE (image collection id: users/potapovpeter/GEDI\_V27). Data download <https://glad.umd.edu/dataset/gedi>. A minimum canopy height of 3 m was selected. Data evaluation from this mosaic was performed digitally through elevation data (see Chap. 6 in this book), and external data sources were used to derive a forest/non-forest mask (FNF) from Blanco et al. (2013), ESA (2017), and JAXA (2018). From these datasets, it was possible to determine where the forests are located, and where it was desirable to estimate FCH.

In Fig. 5.3a–b, the main vegetation types occurring in the study region can be distinguished based on the canopy height. Canopy heights in the range of  $\geq 30$ –15 m (dark green) correspond to terra-firme and tall caatinga forests. Canopy heights below 15 m (light green) include varieties of medium-high to low caatinga forests and other kinds of woodland (e.g., riparian forest, palm swale) as well as bana scrublands. Whitish colors correspond to dry or flooded open white-sand herbaceous formations, in particular meadows and shrubby meadows (specific areas of interest).

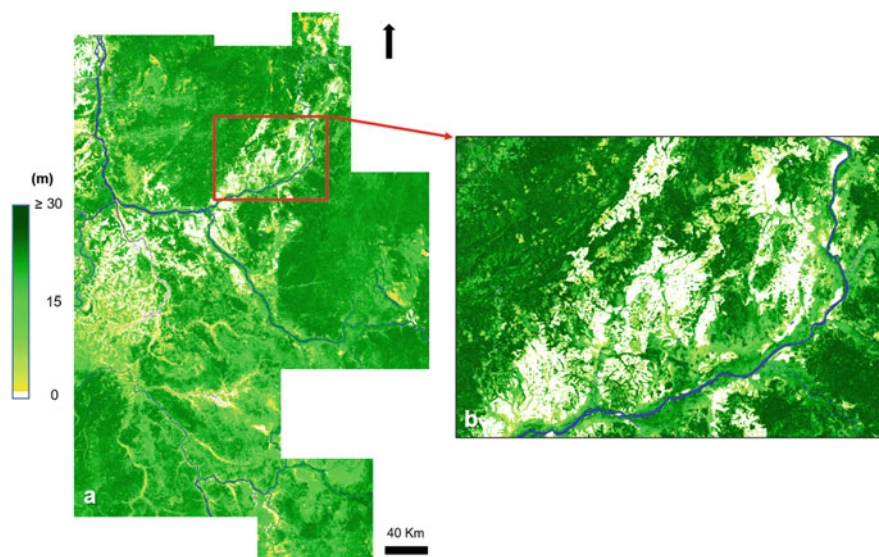


**Fig. 5.3** (a–b) Forest canopy height (FCH) 2019 (Source: Potapov et al. 2020). Data download: <https://glad.umd.edu/dataset/gedi>. The minimum canopy height selected was 3 m. (a) Study region and areas ( $23.4 \pm 6.8$  m). (b) Details of forest canopy height (m) generated in this study

### 5.2.2.6 Tree Cover Loss Dataset

The ENSO is the main driver of interannual climate extremes in Amazonia and other tropical regions. *Tree mortality increases and tree growth decreases during severe droughts, with implications for the global carbon cycle.* Droughts and high temperatures also increase the risk of forest fires. During the last decade, two major drought events, one in 2005 and another in 2010, occurred in the Amazon basin (Lewis et al. 2011). The Amazon rainforest also experienced high-temperature records and severe droughts during ENSO in 2015–2016, and the area of forest impacted by drought was 20% larger than during other extreme ENSO events (Núñez Cobo and Verist 2018).

Tree cover loss dataset from Global Forest Change (Hansen et al. 2013) for the 2001–2018 period was sourced from GEE.<sup>1</sup> Tree cover is defined in this dataset as all vegetation taller than five meters. It may take the form of natural forests or plantations across a range of canopy densities. “Loss” indicates the removal or mortality of tree cover and can be due to a variety of factors. As such, “loss” does not equate to deforestation only. This dataset was used with caution, as suggested by Hansen et al. (2013). The analysis was based on the visual and digital interpretation of forest disturbance sites in the available Landsat mosaics (see Sect. 5.2.3.4). Forest disturbance data were compared with NDVI values and the LC-LUC classes. The global forest/non-forest maps (FNF) of the JAXA (2018) and the ESA (2017) with average overall accuracies ( $77.5\% \pm 3.2\%$ ) and ( $85.4\% \pm 1.6\%$ ), respectively, were assembled in the Sentinel Application Platform (SNAP) software environment, as suggested by Van Thinh et al. (2019).

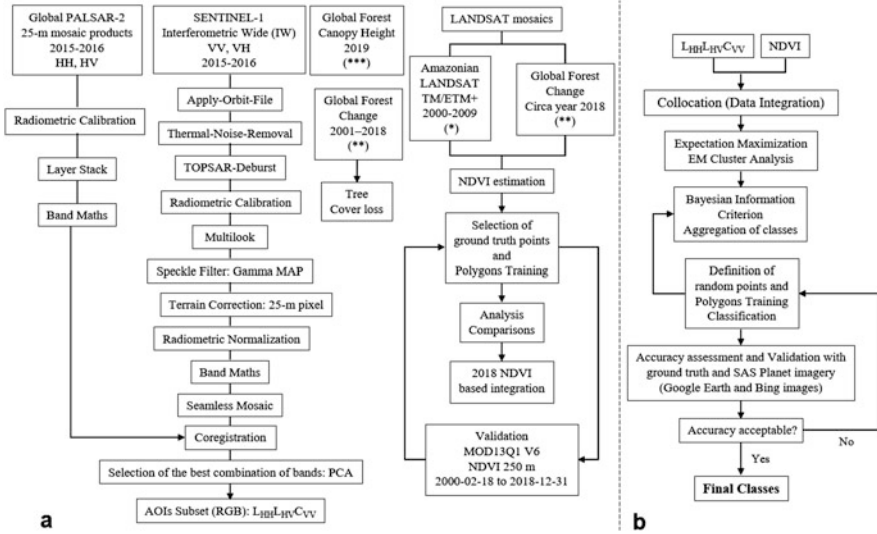
## 5.2.3 Methodology

Figure 5.4a–b presents the data processing workflows, which involve preprocessing and data integration, product improved Expectation-Maximization (EM) classification, and accuracy assessment and validation. Digital processing was performed using the following open-source software packages: SNAP v7.0 (Scientific Exploitation of Operational Missions 2018), Google Earth Pro v7.3.2.5491 (Google LLC 2019), QGIS Development Team (2018), SAS Planet v180518.9750 Nightly (SAS Planet Development Team 2018), Google Earth Engine platform (Gorelick et al. 2017), and R statistic packages (v3.5.0) (R Core Team 2018).

### 5.2.3.1 SAR Data Processing

The Global PALSAR-2 dataset is distributed as amplitude data, and therefore digital numbers (DN) need to be converted to normalized radar cross-section (NRCS) in [ $\text{m}^2/\text{m}^2$ ] expressed in decibels (dB), applying a sensor-specific calibration factor (CF) according to the following equation (JAXA 2018):

<sup>1</sup><http://earthenginepartners.appspot.com/science-2013-global-forest>



**Fig. 5.4 (a–b)** Methods and workflow for implementing the multi-data classification: **(a)** Data preprocessing, band math's, image stacking, combination of SAR bands (PALSAR-2 and Sentinel-1), NDVI estimation (Landsat data), NDVI validation. **(b)** Data integration, EM cluster analysis, training classification, Bayesian information, validation. 2015–2016 (ENSO). \* Van doninck and Tuomisto (2018), \*\* Hansen et al. (2013), \*\*\* Potapov et al. (2020)

$$\gamma^0 \text{ (gamma naught) [dB]} = 10 \times \log_{10} [DN^2] + CF$$

where  $CF = -83.0$  dB for both HH and HV polarizations (PALSAR-2/PALSAR mosaic).

Speckle reduction was a minor issue since PALSAR data are multi-looked (four looks) by JAXA (Shimada et al. 2014).

The processing of Sentinel-1A IW-SLC images was first split into individual IW because the study area lies in different sub-swaths. The precise orbit files were applied to the IWs to determine an accurate satellite position. The sub-swaths were then deburred to remove the demarcation. The IWs were merged to obtain a seamless tile for each test site or area of interest (AOI).

The mosaic data performed were also expressed in the form of the normalized radar cross-section with gamma naught ( $\gamma^0$ ) rather than sigma naught ( $\sigma^0$ ) or beta naught ( $\beta^0$ ) adopted as the expression unit (Small 2011), since the backscatter is normalized by the realistic illumination area under an assumption of scattering uniformity, where:

$$\gamma^0 [\text{dB}] = 10 \times \log_{10} \frac{DN}{\theta} + CF \text{ or } \gamma^0 = \frac{\sigma^0}{\theta}$$

and  $\cos \theta$  is the cosine from the local incidence angle.

**Table 5.2** Correlation coefficients between Global PALSAR-2 (L-band) and Sentinel-1 (C-band)

	$L_{HH}$	$L_{HV}$	$C_{VV}$	$C_{VH}$
$L_{HH}$	1	0.97	0.90	0.80
$L_{HV}$		1	0.89	0.81
$C_{VV}$			1	0.82
$C_{VH}$				1

The product was filtered with Gamma Map  $3 \times 3$  window size. For the terrain correction, a Range Doppler Terrain Correction with a digital elevation model of 30 m was used (Shuttle Radar Topography Mission, SRTM).

Following the preprocessing, all SAR data were statistically analyzed with the R statistic packages (v3.5.0) (R Core Team 2018) establishing mean and variance images of  $\gamma^0$  for each polarization band.

Algebraic operations between bands ( $L_{HH}$  and  $L_{HV}$ ) and ( $C_{VV}$  and  $C_{VH}$ ) in this phase were used to improve visual image interpretation. Image ratio and difference of the polarimetric bands served to emphasize signal–target interactions and, hence, interpret land targets of interest. The  $L_{HH}$ ,  $L_{HV}$ , and  $L_{HH/HV}$  and  $C_{VV}$ ,  $C_{VH}$ , and  $C_{VV/VH}$  combinations used here for red-green-blue (RGB) for PALSAR-2 and Sentinel-1, respectively, are frequently utilized by remote sensing users (Shimada et al. 2010; CEOS 2018). By expressing differences through changes in color hue, it was possible to visually enhance the surface conditions of the test sites and training areas.

Surface roughness refers to the unevenness of the earth’s surface due to natural processes and/or human activities. The root means square (RMS) height, the correlation length, and an autocorrelation function statistically describe it (Ulaby and Long 2014). Microscale and mesoscale roughness were described, associated respectively with image brightness (tone) and image texture. Besides, we used complementary spatial context, understanding of backscattering characteristics, and expert knowledge.

### 5.2.3.2 Analysis and Interpretation of the SAR Backscatter

Variables related to radar design and environmental settings were analyzed to better understand the behavior of the radar signal backscattering. Visual interpretation of the processed images was used to that end, as surface roughness depends on the soil/vegetation conditions and the presence of direct indicators at the ground surface (sand deposits, water, rock outcrops, land degradation). The qualitative interpretation applied in this research did not only require detailed roughness measurements but also knowledge about the landscape and land management variables that influence changes in image brightness.

### 5.2.3.3 Selection of Best RGB SAR Band Combination

The Global PALSAR-2 and the Sentinel-1A, including two different wavelengths (L- and C-bands) and four polarization modes ( $L_{HH}$ ,  $L_{HV}$ ,  $C_{VV}$ , and  $C_{VH}$ ), for all areas of interest (AOI) together, were highly correlated (Table 5.2). This suggests that the intrinsic dimensionality of the data is small, certainly smaller than the number of physical variables that potentially affect the signal (Amitrano et al.

**Table 5.3** Eigenvectors of the principal component analysis of Global PALSAR-2 (L-band) and Sentinel-1 (C-band)

	$L_{HH}$	$L_{HV}$	$C_{VV}$	$C_{VH}$
PC1	0.31	-0.75	-0.54	-0.33
PC2	0.85	0.60	-0.38	0.32

**Table 5.4** Color and texture assignments and output colors for multidimensional SAR image composites (modified from Henderson and Lewis 1998)

$L_{HH}$		$L_{HV}$		$C_{VV}$		Color RGB
Tone	Texture	Tone	Texture	Tone	Texture	
<i>Tonal and texture change on image</i>						Blue
Black	Smooth	Black	Smooth	White	Rough	
Black	Smooth	White	Rough	Black	Smooth	Green
White	Rough	Black	Smooth	Black	Smooth	Red
Black	Smooth	White	Rough	White	Rough	Cyan
White	Rough	Black	Smooth	White	Rough	Magenta
White	Rough	White	Rough	Black	Smooth	Yellow
<i>No tonal and texture change on image</i>						
White	Rough	White	Rough	White	Rough	White
Black	Smooth	Black	Smooth	Black	Smooth	Black
Gray	Medium	Gray	Medium	Gray	Medium	Gray

2016). Thus, given the high correlation ( $>0.9$ ) between both SAR satellites, a principal component analysis (PCA) was applied to remove redundant information.

The analysis revealed that the first components explained 78.4% and 20.7% of the data variability, and a better combination among  $L_{HH}$ ,  $L_{HV}$ , and  $C_{VV}$  (Table 5.3). Thus, they were selected as the raw bands to be included in the production of false-color composites (FCC) showing an optimal combination of wavelength and polarization modes.

Table 5.4 describes how the combination of grayscale imagery assigned to the red-green-blue (RGB) bands would lead to the resulting colors when the extreme dark (black, smooth) and bright (white, rough) colors and textures are combined (modified from Henderson and Lewis 1998).

### 5.2.3.4 Spectral Vegetation Index: NDVI

The Landsat mosaics were used to calculate Normalized Difference Vegetation Index (NDVI), and subsequently for NDVI differencing. Index-based classification requires NDVI as a feature vector; consequently, this was calculated in the SNAP environment using bands 3 (red) and 4 (NIR) for Landsat 7 ETM+, and band 4 (red) comes with band 5 (NIR) for Landsat 8.

Detection of LC-LUC during the period 2000–2009 and in 2018 was undertaken using the NDVI differencing technique (Singh, 1989). The resulting images were

subtracted to assess the  $\Delta$  NDVI image with positive (NDVI increase) and negative (NDVI decrease) changes on a  $30 \times 30$  m pixel resolution:

$$\Delta \text{NDVI} = \text{NDVI}_{2018} - \text{NDVI}_{2000-2009}$$

The NDVI difference image was also tested to determine goodness of fit to a normal distribution. Mean, standard deviation (sigma), median, coefficient of variation, and percentiles (75%, 80%, 85%, and 90%) were generated. Threshold identification for the detection of vegetation changes represents a key issue in the NDVI differencing method. The sigma approach is one of the most widely applied threshold identification techniques for different natural environments (Lu et al. 2005).

Additionally, NDVI values were classified into seven classes using equal intervals. Furthermore, changes in vegetation greenness were computed for the period 2000–2009 and 2018. Therefore, vegetation greenness for types of white-sand LC-LUC was identified (forest, scrubland, grass, sand accumulation). The percentage of greenness within the pixel was validated by ground truth, Google Earth, and Bing images of high resolution. For the integration with radar data, we chose to use the NDVI of the year 2018, because it is closer to the date of the SAR images acquisition.

### 5.2.3.5 Data Integration

The Collocation Tool in SNAP software allows collocating spatially overlapping products. As such, the pixel values of slave products (2018 NDVI data) were resampled into the geographical raster of the master product (SAR data:  $L_{HH}$ - $L_{HV}$ - $C_{VV}$ ). The output product contains a copy of all components of the master and slave products, i.e., band data, tie-point grids, flag coding, bitmask definitions, and metadata.

The geographic position was used to identify the correspondence between samples in the master and the slave raster images. If there was no sample for a requested geographical position, the master sample was set to the no-data value uses which were defined for the slave band. The collocation algorithm required accurate geopositioning information for both master and slave products.

### 5.2.3.6 Feature Extraction and Classification

Unsupervised classification is an important technique especially for the automatic analysis of SAR data. Several unsupervised classification approaches for polarimetric SAR data have been proposed (Liu et al. 2002; Bruzzone et al. 2004; Ince 2010). One approach to unsupervised classification is based on statistical clustering, which has the advantage of identifying classes that do not perfectly align with pure or isolated physical scattering mechanisms. Instead, objects with an arbitrary but similar backscattering and NDVI value are grouped. To this end, the improved Expectation-Maximization (EM) algorithm (Yang et al. 2012) was used, where each pixel is assigned with different degrees of class membership to all classes in a way that maximizes the posterior probability of the assignment concerning a mixture model.



The EM algorithm was implemented in SNAP using an initial number of 60 clusters, 100 iterations, and random seed (used to generate initial clusters; the default was 31,415). A region of interest (ROI) mask was used to restrict cluster analysis to a specific area of interest and the addition of probability.

The Bayesian Information Criterion (BIC), also known as Schwarz's Bayesian criterion (SBC) (Yang et al. 2012), was used to determine the number of final clusters (classes) present in each test site. This criterion gives an indication of which classes are statistically closer and how classes split and merge (Zanetti and Bruzzone 2018). This generic function was implemented in the R statistic packages (R Core Team 2018). Cluster labeling was the final step undertaken with the assistance of available ground truth data.

We identified fifteen LC-LUC classes namely closed to open forest (F1), open forest (F2), upland rocky slope forest (F3), mosaic of natural vegetation and crops (M1), mosaic of trees and shrubs (M2), mosaic of herbaceous cover (M3), dry or flooded open white-sand scrublands (Ws), water bodies (W0), shrubby meadows (W1), shrubby or herbaceous cover, regularly flooded (W2), tree cover, regularly flooded (W3), sparse vegetation (Sp), bare rocky areas (B), sandbanks and sandridges (B2), and built-up area/small towns (U).

### 5.2.3.7 Object-Oriented Approach

An object-based segmentation method was applied to the color composite of the high-resolution imagery subsets, using the object-oriented multi-scale image analysis method embedded in the software SNAP. The Generic Region Merging Processor algorithm (Lassalle et al. 2015) that allows the segmentation of images of arbitrary size was used. The criterion of Baatz and Schäpe (2000) was considered for the region-merging algorithm (Local Mutual Best Fitting) with 100 total iterations, a spectral and a shaped weight of 0.7 and 0.3, respectively, and a scale threshold of 200. In a post-classification phase, classified objects underwent a generalized process of correction of the LC-LUC information assigned to each class supported by ancillary information and expert knowledge.

### 5.2.3.8 Accuracy Assessment

A mixed-method approach was used for assessing the accuracy of the classification results; available ground truth data were combined with a systematic sampling grid of manual interpretations of very-high-resolution optical satellite data (Bing Maps Satellite), Google Satellite (Google maps), and ancillary information (Aymard et al. 2009; Olivero et al. 2016). The latter were gathered from remotely sensed data of moderate accuracy existing over the study area (see Blanco et al. 2013; and the websites Land Cover Map 1992–2018, Climate Change Initiative, ESA, <http://maps.elie.ucl.ac.be/CCI/viewer/>, and <https://www.esa-landcover-cci.org/>).

A stratified-random selection of validation sites was used to construct the error matrix ensuring at least 20 samples per class in each test site. This information was then compiled in a contingency table so that the accuracy of each class could be determined. Furthermore, the classified image maps were displayed in image windows and linked to Google Earth for a visual evaluation of class distributions.

As a result of the accuracy analysis, 83% accuracy and Kappa index of 0.77 were reported.

---

## 5.3 Results and Discussion

### 5.3.1 Mapping Eco-Chorological Areas of the White Sands

The total backscatter from forest land in the wavelengths of the Sentinel-1 and Global PALSAR datasets used includes response from several components: (1) crown volume scattering (dominant in C-band), (2) backscattering from secondary branches and trunks (dominant in L-band), (3) backscattering from the ground, especially if the canopy is sparse (L-band) or there is a gap in the canopy (both C- and L-bands), and (4) crown-ground (mostly in C-band) or trunk-ground (L-band) backscattering, often termed as double bounce (Ulaby and Long (2014).

Three factors were significant when determining the variations in the backscattering coefficient for the environmental setting of the white sands: (1) vegetation type (texture and structure), (2) surface aspect or soil/vegetation conditions (tone, roughness), and (3) surface water/flooded vegetation. The backscattering intensity changes with these parameters produce a range of image brightness variations, expressed as changes in the pixel gray levels or color of the images analyzed. Furthermore, time-series of SAR data are necessary to better characterize the highly dynamic processes associated with the LC-LUC of the white-sand ecosystems, such as wetland inundations or anthropic activities (CEOS 2018; Adeli et al. 2020; Hansen et al. 2020). Hereafter follows a discussion on the main findings related to the mapping of each of the six eco-chorological areas.

#### 5.3.1.1 Sipapo Area

The Sipapo area is a regional depression lying between highlands and hills to the east and a strip of peneplain terrains bordering the course of the Orinoco river to the west. The relief is highlighted in the C-band by the angular resolution of Sentinel-1 ( $34^{\circ}$ - $39^{\circ}$ ), which interacts with the local relief (Fig. 5.5). The classified SAR images show this eco-chorological area as a mixture of forests (from closed to open), meadows, dry or flooded open white-sand scrublands, agricultural land, bare soils, exposed bedrock, water bodies, and small towns, among others.

Despite C-band backscatter ( $\gamma^0$ ) occurring at the top of the canopy, the interaction provides for increased sensitivity to canopy structure and consequently a certain potential for the distinction between meadows and other vegetation types with different canopy (“tone or color” and “spatial texture”), such as white-sand covers. Smoother canopies typically display a lower backscatter (black color, smooth surfaces) at both  $C_{VV}$  and  $C_{VH}$  polarization ( $-22.44$ ,  $-26.39$ , respectively) than “rougher” (white color) canopies ( $-5.93$ ,  $-12.13$ , respectively) with a higher degree of structural variation.

Flooded forests cannot be distinguished from other forest types in the  $C_{VV}$  and  $C_{VH}$  polarizations (Henderson and Lewis 2008). However, in areas with sparser

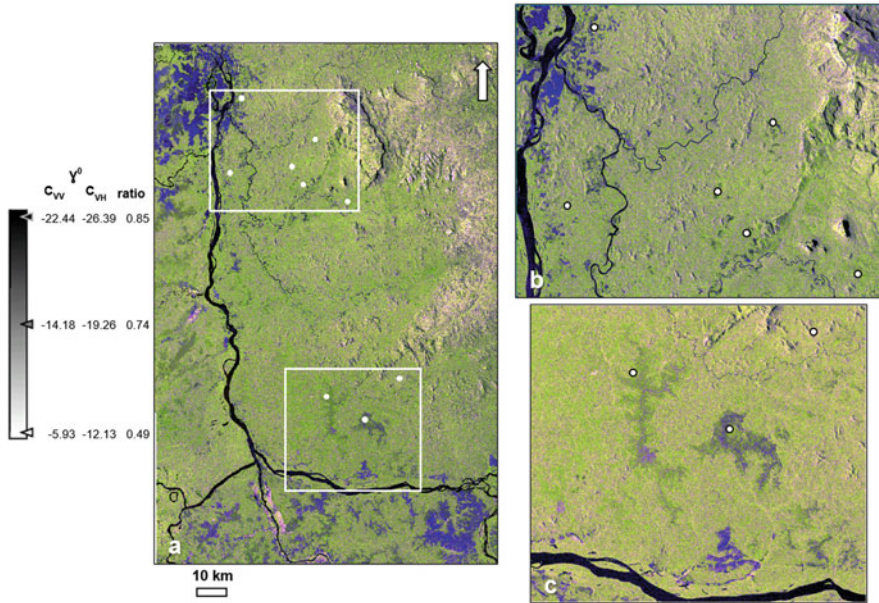


**Fig. 5.5** (a–c) Sentinel-1A, RGB  $C_{VV} / C_{VH}$  ratio: (a) Sipapo area, (b) Sipapo 1 training area, (c) Sipapo 2 training area. White dots indicate field observation sites including vegetation and soil descriptions; sites are identified in Chap. 6

vegetation, where the C-band signal can reach the water surface through gaps in the canopy, relative specular double-bounce reflection can be observed (mostly shades of blue and purple appearance, detected by the ratio band). These areas correspond mostly to bare sand patches and flooded open white-sand scrublands with herbaceous cover (Fig. 5.5b–c).

L-band signals (Fig. 5.6a–c) penetrate deeper into the vegetation volume bordering secondary river courses (pink shades), influenced by the density of the canopy and volumetric soil moisture (surface and subsurface). These areas appear very bright (rough) in  $L_{HH}$  polarization and can be recognized as flooded herbaceous cover with trees and shrubs. The combination of  $L_{HH}$  polarization and the ratio  $L_{HH} / L_{HV}$  has been reported as efficient to discriminate flooded vegetation from unflooded vegetation and open water (Li et al. 2012; CEOS 2018). On the other hand, at  $L_{HV}$  polarization controlled by volumetric soil moisture only, the flooding extent is not as visible and backscatter levels are like that of non-flooded areas. Dry or flooded open white-sand vegetation is better expressed in the L-band than in the C-band (bluish tones), and sand deposits can be confused with flooded areas because of their smooth texture (Rosenqvist 2016). Our results show L-band backscatter ( $\gamma^0$ ) at both  $L_{HH}$  and  $L_{HV}$  polarization lower for white-sand vegetation flooded or non-flooded.  $L_{HV}$  polarization improves sensitivity to bare soil areas and sparse herbaceous/sparse shrub cover (very low backscatter) and displays a wider radiometric dynamic range than the  $L_{HH}$  polarization.

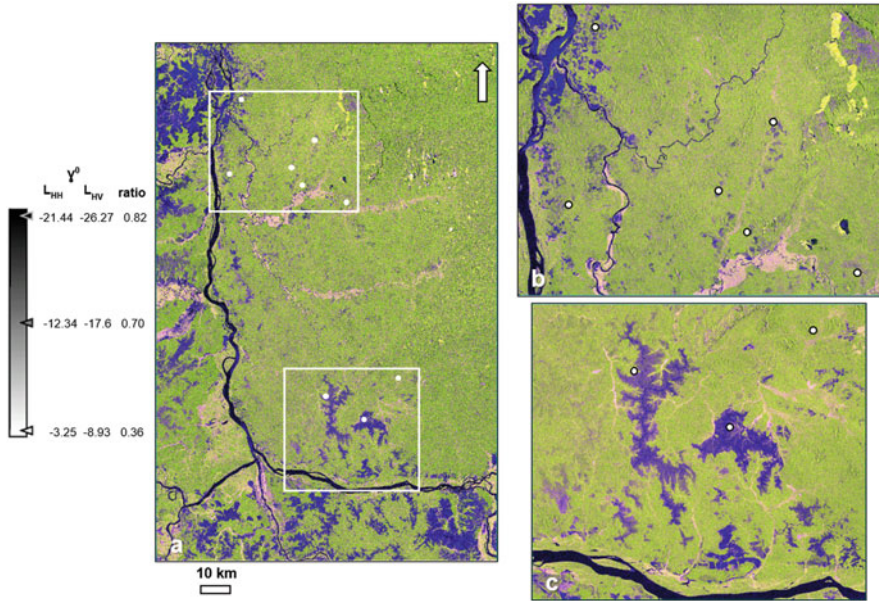


**Fig. 5.6** (a–c) Global PALSAR-2, RGB  $L_{HH}$   $L_{HV}$  ratio: (a) Sipapo area, (b) Sipapo 1 training area, (c) Sipapo 2 training area. White dots indicate field observation sites including vegetation and soil descriptions; sites are identified in Chap. 6

Open water has very dark image characteristics because most of the energy is scattered in the forward direction away from the sensor (both with PALSAR-2 and Sentinel-1). However, the blue color of the Orinoco river visible in the upper left image (Fig. 5.6b) is caused by the different incidence angles of the two images making up the PALSAR-2 mosaic or due to changes in ground conditions between overpasses. A steeper incidence angle (near range) results in stronger direct scattering and a higher  $L_{HH}$  backscatter (Lee and Pottier 2009). Non-flooded forests tend to appear in shades of green, and typically the brightness of green corresponds to the amount of biomass. There are differences in the appearance of some dark green colors in alluvial flat areas in the C-band composite. This stems from a higher sensitivity to volume scattering of shrubs, herbs, and grasses, which have a lower volume scattering component at the L-band (CEOS 2018).

Pixels on upland slopes that face the radar observation direction (yellowish color) have higher backscatter than those on opposite slopes, which causes changes in the return from both  $C_{VV}$  and  $L_{HH}$  (upland rocky slope forest areas) (Fig. 5.6b). Cropland and bare-soil areas can also be observed. The class of bare soil usually represents cultivable agricultural land in the plain landscape. Bare soils on hills could result from repeated forest disturbances. In the C-band, crops with different vegetation structures or growth stages produce a range of different responses at both  $C_{VV}$  and  $C_{VH}$  polarizations, as manifested by the variety of colors in the C-band RGB composite (red, yellow, purple, white). Non-vegetated fields with smooth



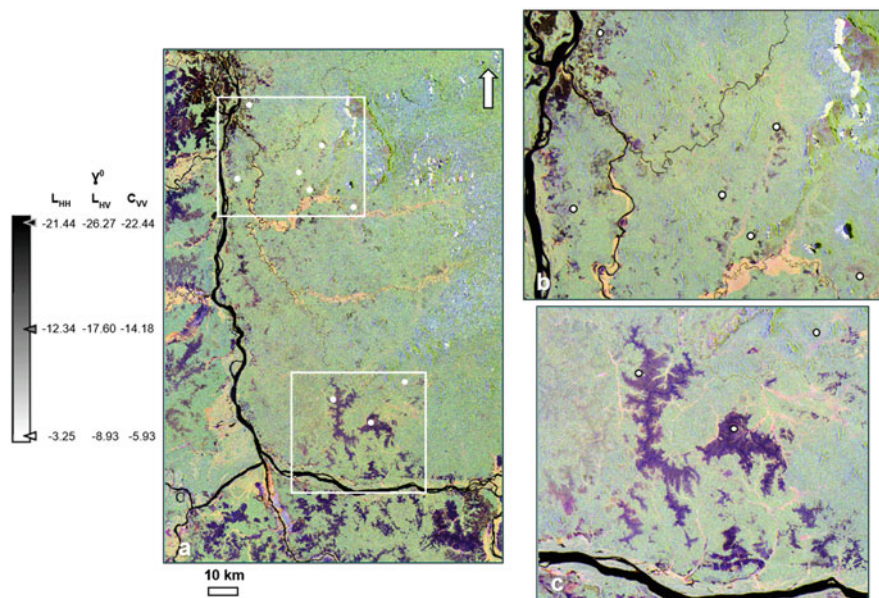


**Fig. 5.7** (a–c) Layer stack RGB  $L_{HH}$   $L_{HV}$   $C_{VV}$ : (a) Sipapo area, (b) Sipapo 1 training area, (c) Sipapo 2 training area. White dots indicate field observation sites including vegetation and soil descriptions; sites are identified in Chap. 6

surfaces that were not distinguishable from herbaceous fields at L-band can be identified by their low response at both  $C_{VV}$  and  $C_{VH}$  and blue color in the RGB image. Agricultural areas typically have a purple appearance. Small tree patches appear green due to higher  $L_{HV}$  backscatter. The bright areas surrounding the fields in the image are remaining forests yet to be cleared.

The color composite that uses two L-polarization bands and one C-polarization ( $L_{HH}$  as red,  $L_{HV}$  as green, and  $C_{VV}$  as blue) in Fig. 5.7a–c shows that in both  $L_{HH}$  and  $C_{VV}$ , large gray value ambiguities exist between forest canopies and non-forest areas. The cross-polarized band facilitates the separation of forest and non-forest areas with less ambiguity (Kellndorfer et al. 2014). The light cyan color of medium texture (Fig. 5.7a) corresponds to the wet evergreen and semi-evergreen forests in hilly terrains of the Cuao-Sipapo massif, where topographic features are visible on the image.

### 5.3.1.2 Camani Area

Camani is a small area that lies south of a narrow mountain gap that divides between watersheds draining to the north and those draining to the south. Several LC-LUC classes can be visualized such as closed to open forests, mosaics of vegetation types, scrublands, flooded tree covers, dry or flooded open white-sand scrublands, water bodies, sparse vegetation, and bare rocky areas.

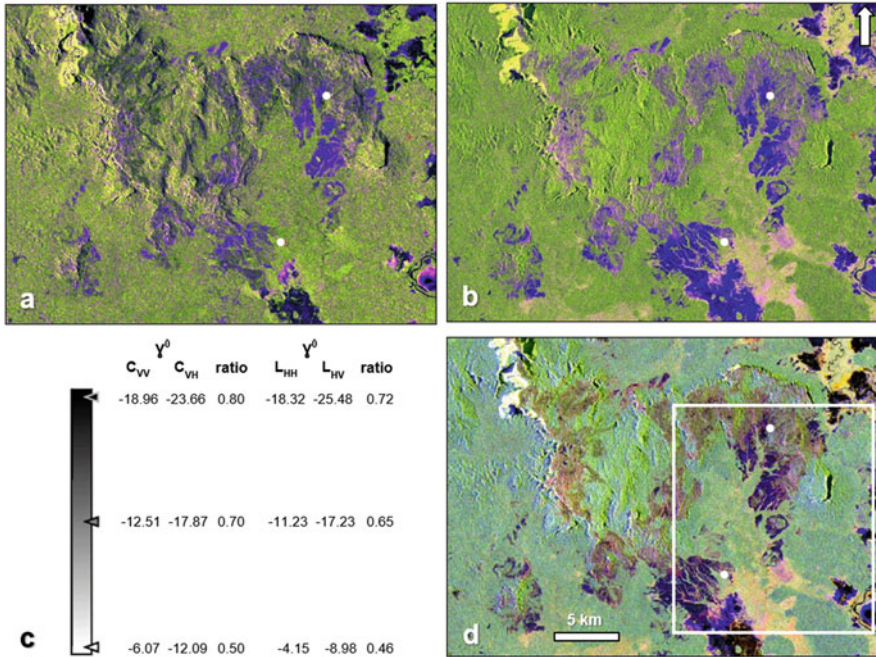


**Fig. 5.8** (a–d) Camani area. (a) Sentinel-1A, RGB  $C_{VV}$   $C_{VH}$  ratio, (b) Global PALSAR-2, RGB  $L_{HH}$   $L_{HV}$  ratio, (c) Backscattering coefficient ( $\gamma^0$ ) measured in decibel (dB) units (gray levels), (d) Layer stack RGB  $L_{HH}$   $L_{HV}$   $C_{VV}$ . White dots indicate field observation sites including vegetation and soil descriptions; sites are identified in Chap. 6

Wet areas and flooded forests show magenta, purple, and blue colors (Fig. 5.8a–b and d). Open water in meadows, rivers, and streams is dark or dark blue. Radar signal registers also water features such as very moist and water-saturated ground, marshy soils, and dunes. Forest areas appear green and light yellowish-green. Texture roughness helps distinguish tree cover from the degraded forest. Both C- and L-bands show blue color for strong changes ( $C_{VV}/C_{VH}$  and  $L_{HH}/L_{HV}$  ratios). Upland rocky slope forest areas facing the incident radar direction appear very bright (yellow), while the shade side appears very dark (black).

The ability of the L-band SAR to penetrate through dense vegetation facilitates distinguishing between vegetated and non-vegetated areas and provides information on vegetation structures and sub-canopy conditions, enhancing mapping and monitoring of wetlands and flooded vegetation. Figure 5.8c shows the  $\gamma^0$  values (gray levels), with white color for very bright objects (rough surfaces) to black color for very dark objects (smooth surfaces). Burnt areas have a strong increase at L-band because stronger soil contribution enhances double bounce and hence brightens the backscatter signal (del Valle et al. 2016; Kellndorfer 2019). The SAR signal follows a pattern of backscatter decrease in degraded forests (Kellndorfer et al. 2014).

However, the severity of forest degradation and bedrock exposure also determine the scattering mechanisms.

The SAR images show that sand deposits, meadows, and water surfaces present extremely low volume scattering in all polarizations and bands.  $C_{VH}$  and  $L_{HV}$  backscatters are closely correlated with forest structure and above-ground biomass, with  $L_{HV}$  reaching higher  $\gamma^0$  values ( $-8.98$  dB) than for any other land cover. Nevertheless,  $L_{HH}$  appears more sensitive to inundated areas; this can be explained by the double-bounce effect from the surface of the water to the tree trunks causing higher backscatter signatures ( $-4.15$  dB). Both images of Sentinel-1A and PALSAR-2 show differences in the state of land features that could indicate temporary inundation or changes in wetland conditions in white-sand vegetation. C-band data also seem less useful than L-band data in identifying white-sand vegetation, including bare sand patches.

### 5.3.1.3 Ventuari Area

The Ventuari area is a glacial landscape, better drained than the alluvial flats of the other eco-chorological areas, and with large proportions of savanna and mixed savanna-meadow vegetation. Distal parts of the glacial are usually bordered by narrow vales and swales covered by morichal vegetation with palm trees on poorly drained sandy soils. The SAR images show land covers of closed to open forests, mosaics of different vegetation types, meadows, flooded tree areas, dry or flooded open white-sand scrublands, water bodies, sandbanks, and sandridges. More to the point, Sentinel-1 C-band and PALSAR-2 L-band data (Fig. 5.9a–b and 5.10a–b, respectively) show characteristic backscatter for the different frequencies and polarizations of these land covers.

In the Sentinel-1 C-band, non-forest cover types with variable characteristics (structure, growth stages) produce a range of different responses at both  $C_{VV}$  and  $C_{VH}$  polarizations, as manifested by the variety of colors in the C-band RGB

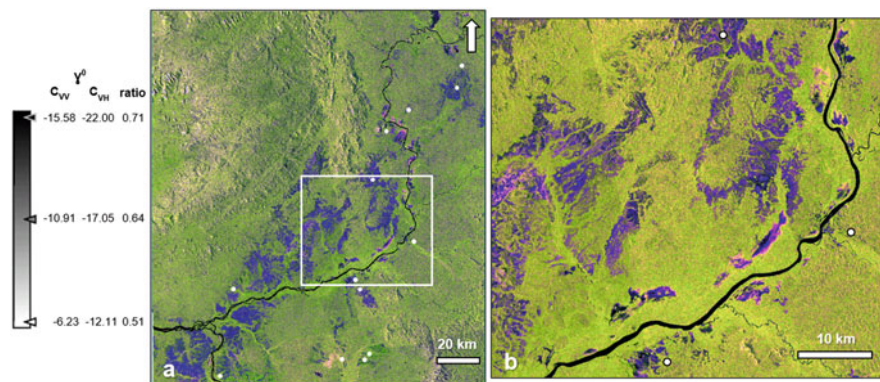


**Fig. 5.9** (a–b) Sentinel-1A, RGB  $C_{VV}$   $C_{VH}$  ratio: (a) Ventuari area, (b) Ventuari training area. White dots indicate field observation sites including vegetation and soil descriptions; sites are identified in Chap. 6



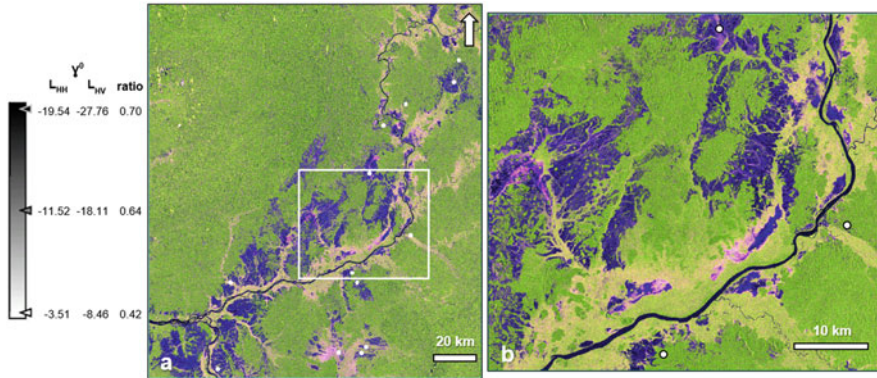


**Fig. 5.10** (a–b) Global PALSAR-2, RGB  $L_{HH}$   $L_{HV}$  ratio: (a) Ventuari area, (b) Ventuari training area. White dots indicate field observation sites including vegetation and soil descriptions; sites are identified in Chap. 6

composite (Fig. 5.9a–b). Non-vegetated terrains (sand deposits or inundated vegetation) with smooth surfaces can be identified by their low response (depending on vegetation density, lots of forward scattering) at both  $C_{VV}$  and  $C_{VH}$  (blue-purple color in the RGB image).

Due to the absence of vegetation at the size of the L-band wavelength and larger, backscatter is very low at both  $L_{HH}$  and  $L_{HV}$  polarizations. The herbaceous cover is hardly distinguishable from bare soil, which both render a bluish color in the L-band RGB composite image (Fig. 5.10a–b). The herbaceous vegetation is also transparent at L-band and results in an extremely low return at both  $L_{HH}$  and  $L_{HV}$  polarizations. Due to the lack of volume scattering, the  $L_{HV}$  backscatter is close to the noise floor of the radar. The slightly brighter features (shades of magenta, reddish-purple color) are caused by riparian vegetation along river channels and by clumps of shrubs and trees (Hansen et al. 2020).

The intensity of the backscatter  $L_{HH}$ ,  $L_{HV}$ , and  $C_{VV}$  polarizations is shown in Fig. 5.11a–b with shades of green (closed to open forests), violet-blue (shrubby meadows), dark purple (dry or flooded open white-sand scrublands), yellow (mosaic of trees and shrubs/herbaceous cover), and magenta (tree cover, regularly flooded) colors. The combination of C- and L-bands allows detecting water under the canopy (Townsend 2001, 2002); furthermore, the weak sensitivity to smooth surfaces of the L-band allows separation between inundated and non-inundated forest areas (Martinis and Rieke 2015; Tsyganskaya et al. 2018).

### 5.3.1.4 Yapacana Area

The Yapacana area is a contrasting environment of alluvial flats, glacia, and fan-glacia. Vegetation varies mostly from open meadow to savanna meadow to shrubby meadow. This area shares much of the LC-LUC classes observed in the Ventuari area. There are relationships between vegetation types and soilscape conditions: for instance, shrubby meadow and meadow on alluvial flats; open

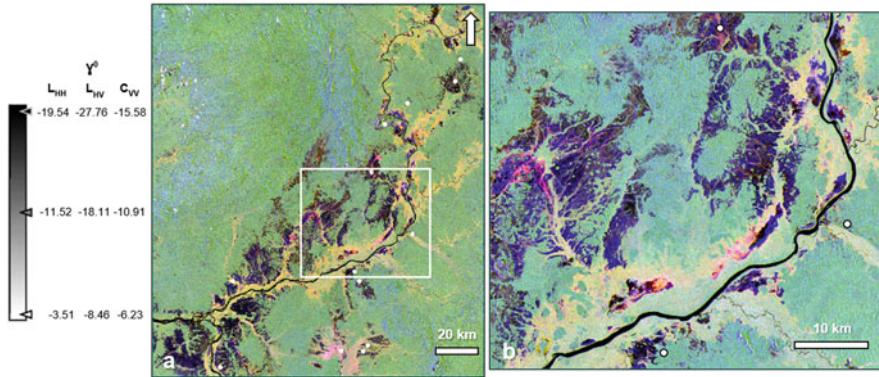


**Fig. 5.11** (a–b) Layer stack RGB  $L_{HH}$   $L_{HV}$   $C_{VV}$ : (a) Ventuari area, (b) Ventuari training area. White dots indicate field observation sites including vegetation and soil descriptions; sites are identified in Chap. 6

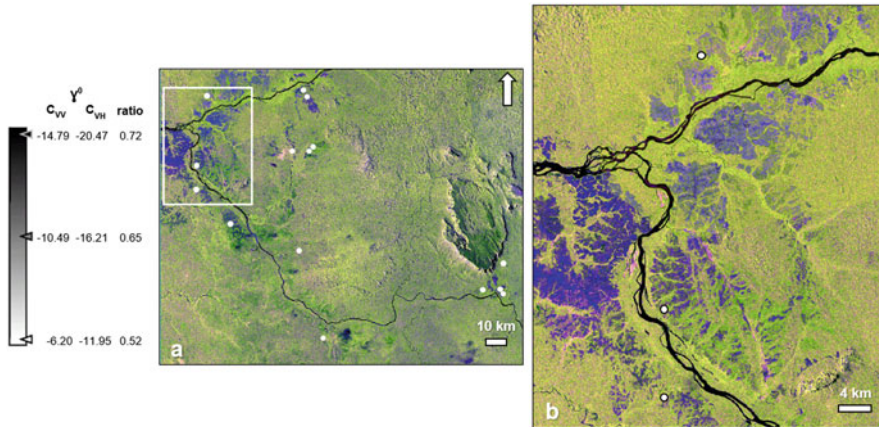


**Fig. 5.12** (a–b) Sentinel-1A, RGB  $C_{VV}$   $C_{VH}$  ratio: (a) Yapacana area, (b) Yapacana training area. White dots indicate field observation sites including vegetation and soil descriptions; sites are identified in Chap. 6

meadow, savanna-meadow, and savanna on glacis; and shrubby meadow and bana scrubland on fan-glacis.

As shown in Fig. 5.12a–b, the C-band is appropriate for the detection of moist or temporary flooded soils under shrubby and herbaceous vegetation (purple and magenta colors), since the wavelength of the C-band allows us to appreciate the depth of the observed scattering (Townsend 2001, 2002; Li et al. 2012). Karszenbaum et al. (2000) showed that  $C_{VV}$  polarizations can detect changes in hydrological conditions in wetlands (e.g., variable flood levels). However, the L-band is more suitable than the C-band for the identification of wetlands covered by forests or dense shrubby herbaceous vegetation (dark blue and magenta colors,

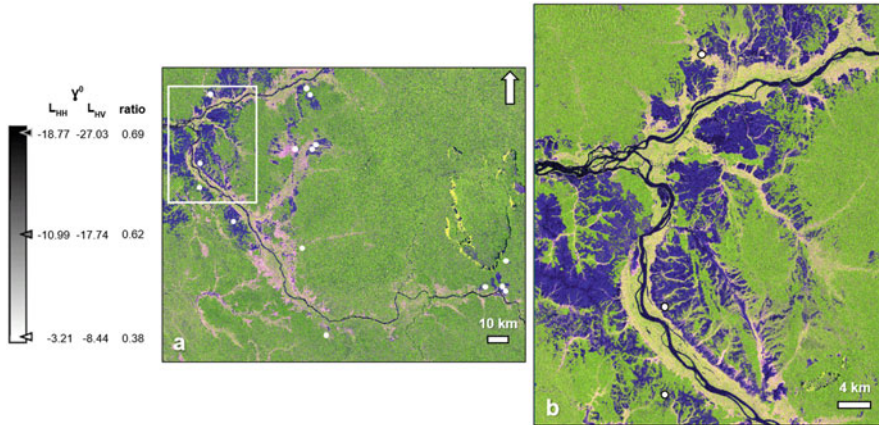


**Fig. 5.13** (a–b) Global PALSAR-2, RGB  $L_{HH}$   $L_{HV}$  ratio: (a) Yapacana area, (b) Yapacana training area. White dots indicate field observation sites including vegetation and soil descriptions; sites are identified in Chap. 6

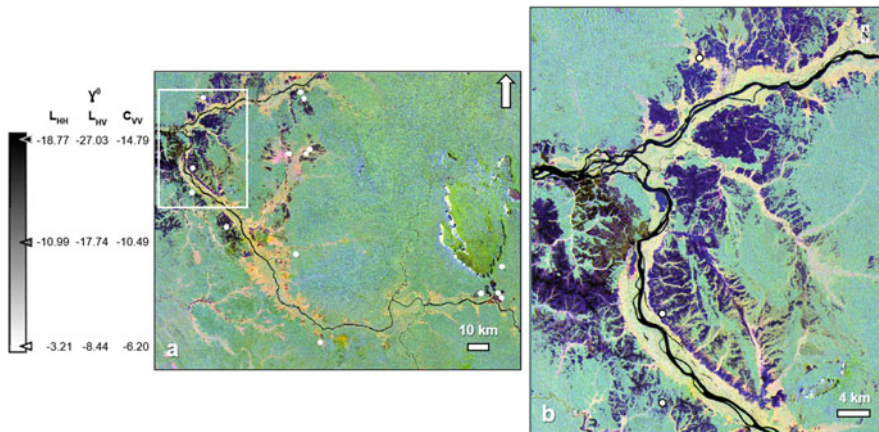


**Fig. 5.14** (a–b) Layer stack RGB  $L_{HH}$   $L_{HV}$   $C_{VV}$ : (a) Yapacana area, (b) Yapacana training area. White dots indicate field observation sites including vegetation and soil descriptions; sites are identified in Chap. 6

Fig. 5.13a–b). The C-band can be useful when the canopy is scarce or during the deciduous season.

The combination of C-band and L-band is more efficient for detecting water under the canopy (Fig. 5.14a–b). For the detection of flooded forest vegetation, polarization  $L_{HH}$  is highly effective. In the C-band, the polarized  $C_{VH}$  produces a backscatter signal strongly influenced by the presence of water beneath woody vegetation, while swamps always have a similar signal regardless of hydrological conditions (Martinis and Rieke 2015; Manavalan et al. 2017). Hess et al. (1990)



showed that the detection of wetlands under canopy is facilitated by incidence angles of less than  $35^\circ$  ( $34.3^\circ$  in our case for the ALOS PALSAR-2). This generalization can be related to a shorter path of the SAR signal through the canopy. Cross polarization ( $C_{VH}$  or  $L_{HV}$ ) is usually more adapted for the distinction between wetlands with forest vegetation and wetlands with herbaceous vegetation due to the sensitivity of cross-polarization to biomass (Ulaby and Long 2014; Thibault et al. 2018).

### 5.3.1.5 Atabapo Area

The Atabapo area is an elongated, flat lowland expanse drained by several east-west oriented rivers and streams. The most common landscape units with meadow and shrubby meadow cover are alluvial plain flats and glacia. The differential hydrological features between alluvial plain flats and glacia can be visualized in the variations of tone and texture observed in the SAR images.

In Fig. 5.15a–b, the C-band backscatter ( $\gamma^0$ ) remains confined to the upper levels of the canopy, and therefore, the floodplain forest presents a backscattering similar to other forest types, regardless of the polarization. However, the C-band signal can reach the water surface through gaps in the canopy, and a VV-polarized double-rebound specular reflection can also be observed in the C-band (shades of pink and magenta colors). Dry or flooded open white-sand scrublands and meadows with smooth surfaces can also be identified by their low response at both  $C_{VV}$  and  $C_{VH}$  in the RGB image (shades of dark blue and purple). Both  $C_{VV}$  and  $C_{VH}$  backscatters are larger for forested areas than for non-forested areas, on average. The  $C_{VV}/C_{VH}$  ratio did not suffice to detect sub-canopy water bodies in flooded forests.

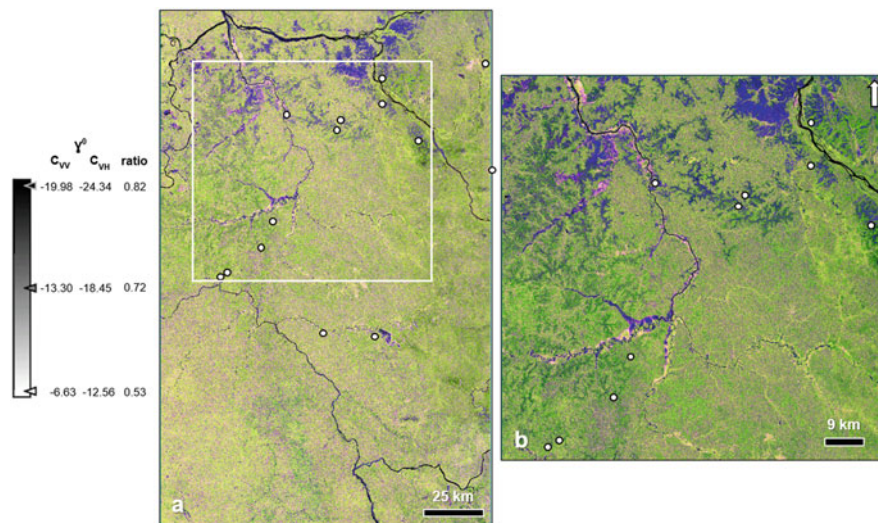


**Fig. 5.15** (a–b) Sentinel-1A, RGB  $C_{VV}$   $C_{VH}$  ratio: (a) Atabapo area, (b) Atabapo training area. White dots indicate field observation sites including vegetation and soil descriptions; sites are identified in Chap. 6

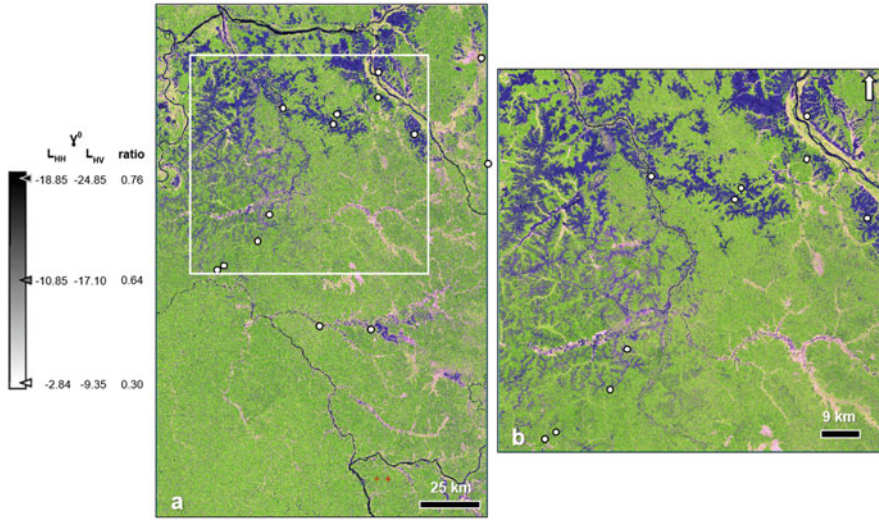


**Fig. 5.16** (a–b) Global PALSAR-2, RGB  $L_{HH}$   $L_{HV}$  ratio: (a) Atabapo area, (b) Atabapo training area. White dots indicate field observation sites including vegetation and soil descriptions; sites are identified in Chap. 6

In seasonally flooded forests in floodplains, water covers parts of the forest floor when river levels are high. With the L-band signal (Fig. 5.16a–b) penetrating the canopy, the vertical stems and the horizontal surface of the water give rise to a strong double-bounce reflection that produces an extremely high  $L_{HH}$  backscatter response. On the other hand, in  $L_{HV}$  polarization, which is dominated only by volume scattering, the extent of the flood is not easily observable, and the backscatter levels are like those of non-flooded forests (Hansen et al. 2020). Herbaceous covers with trees and shrubs show a backscatter low in both  $L_{HH}$  and  $L_{HV}$  polarization. Herbaceous land is virtually indistinguishable from bare soil, both of which are bluish in the L-band RGB composite image.

Remarkably, both false-color SAR composites (Figs. 5.15a–b and 5.16a–b, respectively) exhibit different color impressions (mostly shades of green and blue-purple). Differences are notable foremost by  $L_{HH}$  polarization that is most suitable to distinguish flooded from non-flooded vegetation, while  $L_{HV}$  polarization allowed better separation between woody and non-woody vegetation.

Figure 5.17a–b shows the layer stack RGB  $L_{HH}$   $L_{HV}$   $C_{VV}$ . Hence, green and yellow tones correspond to instances where both  $L_{HH}$  and  $L_{HV}$  information channels have high energy returns (forest areas). Blue-purple and magenta colors are found in the non-forested areas, where the  $L_{HH}$  polarized energy often exhibits a higher return from the surface than the  $L_{HV}$  polarized energy. L-band backscatter ( $\gamma^0$ ) at both  $L_{HH}$  and  $L_{HV}$  polarizations is several dB lower for flooded forests than for other forest types and other kinds of vegetation (pure meadows, white-sand scrublands, and flooded tree areas). Smoother canopies typically display a lower backscatter at  $C_{VV}$  polarization than “rougher” canopies with a higher degree of structural variation.

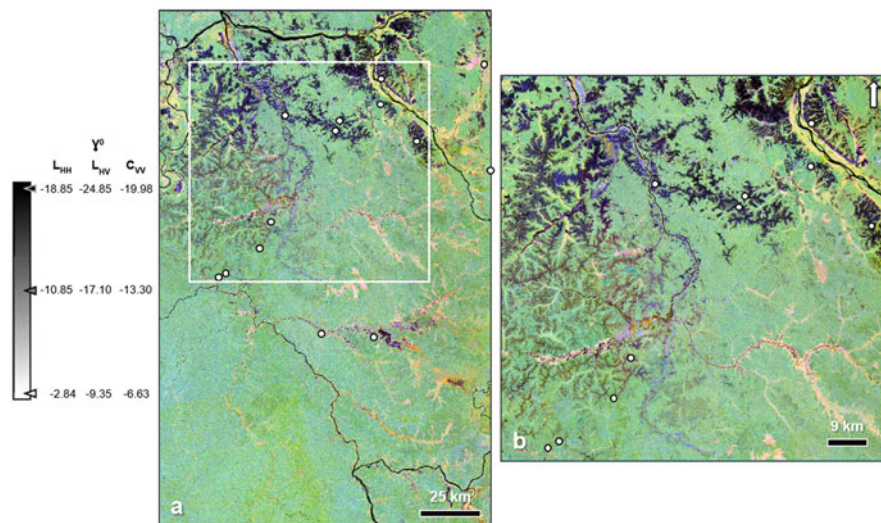


**Fig. 5.17** (a–b) Layer stack RGB  $L_{HH}$   $L_{HV}$   $C_{VV}$ : (a) Atabapo area, (b) Atabapo training area. White dots indicate field observation sites including vegetation and soil descriptions; sites are identified in Chap. 6

### 5.3.1.6 Pasimoni Area

The Pasimoni area is structured by a fluvial system with terraces, levees, backswamps, and floodplains. Meadow patches are small islands, surrounded by caatinga forest. This landscape structure appears less grainy in the PALSAR-2 (Fig. 5.18a–b) as compared to the Sentinel-1 (Fig. 5.19a–b). Noteworthy is a difference in the floodplain area discrimination depending on the polarization in C- and L-bands. Visual comparison between the SAR images shows that in  $L_{HH}$  polarization the double bounce contributes to medium-high backscatter with a ratio ( $L_{HH}/L_{HV}$ ) that is high (shades of blue) in contrast to shades of green of the  $C_{VH}$  polarization.  $L_{HH}$  polarization is less attenuated by the vertical structure of the fluvial system compared also to  $C_{VV}$  polarization, due to the sensitivity of  $L_{HH}$  polarization to double-bounce scattering (Evans and Costa 2013). Likewise, the  $L_{HH}$  polarization produces the greatest contrast between terraces and floodplains. The combination of L- and C-bands (Fig. 5.20a–b) provides a well-balanced compromise of penetration and relevant scattering.

### 5.3.2 Land-cover Classification

Fourteen significant land-cover classes were distinguished based on the cluster centers of the  $L_{HH}$ ,  $L_{HV}$ ,  $C_{VV}$ , and NDVI values (Table 5.7). Classes were defined by a priori probability, a cluster center, and a cluster covariance matrix. The classification technique considers differences between pixels and means of changed



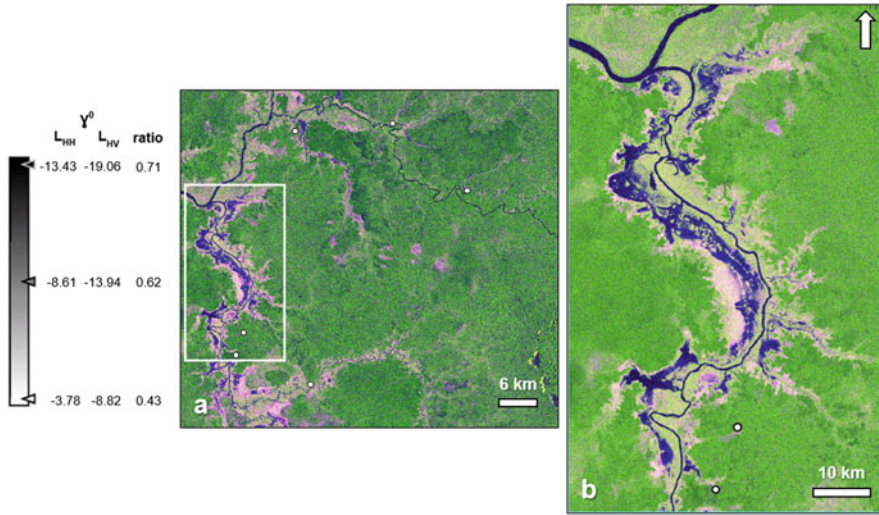


**Fig. 5.18** (a–b) Global PALSAR-2, RGB  $L_{HH} L_{HV}$  ratio: (a) Pasimoni area, (b) Pasimoni training area. White dots indicate field observation sites including vegetation and soil descriptions; sites are identified in Chap. 6

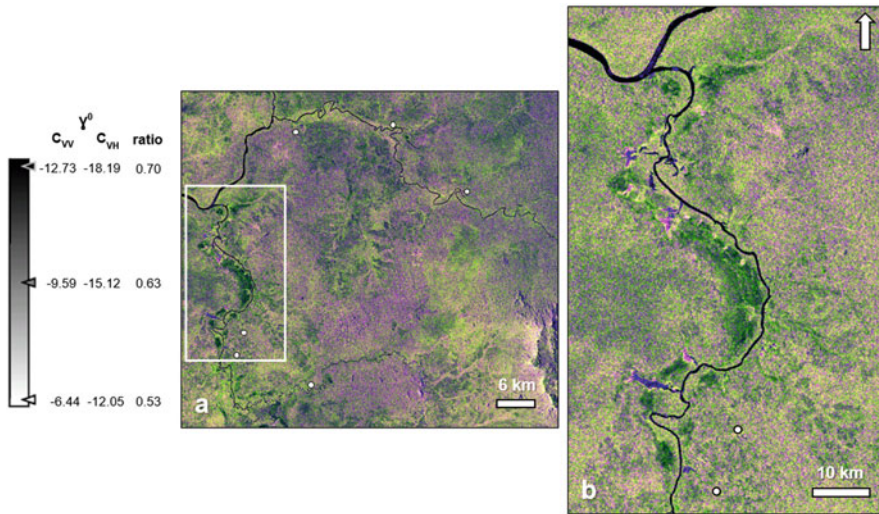


**Fig. 5.19** (a–b) Sentinel-1A, RGB  $C_{VV} C_{VH}$  ratio: (a) Pasimoni area, (b) Pasimoni training area. White dots indicate field observation sites including vegetation and soil descriptions; sites are identified in Chap. 6

and unchanged pixels, which are added to the initial level set to strengthen the correctness of the classification output (Hao et al. 2014). If cluster centers are close to each other, this describes a heterogeneous and complex study region (Yang et al.



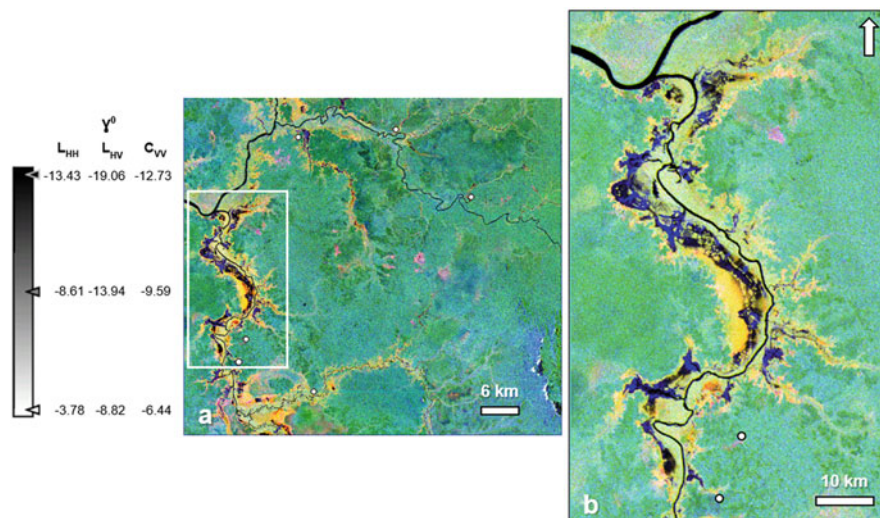


**Fig. 5.20** (a–b) Layer stack RGB  $L_{HH}$   $L_{HV}$   $C_{VV}$ : (a) Pasimoni area, (b) Pasimoni training area. White dots indicate field observation sites including vegetation and soil descriptions; sites are identified in Chap. 6

2012; Zanetti and Bruzzone 2018). Although volume scattering ( $L_{HV}$ ) in both vegetation and soils is important, the clustering centers reveal the predominance of surface scattering ( $L_{HH}$  and  $C_{VV}$ ). This could result from rough ground conditions where backscatter can be significantly enhanced by natural heterogeneity and human disturbances (Kellendorfer 2019, and the sensitivity of  $L_{HH}$  polarization to double-bounce scattering (Evans and Costa 2013).

Table 5.8 shows the percentage of LC-LUC classes by training area. Classes with the highest potential of having Amazonian meadow species, including herbs, forbs, and shrubs, are the units Ws, W1, W2, M1, and Sp. Unit W1 (shrubby meadows frequently interspersed with wooded strips) is specifically recognized to show shrubby meadow vegetation. However, the seasonally flooded units Ws and W2 might encompass relevant inclusions with meadow vegetation, in the areas of Camani, Ventuari, Yapacana, and Atabapo.

The classified LC-LUC classes, together with the segmented and classified high-resolution images (test validation), are shown and described in Appendix (Plates 5.1, 5.2, 5.3, and 5.4). Forest canopies (F1, F2, and F3 classes) are closed (F1) to open (F2 and F3). When open, they show asymmetrical crown configurations, moderate to low foliage density, and dynamic phenological processes in understory vegetation (Huber 2005). Canopy foliage is often clumped; leaves tend to concentrate around crown perimeters and exhibit a vertical leaf angle distribution that is characteristic of sclerophyllous caatinga vegetation. F1 and F2 classes are associated with interfluvial wetlands (Junk et al. 2011). In the  $L_{HH}$  and  $C_{VV}$  bands, higher values were observed for slopes oriented toward the sensors (F3 class), whereas in cross-polarized data ( $L_{HV}$ ), the values were higher for slopes oriented away from the sensors. Forests on

**Table 5.7** Expectation-Maximization (EM) clustering: final cluster centers

ID	Class name	Cluster centers			
		$\gamma^0$ dB			NDVI
		L <sub>HH</sub>	L <sub>HV</sub>	C <sub>VV</sub>	
F1	Closed to open forest, closed crown cover (80–100%) to dense crown cover (50–80%)	−6.422	−10.100	−7.885	0.751
F2	Open forest, dense crown cover (50–80%)	−4.890	−12.200	−7.501	0.664
F3	Upland rocky slope forest	−0.500	−5.303	−3.758	0.632
M1	Mosaic of natural vegetation (trees, shrubs, herbaceous cover) (>50%)/ cropland (<50%)	−6.103	−11.704	−8.600	0.510
M2	Mosaic of trees and shrubs (>50%)/ herbaceous cover (<50%)	−6.100	−10.980	−7.940	0.602
M3	Mosaic of herbaceous cover (>50%)/ trees and shrubs (<50%)	−4.080	−12.450	−8.840	0.554
Ws	Dry or flooded open white-sand scrublands, including bare sand patches	−14.515	−21.862	−11.954	0.239
W0	Water bodies	−16.123	−24.345	−19.221	−0.161
W1	Shrubby meadows frequently interspersed with wooded strips	−6.443	−13.829	−9.143	0.350
W2	Shrubby or herbaceous cover, regularly flooded	−9.333	−16.967	−9.000	0.333
W3	Tree cover, regularly flooded	−5.114	−12.100	−8.500	0.439
Sp	Sparse vegetation (trees, shrubs, herbaceous cover) <20%	−6.710	−13.720	−9.345	0.291
B1	Bare rocky areas	−6.700	−13.800	−9.300	0.150
B2	<i>Sandbanks</i> and <i>sandridges</i>	−21.200	−25.507	−21.320	0.104
U	Built-up area/small towns (Sipapo 1)	−4.740	−14.789	−7.024	0.145

step slopes of limited accessibility are less exposed to human disturbance. Forests are moderately stable communities according to their NDVI values (0.751, 0.664, and 0.632). NDVI has higher sensitivity to crown density differences than other vegetation indices.

The sparse vegetation class (Sp) consists of scattered trees and shrubs in herbaceous cover (<20%). The NDVI value of 0.291 results from the fact that features are reflected more in the visible band than they do in the near-infrared band, indicating areas of low vegetation cover. Woody and herbaceous species intermingle with exposed soil, sand, or rocks differently so that the NDVI results in a mixed signal at the subpixel scale.

Mosaic classes (M1, M2, and M3) signal forest losses resulting from deforestation and/or forest degradation.

The dry or flooded open white-sand scrubland class (Ws) represents a mosaic of shrubby and herbaceous vegetation scattered on the lowland landscape. Recent sedimentary dynamics have caused substantial changes in the landscape of the

**Table 5.8** LC-LUC classes and their distributions on the study areas

ID	Class name	(%)									
		Sipapo1	Sipapo2	Camani	Ventuari	Yapacana	Atabapo	Pasimoni			
F1	Closed to open forest, closed crown cover (80–100%) to dense crown cover (50–80%)	58.1	53.6	39.7	36.0	44.4	46.8	64.7			
F2	Open forest, dense crown cover (50–80%)	14.7	14.5	11.7	12.3	7.4	2.5	7.1			
F3	Upland rocky slope forest	1.0	–	–	–	–	–	–			
M1	Mosaic of natural vegetation (trees, shrubs, herbaceous cover) (>50%/cropland (<50%))	6.3	–	–	–	–	–	–			
M2	Mosaic of trees and shrubs (>50%/herbaceous cover (<50%))	–	8.2	8.5	10.9	6.5	7.9	17.8			
M3	Mosaic of herbaceous cover (>50%/trees and shrubs (<50%))	–	4.4	4.3	9.0	7.1	15.4	2.3			
Ws	Dry or flooded open white-sand scrublands, including bare sand patches	3.4	3.8	10.2	9.6	15.4	7.8	1.8			
W0	Water bodies	4.0	3.2	0.8	1.6	2.8	0.9	1.6			
W1	Shrubby meadows frequently interspersed with wooded strips	1.7	1.7	1.1	7.5	2.0	4.5	4.7			
W2	Shrubby or herbaceous cover, regularly flooded	–	–	3.1	8.5	8.1	5.8	–			
W3	Tree cover, regularly flooded	4.3	–	6.0	4.5	6.2	8.4	–			
Sp	Sparse vegetation (trees, shrubs, herbaceous cover) <20%	2.9	7.9	9.9	–	–	–	–			
B1	Bare rocky areas	3.5	2.3	4.7	–	–	–	–			
B2	Sandbanks and sandridges	0.1	0.4	–	0.1	0.1	0.01	–			
U	Built-up area/Small towns (Sipapo 1)	0.01	–	–	–	–	–	–			

Amazonian lowlands, thereby defining the characteristics of the substrates where white-sand vegetation is now found (Higgins et al. 2011; Rossetti et al. 2019; Zinck, Chap. 10 in this book). Differences in canopy cover show that this class has low herbaceous species richness but high shrub species richness, together with bare sand patches (dark and smooth). Dry and wet scrubland patches have high significant woody stem densities (influence of the  $C_{VV}$  polarization).

Permanent water bodies correspond mostly to white-water and black-water rivers, as well as lagoons and permanent swamps.

Three wetland classes (W1, W2, and W3) were distinguished based on greenness and topo-hydrological characteristics. HH polarization is sensitive to inundated areas resulting in that the double-bounce effect from the water surface to the tree/shrub trunks causes higher backscatter signatures. Wetland areas may indicate temporary water bodies with underlying white-sand vegetation, especially the W3 class that consists of white-sand forests with high light penetration into the forest floor. This class also includes LC-LUC such as floodable scrublands with scattered trees and narrow gallery forests, floodable evergreen forest edges in contact with gallery forests, and seasonally flooded evergreen forests (Junk et al. 2011; Olivero et al. 2016). According to Rosenqvist (1996), the comparison between C- and L-band data would also show a difference in biomass saturation where C-band was found to have a lower threshold, while L-band had a higher one. NDVI values corresponding to the wetland classes are as follows: 0.350 (W1), 0.333 (W2), and 0.439 (W3).

Bare rocky areas consist of exposed rocks and have not more than 10% vegetation cover. *Sandbanks and sandridges (B2 class) are landforms, mostly transient, where sediments accumulate in river channels or the margins thereof.* They have low moisture content and thus lower microwave signal return. Some trees or shrubs can be found on stabilized river sandbanks.

### 5.3.3 Change Detection

LC-LUC performed using the NDVI difference technique evidence that vegetation greenness in the Amazonas state decreases between the period 2000–2009 and the year 2018 (Fig. 5.21a–b). The NDVI maps for the period 2000–2009 and the year 2018, respectively, are displayed in Figs. 5.22, and 5.23. The histograms of both periods show a right-skewed distribution (positive-skew distribution) with a long tail in the positive direction on the number line. The means  $0.80 \pm 0.11$  and  $0.66 \pm 0.16$ , respectively, are also to the right of the peaks.

The areas of interest were examined using the  $\Delta$ NDVI differencing approach (Table 5.5 and Fig. 5.24). The greatest changes in greenness decrease occur in the forest cover in parallel with the expansion of the non-forest covers. The histogram shows a left-skewed distribution (negative-skew distribution). The mean  $-0.14 \pm 0.07$  is to the left of the peak. The goodness of fit of the  $\Delta$ NDVI image values to a normal distribution was verified using Kolmogorov-Smirnov (KS) non-parametric test. Although the KS test indicates a departure from a normal distribution ( $p > 0.01$ ), it is still within the range usually accepted in the literature

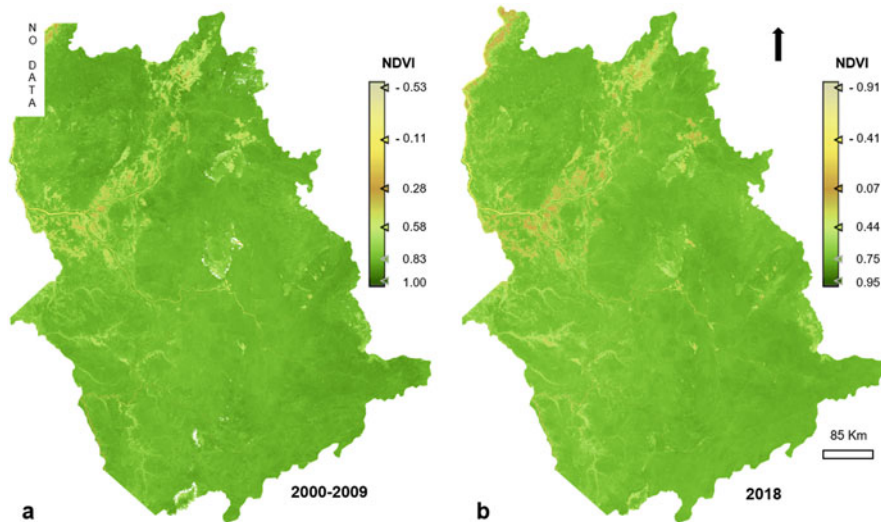


**Fig. 5.21 (a–b)** Amazonas state (Venezuela). Comparison of NDVI derived from available Landsat mosaics. (a) Amazonian LANDSAT TM/ETM+ composite July–September 2000–2009. (b) Circa year 2018 mostly LANDSAT 8 cloud-free image composite

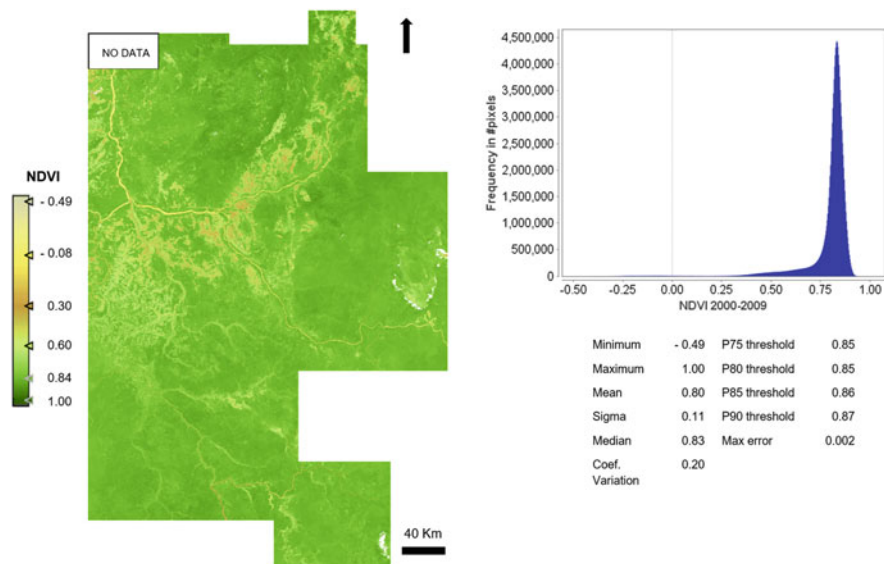


**Fig. 5.22** NDVI map of the study area for the 2000–2009 period. The histogram shows right-skewed distribution (positive-skew distributions), with a long right tail. That is because there is a long tail in the positive direction on the number line. The mean is also to the right of the peak

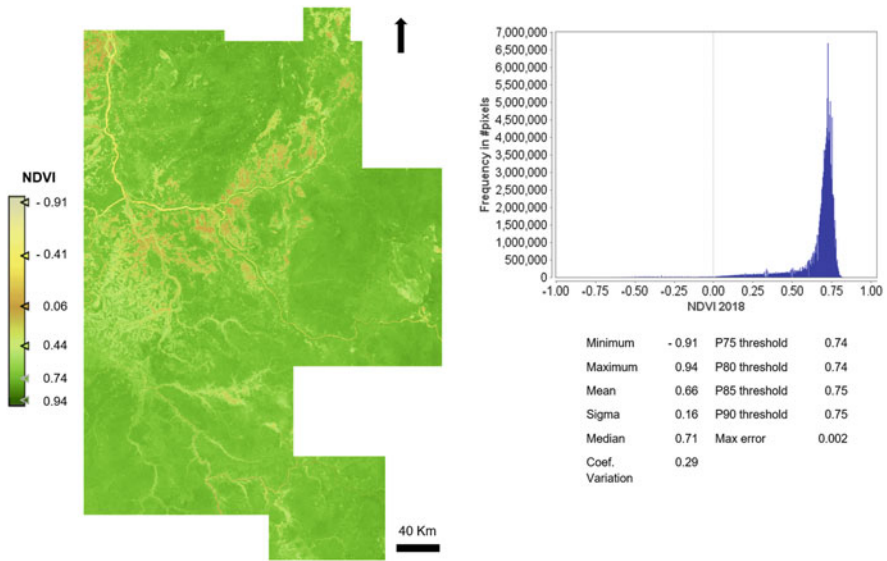


**Fig. 5.23** NDVI map of the study area for the year 2018. The histogram shows right-skewed distribution (positive-skew distributions with a long right tail). That is because there is a long tail in the positive direction on the number line. The mean is also to the right of the peak

(Montanher et al. 2018; O’Connor et al. 2019) to be considered a near-normal distribution.

Decrease in greenness levels can be related to natural disturbances (drought, floods) and anthropic causes (wildfires, deforestation). Since 2007, there has been an irregular rainfall decrease well below the yearly average of 3500 mm. Major drought events occurred in the Amazon basin during the last decade (i.e., in 2005, 2010, 2015, and 2016) as reported in prior research (Lewis et al. 2011; Olivares et al. 2015; Núñez Cobo and Verbist 2018). Referring specifically to the period 2000–2009, Olivero et al. (2016) noted that the greenness of the herbaceous and scrubland classes slightly increased, while that of the forest classes slightly decreased. Atkinson et al. (2011), on the other hand, report a significant long-term decadal decline in vegetation index values, which they decouple from drought occurrence.

Our results indicate that the extent of forest loss in the six study areas during the period 2001–2018 was in decreasing order as follows: Sipapo > Atabapo > Ventuari > Yapacana > Camani, and Pasimoni (Table 5.6; Fig. 5.25).

The NDVI ranges of LC types in different years indicate LUC (Fig. 5.26a–b). For example, in the Ventuari subset, forest coverage and density have decreased over the last 18 years, while dry open white-sand areas with or without shrubs have expanded, reaching the lowest NDVI value range (−0.10–0.24) in the year 2018. This transition of landscape types indicates forest degradation, despite that forest coverage has NDVI values higher than other LC because of high crown density.

**Table 5.5** Statistics of the Normalized Difference Vegetation Index (NDVI) derived from available Landsat mosaics

Areas of interest (AOI)	NDVI scale 2000–2009 * (first rows)/2018 ** (second rows) $\Delta \text{NDVI} = \text{NDVI}_{2018} - \text{NDVI}_{2000-2009}$												Mean	Std dev	Median	CV %
	(1)	$\Delta$	(2)	$\Delta$	(3)	$\Delta$	(4)	$\Delta$	(5)	$\Delta$	(6)	$\Delta$				
Sipapo	-0.48	-0.43	-0.07	-0.35	0.29	-0.25	0.61	-0.21	0.82	-0.13	1.00	-0.11	0.77	0.27	0.82	26
	-0.91		-0.42		0.04		0.40		0.69		0.89		0.62	0.22	0.71	37
Camani	0.12	-0.76	0.36	-0.60	0.58	-0.45	0.76	-0.34	0.90	-0.24	1.00	-0.18	0.79	0.13	0.84	28
	-0.64		-0.24		0.13		0.42		0.66		0.82		0.61	0.17	0.69	44
Ventuari	-0.40	-0.42	-0.02	-0.34	0.34	-0.28	0.62	-0.22	0.85	-0.18	1.00	-0.15	0.80	0.13	0.84	24
	-0.82		-0.36		0.06		0.40		0.67		0.85		0.66	0.18	0.72	33
Yapacana	-0.39	-0.43	-0.01	-0.33	0.33	-0.22	0.62	-0.16	0.84	-0.09	1.00	-0.06	0.80	0.12	0.83	19
	-0.82		-0.34		0.11		0.46		0.75		0.94		0.68	0.15	0.72	26
Atabapo	-0.34	-0.57	0.01	-0.44	0.33	-0.31	0.58	-0.21	0.79	-0.13	0.93	-0.07	0.79	0.12	0.82	22
	-0.91		-0.43		0.02		0.37		0.66		0.86		0.64	0.17	0.70	32
Pasimoni	-0.15	-0.67	0.16	-0.54	0.46	-0.38	0.69	-0.26	0.87	-0.14	1.00	-0.08	0.82	0.09	0.83	11
	-0.82		-0.38		0.08		0.43		0.73		0.92		0.70	0.08	0.71	16
AOIs total	-0.49	-0.42	-0.08	-0.33	0.30	-0.24	0.60	-0.16	0.84	-0.10	1.00	-0.06	0.80	0.11	0.83	20
	-0.91		-0.41		0.06		0.44		0.74		0.94		0.66	0.16	0.71	29
Amazonas state	-0.53	-0.38	-0.11	-0.30	0.28	-0.21	0.58	-0.14	0.83	-0.08	1.00	-0.05	0.82	0.09	0.84	16
	-0.91		-0.41		0.07		0.44		0.75		0.95		0.70	0.13	0.73	23

Source: \* Amazonian LANDSAT TM/ETM+ composite July–September 2000–2009 (Van doninek and Tuomisto 2018) \*\* Circa year 2018 LANDSAT cloud-free image composite (Last), Global Forest Change v1.6 (Hansen et al. 2013), Std dev: standard deviation, CV: coefficient of variation. (1) to (6) = NDVI scale 2000–2009 (first rows)/2018 (second rows).  $\Delta \text{NDVI} = \text{NDVI}_{2018} - \text{NDVI}_{2000-2009}$



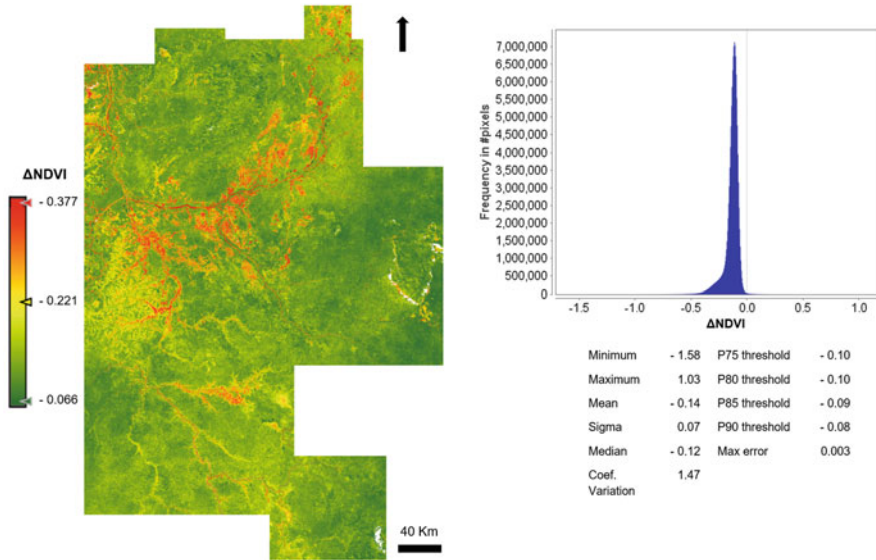


**Fig. 5.24** NDVI differencing technique: change detection in land-use alterations during the 2000–2009 period versus 2018. Left-skewed distribution (*negatively skewed* distributions) has a long left tail. That is because there is a **long tail** in the negative direction on the number line. The mean is also to the left of the peak

### 5.4 Concluding Remarks

This research demonstrated that multi-band SAR data and NDVI integration can be used to map the vegetation of white-sand ecosystems of tropical regions with reasonable accuracy. The use of SAR and optical data has been enabled by the availability of free and open data, well-known image processing, and analysis methods.

The results show that SAR data are an important information source for white-sand ecosystem studies. Our findings show that L-band images explain a greater proportion of feature variability (PCA) appropriate for interpretation than C-band images. For PALSAR-2,  $L_{HH}$  and  $L_{HV}$  presented the highest polarization importance, while for Sentinel-1 the most valuable polarization was  $C_{vv}$ . These findings align with previous research that posits that L-band SAR is, in general, better suited for forest mapping than C-band SAR, since the latter is saturating at much lower biomass vegetation than L-band.

As the C-band dual-polarimetric data are characterized by some limitations regarding the above-described interpretation, the L-band dual-pol enables better separation of different LC-LUC types. L-band SAR data show higher penetration depth into vegetation resulting in better differentiation of flooded and non-flooded

**Table 5.6** Gross loss in forest cover and annual rainfall in the study area

Year	Gross forest cover loss in hectares per year *										Rainfall mm **			
	Sipapo	Camani	Ventuari	Yapacana	Atabapo	Pasimoni	Total	Max	Min	Mean	Median			
2001	1755	1283	2438	992	1217	23	7708	4419	1036	3250	3510			
2002	827	96	457	396	745	34	2555	5168	1497	3790	4025			
2003	1593	122	1329	607	1333	94	5078	4690	1343	3540	3715			
2004	2296	36	1079	764	2213	66	6455	4570	1427	3307	3420			
2005	1247	56	639	370	1318	37	3668	4642	1429	3181	3218			
2006	882	59	440	262	725	35	2403	4917	1516	3372	3422			
2007	4103	250	3894	1618	3321	101	13,287	5058	1307	3427	3412			
2008	1606	205	1847	858	1429	17	5962	3862	1162	2672	2687			
2009	1568	102	1102	605	1542	80	4999	3860	853	2618	2729			
2010	2581	213	3389	2390	2098	132	10,804	4573	1277	2944	2950			
2011	1119	23	607	531	1035	38	3352	4481	1409	3194	3417			
2012	1488	25	739	637	1114	56	4059	4319	993	2972	3017			
2013	1894	88	955	1044	1968	59	6008	3964	891	2537	2549			
2014	2081	143	1191	708	1949	133	6205	3770	810	2570	2695			
2015	1621	49	649	503	1413	97	4331	3385	513	2246	2325			
2016	3544	205	3232	3933	3883	194	14,991	4731	1002	3067	3160			
2017	3094	234	1299	1594	2822	123	9167	4090	858	2716	2808			
2018	5793	634	5862	3912	5953	92	22,246	3827	878	2596	2802			
Total	39,095	3823	31,147	21,724	36,077	1410	133,276	4351	1122	3000	3103			

Source: \* Data extracted from annual 30 m global (Hansen/UMD/Google/USGS/NASA) \*\* Amazonas state: Precipitation Estimation from Remotely Sensed Information using Artificial Neural Networks (PERSIANN) data

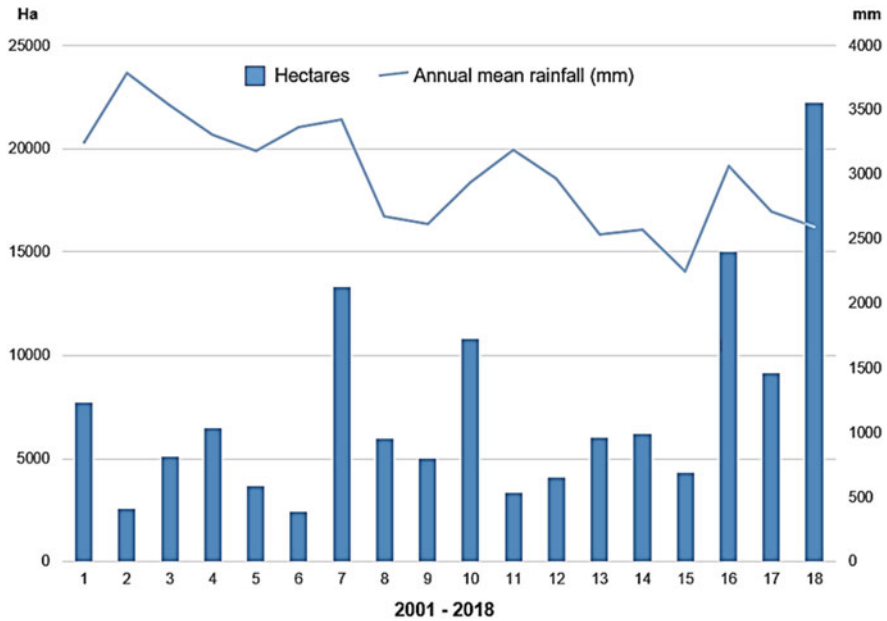


**Fig. 5.25** Study area: tree cover loss (hectares) extracted from Hansen et al. (2013) and mean annual rainfall (mm)

vegetation. However, there was ambiguity in discerning some inundated white sand from non-white-sand areas due to similar smooth roughness (tone and texture).

Our results show and confirm arguments of prior research regarding the two radar systems analyzed having different capabilities to identify landscape features. The approach of combining two different microwave sensors is a sound one, given that orbital sensors can acquire multi-frequency and multi-polarization data.

The method of using an integrated image classification approach (L and C-band with NDVI data) allowed grouping spectral combinations of classes, being an operative way for mapping complex units. Using only observed variations in NDVI values to characterize the LC-LUC classes could lead to circular reasoning because the classification in either one class or another is itself a consequence of the temporal variations of greenness. However, the integrated NDVI and SAR data for classification purposes have the potential to assess the effects of greenness detection in the area of interest with detailed spatial resolution, supported by the temporal variations identified by the MODIS data.

The methodology based on SAR and optical data integration can be transferred and adopted in other regions and countries by researchers or practitioners, since ALOS PALSAR-1, Sentinel-1, Landsat 8, and Sentinel-2 images, among others, are freely available and can be processed and manipulated in free open-access software such as SNAP, PolSARpro, SARbian OS, and QGIS. In extending this framework to other geographies and through time, it is important to highlight the potential of

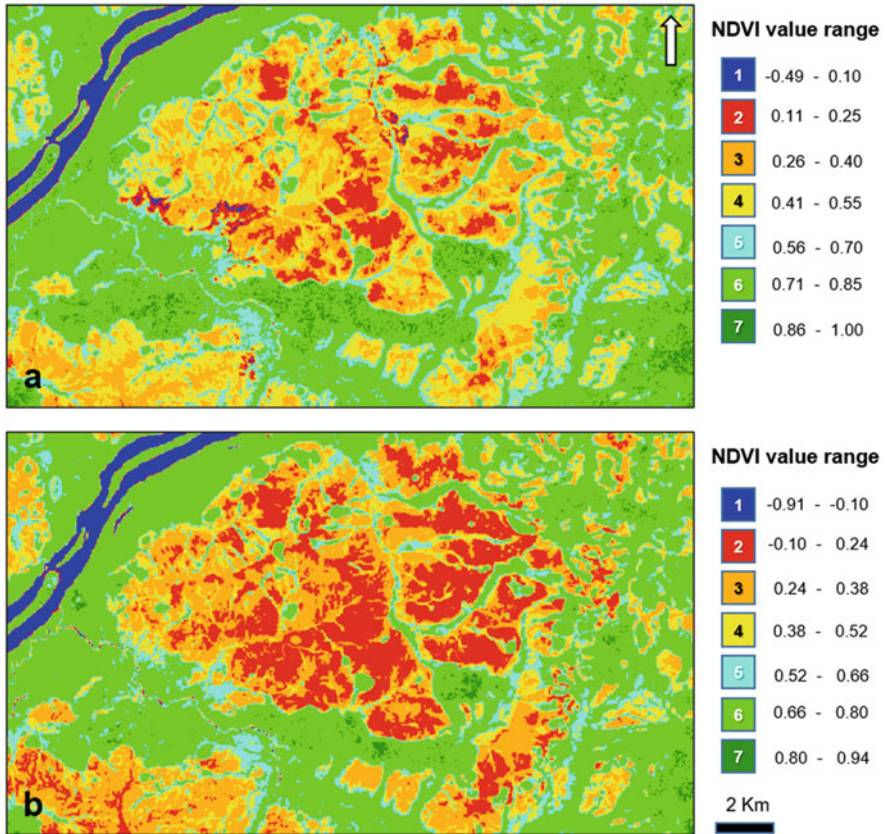


**Fig. 5.26** (a–b) Subset from the Ventuari area: NDVI range values of different land-cover types for the 2000–2009 period (a) and the year 2018 (b). (1) Water bodies, including small shallow inland water bodies. (2) Dry open white sand (bare sand patches). (3) Dry open white-sand scrublands. (4) Flooded open white-sand scrublands. (5) Shrubby meadows. (6) Closed to open forest. (7) Closed forest; classes (3) and (4) include scattered trees and narrow gallery forests

Platforms for Big Earth Observation (EO) data management and analysis, such as GEE used in this study and NASA Earth Exchange, and Amazon's Web Services.

**Acknowledgments** The authors would like to thank the available Amazonian Landsat TM/ETM+ composite mosaic provided by Dr. Van Doninck J.

## Appendix: Classified Land-Cover-Land-Use Cover Classes, Together with the Segmented and Classified High-Resolution Images, Per Study Area

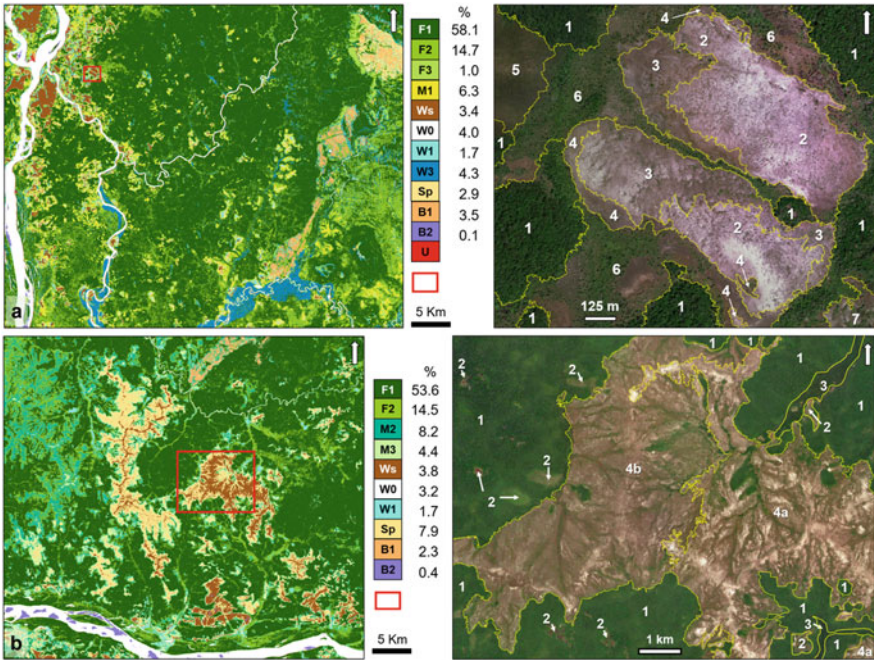


**Plate 5.1** Sipapo areas. (a–b) **F1** Closed to open forest (closed to dense crown cover), **F2** Open forest (dense crown cover), **F3** Upland rocky slope forest, **M1** Mosaic of natural vegetation (trees, shrubs, herbaceous cover) (>50%/cropland (<50%), **M2** Mosaic of trees and shrubs (>50%/herbaceous cover (<50%), **M3** Mosaic of herbaceous cover (>50%/trees and shrubs (<50%), **Ws** Dry or flooded open white-sand scrublands (including bare sand patches), **W0** Water bodies, **W1** Shrubby meadows frequently interspersed with wooded strips, **W3** Tree cover, regularly flooded, **Sp** Sparse vegetation (trees, shrubs, herbaceous cover) (<20%), **B1** Bare rocky areas, **B2** Sandbanks and sandridges, **U** Urban areas. (a) Land cover of the Sipapo 1 training area. Box red (image of right upper corner): Subset of a Bing Maps Satellite image in the Sipapo 1 lowlands (northern sector); Credit: <https://www.bing.com/maps/aerial>. (1) Forest, (2) Dry open white-sand scrublands (with bare sand patches), (3) Flooded open white-sand scrublands, (4) Bare ground with sand sheets and shrub patches, (5) Rounded grayish areas corresponding to a poorly drained depression, (6) Shrubby meadow vegetation interspersed with wooded strips, (7) Penneplain landscape; rounded low hill (crystalline bedrock), sparse vegetation and rock outcrops. (b) Land cover of the Sipapo 2 training area. Box red (image of right lower corner): Subset of a Bing Maps Satellite image (high resolution) showing the alluvial plain flats in the Sipapo 2 lowlands (southern sector); Credit: <https://www.bing.com/maps/aerial>. (1) Forest associated with interfluvial meadows. Note the deforestation patches (2) and the meadows (3). Meadow glades within caatinga forest occur on terrace levels and savanna on floodplains. Alluvial depression (4) of low gradient can be subdivided into two sectors, one with scattered sand dune-like mounds (4a) and another without (4b)



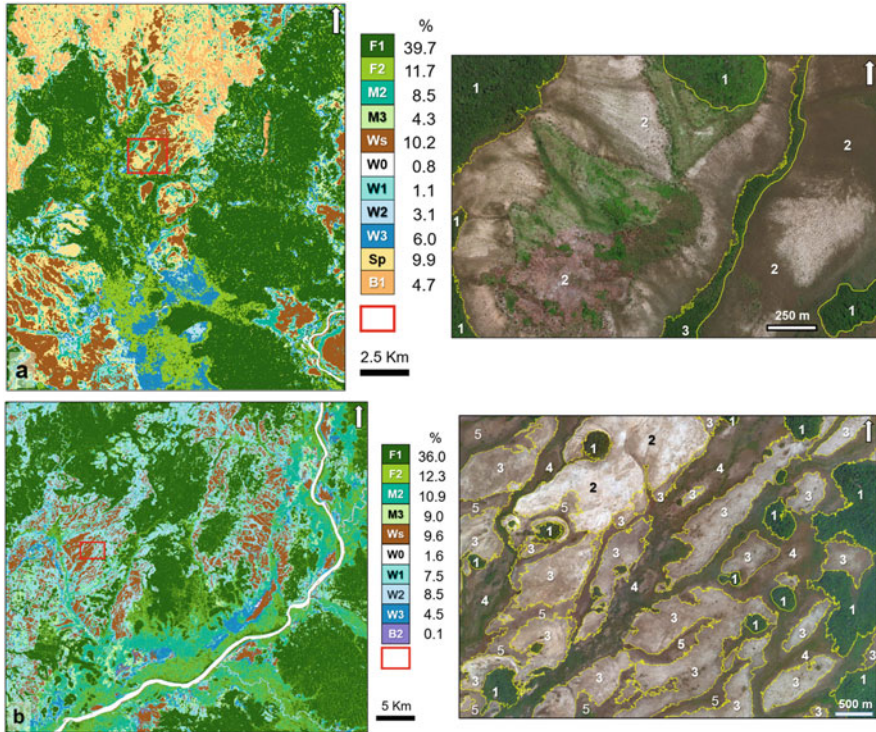


**Plate 5.2** Camani and Ventuari areas. **(a-b)** **F1** Closed to open forest (closed to dense crown cover), **F2** Open forest (dense crown cover), **M2** Mosaic of trees and shrubs (>50%)/herbaceous cover (<50%), **M3** Mosaic of herbaceous cover (>50%)/trees and shrubs (<50%), **Ws** Dry or flooded open white-sand scrublands (including bare sand patches), **W0** Water bodies, **W1** Shrubby meadows frequently interspersed with wooded strips, **W2** Shrubby or herbaceous cover, regularly flooded, **W3** Tree cover, regularly flooded, **Sp** Sparse vegetation (trees, shrubs, herbaceous cover) (<20%), **B1** Bare rocky areas, **B2** Sandbanks and sandridges. **(a)** Land cover of the Camani training area. Box red (image of right upper corner): Subset of a Bing Maps Satellite image (high resolution) from the Camani area; *Credit: <https://www.bing.com/maps/aerial>*. Note the distinct valley landforms, gully erosion, and sand deposits. The surface is covered by open shrubby herbaceous formations severely degraded (deforestation, wildfires); (1) Forest, (2) dry or flooded open white-sand scrublands and herbaceous cover, (3) shrubby meadow vegetation interspersed with wooded strips. **(b)** Land cover of the Ventuari training area. Box red (image of right lower corner): Subset of a Bing Maps Satellite image (high resolution) showing an alluvial depression/floodplain in the Ventuari lowlands (northwest sector); *Credit: <https://www.bing.com/maps/aerial>*. (1) Forest, (2) dry open white-sand scrublands (with bare sand patches), (3) flooded open white-sand scrublands, (4) mixed savanna-meadow vegetation, (5) herb-forb savannas, and meadow-savanna with low density of shrubs

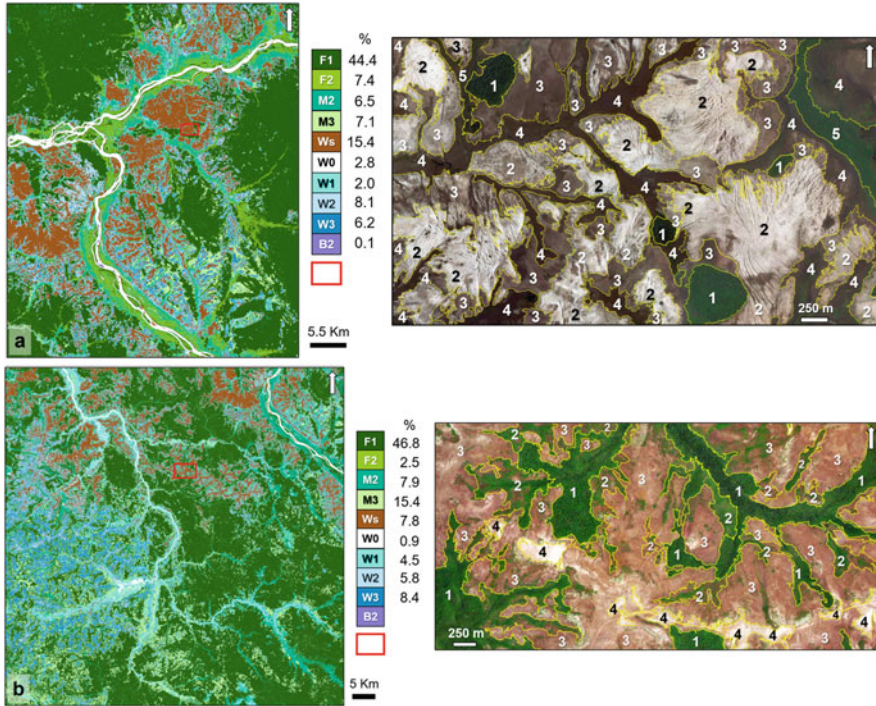


**Plate 5.3** Yapacana and Atabapo areas. **(a-b)** **F1** Closed to open forest (closed to dense crown cover), **F2** Open forest (dense crown cover), **M2** Mosaic of trees and shrubs (>50%)/herbaceous cover (<50%), **M3** Mosaic of herbaceous cover (>50%)/trees and shrubs (<50%), **Ws** Dry or flooded open white-sand scrublands (including bare sand patches), **W0** Water bodies, **W1** Shrubby meadows frequently interspersed with wooded strips, **W2** Shrubby or herbaceous cover, regularly flooded, **W3** Tree cover, regularly flooded, **B2** Sandbanks and sandridges. **(a)** Land cover of the Yapacana training area. Box red (image of right upper corner): Subset of a Bing Maps Satellite image (high resolution) of the Yapacana lowlands (northeast sector); Credit: <https://www.bing.com/maps/aerial>. (1) Forest, (2) bare sand patches, (3) flooded open white-sand scrublands, (4) shrubby meadow, (5) mixed savanna-meadow vegetation. **(b)** Land cover of the Atabapo training area. Box red (image of right lower corner): Subset of a Bing Maps Satellite image (high resolution) showing a flat lowland expanse drained by several streams in the Atabapo area (northern sector); Credit: <https://www.bing.com/maps/aerial>. White-sand forest associated with interfluvial wetlands: slightly degraded (1), moderately to severely degraded (2), and severely degraded (3); (4) dry open white-sand scrublands including bare sand patches



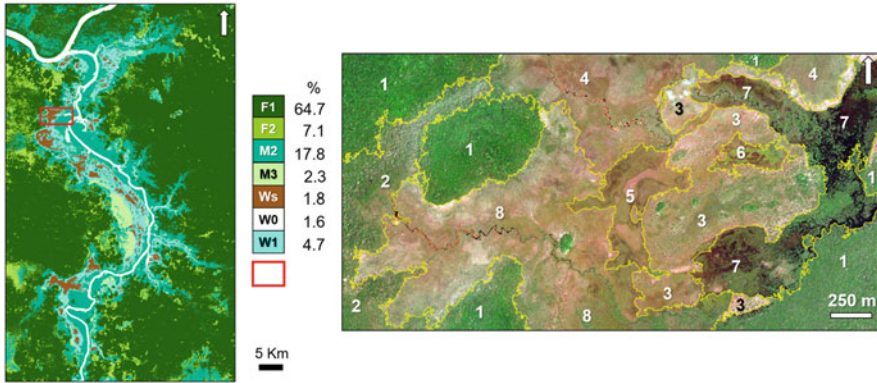


**Plate 5.4** Pasimoni area. **F1** Closed to open forest (closed to dense crown cover), **F2** Open forest (dense crown cover), **M2** Mosaic of trees and shrubs (>50%)/herbaceous cover (<50%), **M3** Mosaic of herbaceous cover (>50%)/trees and shrubs (<50%), **Ws** Dry or flooded open white-sand scrublands (including bare sand patches), **W0** Water bodies, **W1** Shrubby meadows frequently interspersed with wooded strips. Land cover of the Pasimoni training area. Box red (image of right): Subset of a Bing Maps Satellite image (high resolution) from the Pasimoni area (northwest sector) showing terrain spatial variability, flooding regime, and topography of white-sand vegetation; *Credit:* <https://www.bing.com/maps/aerial>. (1) Forest growing on white sands, (2) mosaic of trees and shrubs (>50%)/herbaceous cover (<50%), (3) dry open white-sand scrublands, (4) mosaic of herbaceous cover (>50%)/trees and shrubs (<50%), (5) poorly drained depression, (6) flooded open white-sand scrublands, (7) flooded shrubby meadows in very poorly drained places such as infilled river channels and backswamps, (8) mosaic of bare sand and bare soil patches (>50%)/dry or flooded open white-sand scrublands (<50%)

## References

- Adeli S, Salehi B, Mahdianpari M, Quackenbush LJ, Brisco B, Tamiminia H, Shaw S (2020) Wetland monitoring using SAR data: a meta-analysis and comprehensive review. *Remote Sens* 12:1–28. <https://doi.org/10.3390/rs12142190>
- Adeney, JM (2009) Remote sensing of fire, flooding and white-sand ecosystems in the Amazon. Ph. D. Dissertation, Duke University
- Adeney JM, Christensen NL, Vicentini A, Cohn-Haft M (2016) White-sand ecosystems in Amazonia. *Biotropica* 48(1):7–23
- Akar Ö, Güngör O (2015) Integrating multiple texture methods and NDVI to the random Forest classification algorithm to detect tea and hazelnut plantation areas in Northeast Turkey. *Int J Remote Sens* 36:442–464
- Amitrano D, Di Martino G, Iodice A, Riccio D, Ruello G (2016) RGB SAR products: methods and applications. *European Journal of Remote Sensing* 49(1):777–793
- Arvor D, Funatsu BM, Michot V, Dubreuil V (2017) Monitoring rainfall patterns in the southern Amazon with PERSIANN-CDR data: long-term characteristics and trends. *Remote Sens* 9:889. <https://doi.org/10.3390/rs9090889>
- Atkinson PM, Dash J, Jeganathan C (2011) Amazon vegetation greenness as measured by satellite sensors over the last decade. *Geophys Res Lett* 38:L19105. <https://doi.org/10.1029/2011GL049118>

- Aymard CG, Schargel R, Berry P, Stergios B (2009) Estudio de los suelos y la vegetación (estructura, composición florística y diversidad) en bosques macrotérmicos no-inundables, estado Amazonas, Venezuela. In: Aymard GA, Schargel R (eds) *Biollania edic esp 9*. UNELLEZ, Guanare, Venezuela, pp 6–251
- Baatz M, Schäpe A (2000) Multiresolution segmentation: an optimization approach for high quality multi-scale image segmentation. In: *Angewandte Geographische Informationsverarbeitung XII*. Wichmann, Heidelberg, Germany, pp 12–23
- Blanco PD, López Saldaña G, Colditz R, Hardtke L, Llamas RM, Mari NA, Fischer A, Caride C, Aceñolaza P, del Valle HF, Lillo-Saavedra M, Coronato FR, Opazo S, Morelli F, Anaya J, Sione W, Zamboni P, Barrena Arroyo V (2013) A land cover map of Latin America and the Caribbean in the framework of the SERENA project. *Remote Sens Environ* 132:13–31
- Bruzzone L, Wegmüller U, Wiesmann A (2004) An advanced system for the automatic classification of multitemporal SAR images. *IEEE Trans Geosci Remote Sens* 42:1321–1334
- CEOS (2018) A layman's interpretation guide to L-band and C-band synthetic aperture radar data. Version 2.0. 15 November 2018. Global Forest observation initiative (GFOI). Committee on earth observation satellite (CEOS), systems engineering office (SEO), pp 31
- Channan S, Collins K, Emanuel WR (2014) Global mosaics of the standard MODIS land cover type data. University of Maryland and the Pacific Northwest National Laboratory, College Park, Maryland, USA
- Cordeiro CLO, Rossetti DF, Gribel R, Tuomisto H, Zani H, Ferreira CA, Coelho L (2016) Impact of sedimentary processes on white-sand vegetation in an Amazonian megafan. *J Trop Ecol* 32: 498–509
- Damasco G, Vicentini A, Castilho CV, Pimentel TP, Nascimento HEM (2012) Disentangling the role of edaphic variability, flooding regime, and topography of Amazonian white-sand vegetation. *J Veg Sci* 1-11
- del Valle HF, Blanco PD, Hardtke LA, Metternicht G, Bouza PJ, Bisigato A, Rostagno CM (2016) Contribution of open access global SAR mosaics to soil survey programs at regional level: a case study in North-Eastern Patagonia. Chapter XIX, pp. 321-346. In: Zinck JA, Metternicht G, Bocco G, del Valle HF (eds) *Geopedology: an integration of geomorphology and pedology for soil and landscape studies*. Springer, Switzerland
- Deus D (2016) Integration of ALOS PALSAR and Landsat data for land cover and forest mapping in northern Tanzania. *Land, MDPI* 5(4):1–19
- ESA (2017) Land cover CCI product user guide version 2. Technical report. available at: [maps.elie.ucl.ac.be/CCI/viewer/download/ESACCI-LC-Ph2-PUGv2\\_2.0.pdf](https://maps.elie.ucl.ac.be/CCI/viewer/download/ESACCI-LC-Ph2-PUGv2_2.0.pdf)
- Evans TL, Costa M (2013) Landcover classification of the lower Nhecolândia subregion of the Brazilian Pantanal wetlands using ALOS/PALSAR, RADARSAT-2, and ENVISAT/ASAR imagery. *Remote Sens Environ* 128:118–137. <https://doi.org/10.1016/j.rse.2012.09.022>
- Fisher JL, Mustard JF (2007) Cross-scalar satellite phenology from ground, Landsat and MODIS data. *Remote Sens Environ* 109:261–273
- Friedl MA, Sulla-Menasse D, Tan B, Schneider A, Ramankutty N, Sibley A, Huang X (2010) MODIS collection 5 global land cover: algorithm refinements and characterization of new datasets, 2001–2012. In: *Collection 5.1 IGBP land cover*. Boston University, Boston, MA, USA
- Furtado LF, Silva TS, Fernandes PJ, Novo EM (2015) Land cover classification of Lago Grande de Curuai floodplain (Amazonia, Brazil) using multi-sensor and image fusion techniques. *Acta Amazon* 45(2):195–202
- Google LLC (2019) Retrieved March 5, 2019
- Gorelick N, Hancher M, Dixon M, Ilyushchenko S, Thau D, Moore R (2017) Google Earth Engine: planetary-scale geospatial analysis for everyone. *Remote Sens Environ* 202:18–27. <https://doi.org/10.1016/j.rse.2017.06.031>
- Hagensieker R, Waske B (2018) Evaluation of multi-frequency SAR images for tropical land cover mapping. *Remote Sens* 10(2):257. <https://doi.org/10.3390/rs10020257>
- Hansen MC, Potapov PV, Moore R, Hancher M, Turubanova SA, Tyukavina A, Thau D, Stehman SV, Goetz SJ, Loveland TR, Kommareddy A, Egorov A, Chini L, Justice CO, Townshend JRG

- (2013) High-resolution global maps of 21st-century forest cover change. *Science* 342 (15 November):850–53. Data available online from. <http://earthenginepartners.appspot.com/science-2013-global-forest>
- Hansen JN, Mitchard ETA, King S (2020) Assessing Forest/non-Forest separability using Sentinel-1 C-band synthetic aperture radar. *Remote Sens* 12(11):1–21. <https://doi.org/10.3390/rs12111899>
- Hao M, Shi W, Zhang H, Li C (2014) Unsupervised change detection with expectation-maximization-based level set. *IEEE Geosci Remote Sens Lett* 11(1):210–214
- Henderson FM, Lewis AJ (eds) (1998) Principles and applications of imaging radar. Manual of remote sensing, vol 2, 3rd edn. John Wiley and Sons, New York
- Henderson FM, Lewis AJ (2008) Radar detection of wetland ecosystems: a review. *Int J Remote Sens* 29:5809–5835
- Hess LL, Melack JM, Simonett DS (1990) Radar detection of flooding beneath the forest canopy: a review. *Int J Remote Sens* 11:1313–1325
- Higgins MA, Ruokolainen K, Tuomisto H, Llerena N, Cardenas G, Phillips OL, Vásquez R, Matti R (2011) Geological control of floristic composition in Amazonian forests. *J Biogeogr* 38:2136–2149
- Huber O (2005) Diversity of vegetation types in the Guayana region: an overview. In: Friis I, Balslev H (eds) plant diversity and complexity patterns: local, regional and global dimensions. *Biologiske Skrifter* 55:169–188
- Ince T (2010) Unsupervised classification of polarimetric SAR image with dynamic clustering: an image processing approach. *Adv Eng Softw* 41:636–646
- JAXA (2018) Global 25-m resolution PALSAR-2/PALSAR mosaic and Forest/non-Forest map (FNF). Dataset description. Japan Aerospace Exploration Agency (JAXA). Earth observation research center (EORC). Version H, May 7, 2018, pp 9
- Jesus JB, Kuplich TM (2020) Applications of SAR data to estimate forest biophysical variables in Brazil. *Cerne* 26(1):88–97
- Joshi N, Baumann M, Fensholt R, Grogan K, Hostert P, Jepsen MR, Kuemmerle T, Meyfroidt P, Mitchard ETA et al (2016) A review of the application of optical and radar remote sensing data fusion to land use mapping and monitoring. *Remote Sens* 8(1):70
- Junk W, Piedade MT, Schöngart J, Cohn-Haft M, Adeney J, Wittmann F (2011) A classification of major naturally-occurring Amazonian lowland wetlands. *Wetlands* 31:623–640. <https://doi.org/10.1007/s13157-011-0190-7>
- Karszenbaum H, Kandus P, Martinez JM, Le Toan T, Tiffenberg J, Parmuchi G (2000) ERS-2, RADARSAT SAR backscattering characteristics of the Paraná River Delta wetland, Argentina; European Space Agency (ESA), publication SP-461. Gothenburg, Sweden
- Kellndorfer J (2019) Using SAR data for mapping deforestation and forest degradation. Chapter 3, pp 65–172. In: Flores a, Herndon K, Thapa R, Cherrington E (eds). *The SAR handbook: comprehensive methodologies for forest monitoring and biomass estimation*. <https://doi.org/10.25966/nr2c-s697>
- Kellndorfer J, Cartus O, Bishop J, Walker W, Holecz F (2014) Large scale mapping of forests and land cover with synthetic aperture radar data. *Land Applications of Radar Remote Sensing*. <https://doi.org/10.5772/58220>
- Lassalle P, Inglada J, Michel J, Grizonnet M, Malik J (2015) A scalable tile-based framework for region-merging segmentation. *IEEE Trans Geosci Remote Sens* 53(10):5473–5485
- Lee JS, Pottier E (2009) *Polarimetric radar imaging: from basics to applications*. CRC Press, Boca Raton, FL, USA
- Lewis SL, Brando PM, Phillips OL, van der Heijden GMF, Nepstad D (2011) The 2010 Amazon drought. *Science* 331(6017):554. <https://doi.org/10.1126/science.1200807>
- Li G, Lu D, Moran E, Dutra L, Batistella MA (2012) Comparative analysis of ALOS PALSAR L-band and RADARSAT-2 C-band data for land-cover classification in a tropical moist region. *ISPRS Journal of Photogrammetric Remote Sensing* 70:26–38

- Liu X, Skidmore AK, Osten HV (2002) Integration of classification methods for improvement of land-cover map accuracy. *ISPRS Journal of Photogrammetric Remote Sensing* 56:257–268
- Lu D, Mausel P, Batistella M, Moran E (2005) Land cover binary change detection methods for use in the moist tropical region of the Amazon: a comparative study. *Int J Remote Sens* 26:101–114
- Manavalan R, Rao Y, Buddhiraju KM (2017) Comparative flood area analysis of C-band VH, VV, and L-band HH polarizations SAR data. *Int J Remote Sens* 38:4645–4654
- MARNR-ORSTOM (1986) Atlas del inventario de tierras del Territorio Federal Amazonas (Venezuela). Dirección de Cartografía Nacional, MARNR-ORSTOM, Caracas
- Martinis S, Rieke C (2015) Backscatter analysis using multi-temporal and multi-frequency SAR data in the context of flood mapping at river Saale, Germany. *Remote Sens* 7:7732–7752. <https://doi.org/10.3390/rs70607732>
- Montanher OC, Morais Novo EML, Souza Filho EL (2018) Temporal trend of the suspended sediment transport of the Amazon River (1984–2016). *Hydrol Sci J* 63(13–14):1901–1912. <https://doi.org/10.1080/02626667.2018.1546387>
- Nguyen P, Shearer EJ, Tran H, Ombadi M, Hayatbini N, Palacios T, Huynh P, Updegraff G, Hsu K, Kuligowski B, Logan WS, Sorooshian S (2019) The CHRS data portal, an easily accessible public repository for PERSIAN global satellite precipitation data. *Nature Scientific Data* 6: 180296. <https://doi.org/10.1038/sdata.2018.296>
- Núñez Cobo J, Verbist K (eds) (2018) Atlas de sequía de América Latina y el Caribe. UNESCO PHI, CAZALAC, p 204
- O'Connor J, Santos MJ, Rebel KT, Dekker SC (2019) The influence of water table depth on evapotranspiration in the Amazon arc of deforestation. *Hydrol Earth Syst Sci* 23:3917–3931. <https://doi.org/10.5194/hess-23-3917-2019>
- Olivares I, Svenning J, van Bodegom PM et al (2015) Effects of warming and drought on the vegetation and plant diversity in the Amazon Basin. *Bot Rev* 81:42–69. <https://doi.org/10.1007/s12229-014-9149-8>
- Olivero J, Ferri F, Acevedo P, Lobo JM, Fa JE, Farfán MA, Romero D, The Amazonian communities of Cascaradura, Niñal, Curimacare, Chapazón, Solano, Blanco G, Real R (2016) Using indigenous knowledge to link hyper-temporal land cover mapping with land use in the Venezuelan Amazon: the Forest pulse. *Rev Biología Tropical* 64(4):1661–1682
- Pereira LO, Freitas CC, SantaAnna SJS, Reis MS (2018) Evaluation of optical and radar images integration methods for LULC classification in Amazon region. *IEEE Journal of Selected Topics in Applied Earth Observations and Remote Sensing*:1–13
- Potapov P, Li X, Hernandez-Serna A, Tyukavina A, Hansen MC, Kommareddy A, Pickens A, Turubanova S, Tang H, Silva CE, Armston J, Dubayah R, Blair JB, Hofton M (2020) Mapping and monitoring global forest canopy height through integration of GEDI and Landsat data. *In review*. Data download: <https://glad.umd.edu/dataset/gedi>
- QGIS Development Team (2018) QGIS geographic information system. Open Credit Geospatial Foundation. URL <http://qgis.osgeo.org>
- R Core Team (2018) R: a language and environment for statistical computing. R Foundation for Statistical Computing, Vienna, Austria. Available online at <https://www.R-project.org/>
- Reiche J, Lucas R, Mitchell AL, Verbesselt J, Hoekman DH, Haarpaintner J, Kellendorfer JM, Rosenqvist A, Lehmann EA, Woodcock CE, Seifert FM, Herold M (2016) Commentary: combining satellite data for better tropical forest monitoring. *Nat Clim Chang* 6:120–122
- Rosenqvist A (1996) Evaluation of JERS-1, ERS-1, and Almaz SAR backscatter for rubber and oil palm stands in West Malaysia. *Int J Remote Sensing* 17(16):3219–3231
- Rosenqvist J (2016) Assessing the utility of imaging radar for identifying white-sand vegetation structure. The City College of new York (CUNY), *academic works. Master's thesis*. [https://academicworks.cuny.edu/cc\\_etds\\_theses/611](https://academicworks.cuny.edu/cc_etds_theses/611)
- Rossetti DF, Moulatlet GM, Tuomisto H, Gribel R, Toledo PM, Valeriano MM, Ruokolainen K, Cohen MCL, Cordeiro CLO, Rennó CD, Coelho LS, Ferreira CAC (2019) White-sand vegetation in an Amazonian lowland under the perspective of young geological history. *An Acad Bras Cienc* 91(4):e20181337. <https://doi.org/10.1590/0001-3765201920181337>
- SAS Planet Development Team (2018) SAS.Planet v180518.9750 Nightly. <http://sasgis.org/>

- Scientific Exploitation of Operational Missions (2018) Sentinel Application Platform (SNAP). European Spatial Agency (ESA)
- Shimada M, Tadono T, Rosenqvist A (2010) Advanced land observing satellite (ALOS) and monitoring global environmental change. *Proc IEEE* 98(5):780–799
- Shimada M, Itoh T, Motooka T, Watanabe M, Shiraishi T, Thapa R, Lucas R (2014) New global forest/non-forest maps from ALOS PALSAR data (2007–2010). *Remote Sens Environ* 155:13–31
- Singh A (1989) Digital change detection techniques using remotely sensed data. *Int J Remote Sens* 10:989–1003. <https://doi.org/10.1080/01431168908903939>
- Small D (2011) Flattening gamma: radiometric terrain correction for SAR imagery. *Transactions on Geoscience and Remote Sensing* 49(8):3081–3099
- Thibault C, Li Z, Roux E, Herbreteau V, Gurgel H, Mangeas M, Seyler F, Dessay N (2018) Wetlands and malaria in the Amazon: guidelines for the use of synthetic aperture radar. *Remote Sensing International Journal of Environmental Research and Public Health, MDPI* 15:468. <https://doi.org/10.3390/ijerph15030468>
- Townsend PA (2001) Mapping seasonal flooding in forested wetlands using multi-temporal Radarsat SAR. *Photogramm Eng Remote Sens* 67:857–864
- Townsend PA (2002) Relationships between forest structure and the detection of flood inundation in forested wetland using C-band SAR. *Int J Remote Sens* 23:443–460. <https://doi.org/10.1080/01431160010014738>
- Tsyganskaya V, Martinis S, Marzahn P, Ludwig R (2018) SAR-based detection of flooded vegetation- a review of characteristics and approaches. *Int J Remote Sens* 39(8):2255–2293. <https://doi.org/10.1080/01431161.2017.1420938>
- Tuomisto H, Van Doninck J, Ruokolainen K, Moulatlet GM, Figueiredo FOG, Sirén A, Cárdenas G, Lehtonen S, Zuquim G (2019) Discovering floristic and geoeological gradients across Amazonia. *J Biogeogr* 46:1734–1738
- Ulaby FT, Long DG (2014) Microwave radar and radiometric remote sensing. University of Michigan Press, Ann Arbor
- Van Doninck J, Tuomisto H (2018) A Landsat composite covering all Amazonia for applications in ecology and conservation. *Remote Sensing in Ecology and Conservation* 4(3):197–210
- Van Thinh T, Tadono T, Hoang TT, Cao DP, Hayashi M, Nasahara KN (2019) JAXA annual Forest cover maps for Vietnam during 2015–2018 using ALOS-2/PALSAR-2 and auxiliary data. *Remote Sens* 11(20):2412. <https://doi.org/10.3390/rs11202412>
- WonMoo K, Sang-Wook Y, Joo-Hong K, Kug JS, Minho K (2011) The unique 2009–2010 El Niño event: a fast phase transition of warm pool El Niño to La Niña. *Geophys Res Lett* 38. <https://doi.org/10.1029/2011GL048521>
- Yang H, Peng J, Xia B, Zhang DX (2012) An improved EM algorithm for remote sensing classification. *Chin Sci Bull* 58(9):1060–1071. <https://doi.org/10.1007/s11434-012-5485-4>
- Zanetti M, Bruzzone L (2018) A theoretical framework for change detection based on a compound multiclass statistical model of the difference image. *IEEE Trans Geosci Remote Sens* 56:1129–1143



J. A. Zinck, H. F. del Valle, O. Huber, and P. García Montero

## 6.1 Introduction

Earlier studies on Amazonian lowland ecosystems concentrated on forest biomes. This study focuses on non-forested white-sand ecosystems that have attracted less attention. Exploration visits revealed the specificity of meadow vegetation, including a large number of endemic plants. In this chapter and the following four chapters that form an interrelated sequence, meadow vegetation refers to non-graminaceous herbaceous plant communities that typically live on lowland white sands. Meadow vegetation consists mainly of herbaceous species belonging to highly specialized families such as Rapateaceae, Bromeliaceae, Xyridaceae, Eriocaulaceae, and Cyperaceae, in contrast to grassland (i.e. savanna) that consists mainly of graminaceous herbs (Poaceae) (Huber 2005).

Working in meadow landscape presented the advantage of easy access via helicopter and facilitated on-the-ground displacement for transect studies. Surface features, especially those related to stream and river activity and its influence on vegetation and cover sand distribution could be directly observed on the terrain and from air.

---

J. A. Zinck

Faculty of Geo-Information Science and Earth Observation (ITC), University of Twente, Enschede, The Netherlands

H. F. del Valle (✉)

Centro Regional de Geomática (CeReGeo), Facultad de Ciencia y Tecnología (FCyT), Universidad Autónoma de Entre Ríos (UADER), Oro Verde, Argentina

e-mail: [delvalle.hector@uader.edu.ar](mailto:delvalle.hector@uader.edu.ar)

O. Huber

Merano, Südtirol, Italy

P. G. Montero

Private Activity, Soil Survey and Environmental Planning, Caracas, Venezuela



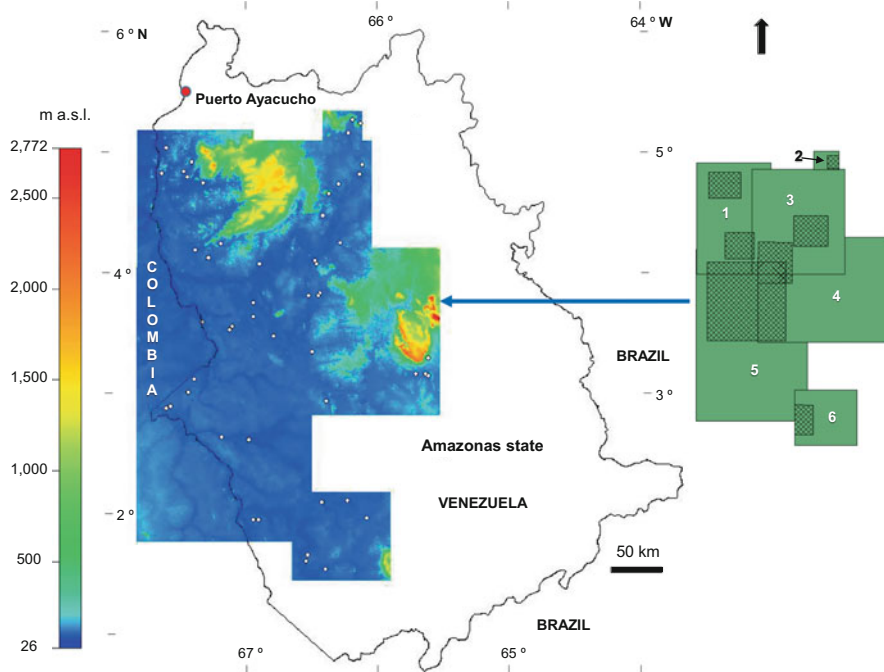


**Fig. 6.1** Digital Elevation Model (DEM) obtained from ASF RTC DEM (12.5-m) with disabled hill shading. Areas of Interest (AOI) from Amazonas State, Venezuela: 1 Sipapo (18,754 sq. km), 2 Camani (1056 sq. km), 3 Ventuari (22,071 sq. km), 4 Yapacana (30,883 sq. km), 5 Atabapo (43,523 sq. km), and 6 Pasimoni (7798 sq. km); crosshatched areas are training-areas (test sites); white dots are field observation sites including soil profile descriptions

The study region encompasses the lowlands lying between the Orinoco and the Rio Negro rivers to the west and the borders of the Guayana highlands to the east, approximately between  $5^{\circ}\text{N}$  and  $2^{\circ}\text{N}$  (Figs. 6.1 and 6.2). The study region as a whole was divided into six eco-chorological lowland areas based on general criteria such as belonging to a major watershed, distinctive physiographic and drainage features, and botanical information collected during earlier visits to the region (Huber 2015). These areas were used to describe the relationships between geomorphic landscapes and soils as a basis to identify physiognomic and floristic variations in meadow vegetation. The study areas are labelled after the name of the main river draining each area or a relevant relief feature, including from north to south: Sipapo, Camani, Ventuari, Yapacana, Atabapo, and Pasimoni. These six eco-chorological study areas are extensively described in Sect. 6.3 (Fig. 6.2). Area boundaries are not solid cartographic limits but rather fuzzy exploration fringes. The areas have core differentiating features as well as transitional and overlapping characteristics. The present chapter describes the white-sand landscapes and soils that occur in these selected areas under a variety of meadow covers from strict herb-forb meadow to



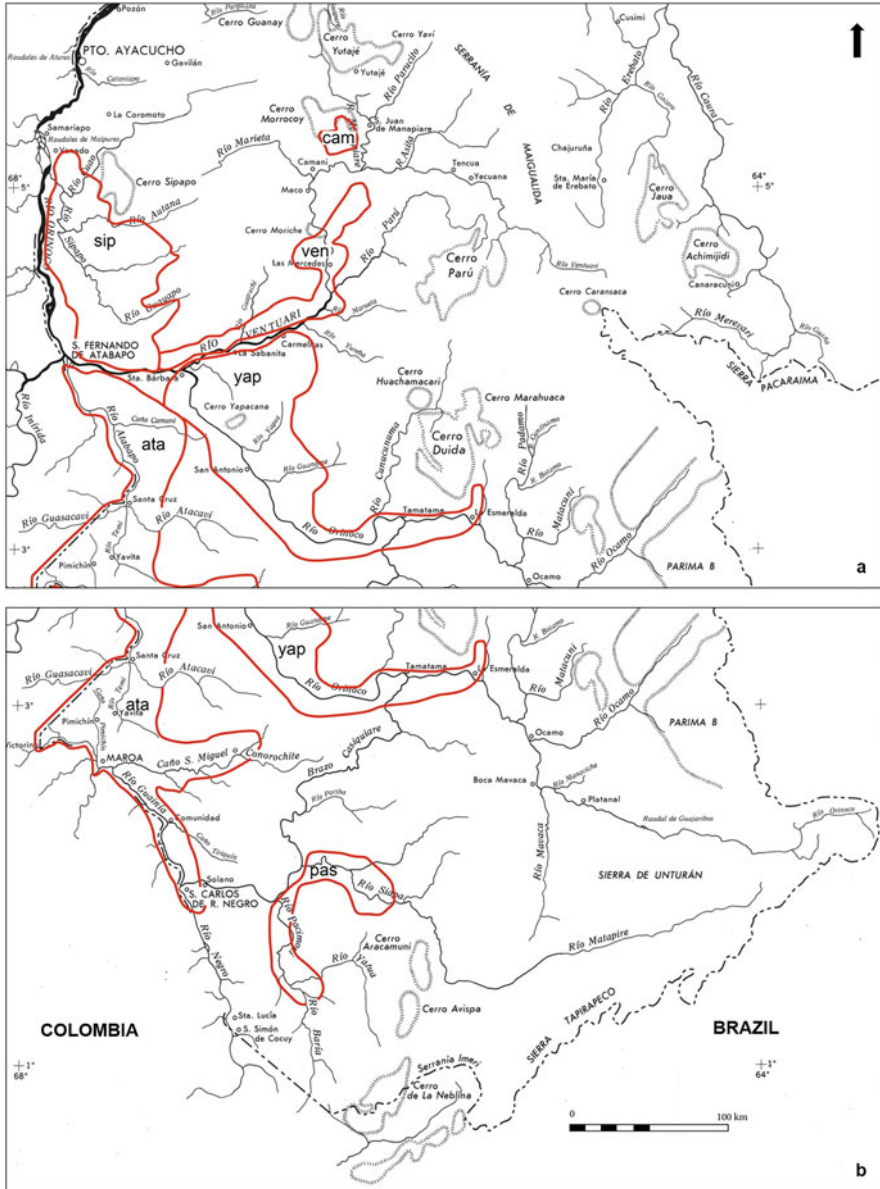


**Fig. 6.2** Study areas delineated in the northern sector (a) and southern sector (b) of the study region: sip, Sipapo; cam, Camani; ven, Ventuari; yap, Yapacana; ata, Atabapo; pas, Pasimoni. Definition and boundaries of the study areas according to Huber (unpublished Mapa de Puntos 2015). Basemap from Atlas del Territorio Federal Amazonas y Distrito Cedeño del Estado Bolívar, MOP-CODESUR (1973)

shrubby meadow. Scrubland (e.g. bana) and forest vegetation (e.g. caatinga, palm swale, terra-firme rainforest) are not considered in this analysis, although a few sites located in meadow-caatinga ecotones are included in the descriptive data tables.

A complete overview of landscape and soil distribution in the Venezuelan territory of the Amazon basin can be found in the soil atlas prepared and published by MARNR-ORSTOM (1986) and Dubroeuq and Volkoff (1998). A general description of the landscape units and soils in the region north of river Autana, thus mainly outside our study region, is provided by Blancaneaux et al. (1978).

---

## 6.2 Materials and Methods

### 6.2.1 Digital Elevation Modelling and Terrain Analysis

By the time field observations were carried out (1979–81), little geospatial support was available (e.g. historical MSS Landsat images). This information gap has been filled now working on digital elevation modelling and terrain analysis of each study area.

#### 6.2.1.1 Construction of Elevation Models

The use of digital elevation models (DEM) to describe the terrain features of the lowlands was appropriate about the topographic characteristics of the areas (slopes, rugged surfaces), scarcity of data, limited field visits, and extent of the study region. The Digital Elevation Model (DEM) was obtained from the Radiometric Terrain Corrected (RTC) products (ASF 2015) included in the files from ALOS PALSAR-1 images (Fine Beam Single polarization). In the absence of ground control data, a higher resolution surface was considered as a reference of ‘true’ elevation. The Shuttle Radar Topography Mission (SRTM) DEM (30 m) and Alaska Satellite Facility (ASF) RTC DEM (12.5 m) show different elevations over the same area. The DEM improved the terrain analysis resolution detail because it allowed an accurate determination of drainage slopes and the location of channels and ridges, among other parameters (Her et al. 2015). The RTC product was converted from DEM orthometric height to ellipsoid height using the ASF Map Ready geoid adjust tool (ASF 2015). This tool applies a geoid correction so that the resulting DEM relates to the ellipsoid.

Digital processing was performed with the following open-source software packages: System for Automated Geoscientific Analyses (SAGA GIS) v7.0.0 (Conrad et al. 2015), Sentinel Application Platform (SNAP) v6.0.4 (SEOM 2018), and Google Earth Pro v7.3.2.5491 (Google LLC 2019). Visualization of maps generated in Google Earth was relevant for terrain analysis because it allowed checking the correctness of the coordinate system definition, evaluating and interpreting mapping results using high-resolution satellite imagery, and exploring 3D data modelling (Hengl 2007).

Study areas have an irregular configuration with contours enclosing observation sites that have affine meadow vegetation characteristics. They were given

quadrangular shapes for spatial analysis using geo-information techniques and served as a basis to select training-areas. These study frames comprise land tracts that have cover types different from meadow vegetation and lack field observations. Their inclusion however is useful because they provide a comprehensive view on the geomorphic landscape distribution and terrain characteristics in the regional context.

Dense vegetation cover defines to some extent the surface that the DEM perceives as it maps the terrain. Much of the local 'topography' in the study areas is a measure of tree height, especially in areas where the ground surface relief is very low. Interpretative separation of the ground surface and vegetative features typically relies upon recognition of their characteristic patterns. In the case of SRTM, it has been shown that the C-band data penetrated significantly into the vegetation canopy (Carabajal and Harding 2006; Hofton et al. 2006). Transitions caused by elevation increasing through DEM reflect the canopy effect, as the tree density is expected to affect the average altimetry (Kellendorfer et al. 2004).

### 6.2.1.2 Extraction of Landscape Features

The terrain algorithms of interest selected were hypsometry (m a.s.l.), hillshade, view in 3D, elevation profile along a transect, density slice ranges (terrain surface classification), slope (flat and slopes <5%), Multiresolution Index of Valley Bottom Flatness (MRVBF), and drainage network and flow accumulation (flow tracing). Transect elevation values capture small- and large-scale variations in the surface topography, separate areas of river drainage from other geomorphic surfaces, and show the relative abundance of streams and rivers at the landscape scale. Standard deviation of residual topography tends to highlight local features such as microrelief or slope breaks but does not detect regional relief.

The hillshade image of the study areas was generated to enhance the aesthetic qualities of the elevation grid and help quick identification of the lowlands. DEM colour codes were: (1) blue-cyan representing the lowest ground, (2) green and yellow for increasing elevation, and (3) orange to red for the highest ground. Thus, DEM allowed distinguishing between geomorphic landscapes imitating the mapping method of a manual interpreter in an automated and reproducible way for a class of features (Hillier and Watts 2004). It was used to describe the surface roughness of the areas, a parameter referring to the variability in elevation within a defined radius and therefore very sensitive to the selected scale.

Geomorphic landscape units were distinguished based on elevation ranges (hypsometric slicing algorithm), using an iteration procedure to obtain best fits from several trials of elevation ranges. Expert knowledge and contour lines were used for demarcating the unit extents.

Two slope classes were selected to distinguish between flat to nearly level areas (<1%) in alluvial plains and gently sloping areas (1–5%) in peneplain and piedmont landscapes. Sand deposits are more likely to occur in these two slope gradient classes.

The MRVBF index identifies gradations of valley bottom flatness, which may be related to depth of deposits. The index classifies terrain units such as, for instance, areas without flat bottoms (<0.5), small valley bottom flats (0.5–1.5), small flats

(1.5–2.5), followed by units with increasing slope gradients. The index can also be used to identify groundwater confinement and delineate hydrologic and geomorphic units (Gallant and Dowling 2003). Values between zero and one indicate erosional terrains, while larger values (>3.2) indicate progressively larger areas of deposition. High MRVBF values (bluish colours) identify broad flat valley bottoms and more extensive alluvial compartments, often confined within the peneplain landscape, where white-sand ecosystems are likely to occur. However, the algorithm does not identify valley areas in steep first- and second-order sub-catchments and steep narrow valleys near catchment outlets.

The D8 method was used for automated extraction of stream paths based on line and point features from raster DEM (Conrad et al. 2015). The algorithm detects only convergent flows and allocates them through a cell to the steepest downslope neighbour. It works well for identifying first- and second-order catchments, but not higher-order catchments. It does not characterize valleys as areas.

### 6.2.1.3 Elaboration of Representative Figures

Figures representative of each study area illustrates relief variations and descriptive landscape features. Digital elevation models are based on data from Alaska Satellite Facility (ASF), <https://www.asf.alaska.edu/>. A 3D training-area was selected in each study area to describe the terrain features in a set of images depicting geomorphic landscape units, slope gradients, index values of valley bottom flatness (MRVBF), and drainage network. Representative transects show elevation and topographic variations along with associated landscape units. The blue shade around the plot line indicates the standard deviation of relief elevations within a square box, with the edge length of the box set to an odd value of 21. Numbered dots are field observation sites including vegetation and soil descriptions.

## 6.2.2 Field and Laboratory Data

Areas covered by meadow vegetation were identified on historical MSS Landsat images and visited using a helicopter facility (1979–81). The location of observation sites depended on landing conditions and was shared for vegetation inventory and soil inventory. Soil description and sampling were carried out in pits to a depth of 80–100 cm, followed by auger boring. Description and classification of the original field data collected by the time of the inventory were updated using FAO guidelines (FAO 2006) and Soil Taxonomy (Soil Survey Staff 2014). Soil laboratory data described in Chaps. 6–10 were obtained using the following methods: pipette method for particle size distribution (Table 6.1), pH in water 1:1. Walkley–Black for organic carbon; Bray–Kurtz for available phosphorus, and ammonium acetate and photometry for exchangeable potassium. Sediment and soil colours conform to Munsell Soil Colour Charts (m = moist; d = dry).

Relevant landscape and soil characteristics of visited sites are summarized in tables, with one table per study area (Tables 6.2, 6.3, 6.4, 6.5, 6.6, and 6.7). Observation sites are identified in the first column of each table and plotted on the

**Table 6.1** Particle size classes in the legend of the bar diagrams

Denomination		Size (mm)
Coarse fragments	cfg	>2
Very coarse sand	vcs	2–1
Coarse sand	cs	1–0.5
Medium sand	ms	0.5–0.25
Fine sand	fs	0.25–0.125
Very fine sand	vfs	0.125–0.05
Total sand	tots	2–0.05
Silt	si	0.05–0.002
Clay	cl	<0.002

DEM images. Each observation site can have more than one soil profile description as identified in the third column of the tables. The majority of the described soil profiles are less than 1 m deep; deeper observation profiles are limited in number because of logistics constraints.

In total, 83 profiles are referred to, out of which 68 profiles are under meadow vegetation *sensu lato*, unevenly distributed in space according to the size and physiographic variability of the study areas, as follows: Sipapo (15), Camani (2), Ventuari (11), Yapacana (26), Atabapo (17), and Pasimoni (12). Description of representative soil sites and profiles is provided in Chap. 7.

### 6.2.3 Landcover Products

In this study, we characterize the key landcover mapping gaps and challenges in the Amazonas State. We compiled and assessed two new global high-resolution landcover products: Esri Land Cover (Karra et al. 2021) and European Space Agency (ESA) WorldCover (Zanaga et al. 2021). Both maps were derived from ESA Sentinel-2 imagery at 10-m resolution. These are a composite of landuse and landcover (LULC) predictions for 10 and 11 classes, respectively, throughout the year to generate a representative snapshot of 2020. This chapter summarizes the details and findings of those efforts and proposes a discuss framework for addressing the identified challenges.

### 6.2.4 Estimation of the Total Area of White-Sand Ecosystem

The main vegetation types occurring in the Amazonas State can be distinguished based on the canopy height (see Sect. 5.2.2.5, Chap. 5). We use the 30-m spatial resolution global forest canopy height (FCH) map (Potapov et al. 2020) that relates as an alternative indicating where units of white-sand ecosystems are expected to occur.

The unit types identified on the FCH map and their estimated percent cover were: (1) ‘Terra-firme’ and Tall caatinga forest ( $\geq 30$ –15 m) (53.2%), (2) White-sand forest (low caatinga forests or bana) (15–7 m), upland rocky slope forest ( $\leq 10$  m) (22.0%), (3) Riparian forest and sparse vegetation (7–3 m) (14.1%), and (4) White-sand meadows/shrublands and water bodies (below 3 m) (10.7%).

The reference data are logistically challenging to collect for large area landcover products. Therefore, we use the data based on the classes defined by the synergistic integration of Global PALSAR-2 and Sentinel-1 satellite products, with the Normalized Difference Vegetation Index (NDVI) derived from Landsat data (see Sect. 5.2.3.6, Chap. 5). The reference classes were mostly grouped into categories based on their high semantic similarity in the units of the FCH map. A total of 400 stratified-random spots were used to construct a frequency table, linked to Google Earth for a visual evaluation of class distributions. The percent area was calculated for each of the six FCH classes, including the grouped classes. We focus on the white-sand forest and meadows/shrublands that showed 75% and 77% accuracy, respectively.

---

## 6.3 Sipapo Area

### 6.3.1 Geographical Setting

The Sipapo area is a regional depression lying between the sandstone highlands of the Cuao-Sipapo massif and crystalline foreland hills to the east and a strip of peneplain terrains (100–200 m a.s.l.) bordering the course of river Orinoco to the west. The latter are formed by low residual hills and the large levee complex of the Orinoco (Table 6.2). The Sipapo area covers the lowlands extending in front of the Cuao-Sipapo massif, roughly between the Cuao river in the north, the Orinoco-Ventuari rivers in the south, and the Orinoco river in the west. Several rivers originating from the Cuao-Sipapo massif, the most important of them being Guayapo, Sipapo, Autana, and Cuao, drain the lowlands and move sands from the erosion of the Roraima sandstone mesetas in the highlands (Plate 6.1a). In the lowlands dominate a peneplain landscape (100–140 m a.s.l.) with flat depositional areas (70–110 m a.s.l.) intermingled with hilland areas (140–200 m a.s.l.). Hilly reliefs developed in igneous-metamorphic rocks (Parguaza rapakivi granite), have rounded summits and steep slopes. Bare rocky crystalline domes are frequent. Locally, crystalline bedrock hills are capped by Roraima sandstone layers forming escarpments. Rugged hilly topography is most frequent between the Sipapo and Guayapo rivers as a westward extension of the Guayapo Serranía range.

The Sipapo area (Plate 6.1a–c) is a regional depression lying between the sandstone highlands of the Cuao-Sipapo massif and crystalline foreland hills to the east and a strip of peneplain terrains (100–200 m a.s.l.) bordering the course of river Orinoco to the west. The latter are formed by low residual hills and the large levee complex of the Orinoco. The configuration and orientation of the regional hydrographic network show that rivers coming from the east cannot join the Orinoco straight away because of the western physiographic barrier. This obliges the Guayapo and Sipapo rivers to bend northward and causes the rivers in their lower courses to run parallel to the Orinoco until their junction in Isla Ratón. Therefore, water is retained and stored along this large trough between eastern and western higher terrains, resulting in a regional confined drainage basin. The evacuation of



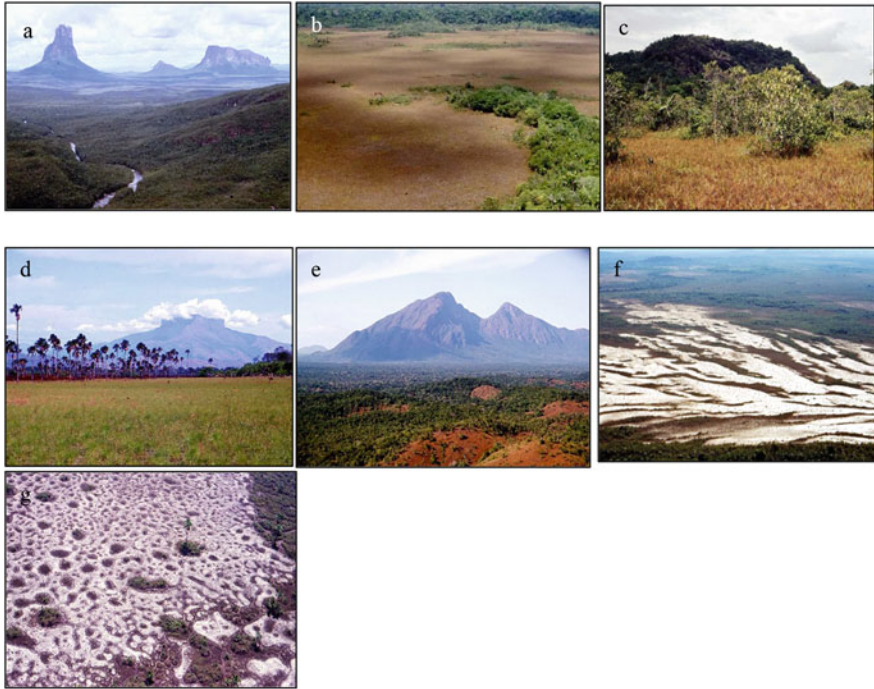


**Plate 6.1** Study areas. (a) Sipapo area: isolated mesetas (tepuis) at the western forefront of the Cuao-Sipapo massif in contact with the Sipapo lowlands; mosaic of meadow and woody covers in the alluvial plain; Cerro Autana (1220 m a.s.l.) in the left background; (b) Sipapo area: meadow vegetation on alluvial plain flat in the southern lowlands; dark brownish areas are poorly drained depressions with Oxyaquic Quartzipsamments, often burying truncated Spodosols; (c) Sipapo area: peneplain landscape in the northern lowlands; glacia head at the foot of a residual crystalline bedrock hill; contact between meadow vegetation and bana scrub; (d) Camani area: Manapiare Valley at the northern edge of the study region; anthropized savanna vegetation; Cerro Guanay in the background; (e) Ventuari area: Cerro Moriche is a landmark in the middle Ventuari valley; at the foot of the massif, piedmont fans enlarge into glacia in contact with the valley bottom; (f) Ventuari area: large peneplain glacia covered by low-density meadow vegetation with isolated shrubs; eroding landscape upon degradation of the original wooden cover through repeated fires; (g) Ventuari area: picturesque, speckled pattern caused by dense concentration of suffusion pans on a white-sand glacia in the middle Ventuari watershed

flood and rainwater during the rainy season is thus retarded, causing groundwater levels to remain high, with some seasonal fluctuations, even during the lower rainfall period in January–March. The frequency of Oxyaquic Quartzipsamments in the Sipapo area is related to this regional situation of impeded drainage.

### 6.3.2 Terrain Features

The DEM image of the Sipapo area (Fig. 6.3a) shows the contrast between the highlands of the Cuao-Sipapo massif and the lowlands of the fluvial network. The







**Table 6.2** (continued)

Sipapo		Prof (15)	Vegetation cover %	Landscape slope %	Soil class	Text	sa-si-cl %	cs-ms-fs 100% s	Colour moist	Mottles features depth cm	Pedogenic features depth cm	A horizon cm	Root depth cm	OC % A Bh Bhs	Groundwater cm	Moisture obs period dry/moist	Microrelief	Obs depth cm	
Site	Locality																		
123		98	Open scrub	Glacis 3-5	Typic Qps		97-1-2	27-46-27	Light grey/white	Fossil roots 44-75	-	23	44	0.21	-		Reticular	130	
04° 51' N		99	Bare soil + shrub patches	Plain flat stream levee			100-0-0	38-56-7		Charcoal 11-35	-	11	70	0.31	-		-	70+	
67° 34' W																			

Prof, description and sampling profile; Qps, Quartzipsamment; Text, texture; sa-si-cl, sand-silt-clay; cs-ms-fs, coarse sand-medium sand-fine sand; A, soil surface horizon; Ch, humic sandy layer; Bh, Bhs, Bhs, spodic horizons; OC, organic carbon; obs, observation; m, moist; d, dry (cm from soil surface); feb, February; mar, March; jul, July

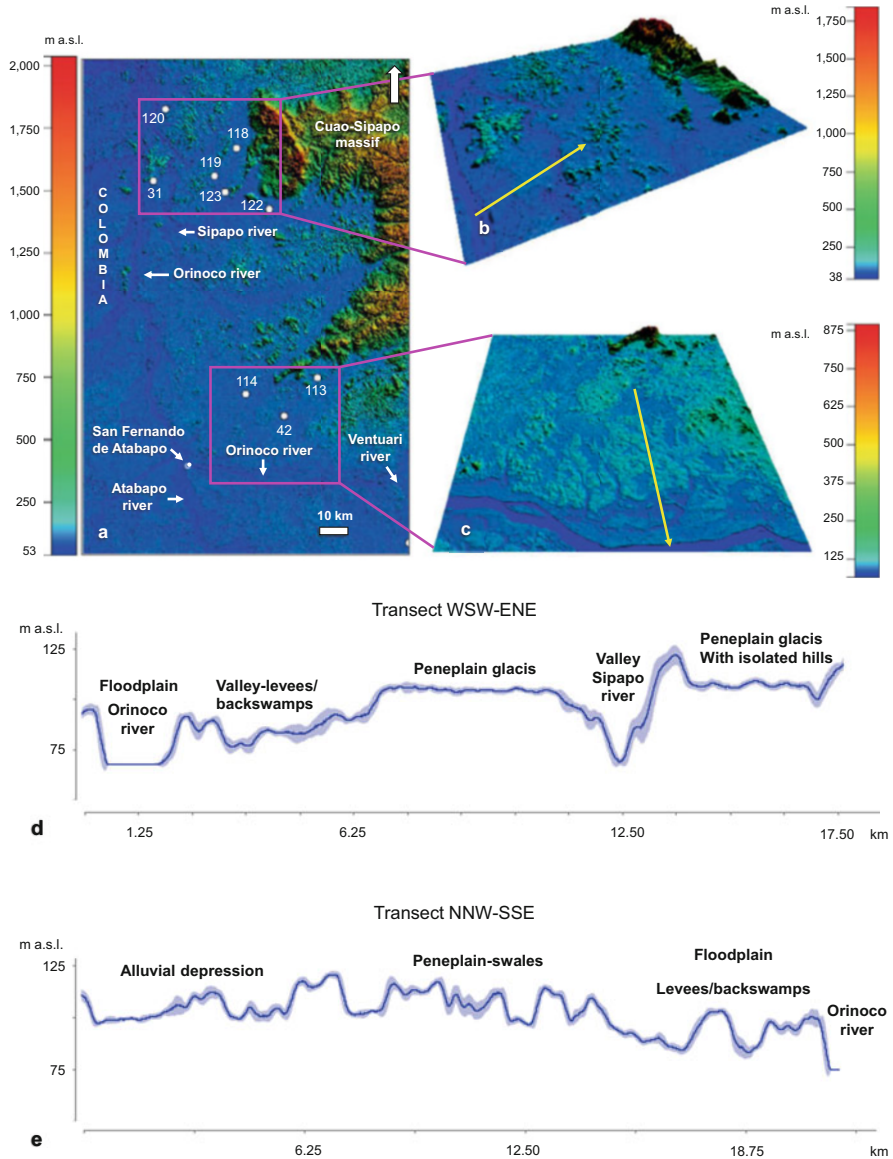


**Fig. 6.3** (a) Hill-shaded DEM of the Sipapo area, pixel 12.5 m; shaded relief illumination from 315° N, 45° above horizon; (b) DEM 3D view of the Sipapo 1 training-area (1897 sq. km), located between 5°22'40.5"N, 68°22'39.5"W and 4°53'23.5"N, 67°25'19.7"W; (c) DEM 3D view of the Sipapo 2 training-area (1743 sq. km), located between 4°19'22.8"N, 67°47'24.4"W and 3°56'47.7" N, 67°03'07.1"W. Transects showing elevation and topographic variations along landscape units in the Sipapo 1 training-area (d) and Sipapo 2 training-area (e)

roughness of elevation detects breaks in terrain steepness, while the roughness of slope enhances noise in the data. River Orinoco has a narrow, incised channel, of straight configuration and moderate gradient in the western and southern part of the image, grading to broad and meandering in the north-western part with a much gentler surface gradient.

The hillshade images of the training-areas show relief heterogeneity in the lowlands (approximately <150 m a.s.l., blue-cyan colour-coded DEM). They allow identifying low hillands and isolated hills, peneplain areas, alluvial plain flats, and the valleys of the Orinoco and Sipapo rivers in the northern sector of the Sipapo study area (Fig. 6.3b), and large peneplain areas and alluvial flats especially along the Orinoco river in the southern sector of the same study area (Fig. 6.3c). Representative features of these landscapes are shown in the elevation transects of Fig. 6.3d, e.

In the northern sector of the Sipapo lowlands, peneplain glacis with scattered low hills is the dominant landscape feature. From Fig. 6.4a, the sequence per the importance of spatial distribution is peneplain glacis > plain, valley > floodplain > piedmont fan-glacis. A large part of the area has a relatively rugged mesotopography with slopes higher than 5% (Fig. 6.4b). This results from the predominance of erosional terrains (Fig. 6.4c) and the high density of short drainage incisions (Fig. 6.4d).

The southern sector of the Sipapo lowlands has a regional landscape less contrasted than that of the northern sector. Alluvial depressions are more extensive than peneplain areas. From Fig. 6.5a, the sequence per the importance of spatial distribution is alluvial depression, floodplain > peneplain-swailes > plain, valley > riverbed, backswamp, stream > piedmont fan-glacis. In general, slopes are lower than 5% (Fig. 6.5b). The presence of many closed depressions of variable dimensions (Fig. 6.5c) that correspond to convergent drainage confinement areas (Fig. 6.5d) indicates that these lowlands are subject to flooding and hindrance of water evacuation. The water flow in valley bottoms does not faithfully follow surface topography, particularly in high flow conditions. The groundwater level is relatively high (less than 1 m).

In these low relief areas where drainage divides between waterways are indistinct, the channel network relates poorly to catchment geometry, and the surface topography is an unreliable indicator of subsurface flow pathways. The valley bottoms of the closed depressions are the key hydrologic feature rather than channels and provide a suitable basis to estimate subsurface flow path width, as suggested by Gallant and Dowling (2003).

Three kinds of landscape in which meadow vegetation occurs, are distinguished, namely alluvial plain flats, glacis, and vales, each characterized by dominant soil classes (Table 6.2).

### 6.3.2.1 Alluvial Plain Flats in the Northern Lowlands

The Sipapo lowlands are overall poorly drained, except for the north-western sector around Munduapo, along the lower stretch of river Sipapo that has a shallow, well-drained valley configuration. All sites of the alluvial plain flats have groundwater at less than 1 m depth by the end of February or beginning of March, in the lower

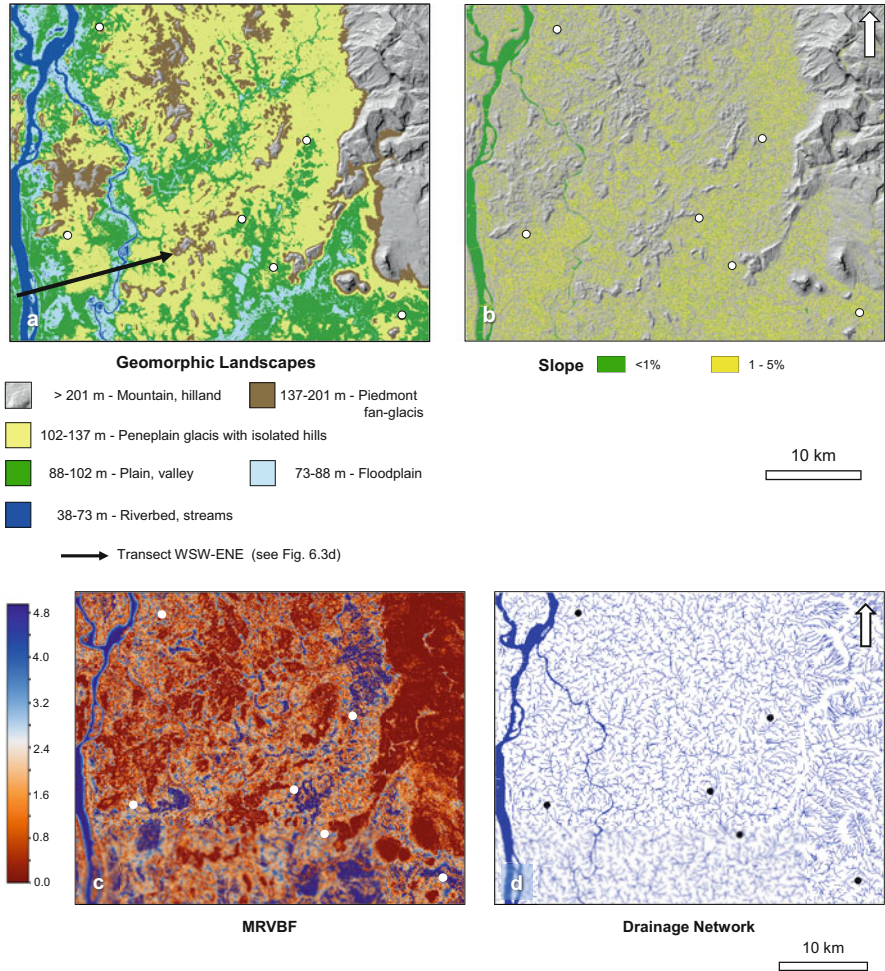


**Fig. 6.4** Sipapo 1 training-area: (a) Geomorphic landscapes; (b) slope gradient classes; (c) multiresolution index values of valley bottom flatness (MRVBF); (d) Stream paths and drainage patterns

rainfall period. By the same time of the year, high groundwater is rather infrequent in the alluvial flats of the other study areas. During the maximum of the rainy season in July, the water table raises commonly to about 10–15 cm from the soil surface.

White-sand meadow vegetation is common on alluvial plain flats in the northern as well as in the southern lowlands (Plate 6.1b). Cover type and density are variable, including pure meadow, savanna-meadow, shrubby meadow, and scrub. Oxyaquic Quartzipsamment soils are dominant in these conditions. Similar white-sand Oxyaquic Quartzipsamments with groundwater within 1 m depth in February have been reported earlier from the Autana and Sipapo lowland watersheds (Zinck 2011).



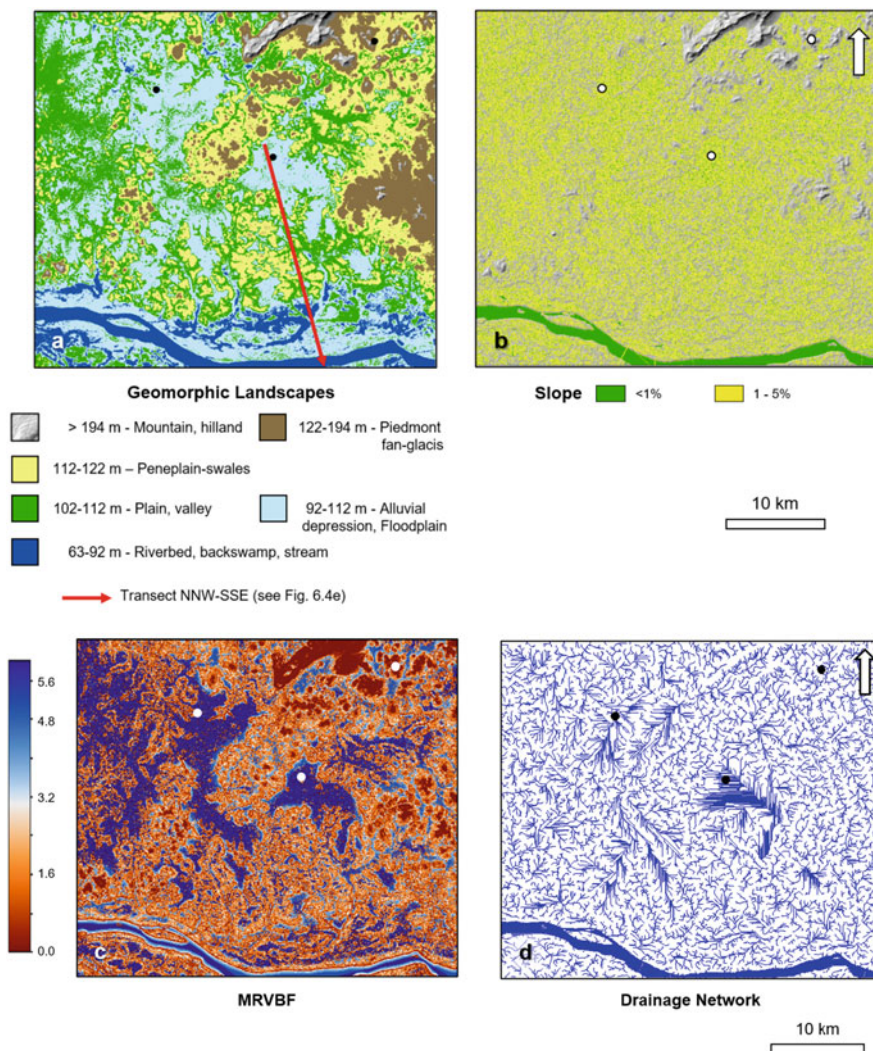


**Fig. 6.5** Sipapo 2 training-area. (a) Geomorphic landscapes; (b) slope gradient classes; (c) multiresolution index values of valley bottom flatness (MRVBF); (d) stream paths and drainage patterns

The soil colour is light grey or light brown in the upper layer, and then fully white with depth, in general without redoximorphic features. At some sites, deep layers are dark-coloured, and the groundwater is brown, but with low organic carbon content, suggesting intergradation towards Aquodic Quartzipsamments. Average sand content per entire profile varies between 95 and 100%, with an overall average of 97%. Average silt content is 0–2% and average clay content is 0–3%. Medium sand dominates in association with fine sand in overflow deposits and with coarse sand in more undifferentiated splay deposits. On average, the thickness of the A horizon is



12 cm (7–20 cm), the organic carbon content in the A horizon is 0.4% (0.2–0.56%), and root penetration depth is 39 cm (15–70 cm). Reticular microrelief was observed only at a few sites. Intricate rill pattern incision is caused by surficial water evacuation during the rainy season from slightly higher positions, often occupied by caatinga, to slightly lower terrain surfaces, in general, less than 1 m elevation difference. Undifferentiated and depressed topography restrains surface drainage. Water retires mainly via groundwater fluctuation.

### 6.3.2.2 Alluvial Plain Flats in the Southern Lowlands

The middle Guayapo river occupies an east-west depression between slightly higher terrains along the Sipapo river in the north and the Orinoco river in the south. In this area, Spodosols were identified together with Oxyaquic Quartzipsamments. Although the groundwater level is relatively high (less than 1 m), Spodosols under meadow vegetation do not show the distinctive characteristics of Aquods such as histic epipedon or redoximorphic features within 50 cm of the soil surface as required by Soil Taxonomy (Soil Survey Staff 2014) because meadow plants produce little organic matter and white sands are depleted of iron oxides. However, Aquods have been reported to occur extensively in the lowlands of the region, especially in the areas of San Carlos de Rio Negro and Maroa-Yavita but always under forest vegetation (caatinga and rainforest) (Schargel and Marvez 2009).

Two profiles classify as Durorthod with ortstein and one profile as Haplorthod. Possibly the Sipapo-Orinoco interfluvium drained by river Guayapo is older than the surrounding areas that have received recent sand deposition from the hinterland of the Cuao-Sipapo massif. Soils are light grey followed by white over dark brown on the spodic horizon. Organic carbon content in the spodic horizon varies between 0.7 and 2.97%. Average sand content per entire profile varies between 92 and 99%, with an overall average of 96%. Average silt content is 1–3%, and average clay content is 0–5%. Medium sand dominates in relatively undifferentiated combinations with coarse and fine sand. Splay deposits are more frequent than overflow deposits. On average, the thickness of the A horizon is 23 cm (20–30 cm), organic carbon content in the A horizon is 0.24% (0.1–0.54%), and depth of root penetration is 47 cm (40–53 cm). Spodosols can be dry in the upper layers (20–30 cm) for some days in February–March. During this period, the presence of the indurated spodic horizon (i.e. ortstein) may play a role in limiting water supply from depth.

### 6.3.2.3 Peneplain Glacis

Sloping glacis terrains (2–5% slope) have formed at the foot of longitudinal sandstone outcrops and at the periphery of rounded to oval crystalline hills (Plate 6.1c). Light pinkish sands produced by physical disaggregation of sandstones or chemical weathering of crystalline rocks turn into white sands over distances of a few tens of metres. Vegetation varies from savanna to open scrub. Soils are white Typic Quartzipsamments. Sand content is 97% or more, with variable combinations of sand separates. The A horizon has an average thickness of 19 cm (15–23 cm) and average organic carbon content of 0.21%. Average root penetration depth is 35 cm (25–44 cm). Reticular microrelief is common.

#### 6.3.2.4 Vales (Small Valleys)

The junction of rivers and local streams with the Orinoco river causes the incision of small valleys to cross the levee complex of the Orinoco. Meadow glades within caatinga forest occur on terrace levels and savanna on floodplains. Light grey over pale brown Udoxic Quartzipsamments are the dominant soils. Sand content varies between 93 and 97% with medium and fine sand. On average, the A horizon has a thickness of 18 cm (8–27 cm) and organic carbon content of 0.69% (0.27–1.1%). Average root penetration depth is 35 cm (20–50 cm). These Udoxic Quartzipsamments lying between the Orinoco and Sipapo rivers have slightly higher silt and clay contents than the typical Quartzipsamments. This may provide a small advantage in terms of water-holding capacity, allowing the occurrence of savanna vegetation.

### 6.3.3 Relevant Features of the Sipapo Area

The meadow environment in the Sipapo area is mainly an alluvial plain landscape. Splay and overflow sediments coexist in the north, while splay deposits dominate in the south. Glacis positions occur at the periphery of hilly reliefs in contact with the flat lowlands. Riverine features have developed in the confluence area between rivers Sipapo and Orinoco. In general, reticular microrelief is infrequent except on peneplain glacis.

Particle size distribution is similar among the meadow soil profiles described in this area. Average sand fraction varies between 92 and 100%, with mostly 95% or more sand. Medium and fine sand compose overflow sediments, while coarse, medium, and fine sand compose splay sediments (Table 6.2). Including all sites regardless of geomorphic position, soil class, and type of meadow vegetation, the overall average of silt is 1.4% (0–4%) and that of clay is 2.1% (0–5%). Among the six study areas, the Sipapo area has the lowest proportion of fines remaining in the environment (3.5%). It is a silt-clay-free area, an almost pure sand reservoir.

In general, the A horizons are less than 20 cm thick. Organic matter (0.2–0.4% OC) concentrates in these shallow surface layers, although a few roots penetrate the soil down to about 40–50 cm depth.

Soils are moist but not wet above the groundwater level. The upper 20–30 cm can dry up during the lower rainfall period. Except in the northwest (Munduapo area), groundwater rises close to the soil surface during the rainy season and stays usually within 1 m depth in February–March. The Sipapo area seems to be one of the poorest drained in the regional context.

The dominance of Oxyaquic Quartzipsamments in the north contrasts with the occurrence of Spodosols in the south. Despite poor drainage, Spodosols have no histic epipedon under meadow vegetation and no redoximorphic features because sands are bleached out of iron hydroxides upon repeated reworking by shifting streams and rivers. It is hypothesized that the Spodosols have formed under caatinga,

have subsequently been truncated upon degradation of the wooden cover, and then buried by a more recent sand cover.

The proximity of this study area to Puerto Ayacucho, the capital city of the Amazonas State, has led to increased intervention of the natural resources for farming and logging.

## 6.4 Camani Area

### 6.4.1 Geographic Setting

Camani is a small area located at the northern edge of the study region, northwest of San Juan de Manapiare. It lies south of a narrow mountain gap between the Guanay range to the west and Yutajé range to the east (Plate 6.1d). The gap is the divide between the watershed of the Suapure river draining to the north and that of the Manapiare river draining to the south.

### 6.4.2 Terrain Features

The DEM in Fig. 6.6a shows the regional contrast between the highlands of the eastern Cuao-Sipapo massif and the surrounding lowlands (<150 m a.s.l., blue

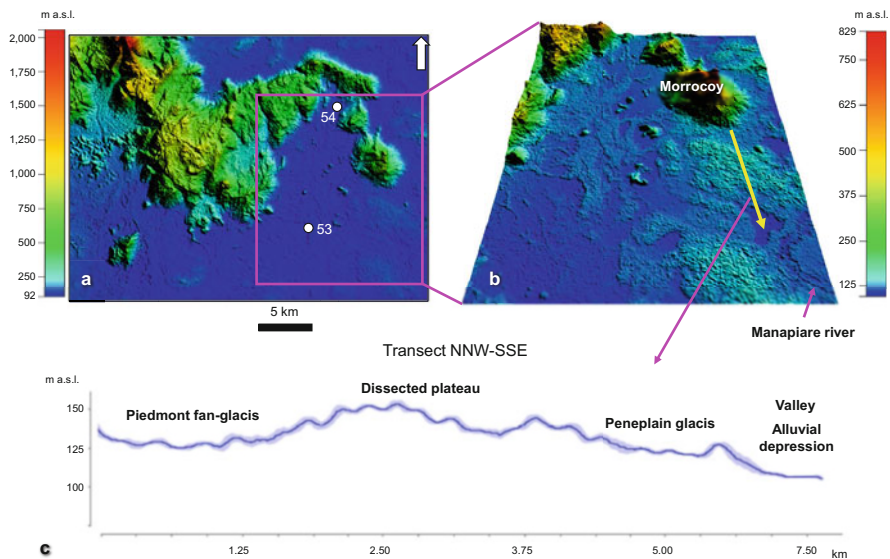


**Fig. 6.6** (a) Hill-shaded DEM of the Camani area, pixel 12.5 m; shaded relief illumination from 315° N, 45° above horizon; (b) DEM 3D view of the Camani training-area (334 sq. km), located between 5°21'44.9"N, 66°14'16.8"W and 5°11'07.8"N, 66°04'58.2"W; (c) Transect showing elevation and topographic variations along landscape units

colour-coded DEM). The eastern part of the training-area (Fig. 6.6b) has a relatively rugged relief as shown in the topographic transect profile (Fig. 6.6c), while the western part is much flatter. Relief amplitude between the associated geomorphic landscapes is not significant in the lowlands, but surface roughness is high as shown by the fairly large standard deviation of the elevation values in Fig. 6.6c (blue shade around the plot line).

The lowlands (<130 m a.s.l.) between Cerro Morrocoy to the north, river Manapiare to the east, and river Ventuari (not shown) to the south include piedmont fan-glacis at the foot of mountains and hillands, and dissected plateaus to the east (light green-cyan colours; approximately 130–150 m a.s.l.), peneplain glacis with some isolated hills in the centre, and alluvial depressions (cyan-blue colour) in the south-west.

The spatial distribution of the geomorphic landscapes is shown in Fig. 6.7a. Peneplain glacis and alluvial depressions are the environments where white sands are most likely to occur. They can be related to flooding gradients, with the forest being replaced by open vegetation as flooding level increases or groundwater depth decreases. These features reveal structural variations in white-sand vegetation (Damasco et al. 2013).

Dominant slope gradient is 1–5% in the flat lowland alluvial plains. Slope is more variable in the dissected plateaus, peneplains, and piedmont areas (Fig. 6.7b). Mesotopographic variations are enhanced in Fig. 6.7c showing the contrast between

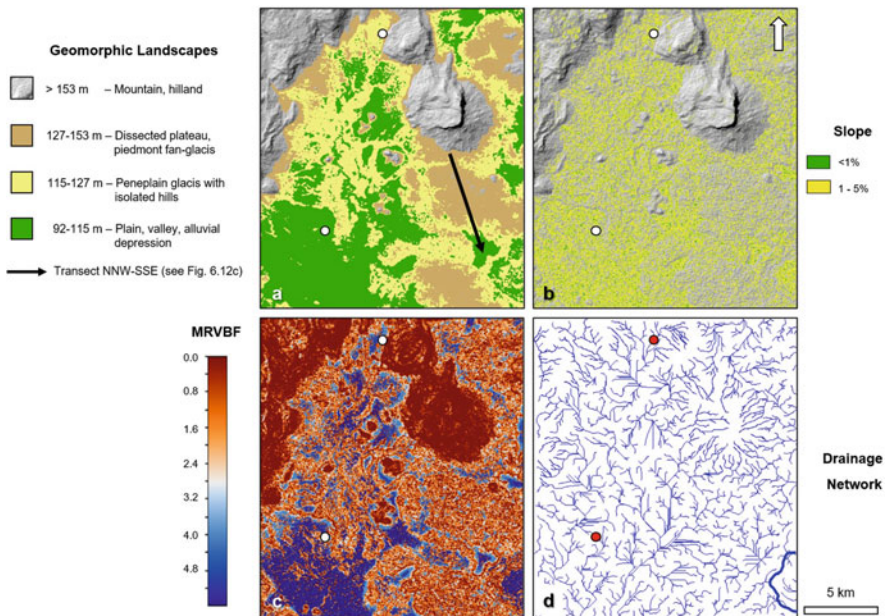


**Fig. 6.7** Camani training-area: (a) geomorphic landscapes; (b) slope gradient classes; (c) multiresolution index values of valley bottom flatness (MRVBF); (d) stream paths and drainage patterns

relief homogeneity of the alluvial depressions (light blue and blue) and relief heterogeneity of the dissected plateaus, as well as the frequency of small depressions within the peneplain landscape.

Figure 6.7d shows the potential flow directions and soil moisture distribution in the area. Since the amount of moisture along the hillslope tends to increase from upslope to downslope, additional moisture is contributed from upslope as the catchment area increases to the bottom of the lowlands. During the dry season, soil moisture is low, and savannas are frequently burned due to increasing human activities.

### 6.4.3 Landscapes and Soils

Gently sloping glacis (0.5–1% slope; 120–150 m a.s.l.) have developed at the foot slopes of structural sandstone reliefs bordering the valley of Caño Camani, a tributary of river Ventuari. Sediments covering the glacis have remarkably high fine sand, very fine sand, and silt contents (88–93%), suggesting aeolian origin. The sediments may have been transported by wind from the north, possibly through the Guanay pass, and deposited as aeolian blankets (sheets), and preserved in sheltered positions. This might also explain northern influence from the Llanos in the vegetation composition south of the Guanay gap.

Very few observations were made in this marginal area. Soils are pinkish grey or light grey Udoxic Quartzipsamments. Values of particle size distribution are 80–87% sand, 13–14% silt, and 0–6% clay. Under shrubby meadow vegetation, the A horizon is 15 cm thick and contains very little organic carbon (0.02%). Under open forest, the A horizon is 27 cm thick and contains 0.6% organic carbon. Depth of root penetration is similar in both cover conditions (50–60 cm). The topsoil can dry up during the lower rainfall period. Suffusion pans and surficial runoff rills are frequent (Table 6.3).

---

## 6.5 Ventuari Area

### 6.5.1 Geographic Setting

The Ventuari area is an elongated strip that corresponds approximately to the middle and lower stretches of the Ventuari river valley (90–130 m a.s.l.). Large glacis has developed on both sides of the valley from the surrounding hilllands that are the source of the sandy materials deposited on the glacis. Cerro Moriche is a landmark in this part of the Ventuari valley (Plate 6.1e). The vegetation cover of the white-sand patches is variable, including savanna, meadow, meadow-savanna, and shrubby meadow (Table 6.4).

**Table 6.3** Camani area: landscape and soil characteristics

Camani		Prof (2)	Vegetation cover %	Landscape slope %	Soil class	Text	sa-si-cl %	cs-ms-fs 100% s	Colour moist	Mottles features depth cm	Pedogenic features depth cm	A horizon cm	Root depth cm	OC % A	Groundwater cm	Moisture obs period dry/moist	Obs depth cm
Site Lat Lon	Locality																
53	Camani valley	32	Shrubby meadow 50-60	Glacis aeolian blanket	Udoxic Qps	s-ls/ s	87-13-0	0-13-87	Pinkish grey	-	-	15	60	0.11	-	m-feb	60
05° 14' N																	
66° 12' W						ls	80-14-6	0-3-97	Grey	-	-	27	50	0.48	-	d/m-feb 10	70
54		33	Open forest														
05° 21' N																	
66° 10' W																	

Prof, description and sampling profile; Qps, Quartzipsamment; Text, texture; s, sand; ls, loamy sand; sa-si-cl, sand-silt-clay; cs-ms-fs, coarse sand-medium sand-fine sand; A, soil surface horizon; OC, organic carbon; obs, observation; m, moist; d, dry (cm from soil surface); feb, February

**Table 6.4** Ventuari area: landscape and soil characteristics

Ventuari		Site	Locality	Prof (11)	Vegetation cover %	Landscape slope %	Soil class	Text	sa-st-cl %	cs-ms-fs 100% s	Colour moist	Mottles features depth cm	Pedogenic features depth cm	A horizon cm	Root depth cm	OC % A	Groundwater cm	Moisture obs period dry/moist	Microrelief	Obs depth cm
Lat	Lon																			
36	04° 43' N	66° 22' W	Cerro Moriche	7	Savanna	Glacis	Udoxic Qps	Sand	85-12-3 87-12-1	5-27-68 3-23-74	Light grey/ pinkish grey	Yellowish-brown along roots	-	13	13	0.36	-	m-feb	-	100
				8	Meadow-savanna									8	23	0.42	-	m-feb	Reticular	
				9	Meadow-savanna	Glacis 1-2			93-6-1	3-17-80	Light grey/ white			9	45	0.18	-	m-feb		
37	04° 32' N	66° 25' W	Río Coroco	10	Morichal	Swale channel	Oxyaquic (Udoxic) Qps		85-14-1	28-30-42	Grey/light grey	-	Densipan 50+	6	6	0.16	-	m-feb		50
				11	Morichal	Swale area inter-channels	Oxyaquic Udorthent	sl	61-35-4	12-20-68		-		50	50	0.77	-	m-feb		
				12	Savanna-meadow	Glacis	Udoxic Qps	ls	75-24-1	37-10-53	Light grey	-		25	50	0.77	-	m-feb	-	
38	04° 07' N	66° 57' W	In front of Maraya stream	13	Shrubby meadow	Glacis 0.5-1	Typic Qps	Sand	97-3-0	28-28-44	Light grey/ white	Yellowish-brown along roots	-	15	50	0.38	-	d/m-feb 15	Reticular	50+
50	04° 48' N	66° 17' W	Cerro Moriche	29		Glacis 0.5-1			97-3-0	11-40-49	Light grey/ very pale brown	-	Densipan 50+	30	50	0.15	-	d/m-feb 15		

(continued)



**Table 6.4** (continued)

Ventuari		Prof (11)	Vegetation cover %	Landscape slope %	Soil class	Text	sa-si-cl %	cs-ms-fs 100% s	Colour moist	Mottles features depth cm	Pedogenic features depth cm	A horizon cm	Root depth cm	OC % A	Groundwater cm	Moisture obs period dry/moist	Microrelief	Obs depth cm	
Site Lat Lon	Locality																		
51	04° 58' N	30	Meadow- savanna 20-30	Glacis 1-1.5			98-2-0	19-33-48	Light grey/ white	Termite mounds	-	28	40	0.15	-	d/m-feb 40		70	
52	04° 53' N	31	Meadow 30-35				96-4-0	12-46-42	Light grey/ very pale brown	-	-	25	70	0.13	-	d/m-feb 25		70+	
66° 06' W																			
148	04° 18' N	131	Meadow- savanna 40-50	Plain mound	Plinthic Qps	s/sl/ sl	90-4-6	19-38-43	Very pale brown/ white/ strong brown	Reddish- yellow	Plinthite 105-130 petroferric 130+	14	58	0.18	-	m-feb	-	130	
66° 16' W																			

Prof, description and sampling profile; Qps, Quartzipsamment; Text, texture; s, sand; ls, loamy sand; sl, sandy loam; sa-si-cl, sand-silt-clay; cs-ms-fs, coarse sand-medium sand-fine sand; A, soil surface horizon; OC, organic carbon; obs, observation; m, moist; d, dry (cm from soil surface); feb, February

### 6.5.2 Terrain Features

The SRTM data unravelled morphological features that occur under forest cover in the Ventuari area (Fig. 6.8a, b). Multi-scale negative relief components form enclosed depressions that are connected to linear systems. The sequence of landscape units per the importance of spatial distribution is peneplain glacis with isolated hills > alluvial depression, floodplain > dissected plateau > plain, valley > river, backswamp, stream > piedmont fan-glacis (Fig. 6.9a). In general, the terrain slope is low (Fig. 6.9b), and this influences surface hydrology and sediment deposition.

River Ventuari crosses a peneplain glacis landscape. The position of the river channel seems to be a relatively recent one as it is not fringed by conspicuous floodplains. To the west of this stretch, an elongated floodplain strip running parallel to the rim of the peneplain landscape can be recognized as an earlier valley floor of the river. In its lower watershed, the Ventuari has shifted position several times alternating erosion and sedimentation. The river has a large upper watershed in highlands and uplands producing discharge peaks that may conflict with concomitant discharge peaks from Orinoco. Flat, open valley bottoms are more extended in the Ventuari area than in the other study areas (Fig. 6.9c). Areas subject to periodic waterlogging in very flat interfluvial forest and riparian vegetation along streams may be much larger than the areas affected by flooding. The flow tracing consists of elongated morphologies and related tributaries that are arranged into a complex network. While some channels are continuous, others are discontinuous, configuring a series of isolated segments. Drainage pattern seems to be unstructured in the flat valley bottoms with a tendency to confinement (Fig. 6.9d).

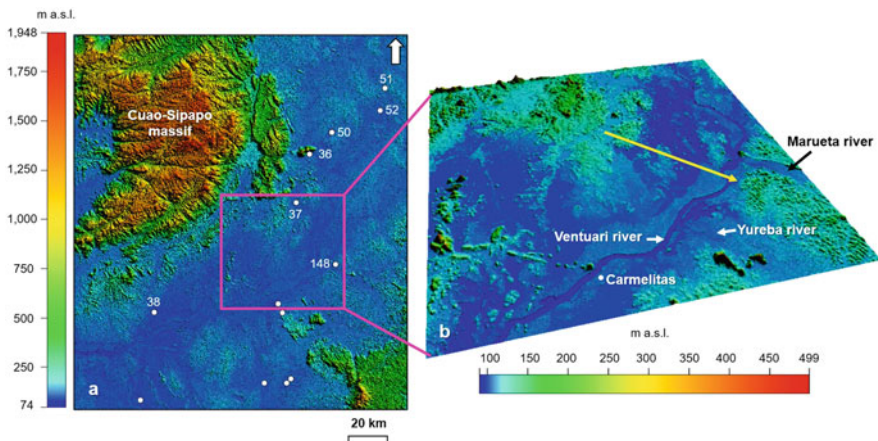


**Fig. 6.8** (a) Hill-shaded DEM of the Ventuari area, pixel 12.5 m; shaded relief illumination from 315°N, 45° above horizon; (b) DEM 3D view of the Ventuari training-area (2388 sq. km), located between 4°33'43.9" N, 66°53'43.3" W and 4°06'59.5" N, 66°01'11.4" W

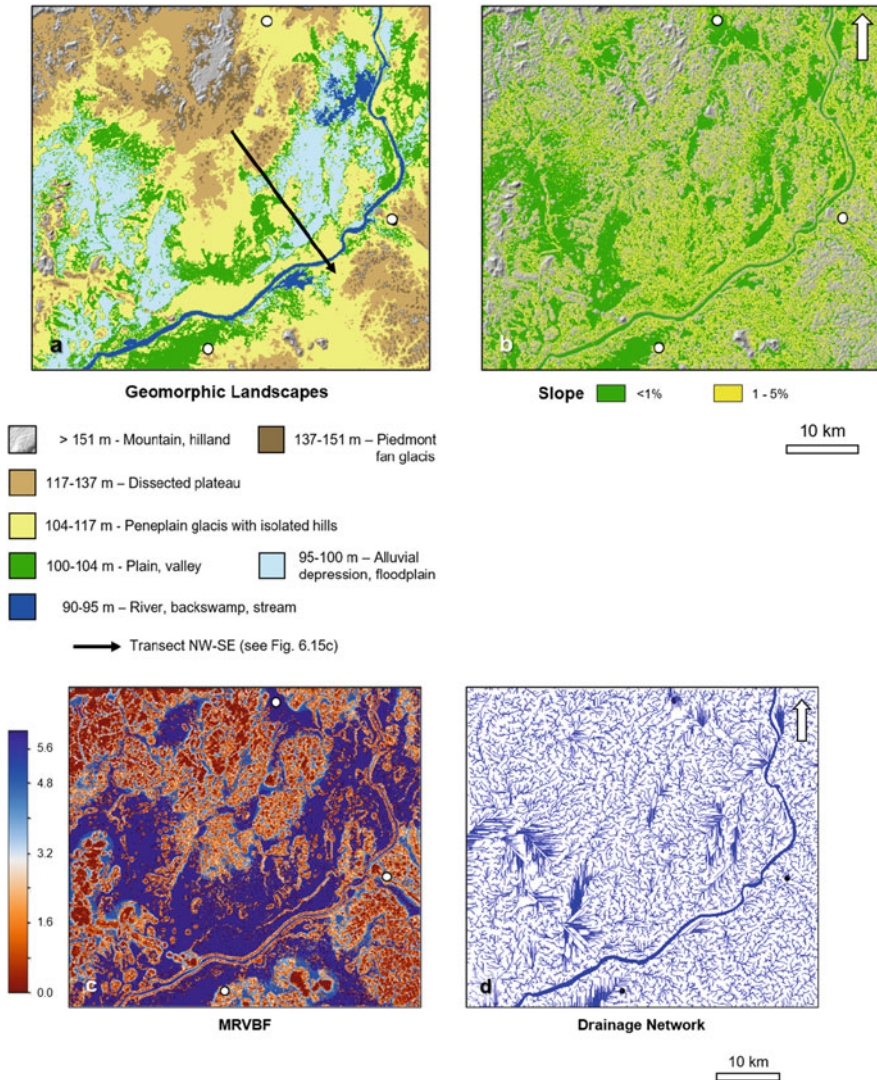


**Fig. 6.9** Ventuari training-area: (a) geomorphic landscapes; (b) slope gradient classes; (c) multiresolution index values of valley bottom flatness (MRVBF); (d) stream paths and drainage patterns

### 6.5.2.1 Large Peneplain Glacis

On large glacis (0.5–1.5% slope) covered in general by low-density shrubby meadow vegetation, soils are light grey over white or over very pale brown Typic Quartzipsamments. Sand content is on average 97% (96–98%), with 3% silt and no clay. Medium and fine sands dominate. On average, the A horizon is 25 cm thick (15–30 cm) and has 0.2% (0.13–0.38%) organic carbon content. Root penetration

depth is 53 cm (40–70 cm). Commonly the upper layers get dry in February–March down to 15–40 cm, causing roots to penetrate deeper here than in other areas having permanently moist topsoils.

### 6.5.2.2 Short Peneplain Glacis

Soils on the short glacis and proximal parts of glacis (1–2% slope) are influenced by the proximity of the hills where sands are coming from. This is also the case of the soils developed on recent sediments deposited by the Ventuari on its lateral banks (Plate 6.1e). Vegetation is mainly herb-forb savanna and meadow-savanna without shrubs. Soils are light grey over pinkish grey or white Udoxic Quartzipsamments that differentiate from the large glacis soils for having lower total sand content (85% on average), higher silt content (14% on average), and remarkably high fine sand content (69% on average). On average, the A horizon is 14 cm thick (8–25 cm) and has an organic carbon content of 0.36% (0.18–0.46%). Root penetration depth is on average 33 cm (13–50 cm). Surface layers of these soils do not dry up during the lower rainfall period.

### 6.5.3 Relevant Features of the Ventuari Area

The Ventuari area is essentially a glacis landscape where fine to medium sand sediments dominate. Overall, sand content is 91% (75–98%), silt content is 8% (2–24%), and clay content is 1% (0–6%). This area is better drained than the alluvial flats in the other areas. Groundwater was not observed within 1 m depth. Topsoils are susceptible to dry up during the lower rainfall period. The area distinguishes from the others by the large occurrence of savanna and mixed savanna-meadow. Vegetation is repeatedly burned by wildfires that progress freely on large glacis (Plate 6.1f). Reticular and suffusion microrelief is a characteristic feature of the Ventuari landscape (Plate 6.1g).

Distal parts of the glacis are usually bordered by narrow vales and swales covered by morichal vegetation with palm (*Mauritia sp.*) and picatón (*Platycarpum sp.*) trees on somewhat poorly drained sandy soils (Oxyaquic-Udoxic Quartzipsamments and Oxyaquic Udorthents).

---

## 6.6 Yapacana Area

### 6.6.1 Geographic Setting

The Yapacana area borders the middle Orinoco river valley from La Esmeralda upstream to Santa Barbara downstream where the Orinoco and Ventuari rivers merge, with a sensible enlargement north-east of Cerro Yapacana (Plate 6.2a). Three main landscape units can be distinguished, including alluvial plain flats, peneplain glacis, and piedmont fan-glacis (Plate 6.2b, c). Main features of the Yapacana area are shown in Table 6.5.

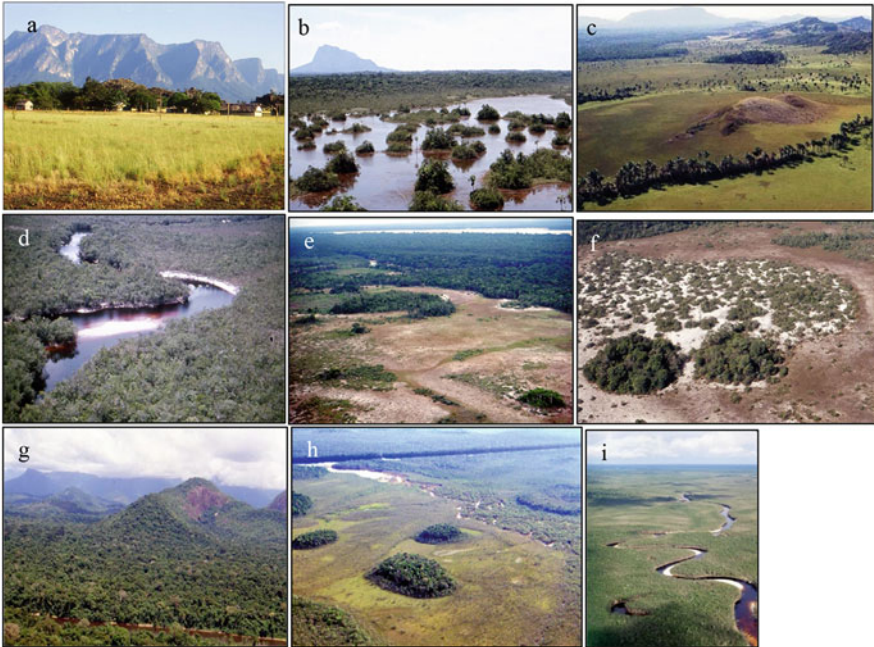


**Plate 6.2** Study areas. (a) Yapacana area: anthropized savanna on alluvial plain, west of La Esmeralda; Duida massif in the background; (b) Yapacana area: flooded depression along the Orinoco floodplain in the confluence area between Orinoco and Ventuari rivers; Cerro Yapacana in the left background; (c) Yapacana area: variety of meadow cover in penneplain landscape east of La Esmeralda; rounded crystalline bedrock hill surrounded by annular glacia and peripheral palm swale (morichal). (d) Atabapo area: blackwater stream at low water stage (February–March), crossing thick white-sand sediment under caatinga vegetation; (e) Atabapo area: herbaceous meadows and shrubby meadows on periodically active alluvial plain flats adjoining a stream tributary to river Guasacavi (in the background); (f) Atabapo area: dune-like mound overlying alluvial flat, fed by sand deflated from close by river bed at low water stage; open scrub of shrub clumps; Caname watershed; (g) Upper watersheds of Pasimoni and Siapa rivers in the Aracamuni massif; blackwater river Siapa in the foreground. Pasimoni area: (h) Pasimoni area: valley of blackwater river Siapa showing meadow islands within a scrubland matrix; (i) blackwater channel of river Pasimoni meandering through backswamps

## 6.6.2 Terrain Features

The DEM (Fig. 6.10a) covers an expanse of the middle Orinoco basin, stretching from Duida-Huachamacari massif in the east to the isolated Cerro Yapacana in the west. The northeast quarter of the picture corresponds to upland reliefs including hilllands, dissected plateaus, and the range of Serranía de El Tigre forming the western border. The light green central sector is a penneplain landscape and the large bluish areas are alluvial plain flats.

The training-area (Fig. 6.10b) depicts the confluence triangle between Orinoco and Ventuari rivers. The elevation profile of Fig. 6.10c crosses the large alluvial

**Table 6.5** Yapacana area: landscape and soil characteristics

Yapacana		Site Lat Lon	Prof (26)	Vegetation cover %	Landscape slope %	Soil class	Text	sa-si-cl %	cs-ms-fs 100% s	Colour moist	Mottles features depth cm	Pedogenic features depth cm	A horizon cm	Root depth cm	OC % A	Ground water cm	Moisture obs period dty/moist	Microrelief	Obs depth cm
33 03° 30' N	5																		
66° 50' W	6	Open meadow	Glacis prox 0.5-1/ sandstone	Udoxic Qps	Sand rock 55	95-4-1	8-31-61	-	-	-	-	-	13	33	0.05	-	m-feb	Reticular	55
39 04° 07' N	14	Savana- meadow 60-70	Glacis prox 0.5-1/ sandstone	Typic Qps	Sand rock 80	89-10-1	5-31-64	Dark grey/grey	-	-	-	-	20	80	1.73	-	-	-	80
66° 28' W	15	Savanna 10-20	Depression inter-glacis/ sandstone	Typic Qps	Sand rock 60	98-2-0	42-31-27	Grey/ light grey	-	-	-	-	15	40	0.54	-	d/m-feb 40	-	60+
40 03° 52' N	16	Shrubby meadow	Plain flat channel	Udoxic Qps	ls	80-19-1	10-23-67	Light grey/ white	-	-	-	Densipan 5-60+	5	35	0.36	-	d/m-feb 5	Reticular suffusion	50+
66° 26' W	17		Plain flat area inter- channels	Typic Udorthent	sl-s	66-33-1	5-13-82	-	-	-	-	Densipan 18-50+	18	50	0.56	-	m-feb	Reticular	50+
41 03° 47' N	18	Perro de Agua	Plain flat	Typic Qps	Sand	99-1-0	28-36-36	-	-	-	-	-	15	40	0.38	-	d/m-feb 15	-	70
67° 00' W	19					98-2-0	52-36-12	-	-	-	-	-	25	25	0.20	-	d/m-feb 60	-	60

(continued)



**Table 6.5** (continued)

Yapacana		Prof	Vegetation	Landscape	Soil class	Text	sa-si-cl	cs-ms-fs	Colour	Mottles	Pedogenic	A	Root	OC	Ground	Moisture	Microrelief	Obs
Site	Locality	(26)	cover %	slope %			%	100% s	moist	features	features	horizon	depth	A	water	obs		depth
Lat	Lon									depth	depth	cm	cm	%	cm	period		cm
43	La Esmeralda	22	Savanna-meadow	Glacis	Typic	s/s	66-32-2	25-36-39	Greyish brown	Vertical OM	Densipan	40	40	1.51	-	d/m-feb	-	70
03° 11' N			60-70	1-2	Udorthents				dark/light grey	streaks	40-70					10		
65° 31' W										40-50								
94	North of Cerro Yapacana	56	Meadow	Plain flat	Grossaemic Plinthic		96-2-2	13-32-55	Pink-brown/ light grey	Yellow	Densipan	7	50	0.26	100-130	m-feb	-	140+
03° 44' N			5-10		Kandiudult					110-140 red	20-50 claybridges				140+			
66° 44' W										140+	130-140							
96	Laguna Yagua	57	Shrubby meadow	Glacis/ saprolite		s/s/s/l	95-2-3	27-32-41	Pink-grey/ yellow/ red white	Variegated Yellow red grey	Bt 100-160	30	65	0.4	-		-	160
03° 51' N											fieldspars muscovite							
66° 32' W																		
97	Caño Yagua	58		Plain flat/ saprolite	Udoxic Qps	s/s	90-8-2	28-28-44	Light grey/ white/ light grey	Yellow	Densipan	4	28	0.40	-		Reticular	205
03° 51' N										4-28	4-53							
66° 27' W		59	Caatinga forest	Plain flat channel			87-12-1	20-28-52	Light grey/ white/ light grey	Yellow Fe nodules	Root mat 4 densipan	10	35	0.33	-		Reticular	150
										130-150	35-80							



97	Caño Yagua	60	Coatinga forest	Plain flat area inter-channels	Entic Humudept	s/s/ls	77-20-3	13-23-64	Dark brown/light grey	charcoal 45+	Root mat 45 densipan 85-130	(30)	45	7.39 O	-	m-feb	Reticular	200
98	03° 51' N 66° 27' W	61	Shrubby meadow		Udoxic Qps (Plinthic)	s/s/sl	81-16-3	24-34-42	Light grey/white/light grey	Variogated yellow, red grey 100+	Fe nodules 100-150	25	40	0.52	-		Reticular suffusion	150
99	04° 09' N 66° 29' W	62	Meadow	Plain flat shallow pan		ls	81-14-5	17-30-53	Grey/light grey	Yellow-reddish 30-115	Nodular petroferic contact 115	30	70	0.24	-			115
108	03° 11' N 65° 37' W	63	Shrubby meadow 40-50	Plain flat	Oxyauiq Haplorhod	Sand	98-0-2	67-20-13	Pink-grey/reddish brown dark	lith dis 40 charcoal 10-40	Bhs 40-120	10	40	0.43 1-1.47	100+ black		-	120+
108	03° 11' N 65° 37' W	73	Shrubby meadow	Fan-glacis	Typic Udorthent	s/s/ stones 74+	82-15-3	7-28-65	Brown/pink-grey	-	-	25	64	0.60	-	m-mar	-	74+
110	03° 11' N 65° 37' W	74	Bana scrub			ls/s/ stones 50+	88-10-2	13-37-50	Grey/pink-grey	-	-	14	37	0.31	-		-	50+
110	03° 11' N 65° 37' W	77	Shrubby meadow 80-90	Plain flat area inter-channels		sl	70-26-4	2-22-76	Black/brown/pink-grey	Greyish brown OM lenses 65-160	Root mat 13 densipan 39-65 115-145	26	39	2.64	150+	d/m-mar 13	Reticular suffusion	160

(continued)

**Table 6.5** (continued)

Yapacana		Prof (26)	Vegetation cover %	Landscape slope %	Soil class	Text	sa-si-cl %	cs-ms-fs 100% s	Colour moist	Mottles features depth cm	Pedogenic features depth cm	A horizon cm	Root depth cm	OC % A	Ground water cm	Moisture obs period dry/moist	Microrelief	Obs depth cm
Site	Locality																	
111	Río Iguapé	79	Shrubby meadow 60-70	Fan-glacis 1-2	Sand/ stones 10-15+	97-1-2	15-46-39	Pinkish grey	-	-	-	13	13+	0.48	-	m-mar	-	13
03° 19'																		
65° N		80	Shrubby meadow 90-95	Fan-glacis 0.5-1	Sand/ stones 40/50	95-4-1	10-28-62	Reddish grey dark/ pink-grey	-	-	-	16	22	1.03	-	-	-	40/50
31° W																		
112	Río Punname	81	Shrubby meadow 40-50	Plain flat	s/sl	95-2-3 /105+ cm 74-11-15	35-37-28 /105+ cm 34-30-36	Pink-grey/ white/ light grey	Brown 105-120 lith dis 105	Densipan 120-150 feldspars 105+	15	43	0.30	75-105 milky	-	-	-	150
03° 22'																		
66° N																		
30° W																		
147	Cerro Cariche	128	Shrubby meadow 80-90		Oxyaquic Qps (Aquadic)	97-1-2	37-24-39	Pink white/ pink, grey	-	Feldspars 44-90	8	44	0.38	60+ black	m-feb	-	-	100
02° 57'																		
66° N		129	Caatinga forest	Plain flat channel	s-ls	87-8-5	18-34-48	Dark grey/light brown/ light grey	-	Root mat 7 densipan 27-40+	20	40	22.1 O 0.43 A	29+ black	-	Reticular	40	
23' W																		
		130	Caatinga forest	Plain flat area inter-channels	Oxyaquic Humudept	59-36-5	7-22-71	Dark brown/ pale brown	-	Root mat 45 densipan 45-60+	(25)	60	6.14 O	70+	-	Reticular	70	

Prof, description and sampling profile; Qps, Quartzipsamment; Text, texture; s, sand; ls, loamy sand; sl, sandy loam; l, loam; sil, silt loam; sa-si-cl, sand-silt-clay; cs-ms-fs, coarse sand-medium sand-fine sand; lith dis, lithological discontinuity; A, soil surface horizon; O, organic horizon; Bt, subsurface illuvial horizon; Bs, spodic horizon; OC, organic carbon; obs, observation; m, moist; d, dry (cm from soil surface); feb, February; mar, March

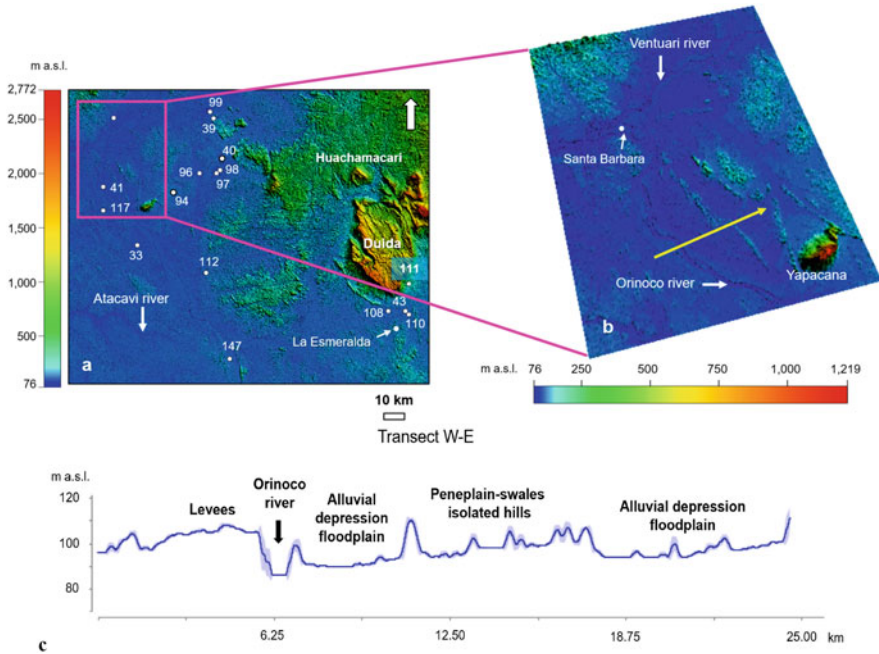


**Fig. 6.10** (a) Hill-shaded DEM of the Yapacana area, pixel 12.5 m; (b) DEM 3D view of the Yapacana training-area (348 sq. km), located between  $4^{\circ}11'45.2''$  N,  $67^{\circ}31'15.2''$  W and  $3^{\circ}36'41.9''$  N,  $66^{\circ}21'39.9''$  W; (c) transect showing elevation and topographic variations along landscape units in the Yapacana training-area

plain of river Orinoco. From west to east, the cross-section shows consecutively conspicuous overflow levees rising above the floor of the plain, the river channel, the current floodplain, a strip of low residual peneplain hills, and an earlier floodplain abandoned after the river shifted to its present position (see palaeo-valley fringed on both sides by lines of hills in Fig. 6.10b).

Orinoco and Ventuari rivers have developed large valleys and alluvial flats, larger than those of the other rivers in the study region, reflecting extensive watersheds and abundant water discharges. The sequence of geomorphic landscapes per the importance of spatial distribution is alluvial depression, floodplain > peneplain glaci > plain, valley > piedmont fan-glaci > dissected plateau > river, backswamp, stream (Fig. 6.11a).

The confluence area between Orinoco and Ventuari rivers is flat to slightly concave alluvial plain, possibly subsiding under the weight of abundant sediment discharge (Fig. 6.11b). Closed depressions and other flat bottom areas are flooded the largest part of the rainy season (Fig. 6.11c). Concomitant floods by both rivers and high discharge events cause severe drainage confinement (Fig. 6.11d).

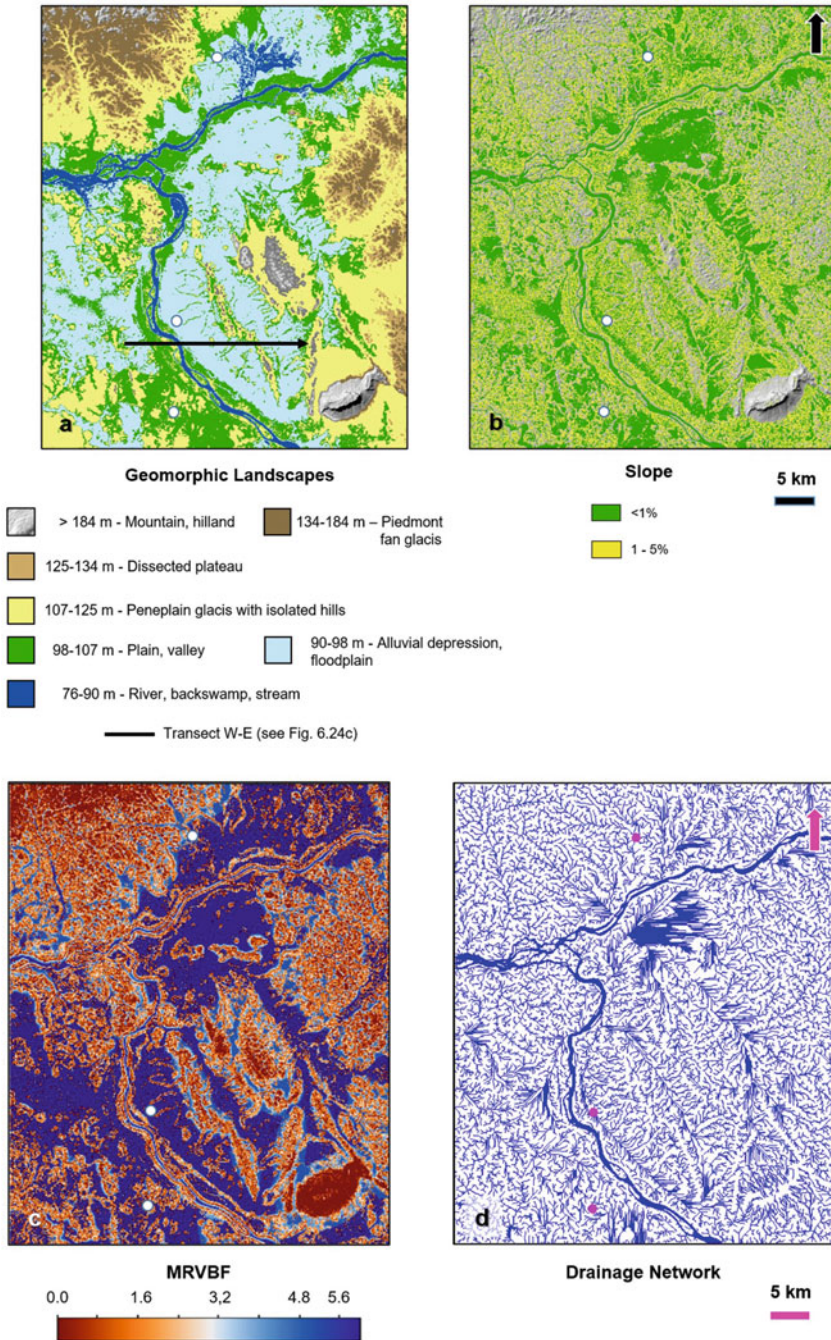


**Fig. 6.11** Yapacana training-area: (a) Geomorphic landscapes; (b) slope gradient classes; (c) multiresolution index values of valley bottom flatness (MRVBF); (d) stream paths and drainage patterns

### 6.6.2.1 Alluvial Plain Flats

Alluvial flats are extensive, especially around Cerro Yapacana (100–130 m a.s.l.). Shrubby meadow is the dominant vegetation cover. The most common soils in these conditions are Udoxic and Typic Quartzipsamments, and subsequently Oxyaquic Quartzipsamments and Typic Udorthents. Deep sandy soils classified as Oxyaquic Haplorthod and Grossarenic Kandiuult occur locally. Weakly developed plinthic, petroferic, and aquodic features appear in-depth at a few sites. In several places, compact sandy layers (i.e. densipan) were identified at variable depth, usually within 1 m from the surface, frequently together with reticular microrelief resulting from the incision of erosion and suffusion channels.

On average, sand content is 97% (95–99%) and silt content is 1% (0–2%) in sites free of reticular microrelief, while sand is 78% (66–90%) and silt is 19% (8–33%) in sites with reticular microrelief. Clay content is overall very low (0–5%). Sites without channel incisions show undifferentiated sand separates, reflecting the splay depositional process. Soils are light grey or pinkish grey over white or very pale brown. On average, the A horizon is 18 cm thick (5–30 cm), and its organic carbon content is 0.56% (0.2–2.6%). Root penetration varies between 25 and 70 cm, with an average of 43 cm. At some of the visited sites, the upper layers were dry down to 10–25 cm depth in February–March.

Within this regional context, some areas have distinctive features, for instance, the watershed of Caño Yagua that has its headwaters in Serranía de El Tigre in the east and joins the Orinoco river in the west in the surroundings of Cerro Yapacana, an alone-standing meseta of 826 m a.s.l. Dominant soils are Udoxic Quartzipsamments with subordinate Typic Udorthents, two taxonomically similar soil classes. These soils differentiate from the other soils in the alluvial plain landscape by their relatively high silt content (19% average, 8–33%). Presumably, silt is related to fresh alluvial sediments coming from erosion in the uplands of Serranía de El Tigre. This granulometric particularity is associated with compact densipan layers, often at shallow depth (truncated soils), and with erosional microrelief and suffusion pans. In this area, channel incision is deeper (80–100 cm) than in other lowland areas and causes a characteristic labyrinthine pattern of channels and inter-channel terrain surface heads.

Other alluvial plain flats distinguish by specific soil features. This is the case of the Perro de Agua area lying between Cerro Yapacana and river Orinoco, where thoroughly washed-out Typic Quartzipsamments dominate (98–99% quartz sand). In the poorly drained area along the Orinoco between river Purunami and Cerro Cariche dominate Oxyaquic Quartzipsamments with high groundwater.

### 6.6.2.2 Peneplain Glacis

Glacis (0.5–2% slope; 100–150 m a.s.l.) covered by open meadow and savanna-meadow vegetation has developed around low granitic hills (La Esmeralda, Laguna Yagua) and hummocky sandstone outcrops (San Antonio, Carmelitas) (Plate 6.2a). Udoxic Quartzipsamments and Typic Udorthents with densipan layers are frequent. Lithic Quartzipsamments occur in the proximity of sandstone outcrops and Ultisols (e.g. Grossarenic Plinthic Kandiuults) close to the base of granitic outcrops. In

general, glacis sites have high sand (89–99%), low but variable silt (1–10%), and very low clay contents. In some glacis, sand separates are undifferentiated reflecting poor sediment sorting, while in others fine sand is dominant. Soils are grey or light grey over white, locally pinkish grey close to rock outcrops. On average, the A horizon is 14 cm thick (3–30 cm) and contains 0.94% (0.05–2.26%) organic carbon. Root penetration varies between 25 and 80 cm, with an average of 49 cm; this is relatively deep penetration to explore deeper layers for water supply in a sloping glacis environment. Upper layers (10–20 cm) were dry in some places in February.

### 6.6.2.3 Piedmont Fan-Glacis

Fan-glacis (0.5–2% slope; 130–300 m a.s.l.) have formed at the foot of the high sandstone plateaus (tepui), at the intersection between piedmont and alluvial plain. This is the case, for instance, of the gently undulating lowlands south and southeast of the Cerro Duida tepui (La Esmeralda, Rio Iguape). These are places where sediments coming from the uplands accumulate in fans that enlarge into glacis through fan coalescence. Vegetation is a shrubby meadow. Soils are sandy Typic Udorthents with gravelly/stony substratum starting at variable depths within 1 m (13–74 cm). Sand content varies from 82 to 97%. Clay is very low (1–3%); silt can be as high as 10–15%. Fine sand is dominant. Soils are brown or grey over pinkish grey. On average, the A horizon is 17 cm thick (13–25 cm) and contains 0.6% (0.3–1%) organic carbon. Root penetration varies between 13 cm and 64 cm, with an average of 34 cm.

## 6.6.3 Relevant Features of the Yapacana Area

Yapacana is the most diverse of the study areas in terms of soil-landscape conditions. Alluvial flats, glacis, and fan-glacis are contrasting environments (Plate 6.2b) (Table 6.5). This is reflected in the large ranges of variation that show the generalized figures of particle size distribution when lumping together the 22 meadow profiles: 89% (66–99%) sand, 9% (0–33%) silt, and 2% (0–5%) clay. There are relevant soil texture and drainage variations within the extensive alluvial flats. Some areas are pure white sands; others have substantial silt contents. Piedmont fan-glacis has gravelly/stony substrata at shallow to moderate depth.

Although reticular microrelief is common in many of the study areas, the most expressive and deepest erosion channels and suffusion depressions were found in the Yapacana area. Characteristic labyrinthine channel networks occur in the lowlands of Caño Yagua, west of Serranía de El Tigre.

Soil classes and their spatial distribution are related to the variations of the geomorphic landscape. For instance, Typic and Oxyaquic Quartzipsamments alternate according to variations of the drainage conditions in the alluvial flats. Udoxic Quartzipsamments and Typic Udorthents with densipan layers are found associated in alluvial flat and glacis areas. The presence of some fines (>5%) in these soils may slightly improve water-holding capacity.



Vegetation varies from open meadow to savanna-meadow to shrubby meadow (Plate 6.2c). There are relationships between vegetation types and soil conditions: for instance, shrubby meadow and meadow on alluvial flats; open meadow, savanna-meadow, and savanna on glacis; shrubby meadow and bana scrub on fan-glacis.

---

## 6.7 Atabapo Area

### 6.7.1 Geographic Setting

The Atabapo area stretches from San Carlos de Rio Negro in the south to San Fernando de Atabapo in the north. It is an elongated, flat lowland expanse drained by a dense network of blackwater rivers (Rio Negro, Guainía, Atabapo, Pimichín, Temi, Guasacavi) and streams (Caño San Miguel, Caño Caname) (Plate 6.2d). The most common landscape units with meadow and shrubby meadow cover are alluvial plain flats and glacis (Table 6.6).

### 6.7.2 Terrain Features

The study area fairly covers the extent of the Atabapo river watershed that is separated by low divides from Orinoco basin to the east, Rio Negro basin to the south, and Inírida basin to the west (Fig. 6.12). It is the lowest-lying study area in the regional context, with hydrographic base level controlled by river Atabapo at about 70–80 m a.s.l. The area is drained by a dense network of short rivers and streams that all originate in the lowland depression itself.

The area includes intermingled peneplain and alluvial plain landscapes. The background landscape of the area is a strongly downgraded, rolling peneplain with low hills and very gentle glacis surrounded by poorly drained vales and swales (Fig. 6.13a, b). This geomorphology causes a finely divided slope mosaic, many flat bottom areas scattered between hilly terrains, and a high density of short drainage ways (Fig. 6.13c, d). Alluvial flats along rivers and streams show indented configurations and contours and traverse irregularly the peneplain landscape suggesting impeded drainage. In the area of the transect the deep incision of river Atabapo in the peneplain (by about 40 m) with a narrow floodplain indicates a new channel position after abandoning the alluvial depression in the west. This causes water retention in a flooded area on the left bank upriver (Fig. 6.13a). The large backswamps bordering the Atabapo channel downriver show the difficulty of water evacuation from the watershed into the Orinoco. From Fig. 6.13a, the sequence of geomorphic landscapes per the importance of spatial distribution is peneplain glacis > alluvial depression, floodplain > plain, valley > river, backswamp, stream.



**Table 6.6** Atabapo area: landscape and soil characteristics

Atabapo		Prof (17)	Vegetation cover %	Landscape slope %	Soil class	Text	sa-si-cl %	es-ms-fs 100% s	Colour moist	Mottles features depth cm	Pedogenic features depth cm	A horizon cm	Root depth cm	OC % A Bh Bhs	Ground water cm	Moisture obs period dry/moist	Microrelief	Obs depth cm	
44	03° 37' N	Guarinuma	Meadow 50-60	Glacis 2-3	Udoxic Qps	ls-sl	80-13-7	4-9-87	Grey-brown/light grey	-	-	50	50	1.47	-	m-feb	Reticular	60+	
67° 26' W		24	Meadow 10-20	Glacis distal 0.5-1	Typic Udorthent	s/sl-s	90-7-3	9-23-68	Light grey/white	Fe nodules 45-60	Ironstone 60-80	15	45	0.31	-			80+	
45	02° 37' N	Caño San Miguel	Shrubby meadow 10-15	Floodplain	Oxyaquic Qps	Sand	97-2-1	39-33-28	Pale brown/white	Yellowish brown 12-35	-	12	12	0.24	-	d/m-feb 5	-	65	
67° 02' W		26	Savanna-meadow 10-20	Floodplain point bar mound	Typic Qps		95-5-0	35-34-31	Grey-brown/white	Charcoal 5-26	-	26	26	0.52	-		-		
46	02° 38' N																		
67° 16' W		27	Savanna-meadow 10-15	Glacis distal 1-1.5	Typic Udorthent	sl/s	87-13-0	38-35-27	Light grey/white	-	-	10	35	0.70	-	d/m-feb 10	-	70+	
48	02° 57' N	Río Temi	Savanna-meadow 10-15	Glacis distal 1-1.5	Typic Qps	Sand	98-2-0	29-43-28	Light brown/white	-	Root mat 0-5/10		35	14.5 O 1.89 A	-	m-feb	-	50	
67° 29' W		28	Catanga forest	Glacis 1-1.5	Typic Qps	Sand	98-2-0	29-43-28	Light brown/white	-	Root mat 0-5/10		35	14.5 O 1.89 A	-	m-feb	-	50	

100	Lower Rio Pimichín	64	Shrubby meadow	Plain flat	Oxyaquic Qps		97-2-1	9-54-37	Light grey/ white	Sand lenses with OM	-	7	30	5.08	77+	m-mar	Reticular	90+	
02° 53' N																			
67° 44' W																			
101		67	Bare sand	Riverbed sand bar	Typic Qps		100-0-0	11-78-11	White	-	Muscovite flakes	15	15	0.12	-	d/m-mar 15	-	15	
02° 54' N																			
67° 42' W																			
102		65	Open scrub	Dune-like mound			98-0-2	73-21-6	Light grey/ white	Charcoal 30-125	-	8	30	2.22	-	d/m-mar 60	-	160	
03° 35' N																			
67° 11' W																			
115		66	Shrubby meadow	Plain flat			98-1-1	54-22-24	Light grey/ white	-	Root mat 0-7	7	33	0.45	114+	m-mar	Reticular	130	
03° 08' N																			
67° 30' W																			
116		84	Shrubby meadow	Plain flat aeolian sand sheet	Typic Durifhumod	s/s	93-4-3	4-65-31	Grey/ white/ very dark brown	Indurated 90-105 150-160	Bh 80-120 Bhs 120+	30	30	2.77 2.7- 5.7	80-90 135- 150 160+			170	
03° 08' N																			
67° 30' W																			
116		85	Open scrub	Dune-like mound	Udoxic Qps	Sand	92-6-2	57-32-11	Light grey/ white	Fossil roots horizontal	-	20	20	0.48	130+	d/m-feb 53	-	160	
03° 33' N																			
67° 12' W																			
116		86	Meadow	Plain flat	Oxyaquic Qps		99-0-1	33-42-25	-	-	-	1.3	23	0.68	75+	m-mar	Reticular	125	
03° 33' N																			
67° 12' W																			

(continued)

**Table 6.6** (continued)

Atabapo		Prof (17)	Vegetation cover %	Landscape slope %	Soil class	Text	sa-si-cl %	es-ms-fs 100% s	Colour moist	Mottles features depth cm	Pedogenic features depth cm	A horizon cm	Root depth cm	OC % A Bh Bhs	Ground water cm	Moisture obs period dry/moist	Microrelief	Obs depth cm
Site Lat Lon	Locality																	
117	NW San Antonio	87	Shrubby meadow 40-50	Glacis 1-1.5/ sandstone	Typic Udothent	s/sl/ rock 63	83-13-4	3-21-76	Pinkish grey/ white	-	Weathered subsoil	6	22	0.31	-	-	-	63
67° 00' N		88	Bare sand	rocky bar hummock	Lithic Qps	Sand/ rock10	94-5-1	1-12-87	Pinkish grey	-	Weathering pocket	10	10	0.65	-	-	-	10
140 03° 01' N	Upper Rio Pimichin	112	Shrubby meadow 30-40	Plain flat aeolian silt sheet	Oxyaquic Alorthod	s/sl	54-42-4	15-7-78	Pinkish white/ brown	-	Densipan 50-72 Bhs72-102	8	28	0.29 0.62	28-50	m-feb d 50-102	Reticular suffusion	102+
67° 33' W		113	Caatinga forest		Histic Humaquept	sil/sl	74-4-22	-	Dark brown/ white	-	Root mat 0-7	28	50	13.3 O	35-50	m-feb	Reticular	50

Prof, description and sampling profile; Qps, Quartzipsammite; Text, texture; s, sand; ls, loamy sand; sl, sandy loam; sil, silt loam; sa-si-cl, sand-silt-clay; cs-ms-fs, coarse sand-medium sand-fine sand; A, soil surface horizon; O, organic horizon; Bh, Bhs, spodic horizons; OC, organic carbon; obs, observation; m, moist; d, dry (cm from soil surface); feb, February; mar, March

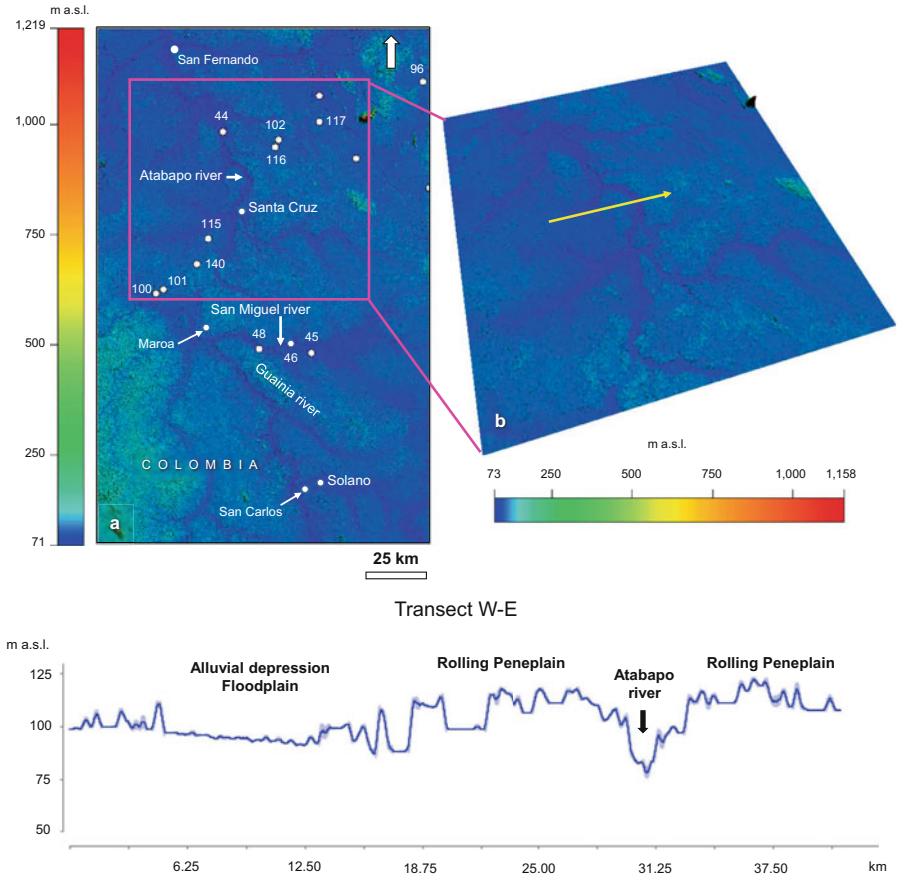


**Fig. 6.12** (a) Hill-shaded DEM of the Atabapo area, pixel 12.5 m; (b) DEM 3D view of the Atabapo training-area (11,114 sq. km), located between 4°14'0.9"N, 67°41'52.5"W, and 3°34'24.2"N, 66°18'57.7"W. (c) Transect showing elevation and topographic variations along landscape units in the Atabapo training-area

**6.7.2.1 Alluvial Plain Flats**

Overall, alluvial flats are poorly drained low-lying areas (90–100 m a.s.l.). During the discharge peaks of Rio Negro and Atabapo rivers, the main regional collectors, water remains stored or is only slowly evacuated from the tributary watersheds in the low-lying hinterland. This causes high groundwater in large parts of the area, more frequent than elsewhere in similar alluvial plain landscapes. Locally, the water level can vary between 30 cm in the Pimichín area and 135 cm in the Guasacavi and Caname areas during the lower rainfall period.

Alluvial flats covered by shrubby meadow vegetation are extensive (Plate 6.2e). Stratified Typic and Oxyaquic Quartzipsamments are the most common soils. In some places, Spodosols (e.g. Durikumods and Alorthods) have developed in white

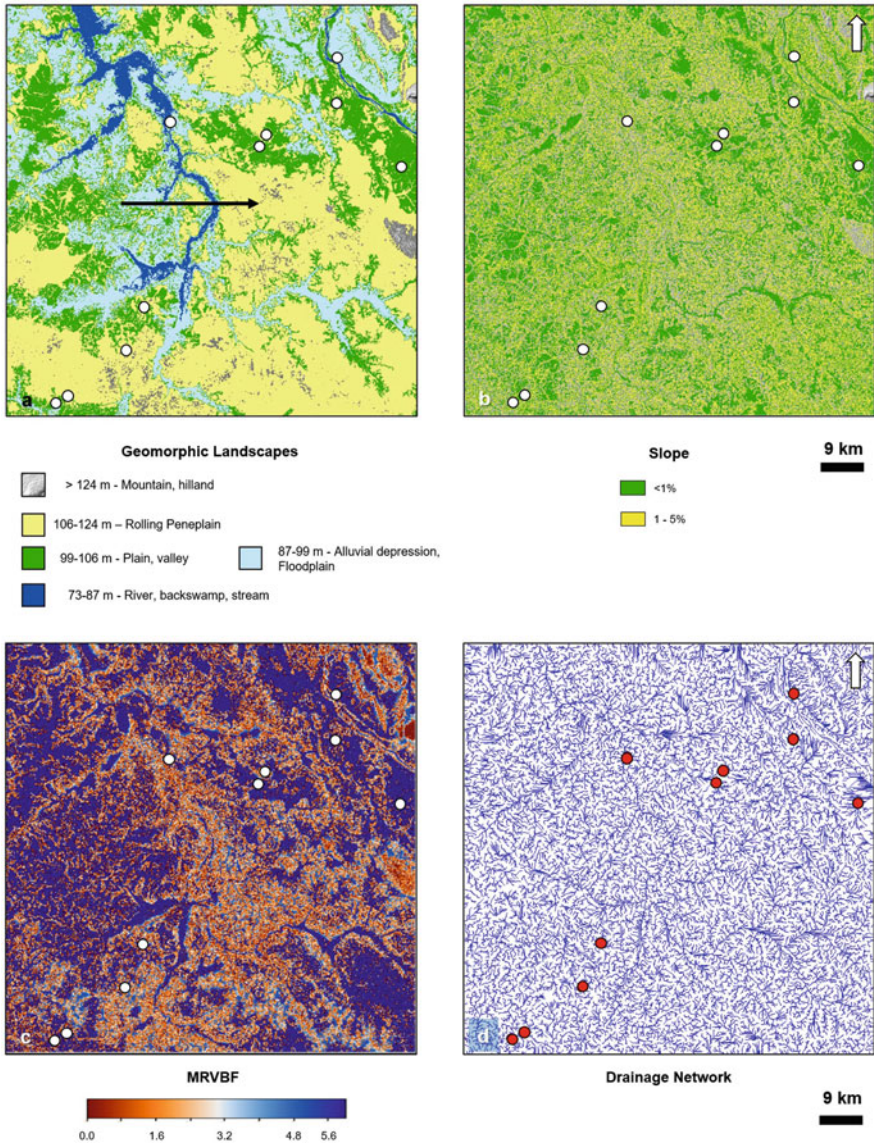


**Fig. 6.13** Atabapo training-area: (a) Geomorphic landscapes; (b) slope gradient classes; (c) multiresolution index values of valley bottom flatness (MRVBF); (d) Stream paths and drainage patterns

sands with groundwater at variable depths but without redoximorphic features. In general, soils have very high sand contents, commonly more than 95%. There is no clear sand sorting trend. At some sites, sand separates are undifferentiated, while medium to coarse sand dominates at others. In general, the sandy material is light

grey or pale brown over white. On average, the A horizon is 8 cm thick (5–13 cm), one of the lowest average thickness found in all study areas. Root penetration depth varies between 5 and 33 cm, with an average of 25 cm, one of the shallowest in the whole study region. Organic matter concentrates in the thin A horizon, with an average organic carbon content of 1.6% and large spatial variations (0.24–5.1%). Reticular microrelief is a common feature in the alluvial flats.

River and especially smaller stream channels are unstable. Frequent shifting of channels creates a network of active and abandoned sand-filled riverbeds and waterways in ever-moving floodplains. White-sand sediments are periodically spread along the stream banks through overflow and crevasse splay. White or pale brown over white Typic Quartzipsamments is dominant in migrating river areas. The river dynamics, together with undifferentiated sand separates and stratified deposits, indicate that the sand cover is frequently reworked by overflow, avulsion, and splay. From the geomorphic point of view, the Atabapo area seems to be currently the most active among the selected study areas.

In several places within the alluvial plain, especially in the lower watershed of Caño Caname, there is evidence of wind-blown sand accumulation in the form of dune-like mounds, covered by scattered clumps of shrubs (Plate 6.2f). Soils are light grey over white Typic and Udoxic Quartzipsamments. They commonly contain charcoal fragments at variable depths and horizontally lying fossil roots that reflect sand cumulation. Sand content is high (92–98%) but with atypical sand separates (unsorted sand or dominant coarse sand), suggesting local episodic sand reworking during the period of lower rainfall (January–March).

The past aeolian activity was also detected in the Pimichín watershed, north of Yavita. Large silt sheets blanket the poorly drained lowlands under shrubby meadow as well as under caatinga. Soils are stratified and can have up to 70–80% very fine sand and silt, a feature that underscores aeolian origin. Groundwater remains high during the lower rainfall season (February–March). Oxyaquic Alorthods and Histic Humaquepts are common soils.

### 6.7.2.2 Peneplain Glacis

The peneplain landscape in the Atabapo area is downgraded to an advanced level of evolution. It shows a policonvexe relief geometry and slope pattern of low rounded hills that in Brazilian geomorphic vocabulary is called ‘mamelonization’ or ‘mar de morros’ (Ab’Sáber 2000). Crystalline bedrock often outcrops along river shores and at channel floors (Plate 6.2c). Low hills scattered over the area (e.g. Guarinuma, Temi, San Antonio) are surrounded by glacis (0.5–3% slope; 100–120 m a.s.l.) with Typic Udorthents and Udoxic Quartzipsamments, covered by a low-density meadow or savanna-meadow vegetation. Close to the foot of the hills, the weathering bedrock can be at shallow depth, causing the occurrence of Lithic Quartzipsamments. Glacis soils have higher silt contents (7–13%) than alluvial plain soils (0–4%) because of their proximity to the periphery of the hills where rock weathering takes place, and because of sand grain attrition through colluviation (Plate 6.2c). The colour of the material varies from pinkish grey over white in the proximal parts of the glacis, close to weathering rocks, to light grey over white in the distal parts. On average, the

organic carbon content in the A horizon is 0.88% (0.31–2.1%), which is about half the organic carbon content in the A horizons of alluvial plain soils. The A horizon is only 10 cm thick (6–15 cm); that is less than in other areas. In contrast, roots penetrate deeper in glaciais conditions than in alluvial plains to counteract the susceptibility of the glaciais soils to dry up in the upper layers. Except for shallow soils close to the footslope of the hills, root penetration is 38 cm (22–50 cm).

### 6.7.3 Relevant Features of the Atabapo Area

The Atabapo area shows an intermingled pattern of peneplain and alluvial plain landscapes. The peneplain is strongly downgraded to low rounded hills surrounded by fine sand glaciais while shifting rivers tend to concentrate coarse sand in the alluvial flats (Table 6.6).

The area is drained by a dense fluvial network of east-west oriented waterways that join river Atabapo flowing northward and rivers Guainía and Rio Negro flowing southward. The sedimentation process through erosion and deposition of sands by laterally migrating rivers and streams is more active than in the other study areas. The sand cover is periodically reworked because of river shifting and avulsion. Therefore, the soil surface tends to be unstable, exposed to alternating truncation and burying. This affects topsoil features, as reflected by thin A horizons and shallow root penetration in alluvial flats. It explains also why there are large variations of organic carbon content between stable areas with high values and unstable areas with low values. Vegetation must adapt to periodically changing topsoil conditions. The topsoil environment is always changing, and vegetation must adapt. This might lead to a decline in plant diversity and an increase in endemism.

A particularity of the Atabapo area is the presence of geofoms such as dune-like mounds and silt sheets that evidence past aeolian activity (Plate 6.2f). The large interfluvium between Caño Caname to the north and river San Miguel to the south lies in front of an area on Colombian territory where dunes can be observed on the leeward side of river Atabapo.

---

## 6.8 Pasimoni Area

### 6.8.1 Geographic Setting

The Pasimoni area encompasses the lower valleys of the Siapa and Pasimoni rivers that have their upper watersheds in the southern uplands and highlands (northern slope of Sierra de la Neblina) (Plate 6.2g). They are tributaries of river Casiquiare (90–130 m a.s.l.). The landscape shows geofoms related to river activity, including floodplains with pointbars and meander lobes, levees, backswamps, and terraces. A shrubby meadow is the most common vegetation cover. Flooded meadows occur in very poorly drained places such as infilled river channels and backswamps (Plate 6.2h). Groundwater is present in all positions, even during the lower rainfall period, below 1 m depth in higher terrains and above 1 m in lower terrains (Table 6.7).



**Table 6.7** Pasimoni area: landscape and soil characteristics

Pasimoni		Site Lat Lon	Prof (12)	Vegetation cover %	Landscape slope %	Soil class	Text	sa-si-cl %	cs-ms-fs 100% s	Colour moist	Mottles features depth cm	Pedogenic features depth cm	A horizon cm	Root depth cm	OC % A Bh	Ground water cm	Moisture obs period dry/moist	Micronielief	Obs depth cm
Locality	Soil class																		
133	Lower Rio Stapa	01° 57' N	100	Shrubby meadow 30-60	River terrace levee	Arenic Alorthod	Sand	96-2-2	29-34-37	Grey-brown/white/dark brown	OM spots 22-54 gravel 54-104	Litho disc 54 Bh 122-150 Bhsm 150+	22	54	0.65 0.7-1	140-150	m-feb	Reticular	165+
135	02° 05' N	66° 02' W	101	Caatinga forest	River terrace overflow mantle			92-4-4	19-23-58	Dark brown/white/black	Densipan 25-80	Root mat 0-25 Litho disc 105 Bh 105-130	-	25	11.120 2.79	-			130
136	02° 06' N	66° 25' W	103	Shrubby meadow	Point bar meander lobe	Oxyaquic Alorthod		93-4-3	22-38-40	Pinkish grey/white/dark brown	OM lamellae 85-115	Litho disc 44 Bh 122-150	27	44	0.38 1.8	85-150			150
137	02° 06' N	66° 12' W	104	Caatinga forest	River terrace	Udoxic Qps		88-8-4	17-33-50	Dark grey/grey/light grey	-	Root mat 0-12	13	42	3.41 O 1.45 A	-			
138	02° 06' N	66° 12' W	105	Shrubby savanna 40-50	River levee meander lobe	Oxyaquic Qps		92-5-3	10-24-66	Grey/white	-	Litho disc 90	18	31	0.64	90+			120
139	02° 06' N	66° 12' W	106	Flooded meadow	Infilled river channel	Psammaquent		98-0-2	19-44-37	Grey	-	-	23	23	6/0.2	23+			23

(continued)

**Table 6.7** (continued)

Pasimoni		Prof (12)	Vegetation cover %	Landscape slope %	Soil class	Text	sa-si-cl %	cs-ms-fs 100% s	Colour moist	Mottles features depth cm	Pedogenic features depth cm	A horizon cm	Root depth cm	OC % A Bh Bhs	Ground water cm	Moisture obs period dry/moist	Microrrelief	Obs depth cm
Site	Locality																	
137	Río Pasimoni	107	Shrubby meadow	Depression backswamp	Hydric Haplohemist		87–10–3	13–28–59	Black/white	–	Histic material 0–60	60	60	OM	40+	–	–	80
01° 35' N		108		River terrace levee	Udoxic Qps		86–11–3	18–29–53	Brown/white/pale brown	Yellow 100–150	Densipan 35–100	20	35	0.67	–	d/m-feb 20	Reticular	150
66° 33' W		109	Shrubby savanna 60-70	River levee 2-4 lateral	Arenic Alorthod		94–3–3	16–32–52	Brown/white/reddish brown dark	Soilfluction ripples on lateral slope	Bhs 120–140+	19	45	1.03 1.0	110+	m-feb	–	140
66° 32' W		110	Scrub	Floodplain	Psammaquent	ls/s	97–0–3	19–36–45	Dark grey/brown/dark brown	–	Histic material 0–10	10	37	25.4 0.27	37+ brownish	–	–	50+
146	Lower RíoYatúa	124	Caatinga forest	River terrace	Kanhapludult	l/s /sil/c	Stratified profile	Strong textural variations	Dark grey/reddish yellow	–	Root mat 0–8 Bt 40–75	32	40	11.980 4.06 A	–	m-feb	–	75
01° 31' N		125	Flooded meadow	Floodplain backswamp lagenocarpus	Hydric Haplohemist	–	No mineral material	–	Dark greyish brown	–	–	OM	OM	OM	35+	–	–	50
66° 23' W																		

Prof, description and sampling profile; Qps, Quartzipsamment; Text, texture; s, sand; ls, loamy sand; l, loam; sil, silt loam; c, clay; sa-si-cl, sand-silt-clay; cs-ms-fs, coarse sand-medium sand-fine sand; A, soil surface horizon; O, organic horizon; Bt, subsurface illuvial horizon; Bh, Bhs, Bhsm, spodic horizons; OM, organic matter; litho, lithological discontinuity; OC, organic carbon; obs, observation; m, moist; d, dry (cm from soil surface); feb, February

### 6.8.2 Terrain Features

The DEM image of the Pasimoni area (Fig. 6.14a) shows the enlarged valleys of rivers Siapa, Pasimoni, and Yatúa crossing low hilllands and dissected plateaus in a little contrasted regional landscape, except the tablet-shaped plateau of Cerro Aracamuni in the south-east corner. The relevant feature depicted in the training-area (Fig. 6.14b) is the water-engorged floodplain of river Pasimoni in the confluence area with river Casiquiare. The floodplain is blocked by scrollbar-swale deposits and flooded backswamps (Fig. 6.14c). The valley is flanked on both sides by river terraces and undifferentiated benches, followed to the east by low dissected plateaus (Fig. 6.15a, b). The sequence of geomorphic landscapes per the importance of spatial distribution is river terrace > alluvial depression, floodplain > dissected plateau > river, backswamp, stream > piedmont fan-glacis. The spotty distribution of the MRVBF index values on the terrace strips bordering both sides of the floodplain indicates that these terrains are eroding (Fig. 6.15c). The river channel

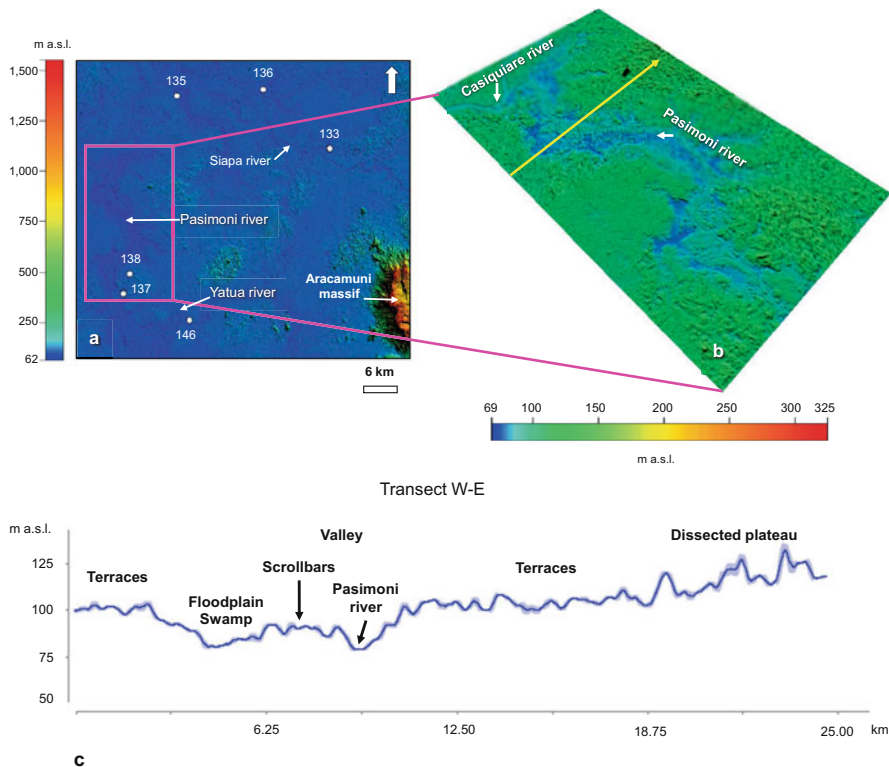


**Fig. 6.14** (a) Hill-shaded DEM of the Pasimoni area, pixel 12.5 m; (b) DEM 3D view of the Pasimoni training-area (232 sq. km), located between 1°58'46.8"N, 66°57'56.6"W, and 1°33'16.7" N, 66°07'19.2"W; (c) Transect showing elevation and topographic variations along landscape units in the Pasimoni training-area

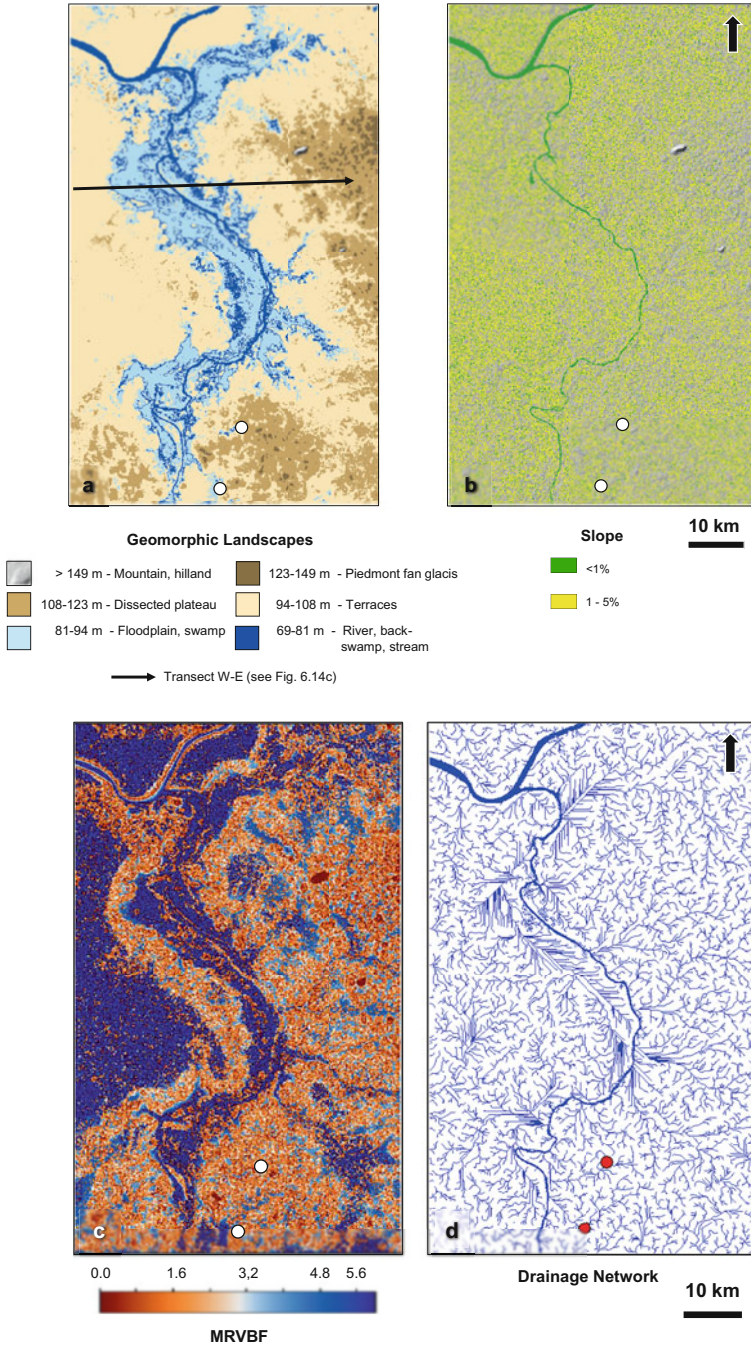


**Fig. 6.15** Pasimoni training-area: (a) geomorphic landscapes; (b) slope gradient classes; (c) multiresolution index values of valley bottom flatness (MRVBF); (d) stream paths and drainage patterns; (e) transect showing elevation and topographic variations along landscape units in the Pasimoni training-area

has shifted to the right margin of the floodplain, leaving large areas without an organized drainage network and causing drainage confinement in backswamps (Fig. 6.15d).

### 6.8.3 Geoforms and Soils

On the higher landscape positions corresponding to older levees and other river benches that lack the typical convexity of levees, Spodosols (Arenic and Oxyaquic Alorthods) are the most common soils, with groundwater in general below 1 m depth. Colour-contrasted horizon sequences include a greyish brown or brown A horizon, a thick (about 1 m) albic E horizon, and a very dark brown or dark reddish-brown spodic horizon. The A horizon has an average thickness of 23 cm (19–27 cm) and average organic carbon content of 0.73% (0.35–0.95%). Root penetration is on average 48 cm (44–54 cm). The spodic Bh<sub>s</sub> horizons occur at a remarkably constant depth of about 120 cm all along the study area. They are 20–40 cm thick and contain 0.7–1.8% organic carbon.

On recent river levees and pointbars, Udoxic and Oxyaquic Quartzipsamments are the most common soils. They have a greyish or light brown surface horizon lying atop the white sandy subsoil. The A horizon is 18–20 cm thick and contains 0.6–1% organic carbon, with roots penetrating to 30–35 cm depth.

A variety of soils was identified in depressed, poorly drained areas, including Psammaquents in infilled river channels, Hydric Haplohemists in backswamps, and Histic Alaquods in floodplains. Groundwater stands at 20–40 cm depth.

Whatever the taxonomic soil class, whether Spodosol, Histosol, or Entisol, all soils have high sand contents, above 86% (86–98%) with largely dominant fine sand, and low clay contents (2–4%). For instance, profiles P107 (backswamp) and P108 (levee) represent, respectively, low and high landscape positions contiguous in space and with 1–1.5 m elevation difference (Table 6.8). The backswamp has an accumulation of 60 cm organic matter on top of the mineral substratum. Particle size distribution of the white sand is remarkably similar at both sites. The low position seems to have been excavated in a generalized sand cover by river shift before becoming a backswamp with organic matter accumulation.

### 6.8.4 Relevant Features of the Pasimoni Area

The Pasimoni area is different from the other study areas. Instead of large alluvial plain flats with dominantly white Quartzipsamments, the landscape of the Pasimoni area is structured by a fluvial system with terraces, levees, backswamps, and floodplains possibly of different ages (Plate 6.2h, i) (Table 6.7). Meadow patches are relatively small islands, surrounded by caatinga forest on Ultisols, Spodosols, and Quartzipsamments. The Pasimoni area encompasses a variety of soil taxa under meadow vegetation, including Entisols, Spodosols, and Histosols. Udoxic and Oxyaquic Quartzipsamments are found on well to moderately well-drained sites

**Table 6.8** Backswamp and levee soils in the Pasimoni area

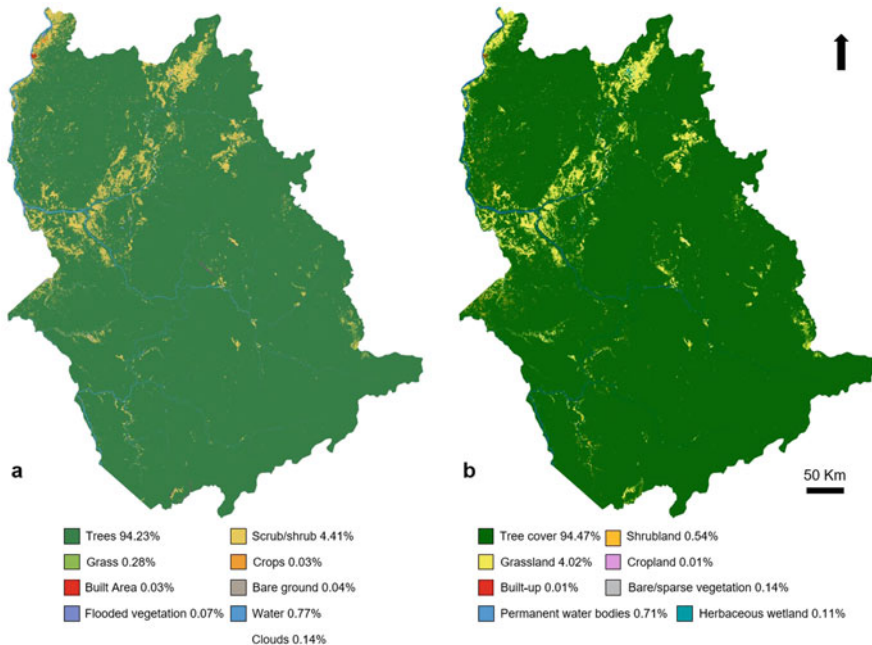
Site	Geomorphic position	Soil class	Topsoil	Mineral material	Sand %	Silt %	Clay %	Coarse sand %	Medium sand %	Fine sand %	Groundwater
P107 01° 35'N 66° 33' W	Backswamp	Hydric Haplohemist	O horizon 0–60 cm	60+ cm	87	10	3	13	28	59	40+ cm black
P108 01° 35'N 66° 33' W	Levee	Udoxic Quartzipsamment	A horizon 0–20 cm	0–150 cm	86	11	3	18	29	53	None

on pointbars, levees, and terraces. In poorly drained conditions, there are Psammaquents, Hydric Haplohemists, and Histic Alaquods. Arenic and Oxyaquic Alorthods show up on levees and slightly higher positions in the landscape that belong to an earlier terrain surface and may be thus anterior to the current fluvial system.

## 6.9 Landcover Amazonas State

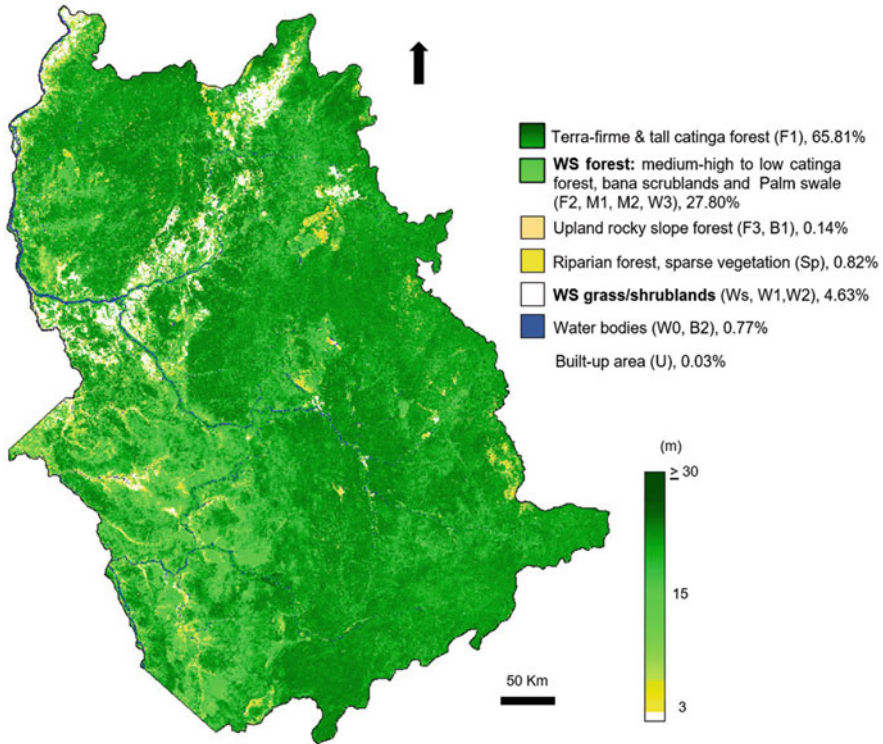
Landcover at the global scale is highly useful information and has already found wide use within the scientific community. However, is often that conventional sources of landcover information are so widespread that anything is an improvement. Another factor leading to unquestionable use is that other uncertainties may have a greater effect on the modelled result than errors in the landcover information. Despite the global overall accuracy of 85.9% and 74.4% for Esri Land Cover and ESA WorldCover, respectively, the results are not adequate to the regional and local reality studied.

Figure 6.16a, b shows the results of landcover for the state of Amazonas, both with an excellent quality of the input data (Sentinel-2, pixel 10-m) but with some discrepancies in the classification algorithm used to produce them, as well as legend



**Fig. 6.16** High-resolution Landcover 2020: (a) Esri 2020 Land Cover (Karra et al. 2021); (b) ESA WorldCover project 2020. Contains modified Copernicus Sentinel data (2020) processed by ESA WorldCover consortium (Zanaga et al. 2021)





**Fig. 6.17** Amazonas State. Global forest canopy height (FCH) map that correlates as a proxy to indicate where units of white-sands ecosystems likely occur (adapted from Potapov et al. 2020). In parentheses landcover classes determined by the optical radar synergy

(Karra et al. 2021; Zanaga et al. 2021). The identification of the dominant landcover types such as forest (trees/tree cover) and water bodies was fairly consistent; but mostly for the meadow and shrubland, the consistency was very low.

Figure 6.17 shows the forest canopy height (FCH) map that correlates as an alternative to indicate where units of white-sand ecosystems possible occur (adapted from Potapov et al. 2020). In parentheses, landcover classes determined by the optical radar synergy.

## 6.10 Conclusions

In the six selected study areas, meadow vegetation including pure herbaceous meadow, shrubby meadow, and mixed meadow-savanna occurs mainly in two landscape types: (1) alluvial flats formed by river and stream deposition in a plain landscape and (2) slightly sloping glacia formed by colluviation in penneplain landscape. Regardless of their taxonomic classification, soils are quartzose sand and

loamy sand sediments, white to light grey when dry and deficient drainage. Bleached sands in C layers are devoid of nutrients; the latter concentrate in the surface ochric epipedon that is the living part of the meadow soils.

Because of the origin and nature of the parent material of the meadow soils, there are commonalities among the various study areas, such as:

- Fragmented white-sand flats and depressions, discontinuously interspersed with residual peneplain reliefs
- Meadow vegetation, often with low cover density and variable proportion of shrubs
- Alluvial plain flats and glaciais landscapes with common reticular microrelief patterns
- White-sand cover and substratum (in general >90% sand, mainly medium and fine sand)
- Low organic matter contents (in general <0.5% OC in A horizon <20 cm thick)
- Very low nutrient availability (0–3 mg kg<sup>-1</sup> phosphorus and potassium, respectively)
- Low water-holding capacity
- Imperfect to poor drainage; upper layer susceptible to dry up during the lower rainfall season
- Quartzipsamments dominant; Udorthents and Spodosols subordinate

However, study areas show also relevant differentiating features summarized hereafter:

- Sipapo: water storage area confined between slightly higher terrains to the west and the east; low-lying, poorly drained alluvial plain landscape; Oxyaquic Quartzipsamments largely dominant, especially in the northern part (Sipapo watershed); truncated buried Spodosols in the southern part (Guayapo watershed).
- Camani: glaciais developed at the foot of structural reliefs and covered by aeolian blankets.
- Ventuari: glaciais landscape on both sides of the Ventuari river valley; Typic and Udoxic Quartzipsamments dominant; generalized reticular microrelief.
- Yapacana: large area, less homogeneous than the others; diversity of environments with distinctive characteristics including (a) fresh sediment deposition and incision of anastomosed channels forming labyrinthine patterns in the Yagua watershed; (b) washed-out recycled sands in the area of Perro de Agua; (c) poor drainage in the Puriname watershed; and (d) fan-glaciais with coarse fragments in the area of La Esmeralda; in general, more soil variety than in the other areas and frequency of compact sandy layers at variable depths.
- Atabapo: shifting fluvial system with a sustained reworking of the white-sand pool, originating stratified Typic and Oxyaquic Quartzipsamments; water storage and obstructed drainage; evidence of past aeolian activity.

**Table 6.9** Generalized values of the A horizon in meadow soils of alluvial plain flats (average and range of variation)

Study areas	Thickness cm	Organic carbon %	Rooting depth cm	Samples
Sipapo north	12 (7–20)	0.40 (0.20–0.56)	39 (15–70)	7
Sipapo south	23 (20–30)	0.24 (0.10–0.54)	47 (40–53)	4
Yapacana	18 (5–30)	0.56 (0.20–2.6)	43 (25–70)	12
Atabapo	8 (5–13)	1.60 (0.24–5.1)	25 (5–33)	7
Pasimoni	23 (19–27)	0.73 (0.35–0.95)	48 (44–54)	9

**Table 6.10** Generalized values of the A horizon in meadow soils of glacis and fan-glacis (average and range of variation)

Study areas	Thickness cm	Organic carbon %	Rooting depth cm	Samples
Sipapo G	19 (15–23)	0.21 (0.20–0.21)	35 (25–44)	2
Ventuari LG	25 (15–30)	0.20 (0.13–0.38)	53 (40–70)	4
Ventuari SG	14 (8–25)	0.36 (0.18–0.46)	33 (13–50)	4
Yapacana G	14 (3–30)	0.94 (0.05–2.26)	49 (25–80)	6
Yapacana FG	17 (13–25)	0.60 (0.3–1.0)	34 (13–64)	4
Atabapo G	10 (6–15)	0.88 (0.31–2.1)	38 (22–50)	4

G, glacis; LG, large glacis; SG, short glacis; FG, fan-glacis

- Pasimoni: river-controlled geomorphic features with a variety of positions and soil classes; Spodosols possibly remnant of an earlier terrain surface.

The A horizon is the living and vital part of the meadow soils. Generalized values of three relevant properties of the A horizon, including thickness, organic carbon content, and depth of root penetration, are reported in Tables 6.9 and 6.10 for rough comparison. In soils on alluvial flats, the A horizon is in general not more than 30 cm thick and can be as shallow as 5 cm. Organic carbon content is low to very low. Values such as 2.6% in Yapacana and 5.15% in Atabapo are infrequent outliers. Roots penetrate in general less than 50 cm deep and explore layers beneath the A horizon for water supply. The values of the Atabapo area deviate from the general trend: the A horizon is shallower and root penetration is more surficial than in the other study areas. This results from periodic truncation of the topsoil by shifting streams. In a penepplain environment, soils of large glacis have slightly thicker A horizon, roots penetrate a bit deeper, but organic carbon content is somewhat lower than in the other kinds of glacis.

Sand is the surface, subsurface, and substratum material in all meadow areas whatever the cover type from pure herbaceous to shrubby. However, there is a differentiation in particle size classes according to landscape type: coarse sand dominates in alluvial plain flats, while fine sand is more frequent in penepplain glacis. This causes the distinction between the study areas according to the predominance of one or the other landscape type. Whether sand grain size influences the kind of meadow vegetation is unclear.

Whether Quartzipsamments or Spodosols, differences in soil types are possible of little relevance to generate variations in vegetation growth and cover density. Deep quartzose sand is an almost sterile substrate that has no influence on meadow vegetation with very surficial rooting. Forbs, herbs, and shrubs live mainly in the upper soil layer and commonly do not explore more than 50 cm depth.

## References

- Ab'Sáber AN (2000) The natural organization of Brazilian inter- and subtropical landscapes. *Revista do Instituto Geológico de São Paulo* 21(1/2):57–70
- ASF (2015) Alaska Satellite Facility radiometric terrain corrected products. Algorithm Theoretical Basis Document, ASF Engineering, Revision 1.2, pp 2–16
- Blancaneaux P, Pouyllau M, Ségalen P (1978) Les relations géomorpho-pédologiques de la retombée nord-occidentale du massif guyanais (Venezuela). *Cahiers ORSTOM, Série Pédologie XVI*(3):293–315
- Carabajal CC, Harding DJ (2006) SRTM C-band and ICESat laser altimetry elevation comparisons as a function of tree cover and relief. *Photogramm Eng Rem Sens* 72(3):287–298
- Conrad O, Bechtel B, Bock M, Dietrich H, Fischer E, Gerlitz L, Wehberg J, Wichmann V, Böhner J (2015) System for automated geoscientific analyses (SAGA) v. 2.1.4. *Geosci Model Dev* 8: 1991–2007. <https://doi.org/10.5194/gmd-8-1991-2015>
- Damasco G, Vicentini A, Castilho CV, Pimentel TP, Nascimento HEM (2013) Disentangling the role of edaphic variability, flooding regime, and topography of Amazonian white-sand vegetation. *J Vegetation Sci* 24(2):384–394
- Dubroeuq D, Volkoff B (1998) From Oxisols to Spodosols and Histosols: evolution of the soil mantles in the Rio Negro basin (Amazonia). *Catena* 32:245–280
- FAO (2006) Guidelines for soil description, 4th edn. Food and Agriculture Organization of the United Nations, Rome
- Gallant JC, Dowling TI (2003) A multiresolution index of valley bottom flatness for mapping depositional areas. *Water Resour Res* 39(12):1347–1360. <https://doi.org/10.1029/2002WR001426>
- Google LLC (2019) Retrieved March 5, 2019
- Hengl T (2007) A practical guide to geostatistical mapping of environmental variables. *Geoderma* 140:417–427
- Her Y, Heatwole CD, Kang MS (2015) Interpolating SRTM elevation data to higher resolution to improve hydrologic analysis. *J Am Water Resour Assoc* 51(4):1072–1087
- Hillier JK, Watts AB (2004) Plate-like subsidence of the East Pacific Rise - South Pacific Superswell system. *J Geophys Res* 109:B10102. <https://doi.org/10.1029/2004JB003041>
- Hofton M, Dubayah R, Blair JB, Rabine D (2006) Validation of SRTM elevations over vegetated and non-vegetated terrain using medium footprint Lidar. *Photogramm Eng Rem Sens* 72(3): 279–285
- Huber O (2005) Diversity of vegetation types in the Guayana Region: an overview. *Biol Skr* 55: 169–188
- Huber O (2015) Definition and boundaries of eco-chorological areas for the meadow inventory project in Amazonas state (Mapa de Puntos, unpublished)
- Karra K, Kontgis C, Statman-Weil Z, Mazzariello JC, Mathis M, Brumby SP (2021) Global land use/land cover with Sentinel 2 and deep learning. In: 2021 IEEE international geoscience and remote sensing symposium IGARSS 2021 July 11. IEEE, pp 4704–4707
- Kellndorfer JM, Walker WS, Pierce LE, Dobson MC, Fites J, Hunsaker C (2004) Vegetation height derivation from shuttle radar topography mission and national elevation data sets. *Rem Sens Environ* 93:339–358

- MARNR-ORSTOM (1986) Atlas del inventario de tierras del Territorio Federal Amazonas (Venezuela). Dirección de Cartografía Nacional, MARNR-ORSTOM, Caracas
- Potapov P, Li X, Hernandez-Serna A, Tyukavina A, Hansen MC, Kommareddy A, Pickens A, Turbanova S, Tang H, Silva CE, Armston J, Dubayah R, Blair JB, Hofton M (2020) Mapping and monitoring global forest canopy height through integration of GEDI and Landsat data. *Rem Sens Environ*. <https://doi.org/10.1016/j.rse.2020.112165>. Data download: <https://glad.umd.edu/dataset/gedi>
- Schargel R, Marvez P (2009) Suelos. In: Aymard GA, Schargel R (eds) Estudio de los suelos y la vegetación (estructura, composición florística y diversidad) en bosques macrotérmicos no-inundables, Estado Amazonas, Venezuela. *BioLlania edic esp* 9. UNELLEZ, Guanare, Venezuela, pp 99–125
- SEOM (Scientific Exploitation of Operational Missions) (2018) Sentinel Application Platform (SNAP software). European Space Agency (ESA)
- Soil Survey Staff (2014) Keys to soil taxonomy, 12th edn. USDA, Washington, DC
- Zanaga D, Van De Kerchove R, De Keersmaecker W, Souverijns N, Brockmann C, Quast R, Wevers J, Grosu A, Paccini A, Vergnaud S, Cartus O, Santoro M, Fritz S, Georgieva I, Lesiv M, Carter S, Herold M, Li L, Tsendbazar NE, Ramoino F, Arino O (2021) ESA WorldCover 10 m 2020 v100. <https://doi.org/10.5281/zenodo.5571936>
- Zinck JA (2011) Synthesis: The peatscape of the Guayana Highlands. In: Zinck JA, Huber O (eds) Peatlands of the Western Guayana Highlands, Venezuela. Properties and paleogeographic significance of peats. *Springer ecological studies* 217, Heidelberg, pp 247–259



# Soil Properties, Formation, Distribution, and Classification

# 7

J. A. Zinck and P. García Montero

## 7.1 Introduction

At regional level, the territory of the Venezuelan Amazonas State, formerly Territorio Federal Amazonas, is covered by a small-scale soil inventory that was performed in the framework of a joint project between the Venezuelan Ministry of Environment (MARNR) and the French agency of ORSTOM (now Institut de Recherche pour le Développement—IRD). Survey results were published in the “Atlas del Inventario de Tierras del Territorio Federal Amazonas (Venezuela)” at the scale of 1:250,000 (MARNR-ORSTOM 1986). Map units were delineated on radar image sheets and reported in an extended descriptive legend. Soils were classified at subgroup or great group levels according to Soil Taxonomy (Soil Survey Staff 1975). The information was organized per physiographic landscape units and relief types. Selected cross sections highlight the relationships between relief, soil, vegetation, and drainage conditions. A variety of soil classes was identified in the lowlands under different kinds of vegetation cover. As meadow areas are often small, they are under-represented in the soil cartography. Vegetation units identified as “sabana” and “matorral muy bajo” in the legend are the most likely to correlate with meadow and shrubby meadow, respectively. Soils reported in these kinds of vegetation cover include Quartzipsamments, Psammaquents, Aquepts, Tropaquods, Tropohemists, among others.

At local level, cross-sectional studies focusing on soil–vegetation relationships are reported for a few selected areas, particularly in San Carlos de Rio Negro and Solano, in the lower and middle stretches of Casiquiare river (Dubroeuq and

---

J. A. Zinck (✉)

Faculty of Geo-Information Science and Earth Observation (ITC), University of Twente, Enschede, The Netherlands

P. G. Montero

Private Activity, Soil Survey and Environmental Planning, Caracas, Venezuela

Sanchez 1981; Schargel et al. 2001; Schargel and Marvez 2009) and along a trail between Maroa and Yavita, in the watersheds of rivers Pimichin and Temi. Observations were made in hilly and flat areas. Spodosols, mainly Alaquods were identified in flat sandy areas under wooded cover (caatinga, bana, and rainforest) (Blancaneaux and Dubroeuq 1983; Schargel et al. 2000; Schargel and Marvez 2009). None of these studies reports data on soils under meadow cover. At site level, ecological studies of forest vegetation, especially caatinga, have been conducted in the area of San Carlos de Rio Negro focusing on nutrient cycling, water regime, forest recovery upon disturbance, among other subjects. Abundant publications are available on these subjects but unrelated with meadow vegetation and soils as reported in Chap. 2 of this book.

So far, ecosystem inventory and research in the Venezuelan lowlands drained by the Orinoco and Rio Negro watersheds have concentrated on forest ecosystems. In contrast, there is no previous information on the nature and properties of the soils associated with the lowland meadow biome. The meadow soil characterization that follows is mainly based on field observations with limited support of laboratory data.

---

## 7.2 General Soil Characteristics

### 7.2.1 Soil Taxa: Diversity, Similarity, Difference

#### 7.2.1.1 Sites and Soils Profiles

In total, 68 soil sites and profiles comprising 4–8 layers were described in meadow vegetation, spanning from open meadow to dense shrubby meadow (Table 7.1). Visited sites and described profiles (14) in ecotone areas between meadow and contiguous lowland formations such as grass savanna, bana scrub, caatinga forest, and palm forest (morichal) that occur also on white sands or other kinds of sandy materials, are not formally included in the following analysis but referred to for the sake of comparison. Information on sandy soils observed on higher landscape positions in uplands, hillands, and highland tepui mesetas at the periphery of the lowland basin is reported in Chap. 8 dealing with the origin and sources of sand. Thus, the selected profile population relates quite strictly to meadow vegetation *sensu lato* and does not account for pedodiversity in other lowland ecosystems.

#### 7.2.1.2 Pedotaxa Variety

Soil description and sampling were carried out in pits as described in Chap. 6. Description and classification of the original field data collected by the time of the inventory were updated using FAO guidelines (FAO 2006) and Soil Taxonomy (Soil Survey Staff 2014). Laboratory data were obtained using the following methods: pipette method for particle size distribution, pH in water 1:1, Walkley & Black for organic carbon, Bray–Kurtz for available phosphorus, and ammonium acetate and flame photometry for exchangeable potassium. Particle size classes in the legend of the bar diagrams refer to particle separates in mm: coarse fragments (>2), very coarse sand (2–1), coarse sand (1–0.5), medium sand (0.5–0.25), fine sand (0.25–0.125), very fine sand (0.125–0.05), total sand (2–0.05), silt (0.05–0.002),



**Table 7.1** Variety and abundance of soil classes under meadow cover per study areas (numbers refer to soil profiles as reported in Tables 6.2, 6.3, 6.4, 6.5, and 6.6 in Chap. 6 and tables describing soil classes in this chapter)

Soil classes	Sipapo	Camani	Ventuari	Yapacana	Atabapo	Pasimoni	Profiles total	%	%
<i>Quartzipsammens</i>									64.8
Udoxic Qps	4	32	7 8 9 12	6 14 16 58 61 62	23 85	108	15	22.1	
Typic Qps	3 98 99		13 29 30 31	15 18 19	26 65 66 67		14	20.6	
Oxyaquic Qps	21 90 91 92 93 97			81 128	25 64 86	105	12	17.6	
Lithic Qps				5	88		2	3.0	
Plinthic Qps			131				1	1.5	
<i>Typic Udorthents</i>				17 22 73 74 77 79 80	24 27 87		10	14.7	14.7
<i>Spodosols</i>									13.1
Typic Durorthods	20 83						2	2.9	
Arenic Alorthods						100 109	2	2.9	
Oxyaquic Alorthods					112	103	2	2.9	
Oxyaquic Haploorthods	82			63			2	2.9	
Typic Durihumods					84		1	1.5	
<i>Other soils</i>									7.4
Grossarenic Plinthic Kandiuults				56 57			2	2.9	
Hydric Haplohemists						107	1	1.5	
Psammaquents						106 110	2	3.0	
Total profiles	13	1	9	22	15	8	68	100	100

clay ( $<0.002$ ). Sediment and soil colors conform to Munsell Soil Color Charts (m = moist; d = dry) (Table 6.1).

Described soil profiles belong to 14 different taxa at subgroup level (Table 7.1). At first glance, this shows rather relevant taxonomic diversity, but in fact four subgroups alone encompass 75% of the taxa population, including Udoxic Quartzipsamments (22.1%), Typic Quartzipsamments (20.6%), Oxyaquic Quartzipsamments (17.6%), and Typic Udorthents (14.7%). All soils have isohyperthermic temperature regime but different moisture regimes.

Quartzipsamments are the most frequently found soil types in meadow conditions. The five different Quartzipsamment subgroups identified constitute 64.8% of the taxa population, while the five different Spodosol taxa identified constitute only 13.1% of the total. Quartzipsamments are in general white when dry in most of the layers. Some are grayish because of more organic matter production by grass mixed with meadow species and deeper root penetration, and some are pinkish in the proximity of sandstone outcrops and along the weathering rim at the foot of crystalline hills. When displaced by runoff, pinkish sands become white over short distance, a few tens of meters. Soils are generally moist the year around because it rains very frequently, except in the period of lower rainfall from January to March and by dry spells during the rainy season that cause surface layers to dry up for a few days or weeks. This is especially the case in Typic Quartzipsamments.

Typic and Udoxic Quartzipsamments are the most frequently identified soils, constituting together 42.7% of the total soil population. With 95% or more quartz sand, Typic Quartzipsamments represent the final residual stage of soil depletion, a mostly inert material without nutrient provision and with very low water holding capacity. Plants living on this kind of impoverished substrate must be very frugal organisms with survival strategy based on recycling scarce nutrients, possibly associated with specialized root morphology (cluster roots) and symbiotic associations, highly efficient in catching any chemical input from organic matter decomposition and rainfall (ecophysiological characteristics described in Chap. 12). Udoxic Quartzipsamments have small amounts of silt and clay (silt + 2× clay  $>5\%$ ), that distinguish them from Typic Quartzipsamments (Soil Survey Staff 2014). This might have a slight influence on improving water retention in the Udoxic subgroup.

Oxyaquic Quartzipsamments have groundwater within 100 cm from the soil surface. Soil layers above the groundwater level are not saturated, just moist. Thus, the Oxyaquic subgroup reflects best the general aquic condition in the lowest-lying meadow positions but without visible redoximorphic features, as white sands are practically iron-free.

Udorthents are grayish sandy soils that deviate from Quartzipsamments because of the presence of sandy loam or finer grained layers and/or coarse fragments within the control section.

Spodosols are also sandy soils, with more than 90% sand in most of the profiles. They are grayish in the surface layers, white in the subsurface layers, and dark-colored in the subsoil. Alorthods, Durorthods, and Haplorthods are the most frequent taxa.

### 7.2.1.3 Relevant Distinctive Characteristics of Soil Taxa

- **Typic Quartzipsamments:** are uncoated white sands, virtually free of silt and clay, well to somewhat excessively drained; lack water supply in the topsoil during the period of lower rainfall (January-March); seem to be mainly reworked and recently moved material; occur on river levees, overflow and splay flats forming the higher terrain units in the alluvial plains, and on glacis.
- **Oxyaquic Quartzipsamments:** are uncoated white sands, virtually free of silt and clay, always moist in the upper layers and saturated in the lower ones, imperfectly to poorly drained; occur in slightly concave depressions that lie behind river levees and in confluence areas where simultaneous flood events between joining streams cause water logging, storage, and stagnation.
- **Udoxic Quartzipsamments:** are light grayish over whitish sands, well to somewhat excessively drained; have slightly more silt and/or clay than Typic Quartzipsamments; occur in or close to areas where subaerial or subsurface rock weathering takes place on glacis or near rocky substratum, and have not been flushed out of fine particles.
- **Udorthents:** are light grayish over whitish sands, well drained, with silt and/or clay contents higher than those of Quartzipsamments, and often stony or gravelly substratum; are somewhat similar to Udoxic Quartzipsamments (taxonomically similar soils).
- **Spodosols:** are sandy soils with contrasted white over dark-colored layers, in low-lying landscape positions, poorly drained, often on older terrain areas or truncated remnants of older surfaces buried by more recent sand cover.

Figure 7.1 displays the average particle size distribution of selected soil profiles representing Typic Quartzipsamments (P66), Oxyaquic Quartzipsamments (P21), Udoxic Quartzipsamments (P23), and Typic Udorthents (P22). Average values were calculated on full profiles including three to five horizons/layers, respectively. Profiles P66, P21, and P22 show similar patterns of poorly sorted sand fraction, with up to four sand separates from very coarse to fine sand that reflect splay deposition. In contrast, P23 shows well sorted overflow sediment with dominance of fine and very fine sand (sedimentological interpretation of these profiles is given in Chap. 9). Typic and Oxyaquic Quartzipsamments are 98–99% sand with only traces of silt and clay. In contrast, the proportion of fines is significant in the Udoxic Quartzipsamment of P23 (20%) and the Typic Udorthents of P22 (34%), providing better water holding capacity and favoring denser vegetation cover. Organic carbon contents in the A horizon are significantly higher in the Udoxic Quartzipsamment and Typic Udorthents than in the Typic and Oxyaquic Quartzipsamments (Table 7.2). Soil reaction is strongly acid ( $\text{pH} < 5.5$ ) in all soils, and there are only traces of phosphorus and potassium (Table 7.3).

### 7.2.1.4 Quartzipsamments Versus Spodosols

The strong dominance of Quartzipsamments and low occurrence of Spodosols in meadow environment depart from earlier soil information gathered in the study region (MARNR-ORSTOM 1986; Schargel and Marvez 2009). Soils on white

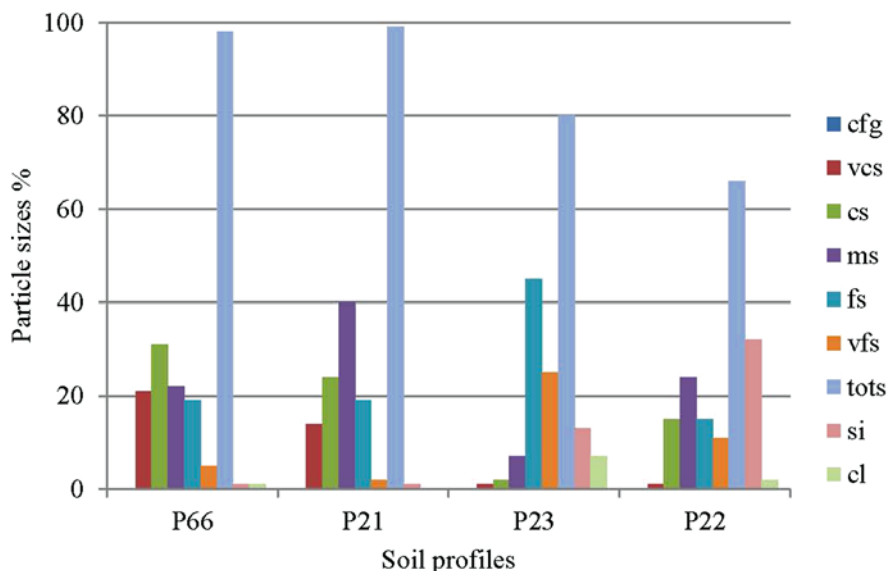


**Fig. 7.1** Average particle size distribution of soil profiles representing Typic Quartzsammments (P66), Oxyaquic Quartzsammments (P21), Udoxic Quartzsammments (P23), and Typic Udorthents (P22)

**Table 7.2** Selected characteristics of representative soil profiles

Profile	Soil class	Vegetation type	Cover density %	Rooting depth cm	A horizon thickness cm	A horizon org. carbon %
P66	Typic Quartzsammment	Shrubby meadow	20–30	33	7	0.45
P21	Oxyaquic Quartzsammment	Meadow	20–25	50	20	0.13
P23	Udoxic Quartzsammment	Meadow	50–60	50	10	2.11
P22	Typic Udorthent	Savanna-meadow	60–70	40	10	2.26

sands reported so far have been described mainly in rainforest, caatinga forest, and bana scrub environments, and very seldom in meadow conditions. Under meadow cover, Spodosols are infrequent because herb-forb-shrub vegetation produces little organic matter and rooting is often shallow. In general, roots do not penetrate deeper than 40–50 cm from the soil surface, making plants vulnerable to dry spells. Thus, current podzolization in meadows is limited, although spodic horizons were found within 2 m from the soil surface and may possibly occur also below that depth (e.g., in giant podzols). At some deep observation sites (150–160 cm), no traces of organic matter and/or iron concentration/cementation were detected, and no redoximorphic features were observed except yellowish brown mottles along roots in some profiles.

**Table 7.3** Averaged values of selected properties in A horizons and C layers of main soil classes

Soil classes	A horizon cm	Rooting depth cm		Organic carbon %	pH 1:1 water	P ppm	K ppm
Typic Quartzipsamments (14)	18 (7–30)	40 (15–70)	A	0.29 (0.12–0.54)	5.2 (3.9–5.8)	0–1	1–3
			C	0.16 (0.03–0.34)	5.6 (5.3–6.1)	0–1	0–2
Oxyaquic Quartzipsamments (12)	12 (7–20)	33 (12–50)	A	0.41 (0.13–0.68)	4.6 (3.5–5.8)	0–1	1–8
			C	0.14 (0.03–0.32)	5.2 (4.2–6.5)	0–1	0–3
Udoxic Quartzipsamments (15)	19 (4–50)	42 (13–80)	A	0.59 (0.05–1.73)	5.2 (4.6–5.9)	0–4	0–7
			C	0.22 (0.03–0.54)	5.5 (4.8–6.1)	0–1	0–3
Typic Udorthents (10)	18 (6–40)	37 (13–64)	A	0.85 (0.31–2.64)	5.2 (4.4–5.9)	0–2	0–6
			C	0.19 (0.09–0.37)	5.8 (5.0–6.2)	0–1	0–3
Spodosols (9)	18 (7–30)	42 (28–54)	A	0.73 (0.15–2.77)	5.1 (4.6–5.9)	0	1–15
			C	0.14 (0.04–0.47)	5.4 (4.4–6.4)	0	0–1

(14) = number of profiles; C in Spodosols refers to the sand layers covering truncated spodic horizons

The infrequency of spodic horizons and Spodosols in meadow areas can be related to the following conditions:

- Meadow vegetation occupies mainly new depositional areas, exposed to frequent sediment reworking. Some sandy materials partly result from the erosion/degradation of caatinga or bana areas. Thus, meadow substrate is mainly white sand depleted of oxides and organic matter, except in the surroundings of crystalline hills and close to pinkish sandstone outcrops. Materials resulting from rock weathering are fully bleached over short colluviation distance. Thus, in newly weathered material that is incorporated in the depositional system, iron and organic matter are stripped out at the source. However locally, Quartzipsamments intergrading with Spodosols were observed (Aquodic subgroup).
- Meadow vegetation has usually low cover density, and even when dense, there is little production of organic matter (see Table 6.9 in Chap. 6). It can be assumed that the specialized plants living in meadow environment, in particular endemic species have developed mechanisms to avoid loss of nutrients and are able to recycle them, in addition to some nutrients captured from rainfall. Thus, there is little leaching of organic matter to feed spodic horizons. Podzolization develops in other conditions, those of caatinga and bana.

Spodic horizons may occur below usual observation depths, for instance below 1.5–2 m. Therefore, some soils classified as Quartzipsamments could actually belong to the class of Spodosols. Shallow field observations may not have allowed reaching the spodic horizon within 2 m depth and may not provide full information for taxonomic classification of the soils, but are sufficient to describe the relationship between soil condition and meadow vegetation life. In situations of deep spodic horizons, the behavior of the upper sandy soil in terms of water holding capacity, depth to groundwater, nutrient availability, and nutrient recycling mechanisms would not be very different from that of a Quartzipsamment in relation to the requirements of the usually short-rooted meadow plants.

The classification and formation of Spodosols in meadow environment are addressed in Sect. 7.3.5, and the relationship between Spodosols and landscape evolution is further developed in Chap. 10.

### 7.2.1.5 Spatial Variability

Although field observation points were distributed as even as possible over the study areas, access by helicopter was in fact determinant for site location. Thus, the possibility to extrapolate point data for cartographic purpose is limited. For the same reason it cannot be concluded that soil taxa identified only occasionally are definitively of low occurrence.

There is no strong trend of spatial soil distribution to differentiate among the six study areas. However, on basis of the relative importance of Typic, Oxyaquic, and Udoxic Quartzipsamments, together with the Udorthents (Table 7.1), there is some pedotaxonomic affinity between the Yapacana and Atabapo areas that happen to have large proportions of endemic species (see Chap. 11). The Ventuari area shares

some features with the former two areas. Imperfectly drained Oxyaquic Quartzipsamments dominate in the Sipapo area, while Spodosols are more frequent in the Pasimoni area.

In terms of geographic distribution, Oxyaquic Quartzipsamments, although not the most frequently identified soils, are presumably the most extensive soils in meadow covered areas, especially in open meadow on alluvial flats. They best reflect the quartzose white-sand environment in most of the plain lowlands, being humus and iron poor, nutrient depleted, with low silt and clay contents (sometimes no clay at all, completely washed away), saturated most of the year in parts of 1 m depth, and with fluctuating groundwater.

## 7.2.2 Soil Moisture and Drainage

### 7.2.2.1 Moisture Regime

Annual rainfall varies from 3500 to 3600 mm in the south to 2500–3000 mm in the north (see Fig. 5.2, Chap. 5). Monthly rainfall is in general higher than 150 mm. About 60% of the annual rainfall takes place between May and September. The soil moisture regime is udic in the northern part of the study region (Sipapo, Camani, and Ventuari areas), and perudic in the southern part (Yapacana, Atabapo, and Pasimoni areas), except for poorly drained soils that have aquic regime. In general, water holding capacity is low to very low. The isohyperthermic temperature regime causes abundant soil water loss through evapotranspiration in the whole study region.

Most field observations, including data on soil moisture regime and groundwater level, were recorded in February–March when monthly rainfall is somewhat lower than during the rest of the year. A few observations were made in July corresponding to the peak of the rainy season. During the short period of lower rainfall (January–March), mean rainfall remains usually above 150 mm/month (Franco and Dezzio 1994). However, repeated dry spells commonly occur for a few consecutive days that affect meadow herbs and forbs much more than caatinga trees. Thus, our observations may not fully account for the soil moisture condition prevailing during the high rainy season. Saturated layers and free groundwater within 100 cm from the soil surface were observed at sites visited in the middle of the rainy season (July). In the period of February–March, aquic condition was observed in saturated deep subsoil layers, below 100 cm depth, by free water forming in boring holes without redoximorphic features, but this was much less frequent in subsurface tiers. In low-lying alluvial flats, groundwater levels can be higher than the observed ones, showing important seasonal fluctuations. Therefore, some soils classified as Typic Quartzipsamments may be in fact Oxyaquic Quartzipsamments. In higher positions, such as for instance peneplain glacis, no groundwater was observed.

There are no published data on the soil water regime in meadow environment but well on that of the sclerophyllous woody caatinga-bana ecosystems with which the meadow areas are spatially associated. Medina and Cuevas (2011), for instance, report from sites of San Carlos and La Esmeralda that tall caatinga is exposed to flooding, while low caatinga has high groundwater level that drops rapidly in dry



days. Franco and Dezzeo (1994) monitored the soil water regime in a terra-firme and caatinga forest complex along an undulating toposequence near San Carlos de Rio Negro. In that area, the mean annual rainfall is 3500 mm and the mean monthly rainfall is higher than 150 mm in all months. The studied sequence includes segments of caatinga and tall bana on sandy valley fill. The caatinga soil (Histic arenic Tropaquod) has a relatively stable water regime over the year, although water can change from total saturation to very low content upon a few dry days. During the wettest months, the soil is permanently saturated at 75 cm depth and frequently saturated (76%) at 20 cm. In the bana soil (Histic arenic Placaquod), total saturation over the year reaches a frequency of 85% at 75 cm and 31% at 20 cm depth. The groundwater level fluctuates frequently and fast between 20 and 75 cm, and occasionally drops below 1 m depth. The upper 20 cm of the sandy soils are unsaturated most of the year under both caatinga and bana vegetation.

In view of the former data, water saturation probability in meadow environment can be assumed to be lower than that of the bana at similar depths and groundwater fluctuations larger and more frequent, especially north of river Orinoco. In meadow with low vegetation cover density, only part of the incoming rainfall penetrates into the sandy topsoil of Quartzipsamments, while a relevant proportion runs on the terrain surface causing the formation of an intricate pattern of rills, especially in the glacis landscape. In alluvial plains, splay and overflow positions are often flooded after heavy rainfalls but water does not stagnate long on the terrain surface as it is resorbed soon by evaporation, runoff, and infiltration. In general, the infiltration front does not penetrate deep into the sand as it is counteracted by high evaporation. Groundwater in most Quartzipsamments stays below 1 m depth during most of the year. Short dry spells during the high rainfall period are detrimental to meadow plants.

Transect studies in the Maroa-Yavita area, north of San Carlos de Rio Negro, report the predominance of poorly drained Aquods under caatinga vegetation in flat sandy plains with slope  $<2\%$  (Schargel et al. 2000, 2001; Schargel and Marvez 2009). Aquods are saturated with water up to the soil surface during a large part of the year. Observations were seemingly done during a period with relatively lower rainfall. We visited meadow sites of the same area in the lower watersheds of rivers Pimichín and Temi (Atabapo study area) in February–March corresponding to the yearly period of lower rainfall ( $>100$  mm/month). Usually, meadow terrains are slightly lower than contiguous caatinga terrains ( $<1$  m elevation difference in ecotone areas). Dominant soils are Oxyaquic Quartzipsamments with groundwater level not higher than 75 cm from the soil surface in February–March. In similar soils and geomorphic positions in the Sipapo area, the groundwater level rises to 10–15 cm in July–August, during the peak of the rainy season. Thus, groundwater in meadow Oxyaquic Quartzipsamments fluctuates substantially over the year, presumably more than in caatinga Aquods. Meadow soils react fast and deep at diminishing rainfall in the January–March period, while caatinga soils maintain a more stable water regime, a feature also noted by Franco and Dezzeo (1994).

In general, water availability in white-sand meadow soils depends heavily on continuous rainfall as water holding capacity is low to very low and

evapotranspiration is very high. Many soils are moist the year around but not saturated, and susceptible to dry up in the surface layer between rainfall events. This is the case in particular of udic regime soils such as Udoxic Quartzipsamments and Udorthents. Oxyaquic Quartzipsamments and sandy Spodosols benefit additionally from groundwater supply. The most limiting water availability condition is found in Typic Quartzipsamments that can be dry down to 50–60 cm depth in February–March. Other soils that have sandy textures in surface and subsurface layers such as the various Spodosol classes and Grossarenic Ultisol subgroups have similar water regime restrictions as those of Quartzipsamments. Shallow soils such as Lithic Quartzipsamments can dry up after a few dry days and be moistened again by one rainfall, submitting herbs and forbs to extreme stress conditions. In general, the surface water regime has a strong impact on meadow vegetation. Plants must be well adapted to survive water shortages during dry spells. This might contribute to explain high species endemism and low biodiversity in meadow environment, while large groundwater fluctuations may prevent woody plants to establish.

#### **7.2.2.2 Surface Drainage Features**

Meadow is more a physical than a biological environment. There is no dense vegetation cover to intercept rainfall and retard water flow to the soil surface. There is no root mat to absorb water and retard infiltration. Rainfall hits directly the soil surface in bare sand patches. During part of the year, the groundwater level is low, except in confined areas with restricted drainage, and does not impede percolation to deeper layers. During the peak of the rainy season, when heavy rainfalls take place, the topsoil, although very permeable, cannot absorb fast enough the incoming rainwater and may be temporarily flooded. Then surface runoff develops and causes the formation of reticular networks of shallow, flat-bottom rills and channels. This pattern of microtopography is common in glacial positions, where sloping terrain favors rainwater runoff to the detriment of infiltration, regardless of soil type. Udoxic Quartzipsamments constitute the individual soil class most affected by reticular microrelief (in 10 of 15 visited sites). Reticular drainage features develop also in Oxyaquic Quartzipsamments when high groundwater restricts rainwater infiltration. Closed channels and pans form in flooded alluvial plain flats, caused by suffusion entraining silt and very fine sand to subsurface layers. Channel incision is frequent in coating-meadow ecotone areas (in 8 of 14 visited sites). The frequency of runoff microrelief in permeable sandy soils shows that a large part of rain water moves fast on the terrain surface before penetrating into the soil. Internal soil drainage is controlled by the water level in the small streams that cross the meadow landscape. When this level drops in the period of January–March, excess water moves laterally through the soil mantle to the streams.

### 7.2.3 Biological Characteristics, Chemical Elements, and Nutrient Status

Table 7.3 shows averaged values of A horizon thickness, rooting depth, soil reaction, and contents of organic carbon, phosphorus, and potassium for the dominant soil classes of the meadow biome, including Typic, Oxyaquic, and Udoxic Quartzipsamments, Typic Udorthents, and a variety of Spodosols; in total, 60 profiles representing 88% of the soil population reported in Table 7.1. Data of the A horizon thickness and rooting depth are averages of the profiles belonging to each soil class. Data of organic carbon, pH, phosphorus, and potassium were averaged per A horizons and C layers separately, first for each profile and subsequently for all profiles belonging to a given soil class.

#### 7.2.3.1 Variations in Organic Matter

Averages of the A horizon thickness (18–19 cm) and rooting depth (33–42 cm) are remarkably constant among the various soil classes. Oxyaquic Quartzipsamments depart from this general picture as the A horizon is shallower (12 cm) and root penetration is more surficial (33 cm) (Table 7.3). Water saturation close to the soil surface may restrict root deepening and cause biological activity to concentrate in the surface layer. Data on rooting depth reported here refer to meadow herbs and forbs. Shrubs penetrate as deep as 90–100 cm. A particular feature of meadow plants is that they stand directly in the sand substrate, in contrast with the woody white-sand ecosystems (e.g., caatinga) that develop root mats allowing for efficient nutrient recycling.

In general, organic carbon (OC) contents are low to very low (0.29–0.85% = 0.5–1.5% organic matter). Locally, values of 2–3% OC can be found in dense shrubby meadow. There is a trend of OC content increase from Typic Quartzipsamments (0.29%) to Typic Udorthents (0.85%). Variations of organic carbon content in the A horizon seem to be primarily related with soil water holding capacity that allows vegetation to counteract water stress during consecutive dry days in the lower rainfall period (January–March). Open meadow is exposed to high physical evaporation in bare sand patches around plant clusters and bushes. Plants in soils having some proportion of fines (silt + clay) resist better dry spells than those living on pure sand. Udoxic Quartzipsamments and Typic Udorthents have commonly 10–20% fines, mainly silt, and are thus provided with better water holding capacity than Typic and Oxyaquic Quartzipsamments that have usually more than 95% sand. As a consequence, vegetation cover density and organic matter accumulation are higher in the former soil taxa than in the latter (Table 7.2). Typic Udorthents show the best performance, while Typic Quartzipsamments have an organic carbon content in the A horizon that is only slightly higher than that of pure C layers. Values of organic carbon in white-sand C layers are very low and comparable in all soil classes (0.14–0.22%) (Table 7.3).

Many soils have a thin cover layer of loose coarse sand lying atop the soil in situ (Table 7.4). Cover layers are in general less than 2 cm thick, but can be as thick as 5 cm. Color is often pinkish reflecting the influx of fresh colluvial material by rainfall

**Table 7.4** Nutrient availability in loose transferal sand cover layers and underlying A horizon

Soil class	Profile	Sandy cover layer		A horizon	
		OC %	K ppm	OC %	K ppm
Typic Quartzipsamments (ca 1 cm layer)	65	0.45	2	2.22	2
	98	0.49	3	0.21	0
	99	0.24	1	0.31	3
Oxyaquic Quartzipsamments (2–3 cm layer)	90	0.58	10	0.46	2
	91	2.49	11	0.56	1
	92	0.39	4	0.18	1
	97	1.31	12	0.53	8
	128	0.67	11	0.38	4

runoff. The material dries up quickly after each rainfall but is often covered by black alga films that form upon runoff flooding. Cover layers contain frequently carbon fragments resulting from fire and have more organic matter and available potassium than the underlying A horizon. They are more frequent in Oxyaquic Quartzipsamments because these soils occupy slightly lower landscape positions than the other Quartzipsamments and are more likely to receive rainfall overflow that moves loose sand. The difference in organic carbon content between sandy cover layer and A horizon can be substantial. There is even a difference in potassium content, although values are overall very low. Loose transferal sand layers are unstable and exposed to be reworked at each strong rainfall event by runoff or blown away by wind when the soil surface is dry (Table 7.4). Thus, organic matter produced in one place may be moved to another one, impeding decomposition in situ, incorporation in the A horizon, and availability to plants. The fate of this organic matter is to be carried into streams and rivers. This may result in net loss of organic matter on the soil surface.

At sites where vegetation has been recently exposed to fire, burned organic matter has been mixed with the sandy matrix, originating higher organic carbon contents than those of the surrounding soil surface. For instance in the Atabapo area where fires are frequent, organic carbon at a burned site is 2.22% (P65, 0–8 cm), while it is only 0.45% at a neighboring unburned site (P66, 0–7 cm). At another burned place, organic carbon in the surface layer is as high as 5.1% (P64, 0–7 cm).

For the purpose of comparison, the percentages of organic carbon were transformed into  $\text{kg m}^{-2}$  in the 0–25 cm topsoil, in the last column of Table 7.5. Bulk density values of 1.5, 1.4, and  $1.3 \text{ Mg m}^{-3}$  were assumed for sand, loamy sand, and sandy loam textures, respectively. In some profiles, the topsoil includes the upper part of the underlying C layer in addition to the shallow ochric epipedon. Representative profiles of the five main sandy soil classes were selected in the landscapes of alluvial plain and peneplain (Table 7.5). Overall organic carbon content is low to very low and varies in the range of 0.45–2.44  $\text{kg m}^{-2}$ . There are slight differences according to soil class, landscape position, and cover type. Quartzipsamments, for instance, have a narrow organic carbon range of 0.5–1  $\text{kg m}^{-2}$ . Two-thirds of the values are below 1  $\text{kg m}^{-2}$  irrespective of the soil

**Table 7.5** Content of organic carbon and organic matter in kg m<sup>-2</sup> per 0–25 cm topsoil

Soil class	Profile	Geoform	Cover type	OC	OM
Typic Quartzipsamments	98	Penepain glaxis	Open scrub	0.79	1.36
	29	Penepain glaxis	Shrubby meadow	0.56	0.97
	31	Penepain glaxis	Meadow	0.49	0.84
	18	Alluvial plain flat	Shrubby meadow	0.98	1.69
	19	Alluvial plain flat	Shrubby meadow	0.75	1.29
	66	Alluvial plain flat	Shrubby meadow	0.90	1.55
Oxyaquic Quartzipsamments	90	Overflow plain	Meadow	1.10	1.90
	91	Overflow plain	Dense scrub	1.67	2.88
	81	Alluvial plain flat	Shrubby meadow	0.97	1.67
	128	Alluvial plain flat	Shrubby meadow	0.61	1.05
	25	Floodplain	Shrubby meadow	0.45	0.78
Udoxic Quartzipsamments	8	Penepain glaxis	Meadow-savanna	0.75	1.29
	9	Penepain glaxis	Meadow-savanna	0.68	1.17
	58	Alluvial plain flat	Shrubby meadow	0.84	1.45
	61	Alluvial plain flat	Shrubby meadow	1.69	2.91
	62	Alluvial plain flat	Meadow	0.90	1.55
Typic Udorthents	17	Alluvial plain flat	Shrubby meadow	1.46	2.52
	73	Piedmont fan-glaxis	Shrubby meadow	2.03	3.50
	74	Piedmont fan-glaxis	Scrub	0.87	1.50
	24	Penepain glaxis	Meadow	0.87	1.50
	87	Penepain glaxis	Shrubby meadow	0.82	1.41
Spodosols	82	Alluvial plain flat	Shrubby meadow	1.13	1.95
	83	Alluvial plain flat	Shrubby meadow	2.03	3.50
	63	Alluvial plain flat	Shrubby meadow	1.03	1.78
	112	Alluvial plain flat	Shrubby meadow	0.48	0.83
	100	River terrace	Shrubby meadow	2.44	4.21

classes. Poorly drained soils as in the case of some Spodosols tend to have higher values. Alluvial plain soils have more organic carbon in the topsoil than penepain soils. The effect of variation in vegetation on the abundance of organic carbon production is difficult to assess because shrubby meadow is the dominant cover type. The sequence of open scrub to shrubby meadow to meadow corresponding to profiles P98-P29-P31 delivers a decreasing range of values from 0.79 to 0.56 to 0.49 kg m<sup>-2</sup>. Similarly, there is no straightforward relationship between cover density and richness of organic carbon. Shrubby meadow at P25 with 10–15% cover provides 0.45 kg m<sup>-2</sup>, while pure meadow at P24 with 10–20% cover generates 0.87 kg m<sup>-2</sup> (Table 7.5). Obviously more samples would be needed to establish a more conclusive relationship.

Working in the upper Rio Negro and Casiquiare watersheds, Schargel and Marvez (2009) have evaluated the organic matter content in poorly drained Spodosols under forest cover. They obtained figures as high as 18–20 kg m<sup>-2</sup> in the 0–25 cm top horizon. The highest values obtained in Spodosols under shrubby meadow in our study area are 3.5–4.2 kg m<sup>-2</sup>.

### 7.2.3.2 Variations in Chemical Soil Composition and Nutrients

Soil reaction is in general strongly acid in the A horizon with pH less than 5.5 in all soil classes (Table 7.3). Values of pH are steadily half a unit higher in C layers than in A horizons. Organic matter produced by meadow herbs and forbs possibly increases acidity in the A horizon. In spodic horizons, pH is usually one to two units lower than in the overlying C layers or E horizons. Phosphorus and potassium availability is very low, in many cases not detectable or only at the level of traces (Table 7.3). Values of electrical conductivity are insignificant, on average 0.02–0.05 ds m<sup>-1</sup>.

In Table 7.6, selected chemical elements (cations) of three Quartzipsamments are reported. Soils are different in color, geomorphic landscape position, and type of vegetation cover:

- P8 is a pinkish gray Udoxic Quartzipsamment on penepain glacis under mixed vegetation cover including meadow and savanna species (e.g., within the genera *Xyris*, *Schoenocephalum*, and *Mesosetum*). The color reflects the origin of the sediment from pinkish Roraima sandstones of Cerro Moriche. Material is 90% sand, mainly fine and very fine sand, and 10% silt. Organic carbon content is 0.42% in the A horizon (0–8 cm) and 0.15% in the underlying C layers. Root penetration is limited to the upper 23 cm. Profile P8 represents a typical colluvial glacis sediment in penepain landscape.
- P18 is a white Typic Quartzipsamment on alluvial plain flat under shrubby meadow vegetation (e.g., *Terminalia yapacana*, *Xyris* sp.). Material is 99–100% sand with unsorted particle size distribution, including coarse, fine, and very fine sand. Organic carbon content is 0.38% in the A horizon (0–15 cm) and 0.11% in the underlying C layers. Herb and forb roots concentrate in the upper 15 cm. Profile P18 represents a typical washed out alluvial splay sediment.

**Table 7.6** Chemical elements in three color-differentiated Quartzipsamments

Site	Profile	Geomorphic position	Vegetation	Soil class	Depth cm	Na	K	Ca	Mg	Mn	Al
Cerro Moriche	P8 pinkish gray	Peneplain glaxis	Meadow-savanna	Udoxic Quartzipsamment	0-8	1.77	9.72	10.59	1.98	0.45	5.40
					8-23	0.54	1.68	3.93	0.72	0.36	0.91
					23-50	0.57	1.08	2.79	0.54	0.39	0.31
Perro de Agua	P18 white	Alluvial plain flat	Shrubby meadow	Typic Quartzipsamment	0-15	3.00	3.33	0.84	0.96	0.36	0.06
					15-40	0.51	0.81	0.45	0.42	0.39	0
					40-70	1.02	0.75	0.96	0.36	0.36	0
Yutajé	P36 grayish	Piedmont glaxis	Shrubby savanna	Udoxic Quartzipsamment	0-20	0.63	7.86	6.51	1.95	2.16	16.20
					20-50	0.54	3.90	1.32	0.90	0.51	21.79
					50-70	0.75	2.04	1.95	0.63	0.42	8.40

Values determined using 1N NH<sub>4</sub>Cl and expressed in ppm (mg kg<sup>-1</sup>); unpublished data; courtesy of H. Fölster, University of Göttingen, Germany



- P36 is a grayish Udoxic Quartzipsamment on piedmont glacis under shrubby savanna. Grass species from genera such as *Andropogon*, *Axonopus*, and *Trachypogon* are mixed with Al-tolerant short savanna trees such as *Curatella americana* and *Byrsonima* sp., a vegetation cover somewhat similar to the cerrado biome in Brazil. Material is 90% sand, 7% silt, and 3% clay. Organic carbon content is 0.49% in the A horizon (0–20 cm) and 0.18% in the underlying C layers. The dense fibrous roots of the savanna grasses penetrate to 60 cm depth, promoting the grayish soil color. Profile P36 is not a lowland meadow soil but is provided here for the sake of comparison between alluvial flat, glacis, and piedmont soils.

Concentrations of the selected elements are very low, a few milligrams per kilogram soil. Grass species at sites P8 and P36 concentrate some potassium and calcium in the A horizon, while P18 is thoroughly impoverished. Element values in the subsurface C layers are very low among the three sites. At site P36 aluminum is significantly higher than elsewhere, possibly related with the presence of Al accumulating savanna species, similarly to cerrado species in Brazil (Haridasan 2008) (Table 7.6).

Aluminum was also found to accumulate in meadow shrubs growing on Spodosols that have Al-humus complexes in the spodic horizon (Aymard et al. 2014). Soil at P18 is overwhelmingly depleted in all elements. P8 and P18 can be considered as paradigm of the nutrient-poor, quartzose sandy meadow soils, representing, respectively, the two main landscape types of the lowlands, i.e. alluvial plain flats and peneplain glacis. With their extreme levels of nutrient deficiency and bleached sandy textures, they typify appropriately the soil environment of the meadow psammic peinobiome.

Referring to the coarse-grained, nutrient-poor herbaceous Amazon biome, Walter (1985) considers that it is remarkable that so many species grow on such impoverished sandy soils. Similarly, Huber (1988, 2006) and Huber and Zinck (2000) point out that severe nutrient stress, together with alternating hydrological conditions causes strong limitations to the implantation and growth of vegetation (more details in Chap. 12).

#### **7.2.4 A Special Feature: The Occurrence of Densic Layers (Densipan)**

Compact sandy layers were found at 15 visited places, in soils under meadow and also in bordering caatinga forest. Ten out of 68 meadow profiles (15%), four caatinga profiles, and one palm swale profile show such layers. Ten of the 15 profiles occur in the Yapacana area, two in Ventuari, two in Pasimoni, and one in Atabapo. The concentration of two-thirds of the compact layer profiles in the Yapacana area calls the attention. Densic layers occur mainly in alluvial flats, seldom in glacis.

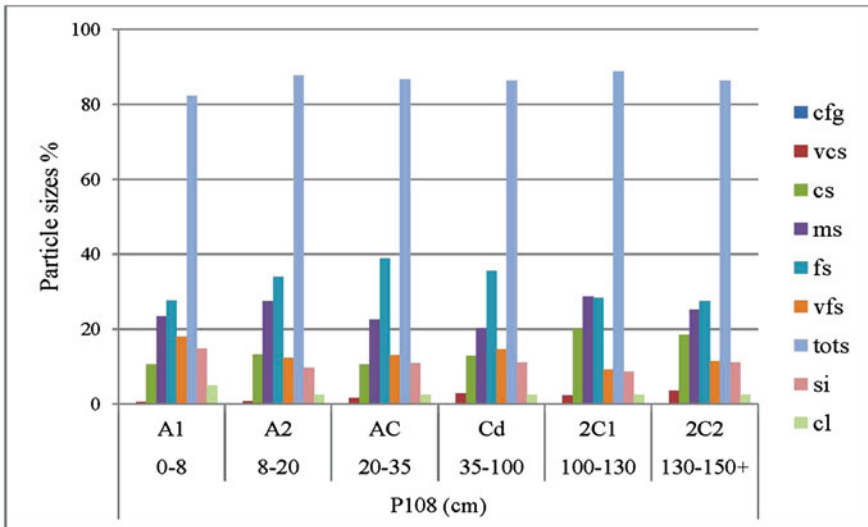
### 7.2.4.1 Characteristics and Properties

The occurrence of a compact layer is a contrasting feature in profiles that causes lithological discontinuity with the overlying and underlying looser layers. The compact layer is non-cemented white sandy material that is difficult to penetrate with spade or auger, but can be cut into blocks with a knife (Fig. 7.2). Colors are whitish with slight variations from very pale brown (10YR7.5/3 moist, 10YR8/1.5 dry) to pinkish gray (5YR7/2 moist, 5YR8/1 dry) to white (10YR8/1 m, 7.5YR8/1 d). Dominant textures are sandy loam and loamy sand. Profiles with compact layers have comparatively higher silt contents together with fine and very fine sand than the usual white-sand alluvial sediments. Silt content varies from 4 to 31%, with an average of 16%, disregarding two outliers, one with no silt (Grossarenic Kandiudult) and the other with 62% (eolian silt sheet). The material has soft, powdery touch, and gives the feeling of talc. It is usually moist the year around, unless when occurring close to the soil surface. Saturation water is milky and stains the fingers white. Compact layers often sustain a perched water table. Hereafter, it is referred to this kind of compact layer as densipan (from *densus* meaning closely compacted in substance).

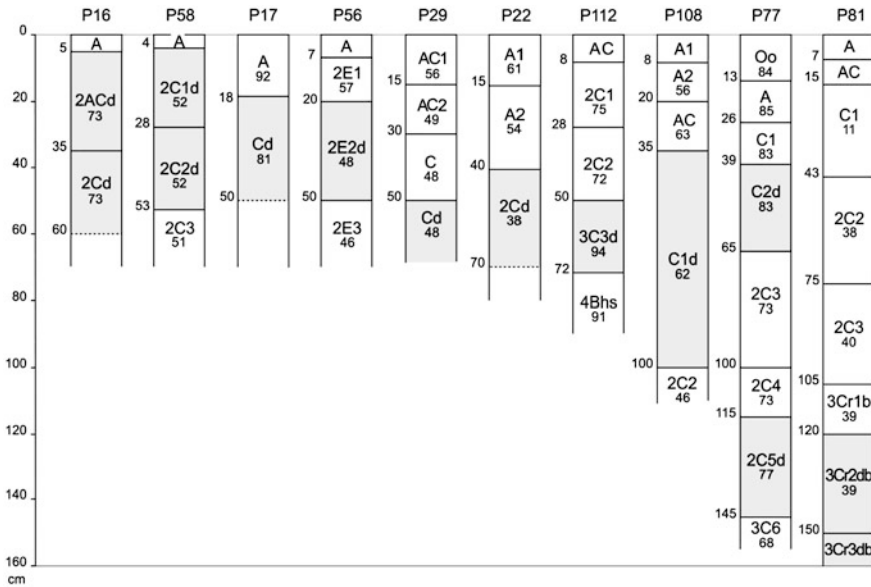
Compactness is such that only few fine roots enter the layer. This is particularly limiting when the densipan occurs close to the terrain surface (in a few cases at 4–5 cm, in others at 18–20 cm). Rooting depth is then very limited and vegetation suffers water stress during the lower rainfall period (January–March) and by dry spells in the rainy season. In these situations, meadow cover density is very low (e.g., 10–20%). Although resistant to mechanical penetration, the material is structureless and friable in the prevailing moist natural condition. Air-dry fragments are slightly hard to hard but slake easily, almost instantaneously when submerged in water. Bulk density tests performed on a set of samples of variable sizes provided data ranging from  $1.65 \text{ Mg m}^{-3}$  to  $1.75 \text{ Mg m}^{-3}$ . One determination provided an extreme value of  $1.86 \text{ Mg m}^{-3}$ . An average value of  $1.7 \text{ Mg m}^{-3}$  would be a fair approximation to densipan bulk density of the loamy sand and sandy loam samples analyzed. Such high bulk density values in sandy materials are usually recognized as causing hindrance to root penetration.

Low porosity restrains water percolation and retards water evacuation through internal drainage. Rain water tends to remain longer on the soil surface and even stagnate. Flood water is resorbed via incision of reticular surface drainage channels.

The depth to the top of the densipan layer is very variable in meadow environment: it can be as shallow as 4 cm from the soil surface or as deep as 120 cm (Fig. 7.3). Disregarding three outliers (P16, P58, at less than 5 cm depth), and P81 (at 120 cm depth), starting depth of seven layers varies between 18 and 50 cm, with an average of 36 cm. This could correspond to the top of the groundwater level during the high rainfall season. Densipan thickness is 26–65 cm, with an average of 37 cm for ten profiles. This could correlate with the fluctuation margin of the groundwater during the rainy season. Under caatinga, the densipan layer underlies directly the root mat of the O horizon at depths variable between 25 and 45 cm as in profiles P101 and P130 (Fig. 7.4). Under channels incised in the caatinga terrain,

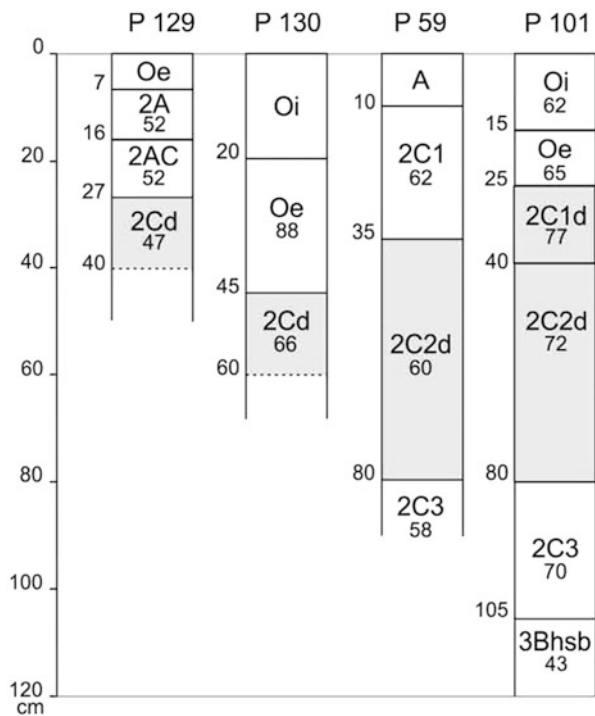


**Fig. 7.2** Thick densipan layer (35–100 cm) and sample from an Udoxic Quartzipsamment (P108) on a river terrace in the lower Pasimoni valley; dry densipan can be cut into blocks that slake easily, almost instantaneously when submerged in water; talcose aspect of the block surface



**Fig. 7.3** Soil profiles with densipan layers in meadow environment; numbers below the horizon designations correspond to the sum of fine sand, very fine sand, and silt % Explain the meaning of the letters

**Fig. 7.4** Soil profiles with densipan layers in caatinga environment; numbers below the horizon designations correspond to the sum of fine sand, very fine sand, and silt %



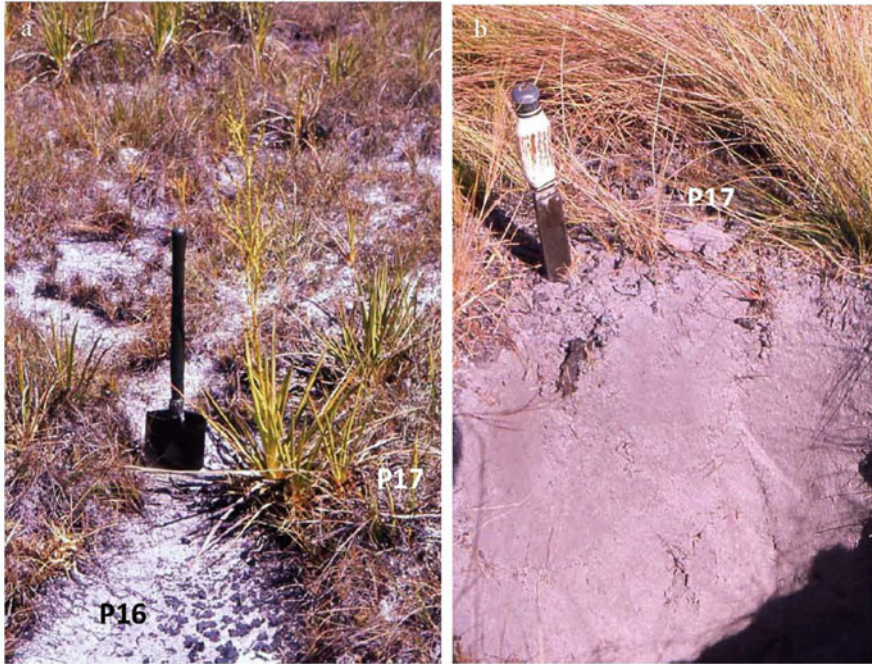
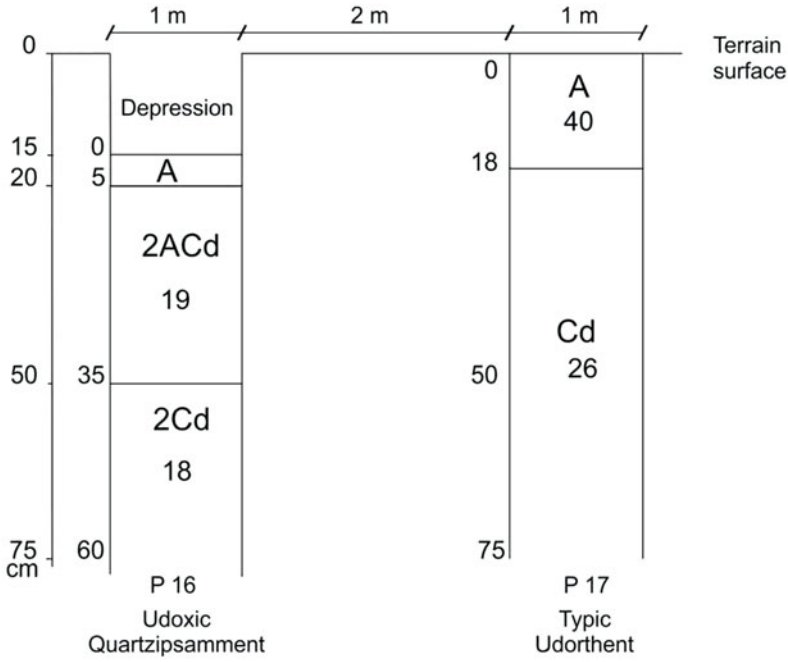


**Fig. 7.5** Adjacent soil profiles with densipan layers under shrubby meadow; (a) P16 at the bottom of a suffusion depression; enlargement and narrowing of suffusion depressions; closed pan to the center left; (b) P17 on the terrain surface; the darker surface horizon of P17 (0.56% OC) is missing at P16; numbers below the horizon designations correspond to the sum of fine sand, very fine sand, and silt %

densipan layers occur beneath mineral layers (e.g., P59, P129). Densipan layers in Spodosols, if any, overlie the spodic horizons (e.g., P101, P112).

Generalization from individual profiles may be of limited scope; however when the densipan is interpreted in the context of the profile on the landscape it can contribute to understand spatial and vertical variations. A few examples are reported hereafter:

- Profiles P16 and P17 are 2 m distant from each other, the former at the bottom of a suffusion depression and the latter on the terrain surface in meadow environment (Fig. 7.5). The difference of depth to the top of the densipan layer (5 cm and 18 cm, respectively) corresponds to the depth of the depression (about 13 cm). This is also the case of the two adjacent profiles P129 and P130, the former at the bottom of a drainage channel and the latter on the terrain surface under caatinga, with depth to the top of the densipan layer of 27 cm and 45 cm, respectively (Fig. 7.4).
- Profile P58 has possibly been truncated by lateral stream migration, causing the densipan to appear at shallow depth from the soil surface. In contrast, at site P81 new sediment accumulation has taken place, burying the densipan at deeper depth (Fig. 7.3).
- Profile P77 has two densipan layers separated by loose white-sand layers, showing bimodal repetition of the densification process over time in two consecutive depositional tiers separated by a lithological discontinuity at 65 cm depth (Fig. 7.3).

This is a particularity of the Yapacana area in the regional context. Yapacana is the easternmost of the study areas at the foot of the upland periphery that contributes new sediments to the lowlands. Comparatively, the areas lying to the west have been thoroughly washed out of fines in the lower watersheds of the tributaries to the Orinoco and Rio Negro rivers. Part of the Yapacana area is also poorly drained, especially in the confluence triangle between Orinoco and Ventuari rivers where Oxyaquic condition is frequent in a variety of soils with densipan including Quartzipsamments, Udorthents, and Alorthods.

#### **7.2.4.2 Formation Modes**

What causes the formation of densipan layers? Several hypotheses explaining densification can be contemplated such as fragmentation of sand grains into smaller particles, translocation of fine sand and silt via suffusion through the coarse-sand matrix, and re-arrangement of the particle fabric.

##### **(a) Translocation of Fine Sand Particles**

Field observations show that heavy rainfalls, frequent at the peak of the rainy season, are followed by instantaneous infiltration of large amounts of water into the bare sandy soil surface under open meadow in flat areas, before excess water starts flooding the terrain. This causes turbulent percolation flow able to entrain fine sand, very fine sand, and silt through the macro-pores of the coarse-sand matrix.



Sums of these particle separates per layers are reported in Figs. 7.3 and 7.4. It can be hypothesized that the particles dragged by leaching will deposit in layers where water percolation stops, lowering porosity upon repeated events over time.

Often, silt content and sometimes very fine sand and clay contents are higher in the organic topsoil than in the sandy substratum. Sand grains may have been fragmented into smaller particles in the acid environment of the root mat. Sand grains show alveoli caused by silica dissolution, a feature also reported from other areas in the upper Rio Negro basin (Schnütgen and Bremer 1985; Dubroeuq and Volkoff 1998)

Similarly in meadow environment, there are no significant textural differences between densipan and overlying layers, thus no evidence of mechanical translocation and enrichment of the densipan layer in fine particles (Fig. 7.3). Profile P77 is a two-tier profile with a lithological discontinuity at 65 cm depth. In the upper tier (0–65 cm), the pattern of particle size distribution does not vary with depth. All layers have similar proportions of silt (28–29%) and very fine sand (14–19%), including the compact layer (39–65 cm). The lower tier (65–160 cm) starts with a layer having less silt content that reflects the separation between the two depositional tiers, but there is no significant change in particle size distribution with depth.

Microtopography of closed channels and pans under meadow cover evidences loss and entrainment of fine particles from the soil surface through suffusion (i.e., seepage) (see Sect. 10.4.3 in Chap. 10). Percolating drainage water drags along the silt particles into depth, possibly together with dissolved silica. Profile P112 shows a substantial silt increase in layer 3Cd (50–72 cm) that could be interpreted as a lithological discontinuity (Fig. 7.3). However, it results most likely from enrichment in fine particles that clog pore space and cause densification. As a consequence, a perched water table has formed on top of the densipan in layer 2C2 (28–50 cm).

### **(b) Re-arrangement of the Particle Fabric**

Compact layers result from filling of macro-pores in the coarse-sand matrix by finer sand particles together with silt. In general, these finer particles constitute more than half of the soil matrix and, except in few cases, there is no significant textural difference between compact and non-compact layers. Thus, densification and compaction are not basically controlled by particle size distribution.

Densipan formation through lessivage of fine particles that accumulate in a subsurface layer is probably limited to places where suffusion operates. This means that a hypothesis of larger scope is needed to embrace the densification process in general. Densification can be seen as resulting from re-arrangement of the particle fabric (Mitchell 1976). White sand single-grain packing can be deranged under the effect of fluctuating groundwater movement. Repeated oscillations of the groundwater level during the high rainy season can mobilize and displace silt and fine sand particles. Water regime monitored in a sandy bana soil (Tropaquod) in the area of San Carlos de Rio Negro showed that groundwater fluctuated frequently and fast between 20 and 75 cm depth (Franco and Dezzio 1994). Over the years, a selective re-settling of particles via sliding and rolling can take place and result in progressive filling of pores of variable sizes. Additionally, silica dissolved in the



milky groundwater contributes to fill small interstices and form bridges between sand grains.

White-sand grains are not rounded. They are irregular because they have been fragmented during repeated reworking by shifting rivers and local streams. They are also fragile because of micro-alveolization in acid environment. As a consequence, sand grains crumble under finger pressure and can be crushed into smaller particles. Quartz comminution results in a single-grain fabric with irregular grains of variable sizes that tend to be tightly interlocked causing dense packing, large friction surface, and low number of connected pores. In oscillating groundwater these particles are susceptible to relocate, increasing compaction and bulk density.

Few of the visited profiles with densipan layers have currently groundwater within 1 m from the soil surface. Thus, the hypothesis that the position of the densipan layer would correspond to the fluctuation fringe of the groundwater could not be verified. However, if the depositional dynamics in meadow environment is taken into account, the internal drainage conditions in alluvial flats may have changed repeatedly over time as a consequence of river and stream migrations. Thus, in some places, densipan layers may be related with earlier groundwater levels. The densipan can then be interpreted as an inherited hydropedologic feature (see reference to profiles P58, P77, and P81 above). As a comparative feature, compaction has been reported to occur in albic horizons of bleached Ultisols in the upper Rio Negro basin (Dubroeuq and Volkoff 1998).

---

### 7.3 Main Soil Types

Hereafter, the main soil types identified in meadow environment are addressed in terms of distribution, setting, and properties. Soils occurring in fringes between meadow areas and wooded formations (i.e., caatinga, bana, palm swale) are also mentioned.

Relevant landscape and soil characteristics of visited sites are summarized in tables, for each pedotaxon. Each profile number is followed by a letter indicating the study site (Sipapo, Camani, Ventuari, Yapacana, Atabapo, and Pasimoni). General characteristics of sites and soils for each profile are given in Tables 6.2, 6.3, 6.4, 6.5, 6.6, and 6.7. Observation sites are identified in the first column of each table and plotted on the DEM images in Chap. 6. Capital letters following the site numbers refer to the study areas from north to south. Each observation site can have more than one soil profile description as identified in the third column of the tables. The majority of the described soil profiles is less than 1 m deep; deeper observation profiles are limited in number because of logistics constraints.

### 7.3.1 Typic Quartzipsamments

#### 7.3.1.1 Distribution and Setting

Typic Quartzipsamments were identified in four of the six eco-chorological areas, i.e. Sipapo, Ventuari, Yapacana, and Atabapo. Their absence in the Pasimoni area is related with the fact that this is a poorly drained depressed area within a low-lying valley landscape, different from the large overflow and splay plains of the other areas (Table 7.1).

Typic Quartzipsamments are substrate of a variety of meadow and meadow-affined vegetation, in which typical Amazonian herbs and forbs (<1 m) dominate, frequently together with shrubs (<2 m) and sometimes with special grass species. Shrubby meadow is the most common cover, in association with related cover types including bare sand with some shrub bushes, open meadow, savanna-meadow, meadow-savanna, transitional savanna, isolated shrubs, and open scrub.

Typic Quartzipsamments occur mainly on three types of well-drained geomorphic positions: (1) long, gently sloping glacis (1–2% slope in general, up to 5%), dominant in the Sipapo and Ventuari areas where they have developed at the foot of crystalline rock hills that are widespread over the lowlands, with reticular microtopography; (2) flat splay and overflow plains that were built by shifting rivers and streams, including local riverine features such as levees, ridges, and beaches, without reticular microtopography, in the lowlands of the Yapacana and Atabapo areas; and (3) elongated, elliptical-shaped mounds (<2 m high) that most likely result from the accretion of locally recycled wind-blown sands.

#### 7.3.1.2 Properties

The average sand content of individual entire profiles is 95% or more. The overall average of the 14 profiles is 97.6% sand, 1.9% silt, and 0.5% clay. In 10 profiles, clay is fully depleted. Typic Quartzipsamment environments are virtually free of fines. This quartzose sandy material lacks water holding capacity and nutrient availability. Thus, plants in Typic Quartzipsamments mostly rely on water supply from rainfall in the glacis environment and from rainfall and flooding by river overflow in the alluvial plain environment. Nutrient supply is based on recycling whatever can be kept in the topsoil or trapped from rainfall, runoff, and flood water.

There is a difference in sand particle size distribution between the Typic Quartzipsamments on glacis and those in plain. Glacis soils show a predominance of medium sand (0.5–0.25 mm) and fine sand (0.25–0.05 mm). This reflects the provision of finer sand materials from local rock weathering and the attrition effect of colluviation that operates usually on glacis. In contrast, plain soils show either a predominance of coarse sand (2–0.5 mm) or undifferentiated sand separates proper to the splay depositional process that operates in the lowland plains of the Yapacana and Atabapo areas..

Some soils are whitish (e.g., 10YR7/1 m, 10YR8/1 d) from the surface, while others have a shallow to moderately thick grayish (e.g., 10YR4.5/1 m, 10YR6.5/1 d) ochric epipedon topping the white layers. The A horizon is 7–30 cm thick, but

mainly 15–25 cm, with an average thickness of 18 cm. The A horizons in some plain soils are comparatively thinner than those of the glacis soils.

Typic Quartzipsamments offer the opportunity to test, from simple field observations, the effect of occasional dry spells (a few days with no or low rainfall) during the period January–March. Glacis and plain environments react differently. The soils on sloping glacis dry up to depths between 15 and 40 cm by the end of February, in the middle of the lower rainfall period (P13 to P31). Soils described in July, at the peak of the rainfall season, are moist from surface layer downwards (P98 and P99). By contrast, soils in low-lying plains suffer less from dry spells and some remain moist from the surface of the soil in February–March.

Organic carbon in the A horizon varies between 0.12 and 0.54%, with an average of 0.29% (or 0.50% organic matter) (Tables 7.3 and 7.7). The value of 2.22% at P65 results from recent fire (Table 7.7). There is a slight difference in organic carbon content between glacis soils (0.20%) and plain soils (0.33%). The more favorable moisture regime in plain environment contributes to higher vegetation density and therefore more organic matter production. Average pH is 5.2 (3.9–5.8). There are only traces of phosphorus (0–1 ppm) and potassium (1–3 ppm).

The C layers are very poor in organic carbon with 0.16% on average (0.03–0.34%). Values of pH are slightly higher than those of the A horizon, with 5.6 on average (5.3–6.1). Roots concentrate mainly in the upper 10–25 cm. In the glacis soils that dry up faster and deeper than the plain soils, a few roots go down to 50–70 cm to explore deeper layers for water supply. The rooting system in the plain soils is comparatively more surficial because there is less water stress during dry spells (Table 7.7).

In summary, Typic Quartzipsamments occur on the higher, best drained, probably most recent or presently most active parts of the depositional areas, essentially on glacis and on the higher overflow and splay mantles, on river levees, and on dune-like mounds. They are well to somewhat excessively drained. The two types of geomorphic environment, i.e. glacis and plain, in which Typic Quartzipsamments occur most commonly, control a large part of their distinctive features and their relationships with the vegetation cover, as shown hereafter.

- In the Sipapo and Ventuari areas, Typic Quartzipsamment soils occur mainly on sloping peneplain glacis on which runoff causes loss of part of the incoming rainwater and favors reticular microtopographic features; they are affected by dry spells during the lower rainfall season, have relatively deep root penetration to compensate for surficial water shortage by exploring deeper moist layers for water supply, have lower vegetation density, and as a consequence lower organic matter production.
- In the Yapacana and Atabapo areas, Typic Quartzipsamment soils occur on low-lying alluvial plain flats where incoming water from rainfall and overflowing rivers promotes a slightly better water economy, diminishing the effect of dry spells and contributing to denser vegetation cover and thus more organic matter production; reticular microtopography is uncommon because shifting rivers and splay process create unstable terrain surface.

**Table 7.7** Typic Quartzipsamments: nutrient availability and soil reaction

Site	Typic Quartzipsamments		Prof (14)	Vegetation cover %	Landscape slope %	A horizon cm	Root depth cm	OC %	pH			P ppm	K ppm	Loose cover sand <2 cm
	Locality								1:1 A	A C	A C			
31S	Río Sipapo		3	Savanna 15–20	Glacis 2–4	15	25	0.20 0.13	5.7 5.6	0 0	1 1	1 1	–	
123S	Río Autana		98	Open scrub	Glacis 3–5	23	44	0.21 0.15	4.2 5.3	0 0	2 1	2 1	OC 0.49	
123S	Río Autana		99	Bare soil + shrub patches	Plain flat stream levee	11	70	0.31 0.08	4.5 5.4	0 0	3 2	3 2	OC 0.24	
38V	In front of Maraya stream		13	Shrubby meadow	Glacis 0.5	15	50	0.38 0.09	5.5 5.6	0 0	1 0	1 0		
50V	Cerro Moriche		29	Shrubby meadow	Glacis 0.5–1	30	50	0.15 0.33	5.3 5.3	1 0	1 1	1 1		
51V	Río Manapiare mouth		30	Meadow-savanna 20–30	Glacis 1–1.5	28	40	0.15 0.28	5.8 5.9	1 1	1 1	1 1		
52V	Río Manapiare mouth		31	Meadow 30–35	Glacis 1–1.5	25	70	0.13 0.15	5.6 6.1	1 1	1 1	1 1		
39Y	Carmelitas		15	Savanna 10–20	Depression inter-glacis /sandstone	15	40	0.54 0.03	5.1 5.6	1 1	1 1	1 1		
41Y	Perro de Agua		18	Shrubby meadow	Plain flat	15	40	0.38 0.11	5.8 5.6	0 0	3 2	3 2		
41Y	Perro de Agua		19	Shrubby meadow	Plain flat	25	25	0.20 0.08	5.8 5.7	0 0	2 2	2 2		
46A	Caño San Miguel		26	Savanna-meadow 10–20	Floodplain point bar mound	26	26	0.52 0.34	5.2 5.7	1 0	2 2	2 2		

(continued)

**Table 7.7** (continued)

Site	Typic Quartzipsamments		Prof (14)	Vegetation cover %	Landscape slope %	A horizon cm	Root depth cm	OC %	pH 1:1			P ppm			K ppm			Loose cover sand <2 cm
	Locality								A	A	A	A	A	A	A	A	A	
101A	Lower Rio Pimichín		67	Bare sand	Riverbed sand bank	15	15	0.12	5.8	—	—	0	—	—	1	—	—	—
102A	Caño Caname		65	Open scrub	Dune-like mound	8	30	2.22	3.9	—	—	0	—	—	2	—	—	OC 0.45
102A	Caño Caname		66	Shrubby meadow	Plain flat	7	33	0.11	5.3	—	—	0	—	—	1	—	—	—
								0.45	4.9	—	—	0	—	—	1	—	—	—
								0.15	5.8	—	—	0	—	—	1	—	—	—

Prof, description and sampling profile; OC, organic carbon; P, phosphorus; K, potassium

Typic Quartzipsamments best represent the end product of the evolution that the lowland sand covers underwent and/or still undergo, leaving only a quartzose white-sand residuum of recycled material with little or no silt and clay.

## 7.3.2 Oxyaquic Quartzipsamments

### 7.3.2.1 Distribution and Setting

Oxyaquic Quartzipsamments were identified in four of the six eco-chorological areas, i.e. Sipapo, Yapacana, Atabapo, and Pasimoni. This soil class is most frequent in the Sipapo area (Table 7.1; Fig. 7.6)

Likewise the Typic subgroup, Oxyaquic Quartzipsamments occur under a variety of meadow and meadow-affined vegetation, in which typical Amazonian herbs and forbs (<1 m) dominate, together with shrubs (<2 m) and sometimes special grass species. Shrubby meadow is the most common cover type south of river Orinoco, in the Yapacana, Atabapo, and Pasimoni areas. In the Sipapo area, north of the Orinoco, the vegetation cover is more diverse, ranging from pure meadow to savanna-meadow, open scrub, and dense scrub.

Reticular microtopography was observed under different vegetation covers, including shrubby meadow and savanna-meadow, on splay flats with high sand contents (>97%) but variable sand separate percentages.

Oxyaquic Quartzipsamments are frequent on imperfectly to poorly drained alluvial flats in low-lying overflow and splay plains. They occur in backswamps beyond river levees but also on low levees. Occasionally, they are found on point bars in floodplain lobes or in abandoned river channels. In some Oxyaquic Quartzipsamments, groundwater is brown to black even at shallow depth (e.g., 10–30 cm), although organic carbon content in the saturated layers is low. Dark groundwater may be influx from neighboring or upstream podzolic caatinga areas or lateral penetration from blackwater streams. These soils limit with Aquodic Quartzipsamments. They also share limit with Psammaquents (brownish groundwater) identified in floodplain and flooded meadow environment of the Pasimoni area.

Oxyaquic Quartzipsamments are more frequent in the Sipapo-Guayapo area than in the others because this is a regional drainage basin confined between eastern and western higher terrains causing water retention and storage in local depressions. The evacuation of flood and rainwater during the rainy season is thus retarded, and groundwater levels remain high even during the lower rainfall period in January–March (see also Sect. 6.3 in Chap. 6).

### 7.3.2.2 Properties

Oxyaquic Quartzipsamments are moist from the soil surface and saturated in deeper layers within 1 m depth throughout the year. Soils at sites visited in February–March are fully moist. The depth to the fluctuating water table varies between about 10 and 100 cm. There are no redoximorphic features as iron oxides have been washed out. Brown groundwater identified at some sites can indicate intergradation toward

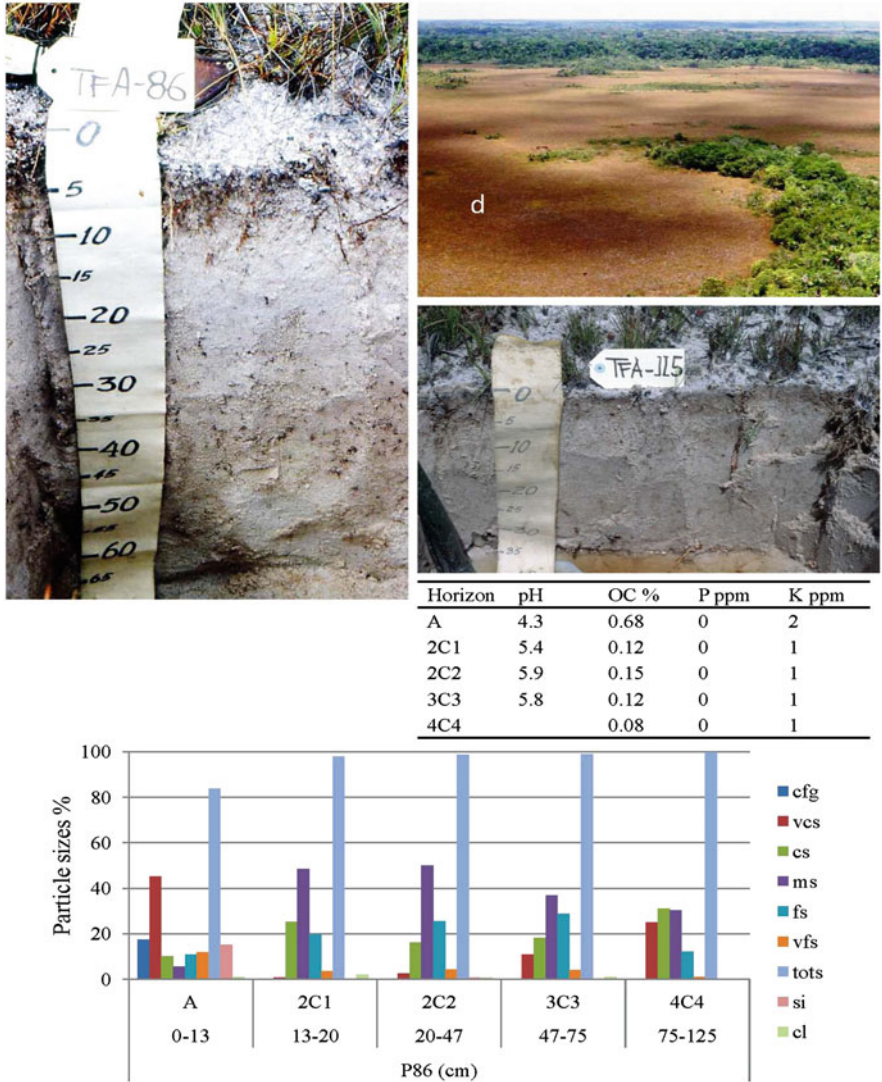


**Fig. 7.6** Oxyaquic Quartzipsamment (P86) on poorly drained alluvial plain flat (d) in the lower watershed of Caño Caname, Atabapo area, site 116; open meadow to shrubby meadow; dense reticular surface drainage network; stratified profile with lithological discontinuities between depositional layers; groundwater at 77 cm in March, rises close to the soil surface at the peak of the rainy season as in P115 (Solano area); A horizon (7.5YR5.5/2 m, 7.5YR7.5/2 d); C layers (7.5YR7/2 m, 7.5YR8/1 d); charcoal fragments at 30-50 cm depth; roots penetrate to 20–25 cm depth; nutrients are depleted



Aquodic Quartzipsamments (e.g., P21) or Spodosols, but dark-colored water can also come from elsewhere as mentioned above (Table 7.8).

The average sand content of individual entire profiles is 95% or more at all sites but one. The overall average of all 12 profiles is 96.5% sand, 1.4% silt, and 2.1% clay. Oxyaquic Quartzipsamment environments are virtually free of silt and clay. This purely quartzose sandy material has neither water retention capacity, nor nutrient availability. Plants rely on water supply from rainfall and flooding but overall from groundwater that remains close to the surface all the year around. Nutrient supply is based on recycling whatever can be kept in the topsoil or trapped from rainfall and flood water (Table 7.8).

Particle size distribution does not show a clear trend that would allow inferring a dominant depositional process. The most common pattern is of undifferentiated sand separates that points at a filling process of the depressed areas occupied by Oxyaquic Quartzipsamments. Filling results from splay reworking and redistribution of the sands brought by river overflow. In some places, the lower layers are derived from weathering of the substratum (Fig. 7.6).

The dominant soil color is whitish (e.g., 10YR7/1 m, 10YR8/1 d) from the surface. Some soils have a shallow to moderately thick grayish (e.g., 10YR4.5/1 m, 10YR6.5/1 d) ochric epipedon topping the white layers. The A horizon is 7–20 cm thick, with an average thickness of 12 cm. Root development takes place mainly in the A horizon, but some roots penetrate commonly down to 40–50 cm depth (Table 7.8).

Organic carbon content in the A horizon varies from 0.13 to 0.68%, with an overall average of 0.41% (or 0.71% organic matter). The value of 5.08% at P64 results from recent fire. Although the average thickness of the A horizon in the Oxyaquic Quartzipsamments is less than that of the Typic soils (12 cm vs. 18 cm), the organic matter content is slightly higher (0.71% vs. 0.50%). Sustained water supply throughout the year leads to higher vegetation density and more organic matter production. Average pH is 4.6 (3.5–5.8). There are only traces of phosphorus (0–1 ppm) and potassium (1–8 ppm). The C layers are very poor in organic carbon with 0.14% on average (0.03–0.32%). Values of pH are slightly higher than those of the A horizon, with 5.2 on average (4.2–6.5) (Table 7.8).

### 7.3.3 Udoxic Quartzipsamments

#### 7.3.3.1 Distribution and Setting

Udoxic Quartzipsamments were identified in all six eco-chorological areas, but with higher frequency in the Yapacana and Ventuari areas (Table 7.1; Fig. 7.7). Together with Typic Quartzipsamments (20.6%), they are the best represented with 22.1% of the profile population.

Likewise the Typic and Oxyaquic subgroups, Udoxic Quartzipsamments occur under a variety of meadow and meadow-affined vegetation, in which typical Amazonian herbs and forbs (<1 m) dominate, together with shrubs (<2 m) and savanna grass species. However, in contrast to Typic and Oxyaquic soils that are mostly

**Table 7.8** Oxyaquic Quartzipsamments: nutrient availability and soil reaction

Oxyaquic Quartzipsamments		Prof (12)	Vegetation cover %	Landscape slope %	A horizon cm	Root depth cm	OC %			pH 1:			K ppm			Loose cover sand <2 cm
Site	Locality						A	C	A	C	A	C	A	C	A	
42S	Río Guayapo	21	Meadow 20–25	Plain flat splay	20	50	0.13	0.03	5.7	5.6	0	0	2	2		
118S	Cerro Cuao toeslope	90	Meadow patch in scrub 40–50	Overflow plain	7	40	0.46	0.25	4.2	5.6	0	0	2	2	OC 0.58 K 10 pH 4.2	
118S	Cerro Cuao toeslope	91	Dense scrub	Overflow plain	13	40	0.56	0.32	4.0	4.2	0	1	1	1	OC 2.49 K 11 pH 4	
119S	Río Autana	92	Open scrub	Plain flat bench	7	50	0.20	0.09	4.6	5.5	0	0	1	1	OC 0.39 K 4	
120S	In front of Isla Ratón	93	Savanna-meadow	Plain flat	7	20	0.43	–	3.5	–	1	1	7	3		
122S	Río Autana	97	Meadow patch in scrub	Floodplain channel	7	15	0.53	0.30	3.8	4.5	0	0	8	1	OC 1.31 K 12 pH 3.5	
112Y	Río Puruname	81	Shrubby meadow 40–50	Plain flat	15	43	0.30	0.15	5.8	6.5	1	0	1	0		
147Y	Cerro Cariche	128	Shrubby meadow 80–90	Plain flat	8	44	0.38	0.12	4.8	4.8	0	0	4	2	OC 0.67 K 11	
45A	Caño San Miguel	25	Shrubby meadow 10–15	Floodplain	12	12	0.24	0.09	5.7	5.9	0	0	3	2		
100A	Lower Río Pimichín	64	Shrubby meadow	Plain flat	7	30	5.08	0.17	4.2	4.7	0	0	3	1		
116A	Caño Caname	86	Shrubby meadow	Plain flat	13	23	0.68	0.12	4.3	5.7	0	0	2	1		
136P	Lower Río Siapa	105	Shrubby meadow 40–50	River levee meander lobe	18	31	0.64	0.20	4.3	4.7	0	0	4	1		

Prof, description and sampling profile; OC, organic carbon; P, phosphorus; K, potassium

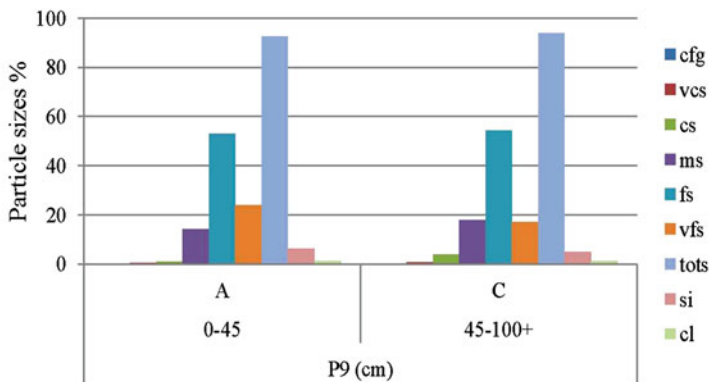
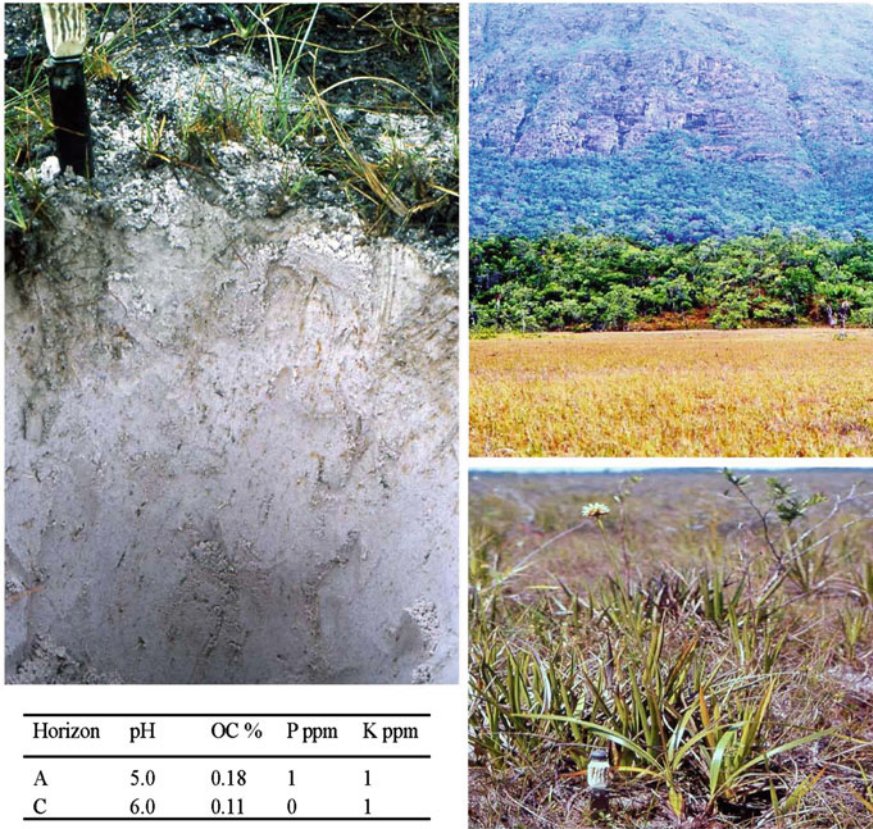


**Fig. 7.7** Udoxic Quartzipsamment (P9); Ventuari area; Cerro Moriche, site 36; penplain glacis in front of a piedmont landscape and Roraima sandstone escarpment in the background; meadow-savanna vegetation with meadow plants dominating (e.g., *Bulbostylis*); A horizon (7% fines; 10YR6/1 m); C layer (6% fines; 10YR7/1 m); meadow plants generate less organic matter (0.18% OC) than savanna plants in P14 (1.73% OC); roots penetrate to 40-50 cm depth; soil is moist in February; nutrients are depleted

associated with shrubby meadow, Udoxic Quartzipsamments occur in similar proportions under three vegetation types on the basis of 15 visited sites: pure meadow, savanna and savanna-meadow, and shrubby meadow. The Ventuari area distinguishes from the others as no shrubby meadow vegetation was identified there.

Udoxic Quartzipsamments occur essentially on two geomorph types: gently sloping glacis (0.5–3%) and plain flats. They were also found locally on elongated, elliptical-shaped mounds (<2 m high) that presumably result from short-distance reworking of splay mantle or riverbed sands by wind (coarse sand dominant). Udoxic and Typic Quartzipsamments occupy similar geomorphic positions but are clearly different in color and particle size distribution pattern.

Reticular microtopography is common especially on plain flats, less on glacis. Anastomosed channels can be as deep as 50 cm. The presence of closed pans suggests suffusion.

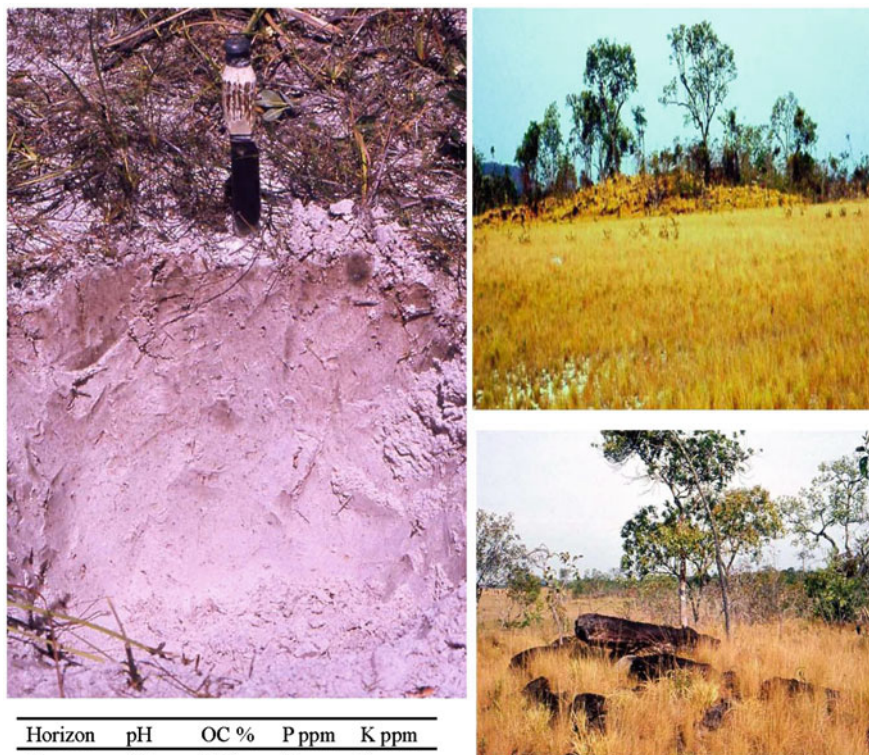
### 7.3.3.2 Properties

The average sand content of individual entire profiles varies from 75 to 95%, but lies usually in the range of 80–90% (in 10 out of 15 profiles), while the average silt content varies from 4 to 24%, but lies commonly in the range of 10–20% (in 9 out of 15 profiles). The overall average of all profiles lumped together is 86.3% sand, 11.5% silt, and 2.2% clay. Some profiles included in this set have sandy texture and are close to Typic Quartzipsamments but classify as Udoxic on the basis of the rule used to separate both subgroups, i.e. Udoxic soils have silt + 2 × clay > 5% (Soil Survey Staff 2014). The average silt content of 11.5% is a distinctive feature of the Udoxic soils, compared to 1.9% in Typic and 1.4% in Oxyaquic subgroups (Figs. 7.7 and 7.8).

The higher silt content in Udoxic Quartzipsamments is related with the position that these soils occupy on the landscape. They are frequent on proximal glacis at the foot of rock outcrops. Rock weathering and erosion provide fresh sediments that still contain argillaceous pinkish matrix impurities of sandstones or weathered saprolite material of crystalline rocks. They occur also on eolian blankets covering piedmont glacis. In situ fragmentation of quartz grains through chemical corrosion is a possible source of silt as suggested by the occurrence of silt-enriched densic layers in several profiles. There is a remarkable predominance of fine sand (0.25–0.05 mm). In 11 out of 15 profiles, the fine sand content is above 50% (53–87%, on average 68%) (Figs. 7.7 and 7.8). Fine sand is especially high in glacis positions possibly related with the weathering of rock outcrops. In more than half of the profile population, coarse-sand content is less than 10%.

Profiles were moist from the surface by the end of February, thus in the middle of the low rainfall season, except at two particular sites corresponding, respectively, to a dune-like mound and a river levee, both about 1 m higher than the surrounding terrain surface.

Light gray, light brownish gray, and pinkish gray are the dominant colors in the topsoil and in large parts of the subsoil, with white sand in deeper layers. Only in a few cases (three profiles) is the material white from the soil surface. Some profiles have yellow mottles in depth and, in two cases, plinthic materials appeared below



Horizon	pH	OC %	P ppm	K ppm
A	4.6	1.73	4	3
C	5.0	0.54	1	1

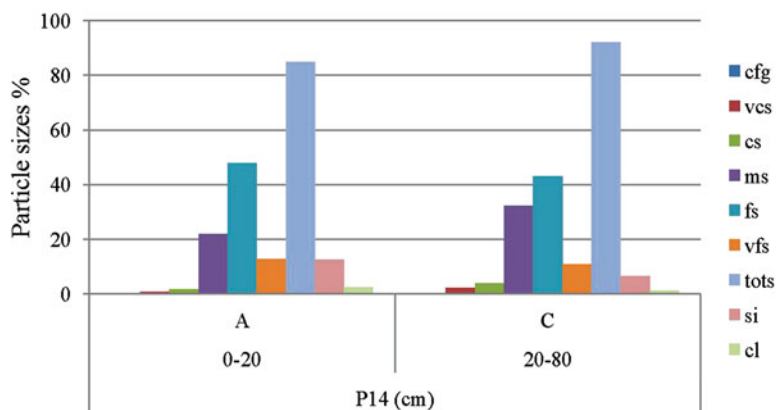


**Fig. 7.8** Udoxic Quartzipsamment (P14); Ypacana area; Carmelitas-Yagua, site 39; peneplain proximal glacia in front of a low sandstone outcrop hill covered by *Platycarpum* trees; glacia with savanna-meadow vegetation (*Mesosetum* dominant); sandstone at 80 cm depth; A horizon (15% fines; 10YR4/2 m); C layer (8% fines; 10YR5/1 m); soil is moist in February; the presence of grass species in the mixed cover generates more organic matter (1.73% OC) than pure meadow vegetation and favors deep root penetration (80 cm), resulting in a grayish variety of Quartzipsamment



1 m depth, followed by petroferic substratum. At two sites densic layers were identified within 1 m depth.

The thickness of the A horizon varies from 4 cm in open, low density meadow with large bare patches, to 30 cm in dense meadow. In 10 out of 15 profiles, the A horizon is thicker than 10 cm with an overall average of 19 cm.

The organic carbon content in the A horizon varies from 0.05 to 1.73%, with an average of 0.59% (or 1.02% organic matter). Average pH is 5.2 (4.6–5.9). Root development takes place mainly in the A horizon but some roots penetrate commonly down to 40–50 cm depth and in some cases to 70–80 cm. There are only traces of phosphorus (0–4 ppm) and potassium (1–7 ppm). The C layers are very poor in organic carbon with 0.22% on average (0.03–0.54%). Values of pH are slightly higher than those of the A horizon, with 5.5 on average (4.8–6.1) (Table 7.9).

Udoxic Quartzipsamments depart significantly from the other Quartzipsamment classes. They are not limited by excess water as the Oxyaquic soils are in the high rainy season. They have higher fine sand and silt contents than Typic and Oxyaquic Quartzipsamments; this contributes to increase meso-porosity and provide a slightly better water holding capacity to counteract the effect of dry spells in the low rainfall period of January–March. This may favor the presence of savanna grasses (Huber 2006). Savanna and more frequently mixed savanna-meadow formations were found mainly on Udoxic Quartzipsamments and additionally on Udorthents in the northern parts of the Sipapo and Ventuari areas.

### 7.3.4 Typic Udorthents

Typic Udorthents were identified in only two eco-chorological areas, i.e. Yapacana and Atabapo, in which Udoxic Quartzipsamments are also frequent (Table 7.1). These soils are in general coarse-textured but have some layers with textures finer than loamy fine sand and/or gravelly-stony layers within the control section (25–100 cm), preventing them to classify as Psamments. Udorthents are thus a heterogeneous soil class in this study region. They are associated with two types of geomorphic position that control some of their properties: fan-glacis in piedmont landscape and annular glacis in peneplain landscape. A few Udorthents were also found in alluvial plain flats.

#### 7.3.4.1 Udorthents on Piedmont Fan-Glacis

Piedmont fans are formed by creeks that originate in the highlands, mainly in the table-shaped tepuis (e.g., Duida massif), cross the piedmont landscape, and deposit their coarse sediment load at the intersection between the sloping piedmont and the flat lowland plains. Neighboring fans frequently coalesce in their distal parts and enlarge into gently sloping glacis (0.5–2% slope).

Udorthents occurring on sandy-skeletal alluvium fan-glacis are covered by shrubby meadow vegetation. Top sandy and loamy sand layers rest on a gravelly-stony substratum with sandy matrix that appears at depths varying between 13 and

**Table 7.9** Udoxic Quartzipsamms: nutrient availability and soil reaction

Udoxic Quartzipsamms Site	Udoxic Quartzipsamms		Prof (15)	Vegetation cover %	Landscape slope %	A horizon cm	Root depth cm	OC %	pH 1:			P ppm			K ppm		
	Locality								1	A	C	A	A	C	A	A	C
31S	Río Sipapo		4	Savanna	Floodplain	27	50	1.08	5.2	5.2	3	3	2				
53C	Camani valley		32	Shrubby meadow 50–60	Glacis 0.5 eolian blanket	15	60	0.11	5.6	5.6	1	1	1				
36V	Cerro Moriche		7	Savanna	Glacis	13	13	0.36	5.7	5.7	1	1	1				
36V	Cerro Moriche		8	Meadow-savanna	Glacis	8	23	0.42	5.0	5.0	0	0	2				
36V	Cerro Moriche		9	Meadow-savanna	Glacis 1–2	9	45	0.15	5.6	5.6	0	0	0				
37V	Río Coro-Coro		12	Savanna-meadow	Glacis	25	50	0.77	4.9	4.9	1	1	1				
33Y	San Antonio		6	Open meadow	Glacis prox 0.5–1 /sandstone	13	33	0.05	5.3	5.3	1	1	0				
39Y	Carmelitas		14	Savanna-meadow 60–70	Glacis prox 0.5–1 /sandstone	20	80	1.73	4.6	4.6	4	4	3				
40Y	Caño Yagua		16	Shrubby meadow	Plain flat channel	5	35	0.36	5.6	5.6	0	0	0				
97Y	Caño Yagua		58	Shrubby meadow	Plain flat/saprolite	4	28	0.29	5.8	5.8	0	0	0				
98Y	Caño Yagua		61	Shrubby meadow	Plain flat area inter-channels	25	40	0.20	5.4	5.4	0	0	3				
								0.52	4.8	4.8	0	0	6				
								0.15	5.8	5.8	0	0	3				

(continued)



**Table 7.9** (continued)

Site	Udoxic Quartzipsamments		Prof (15)	Vegetation cover %	Landscape slope %	A horizon cm	Root depth cm	OC %	pH 1:			K ppm
	Locality								1	A	C	
98Y	Caño Yagua		62	Meadow	Plain flat shallow pan	30	70	0.24	5.0	0	0	2
44A	Guarinuma		23	Meadow 50–60	Glacis 2–3	50	50	0.16	5.3	0	0	2
116A	Caño Caname		85	Open scrub	Dune-like mound	20	20	1.47	5.1	1	1	3
137P	Rio Pasimoni		108	Shrubby meadow	River terrace levee	20	35	0.28	5.3	0	0	2
								0.48	4.8	0	0	1
								0.20	5.9	0	0	1
								0.67	4.9	0	0	7
								0.22	4.8	0	0	1

Prof, description and sampling profile; OC, organic carbon; P, phosphorus; K, potassium

74 cm. The average sand content of individual entire profiles varies between 82 and 95%, with an overall average of 91%. Silt content varies between 1 and 15%, while clay content is very low (1–3%). Fine sand (0.25–0.05 mm) is remarkably dominant. The sandy material is pinkish gray to pinkish white (5YR6/2–8/2 m), reflecting the relationship of the alluvial sediments with the pinkish Roraima sandstones where they originate (Table 7.10; Figs. 7.9 and 7.10).

In spite of being coarse-textured, soils are moist from the surface during most of the lower rainfall season (February–March). The A horizon is light gray and 13–25 cm thick, with an average thickness of 17 cm. Organic carbon content varies between 0.31 and 1.03%, with an average of 0.61% (or 1.05% organic matter). Root development takes place mainly in the A horizon, but some roots penetrate the gravelly-stony substratum down to more than 60 cm. Organic carbon content in the substratum is 0.24% on average (0.17–0.37%).

#### 7.3.4.2 Udorthents on Penepplain Annular Glacis

Annular glacis is a common geomorph type in the penepplain lowlands. They surround low hills, hillocks, and hummocky rock outcrops that have been fragmented by weathering (Fig. 7.10). Rocks can be sandstone or crystalline bedrocks, generally leucocratic (e.g., gneiss, granite). The sandy, quartzose clastic materials originated by weathering are washed away from the rock outcrops and redistributed by rainfall runoff forming gently sloping annular belts (0.5–2% slope) that extend gradually into plain flats. Some sites show reticular microtopography, associated with relatively high silt content (26–33%) and the presence of densipan layers at variable depths, from as shallow as 18 cm to as deep as 115 cm.

Vegetation is mainly meadow and savanna-meadow. Soil profiles are layered with textures varying between sand, loamy sand, and sandy loam. Sometimes limiting substrata (i.e., bedrock, ironstone) appear at less than 1 m depth. There are regional differences in terms of particle size distribution. For instance, in the Yapacana area, the average sand and silt contents are 66% and 33%, respectively, while they are 87 and 11% in the Atabapo area. Clay and iron oxides have been washed out of the sediments. Slightly colored weathering products are fully bleached over short distance from the hill fringes.

Soils were mostly moist by the time of description (February–March). They are light gray over white; some are fully white. The A horizon is 6–40 cm thick with an average thickness of 18 cm. Organic carbon content varies between 0.31 and 1.51%, with an average of 0.71% (or 1.22% organic matter). Root development takes place mainly in the A horizon, but some roots penetrate commonly down to 40–50 cm depth. Organic carbon content in the substratum is 0.17% on average (0.13–0.25%). The value of 2.64% at P77 corresponds to humified organic carbon in a shallow root mat (Table 7.10).

Overall, taking into account all profiles regardless of their geomorphic position on the landscape, the A horizon of Typic Udorthents is on average 18 cm thick (6–40 cm) and contains 0.85% organic carbon (0.31–2.64%). Average pH is 5.2 (4.4–5.9). There are only traces of phosphorus (0–2 ppm) and potassium (0–6 ppm).

**Table 7.10** Typic Udorthents: nutrient availability and soil reaction

Typic Udorthents		Prof (10)	Vegetation cover %	Landscape slope %	A horizon cm	Root depth cm	OC %			pH 1:1			P ppm			K ppm			Loose cover sand <2 cm
Site	Locality						A	C	A	C	A	C	A	C	A	C	A	C	
40Y	Caño Yagua	17	Shrubby meadow	Plain flat area inter-channels	18	50	0.56	0.15	5.4	5.8	0	0	0	0	0	0			
43Y	La Esmeralda	22	Savanna-meadow 60–70	Glacis 1–2	40	40	1.51	0.13	4.7	5.8	2	3	1	1					
108Y	West of la Esmeralda	73	Shrubby meadow	Fan-glacis	25	64	0.60	0.18	5.7	5.7	0	3	0	3					
108Y	West of la Esmeralda	74	Bana scrub	Fan-glacis	14	37	0.31	0.23	4.7	6.1	0	3	0	3	OC 0.75				
110Y	West of la Esmeralda	77	Shrubby meadow 80–90	Plain flat area inter-channels	26	39	2.64	0.09	4.4	5.8	1	6	0	1					
111Y	Río Iguapé	79	Shrubby meadow 60–70	Fan-glacis 1–2	13	13+	0.48	0.37	5.5	6.0	1	1	1	1					
111Y	Río Iguapé	80	Shrubby meadow 90–95	Fan-glacis 0.5–1	16	22	1.03	0.17	4.9	6.2	0	3	0	1					
44A	Guarinuma	24	Meadow 10–20	Glacis distal 0.5–1	15	45	0.31	0.14	5.4	5.6	0	5	0	2	OC 0.46				
48A	Río Temi	27	Savanna-meadow 10–15	Glacis distal 1–1.5	10	35	0.70	0.25	5.2	5.7	1	5	1	2					
117A	NW of San Antonio	87	Shrubby meadow 40–50	Glacis 1–1.5 /sandstone	6	22	0.31	0.17	5.9	5.0	0	1	0	1					

Prof, description and sampling profile; OC, organic carbon; P, phosphorus; K, potassium

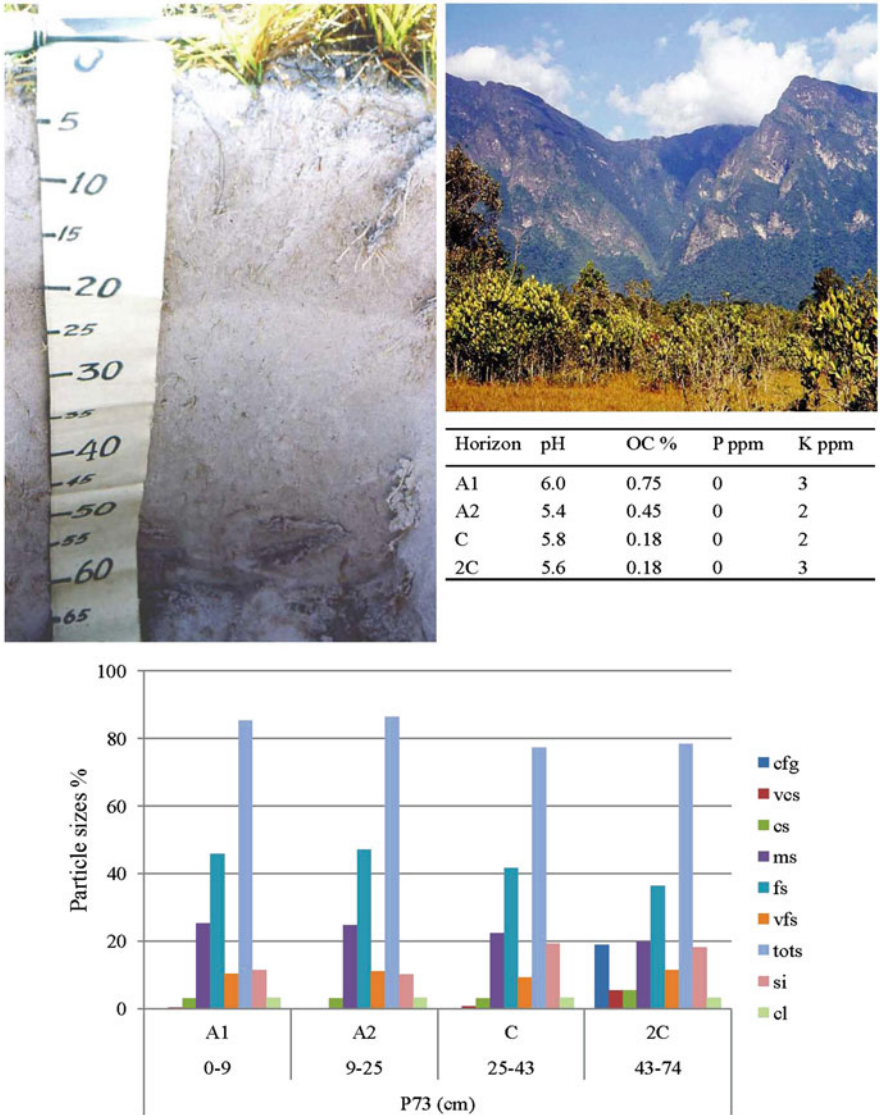


**Fig. 7.9** Typical Udorthents (P73) in the Yapacana area, site 108; in the background, Duida sandstone massif west of La Esmeralda; in the foreground, piedmont fan-glacis starting as fan in the upper piedmont and expanding laterally as glacis in the distal part covered by shrubby meadow and bana scrub; moderately deep loamy sand soil over sandy-skeletal alluvium on the levee of a piedmont creek; sand derived from the pinkish Roraima sandstone is bleached during transport; A horizon (14% fines; 7.5YR5.5/2 m, 5YR7/1 d); C layer (22% fines; 5YR7/2 m, 5YR8/1 d); fine roots penetrate to 60–70 cm depth; residual effect of recent rainfall water penetration to 20 cm depth



Horizon	pH	OC %	P ppm	K ppm
A	5.2	0.70	1	5
2AC	5.3	0.45	1	2
3C	6.0	0.05	0	1

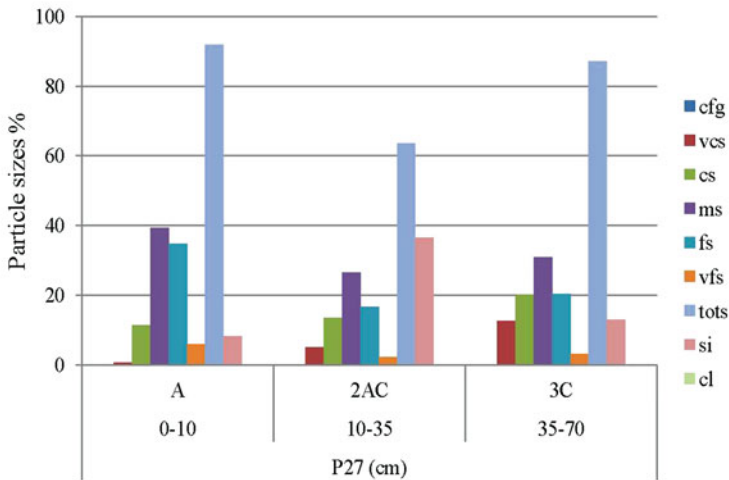


**Fig. 7.10** Typical Udorthents (P27); lower Temi watershed, Atabapo area, site 48; annular peneplain glacis surrounding low crystalline hill covered by rainforest; low-cover density savanna-meadow in front of burned bana; A horizon (8–37% fines; 10YR5/1 m, 10YR6/1 d); C layer (13% fines; 10YR7/1 d); presence of grass species (e.g., *Panicum*) generates more organic matter than pure meadow vegetation; thin transferal white-sand layer on the soil surface

On average, the C horizon contains 0.19% organic carbon (0.09–0.37%) and has a pH of 5.8 (5.0–6.2) (Table 7.10).

### 7.3.5 Spodosols

Spodosols were identified in four of the six eco-chorological areas, i.e. Sipapo, Yapacana, Atabapo, and Pasimoni, with higher frequency in the Sipapo and Pasimoni areas (Table 7.1; Figs. 7.10 and 7.11).

#### 7.3.5.1 Dual Classification

The occurrence of Spodosols under wooded cover, mainly sclerophyllous caatinga forest and bana scrub, in the Amazonian lowlands at large and in the upper Rio Negro basin in particular has been widely reported (Klinge 1965; MARNR-ORSTOM 1986; Dubroeuq and Blancaneaux 1987; Bravard and Righi 1989, 1990; Malagón Castro 1995; Pulido Roa and Malagón Castro 1996; Dubroeuq and Volkoff 1998; Schargel et al. 2000, 2001; Horbe et al. 2004; Do Nascimento et al. 2004; Schargel and Marvez 2009; Quesada et al. 2010, 2011; Medina and Cuevas 2011; IGAC 2014a, b; Mendonça et al. 2014; Adeney et al. 2016; i.a.). In the areas of San Carlos de Rio Negro and Maroa, south and west of our study region, Spodosols were also found in no-caatinga rainforest (Schargel and Marvez 2009). By contrast, the development of Spodosols under meadow vegetation (herbs, forbs, some shrubs) has not yet been documented in the study region.

A typical Spodosol profile under caatinga includes (1) a topsoil litter and raw humus layer that contain the soil nutrients and are the source of the organic substances illuviated into the spodic horizon, (2) a white sandy E horizon, and (3) a dark-colored spodic horizon where organic material and Fe-Al hydroxides accumulate and often form with the sandy matrix an indurated layer. Contrastingly, in meadow environment there is no organic matter layer topping the mineral soil, just a weak ochric epipedon, poor in organic matter. Organic carbon can be as low as 0.2–0.3% in the widespread Typic Quartzipsamments. Below the topsoil, there is a sequence of stratified white-sand C layers that look like E horizons, with one or more lithological discontinuities of depositional origin and irregular variations of organic carbon with depth (i.e., fluventic feature). In general, C layers have 95–100% total sand but with significant variations in the sand separates causing stratigraphic breaks. The sand of the C layers can be reworked E material coming from Spodosols eroded in caatinga areas that have been degraded, for instance by fire, or fresh sand influx from surrounding higher reliefs and deposited by shifting rivers. The underlying spodic horizon starts generally at 70–120 cm depth with a relevant textural change (about 10% less sand) and a strong organic carbon increase (e.g., 2–3%). It is unlikely that the weak surface horizon can supply enough organic substances to form a spodic horizon. Thus, in this kind of Spodosol the upper and lower horizons are not genetically related. The spodic horizon is not in balance with the current low-cover meadow vegetation. It can be assumed to be the remnant of an earlier-formed



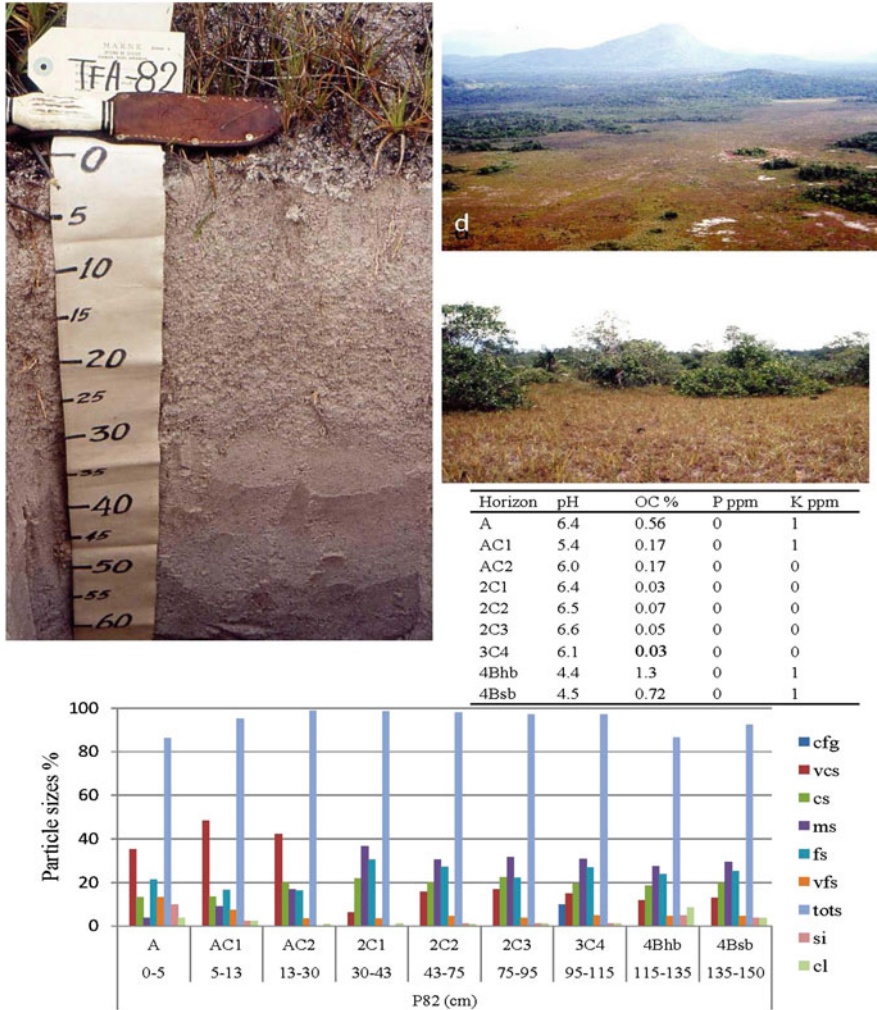


**Fig. 7.11** Oxyaquic Haplorthod (P82) in the lower Guayapo watershed, Sipapo area, site 113; alluvial plain flat including poorly drained depressions (d) where Spodosols occur; P82 is a truncated Spodosol subsequently buried by stratified sand layers with relevant lithological discontinuity at 95–115 cm depth (10% coarse fragments); shrubby meadow with 40-50% cover; A horizon (10YR6/2 m, 10YR8/2 d); C layers (7.5YR7/1 m, 7.5YR8/1 d); spodic horizons (5YR3/2 m, 7.5YR4/4 d; pH two units lower than that of the C layers); groundwater at 95 cm in March; alternative classification is Thapto-spodic Oxyaquic Quartzipsamment

Spodosol under caatinga vegetation that has been truncated by shifting fluvial dynamics and subsequently buried by white-sand sediments.

As a consequence of the former, the question rises of how to classify the Spodosols found under current meadow vegetation. There are two possibilities. One option consists in classifying these composite soils as one soil body including



both the cover and buried soil materials. Then the Spodosols identified in meadow environment of our study region classify as Durorthods, Haplorthods, Durihumods, and Alorthods. The second option consists in classifying the same soils as duplex soils with lithological discontinuity separating cover sand and buried spodic horizon. Then the cover soil (>50 cm deep) determines the soil class and all soils but one (P112) classify as Quartzipsamments. The buried soil can be reflected at subgroup level as Thapto-spodic Quartzipsamment or, more complete, as Thapto-durorthodic Quartzipsamment, for instance. Whether the soils are classified in one way or the other does not make difference in terms of soil characteristics and behavior in relation to plant life requirements (e.g., very low water holding capacity, very low nutrient availability). The soils could also be classified simply as Aquodic Quartzipsamments but this modality would not reflect the nature and origin of the composite profiles.

Spodosols described and classified in the Amazon region were considered so far as full soil bodies (see references above). Either there were no lithological discontinuities in Spodosols under caatinga or, if any, they were not detected or not taken into account. It is generally considered that Spodosols under caatinga have developed in situ from weathering of igneous-metamorphic substratum (e.g., IGAC 2014a).

By reason of simplicity, we use the one-soil-body classification alternative to refer in the text and tables to the meadow Spodosols of our study region. It allows showing the distinctive characteristics of the spodic horizons in the soil names and comparing with similar soils reported in the region under forest vegetation. It disregards the lithological discontinuities within the sand cover and between this and the underlying spodic horizons, and therefore does not account for the history and evolution of the meadow Spodosols. Thus, a hybrid approach was implemented here: soils are classified according to the rules of Soil Taxonomy for Spodosols (Soil Survey Staff 2014), but horizons are designated according to their geogenic-pedogenic origin to reflect the formation of the soil mantle. In this perspective, spodic features and in particular spodic horizons were considered remnants of earlier-formed Spodosols that have been truncated upon degradation of the wooded cover and subsequently buried by white-sand sediments. This statement is further developed when analyzing landscape evolution in Chap. 10.

### 7.3.5.2 Distribution and Setting

Spodosols have been identified and mapped in the regional context of the Amazonas State (formerly Territorio Federal Amazonas). The MARNR-ORSTOM Atlas (1986) reports few Spodosols, only in two landscape map units: i.e. Ultic Placaquods in weathering-erosion peneplain and Typic Tropaquods in erosion plain. According to detailed transect studies done in San Carlos de Rio Negro, San Carlos-Solano, and Maroa-Yavita, the most common Spodosols are Aquods under caatinga forest (Dubroeuq and Sanchez 1981; Blancaneaux and Dubroeuq 1983; Dubroeuq and Blancaneaux 1987; Schargel et al. 2000, 2001; Schargel and Marvez 2009) It is not clear from these publications whether any Spodosols were identified in meadow areas, as such areas are often small and patchy.

In our study, several classes of Spodosols were identified at nine out of 68 meadow sites (13%). They are present in four of the six eco-chorological areas, namely Sipapo, Yapacana, Atabapo, and Pasimoni, the latter being the area with the highest number of Spodosol sites. Usually, Spodosols occur on low-lying level plain flats. In the Pasimoni area, however, Spodosol profiles were found on convex, elongated benches that may be fragments of river levees or meander lobes a few meters higher than the neighboring backswamps, close to blackwater rivers and streams. Overall, the vegetation cover is shrubby meadow. Reticular microtopography was observed at some sites.

### 7.3.5.3 Properties

The average sand content of individual entire profiles is 92% or more, with an overall average of 95.2% sand, 2.1% silt, and 2.7% clay. The patterns of sand separates are diverse, but in general coarse sand dominates in the Sipapo and Yapacana areas, while medium to fine sand dominates in the Atabapo and Pasimoni areas (Table 7.11; Fig. 7.11).

The A horizon is grayish or brownish and 7–30 cm thick with an average thickness of 18 cm. Organic carbon varies between 0.15 and 2.77%, with an overall average of 0.73% (or 1.26% organic matter). Average pH is 5.1 (4.6–5.9). There is no phosphorus and only traces of potassium. Root development takes place mainly in the A horizon, but some roots penetrate commonly down to 40–50 cm depth (Table 7.11).

The top horizon is underlain by one or more white-sand layers that do not show evidence of eluviation and have very low organic carbon contents with an overall average of 0.14% (0.04–0.47%). Average pH is 5.4 (4.4–6.4).

Deep dark-colored horizons (from brown to black) are Bh, Bs, and Bhs horizons enriched in iron oxides and/or organic substances. Organic carbon in the spodic horizons varies between 0.62 and 5.70%. Values of pH are usually low because of the accumulation of aluminum-organic complexes. For instance, profile P84 has a thick spodic horizon (80–170 cm) with 3–6% OC and pH 3.5–3.7, while the overlying white-sand layers have 0.2–0.3% OC and pH 5–6 (Table 7.11). Differences in organic carbon and pH between C layers and buried spodic horizons are abrupt and substantial (1–3% OC and 1–2 pH values) (Tables 7.11 and 7.12) (see Table 10.3 in Chap. 10). Differences can be pedogenic resulting from podsolization (e.g., P84), or geogenic resulting from burying of spodic horizons by new sand cover layers (e.g., P20, P82) (Fig. 7.10) (Table 7.13). There are only traces of phosphorus (0 ppm) and potassium (1–15 ppm). The depth at which spodic horizons start varies from 37 to 122 cm. Similarly, the thickness of the various kinds of spodic horizon varies greatly, from 7 to 90 cm. In two cases, the spodic horizon is indurated forming an ortstein layer (Bhsm).

Most of the profiles were moist by description time, in the middle of the lower rainfall period (February–March). All sites have groundwater that starts at depths variable from 28 to 140 cm. At several sites, a perched water table was sustained by an indurated spodic layer. Groundwater is often brown to black.

**Table 7.11** Spodosols: nutrient availability and soil reaction

Spodosols		Prof (9)	Vegetation cover %	Landscape slope %	A horizon cm	Root depth cm	OC			pH 1:			P			K			Loose cover sand <2 cm
Site	Locality						%	A	C	1	A	C	1	A	C	ppm	A	C	
42S	Río Guayapo	20	Bana scrub	Plain flat eroded	20	40	0.15	0.05	0.30	5.7	5.8	5.9	0	0	0	1	1	1	OC 0.28
113S	Río Guayapo	82	Shrubby meadow 40–50	Plain flat	30	43	0.30	0.04	0.54	5.0	6.4	5.0	0	0	0	1	1	1	
114S	Río Guayapo	83	Shrubby meadow 25–50	Plain flat	22	53	0.47	0.43	0.15	4.4	4.7	5.1	0	0	0	1	1	1	
99Y	Carmelitas	63	Shrubby meadow 40–50	Plain flat	10	40	0.15	2.77	0.25	4.6	5.5	5.0	0	0	0	1	1	1	
115A	Río Guasacavi	84	Shrubby meadow 80–90	Plain flat eolian sand sheet	7	30	0.29	0.07	0.65	5.1	5.6	5.4	0	0	0	1	1	1	
140A	Upper Río Pimichin	112	Shrubby meadow 30–40	Plain flat eolian silt sheet	8	28	0.17	0.38	0.15	5.1	5.1	5.1	0	0	0	1	1	1	
133P	Lower Río Siapa	100	Shrubby meadow 30–60	River terrace levee	22	54	0.15	0.15	1.03	5.6	5.4	5.0	0	0	0	7	3	15	OC 0.29
135P	Lower Río Siapa	103	Shrubby meadow	Point bar meander lobe	27	44	0.12	0.12	0.12	5.3	4.8	5.1	0	0	0	1	1	1	OC 0.79
138P	Río Pasimoni	109	Shrubby savanna 60–70	River levee 2–4 lateral	19	45	0.12	0.12	0.12	5.2	5.2	5.2	0	0	0	1	1	1	K 10

Features of the spodic horizons are reported in Table 7.13; C layers correspond to the sand cover that buries the spodic horizons at variable depths; cover soils behave as Quartzipsamments. Prof, description and sampling profile; OC, organic carbon; P, phosphorus; K, potassium

**Table 7.12** Soils under tree cover: nutrient availability and soil reaction

Soils under tree cover		Prof (14)	Vegetation cover %	Landscape slope %	Soil class	O horizon cm	A horizon cm	Root depth cm	OC % O/A/C	pH 1:1 O/A/C	P ppm O/A/C	K ppm O/A/C
Site	Locality											
31S	Río Sipapo	1	Caatinga forest	Valley terrace	Udoxic Qps limit with Udipsamment	0–15	15–35	50	0.92 A 0.16 C	4.9 5.1	2 1	2 1
31S	Río Sipapo	2	Bare glade in caatinga	Valley terrace	Udoxic Qps limit with Udipsamment	–	0–8	20	0.27 A	5.6	1	1
54C	Camani valley	33	Open forest	Glacis eolian blanket	Udoxic Qps	–	0–27	50	0.48 A 0.17 C	5.3 5.7	1 1	3 2
37V	Río Coro-Coro	10	Morichal	Swale channel	Oxyaquic Qps (Udoxic)	–	0–6	6	0.16 A 0.18 C	4.9 6.0	1 0	1 0
37V	Río Coro-Coro	11	Morichal	Swale area inter-channels	Oxyaquic Udorthent	–	0–50	50	0.77 A	4.9	1	2
97Y	Caño Yagua	59	Caatinga forest	Plain flat channel	Udoxic Qps	0–4	4–14	35	0.33 A 0.20 C	5.1 5.6	0 0	4 3
97Y	Caño Yagua	60	Caatinga forest	Plain flat area inter-channels	Entic Humudept	0–45	(15–45)	45	7.39 O 0.27 C	4.2 5.0	5 0	11 4
147Y	Cerro Cariche	129	Caatinga forest	Plain flat channel	Oxyaquic Qps (Aquadic)	0–7	7–27	40	22.10 O 0.43 A 0.08 C	3.9 4.5 5.0	0 0 0	210 6 1
147Y	Cerro Cariche	130	Caatinga forest	Plain flat area inter-channels	Oxyaquic Humudept	0–45	(20–45)	60	6.14 O 0.66 C	4.3 4.6	5 0	1 1
48A	Río Temi	28	Caatinga forest	Glacis 1–1.5	Typic Qps	0–5/10	5–15	35	14.49 O 1.89 A 0.51 C	3.5 4.5 5.7	1 5 1	8 10 1
140A		113			Histic Humaquept	0–35	–	50	13.31 O	3.7	1	–

	Upper Rio Pimichin		Caatinga forest	Plain flat eolian silt sheet					0.25 C	5.1	0	-
133P	Lower Rio Siapa	101	Caatinga forest	River terrace	Arenic Alorthod	0-25	-	25	11.12 O 0.24 C 2.79 Bhs	3.7 4.9	1 0	- -
135P	Lower Rio Siapa	104	Caatinga forest	River terrace	Udoxic Qps	0-12	12-25	42	3.41 O 1.45 A 0.42 C	3.5 3.5 4.0	4 1 0	52 17 2
146P	Lower Rio Yattia	124	Caatinga forest	River terrace	Kanhapludult	0-8	8-40	40	11.98 O 4.06 A	3.7 3.7	0 0	10 5

Prof. description and sampling profile; Qps, Quartzipsamment; O horizon, rootmat; OC, organic carbon; P, phosphorus; P, potassium

**Table 7.13** Organic carbon and soil reaction in C layers and spodic Bh/Bhs horizons (all horizons have sandy texture)

Profile	Soil class	Horizon (cm)	OC %	pH 1:1 w
P20	Durorthod	C (40–60)	0.0	5.8
		Bhs (60–75)	2.97	4.5
P82	Haplorthod	C (95–115)	0.03	6.1
		Bh (115–135)	1.30	4.4
P84	Durihumod	EC (46–80)	0.28	5.8
		Bh (80–90)	2.67	3.7

### 7.3.5.4 Formation

The Spodosols identified in the study region show diverse features. This diversity is reflected in their taxonomic classification, with four classes at great group level, including Durihumod, Durorthod, Alorthod, and Haplorthod.

In contrast with previous studies that report frequent Aquods in the Amazonian lowlands, mainly under caatinga forest (e.g., Schargel and Marvez 2009), Aquods are uncommon under meadow vegetation. The definition of Aquods requires aquic conditions within 50 cm of the mineral soil surface, and either a histic epipedon or redoximorphic features in an albic or spodic horizon within 50 cm of the mineral soil surface (Soil Survey Staff 2014). In meadow environment of our study region, Spodosols have well aquic conditions (i.e., groundwater), but herbaceous vegetation does not produce enough organic matter to form histic material and soils have no redoximorphic features, especially no reduction mottles, as they are uncoated white sands depleted of iron oxides. As a consequence, Aquods are rare and other spodic features such as induration and accumulation of organic substances overrule the aquic condition and become diagnostic for the classification of these soils.

Are Spodosols under-represented in our soil population? Field observation sites were selected on the basis of two criteria: (1) purpose-oriented, to visit the largest possible number of white-sand areas and patches as identified on satellite images and (2) random-located within the white-sand areas, depending on the landing possibility of the helicopter. As there were no specific terrain features, except the type and density of vegetation cover (i.e., varieties of meadow and related plant formations), the probability of identifying Spodosols was approximately the same as for other soil classes. Thus, low frequency of Spodosols in white-sand meadow environment is possibly not a survey artifact. A limiting factor is that spodic horizons or features can occur in this region at considerable depth, sometimes below the diagnostic limit of 2 m depth (e.g., giant podzols). The fact that Quartzipsamments are overwhelmingly dominant (65%) might result from insufficient observation depth at some sites because of logistics constraints (i.e., short helicopter stops). However, it is quite unlikely that widespread podsolization takes place in the present white-sand meadow environment. Hereafter, some features of the meadow Spodosols are provided to support this hypothesis:

- Quartzose white sands are fully bleached and iron oxides have been largely washed out.

- The production of organic matter by meadow and shrubby meadow vegetation is low, and features showing migration of organic matter such as dark streaks, lamellae, or spots are unusual to detect in the sand layers overlying the spodic horizons.
- In many white-sand areas, new sand cover layers have been deposited through alluvial reworking, making the presumable deep spodic horizons look like paleo-features. Compared to the relatively stable caatinga and bana terrains, meadow areas are dynamic from erosional-depositional point of view. In geomorphic terms, they are the active parts of the lowland landscape. Some of them are periodically reworked, alternatively losing sand through rainwater runoff and river flow sweeping or gaining sand through river overflow and splay deposition, causing stratification in white-sand sediments. These terrain surface disruptions make the process of colonization by vegetation and cover development slow.
- Some Spodosols identified under meadow vegetation have advanced podsolization features (i.e., Durikumods, Durorthods) the formation of which is unlikely to have taken place in unstable, reworked white-sand cover.
- Some meadow areas result from the dismantling of caatinga forest through densification and deepening of reticular channel patterns, causing regressive erosion (see Sect. 10.3 in Chap. 10). The presence of spodic horizons in meadow-caatinga ecotone fringes is presumably inherited from Spodosols earlier formed under caatinga vegetation.
- Spodosols form usually in low-lying terrain positions. Departing from this general formation pattern, three profiles with spodic features at about 120 cm depth (P100, P103, and P109) occur in the Pasimoni area along the banks of blackwater rivers (levees and meander lobes) that dominate the surrounding terrain surface. The spodic features could result from lateral penetration of black river water impregnating deep sand layers.

In view of the former, Spodosols can be interpreted as inherited features related with paleo-environmental conditions different from the current meadow environment. This leads to the hypothesis that some meadow areas may have been originally covered by caatinga under which Spodosols have formed. The degradation of the caatinga forest and the removal of the associated root mat have caused the exposure of the underlying white-sand substratum. This process may have resulted in shrinking of the areas covered by caatinga and expansion of the areas exposed to sand reworking. The presence of charcoal fragments in white-sand Spodosols under caatinga in the upper Rio Negro region indicates that forest vegetation has been degraded during the Holocene by natural and/or human-induced fires (Sandford et al. 1985; Saldarriaga and West 1986).

Thus, Spodosols are key indicators of past evolution (Holocene) in this region, as a paleo-feature under meadow that reflects earlier podsolization under caatinga (see Sect. 10.5 in Chap. 10). Similarly, Buol et al. (1997) note a lack of relationship between vegetation cover and soil when referring to a giant podzol described by Eyk in Surinam (1957), and consider that “the present savanna vegetation may be quite different from that under which this soil has first formed.”



### 7.3.6 Other Soils Under Meadow Vegetation

A few profiles depart from the dominant soil taxa. They are representative of local landscape units and features of lesser extent that however repeat with some frequency.

Lithic Quartzipsamments occur in the proximal parts of the glacis that surround low hills and hummocky rock outcrops, often sandstone or quartzite, in the peneplain landscape with open meadow or bare sand surface. These are mainly recent white or pinkish gray weathering products with sand content above 95%, thin A horizon (<10 cm), and low organic matter content. They are susceptible to dry up repeatedly during the lower rainfall period.

Deep sandy soils with plinthic feature in depth occur close to small streams or above weathering granite substratum. They are white in the upper layers and variegated in depth. Layers are stratified with lithological discontinuities, reflecting depositional origin of the material in which developed soils have formed. Clay content often increases with depth, resulting in the formation of weak illuvial horizons (Plinthic Quartzipsamments with Bt horizon and Grossarenic Plinthic Kandiodults). Vegetation varies from meadow-savanna to shrubby meadow.

In an environment where the configuration of the river system is very dynamic and river channels shift frequently, abandoned water courses are common features of the alluvial plains. They are filled with materials that vary from pure sand layers under flooded meadow (Psammaquents) to organic matter accumulation under shrubby meadow (Hydric Haplohemists).

Thickness of the A horizon and root penetration depth are variable in all these kinds of soil, while nutrient availability is very low everywhere.

A variety of soils occurs in the outer fringe of caatinga forest areas. They depart from the soil taxa usually found under caatinga and prefigure kinds of soil that dominate under meadow vegetation, for instance Udoxic and Oxyaquic Quartzipsamments. Does this suggest that the caatinga fringe is a progressive front colonizing meadow areas or is it, on the contrary, a regressive head where the thick root mat of the caatinga soil is dismantled by reticular erosion, causing the white-sand substratum to come closer to the terrain surface? This issue of contact fringes between meadow and wooded areas is further analyzed in Chap. 10.

Primary waterways in meadow environment are swales, i.e. narrow, shallow, longitudinal depressions with smooth borders, in general less than 100 m wide and a few meters deep, that collect rainwater runoff from the slightly higher-lying terrain surfaces, especially glacis. Swales are filled by colluvial white sands eroded from the surrounding glacis and flooded during large part of the high rainy season. They are covered essentially by palm trees (e.g., moriche, *Mauritia* sp.), sometimes in association with a few other tree species (e.g., picatón, *Platycarpum* sp.). Channels are interconnected in reticulate pattern surrounding isles of the original terrain surface where trees concentrate. A typical soil association includes Oxyaquic Udorthent with thick A horizon on inter-channel areas and Oxyaquic (Udoxic) Quartzipsamment at channel bottom. Histosols occur in poorly drained parts.

## 7.4 Conclusions

Quartzipsamments are the dominant soils under meadow vegetation *sensu lato* (65%), with three subgroups (i.e., Udoxic, Typic, and Oxyaquic) sharing similar proportions. Udorthents and Spodosols are subordinate soil classes. A feature common to all soils is the high content of whitish quartzose sand (usually more than 95%) that has very limited water holding capacity. The regional soil moisture regime as influenced by climatic conditions is udic in the norther part of the region and perudic in the southern part, together with widespread aquic regime soils in poorly drained low-lying alluvial flats. Most of the soils have a weak ochric epipedon with low organic matter content overlying white-sand C layers. Poor water economy and nutrient scarcity make the meadow soils a harsh life support medium for plants to establish and grow. Compact, dense layers were identified in meadow environment and caatinga fringes at variable depths, in general in subsurface layers. They are particularly frequent in the Yapacana area where materials with relatively high contents of fine sand, very fine sand, and silt occur. A particularity in some meadow soils is the presence of compact densic sand layers that restrain root penetration and seem to result from re-arrangement of the particle fabric within the oscillation margin of the groundwater level. Although compact white sandy layers fulfill some of the properties of densic materials, they seem to be a pedogenic part of the soil profile rather than a geogenic material. Therefore, the term densipan is used here to refer to compact, densified white sandy layers that are identified by the suffix “d” in the profile descriptions.

The geographic distribution of the main soil classes is landscape-related. Typic Quartzipsamments occur mainly on three types of well-drained geomorphic positions including: (1) long, gently sloping peneplain glacis, (2) flat splay and overflow plains built by shifting rivers and streams, and (3) elongated, elliptical-shaped mounds of recycled wind-blown sands. Oxyaquic Quartzipsamments are common on imperfectly to poorly drained alluvial flats in low-lying overflow and splay plains with brown to black groundwater. Udoxic Quartzipsamments occur essentially on gently sloping peneplain glacis and alluvial plain flats. They have higher fine sand and silt contents than those of Typic and Oxyaquic Quartzipsamments; this may contribute to slightly improve water holding capacity to counteract the effect of dry spells in the low rainfall period of January–March. Udorthents form a heterogeneous soil class that occurs in piedmont fan-glacis and peneplain annular glacis. Although Spodosols are usually associated with caatinga-bana vegetation, they were also found in current meadow environment with which they do not seem to bear genetic relationship. They are duplex soils, constituted by an upper tier of stratified sand cover with lithological discontinuities and a lower tier corresponding to the remnant of truncated Spodosol. As white-sand meadows occur usually in the form of patches or larger areas surrounded by woody vegetation making together an intricate mosaic of land cover, soils at meadow-caatinga fringes allow analyzing ecotone dynamics as shown in Chap. 10.

Hereafter, some relevant features based on large generalizations are summarized:

- Soil materials and sediments are in general uncoated white quartz sand; pinkish gray sand occurs in areas close to Roraima sediment sources, and grayish sand is common under herbaceous cover including grass species (meadow-savanna and savanna).
- Soil materials and sediments are 95% or more sand, except in the Yapacana area where the silt component is important.
- Medium and fine sand are the dominant sand separates throughout the study region.
- Sandy sediments in meadow environment are periodically reworked by lateral migration of streams and rivers. This results in stratified profiles showing lithological discontinuities.
- Clay is everywhere very low and in some cases fully depleted, especially in Typic and Oxyaquic Quartzipsamments.
- Silt is locally relatively high; it can result from fragmentation of quartz grains upon chemical corrosion and alveolization and from weathering of local rock outcrops.
- Organic carbon is 0.29–0.85% (= 0.50–1.47% organic matter) in A horizons and 0.14–0.22% in C layers.
- Soil reaction is strongly acid, with pH <5.5. In C layers pH values are up to half a unit higher than in the surface A horizon.
- Phosphorus and potassium availability is very low, in many cases not detectable or only at the level of traces.
- Savanna and mixed savanna-meadow formations occur in the northern parts of the Sipapo and Ventuari areas, frequently associated with Udoxic Quartzipsamments.

The majority of the soils identified in meadow environment is sandy (mainly sand, also loamy sand and sandy loam) at least down to one meter depth unless lithic contact. This includes Quartzipsamments, Udorthents, all Spodosol classes, and also less frequent soils such as Grossarenic Ultisols and Psammaquents. Whatever the taxonomic class, all soils lack water holding capacity and nutrient availability. They provide similarly limited life supporting conditions for plants to establish and grow. Aquic conditions in poorly drained soils introduce a difference that can be seen as a source of water supply when needed or, on the contrary, a cause of water excess when detrimental.

---

## References

- Adeney JM, Christensen NL, Vicentini A, Cohn-Haft M (2016) White-sand ecosystems in Amazonia. *Biotropica* 48(1):7–23
- Aymard G, Campbell LM, Romero-Gonzalez GA (2014) *Paypayrola arenacea* (Violaceae), a new species with an unusual life-form from white sand savanna in the Amazon river basin of Venezuela. *Harv Pap Bot* 19(2):175–184
- Blancaneaux P, Dubroeuq D (1983) Características edáficas y ambientes del área muestra Maroa-Yavita. Serie Informes Técnicos DGSIIA/IT/128, MARNR, Caracas

- Bravard S, Righi D (1989) Geochemical differences in an Oxisol-Spodosol toposequence of Amazonia, Brazil. *Geoderma* 44:29–42
- Bravard S, Righi D (1990) Podzols in Amazonia. *Catena* 17:461–475
- Buol SW, Hole FD, McCracken RJ, Southard RJ (1997) Soil genesis and classification, 4th edn. Iowa State University Press, Ames
- Do Nascimento NR, Bueno GT, Fritsch E, Herbillon AJ, Allard T, Melfi AJ, Astolfo R, Boucher H, Li Y (2004) Podzolisation as a deferralization process: a study of an Acrisol-Podzol sequence derived from Palaeozoic sandstones in the northern upper Amazon Basin. *Eur J Soil Sci* 55: 523–538
- Dubroeuq D, Blancaneaux P (1987) Les podzols du Haut Rio Negro, région de Maroa, Venezuela. Environment et relations lithologiques. In: Righi D, Chauvel A (eds) Podzols et podzolization. AFES \$ INRA, Plaisir et Paris, pp 37–52
- Dubroeuq D, Sanchez V (1981) Características ambientales y edáficas del área muestra San Carlos de Río Negro-Solano. Serie Informes Técnicos DGSIIA/IC/12, MARNR, Caracas
- Dubroeuq D, Volkoff B (1998) From Oxisols to Spodosols and Histosols: evolution of the soil mantles in the Rio Negro basin (Amazonia). *Catena* 32:245–280
- FAO (2006) Guidelines for soil description, 4th edn. Food and Agriculture Organization of the United Nations, Rome
- Franco W, Dezzee N (1994) Soils and soil water regime in the terra firme-caatinga forest complex near San Carlos de Rio Negro, State of Amazonas, Venezuela. *Interciencia* 19(6):305–316
- Haridasan M (2008) Nutritional adaptations of native plants of the cerrado biome in acid soils. *Braz J Plant Physiol* 20(3):1–10
- Horbe AMC, Horbe MA, Kenitiro S (2004) Tropical Spodosols in northeastern Amazonas State, Brazil. *Geoderma* 119(1-2):55–68
- Huber O (1988) Guayana highlands versus Guayana lowlands, a reappraisal. *Taxon* 37(3):595–614
- Huber O (2006) Herbaceous ecosystems on the Guayana Shield, a regional overview. *J Biogeogr* 33(3):464–475
- Huber O, Zinck JA (2000) Aspects of stress ecology in white-sand ecosystems of the Venezuelan Guayana region. Oral presentation, Marburg Stress Symposium, Marburg (unpublished)
- IGAC (2014a) Estudio general de suelos y zonificación de tierras del Departamento de Guainía, escala 1:100,000. Instituto Geográfico Agustín Codazzi, Subdirección de Agrología, Bogotá
- IGAC (2014b) Estudio general de suelos y zonificación de tierras del Departamento de Vichada, escala 1:100,000. Instituto Geográfico Agustín Codazzi, Subdirección de Agrología, Bogotá
- Klinge H (1965) Podzol soils in the Amazon basin. *J Soil Sci* 16(1):96–103
- Malagón Castro D (1995) Estudio genético-taxonómico de Espodosoles, Ultisoles y Oxisoles y su relación con el manejo de las tierras en el Departamento del Vaupés (Colombia). Universidad Nacional de Colombia, Bogotá
- MARNR-ORSTOM (1986) Atlas del inventario de tierras del Territorio Federal Amazonas (Venezuela). Dirección de Cartografía Nacional, MARNR, Caracas
- Medina E, Cuevas E (2011) Complejo caatinga amazónica: bosques pluviales esclerófilos sobre arenas blancas. *BioLlania edic esp* 10:241–249. UNELLEZ, Guanare, Venezuela
- Mendonça BAFD, Simas FNB, Schaefer CEGR, Fernandes Filho EI, Vale Júnior JFD, Mendonça JGFD (2014) Podzolized soils and paleoenvironmental implications of white-sand vegetation (Campinarana) in the Viruá National Park, Brazil. *Geoderma Reg* 2– 3:9–20
- Mitchell JK (1976) Fundamentals of soil behavior. Wiley, New York
- Pulido Roa C, Malagón Castro D (1996) Estudio genético y taxonómico de Espodosoles, Ultisoles y Oxisoles y su relación con el manejo de las tierras. In: Aspectos ambientales para el ordenamiento territorial del Municipio de Mitú, Departamento del Vaupés. Instituto Geográfico Agustín Codazzi, Bogotá, Colombia, Tomo I: 307–399
- Quesada CA, Lloyd J, Schwarz M, Patiño S, Baker TR, Czimczik C, Fyllas NM, Martinelli L, Nardoto GB, Schmerler J, Santos AJB, Hodnett MG, Herrera R, Luizão FJ, Arneith A, Lloyd G, Dezzee N, Hilke I, Kuhlmann I, Raessler M, Brand WA, Geilmann H, Moraes Filho JO, Carvalho FP, Araujo Filho RN, Chaves JE, Cruz Junior OF, Pimentel TP, Paiva R (2010)

- Variations in chemical and physical properties of Amazon forest soils in relation to their genesis. *Biogeosciences* 7:1515–1541
- Quesada CA, Lloyd J, Anderson LO, Fyllas NM, Schwarz M, Czimczik CI (2011) Soils of Amazonia with particular reference to the RAINFOR sites. *Biogeosciences* 8:1415–1440
- Saldarriaga JG, West DC (1986) Holocene fires in the northern Amazon basin. *Quat Res* 26:358–366
- Sandford RL, Saldarriaga J, Clark KE, Uhl CH, Herrera R (1985) Amazon rainforest fires. *Science* 227:53–55
- Schargel R, Marvez P (2009) Suelos. In: Aymard GA, Schargel R (eds) Estudio de los suelos y la vegetación (estructura, composición florística y diversidad) en bosques macrotérmicos no-inundables, Estado Amazonas, Venezuela. *BioLlania edic esp* 9:99–125. UNELLEZ, Guanare, Venezuela
- Schargel R, Aymard G, Berry P (2000) Características y factores formadores de Spodosoles en el sector de Maroa-Yavita, Amazonia Venezolana. *Revista Unellez de Ciencia y Tecnología* 18(1): 85–96
- Schargel R, Marvez P, Aymard G, Stergios B, Berry P (2001) Características de los suelos alrededor de San Carlos de Río Negro, Estado Amazonas, Venezuela. *BioLlania edic esp* 7:234–264. UNELLEZ, Guanare, Venezuela
- Schnütgen A, Bremer H (1985) Die Entstehung von Decksanden im oberen Rio Negro-Gebiet. *Z Geomorph NF Suppl -Bd* 56:55–67
- Soil Survey Staff (1975) Soil taxonomy. A basic system of soil classification for making and interpreting soil surveys. *Agriculture Handbook* 436, USDA Soil Conservation Service, Washington, DC
- Soil Survey Staff (2014) Keys to soil taxonomy, 12th edn. USDA, Washington, DC
- van der Eyk JJ (1957) Reconnaissance soil survey in northern Surinam, PhD thesis, Wageningen
- Walter H (1985) *Vegetation of the Earth and ecological systems of the geo-biosphere*. Springer, Heidelberg



# Origin and Sources of Sand: From Highlands to Lowlands

8

J. A. Zinck and P. García Montero

## 8.1 Introduction

In the Amazonian lowland basin of Venezuela, all surface- and ground-waters concentrate toward the west into two main collectors, the Orinoco flowing to the north and the Rio Negro flowing to the south. Both rivers form together a major meridian axis that drains in opposite direction along the divide between the river system of the Guayana Shield from the east and the river system of the Llanos Plains from the west. Both are fringed by levee and point bar systems that form barrier to efficient evacuation of excess water and sediments. As a consequence, the sand load of the rivers and large part of the water tend to remain in the lowland basin, confined in depressed drowning areas. Before being stabilized by woody vegetation (rainforest, caatinga, bana), sand sediments experienced several episodes of reworking, bleaching, and washing. Thus, the sand cover is in fact mainly residual sand. New sand influx to the lowlands comes from the highlands and uplands, and from the hills spread over the lowlands.

Except for piedmont sands (fans and glacis) and hillside sands (glacis) that are derived from *ex situ* rock weathering, the white-sand covers in meadow environment have undergone alternating deposition and erosion through rainwater runoff, river and stream migration, and sediment redistribution via overflow and splay in flat lowlands. In general, they are stratified in layers with variable sand separate combinations that indicate changes in depositional energy. Thus, meadow is an active environment in spite of being apparently stable. Frequent surface soil reworking makes it difficult for meadow vegetation to establish and develop.

---

J. A. Zinck (✉)

Faculty of Geo-Information Science and Earth Observation (ITC), University of Twente, Enschede, The Netherlands

P. G. Montero

Private Activity, Soil Survey and Environmental Planning, Caracas, Venezuela

This chapter describes processes of sand generation in the lowlands themselves and identifies sources of clastic materials in the surrounding higher basin reliefs that contribute sand to the lowlands. A set of visited sites distributed over piedmonts, uplands, and highlands that form the periphery of the lowlands provides information on sand source areas. It refers to the production of sand within the upper basin through physical fragmentation and/or chemical weathering of bedrocks.

Soil description and sampling were carried out in pits as described in Chap. 6.

---

## 8.2 Sands of Multiple Origins

The occurrence of white sands and other kinds of sandy materials has been reported in the Amazon basin at large (Klinge 1965; Herrera et al. 1978; Anderson 1981; Schnütgen and Bremer 1985; MARNR-ORSTOM 1986; Malagón Castro 1995; Pulido Roa and Malagón Castro 1996; Dubroeuq and Volkoff 1998; Do Nascimento et al. 2004; Horbe et al. 2004; Aymard and Schargel 2009; Medina and Cuevas 2011; IGAC 2014a, b; Mendonça et al. 2014; Adeney et al. 2016). Sand sediments covering the lowlands in the Venezuelan Amazonas territory come from different sources and related sand generation processes. Several main sand release areas and mechanisms can be considered (Fig. 8.1):

- The Roraima sandstone/quartzite cover overlying the crystalline shield basement in the Guayana highland plateaus and isolated tepui mesetas: physical fragmentation and physical-chemical weathering via intergranular cement dislocation of the sedimentary and metasedimentary rocks generate sands in the highlands that are stepwise transferred to the lowlands by surface transport via cascading creeks and underground transport via karstic drains.
- The crystalline rocks of the hilly upland reliefs, piedmont hills, and scattered lowland hills: physical disintegration and chemical weathering of granite and gneiss produce saprolites; these loose slope materials are subsequently removed by rainfall runoff and creek transport; selective sorting of the material in piedmont areas leads to depletion of the fines and concentration of sand particles at footslopes.
- The crystalline rock substratum in the large lowland peneplains: in situ weathering generates deep saprolites that are washed out by vertical percolation drainage, leaving a residual sand cover.
- The transformation of Oxisols and Ultisols into Spodosols: podzolization bleaches ferrallitic sands in areas with fluctuating water table, especially at the periphery of crystalline rock hills covered by red Oxisols and Ultisols.

Sand resulting from deep vertical podzolization under forest cover, usually in hydromorphic conditions, is not referred to here as this process does not operate in the current meadow environment, but has been reported to occur elsewhere in the Amazon basin (Horbe et al. 2004; Quesada et al. 2011).



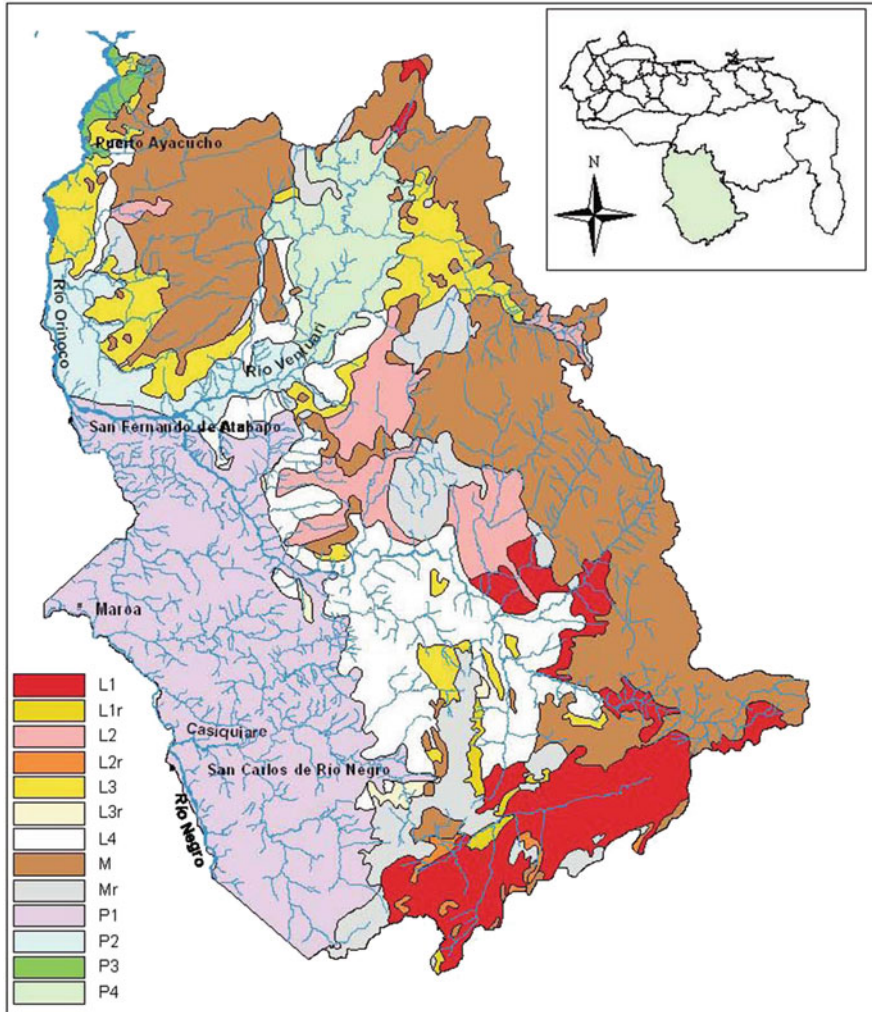


**Fig. 8.1** Physiographic landscapes of Amazonas State, Venezuela. M: mountains on igneous and metamorphic rocks; Mr: mountains and tepuis on sedimentary rocks (Roraima group); L1, L2, and L3: hillands of variable altitude and relative elevation on igneous and metamorphic rocks; L1r, L2r, and L3r: hillands of variable altitude and relative elevation on sedimentary rocks (Roraima group); L4: low hillands; P1: Casiquiare peneplain; P2: lower Ventuari and Sipapo peneplain; P3: northern peneplain; P4: middle Ventuari peneplain. Legend simplified from the original prepared by R. Schargel (Aymard and Schargel 2009)

Sandy products coming from above primary sources are reworked and distributed over the lowlands by fluvial, colluvial, and eolian processes. Tertiary and Pleistocene inland sea and lake beaches in the Amazon basin (Klammer 1978, 1984; Irion 1984; Putzer 1984; Sombroek 1984), ancient river beaches (Prance and Schubart

1978), and sand dunes (Carneiro Filho and Zinck 1994; Carneiro Filho et al. 2002; Mendonça et al. 2014) are areas of sand concentration but not primary sources of sand production.

### 8.3 Sand Sources at the Basin Periphery

The lowland basin is bordered and surrounded by mid- and high-elevation reliefs. Various kinds of crystalline and sedimentary rocks of Proterozoic age constitute the basement of hills, mountain, and plateau landscapes that encircle the lowlands. The map units identified as “peneplains” P1, P2, and P4 in Fig. 8.1 conform the lower basin where sands produced in the peripheral upper basin accumulate. Structural geoforms including mesetas, cuestas, and hogbacks that have developed in Roraima sandstones and quartzites are present at various elevations, but most typically table-shaped geoforms, i.e. the tepui mesetas, occur at the highest elevations (up to 2800 m a.s.l.) (Plate 8.1a, b). Hills and mountains that have developed mainly in igneous-metamorphic rocks are the common landscape types at mid-elevations (up to about

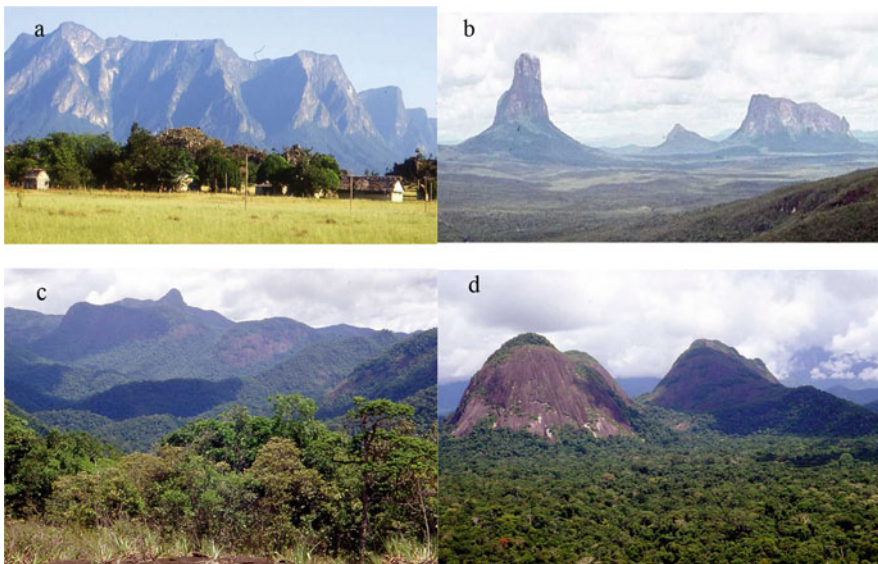


**Plate 8.1** Highlands and lowlands: (a) Duida massif, south-eastern escarpment of the table-shaped sandstone plateau (1400–1500 m a.s.l.) dominating the plain flat of the Orinoco river, in the proximity of La Esmeralda; (b) remains of the earlier quartzitic platform (Roraima group) covering the igneous-metamorphic basement rocks of the Guayana Shield; Cerro Autana to the left (1200 m a.s.l.); lowlands of the Autana river watershed showing meadow islands (light green) within a woody matrix. Uplands and lowlands: (c) hilland landscape resulting from dissection of igneous-metamorphic basement rocks in the upper Siapa river watershed, in the southern edge of the study region; (d) dome-like hills developed in igneous-metamorphic rocks dominating the lowlands of the middle Siapa river watershed

1500 m a.s.l.) (Plate 8.1c, d). After having been uplifted, the crystalline and sedimentary massifs have remained tectonically fairly stable over long periods of time but were submitted to intensive relief fragmentation, dissection, and down-wasting (Mendoza 2005). Acting over millions of years, the dismantling of the Roraima sandstone/quartzite cover, that originally extended over the whole Guayana Shield, and longstanding rock weathering and erosion have produced masses of clastic sediments and especially sands that have filled the lowland basins. Today, the flat-topped highland reliefs of the Roraima sedimentary cover form a relatively small portion of the surrounding mountain belt, while the rugged mid-elevation upland crystalline and sedimentary reliefs constitute the largest extent.

The whole upland and highland periphery surrounding the lowlands is source of sand. Sandstone and quartzite fragment directly into sand. The weathering of the igneous-metamorphic rocks generates a matrix of clastic fragments including ferromagnesian, feldspar, and quartz debris, but further weathering in the warm moist climate of the area depletes most of the minerals and leaves only a quartz-sand residuum. Stained quartz grains are bleached over short distance transport to form white sands.

### 8.3.1 Highland Sand Sources

The Guayana plateau highlands (i.e., tepui mesetas) range in elevation mostly between 1200 and 2800 m a.s.l. At the surface of the table-shaped reliefs, Roraima sandstone and quartzite rocks have been continuously disaggregating over millions of years. Tepui mesetas are an inexhaustible source of sand. Subaerial arenization takes place on bare rock exposures along joints and fissures, and in dissolution alveoli, pans, and runnels. Debris are washed away by rainfall runoff and accumulate temporarily at footslopes of rock outcrops and in vales before disappearing in karstic crevasses or being carried further down by creeks. Sand deposits often thicker than 1 m have been observed as colluvial vale fill at Duida summit (1160 m a.s.l.) and colluvial glacia cover at the foot of a sandstone bar at Autana summit (1210 m a.s.l.) (Fig. 8.2). In both cases, the disaggregation of Roraima sandstone resulted in a well sorted sediment with fine and medium sand dominant (Zinck and Garcia 2011).

Sand generation is also active beneath the peat mantles that cover parts of the tepui summits. Peat forms in low-lying, closed or nearly closed landforms where water stagnates and organic material accumulates faster as it decomposes. At the peat–rock interface, pH values are as low as 3.2, supporting the idea that oligotrophic peatlands act as strong agents of weathering in and underneath them. Active micro-morphogenesis takes place under the peat mantle because of acid organic matter and acid peat water. Rock weathering proceeds along joints and fractures, deepening the incisions and enhancing the original microrelief. This results into intricate cryptolapies (crypto-karren) with rectangular or trellis pattern (Fig. 8.3). Weathering of the siliceous cement of quartzite and quartz sandstone through intergranular dissolution of quartz causes rocks to lose matrix coherence and finally crumble into single sand grains. Quartz-sand grains show surface etch pits reflecting dissolutional rock

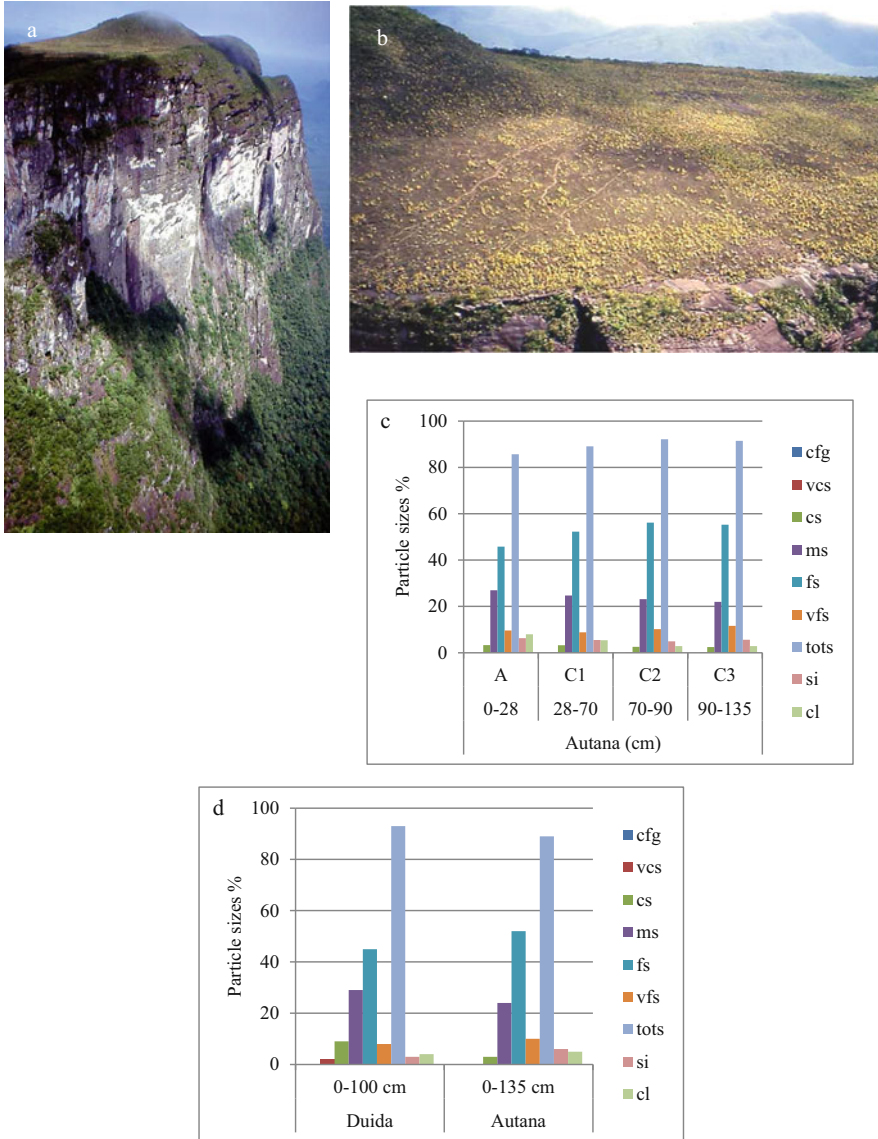


**Fig. 8.2** Cerro Autana (1210 m a.s.l.) (a). (b) sandy colluvial glacia (135 cm thick), resulting from sandstone weathering and erosion of the low hill at the northern edge of the tepui; (c) homogeneous, well sorted particle size pattern with dominant fine sand, showing sustained colluviation over time; (d) similarity of colluvial sand accumulation from sandstone weathering at Duida and Autana summits (1160 m a.s.l.)

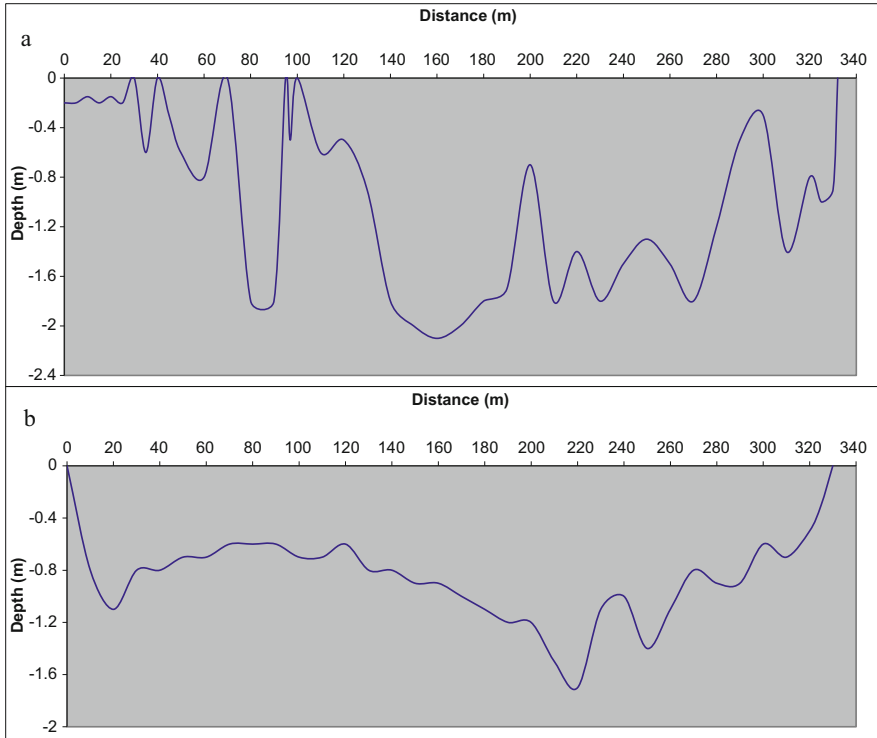


**Fig. 8.3** Microtopography of crypto-lapies (crypto-karren) resulting from rock weathering under peat mantle; **(a)** transect on a sedimentary meseta at the summit of the Cuao-Sipapo massif (1500 m a.s.l.); indented microrelief reflects preferential karstic sandstone weathering along a dense grid of joints and fractures; **(b)** transect on a crystalline hill at the summit of the Maigualida massif (2150 m a.s.l.); slightly undulating microrelief reflects pseudokarstic granodiorite weathering more controlled by rock mineralogy than by structural joints; sand produced by sandstone weathering at the peat–rock interface is evacuated by endokarstic conducts (Zinck and Garcia 2011)

weathering in peat bogs. As a result, small sand strata, mostly of medium and fine sand, up to 25–30 cm thick, form along the interface between the base of the peat deposit and the underlying rock surface (Zinck and Garcia 2011).

As the origin of the siliceous Roraima rocks dates back to Precambrian times, it can be assumed that considerable masses of sand have been produced in the highlands and sunk into the lowlands. Sand removal from the highlands and discharge to the lowlands must have been particularly intense by the end of the Pleistocene before vegetation started establishing at tepui summits at the onset of the Holocene, with peat accumulation initiating around 8400 calBP (Zinck et al. 2011). Clastic debris are mobilized both via internal drainage and surface runoff and stepwise transferred from higher to lower elevations. Sub-peat groundwater fluctuations entrain sand grains through joints and dissolution fissures to underground endokarst drainage systems that resurge at the footslopes of the plateaus.



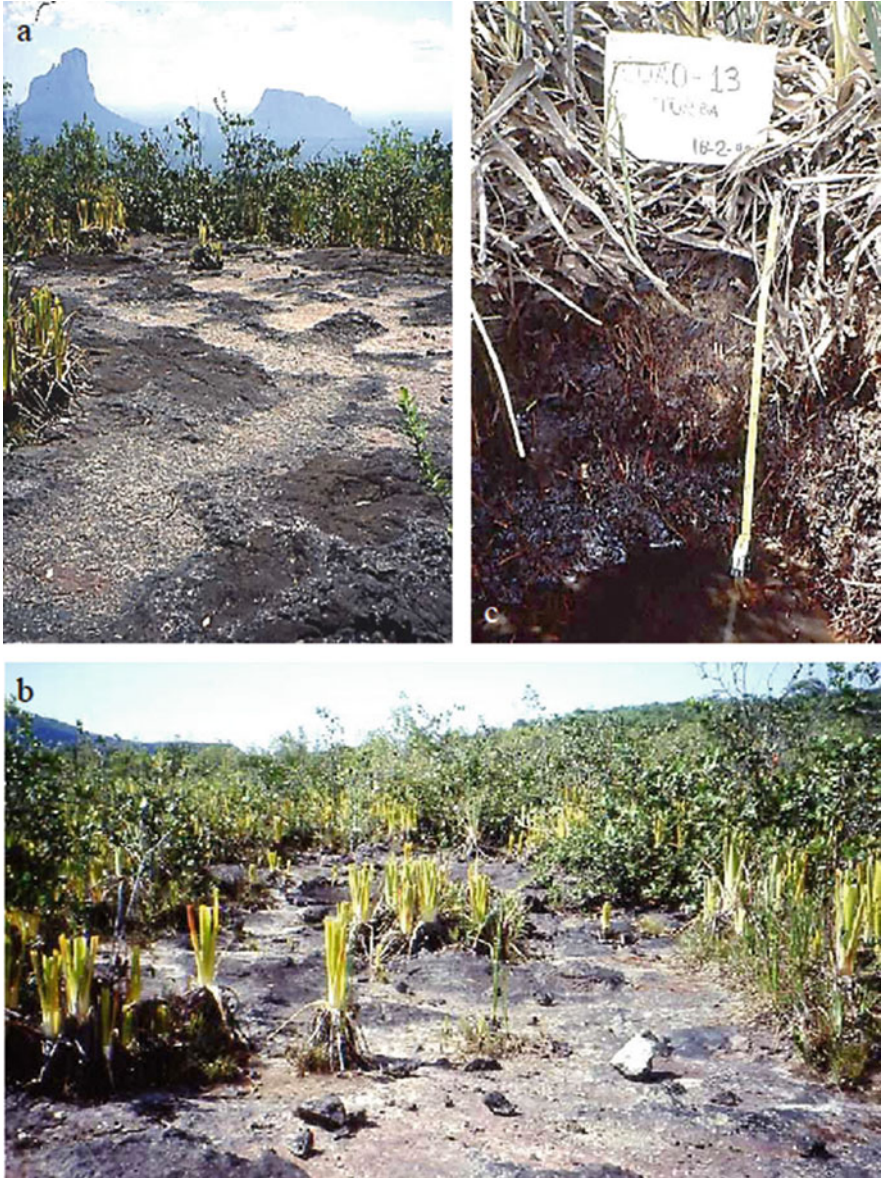


**Plate 8.2** Sandstone meseta in the Cuao-Sipapo massif (720 m a.s.l.); (a, b) karren microtopography of mounds with bare rock and depressions with sandy weathering residues, uncovered upon sliding of the peat mantle (c); sand is removed by runoff and transferred to lowlands via external and internal drainage (Zinck et al. 2011) *Brocchinia* clusters remnant of the original vegetation cover

Sliding of slope peats promoted by water saturation at the peat–rock interface breaks and drags the peat mantle together with the underlying sand debris to pseudokarstic depressions that drain to endokarst or to local creeks that drain directly to piedmont areas (Plate 8.2). As a result, large amounts of sandy materials accumulate and are stored in the piedmonts that circumscribe the base of the tepui escarpment walls before being redistributed to the lowlands. Roraima sedimentary rocks are the most important source of sand feeding the lowland alluvial plains.

More details on karst and pseudokarst morphology in Roraima tepuis and related clastic material production can be found in Zinck and Garcia (2011).

### 8.3.2 Upland Sand Sources

Mountain and hilland landscapes occur at mid-elevations (ca 300–1500 m a.s.l.) forming uplands at the periphery of the lowlands. Typical geofoms are dome-like hills of crystalline bedrocks (granite, rapakivi granite, gneiss) or structural hills (e.g., hogbacks) of (meta)-sedimentary cover rocks (sandstone, quartzite). Some hills have large bare faces and patches, especially on the steepest slopes that are directly exposed to subaerial rock weathering. They often show karst-like features (e.g., runnels) and forms (e.g., dissolution pockets) on siliceous as well as on igneous-metamorphic rocks.

#### 8.3.2.1 Crystalline Domes

Sand production on crystalline domes results from rock weathering on slightly convex summits as well as on steep side flanks (55–60° slope). Sliding and falling of (curved) rock slabs upon exfoliation and splitting expose ledges on lateral cliffs. Pseudokarstic alveolization sculptures cavernous pits, pockets, and pans on the flanks of granitic domes (Zinck and Garcia 2011). These microtopographic terrain irregularities are places where rainwater ponds, acid organic matter accumulate, and weathering takes place. Structure disintegration of the igneous-metamorphic rocks generates sand that is removed and transported by runoff into the flat lowlands.

Dome summits and slope niches and pockets are often covered by dense scrub or forest vegetation including palm trees, where deeper rock weathering takes place. *Profile P102* (350 m a.s.l., 01°41'N, 65°41'W) is located on a crystalline dome summit (10–15% slope) where the Siapa valley exits the Aracamuni massif (Fig. 8.4). A two-layered brownish sandy loam A horizon (1.3–1.9% OC) overlies at 20 cm depth a reddish brown sandy clay loam Bw horizon. The weathering of the leucocratic rapakivi granitoid gneiss has generated a soil material that shows a fairly constant particle size distribution pattern over the whole depth. It is a fully unsorted weathering product in which all particle sizes are represented, reflecting the size variability of primary mineral grains in the rapakivi gneiss. Silt and clay are derived mainly from the chemical alteration of the ferromagnesian minerals and feldspar phenocrysts, while sand results from mechanical fragmentation along joints of the quartz matrix. Average contents of the profile are 60% sand, 22% silt, and 18% clay. During the rainy season, the water-saturated soil-forest cover tends to fragment at the



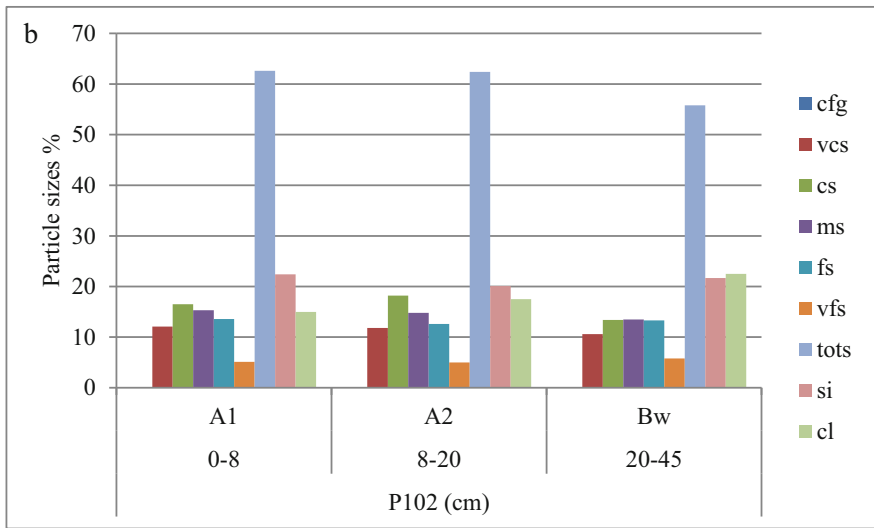


**Fig. 8.4** Aracamuni massif; (a) cavernous weathering pits and pockets on the summit and flanks of a granitic dome; water concentrates and peat forms in the relief niches where rock weathers and residual sand accumulates; (b) mechanical fragmentation leads to unsorted sand formation, while chemical weathering produces silt and clay; episodic overflow and runoff transfer the loose clastic material to the foot of the hill

edges; patches thereof are detached and slide on the convex slope to the foot of the dome. Subsequently, runoff operates a particle selection of the material washing away the fines, while bleaching and reworking the sand. This process, repeated in time and space, is a relevant source of fresh sand that is stepwise incorporated in and redistributed over the lowlands. Weathering products of igneous-metamorphic rocks are also source of nutrients for the adjoining toeslopes (40 ppm K in the A horizon compared to traces in the reworked white sands in the lowlands).

Pseudokarstic depressions occur commonly at the top of bare crystalline domes. They result from rock weathering in terrain concavities where rainwater stagnates and organic matter from colonizing pioneer plants accumulates in thin peat layers. Zinck and Garcia (2011) report the formation of coarse sand and fine gravel layers up to 30 cm thick at the bottom of granodiorite weathering depressions in the Cua-Sipapo massif. Overflow of the depressions during the rainy season spreads the sand debris along the dome flanks.

Although total erosion rates of the Guayana Shield basement rocks evaluated from river data are extremely slow, ca 10 m per million of years, the penetration rate of the weathering front into the fresh substratum is considered to be about twice the denudation rate (Edmond et al. 1995). This indicates sustained production of regolith in the weathering pockets and debris removal at the crystalline dome surfaces.

### 8.3.2.2 Sedimentary Structural Reliefs

Although uplands are mainly the domain of igneous-metamorphic basement rocks, there are also remnants of the original Roraima sedimentary cover. They form sandstone and quartzite plateaus and other structural reliefs the erosion of which delivers clastic materials. Two selected profiles illustrate sand production from quartzite and sandstone, respectively. Both are shallow profiles that reflect the sustained removal of the weathering products by erosion and thus the transfer of sand to the lowlands.

The Aracamuni massif at the southern edge of the study region includes structural mesetas forming stepped levels from 500 to 1500 m a.s.l. *Profile P111* (Lithic Udorthents) is located on a tread position within a large perched syncline at 730–750 m a.s.l. (Plate 8.3a–c). Slope is 3–4% at the observation site, but increases to about 10% downslope. Cover is low shrubby woodland (5–8 m high) including tepui elements (e.g., *Bonnetia* spp.) and lowland elements (e.g., species of *Brocchinia*, *Schoenocephalum*). Below a thin organic top layer, material is light brownish gray very fine loamy sand (Plate 8.3d, e). The soil rests on a hard white quartzite slab at 36 cm depth. Dark colored streaks of organic matter cross obliquely the mineral material and deformed organic lamellae alternate with loamy sand on top of the quartzite, suggesting that the soil material tends to slide on the bedrock. The weathered product is on average 78% sand, 18% silt, and 3% clay. Physical disaggregation of the quartzite generates a large spectrum of sand separates and silt. The mixture of sand from coarse to very fine results from the fracture of the grains that occurred by the time high-grade metamorphism transformed the original sandstone into quartzite.

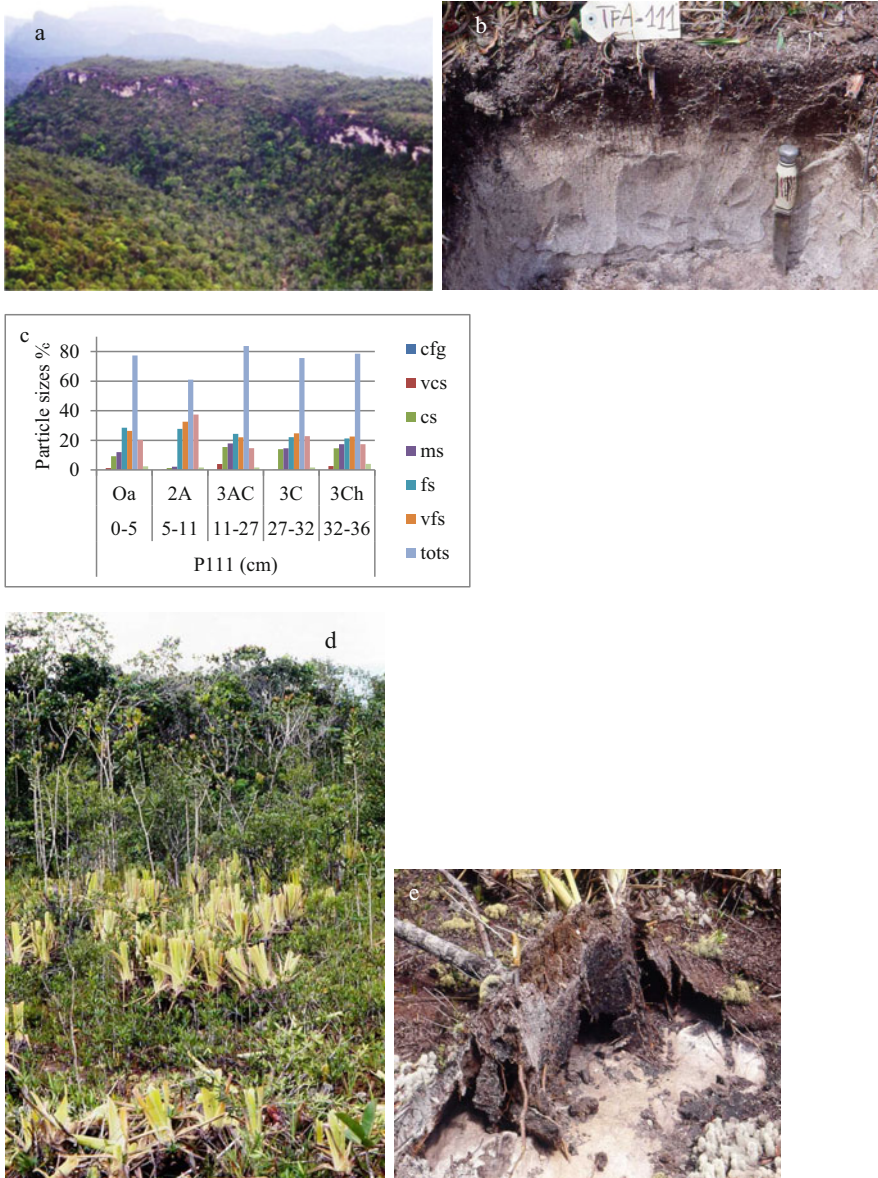


**Plate 8.3** (a) Sedimentary meseta covered by shrubby woodland in the upper watershed of the Siapa river that drains the Aracamuni massif; (b) shallow loamy sand Udorthent formed on the reversal of the meseta; deformation and rupture of organic lamellae suggest that the soil tends to move downslope; (c) unsorted particle size pattern derived from physical weathering of quartzite bedrock. (d) Clearing in the forest cover next to the site of profile P111 in the Siapa watershed, shown in Plate a; (e) upon removal of the sandy soil mantle by sliding, the eroded surface is being recolonized by pioneer vegetation (e.g. *Brocchinia*) and a shallow soil is developing again from the weathering of the quartzite bedrock



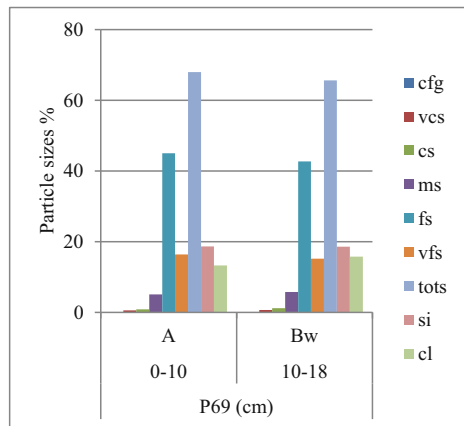


**Plate 8.4** Shallow fine sandy loam Udorthent derived from physical weathering of sandstone on the front face of a structural relief under scrubland on Cerro Mahedi; the top layer is moistened by recent rainfall

Cerro Mahedi is another example of mid-elevation sand production environment, providing sand to the lowlands. Mahedi is a structural plateau massif at 600–900 m a.s.l. that dominates the middle Ocamo river valley, a tributary of the upper Orinoco (Plate 8.4). Important fault tectonics has created a rugged topography of escarpments, cuestas, hogbacks, and excavated anticlines developed in Roraima sandstone. *Profile P69* (Lithic Udorthents) is located on a small flat tread on the front-slope of a cuesta with 30% gradient under shrubby savanna at 650 m a.s.l. The material derived from the weathering of the sandstone above the lithic contact at 18 cm depth is 67% sand, 19% silt, and 14% clay, with a clear predominance of fine sand (44%). Clay impurities are residues of the cement binding together the

sandstone grains. Sandstone weathering produces better sorted sand fraction than quartzite weathering does (see Plate 8.4).

The weathering of both crystalline and sedimentary rocks in the uplands produces substantial amounts of clastic debris that secure continuous influx of fresh sand to the lowlands. Physical fragmentation of sedimentary rocks contributes more sand than chemical weathering of crystalline rocks.

Intense and persistent runoff controlled by 2000–3000 mm rainfall distributed over the largest part of the year causes over-saturation of the hilltop soil mantles that fragment by sliding downslope creating openings in the forest cover. Weathered sandy debris are collected by creeks and moved to the lowlands. This process of sediment transfer contributes abundant amounts of sand that accumulate in piedmont areas before being redistributed to the lowland plains. Fine material (silt and clay) is washed away along the transport and sands are bleached from brownish to whitish. A large part of the white sands in the lowlands is thus allogenic. Highlands and uplands have provided over time and still provide today more sand to the lowlands than any other process of sand generation in the basin at large.

### 8.3.2.3 Intra-mountain Tectonic Depressions

Part of the clastic debris from rock weathering on crystalline domes and sedimentary reliefs is trapped in intra-mountain tectonic depressions that are a common figure in the uplands. According to Mendoza (2005), the last relevant uplift of the Guayana Shield took place in mid-to-upper Eocene, resulting in the formation of grabens, intense dissection, and accelerated erosion. Therefore, tectonic depressions have been acting over time as sediment sinks and storage receptacles (Plate 8.5). Pleistocene dry periods have certainly contributed to sediment filling. Increased rainfall during the Holocene causes now landscape dissection and erosion. Sand is selectively released and remobilized via colluviation into creeks and streams, while remaining coarse fragments concentrate in terrain pavements. Soil and sediment erosion in the upland depressions delivers stepwise new sand influx to the lowlands.

Dark grayish sandy to loamy sand soils similar in morphology to *Profile P38* and *Profile P70* (Plate 8.5) are common on colluvial glacis (2–3% slope) and sediment fillings in upland landscapes, especially in intra-mountain depressions (300–800 m a.s.l.). They are mainly found under grassland with relevant organic matter production and incorporation in profile depth. Data from five selected profiles show that the A horizon is usually as thick as 50 cm. Organic carbon content is on average 1.2% (0.63–2.5%) in the top 10 cm and 0.9% (0.59–1.79%) in the upper 50 cm. Content of fines is always more than 5%, usually 10–15%. When these soils are eroded, a large part of the organic matter and fines is lost in the course of displacement to the lowlands. This results in the impoverished end product of Quartzipsamments in the alluvial plains, with an average organic carbon content of 0.29% (0.12–0.54%) in the ochric epipedon and 0.16% (0.03–0.34%) in the C layers (see Sect. 7.3.1.2 in Chap. 7).

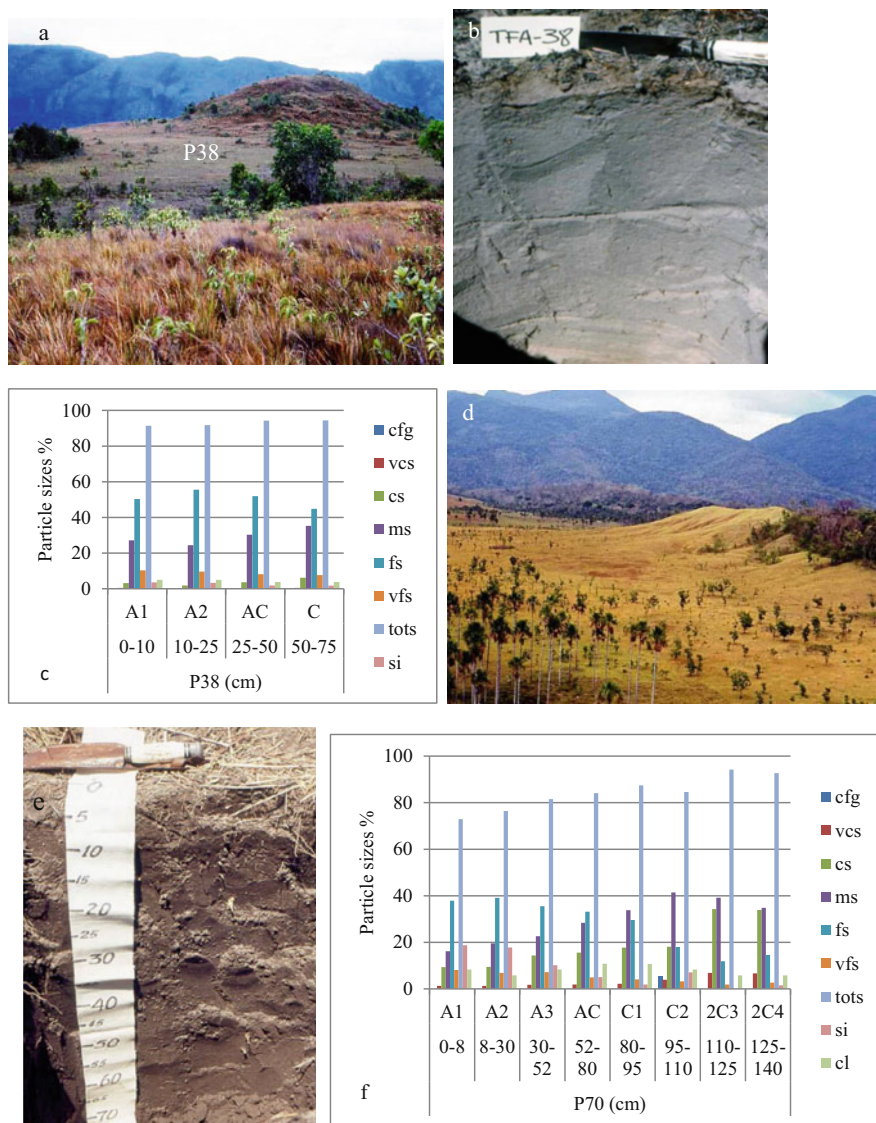


**Plate 8.5** (a) Tectonic depression within the Cerro Parú plateau (800–850 m a.s.l.), incised by the upper watershed of Parú river (450 m a.s.l.); (b, c) dark grayish homogeneous sandy soil with fine and medium sand dominant, developed under grass cover on the colluvial glacia (2–3% slope) that surrounds the sandstone hill in the upper right of the landscape picture. (d) Intra-mountain tectonic basin enclaved in the Mahedi massif (800–900 m a.s.l.); (e, f) Dark grayish loamy sand soil (P70) with medium and fine sand dominant, developed on colluvial sediments filling the bottom of the depression (330 m a.s.l.); dense grass cover (0.8–1 m high) generates relevant organic matter contents (2.5–1.6–1.2% OC in the three consecutive A horizons)

## 8.4 Lowland Sand Sources

### 8.4.1 Subsurface Sand Generation Under Forest and Scrubland in Undulating Lowlands

Lowlands are the sink of sand imported from the surrounding higher relief areas. However, sand is also generated in the lowlands themselves. Two types of processes have been proposed to explain the production of sand in gently sloping landscapes covered by woody vegetation (i.e. “terra-firme” forest, caatinga, and bana) from research carried out in the Rio Negro basin. Hereafter, it is referred to as the weathering model and the transformation model, respectively. Sandy materials resulting from these processes may be subsequently reworked by runoff and creek transport to feed sand covers in flat meadow lowlands.

#### 8.4.1.1 The Weathering Model

The weathering model focusses on quartz sand as a residual product derived from weathering of granitic or gneissic substratum. Deep, subsurface vertical pedodynamics is the central process of this sand production model.

Working in the area of San Carlos de Rio Negro, Schnütgen and Bremer (1985) have considered several possibilities to explain the formation of quartz sand in their study area, referring to hypotheses and conclusions forwarded by earlier research on sand covers in distinct parts of the Amazon basin. They include sands coming from the Guayana highlands and redistributed by lowland rivers, sands derived from a Tertiary shallow sea, and sand influx from eolian activity. In this context of multiple possible origins, the authors privilege the analysis of sands as relicts from weathering of the granitic substratum.

The authors have sampled soils, weathering materials derived from granite, and river sediments in the area between San Carlos de Rio Negro and Solano on river Casiquiare. A detailed toposequence was studied, including a hillslope under rainforest and an adjoining low-lying surface with open bana scrub vegetation. The sand cover is up to 1.8 m thick and lies above kaolinitic saprolite resulting from weathering of Precambrian metamorphic granite. Oxisols occur on the upper segment of the hillslope, Ultisols on the lower segment, and Podzols in the bana area. A poorly drained vale with palm trees, incised by channels (locally called *zuros*), separates the foot of the hill from the bana. The Atlas del Inventario de Tierras del Territorio Federal Amazonas (MARNR-ORSTOM 1986) shows that this kind of landscape is recurrent and thus quite representative of parts of the Amazon territory in Venezuela. Using heavy minerals, particle size distribution, and shape of the sand grains, the authors sustain that sands are residual products of the igneous-metamorphic bedrock weathering and refute the other origin hypotheses.

Among heavy metals minerals, zircon dominates overwhelmingly in Oxisols, Ultisols, bana soils, granite saprolite, and granite rock, as well as in sediments of local creeks draining granitic areas, with only occasional traces of other minerals. By contrast, the mineral spectrum of the sediments of the Rio Negro, Guainía, and Casiquiare rivers is much more diverse, including zircon, but also relevant



proportions of sillimanite, staurolithe, disthene, epidote, hornblende, and pyroxene, together with minor proportions of turmaline, rutile, and andalusite, sometimes also monazite. Although much less resistant than zircon, some of these minerals have been transported from relatively distant areas. Sillimanite in the sediments of rivers Guainía and Rio Negro has undergone a transport of at least 100 km from its source in the Complejo Migmático de Mitú in Colombia. On basis of the heavy mineral analysis, the authors conclude that the bana sands cannot proceed from distant fluvial transport and are most probably weathering products, very similar to the material derived from weathering of granite. White sands in the study area are thus an in situ residual, almost mono-specific (quartz) material related to the granitic substratum.

Grain size was also used by the authors to elucidate the origin of the quartz sands. Bana sands are characterized by a high content of medium sand. The coarse sand fraction is much lower than that of granite saprolite because of stronger solutional quartz weathering as revealed by the analysis of thin section and electron microscope images. Bana sands depart also from eolian sands that lie usually in the fine sand fraction as well as from fluvial and marine sands that are in general better sorted. Overall, particle size distribution of fine earth and sand fraction in bana samples shows affinity with the weathering materials of the study area.

The grain shape was analyzed by the authors on thin section and scanning electron microscope images. Bana sand is made up of elongated to oval grains, with relatively smooth surface and deep alveolar dissolution cavities. This is also the case of the sand grains in the kaolinitic saprolite. Fluvial sand grains are less elongated and have dull surfaces caused by grain impacts. The caverns carved in the sand grains by corrosion, as revealed by the electron microscope, are particularly striking and show that quartz dissolution is an ongoing process in the bana environment.

The authors conclude that the cover sands of the bana terrains are strongly impoverished relicts of the weathered substratum, formed in situ by vertical dynamics. They assume that the fine saprolite particles have been removed by underground percolation and/or surficial flooding, leaving an almost pure quartz residuum cover. This may have resulted in lowering the original terrain surface by several meters.

In conclusion, weathering causes the acid crystalline rocks of the substratum to disintegrate, followed by depletion of the soluble and colloidal substances through deep leaching or surficial loss through selective removal by water overflow. This process may be prevailing in parts of the lowlands where vertical percolation and deep drainage are dominant as, for instance, in woody peneplain areas, similar to the studied transect setting.

#### **8.4.1.2 The Transformation Model**

In contrast to the weathering model based on vertical pedodynamics, the transformation model postulates a mechanism of sandy albic horizon formation via lateral evolution of a catenary soil mantle involving the podzolization of Ultisol-Oxisol associations. This transformation process has been studied in various tropical areas (e.g., Lucas et al. 1987; Bravard and Righi 1989, 1990; Do Nascimento et al. 2004).

A thorough presentation based on examples from Rio Negro basin has been proposed by Dubroeuq and Volkoff (1998).

The authors have studied sites distributed over the Rio Negro basin from the upper stretches of the river and tributaries in Venezuela and Brazil down to the confluence area with the Amazon. The sites were considered representative of selected landscape types, including ferrallitic convex hills, low hills, low hills with flat interzones, ferrallitic plains, podzolic plains, and peat areas. At each site, a toposequence was described. The features observed in pits and auger holes were extrapolated to show the organization of the soil horizons in continuous soil mantles. Diagnostic horizons previously recognized via soil inventory in the Venezuelan Amazon region (MARNR-ORSTOM 1986) served as reference types. The properties and spatial distribution of the horizon types along the toposequences were used to analyze the dynamic relationships between consecutive landscape segments and the transformation processes of the material. Horizon types included pale to black humic horizons, albic and other eluvial horizons, spodic and alios horizons, argillic horizons, oxic horizons, red to white plinthite, and saprolite, among others. A large array of laboratory analyses was performed, including thin sections examined under optical microscope, particle size distribution, heavy mineral identification, X-ray diffraction, total chemical analyses to separate primary minerals, selective chemical extractions of Al, Fe, and Si oxihydroxides, and ultracentrifugation to separate cryptocrystalline silica grains in E horizons.

Oxisols, Ultisols, and Spodosols were found as members of soil toposequences developed from similar parent materials throughout the Rio Negro basin, more specifically in two landscape types, i.e. low hills and ferrallitic plains on crystalline basement. The authors consider that the occurrence of Spodosols with sandy albic horizons at the foot of ferrallitic hills, in inter-hill colluvio-alluvial depressions, and more largely in ferrallitic plains can be given three explanations: (1) white quartz sands can be alluvial sediments distributed by river overflow; (2) they can be colluvial materials transferred from upslope to hill surroundings; and (3) they can derive from the progressive transformation of Oxisols into Spodosols. The authors focus on the last hypothesis and provide detailed field and laboratory data to substantiate their model. They argue that Spodosols with white quartz sand occurring in the lower sequence position can derive from transformation of Oxisols and Ultisols occupying the upper and middle segments of the landscape.

In hilly landscape, the ferrallitic sequence on high convex hills (40–80 m high) did not provide evidence of Spodosol formation and production of autochthonous sand material in footslope position. However, in low hill areas (<30 m high) on gneissic granite, with adjacent or scattered hills, hydromorphic Ultisols with albic horizon and Spodosols were observed. Upon clay depletion, sand grain contents increased gradually along the slope from Oxisol to Ultisol, becoming pure sand in the albic horizon of the hydromorphic Ultisol and Spodosol, the lower end members of the sequences. Downslope, sand grains became smaller and showed dissolution alveoles. Sand of the albic horizons was considered authigenic material, resulting from soil transformation along the slope. One sequence shows an albic horizon penetrating laterally into and forming at the expense of a yellow oxic horizon. The

black humic horizon of the Ultisols and the spodic horizon of the Spodosols showed mineralogical and micromorphological similarities. In both cases, for instance, the fine material coating the sand grains is composed of micro-quartz, organic matter, and small amount of kaolinite. Authors argue that these features, among others discussed in the paper, advocate in favor of sand layer formation *in situ* rather than allogenic sand deposition by rivers.

The ferrallitic plain is a flat to slightly undulating landscape in the central and eastern parts of the Rio Negro basin. A typical toposequence on very gentle slope includes a yellow Oxisol, a mottled Ultisol, a bleached hydromorphic Ultisol with a compact albic horizon, and finally a waterlogged Spodosol. As in the former case, the sandy albic horizon seems to form at the expense of a yellow oxic horizon and is explained as being related to the upwelling of groundwater to the soil surface in the footslope position.

The authors summarize the process of white-sand formation via lateral evolution of the soil catena as follows. In ferrallitic low hill and plain landscapes, transformation of Oxisols into Spodosols involves clay depletion through acidic hydrolysis and oxide removal. Subsequently, yellow oxic and plinthic horizons are bleached into white sands induced by lateral drainage and upwelling of the groundwater to the soil surface.

The loss of substances from the Oxisols causes a depression of the hill summit terrain and lowering of the hill elevation, while the lateral evolution of the soil catena with transformation of the oxic horizon into albic horizon leads to the retraction of the hillside and shrinking of the basal hill surface area. As a consequence, the inter-hill space tends to expand and white sand mantles to enlarge.

However, the largest extents of Spodosols do not occur in the ferrallitic landscapes but in the podzolic plains that are widespread in the southwest of the basin. Deep white-sand mantles cover the terrain surface which can be interpreted as being the albic horizon of giant Spodosols, but are classified as Quartzipsamments. At depths of up to ten meters, discontinuous hardpan strata of dark-brown sand grains covered by oxides and organic matter reflect the podzolization process. These giant Spodosols are frequently interspersed with patches of Histosols. The authors consider that peat profiles gradually evolve into Spodosols in areas where groundwater is shallow, with the formation of a compact albic horizon. The actual origin of the sandy material is not elucidated. Does podzolization generate sand or is sand the condition for podzolization to develop?

The two modalities of *in situ* sand generation, i.e. through deep substratum weathering and lateral ferrallitic soil transformation, respectively, occur in the Amazon lowlands under different types of woody cover from low bana scrubland to high terra-firme forest in undulating to hilly reliefs. However, they do not account for the sand cover building and dynamics taking place in the extensive, fairly flat meadow areas where river activity plays an important role in distributing and reworking authigenic as well as allogenic sands. Neither of the two models accounts for the sedimentary stratifications and lithological discontinuities observed in meadow sands. The features, formation, and evolution of the sand covers in meadow environment are described in Chap. 9.

## 8.4.2 Subaerial Sand Generation

In the alluvial plain and peneplain lowlands under meadow vegetation, the podzolic transformation model does not apply because there are no Oxisol-Ultisol-Spodosol toposequences, while the bedrock weathering model is superseded by surface sedimentological processes controlled by shifting river activity. The meadow environment is a domain where other processes of authigenic white-sand formation take place and where reworking of allogenic white sand prevails over in situ generation. Sand debris are produced by rock weathering on residual hills and other kinds of rock outcrops frequent in peneplain landscape.

### 8.4.2.1 Sand from Weathering of Residual Reliefs

Residual rocky reliefs are scattered irregularly over the lowlands. They vary in elevation, physiography, and lithology. Typically, residual geofoms are dome-like hills of crystalline rocks (granite, rapakivi granite, gneiss). They occur as small hill clusters and sometimes as larger hilllands of 250–300 m relative elevation. Lines or hummocks of subvertical to vertical bars and slabs/blocks of sedimentary and crystalline rocks, a few meters high are local remnants of incomplete bedrock peneplanation. Widespread hills and other outcropping bedrock structures, including rocky inselbergs, show sand formation in pseudokarstic alveoles and pockets and provide continuous sand supply to the surroundings.

### 8.4.2.2 Sand from Weathering of Rock Bar Outcrops

Sedimentary, metasedimentary, and crystalline rock outcrops on the terrain surface are frequent throughout the peneplain landscape. Sedimentary rocks occur commonly as tectonized subvertical to vertical alignments of sandstone or quartzite bars. Also, gneiss bar alignments were observed in some places. Sandstone bars are generally grouped in fields, but may occur also as isolated flagstones. Height varies from 0.2–0.3 m up to 5–6 m. Sandstone rock is pale, sometimes slightly pinkish, slightly arkosic, with quartz veins, and pseudokarstic alveoles. Physical weathering disintegrates the rock into white sands, sometimes mixed with some gravel, that accumulate between and around the outcropping flags (Plate 8.6). Rocks are not only loosened and disaggregated, but the sand grains themselves are fragmented by corrosion and reduced in size. Subaerial weathering of sandstone outcrops is an important source of authigenic fresh sand that is incorporated into the sand pool of the lowlands via colluviation.

Plate 8.6 shows the particle size distribution of a fine-grained white sandy material resulting from subaerial weathering of coarse-grained arkosic sandstone outcrops in shrubby meadow 20 km north-west of San Antonio, on the interfluvium between river Orinoco and upper Caño Caname (*P5 Lithic Quartzsammant*, 120 m a.s.l.). The arenization product of the flagstones is on average 99% white sand, with 51% fine sand and 34% medium sand, above a thin gravelly Cr layer and the sandstone at 30 cm depth.

In addition to scattered flagstone fields, peneplains and sometimes plains are also crossed by protruding rock alignments often covered by shrubs. Subaerial rock

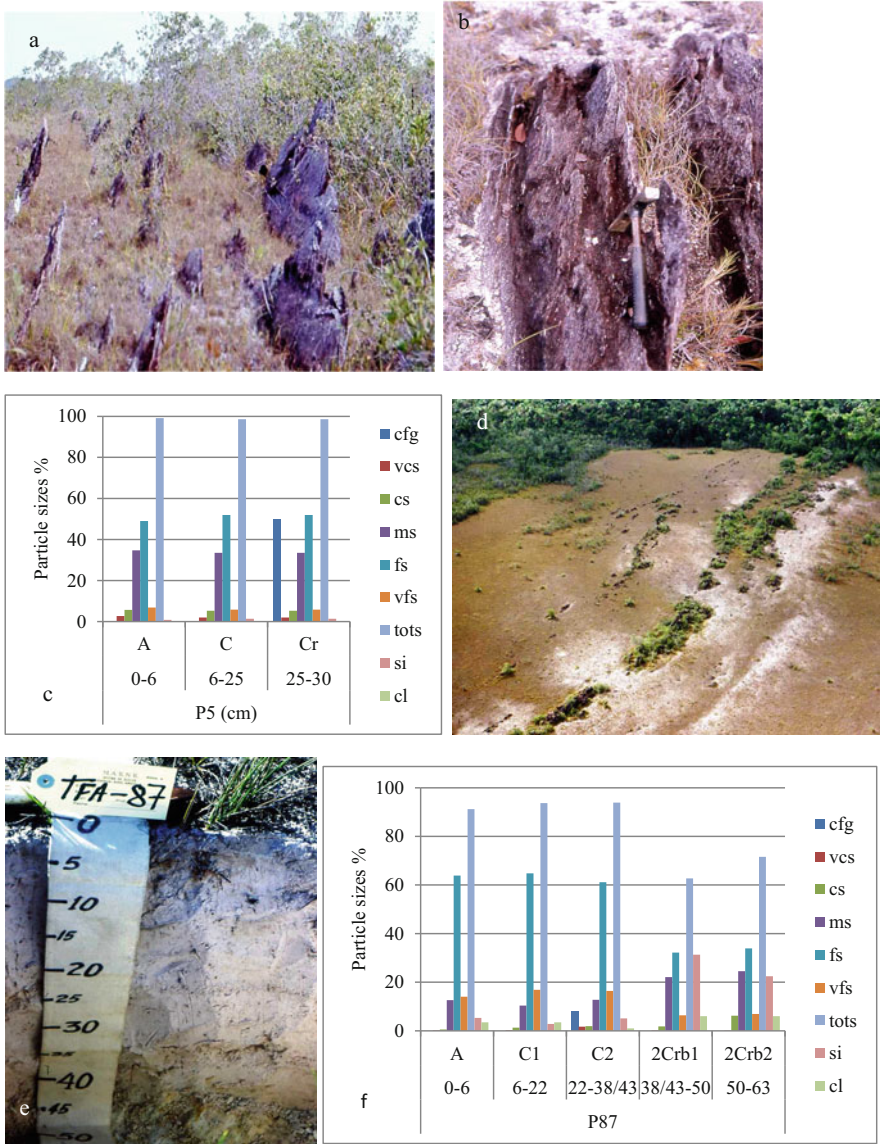


**Plate 8.6** (a, b) Flagstone field under shrubby meadow; (c) the weathering of the thin-bedded gneiss flags leaves a quartz-sand residue forming a shallow Quartzipsammit (P5); area of San Antonio, on the left Orinoco bank. (d) The weathering of outcropping sandstone crests covered by shrubs on a peneplain glacis (1–2% slope); (e, f) generates the white-sand layers of an Udorthent (P87) with more than 60% fine sand, that buries a weathering graywacke substratum at 38/43 cm depth; area of San Antonio, on the left Orinoco bank

weathering releases white sand that is usually redistributed on the gentle slopes surrounding the flagstone fields and rock lines by rill and inter-rill rainfall runoff forming colluvial glacia. Plate 8.6 shows a colluvial sand cover (0–38 cm) burying an unconformable weathering graywacke substratum (*Profile P87*).

Similar rock outcrops called *campo rupestre* (rock field) have been described in Brazilian Amazonia by Anderson (1981). Rock outcrops grade into sandy soils where unusual, often endemic herbs and shrubs with whorled leaves grow.

#### **8.4.2.3 Sand from Soil Movements on Forest-Covered Low Hills**

Colluvial and mass movements of soil materials operating at hill surface contribute sand to the footslopes. *Profile P117* is located on the sideslope (10–15%) of a granite hill about 20 m high, covered by terra-firme forest, close to San Carlos de Rio Negro. It is a complex Kanhapludult profile. The sand separate pattern is unsorted and different in each horizon; this reflects the layering of reworked soil material along the slope (Fig. 8.5). The upper part (0–100 cm) is a mixture of soil material formed in situ and red soil fragments from upslope with iron concretions. The lower part (100–200 cm) is an iron-indurated nodular cuirass with pockets of loose red soil material. The fine-earth matrix is overall sandy loam and sandy clay loam. Sand content remains fairly constant over depth (57–67%) with dominance of coarse, medium, and fine sand. Therefore, soils on low granitic hills represent a potential source of sand. Runoff under forest moves surface material downslope into the adjoining meadow environment. Whitish sands occur at the basis of the hills and in inter-hill areas. Thus, surface colluviation on hill summits and slopes under wooded cover is probably as important as catena soil transformation in transferring sands from hills to lowlands.

### **8.4.3 Piedmont Sand: From Storing to Redistributing Allogenic Sand**

The piedmont landscape, especially piedmont at the foot of tepui plateaus, represents a geomorphic connection between highlands and lowlands: the piedmont receives, stores, reworks, and redistributes sediments provided by rock weathering and erosion in higher reliefs.

Uplands and highlands surround the Orinoco basin lowlands to the north, east, and south (see Fig. 8.1 and DEM images in Chap. 6). This peripheral amphitheater of higher reliefs is a source of sediments that has provided sand influx to the lowlands over time. Although weathering and disintegration of crystalline rocks contribute sand production, the most important sand sources however are the Roraima sandstone and quartzite strata that form the tepui plateau landscape covering the crystalline shield basement.

Typically, the slope connecting the summits of the tepui mesetas with the lowlands is composed of three segments: an upper segment corresponding to a fault escarpment of sandstone/quartzite that can be as high as 1000 m; a middle segment mostly covered by low forest corresponding to debris talus (35–40°) where



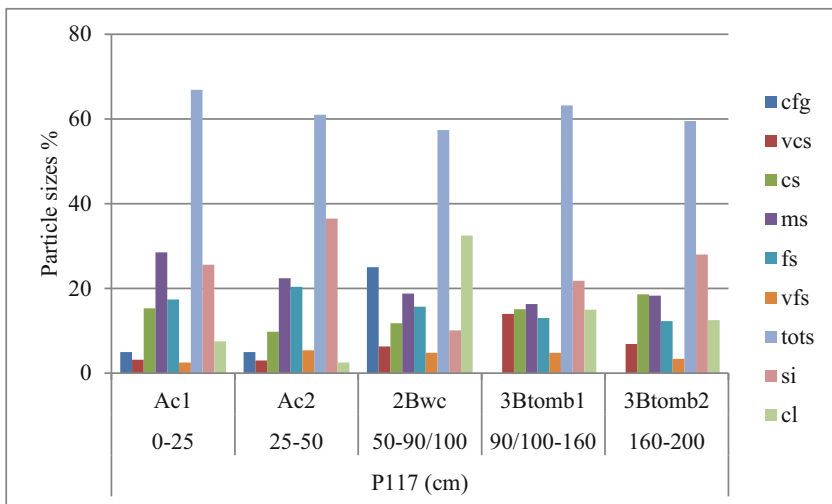


**Fig. 8.5** Heterogeneous hillslope profile; the upper part of profile P117 (0–90/100 cm) is sandy loam to sandy clay loam colluvial soil material moving on an iron-indurated nodular cuirass along the slope of a granite hill under forest cover in the area of San Carlos de Río Negro



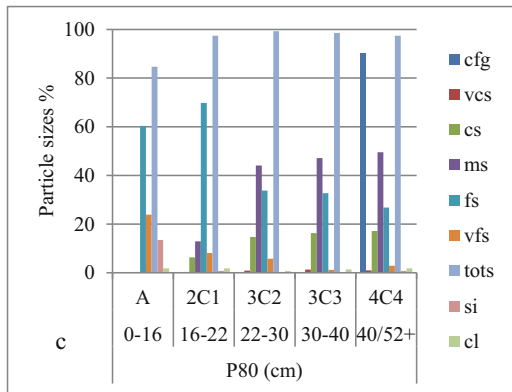


**Plate 8.7** (a) Contact landscape between the south-eastern sandstone escarpment of the Duida massif and the adjoining piedmont area north of La Esmeralda; the upper section of the piedmont (1) corresponds to debris talus (40–45° slope) covered by woodland; the lower section (2) is a fan-glacis of sediment deposited by the creek that incises the escarpment; (b, c) P80 is a sandy over sandy-skeletal Udorthent located on the distal part of the fan-glacis

coarse fragments including large blocks dislodged and falling from the overlying scarp land and accumulate; and a lower segment with a much gentler slope (1–5%) where creeks incising the escarpment deposit part of their load and form a piedmont landscape at the fringe of the alluvial lowland plains. In piedmont areas, sediments especially cobbles, gravel, and sand coming from the uplands accumulate in

fans that enlarge into glacis through fan coalescence (Plate 8.7a). Piedmont areas are the entry door of allogenic sand to the lowlands.

Creeks usually start draining the peat depressions at the concave summits (i.e., perched synclines) of the tepuis. They cascade along the scarp walls and the debris talus or rush into dissolution shafts (i.e., sima) via karstic pipes and galleries and re-emerge at the level of the debris talus. Tepui drainage drags sand produced by subaerial sandstone arenization and pseudokarstic sandstone weathering taking place beneath the acid peat mantles (Zinck and Garcia 2011). This process operating continuously transfers important quantities of sand from top to the foot of the tepui mesetas. Sand accumulates and is temporarily stored in the piedmont before being distributed to the lowlands. A similar process of sand transfer takes place in the upland hills. The summits of the mid-elevation crystalline domes are frequently covered by peat that develops in weathering depressions the drainage of which carries sand to the lowlands. This process takes place all along the periphery of the lowland basin introducing allogenic sand into the lowlands. The piedmont is not a primary source of sand generation but a reservoir of allogenic sand.

*Profile P80* (Typic Udorthents, 300 m a.s.l., 03°19'N, 65°31'W) is located on a piedmont fan-glacis (0.5–2% slope) under shrubby meadow at the south-eastern foot of the Duida tepui massif, about 15 km north of La Esmeralda in the middle Orinoco watershed (Plate 8.7b, c). The soil is stratified including pinkish gray sandy and sandy loam layers that reflect the color of the Roraima sandstone, over a gravelly/stony substratum with sandy matrix at 40/52 cm depth. Organic carbon is 1% in the A horizon (0–16 cm) and 0.1–0.2% in the C layers. On average, the material is 95% sand (85–99%), 4% silt, and 1% clay. Fine sand (49%) and medium sand (26%) dominate. The proportion of the sand separates changes slightly with depth, but the pattern remains fairly the same.

In piedmont places similar to that of profile P80, coarse fragment strata of gravel, cobbles, and stones constitute the base of the fan deposits. Many of the fan-glacis are nowadays stabilized. Their spatial extent and the presence of stony basal deposits reflect an earlier period of geomorphic activity with strong erosion in the highlands and abundant deposition in the lowlands. Torrential accumulations have taken place possibly in contrasted climatic conditions by the end of the Pleistocene, before peat formation started at tepui summits at the onset of the Holocene and before the sand cover layers were deposited more recently (Zinck et al. 2011). Depth to the gravelly/stony substratum varies, usually around 40–50 cm, but can be as shallow as 10–15 cm and as deep as 70–75 cm.

Changes in particle size distribution between sand deposits resulting from sandstone fragmentation at tepui summits and sand deposits in piedmont lying at the foot of tepui plateaus could be expected. Transport of clastic particles from high elevations (ca 1500–2500 m a.s.l.) to low elevations (ca 130–150 m a.s.l.) should result in some fragmentation of the coarse particles, increasing the proportions of fine sand and silt. In Fig. 8.6, averaged particle size distribution values of the five piedmont profiles are compared with those of two tepui summit profiles (Duida and Autana). In all profiles, medium sand and especially fine sand dominate overwhelmingly. There is evidence of silt increase in some piedmont profiles, but there is no

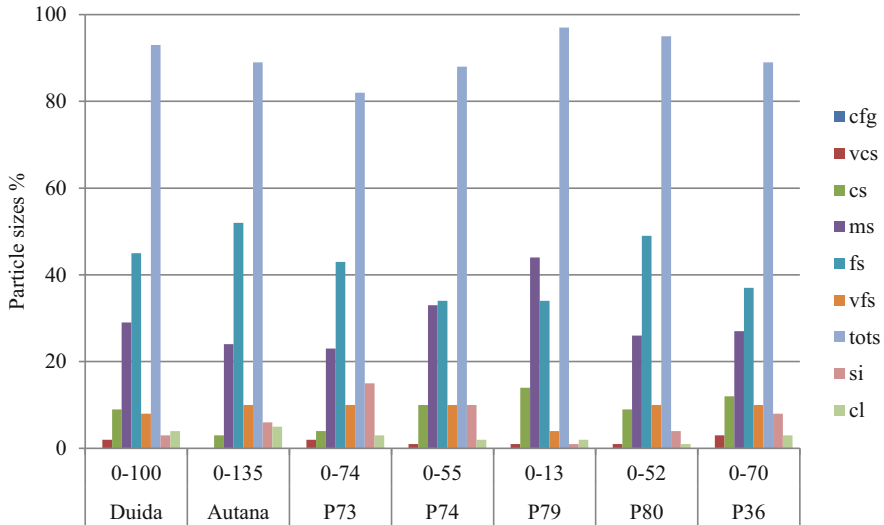


**Fig. 8.6** Similarity of particle size distribution with dominance of medium and fine sand between highland profiles (Duida and Autana) and lower piedmont profiles (P73 to P36)

significant difference in particle size distribution pattern between emitting sand sources at tepui summits and sand receiving places in the piedmont. Color is reddish gray to pinkish gray (5YR5/2–7/2 m) inherited from Roraima rocks.

The fact that particle size distribution is not substantially modified suggests that the transfer of sand from high to low elevations takes place mainly through internal rock drainage. This causes less friction and grain attrition than external drainage along steep rocky creeks. Sand produced at tepui summits results principally from rock fragmentation in crypto-lapies under acid peat cover. Sand is then drained via joints at the bottom of the peat depressions into endokarstic conducts that resurge at piedmont level where sand is mixed with coarse fragments falling from the debris talus.

Connecting highlands and lowlands, the piedmont functions as a geomorphic transit and filter system for incoming sediments. It receives clastic materials of variable sizes from highlands and uplands, retains the coarser fragments, and releases mainly sand to feed lowland sand covers.

## 8.5 Conclusion

Highlands and uplands form a peripheral mountain belt that makes water and sediments converge toward the lowland basin drained by the Orinoco and Rio Negro rivers and their tributaries. These high relief areas are sources of sand produced by rock weathering. In highlands, Roraima sandstone/quartzite plateaus are exposed to subaerial arenization of bare rock terrains and rock fragmentation

under peat mantles. Sand is removed by creeks and underground karstic drainage, and ends up accumulating in piedmonts that surround the basis of the tepui plateaus. In uplands, igneous-metamorphic rocks of the Guayana Shield basement form dome-like hilly massifs. The weathering of the crystalline rocks generates multi-mineral clastic debris, but mafic minerals and feldspars are quickly depleted, leaving a quartz-sand residuum that accumulates at the basis of the hills. These processes of rock weathering acting over millions of years have generated considerable masses of sand that have been mobilized by runoff and streams from their transitory storage at footslopes and in piedmonts and distributed as allogenic sands over the lowlands. Sand is fully bleached from original pinkish or brownish staining in acid runoff water over short distance transport.

There is also authigenic sand production in the lowlands themselves. Subsurface processes acting in undulating landscapes under woody vegetation cover generate white sands. The transformation model explains the formation of sandy albic horizons through lateral evolution of Oxisol-Ultisol toposequences. In ferrallitic low hill and plain landscapes, transformation of Oxisols into Spodosols involves clay depletion through acidic hydrolysis and oxide removal, and correlative increase of sand content. Yellow oxic and plinthic horizons are bleached into white sands induced by lateral drainage and upwelling of the groundwater to the soil surface. In contrast, the weathering model focusses on quartz sand as a residual product derived from weathering of granitic or gneissic substratum. Deep, subsurface vertical pedodynamics causes the acid crystalline bedrocks to disintegrate, followed by depletion of the soluble and colloidal substances through deep leaching or surficial loss through selective removal by water overflow. This process may be prevailing in peneplain areas under woody cover where vertical percolation and deep drainage are dominant.

These two modalities of in situ sand generation occur in the Amazon lowlands under different types of forest cover from low bana scrubland to high terra-firme forest in undulating to hilly reliefs. They do not account for the sand cover generation and dynamics taking place in the extensive, fairly flat areas covered by meadow vegetation. In alluvial plains, river activity plays an important role in distributing and reworking authigenic and allogenic sands in layered deposits showing sedimentary stratifications and lithological discontinuities. In peneplains, glacia is the most common geomorphic setting of colluvial sands derived from weathering of rock outcrops and rocky hills. The features, formation, and evolution of the meadow sand covers are described in Chap. 9.

---

## References

- Adeney JM, Christensen NL, Vicentini A, Cohn-Haft M (2016) White-sand ecosystems in Amazonia. *Biotropica* 48(1):7–23
- Anderson AB (1981) White-sand vegetation of Brazilian Amazonia. *Biotropica* 13(3):199–210
- Aymard GA, Schargel R (eds) (2009) Estudio de los suelos y la vegetación (estructura, composición florística y diversidad) en bosques macrotérmicos no-inundables, Estado Amazonas, Venezuela. *BioLlania edic esp* 9, UNELLEZ, Guanare, Venezuela

- Bravard S, Righi D (1989) Geochemical differences in an Oxisol-Spodosol toposequence of Amazonia, Brazil. *Geoderma* 44:29–42
- Bravard S, Righi D (1990) Podzols in Amazonia. *Catena* 17:461–475
- Carneiro Filho A, Zinck JA (1994) Mapping paleo-aeolian sand cover formations in the northern Amazon basin from TM images. *ITC J* 1994-3:270–282
- Carneiro Filho A, Schwartz D, Tatumi SH, Rosique T (2002) Amazonian paleodunes provide evidence for drier climate phases during the Late Pleistocene-Holocene. *Quat Res* 58:205–209
- Do Nascimento NR, Bueno GT, Fritsch E, Herbillon AJ, Allard T, Melfi AJ, Astolfo R, Boucher H, Li Y (2004) Podzolisation as a deferrallitization process: a study of an Acrisol-Podzol sequence derived from Palaeozoic sandstones in the northern upper Amazon Basin. *Eur J Soil Sci* 55:523–538
- Dubroeuq D, Volkoff B (1998) From Oxisols to Spodosols and Histosols: evolution of the soil mantles in the Rio Negro basin (Amazonia). *Catena* 32:245–280
- Edmond JM, Palmer MR, Measures CI, Grant B, Stallard RF (1995) The fluvial geochemistry and denudation rate of the Guayana Shield in Venezuela, Colombia, and Brazil. *Geochimica et Cosmochimica Acta* 59(16):3301–3325
- Herrera R, Jordan C, Klinge H, Medina E (1978) Amazon ecosystems. Their structure and functioning with a particular emphasis on nutrients. *Interciencia* 3:223–232
- Horbe AMC, Horbe MA, Kenitiro S (2004) Tropical Spodosols in northeastern Amazonas State, Brazil. *Geoderma* 119(1-2):55–68
- IGAC (2014a) Estudio general de suelos y zonificación de tierras del Departamento de Guainía, escala 1: 100,000. Instituto Geográfico Agustín Codazzi, Subdirección de Agrología, Bogotá
- IGAC (2014b) Estudio general de suelos y zonificación de tierras del Departamento de Vichada, escala 1: 100,000. Instituto Geográfico Agustín Codazzi, Subdirección de Agrología, Bogotá
- Irion G (1984) Sedimentation and sediments of Amazonian rivers and evolution of the Amazonian landscape since Pliocene times. In: Sioli H (ed) *The Amazon. Limnology and landscape ecology of a mighty tropical river and its basin*. Kluwer, Dordrecht, pp 201–214
- Klammer G (1978) Reliefentwicklung im Amazonasbecken und plio-pleistozäne Bewegungen des Meeresspiegels. *Z Geomorph NF* 22:390–416
- Klammer G (1984) The relief of the extra-Andean Amazon basin. In: Sioli H (ed) *The Amazon. Limnology and landscape ecology of a mighty tropical river and its basin*. Kluwer, Dordrecht, pp 47–83
- Klinge H (1965) Podzol soils in the Amazon basin. *J Soil Sci* 16(1):96–103
- Lucas Y, Boulet R, Chauvel A, Veillon L (1987) Systèmes sols ferrallitiques-podzols en région amazonienne. In: Righi D, Chauvel A (eds) *Podzols et podzolisation*. AFES et INRA, Plaisir et Paris, pp 53–65
- Malagón Castro D (1995) Estudio genético-taxonómico de Espodosoles, Ultisoles y Oxisoles y su relación con el manejo de las tierras en el Departamento del Vaupés (Colombia). Universidad Nacional de Colombia, Bogotá
- MARNR-ORSTOM (1986) Atlas del inventario de tierras del Territorio Federal Amazonas (Venezuela). Dirección de Cartografía Nacional, MARNR, Caracas
- Medina E, Cuevas E (2011) Complejo caatinga amazónica: bosques pluviales esclerófilos sobre arenas blancas. *BioLlania edic esp* 10:241–249. UNELLEZ, Guanare, Venezuela
- Mendonça BAFD, Simas FNB, Schaefer CEGR, Fernandes Filho EI, Vale Júnior JFD, Mendonça JGFD (2014) Podzolized soils and paleoenvironmental implications of white-sand vegetation (Campinarana) in the Viruá National Park, Brazil. *Geoderma Reg* 2-3:9–20
- Mendoza V (2005) Geología de Venezuela: Escudo de Guayana, Andes Venezolanos y Sistema Montañoso del Caribe. Universidad de Oriente, Ciudad Bolívar
- Prance GT, Schubart HOR (1978) Notes on the vegetation of Amazonia. I. A preliminary note on the origin of the open white sand campinas of the lower Rio Negro. *Brittonia* 30(1):60–63
- Pulido Roa C, Malagón Castro D (1996) Estudio genético y taxonómico de Espodosoles, Ultisoles y Oxisoles y su relación con el manejo de las tierras. In: *Aspectos ambientales para el*

- ordenamiento territorial del Municipio de Mitú, Departamento del Vaupés. Instituto Geográfico Agustín Codazzi, Bogotá, Colombia, Tomo I:307–399
- Putzer H (1984) The geological evolution of the Amazon basin and its mineral resources. In: Sioli H (ed) *The Amazon. Limnology and landscape ecology of a mighty tropical river and its basin*. Kluwer, Dordrecht, pp 15–46
- Quesada CA, Lloyd J, Anderson LO, Fyllas NM, Schwarz M, Czimczik CI (2011) Soils of Amazonia with particular reference to the RAINFOR sites. *Biogeosciences* 8:1415–1440
- Schnütgen A, Bremer H (1985) Die Entstehung von Decksanden im oberen Rio Negro-Gebiet. *Z Geomorph NF Suppl Bd* 56:55–67
- Sombroek WG (1984) Soils of the Amazon region. In: Sioli H (ed) *The Amazon. Limnology and landscape ecology of a mighty tropical river and its basin*. Kluwer, Dordrecht, pp 521–535
- Zinck JA, Garcia P (2011) Tepui peatlands: setting and features. In: Zinck JA, Huber O (eds) *Peatlands of the western Guayana highlands, Venezuela. Properties and paleogeographic significance of peats*. Ecological studies 217. Springer, Heidelberg, pp 91–126
- Zinck JA, Garcia P, van der Plicht J (2011) Tepui peatlands: age record and environmental changes. In: Zinck JA, Huber O (eds) *Peatlands of the western Guayana highlands, Venezuela. Properties and paleogeographic significance of peats*. Ecological studies 217. Springer, Heidelberg, pp 189–236



# Sand Dynamics and Distribution in Meadow Environment: A Geo-Pedological Approach

# 9

J. A. Zinck and P. García Montero

## 9.1 Introduction: The Lowland Sandscapes

Lowland meadows *sensu lato* include vegetation variations from nearly pure herbaceous to shrubby formations. Vegetation and sand combine in a variety of sandscapes. The most striking sandscapes are those that are practically bare or have very scattered vegetation. They appear as shiny white surface areas of variable dimensions, from small islands surrounded by woodland to large stretches separated by palm tree swales. The largest open white sand areas result commonly from vegetation cover degradation by yearly repeated and expanding fires; others result from new sand deposition by shifting rivers and streams.

It is uncommon to find deep weathering profiles at the terrain surface in the flat meadow lowlands, as the weathering front of the bedrock substratum is generally buried under cover sands.

In this chapter, a geopedological approach is used to describe the variety of sandy materials included in the general term of “white sands” and to analyze the spatial distribution of the sands in a geomorpho-dynamic context in relation to different types of geoforms. In addition to the spatial dimension, this analysis establishes a typology of geoforms that can be used as reference sites to identify correlations between geophysical environment and variations of the vegetation cover in physiognomic and floristic terms.

Core objectives of the geophysical study of the meadow environment are (1) compare and correlate point data including field observations and supporting laboratory data, (2) generate general knowledge about landscape settings and soil-sediment

---

J. A. Zinck (✉)

Faculty of Geo-Information Science and Earth Observation (ITC), University of Twente, Enschede, The Netherlands

P. G. Montero  
Caracas, Venezuela



characteristics, and (3) finally establish a typology of soil-landscape situations that allow correlations with floristic variations of the meadow vegetation cover. Basic to these objectives is investigating the origin and spatial distribution of the (white) sands on which meadow plants, especially endemics have established.

Field descriptions of site settings and morphology of soil-sediment profiles, together with laboratory analyses of particle size distribution, organic carbon, and pH values, are interpreted to reconstitute the sedimentological dynamics and history of the surficial white sand covers to the depth of about 2 meters. Site analysis and correlation of point data are geared toward generating information that is further transformed and generalized into knowledge about geomorphic processes and resulting geofoms in sand covers.

Bar graphs are used to analyze sedimentological and pedological features in depositional environments. They were used here to identify:

- Stratifications and lithological discontinuities in the sand covers to understand the sedimentological history and evolution of the landscape
- Particle size distribution patterns leading to determining the main depositional facies of the area (e.g., alluvial splay, alluvial overflow, eolian, colluvial) and unraveling features of Holocene sedimentation
- Truncation or fossilization of soil profiles to reveal the history of soil formation

Sand cover sediments vary from well to poorly sorted according to the depositional process involved. The relative importance of the sand separates as shown in the particle size distribution diagrams (i.e., bar graphs) reflects the degree of sediment sorting. As a general rule, the following criteria were implemented: one or two dominant sand separates indicate good sorting, while more than two dominant sand separates indicate a trend to poor sorting. This allows distinguishing, for instance, between the two main depositional processes and resulting sediment facies in the alluvial plains, i.e., overflow and splay, respectively.

First, an inventory was made of the main landscape types and geofoms that sustain meadow vegetation, and subsequently, the sand covers were characterized in a selection of representative geomorphic units. Table 9.1 shows (1) the variety of sand sources in the highlands and uplands that surround the lowlands and in the lowlands themselves (described in Chap. 8), (2) the geomorphic landscapes and forms in which the sands settle in the lowland sand, and (3) the sedimentological processes by means of which primary sands are reworked and redistributed in the lowlands as residual sands, analyzed in this chapter.

---

## 9.2 Sands in Alluvial Plains

### 9.2.1 Floodplain Dynamics

Alluvial plains are the lowest areas in the lowlands where sands accumulate and are redistributed. Meade (1994) describes the alluvial plain dynamics in the lowlands as characterized by increased storage and reduced transport of sediments during periods

**Table 9.1** Diversity of pathways: from sand generation in the periphery and center of the basin to types of sand settings in meadow lowlands

---

Allogenic sand sources in highlands and uplands:

- Weathering of sedimentary and metasedimentary rocks (sandstone and quartzite of the Roraima group), especially on the table-shaped highland tepuis
- Weathering of crystalline shield bedrocks (acid granites, gneiss), especially in mid-elevation hilly uplands

Authigenic sand sources in the lowlands:

- Deep in situ weathering of crystalline and sedimentary basement rocks
- Lateral transformation of Oxisols-Ultisols into Spodosols along low hill soil catenas
- Surface weathering on rocky hills and local rock outcrops in peneplain landscape

Sedimentological processes of distributing and reworking sands in the lowlands:

- Alluvial (e.g., splay mantles, overflow mantles, splay glacis, depression fillings and avulsion, confluence fans, drainage swales)
- Colluvial-alluvial (e.g., large glacis)
- Colluvial (e.g., short glacis)
- Eolian (e.g., dunes, sheets)

Geomorphic landscapes and forms on which sands are distributed and reworked in the meadow lowlands:

- Piedmont: fan-glacis
  - Peneplain: colluvial-alluvial splay glacis, colluvial glacis, weathering glacis
  - Alluvial plain: floodplain, splay plain, overflow plain, minor geofoms (terrace, river levee, meander lobe, floodplain scroll, scroll bar, sand bar)
  - Eolian activity: dune-like mounds, sand sheets, blanket silt covers
- 

of river peak water discharge. Meade (1994) writes: “A peculiar pattern of seasonal storage and remobilization of suspended sediments occurs in the Orinoco river. When the river stage is near its annual peak, the middle Orinoco reach forms a large area of backwater that includes the lower reaches of a number of tributaries as well as large tracts of intervening floodplains, an area described as an inland delta by Alexander von Humboldt when he visited it in 1800. Floodplains are dynamic, continually gaining sediment by vertical accretion during periods of overflow and losing by lateral erosion. Considerable fine-grained sediment is exchanged between rivers and floodplains by the combination of overbank deposition and bank erosion.”

Meade (2007) refers essentially to the tributaries of the Orinoco’s left bank draining the Llanos plains and carrying sediments from the Andes, in northern Venezuela. But the process described is also true for the tributaries of the right bank of the Orinoco mainstem. Rivers from the Guayana side are blocked by the abundant discharge and sediment load of the rivers coming from the Llanos side. This causes the lower Guayapo, Sipapo, and Autana rivers to run parallel to the Orinoco before being able to join it close to Isla Ratón. As a consequence, water and sediment are stored in the lowlands confined between the lower Ventuary to the south, the Orinoco to the west from San Fernando de Atabapo to Isla Ratón, Cuao river to the north, and the piedmont of the Cuao-Sipapo massif to the east. These lowlands function as a vast storage compartment where water and sediments are retained until the flow in the Orinoco channel decreases and allow the evacuation of stored water. This is also the case of the Atabapo area as a whole and that of smaller stream watersheds. For instance, “caño” Yagua has formed a sort of inland delta east

of Cerro Yapacana where silty sediments are trapped in flooded forest environment. All these areas have high groundwater.

Repeated episodes of storage and remobilization increase the weathering of minerals and rock fragments. As a result, the amounts of quartz increase, and fine particles are removed by the water (Meade 2007). This is true for the Andean sediments on the left bank of the Orinoco but also for the sediments coming from weathering of crystalline rocks on the right bank. Thus, there is a sort of sieving effect leaving quartz sand as a residual end product. Meade (2007) estimates that a considerable amount of sediment might be recycled in a few hundred to thousands of years. This leads to increasing sand concentration in the lowlands.

Alluvial plain landscape is drained by an intricate network of waterways bordered by riparian forest and intertwined with interfluvial woodland. Upon intervention by human activities, including extensive use of fire, woodland is often replaced by meadow vegetation (Plate 9.1). Alluvial plains under meadow cover are dynamic, unstable areas. Herbs, forbs, grass, and small shrubs are unable to fix and stabilize the terrain surface. As a consequence, old stream channels are periodically abandoned and new ones are created by avulsion. Through lateral migration, shifting streams erode sand here and deposit it there. During high water periods, amounts of sand are transported by a dense network of waterways and discharged over the lowlands in riverine and interfluvial areas. Some sediments settle in the proximity of the channels in a variety of riverine features. Most of the sediments are spread over the low-lying interfluvial areas by overflow and splay processes. Present sand covers under meadow result from this past and ongoing sedimentological dynamics that have possibly been active over most of the Holocene. Sand deposits sustaining the meadow environment are polygenic and polychronic. The whole area is a sedimentological palimpsest.

## 9.2.2 Riverine Features and Geofoms

### 9.2.2.1 The Lowland Fluvial Network: Streams and Rivers

The lowlands are drained by rivers (“ríos”) and streams (“caños”), together with creeks (“quebradas”) in hilly and piedmont areas. In alluvial plain environment waterways usually carry black water and white sand except for larger rivers such as the Orinoco and the Ventuari (Plate 9.1c). Because of relief flatness, rivers and streams develop meander belts (Plate 9.1f). They are only slightly incised in the terrain surface (3–4 m) which causes them to overflow frequently during high water stages. At low water levels in January–March, point bars, scroll bars, and other sand benches with no or ephemeral vegetation occupy parts of the larger channels. Levees and other overflow ridges formed by larger rivers are in general stabilized by riparian forests. Along smaller rivers, streams, and creeks, levees are usually inconspicuous because they are periodically reworked by bank overflow. Confluence splay fans form at places where smaller rivers or streams join larger ones. Junction is impeded at high waters. This causes tributaries to overspill, flood large confluence areas, and discharge their sand load forming splay fans.



**Plate 9.1** White-sand alluvial plains: (a) pristine forest landscape with distinction between riparian forest along branching fluvial network and lower interfluvial forest; (b) meadow vegetation replacing the original forest in interfluvial areas. River types: (c) Orinoco river in Tamatama, west of La Esmeralda; white water and pinkish sediments originated from erosion of Roraima sandstones; (d) Atabapo river in the proximity of the confluence with caño Caname; blackwater and quartzose white sands. Blackwater rivers and streams; (e) caño San Miguel crossing the peneplain landscape of the Atabapo area with the crystalline shield basement outcropping at shallow depth; (f) Guayapo river meandering through the stabilized, flat, slightly subsiding alluvial plain of the Sipapo area

The “caños” network forms the basic primary drainage system that evacuates rainfall and groundwater from the low-lying terrains to the rivers. “Caños” Pimichin, San Miguel, Temi, and Caname are typical black water lowland streams that drain the Atabapo area (Plate 9.1d, e). During the rainy season, the waterflow spills over the lateral banks and discharges water and sand into the lowland. “Caños” collect the rainwater that percolates through the filter of the white sand mantle and gets loaded with organic substances and hydroxides by crossing spodic horizons. Water is



**Plate 9.2** Atabapo river in the proximity of the junction with the Orinoco river; (a, b) channel enlargement and engorgement through retention of sediments caused by the overwhelming flow of the Orinoco at peak discharge; (c, d) contact front between the white water of the Orinoco and the black water of the Atabapo

tea-colored to black the whole year around. Blackwaters have usually low pH (4.5–4.8). The overbank spill returns to the bordering areas part of the water collected from groundwater until the water level drops substantially in the main river channels.

Channel sediment is pure quartzose white sand (10YR8/1-7.5YR/8/1), mixed sometimes with some mica flakes and feldspar grains that indicate local contribution from crystalline rocks that often outcrop along the channel and in the shores. Large parts of the beds are occupied by sand bars intermingled with braided blackwater channels (Plate 9.2). At bankfull stage during the rainy season, levee overflow and crevassing cause excess water and sand load to invade the neighboring floodplains.

The white sand areas with meadow vegetation that are the object of this study lie on the interfluves between the river and stream network where splay and overflow processes generate large sand mantles. In areas proximal to rivers and streams, channel migration has a direct influence on the building of riverine geomorphs and floodplain sediments.



### 9.2.2.2 Channel-Related and Floodplain Sediments

#### (a) Confluence splay fan (or spill fan)

Soil drainage and water flow in river channels are slow because of the levelness (flatness) of the alluvial plains. At the height of the rainy season, channel flow tends to spill over the neighboring lower-lying landforms. River and stream confluence areas are particularly exposed to flooding. Confluence swamps (“rebalse,” local term for overspill causing water retention and stagnation) tend to form at the junction between larger rivers coming from the uplands and highlands and local streams that have their headwaters in the penepain landscape (Plate 9.3a, b). At high water levels, the regional and the local water drainage systems compete for water evacuation. This impedes smaller tributaries to join the mainstem collectors. In the confluence area, a stream usually develops a succession of short and sharp-bending meanders before reaching the levee of the main river (Plate 9.3c, d). Often the stream channel runs parallel to the outer side of the levee for some stretch before being able to join the main river channel. At high waters, junction is obstructed and the stream discharges water and sand load over the confluence area. When main and secondary waterways have simultaneous high waters, there can even be reflux from the former to the latter. This results in the formation of characteristic, fairly triangular white sand splay fans frequent in the Maroa area and south of river Casiquiare. In these splay fans, a variety of minor riverine geoforms can be found such as meander lobes, point bars, small levees, and boggy areas with various types of sediment and vegetation. Typically, colonies of *Malouetia molongo* and *Lagenocarpus* sp. establish in these white sand-flooded fans (Plate 9.3e, f).

#### (b) Stream levee

The competence of streams to transport detrital material is lower than that of rivers. It results that sediments moved by streams are usually better selected and fit in a relatively narrow size range. *Profile P99* (Typic Quartzipsamment, 150 m a.s.l.; Sipapo area, Table 6.2) is on a levee with 2–3% lateral slope, close to a stream incised 3–4 m in the terrain, and covered by open shrubby vegetation with large bare sand patches. Several layers were separated on the basis of slight differences in color, rooting density, and the presence of charcoal fragments at 11–35 cm depth. The material is overall light grey (5YR7/1) while the surface layer is pinkish grey showing ongoing deposition. The profile is very homogeneous with 100% sand in all layers and well-sorted dominance of medium and coarse sand (90% together) (Plate 9.4a). Deep root penetration (70 cm) suggests sediment aggradation by periodic overflow (Tables 7.3 and 7.10); narrow active levees at low water stage in February–March on both sides of stream channels are shown in the Atabapo area, close to Maroa (Plate 9.4b, c)

#### (c) Stream floodplain

Rivers at fullbank stage usually spill over large areas; therefore, they have no conspicuous floodplain *sensu stricto*, i.e., a low-lying area that borders the waterway channel and is incised by migrating meanders in the surrounding terrain. In contrast, streams (“caños”) have often narrow floodplains where fresh



**Plate 9.3** (a) River and stream junctions are frequent in the dense lowland waterway network and are critical nodes for water movement through the fluvial system. Sediment engorgement in confluence areas causes bottlenecks that decrease the effectiveness of the drainage network. (b) Channel splitting and enlargement through meandering allow smaller streams to join larger ones. The stem river in the two pictures is Rio Negro. (c) Small splay fans in frontal and (d) lateral position in the confluence area between stream and river; (e, f) Large confluence splay fan, partially fixed by “palo de boya” (*Malouetia molongo*) and *Lagenocarpus* (Pasimoni watershed)

sediments are deposited and reworked at each flood event, resulting in ridge-and-swale topography in meander lobes (“orillar,” local term) and water ponding (Plate 9.4d–g).

*Profile P25* (Oxyaquic Quartzipsamment, 100 m a.s.l.) is located in the middle watershed of “caño” San Miguel, around 70 km east of its confluence with river Guainía. The site is on a floodplain that is incised 1–2 m by the stream channel. The



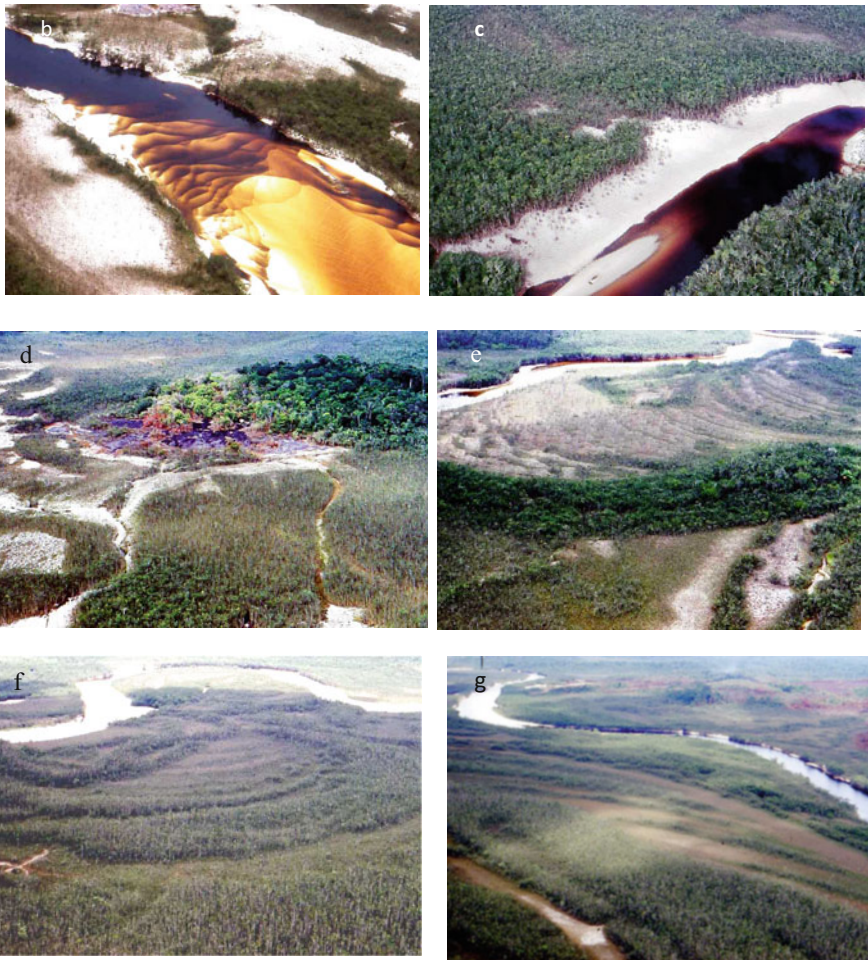
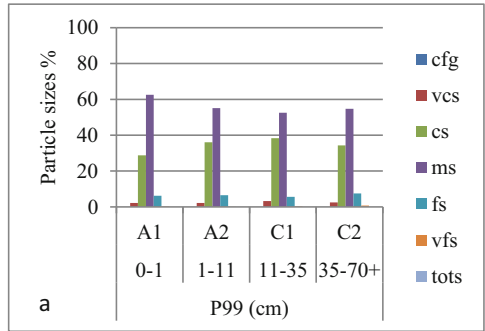


**Plate 9.4** (a) Profile P99 Typical Quartzipsamment; homogeneous soil-sediment profile from a stream levee in the northern Sipapo with well-sorted material, dominance of medium and coarse sand; (b, c) Features of stream floodplains in the Atabapo area, showing (d) white-sand patches of recent overflow, a variety of vegetation cover from low-density meadow to shrubby meadow to scrub, and terra-firme forest on a residual hill; (e) arch-shaped association of scroll bars and

terrain is covered by patches of bare white sand under very open shrubby meadows (10–15% cover) that alternate with areas of higher shrub density and dominance of *Lagenocarpus* sp. (Cyperaceae). Along the river bed, marshy areas with organic soil over white sand are covered by *palo de boyá* (*Malouetia molongo*) (see Plate 9.3e, f).

Root development is limited to the surface layer (0–5 cm). The material is stratified, poorly sorted white sand with 97% sand, 2% silt, and 1% clay. Two loose cover strata (0–12 cm) of recent deposition lie on top of two base layers (12–65+) with dominance of coarse, medium, and fine sand. No primary minerals (e.g., feldspar, mica) were identified in the profile, but the poor sorting of the sediment could be influenced by substratum weathering products, as rock outcrops are frequent in stream beds.

Further down the watershed of “caño” San Miguel, at about 30 km east of its confluence with river Guainía, *profile P26* (Typic Quartzipsamment, 90 m a.s.l.) was described in a savanna-meadow area enclaved in a “yevaro” (*Eperua purpurea*) forest, nearby a blackwater tributary (Plate 9.5a, c). The material is stratified, poorly sorted grey brown sand over white sand with 95% sand, 5% silt, and no clay. Layer 3–25 cm contains horizontally aligned charcoal fragments deposited by flooding. Also, angular fragments of quartz and granite (2–5 cm) are present, suggesting the proximity of weathering substratum in the stream channel. Organic carbon content, somewhat higher than usual in white sands, decreases irregularly with depth.

*Profiles P25* and *P26* have similar particle size distribution patterns and the same sequence of sand separates with dominant medium sand, and codominant coarse and fine sand (Plate 9.5d, e). Both profiles are representative stream floodplain sediments of the Atabapo area in the south of the study region. *Profile P97* (Oxyaquic Quartzipsamment, 100 m a.s.l.) occupies a similar position in a stream floodplain in the north of the study region, in the watershed of river Autana, and shows depositional facies comparable to that of *P25* and *P26* (Plate 9.5f). These poorly sorted splay sediments are commonly found in stream floodplains. However, similar layer sequences can also be found in glacial deposits, for instance in layer 35–70 cm of profile *P27* that is located about 50 km north-west of profile *P25*, in the lower watershed of “caño” Temi. Such a repeating particle size pattern in different geomorph types highlights the large spatial distribution of splay sediments in meadow lowlands.

### 9.2.3 Alluvial Plain Sediments: Splay Mantles

Sedimentation in the lowlands, especially in the Sipapo, Yapacana, and Atabapo areas, is controlled by laterally migrating rivers and streams. As waterways are

---

**Plate 9.4** (continued) intervening swales in a meander lobe; Relief flatness in the alluvial plains causes river channel instability; (f) association of scroll bars and intervening swales resulting from meander migration; (g) parallel depositional strips resulting from lateral shifting of the stream channel

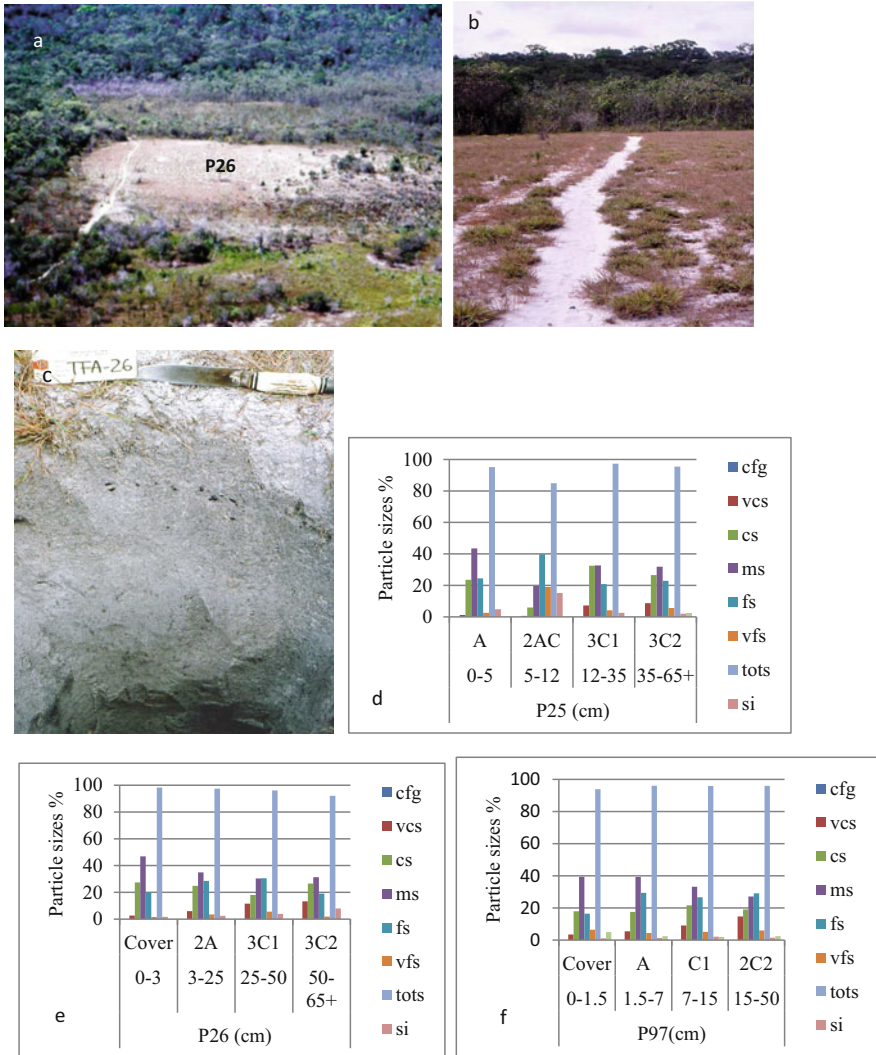


**Plate 9.5** Profile P26: Typic Quartzipsamment; (a) located on a point bar mound in an earlier floodplain of caño San Miguel in the Atabapo area; (b) mixed savanna-meadow vegetation (*Mesosetum, Panicum, Xyris*); (c) charcoal fragments at 20–26 cm depth, some of them horizontally aligned. (d) Profile P25: Oxyaquic Quartzipsamment under open shrubby meadow; (e) Profile P26: Typic Quartzipsamment under savanna-meadow; soil-sediment profiles from the floodplain of caño San Miguel in the Atabapo, showing similar pattern of poorly sorted splay material; (f) Profile P97: Oxyaquic Quartzipsamment; soil-sediment profile from a stream floodplain in the watershed of river Autana, in the north of the study region, that shows a depositional facies similar to that of the soils in the Atabapo area, in the south of the study region (P25 and P26)

frequently shifting over the depositional surfaces, channels are only slightly incised and bordering levees are low. At high water levels, overbank flow and crevasse incision in the levees allow large parts of the sediment load to be spilled without selection over the contiguous flats and depressions (Plate 9.6). Load is mainly sand as fines have been flushed out of the environment by repeated episodes of sediment reworking. This type of depositional process leads usually to poorly sorted splay mantles. Undifferentiated particle size distribution, with fairly similar proportions of material in several sand separates, is characteristic of the splay facies. A variety of depositional situations occurs from stratified to monotonic layer sequences.

### 9.2.3.1 Stratified Splay Mantle

*Profile P66* (Typic Quartzipsamment, 100 m a.s.l.) is located on a flat terrain covered by shrubby meadow dominated by a 4–5 m high species of *Humiria*, south of the middle *caño* Caname. The site is 200 m distant from a dune-like mound (P65). The terrain surface is crossed by reticular drainage rills (5–7 cm deep, 10–15 cm wide) that bifurcate in irregular patterns between shrubs. Groundwater is at 114 cm depth. Below a thin (0–7 cm) light brownish grey A horizon, all C layers are pinkish grey to light grey. Average particle size distribution of the five layers of the deposit is 98% sand, 1% silt, and 1% clay. Although total sand is similar in all layers (95–100%), sand separate pattern varies with depth (Fig. 9.1a). Coarse, medium, and fine sands are codominant in the first two layers (0–33 cm), while very coarse and coarse sands are codominant with medium sand subdominant in the last two layers (63–130 cm). The intermediate layer (33–63 cm) shows a very poorly sorted, torrential depositional pattern, including four main sand separates with relatively similar sand percentages, 12% fine quartz gravel (2–4 mm), and discontinuous horizontal dark grey veins of organic matter. This sediment is a stratified splay mantle with two lithological discontinuities (breaks) at 33 cm and 63 cm depth, respectively. Average sand values of the five layers (0–130 cm) show large variability in all sand separates, reflecting sediment heterogeneity with depth and poorly sorted, undifferentiated particle size distribution that is characteristic of splay deposition (Fig. 9.1b). This implies variations in flow energy between the consecutive splay events.

Often there is little difference between the particle size distribution of the sediment in the stream channel and that of the sediment spread over the adjacent splay area. This suggests that torrential overbank flow and levee crevassing are the main processes of transferring channel bed load to depositional areas with little sediment sorting. *Profile P97* is located in a vegetated (herbs and forbs) paleochannel in the lower watershed of river Autana. It shows unsorted bed load, especially in the 15–50 cm layer that is the source of material feeding splay mantles in the depositional areas (Plate 9.5f).

### 9.2.3.2 Uniform Splay Mantle Layering

Heterogeneous layering with lithological discontinuities is an intrinsic characteristic of most splay deposits as splay sediments are usually spread under a rather torrential deposition regime. However, relatively uniform splay deposits, with monotonic layering, were found in places where presumably the same aggradational process





**Plate 9.6** (a, b) Linear depositional strips resulting from riverbank crevassing at high water stage; (c) Crevasse splay creating an opening in a woodland cover, recently re-activated; (d) older crevasse splay that invaded a poorly drained depression, recently burned. (e) Active crevasse splays along river Atabapo (white patches); (f) abandoned meander. Variety of crevasse splays along streams; (g) active splays with channels free of vegetation; (h) stabilized splays with vegetated channels

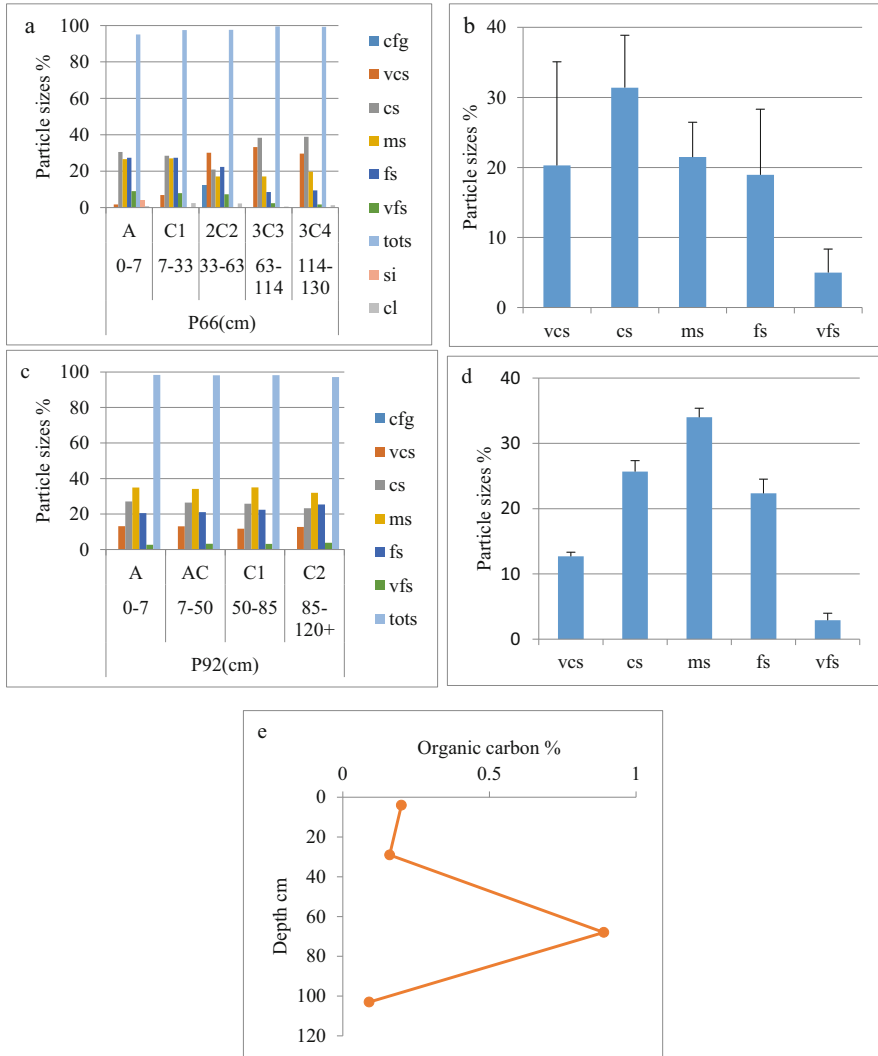


**Fig. 9.1** Profile P66: Typic Quartzsammert; stratified splay sediment): (a) poorly selected particle size distribution showing a torrential event at 33–63 cm depth; (b) averaged sand fraction separates (five layers) with large standard deviation values reflecting poor sediment sorting. Profile P92: Oxyaquic Quartzsammert; uniform splay depositional facies: (c) monotonic sequence of sand layers with similar particle size distribution; (d) averaged sand separates of the four layers showing poor sediment sorting, but with small standard deviation values reflecting unvaried sedimentation process over time; (e) irregular distribution of organic carbon with depth

has been operating over time without significant change in depositional energy. Heterogeneous deposits are possibly more frequent than homogeneous ones in splay mantles (Table 9.2).

**Table 9.2** Characteristics of selected profiles in splay deposits from various study areas

Profile	Soil class	Geoform	Study area	Texture	Udoxic index	Color moist	Vegetation
P18	Typic Quartzipsamment	Splay mantle	Yapacana	Fine sand/medium sand	1	Light grey/white	Shrubby meadow
P19	Typic Quartzipsamment	Splay mantle	Yapacana	Coarse sand	2	Light grey/white	Shrubby meadow
P66	Typic Quartzipsamment	Splay mantle	Atabapo	Coarse sand	3	Light grey/white	Shrubby meadow
P86	Oxyaquic Quartzipsamment	Splay mantle	Atabapo	Medium sand	1	Light grey/white	Meadow
P92	Oxyaquic Quartzipsamment	Splay mantle	Sipapo	Medium sand	4	Light grey/white	Open scrub
P97	Oxyaquic Quartzipsamment	Splay mantle	Sipapo	Medium sand/fine sand	8	Grey/white	Meadow within scrub
P58	Udoxic Quartzipsamment	Splay filling basin	Yapacana	Fine sand/foamy fine sand	12	Light grey/white/light grey	Shrubby meadow

Udoxic index: silt%+2× clay% (Soil Survey Staff 2014)



*Profile P92* (Oxyaquic Quartzipsamment, 100 m a.s.l.) is located 20 km northwest of Cerro Autana on a white sand bench-like terrain with groundwater at 95 cm depth. Vegetation is open scrub with shrubs forming 3–4 m high clusters 5–15 m apart. The terrain under shrub colonies is 10–30 cm higher than the intermingled bare areas. Runoff erosion causes undulating microrelief. Fresh loose pinkish sand covers the irregularities of the terrain. The upper layers, below the loose sand cover, include horizontally lying roots, buried by incoming sand.

The soil is covered by loose sand in transit that is displaced by rainfall runoff (0–1.5 cm). The shallow topsoil (1.5–7 cm) is light grey, followed by white sand layers. All layers show similar particle size distribution patterns (Fig. 9.1c). On average (1.5–120 cm depth), the deposit is 98% sand, 0% silt, and 2% clay. Sand is distributed over four separates, including 13% very coarse sand, 26% coarse sand, 34% medium sand, and 22% fine sand. This reflects poorly sorted, fully undifferentiated particle size distribution that is characteristic of splay deposition. The same disordered particle size distribution pattern of medium sand>coarse sand>fine sand>very coarse sand repeats over depth, with the sand proportions in the four separates remaining fairly constant. Figure 9.1d shows very low standard deviation values, in contrast with those of the heterogeneous splay deposit of P66 (Fig. 9.1b). Vertical homogeneity throughout indicates that the same depositional process has been active over time. There are no textural discontinuities between layers. However, the sediment is not a one-time deposit as organic carbon varies irregularly with depth (Fig. 9.1e) This shows that sedimentation was episodically interrupted, but consecutive layers were formed in a stable environment, different from that of shifting rivers, by a depositional flow of invariant energy. The sediment was possibly built up by non-selective overbank flow occurring at irregular intervals at high channel water levels and resulting in generalized splay accretion on lateral alluvial flats (Table 9.3).

#### **9.2.4 Alluvial Plain Sediments: Overflow Mantles**

The overflow mantle is the main geomorphic component of large alluvial plains that are drained by stable rivers with relatively well-developed channels. It forms usually by overbank flow of the fine-grained load, while the coarse-grained particles remain in the channel or deposit on levees. In the meadow lowlands, medium and fine sand are usually the dominant separates in overflow mantle, reflecting well-sorted sediment. It distinguishes from splay mantle that is on the coarse side of the sand spectrum and includes several sand separates with fairly similar or variable sand proportions, reflecting poorly sorted sediment. The overflow mantle lies in general adjacent to the levee at a slightly lower level and from there expands over large flat areas. Overflow sediments often fill lateral depressions with moderately high to high groundwater (Plate 9.7).

**Table 9.3** Particle size distributions and ranking of sand separates of selected profiles in splay deposits (see Table 9.2)

Profile	Depth cm	Number of layers	Very coarse sand	Coarse sand	Medium sand	Fine sand	Very fine sand	Total sand	Ranking of sand separates (>10% sand)
P18	15-70	2	9	19	36	29	6	99	ms > fs > cs
P19	3-60	2	6	45	35	10	2	98	cs > ms
P66	0-130	5	21	31	22	19	5	98	cs > ms = vcs = fs
P86	13-125	4	10	23	41	22	3	99	ms > cs = fs
P92	2-120	4	13	26	34	22	3	98	ms > cs > fs > vcs
P97	0-50	4	8	19	36	26	6	95	ms > fs > cs
P58	4-100	3	4	19	25	29	12	89	fs > ms > cs > vfs
Average			10	26	33	22	5	97	
Range			4-21	19-45	22-41	10-29	2-12	89-99	

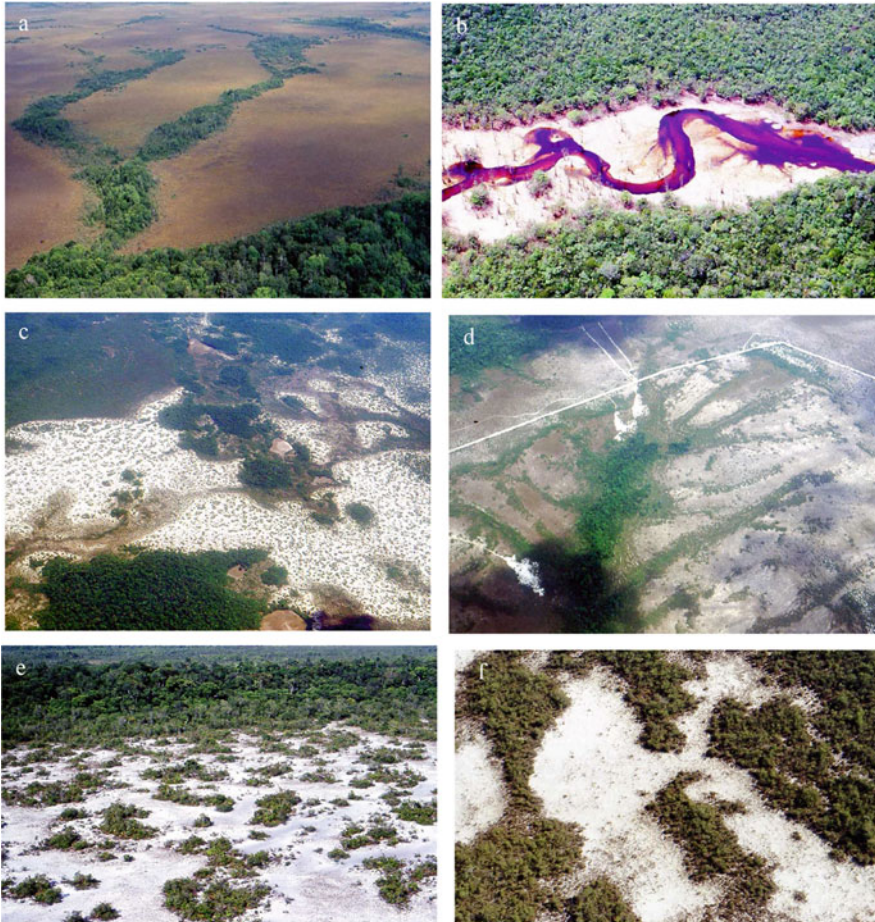


**Plate 9.7** Overflow mantles: (a) stabilized alluvial flats under meadow cover formed by sediment overflow from distributary streams; dark brownish areas are somewhat poorly drained; (b) generalized overflow spreading a mantle of white sand over the floodplain of a blackwater river. White-sand uniform mantle (c) and surficial blanket deposits (d) resulting from overflow of delta-like branching distributary channels. Process of cover sand distribution and mantle formation through overflow and splay; (e) interlaced flow pathways between shrub bushes and sand retention around and within bushes; (f) intrusion of sand flows into woodland areas

#### 9.2.4.1 Representative Sites

*Profile P64* (Oxyaquic Quartzipsamment, 100 m a.s.l.) is located in the western watershed of “caño” Pimichin, a tributary of river Guainía, 10 km north of Maroa in a shrubby meadow area surrounded by caatinga and morichal. Groundwater is at 77 cm depth. A dark reddish brown (5YR2/2 m) surface horizon lies above the white sand. The presence of sand lenses mixed with organic matter (0.5–1 cm thick), especially frequent from 50 cm downwards reflects cumulizacion by fluvial accumulation, a process typical in overflow mantle. Except for the cover layer, the same

particle size distribution pattern dominated by medium and fine sand repeats from 7 to 90 cm depth. On average (7–90 cm), the sediment is 97% sand, 2% silt, and 1% clay. Medium (53%) and fine sand (31%) concentrating 84% of the material characterize a well-sorted deposit. *Profile P64* is a representative profile of overflow mantle. Comparatively profiles P66 and P92 that represent splay mantle deposits have 3–4 separates with similar or variable sand proportions, reflecting poorly sorted, undifferentiated sediment (See Sect. 9.2.3).

*Profile P90* (Oxyaquic Quartzipsamment, 100 m a.s.l.) is located 5 km west of the Cuao range in a poorly drained meadow island, surrounded by bana scrub up to 5 m high (Table 6.2, Chap. 6). The meadow vegetation is composed mainly of species of the genera *Xyris* and *Abolboda* (40–50% cover) reflecting poor drainage, with disseminated shrubs (0.5–1 m high). By the time of description at the height of the rainy season in July, groundwater was at about 10 cm depth, brownish presumably because of the proximity of spodic material. Other meadow patches in the surroundings had a shallow water film on the terrain surface and algae cover. Below pinkish grey loose coarse sand in transit at the soil surface, the sediment is light grey to white. Medium and fine sand dominate the particle size distribution, with fine sand increasing gradually with depth. On average (2–40 cm depth), the sediment is 96% sand, 2% silt, and 2% clay. Medium sand (52%) and fine sand (32%), summing up 84% of the material characterize a well-sorted deposit. This profile shows a particle size distribution pattern strikingly similar to that of profile P64, although both profiles are 300 km apart, one located in the extreme north (Cuao area) and the other in the extreme south (Maroa area) of the study region. When the five sand separates are generalized into three sand classes of coarse sand (2–0.5 mm), medium sand (0.5–0.25 mm), and fine sand (0.25–0.05 mm), the figures of cs-ms-fs are 9–54–37% in P64, and 9–55–36% in P90, respectively. P64 and P90 show homomorphic sediment facies and represent the paradigm of overflow deposits in meadow environment.

The sediment at both P64 and P90 sites could also be interpreted as being eolian, but the site conditions do not favor such a hypothesis. In both cases, the meadow is a low-lying area surrounded by slightly higher terrain surfaces covered by shrubby vegetation.

*Profile P91* (Oxyaquic Quartzipsamment) is located in a dense bana scrub (2–5 m high) that surrounds the meadow island of P90 (Table 6.2). The terrain is about 10 cm higher than the enclosed meadow surface and has similarly high groundwater (at 13 cm). On average (3–40 cm), the sediment is 98% sand, 0% silt, and 2% clay. Medium (37%) and fine sand (44%) sum up 81%, characterizing a well-sorted deposit. Below a dark grey mixed sand cover, the sediment is light grey with similar proportions of medium sand and fine sand (around 40% each). This material is similar to that of the lower layer (20–40 cm) in P90. It confirms a basic characteristic of the overflow facies, i.e., the concentration of particles in a few separates of the sand spectrum, mainly in the range of medium to fine sand. It shows also that herbaceous meadow and scrubby bana vegetation coexist on the same type of sandy substrate.

## 9.2.5 Boundary Conditions

Well-sorted overflow sediments in meadow conditions are on average 95–98% sand with two codominant sand separates, usually medium and fine sand, that concentrate a large part of the sand fraction. Splay mantles have also more than 90% sand content but distinguish from overflow mantles for being in general poorly sorted depositional materials with 3–4 codominant sand separates. Not all visited sites represent clear-cut alluvial depositional types. For instance, typical levees with coarse and medium sand are uncommon in large alluvial plains because reworked sand grains are vulnerable to fragmentation upon micro-alveolization. Transitional situations sharing splay and overflow characteristics may be more frequent than what field observations could identify. Blended depositional patterns occur in places where deposits depart from the typical overflow sediment for having, in addition to two dominant medium and fine sand separates, a background spectrum of all the other particle size classes, including silt and clay, contributing to the total sample composition. Boundary cases were also identified in places where different kinds of sediment, including alluvial and weathering facies, are spatially closely associated either by superposition at the same site, or by adjacency in neighboring sites, or as unusual mixtures of particle classes, for instance sand and silt in an otherwise dominantly sandy environment. For instance, overflow and splay deposits can be adjacent, intermingled, partially overlapping, or fully superposed, making cartographic separation difficult. Such situations may be frequent but evaluating their spatial extent is beyond the scope and possibility of this study. The following are a few of such mixed situations.

### 9.2.5.1 Overflow Deposit Atop Splay Sediment

Overflow and splay deposits can alternate in the same place, one burying the other. Superposition can result from a decrease of flow energy during the same depositional event with splay at the bottom changing to more selective overflow at the top or from two consecutive events of different flow energy.

*Profile P86* (Oxyaquic Quartzipsamment, 100 m a.s.l.) is located in the middle watershed of “caño” Caname, about 20 km south of the stream. Vegetation is meadow with some shrub clusters. Cover density increases from 30 to 70–80% in the center of the area (Tables 6.6, Chap. 6; 9.2 and 9.3).

The material is pinkish grey and pinkish white down to 75 cm, and then white. Groundwater is at 75 cm depth. The profile is capped by a torrential splay layer (0–13 cm), compact, with white powdery silt between the sand grains. Although sand content is 98–100% in all layers except the cover layer, the sand fraction composition varies with depth. The upper member of the sediment (13–47 cm) is a fairly well-sorted overflow material with nearly 50% medium sand. The lower member (75–125 cm) is a poorly sorted splay material with codominance of very coarse, coarse, and medium sand. Very coarse and coarse sand constitute 56% of the layer. The intermediate layer (47–75 cm) has a transitional pattern that shows that deposition was continuous with a gradual shift from higher to lower flow energy.

### 9.2.5.2 Association of Levee and Crevasse Fan Deposits

High water levels in the river channel can cause excess water to flow over the levee or break through the levee. In the first case, usually coarser particles are retained on the levee and finer particles reach the adjacent depression forming an overflow deposit. In the second case, the rupture of the levee allows the full flow, without particle selection, to leave the channel and irrupt into the lateral depression forming a crevasse splay fan. Profiles P18 and P19, 300 m apart, illustrate these two processes of alluvial deposition.

*Profiles P18 and P19* (Typic Quartzipsamments, 100 m a.s.l.) are located on the right bank of river Orinoco, about 30 km south of its junction with river Ventuari. Terrain is flat, incised by a palm tree swale (morichal). Vegetation is shrubby meadow with *Terminalia yapacana* at P18 site and without at P19 site. Below a light grey A horizon, material is white sand at both sites. At P18 average particle values are 99% sand, 1% silt, and no clay. Sand particles are spread over several separates from very coarse to very fine sand, with variable percentages in each layer and between layers, reflecting poorly sorted stratified splay sediment forming a crevasse fan. P19 has similar average values with 98% sand, 2% silt, and no clay, but sand particles concentrate in two codominant separates of coarse and medium sand of a levee deposit (Tables 6.5, Chap. 6; 9.2 and 9.3).

### 9.2.5.3 Silty White Sands

In general, lowland sediments in meadow environments have a very low content of fines. Silt and clay, together with organic matter and iron hydroxides have been depleted by multiple episodes of sediment reworking and translocation. However, in some areas, white sands with considerable amounts of silt were found, for instance in the areas of “caño” Yagua, west of La Esmeralda (Yapacana area), and “caño” Pimichin (Atabapo area). Silty white sands occur in confined, usually poorly drained depressions. Some of these are large enough to simulate small internal deltas as in the Yagua watershed. The Pasimoni area shows a large number of permanently waterlogged marshes and swampy lakes. It can be hypothesized that river overflows have filled the depressions with finer sediments. Silt was trapped and remained stored in the concave topography of drowned areas, often waterlogged. Silt may result from weathering of crystalline and sedimentary rocks in upper watersheds. Piedmont fans and proximal peneplain glacis have up to 20% silt content (e.g., profiles P22, P73).

Two distinctive features characterize sediments with high silt content: the presence of compact layers (densipan) and reticular microrelief of discontinuous channels and closed pans resulting from suffusion. Vegetation cover is shrubby meadow.

*Profile P77* (Typic Udorthent, 125 m a.s.l.) is located in a lateral depression on the right side (north) of the Orinoco (Table 6.5, Chap. 6). It shows below a very dark grey to black topsoil (0–26 cm), layers are pinkish grey with slight variations between 5YR5/2 and 5YR7/2, reflecting the influence of Roraima sandstone of the nearby Duida massif. Dark grey lenses are interstratified within the white sand layers. The sediment is 70% sand, 26% silt, and 4% clay. Silt varies irregularly



with depth in the range of 21–31%. Fine sand (ca 30–40%) and silt (ca 20–30%) are the dominant particle sizes in all layers. Fine sand, very fine sand, and silt sum up 78% of the sediment. The profile is fairly homogeneous over depth but the sand separate sequence changes at 65 cm depth from fine>veryfine>medium sand to fine>medium>veryfine sand. Soil reaction varies irregularly with depth showing that the deposit has been built up by layer aggradation, thus not a weathering profile. The pH values of 6.4–6.6 in the middle and lower layers are unusual in an otherwise dystrophic environment and may result from an influx of reworked saprolite materials, less impoverished than the white sand in the upper layers. Two layers are very compact (densipan) at 39–65 cm and 115–145 cm depth. This suggests that the sediment was built up in two times with a depositional interruption corresponding to the lithological discontinuity at 65 cm depth. Densipan formation may be related to surface suffusion, leaching fine-grained particles from the overlying layers and clogging pores in the illuvial layers. Depressions are not interconnected and do not correspond to channels or rills incised by water flow but result from subsidence upon suffusion.

*Profiles P16 and P17* located in the watershed of “caño” Yagua show particle size distribution patterns similar to that of P77, with 20–40% silt in various layers (see Plate 10.3c in Chap. 10, Sect. 10.4.3).

In Table 9.4 are reported several profiles having relevant silt contents (19–36%) in an alluvial environment that is overwhelmingly sandy. All profiles are on drowned alluvial flats under shrubby meadow vegetation except P130 which is under caatinga forest. All profiles have a kind of silt-related compact layer (densipan) that restricts root penetration and internal drainage. The terrain surface shows characteristic reticular microrelief in the form of unconnected channels and closed pans that are originated by suffusion.

Although silty sands have substantial proportions of very fine sand and silt, the particle size spectrum is not sorted enough to clearly reflect eolian activity. They also distinguish from pure overflow mantle that is characterized by a large codominance of medium and fine sand (ca. 80%).

Similar blended depositional situations were identified in drowned, semi-endorheic alluvial plains, especially in the Pasimoni and Siapa watersheds (P103, P104, P105, P108, P109), but also in some smaller areas with impeded drainage in the Yagua watershed (P56) and Ventuari valley (P131). In all these areas, the weathering front of the substratum lies relatively close to the terrain surface. Profiles show large spans of particle sizes that may correspond to rock weathering residues not fully flushed out by repeated sediment reworking in sunken, concave lowlands. These “sedimentological impurities” contribute to creating hybrid overflow sediments.

#### **9.2.5.4 Reworked White Sands Over Weathered Bedrock**

In the lowlands themselves, white sands are derived from rock weathering under meadow vegetation in the penepplain landscape, for instance at the footslope of crystalline domes or sedimentary structural reliefs, in the immediate surroundings of local rock bar outcrops, and in the proximal stretches of glacia. In the plain



**Table 9.4** Profiles having moderate silt contents in a contextual sandy environment, with densipan layers

Profile	Depth cm	Soil class	Sand%	Silt %	Clay%	Densipan cm	Groundwater cm
P16	5-60	Udoxic Quartzipsamment	80	19	1	5-60+	Deep
P17	0-50	Typic Udorthent	66	33	1	18-50+	Deep
P77	0-160	Typic Udorthent	70	26	4	39-65/115-145	150
P130	20-60	Oxyaquic Udorthent	59	36	5	45-60+	70

landscape, full weathering profiles are unusual to detect as the terrain surface is covered by reworked sandy sediments. However, in some places there is evidence that bedrock is not far in depth as outcrops emerge at the bottom of river and stream channels at low water level.

*Profile P81* (Oxyaquic Quartzipsamment, 100 m a.s.l.) is an example of duplex profile with upper layers of depositional origin and deeper layers resulting from bedrock weathering. Terrain is flat, exposed to flooding, covered by shrubby meadow, and surrounded by bana and caatinga vegetation (Table 6.5).

The upper part of the profile (0–105 cm) is pure white sand (10YR8/1) with 95% sand, 2% silt, and 3% clay (Fig. 9.2a). It is composed of two sets of layers; the upper set is well sorted with coarse and medium sand dominant (86% sand together); the lower set is moderately well sorted with coarse, medium, and fine sand codominant. The lower part of the profile (105–150 cm) is light grey (2.5Y7/2) granitic saprolite with 74% sand, 11% silt, and 15% clay. It is an unsorted weathered rock in place containing fine fragments of feldspar (2–4 mm) and no clayskins. At 105 cm depth, silt and clay increase abruptly, both by more than 10% content. The two layers at 120–150 cm are very dense and sustain a perched water table at 105–120 cm. Water is milky from dissolved silica. At 105 cm, pH drops from 6.6 to 5. Thus, there is a major lithological discontinuity at 105 cm depth between the stratified sand cover and underlying saprolite material. However, the dominance of coarse, medium, and fine sand in the lower part of the sand cover (43–105 cm) suggests that the reworked sand is genetically related with the weathered substratum material that has similar sand spectrum.

*Profile P128* (Oxyaquic Quartzipsamment, limit Aquodic, 120 m a.s.l.) is another example of duplex profile with upper layers of depositional origin and deeper layers resulting from weathering of the substratum. The profile is located on the left bank of the Orinoco. Terrain is flat, flooded during the rainy season. Vegetation is dense shrubby meadow (80–90% cover), with large proportion of *Brocchinia prismatic* frequently assembled in colonies together with species of *Schoenocephalum*, Cyperaceae, Eriocaulaceae, and Xyridaceae. The meadow is surrounded by bana and caatinga vegetation (15–20 m high) (Table 6.5).

The profile is uniformly pinkish white sand to 90 cm depth, then light grey sand. In contrast, particle size distribution changes abruptly at 44 cm depth (Fig. 9.2b). Although total sand is unvarying (98%), the upper layers (1–44 cm) are dominantly fine and medium sand (79%), while the lower layers (44–100 cm) are dominantly very coarse and coarse sand (71%). Figure 9.2c shows the opposite stepwise particle size pattern of the upper and lower segments of the profile. Lower layers contain feldspar fragments probably coming from the weathering of coarse-grained rapakivi granite with feldspar phenocrysts (outcropping in stream channels). Thus, the profile is a composite one, with well-sorted overflow sediment fossilizing a weathered crystalline substratum. In contrast to profile P81 which has up to 26% silt and clay, the weathering of rapakivi granite at site P128 generates very little fines.

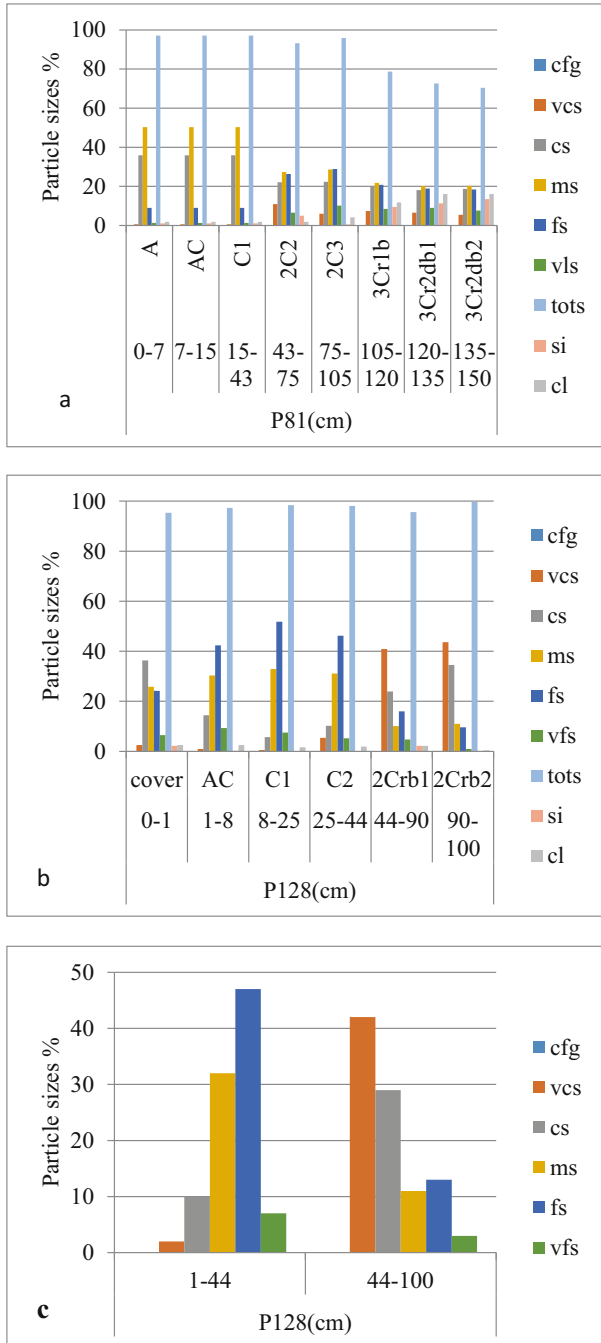


**Fig. 9.2** (a) Profile P81: Oxyaquic Quartzipsammunt; layered white-sand cover (0–105 cm) burying weathered bedrock (105–150 cm); (b) Profile P128: Oxyaquic Quartzipsammunt white-sand cover (0–44 cm) burying weathered bedrock (44–100 cm); (c) contrast of particle size pattern between upper and lower segments of the profile

### 9.2.6 Discussion

Lowland alluvial plains are the end receptacles of the sandy sediments coming from different sources within the lowlands (e.g., peneplain glacis) and outside (e.g., peripheral mountain massifs) that are described in Chap. 8. Currently, parts of the alluvial plains are temporarily stabilized, while others are undergoing different stages of geo-sedimentological activity from surface blanketing by new overflow sediments to more conspicuous changes in terrain morphology caused by river and stream shifting.

Our field observations are limited to 1–2 m depth, describing surface processes and landscape changes. They do not account for the nature, structure, origin, and thickness of the underlying series of sand mantles that fossilize the Archaeozoic igneous-metamorphic basement of the basin. The lowlands lying in front of the eastern peripheral mountainous arc correspond to a subsiding graben-like regional basin, the axis of which corresponds to the meridian alignment of rivers Orinoco, Atabapo, Guianía, and Rio Negro. The sand mantles of the substratum may be considerably thick as sediments have been infilling the basin for millennia, possibly since the mid-to-upper Eocene when the last relevant uplift of the Guayana Shield took place, resulting in the formation of grabens, intense dissection, and accelerated erosion (Mendoza 2005). Besides the sediments entering the basin from the eastern side, sediment load is compounded by the voluminous alluvial materials coming from the Colombian and Venezuelan Llanos plains on the western side.

The mountain massifs such as Cuao-Sipapo and Duida are surrounded at the base by impressive debris talus that evidence past strong morphogenic activity during dry periods of the Pleistocene (Plate 8.7a in Chap. 8). Large-size sandstone blocks were detached from the tepui escarpment walls and accumulated at the base of the table-shaped reliefs. Smaller clastic debris, especially sand, were washed out and moved to the low-lying areas. With such events of predominantly mechanical erosion repeating over time, it can be assumed that large volumes of sand have accumulated in the subsiding foreland. What is the spatial organization of these consecutive sand mantles being a matter of speculation. Possibly, in large areas such as the present Ventuari-Orinoco interfluve, megafans might have formed during the history of the basin sedimentation, similar to the megafans of the Virúa area in northern Amazonian Brazil (Rossetti et al. 2014, 2019).

The current surface sand mantle is discontinuous, fragmented into individual often confined depositional compartments, interrupted by and intermingled with residual peneplain reliefs. There are no extensive meadow alluvial plains but a repetitive spatial distribution of mid-size and smaller units, the largest ones occurring along the river and stream courses. This feature is shown in the geomorphic landscape figures in Chap. 6 (Multiresolution index of Valley Bottom Flatness—MRVBF).

The spatial organization of the alluvial sand covers, especially the differentiation between splay mantles and overflow mantles, is not easy to distinguish from the terrain surface or detect from the air. The geo-sedimentological study based on

distributed profile data and spatial correlation thereof shows the complexity of the sedimentation in the alluvial plains.

---

### 9.3 Sands in Peneplains

The peneplain landscape covers a variety of geomorphic settings from large, fairly flat terrains with few scattered residual hills to denser hill clusters with small interhill areas. In the Atlas de las Tierras del Territorio Federal Amazonas (MARNR-ORSTOM 1986), several kinds of peneplain are recognized and mapped, including peneplain proper, weathering peneplain, erosional weathering peneplain, and erosional plain. The authors consider that the last three landscape types are consecutive evolution stages of the primary peneplain, resulting from progressive dismantling, dissection, and downwasting of the original half-orange and other convex dome-like reliefs. Weathering of the crystalline basement rocks is assumed to be the dominant geopedologic process in peneplain environment.

In our study areas, limited to the meadow environment *sensu lato*, a sequence of peneplain landscape evolution similar to the one proposed above was traced. The original peneplain landscape is a rolling relief with rounded to oval hills of similar height, a network of incised palm tree vales and more surficial swales, and small depositional fringes around the hills (Plate 9.8a). This initial policonvexe relief geometry is called “mamelonization” or “mar de morros” in Brazilian geomorphic vocabulary (Ab’Sáber 2000). Progressive erosion of the hilly topography causes lowering and size reduction of the individual hills, with concomitant enlargement of the inter-hill areas where depositional glacis develop (Plate 9.8b). In a further stage of evolution, only residual hills formed mainly of igneous-metamorphic basement rocks remain from the original landscape, while remnants of the sandstone cover are scarce at low elevations (Plate 9.8c, d). Depositional glacis constitutes the largest parts of this kind of peneplain landscape. Subsequently, the combination of rock weathering and removal of the saprolite causes the downgrading of the residual hills, leaving circular flattened mounds of white sands upon depletion of fines and oxides by runoff (Plate 9.8e, f).

The combination of rock weathering and erosion of the weathered products has lead to the formation and expansion of flattened, slightly slopping terrains in the most advanced evolution stages of the peneplain, including typically glacis formation. It is in these flattened peneplain terrains where white sand areas with meadow vegetation are found (Plate 9.8e, f). In our field observations, the weathering front in contact with the basement rocks has been seldom reached in the first 1–2 m depth in peneplain lowlands. Cover materials in these areas are mainly reworked sandy sediments as shown in the following examples.

The kind of peneplain landscape where meadow white sands are common consists typically of hills, glacis, and drainage swales. Local association of these three geofoms is particularly neat around alone-standing hills. Hills have generally low relative elevation (200–300 m) and occur either as isolated inselbergs, or scattered hill groups, or hilland massifs. Rounded summits are covered with scrub

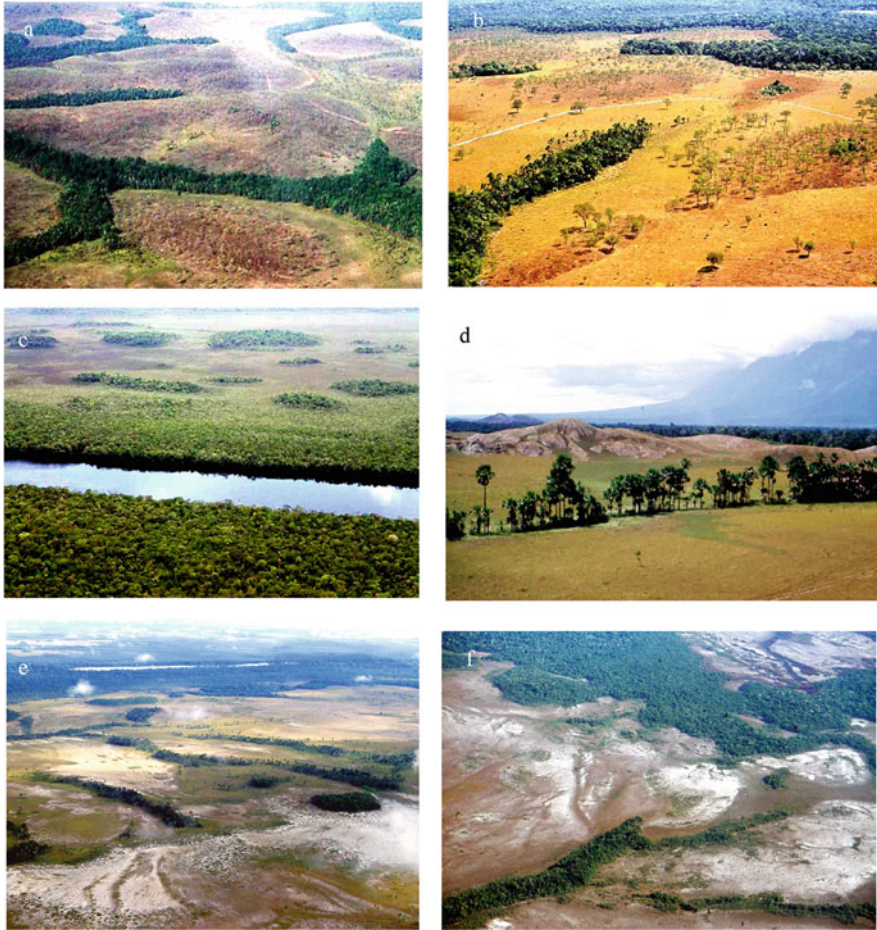


**Plate 9.8** Features of peneplain evolution: (a) rolling peneplain with low bedrock hills of similar height separated by small depositional areas and incised palm tree wales; (b) peneplain in moderately advanced stage of evolution with scattered downgraded bedrock hills separated by large depositional areas (glacis with meadow vegetation). Advanced stage of peneplain evolution with isolated residual hills; (c) rounded dome-shaped hills of igneous-metamorphic rocks (west of Rio Negro); (d) elongated hills of sedimentary rocks in the neighborhood of La Esmeralda; Duida massif in the background; (e, f) Final stage of peneplain evolution; dome-shaped hills are downgraded; the weathering of igneous-metamorphic bedrock delivers large amounts of white sands that are spread over annular glacis

or low forest, and steep sidewalls are often rocky. Glacis are gently sloping terrain surfaces surrounding hills or extending over larger, very gently inclined surfaces between hilly islands. Vegetation cover varies from open meadow to shrubby meadow to dense scrub. Narrow drainage swales with palm trees collect rain and runoff water from hills and glacis. They usually border the distal rims of the glacis.

Focus here is on glacis as these are the peneplain geofoms with white sands under meadow cover.

The Atlas de las Tierras del Territorio Federal Amazonas (MARNR-ORSTOM 1986) emphasizes weathering as the main process responsible for peneplain formation and evolution. However, only in a few visited sites could weathered rock material be identified at observation depths. In the majority of glacis under meadow vegetation, the upper layers (1–2 m) are formed by transported sediments that may rest in depth on some kind of weathering front.

Depositional glacis vary from local colluvial glacis, often related with rock bar outcrops, to more complex colluvio-alluvial glacis. The latter are large gently inclined terrain surfaces, most extensive in the peneplain landscape. Slope gradient is usually 0.5–2% but can be up to 5%. Glacis are covered by sand layers lying above variable kinds of weathered substrata and bedrocks (sedimentary or crystalline). Sand is originated by weathering of crystalline rocks or sandstone-quartzite strata in upslope hills and reliefs, and is transported by colluviation or a combination of colluvial and alluvial processes controlled by rainfall runoff. Between the proximal and distal parts of the glacis, particle size distribution remains fairly the same as the material moves by colluviation, but sometimes particle selection can be observed with more medium and fine sand in the frontal part. Loose surface sands are in transit as the material moves at each rainfall event. Often the terrain is crossed by shallow drainage rills and suffusion channels that create microrelief patterns from linear to reticular.

Two types of depositional glacis were observed in the study area: annular and longitudinal glacis:

- Annular glacis is a geofom that surrounds an individual hill or a small hill cluster with a ring-shaped sloping terrain and is fringed along its distal border by a peripheral circular palm swale/vale.
- Longitudinal glacis is a geofom that develops along the front of a hill range as a broad, elongated, inclined terrain, and is formed by the coalescence of smaller glacis or fans. This kind of large glacis is often subdivided into strips by palm tree swales running parallel to the terrain surface and merging downslope with a (blackwater) stream (local name “caño”).

Bedrock underlies all types of glacis but often at depths such that the weathering products are not recognizable in the sand covers. However, at some places, in annular as well as longitudinal positions, the weathering front is close enough to the terrain surface so that rock fragments and saprolite can influence the surface materials. Weathered clastics are reworked and distributed on the surface by colluviation or splay. A section hereafter is dedicated to these mixed situations.

The most common soils on glacis are Typic and Udoxic Quartzipsamments. These soils are flushed out of fine particles (nearly free of silt and clay) as well as of iron oxides and organic substances that end up in the palm vales. It is thus rare to find spodic features in sandy glacis materials.



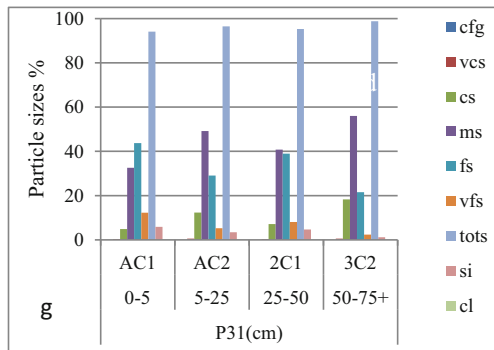


**Plate 9.9** Typical circular association of geofoms in advanced peneplain evolution stage; (a) residual hill in the center of the landscape surrounded by annular glacial and peripheral palm tree swale; (b) hill in sedimentary rock. (c) Annular glacial, wooded rounded dome-shaped hill; sand produced by rock weathering is spread around the hill forming an annular glacial; (d) fragmented peneplain landscape with wooded dome-shaped hills, annular glacial covered by meadow vegetation, and deforested drainage swales (originally morichal with *Mauritia* palms); (e) annular glacial around two hills of different downgrading stages; (f) arched concentric vegetation lines underlining

### 9.3.1 Annular Depositional Glacis

Annular glacis is part of a concentric association of three related relief forms (Plate 9.9):

- At the core of the landscape, a hill or group thereof partially covered by forest or scrub, with large bare rock patches, especially along the steep lateral slopes; bare surfaces are exposed to rock disintegration, especially in pseudokarstic alveoles, generating fine gravelly and sandy materials that are washed downslope by runoff
- Surrounding the hilly core, a gently sloping glacis where hill erosion sediments accumulate and are redistributed by rill and inter-rill runoff (colluviation)
- At the rim of the landscape, a swale or sometimes a more incised colluvio-alluvial vale covered mainly by palm trees that runs along the distal edge of the glacis and collects the excess runoff from the glacis

Evolution of this geofom association over time results usually in downgrading of the hill and expansion of the glacis belt (Plate 9.9). Annular glacis mostly surround granitic dome-like hills. They constitute a common geofom type in the middle Ventuari valley, south of the junction with river Manapiare. Representative book examples are also found in the peneplain landscape south-east of the Duida massif.

#### 9.3.1.1 Proximal Annular Glacis Under Meadow Cover

*Profile P30* (Typic Quartzipsamment, 130 m a.s.l.) is located on an annular glacis east of river Ventuari, at the foot of a circular granitic dome with forest covering the summit and bare lateral flanks. The glacis is uniformly sloping (1–2%) from the rim of the dome to a peripheral palm tree swale. Small domical rock outcrops are spread throughout the glacis. The terrain surface is crossed by rectilinear rills in divergent fan patterns. Rills are on average 5 cm deep, 30 cm large, and distant 5–8 m; they are crusted by black algae. In the proximal part of the glacis, suffusion pans are limited because slope favors surface drainage over infiltration and percolation. In contrast, the distal part shows rounded to elongated suffusion pans, some of them connected by short channels.

The site is in the proximal part of the glacis, 60 m downslope from hill boundary. The material is light grey in the surface layer and white in depth. Close to the border of the dome there are sand spots colored by iron oxides and organic matter washed down from weathering slope cover. Vegetation is a mix of savanna grass and meadow species (20–30% cover) and becomes shrubby toward the dome. A few termite mounds were observed. Loose colluvial sand is in transit on the terrain surface.



**Plate 9.9** (continued) the curved exfoliation joints in the dome-shaped structure of the bedrock, forming a stepped glacis slope; (g) Profile P31: Typic Quartzipsamment on the distal part of an annular glacis, moderately well sorted colluvial material with medium and fine sand dominant; low cover (30%) meadow vegetation

Particle size distribution is homogeneous along the profile with an average 98% sand, 2% silt, and no clay. Variations of all particle size fractions are low in the three layers composing the profile. Fine sand (40%) and medium sand (33%) are the dominant sand separates in all layers with coarse sand as subordinate separates. This sediment is moderately well sorted, reflecting a sustained colluviation process operating over the whole time of sedimentation. Roots penetrate to 40 cm depth, but organic matter content is low (0.2% OC in the topsoil).

### 9.3.1.2 Proximal Annular Glacis in Meadow Glade Surrounded by Forest

Meadow areas are sometimes small insular glades of a few hectares, surrounded by forest in a mosaic of vegetation cover. *Profile P29* (Typic Quartzipsamment, 120 m a.s.l.) is located in such a place about 10 km south of site P30 (former site) and 10 km NE of Cerro Moriche, on the west bank of the middle Ventuari valley. The site is a window within a caatinga-like forest (20–30 m high) that covers a large white sand glacis (0.5–1% slope). Lines of suffusion hollows (20–30 cm deep) are connected by bridges that indicate hypodermic runoff. The lower stems of herbs and forbs are covered by a layer (0–15 cm) of transferral white sand that has little organic carbon (0.16%) but frequent horizontally lying buried roots. Below the cover layer is a light grey A horizon with frequent roots, followed by very pale brown C layers with common roots. A compact densipan layer starts at 50 cm depth.

Particle size distribution is homogeneous along the profile with an average 97% sand, 3% silt, and no clay. Variability is low. Fine sand (42%) and medium sand (39%) are the dominant separates in all three layers. The sediment is well sorted, reflecting colluviation operating over the whole time of deposition. Colluviation is not active today under the caatinga forest where a litter layer (0–10 cm) and a dense root mat (10–20 cm) stabilize the terrain surface. In the meadow enclave, sand is well reworked by runoff (0–15 cm).

The particle size pattern of P29 is remarkably similar to that of P30, with fine and medium sand dominant (approximately 70–80% in all layers), although these profiles are 10 km apart. They have practically the same values of total sand and organic carbon in comparable layers (Table 9.5). Both sites represent proximal glacis sectors, one covered by meadow, the other by forest on similar sand substratum. This raises the following questions. Was P30 originally covered by forest, now degraded into meadow? Was P29 originally covered by meadow, now colonized by forest? The small meadow glade of P29 enclaved in the forest cover may provide some elements of explanation. The loose reworked sand cover (0–15 cm) cannot proceed from within the surrounding forest as the surface is stabilized by a dense root mat. It can only come from the rim of the forest where the protecting root mat is presumably

**Table 9.5** Similarity of sand and organic carbon contents between two soils located on proximal glacis distant in space

Layers	Total sand %		Organic carbon %	
	P29	P30	P29	P30
AC1	97	98	0.16	0.17
AC2	98	98	0.14	0.14
C	95	97	0.33	0.28

perturbated by runoff (or wind) and the underlying white sand is remobilized and redistributed on top of the glade surface. It can then be hypothesized that the forest cover at this place is in regression.

### 9.3.1.3 Distal Annular Glacis Under Meadow Cover

*Profile P31* (Typic Quartzipsamment, 130 m a.s.l.) is also located on an annular glacis, 1 km north-east of site P30, but on the distal part where the terrain surface flattens out in the direction to a peripheral palm tree swale. Surface drainage lines in divergent patterns are successions of open rills 20–30 cm deep, crusted with black algae, and small tunnels dug by hypodermic flow. There are some isolated suffusion pans, the largest of which are covered by colonies of grass and Cyperaceae. Locally crystalline rock slabs with white sand around rise from the terrain surface. Vegetation is meadow (30% cover). The feet of the plants are buried by loose white sand.

Below a 5 cm surface cover of loose transferral white sand, the sediment is very pale brown sand with roots (1–3 mm) down to the bottom of the profile (70 cm). Average sand is 96%, silt 4%, and no clay. Medium and fine sand are the dominant separates as in the case of P29 and P30, but with more variability among the consecutive layers. Standard deviation values are larger than those of P29 and P30. This reflects the variation of the colluvial deposition in the distal part of the glacis where sediments are spread over larger areas than in the transportational part of the proximal sector.

### 9.3.1.4 Annular Glacis Around a Green-Foliated Rock Hill

Associations of central hill, annular glacis, and peripheral swale are frequent in the peneplain east of the Duida massif. The following is an example of how the weathering of a bedrock kind different from the granitic-gneissic rocks that usually outcrop in peneplain landscape influences the particle size pattern. An annular glacis belt surrounding a central hill made of green schistose quartzitic rock was selected in the proximity of La Esmeralda, in the middle Orinoco river valley. The weathering of this kind of rock produces not only sand but also silt. The hill is covered with a heap of large rock boulders without vegetation. Thus, weathering products are not filtered and penetrate the glacis surface without any previous selection. This causes an undifferentiated particle size pattern that deviates from the common colluvial glacis pattern. The glacis (1–2% slope) is covered by relatively dense (70%) meadow vegetation including grass species.

*Profile P22* (Typic Udorthent, 130 m a.s.l.) is a composite one showing two sedimentation phases. The upper set of two layers (0–40 cm) is a well-structured, dark greyish brown sandy loam A horizon, with 66% sand, 32% silt, 2% clay, and undifferentiated sand separates except a slight dominance of medium sand (24%) (Table 6.5). The subsurface layer (40–70 cm) is a light grey loamy sand densipan horizon, with 82% sand, 17% silt, 1% clay, and codominance of coarse sand (24%) and medium sand (26%). This is a sort of glacis material that departs from typical white sand glacis: it is dark colored, unsorted, with significantly lower proportion of sand and higher proportion of silt. Thus, the nature of the weathering rock that produces colluvial sands introduces variations in peneplain glacis.

### 9.3.2 Longitudinal Depositional Glacis

#### 9.3.2.1 Longitudinal Glacis Under Meadow

Longitudinal glacis are large, elongated white sand surfaces, slightly inclined (1–2%) toward a palm tree swale/vale with anastomosed channels. They form usually at the front of larger hilland areas consisting of dome-like reliefs in crystalline rocks or linear structural reliefs in sedimentary rocks (Plate 9.10). The vegetation cover is meadow or shrubby meadow. The terrain is subdivided into parallel; slightly convex interfluve strips by the incision of secondary swales. The surface is crossed by linear rills, sometimes anastomosed, up to 10 cm deep. Sand is much less sorted than that of the annular glacis type. Usually, there is a codominance of several sand separates.

*Profile P13* (Typic Quartzipsamment, 100 m a.s.l.) is a longitudinal glacis site, north of river Ventuari close to the mouth of the Maraya stream. The surface layer is light grey; the subsurface layer is white. On average, the sediment is 97% sand, 3% silt, and no clay. The particle size pattern is unsorted, with 20% coarse sand, 27% medium sand, and 33% fine sand (Plate 9.10e). This reflects a splay-like poorly selective depositional process.

#### 9.3.2.2 Longitudinal Glacis Under Scrub

Large glacis (3–5% slope) have formed at the foot of structural reliefs including fault scarps of Roraima sandstone and quartzite that constitute the border of the Cuao-Sipapo massif in contact with the lowlands. The terrain is covered by open scrub (bana) formed by clusters of shrubs and trees 3–5 m high and interspersed meadow, and bare sand patches. New sand accretion in glacis covered by scrub vegetation is very limited to nill. Such glacis are no longer active. Only locally some pinkish sand can be found spread over the soil surface, above the A horizon, indicating the arrival of fresh material from upslope erosion. Current runoff causes slightly undulating microtopography and surficial sand removal, with sand excavation downslope and accumulation upslope the trees.

*Profile P98* (Typic Quartzipsamment, 150 m a.s.l.) is a site located on a non-active glacis, 12 km WSW of Cerro Autana. The surface layer is light grey, while the subsurface layers are white. On average, the sediment pack is 97% sand, 1% silt, and 2% clay. Seven layers were distinguished on the basis of slight differences in color from greyish white to white, and/or the presence of fossil roots (44–75 cm). The profile is remarkably homogeneous over depth; all layers have similar particle size distribution patterns with medium sand dominant (about 40%), and coarse sand and fine sand subdominant (each 20% or more). Standard deviation values of particle size classes among layers are low. With three sand separates summing up about 90% of the sediment, sorting can be considered moderate, reflecting splay deposition rather than colluviation. The presence of buried roots and irregular variations of organic carbon with depth indicate an effect of cumulation, but the same depositional process was operating the whole time of glacis construction. The absence of conspicuous layering in this profile is a relevant



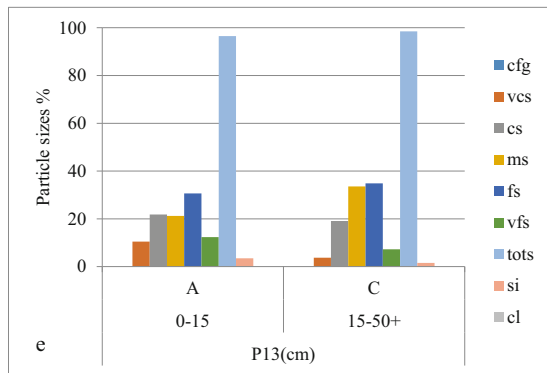
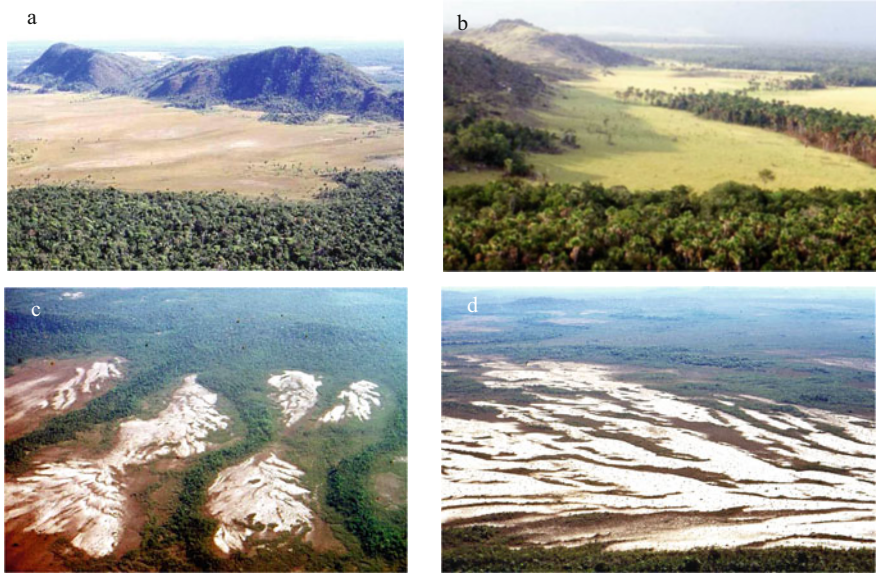


**Plate 9.10** Longitudinal glacis under meadow vegetation developed in front of hilly reliefs: (a) igneous-metamorphic ridge; (b) sedimentary ridge; Longitudinal glacis reactivated by rainfall runoff and sheet erosion upon repeated burning of bana-caatinga mixed cover in the Ventuari area; (c) older glacis surface starting in front of a transversal ridge, fragmented by the incision of creeks with enlarged floodplains; (d) younger glacis surface incised by swales originally covered by *Mauritia* palms (“morichal”); (e) Profile P13: Typic Quartzipsamment on a longitudinal glacis under meadow vegetation; unsorted splay-like depositional facies

feature that distinguishes relatively homogeneous glacis sediments from stratified alluvial plain sediments.

The effect of shifting river deposition in alluvial plains, with reworking of the sand cover, causes granulometric sediment stratification resulting in layers separated by lithological discontinuities, especially in splay sediments. Comparatively, glacis is geomorphically a more stable environment, as it is not exposed to strong river/

stream disruptions. The same process operates over time with only slight variations. It allows a more stable establishment of the vegetation cover. This may explain why glacia soils tend to be rather greyish than white.

Longitudinal glacia under bana scrub and caatinga woodland on white sands is the most vulnerable biome to fire during the period of lower rainfall in January–March because sclerophyllous vegetation is more inflammable than rainforest and fire propagates easily on large flat terrains (Plate 9.10). Upon repeated burning, the terrain is nearly bare allowing the direct impact of rainfall and remobilization of surface sand through runoff.

### 9.3.2.3 Soil-Sediment Toposequence on Longitudinal Glacia

To detect changes in particle size distribution along a glacia slope, a soil toposequence was described on a longitudinal glacia (1–2% slope) lying south-east of Cerro Moriche, a major mid-elevation Roraima sandstone-quartzite relief in the middle valley of river Ventuari. The toposequence (120 m a.s.l) consists of three profiles ca. 250 m apart, located in the proximal (P9), central (P8), and distal (P7) parts of the glacia, respectively. Vegetation cover is mainly meadow with increasing grass species (e.g., *Mesosetum* sp.) from upper to lower glacia. Soils and sediments are light grey over pinkish grey, reflecting their origin from Roraima rocks. They show remarkably similar particle size composition based on averaged layer values. Fine sand is the dominant separate, together with subordinate medium and very fine sand, both in relatively similar proportions. There is no relevant trend of spatial granulometric selection from proximal to distal glacia, except a small decrease of total sand and small increases of medium sand and silt. Particle size distribution is fairly homogeneous with depth in all three profiles with relative dominance of fine sand. The absence of spatial and vertical particle size differentiation shows that the same depositional process with constant flow energy has been operating during the sand cover formation over the whole glacia extent.

The depositional cover of this longitudinal glacia is less sorted than that of short glacia. The latter usually show codominance of two sand separates, often medium and fine sand, a pattern that can be interpreted as resulting from colluviation (see P29 and P31 in Fig. 9.3a, b). In the present case, there is relevant dominance of fine sand (40–50%) but together with medium and very fine sand (ca. 20% each). This reflects a moderately to poorly sorted sediment where splay deposition and reworking have probably played a stronger role than colluviation. Surface transferral of particles by runoff is evidenced by sand removal around plants upslope and accumulation downslope.

All three profiles, P7, P8 and P9, classify as Udoxic Quartzipsamments based on silt + clay contents. It means that these soils have better water holding capacity than Typic Quartzipsamments, and this could explain the presence of grass species together with more frugal, less demanding, more drought-resistant meadow species.



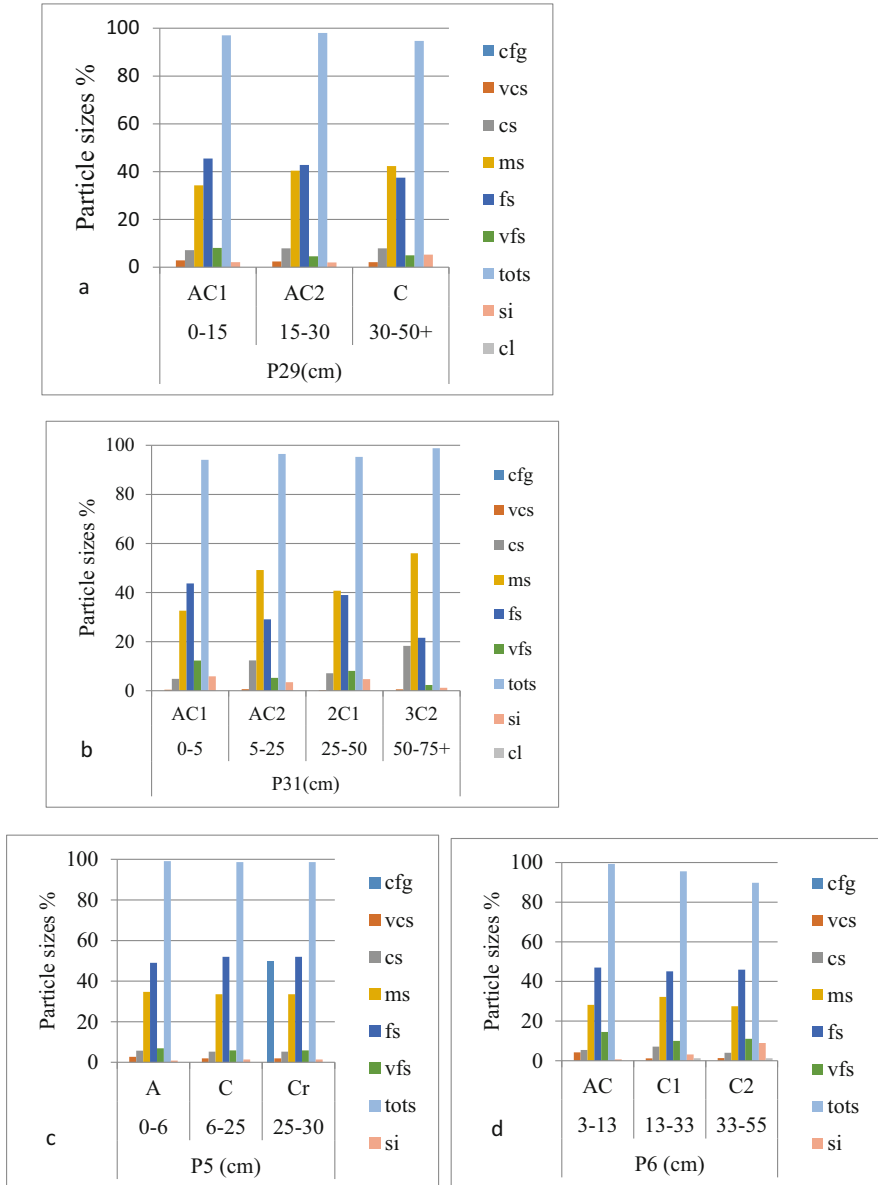


**Fig. 9.3** (a) Profile P29: Typical Quartzipsamment on a proximal glaciis in a meadow glade surrounded by caatinga; well-sorted colluvial material with fine and medium sand dominant. (b) Profile P31: Typical Quartzipsamment on the distal part of an annular glaciis surrounding a low granitic hill covered by rainforest; moderately well-sorted colluvial material with medium and fine sand dominant; low cover (30%) meadow vegetation. White sand generated by weathering of local sandstone outcrops and distributed by runoff to form a colluvial glaciis; (c) sand produced and accumulated around the flagstones including a relevant proportion of coarse fragments in the Cr layer (P5 Lithic Quartzipsamment); (d) sand spread on the glaciis surface by colluviation about 400 m downslope from profile P5 (P6 Udoxic Quartzipsamment); both materials at the site of emission and the site of deposition show similar well-sorted particle size distribution with fine and medium sand dominant

### 9.3.3 Weathering Glacis

#### 9.3.3.1 Characteristics of Sand Produced by Weathering

An investigation carried out in the proximity of San Carlos de Rio Negro by Schnütgen and Bremer (1985) shows that deep weathering of granite on woody peneplain terrains generates strongly impoverished cover sand relicts of the weathered substratum, upon removal of the fine saprolite particles by underground percolation and/or surficial flooding, leaving a nearly pure quartz residuum cover (see Chap. 8, Sect. 8.4.1.1).

In peneplain landscape covered by meadow vegetation complete weathering profiles starting from the terrain surface were not found. In this environment, weathering bedrock is usually covered by sandy material that is not fully related with the substratum. Hereafter glacis are considered weathering glacis in situations where the weathering front is within 1 m depth from the surface.

Weathering glacis occur in annular as well as longitudinal landscape positions. Depth to bedrock varies from shallow (30–50 cm) to moderate (50–100 cm). In these situations, the particle size distribution of the clastic material reflects the nature of the weathered bedrock in the lower profile layers. Surface and subsurface layers result frequently from reworking of the weathered material mixed with sediments coming from upslope, and redistribution of the mix by colluviation or splay. Thus, weathering glacis are usually mixed situations. The saprolite of the weathering front shows usually some of the following characteristics:

- White color except in very poorly drained sites
- Presence of coarse fragments resulting from the physical disaggregation of the bedrock
- Presence of feldspar fragments when the bedrock is crystalline
- Silt increase with depth (weathering product)
- Presence of compact layers (densipan) possibly related with silt content and sand grain fragmentation
- Unsorted particle size distribution with large spectrum of particles reflecting the texture of the bedrock
- Often less than 85% of sand

Similar features characterize materials resulting from bedrock weathering in alluvial plains, usually associated with reticular network of suffusion channels and pans with vertical walls, especially in areas of impeded surface drainage.

Hereafter a few examples are analyzed to show variations in weathering glacis.

#### 9.3.3.2 Surficial Weathering Glacis Around Local Rock Bar Outcrops

Subvertical to vertical alignments of rock bars outcrop on the terrain surface throughout the peneplain landscape. Bars are generally grouped in fields but may occur also as isolated flagstones. Height varies from 0.2–0.3 m up to 5–6 m. Physical weathering disintegrates the rock into white sands, sometimes mixed with some gravel, that accumulate between and around the outcropping flags (see Plate 8.6 in

Chap. 8, Sect. 8.4.2.2). Subaerial weathering of sandstone outcrops is an important source of authigenic fresh sand that is incorporated into the lowland sand cover via colluviation. The weathered sandy material is usually redistributed on the terrain surrounding and downslope the flagstone fields by rill and inter-rill rainfall runoff forming colluvial glacis under open meadow with some shrubs (e.g., *Terminalia yapacana*). *Profile P6* (Udoxic Quartzipsamment, 120 m a.s.l.) is located on a mixed colluvial-weathering glacis (0.5–1% slope), 20 km north-west of San Antonio, on the interfluvium between river Orinoco and the upper *caño* Caname. Weathered white sand covers a 700–800 m long glacis fed concomitantly by clastic debris coming from subaerial disintegration of the sandstone flags at site P5 100 m distant upslope and the weathering in situ of the sandstone substratum. Averaged total sand is 95% (90–99%) with 46% fine sand and 29% medium sand, above the sandstone bedrock at 55 cm depth. Both profiles P5 and P6 show similar particle size distribution patterns with a dominance of fine and medium sand, a kind of pattern also found in annular glacis (Fig. 9.3c, d).

### 9.3.3.3 Cover Glacis Over Unconformable Weathering Substratum

Glacis sediments generated from one kind of sedimentary or crystalline rock upslope cover often other kinds of rock downslope. This causes complex situations where short-distance variations of the substratum generate contrasting sand facies between clastic cover and underlying weathering rock. The following is an example of composite profile showing glacis sediment lying on top of weathered greywacke.

*Profile P87* (Typic Udorthent, 100 m a.s.l.) is located 40 km north-west of San Antonio and 10 km west of the Orinoco left bank, on a glacis (1–1.5% slope) covered by shrubby meadow, at the foot of low sandstone hills. The glacis is crossed by transversal lines of sandstone bars, subvertical (70–80°), bedded (5–15 cm thick strata), up to 4–6 m high, showing strongly weathered rock faces and pseudokarstic alveoles. The profile is about 100 m downslope of the outcropping rock bars (see Plate 8.6 in Chap. 8, Sect. 8.4.2.2).

The cover material (0–38/43 cm) is pinkish white sand coming from pinkish sandstone that forms the upslope hills and the outcropping bars on the glacis. It is composed of 93% sand, 4% silt, and 3% clay, with dominant fine sand (63%). The last layer contains 8% gravel and lies unconformably (undulating contact) on the weathering substratum (Fig. 9.4a). The high content of fine and very fine sand (79%) suggests the possibility of wind activity, but the eolian hypothesis can be discarded because of the presence of gravel.

The substratum (38/43–63 cm) is slightly greenish white sand from strongly weathered greywacke. The rock structure is still visible but crumbles fully by touching. Solid bedrock appears at 63 cm depth. Material is 67% sand, 27% silt, and 6% clay, with only 33% fine sand. A large proportion of silt comes from the matrix of the greywacke.

*Profile P88* (Lithic Quartzipsamment) is located at the same site as P87, 40 m upslope, between two lines of the subvertical rock bars that outcrop across the glacis. It is loose pinkish grey sand 5–10 cm thick, directly formed from weathering of outcropping sandstone bars. The particle size distribution pattern is remarkably

similar to that of the cover material at P87, showing thus geogenetic relationship (Fig. 9.4b). The colluvium that covers the weathered greywacke substratum at P87 originates in fact from the disintegration of sandstone bars outcropping at P87.

#### 9.3.3.4 Cover Sand from Different Bedrocks

Hereafter, two profiles, one on sandstone (P14) and another on granite (P23) are compared.

*Profile P14* (Udoxic Quartzipsamment, 220 m a.s.l.) is located 10 km east of Carmelitas, south of the middle Ventuari river, in the Yapacana area. The glaciais (0.5–1% slope) forms an annular belt around a small hill (8–10 m high) of sandstone outcrops dismantled into a heap of boulders showing pseudokarstic features with white sand between boulders and covered by stunted trees and shrubs. The glaciais is covered by dense herbaceous vegetation (60–70%) consisting of savanna grasses and meadow species. The soil is dark grey over grey, with roots penetrating down to the sandstone at 80 cm depth. On average, the material is 89% sand, 10% silt, and 1% clay. Fine sand is dominant (46%), followed by medium sand (27%) (see Tables 7.3, 7.9 and Fig. 7.8 in Chap. 7).

*Profile P23* (Udoxic Quartzipsamment, 95 m a.s.l.) is located close to Guarinuma village in the Atabapo area, on a long sloping glaciais (2–3%) with savanna-meadow vegetation (50–60% cover). Granite substratum outcrops in the surroundings and ironstone layers (hardened plinthite) formed on granite are sometimes exhumed along palm tree swale incisions. The soil is dark grey over grey, with roots penetrating down to 50 cm depth. On average, the material is 80% sand, 13% silt, and 7% clay. Granite weathering provides moderately sorted mineral soil, with fine sand dominant (54%), followed by very fine sand (25%). The chemical weathering of granite generates a larger spectrum of particle separates than that caused by the physical weathering of sandstone, with more very fine sand, silt, and clay.

Although P14 and P23 are derived from the weathering of two different parent rocks, they have in common some features that distinguish them from other glaciais materials. They classify as Udoxic Quartzipsamments because of slightly higher amounts of fine sand, very fine sand, silt, and clay. P23 is associated in the same glaciais with Udorthents (P24). These soils are less exposed to surface layer drying during the period of lower rainfall in January–March. They are dark grey over grey and have higher organic carbon contents than typical white sand materials, inclusive in deeper layers (2.1/0.8% in P23; 1.7/0.5% in P14). Roots penetrate to 50 cm depth or more. Vegetation cover is usually fairly dense, with savanna grasses and meadow herbs together.

There is no conspicuous weathering front with saprolite material along the contact with the underlying bedrock. This suggests that the substratum has been exposed upon erosion of an earlier soil body (hardened plinthite) and subsequently buried by incoming colluvium from upslope. Thus, alternation of erosion and deposition can be envisaged in weathering glaciais evolution.

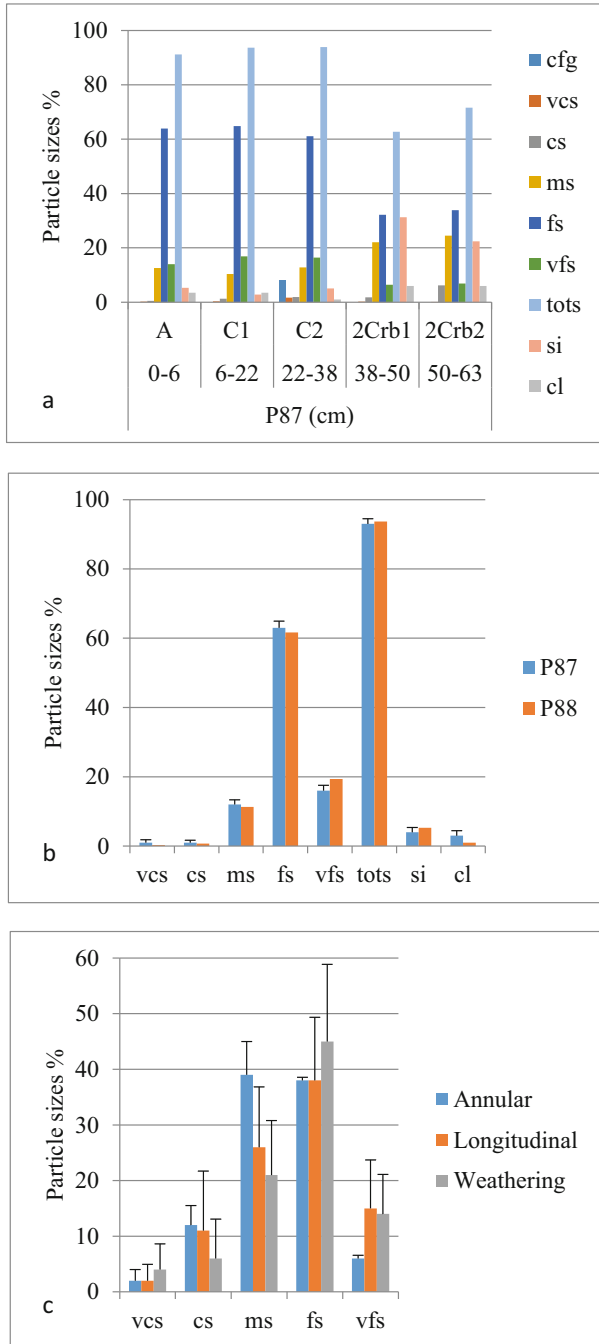


**Fig. 9.4** (a) Profile P87: Typical Udorthent in fine sand (about 60%) of a colluvial glacia (0–38 cm) burying weathered greywacke substratum; (b) similarity of particle size distribution between the sand emission place at P88 upslope and the colluvial deposition at P87 downslope (P87: 0–43 cm, 3 layers; P88: 0–5/10 cm, 1 layer), with relevant dominance of fine sand (ca 60%); (c) generalized

### 9.3.4 Discussion

#### 9.3.4.1 Relationships Between Soil Class, Texture, Color, and Vegetation

Out of the 15 profiles used to describe soil-sediment variations under meadow and shrubby meadow vegetation in peneplain landscape, five are Typic Quartzipsamment white sands, while six are Udoxic Quartzipsamment greyish sands with fine sand and loamy fine sand textures (Table 9.6). The remaining four profiles are Typic Udorthent greyish sands with fine sand, loamy sand, and sandy loam textures. Colors reported are moist Munsell colors. When dry, light grey and very pale brown sands become white, and pinkish grey sands become pinkish white.

In alluvial plain landscapes, sandy materials are mainly pure white sands. In peneplain glaciais landscape, white sands are frequent, but also pinkish grey, greyish, and pale brown sands occur. Color variation depends on several factors such as the proximity to Roraima rock outcrops that provide the pinkish stain, the length of the colluvial transport that causes sand bleaching through deferrugination from proximal to distal glaciais, and the density and composition of the vegetation cover that contribute to greyish color through organic matter incorporation.

Field observations suggest that there might be a relationship between annual rainfall and soil color under savanna and savanna-meadow vegetation. In areas where soils are drier, grass species tend to explore deeper layers searching for water supply. Root decay in depth causes subsurficial sand to be greyish. In southern areas, soils are moist for the largest part of the year, roots penetrate less deep, and subsurficial sand layers are white. This relationship relates more to glaciais environment than to low-lying alluvial plains.

Udoxic Quartzipsamments and Typic Udorthents share some characteristics that distinguish them from other glaciais soils. They are mostly greyish in the upper layers except on some weathering glaciais, they often have a bit more organic matter than Typic Quartzipsamments, they have some content of fines (silt +clay), root penetration goes deeper (>50 cm), and in many cases meadow species are mixed with savanna grass species. In pure meadow vegetation, herbs and forbs show some resistance to water stress that grass species may not have. Soil Taxonomy (Soil Survey Staff 2014) distinguishes Udoxic Quartzipsamments from Typic Quartzipsamments on basis of the criterion that the sum of the weighted average silt plus two times the weighted average clay is more than 5 in the Udoxic subgroup. The implementation of this index shows relevant differences between Typic Quartzipsamments and the other peneplain soils (Table 9.6). The index can be used as an indicator of water-holding capacity in sandy soils and this could explain the presence of grass species mixed with meadow vegetation in Udoxic Quartzipsamments and Typic Udorthents. Deeper soil penetration of grass species and root decay may cause the greyish staining of the sand grains. The highest udoxic

---

**Fig. 9.4** (continued) particle size distributions of annular, longitudinal, and weathering glaciais; averages based on the data reported in Table 9.8



**Table 9.6** Variety of soil classes and features, glacia types, and vegetation covers in penneplain landscape

Profile	Soil class	Glacia type	Texture	Udoxic index	Color moist	Vegetation	Study area
P29	Typic Quartzipsamment	Annular	Fine sand	3	Light grey/very pale brown	Shrubby meadow	Ventuari
P30	Typic Quartzipsamment	Annular	Fine sand	2	Light grey/w/white	Meadow-savanna	Ventuari
P31	Typic Quartzipsamment	Annular	Medium sand	4	Light grey/very pale brown	Meadow	Ventuari
P13	Typic Quartzipsamment	Longitudinal	Fine sand	3	Light grey/white	Shrubby meadow	Ventuari
P98	Typic Quartzipsamment	Longitudinal	Medium sand	5	Light grey/w/white	Open scrub	Sipapo
P7	Udoxic Quartzipsamment	Longitudinal	Loamy fine sand/fine sand	18	Light grey/pinkish grey	Savanna	Ventuari
P8	Udoxic Quartzipsamment	Longitudinal	Loamy fine sand/fine sand	14	Light grey/pinkish grey	Meadow-savanna	Ventuari
P9	Udoxic Quartzipsamment	Longitudinal	Fine sand	8	Light grey/pinkish white	Meadow-savanna	Ventuari
P6	Udoxic Quartzipsamment	Weathering	Fine sand	6	Light grey/white	Open meadow	Yapacana
P14	Udoxic Quartzipsamment	Weathering	Loamy fine sand/fine sand	12	Dark grey/pale brown	Savanna-meadow	Yapacana
P23	Udoxic Quartzipsamment	Weathering	Loamy fine sand -sandy loam	27	Grey brown/light grey	Meadow	Atabapo
P22	Typic Udorthent	Annular	Medium sandy loam /medium loamy sand	36	Grey brown/light grey	Savanna-meadow	Yapacana
P24	Typic Udorthent	Weathering	Fine sand/fine sandy loam	13	Light grey/white	Meadow	Atabapo

(continued)

**Table 9.6** (continued)

Profile	Soil class	Glacis type	Texture	Udoxic index	Color moist	Vegetation	Study area
P27	Typic Udorthent	Weathering	Medium sandy loam/medium loamy sand	13	Light grey/white	Savanna-meadow	Atabapo
P87	Typic Udorthent	Weathering	Fine sand/fine sandy loam	10	Pinkish grey/white	Shrubby meadow-savanna	Atabapo

Udoxic index: silt%+2× clay% (Soil Survey Staff 2014)

**Table 9.7** Relationship between glacis type, udoxic index, organic carbon, and vegetation cover

Profile	Glacis type	Dominant separate	Udoxic index	Subsurface organic carbon %	Vegetation cover
<i>White</i>					
P30	Annular	Fs	2	0.21	Meadow-savanna
P13	Longitudinal	Fs	3	0.09	Shrubby meadow
P98	Longitudinal	Ms	5	0.15	Open scrub
P6	Weathering	Fs	6	0.09	Open meadow
P24	Weathering	Fs	13	0.14	Meadow
P27	Weathering	ms	13	0.05	Savanna-meadow
P87	Weathering	Fs	10	0.13	Shrubby meadow-savanna
<i>Pinkish grey</i>					
P7	Longitudinal	Fs	18	0.18	Savanna
P8	Longitudinal	Fs	14	0.15	Meadow-savanna
P9	Longitudinal	Fs	8	0.11	Meadow-savanna
<i>Pale brown</i>					
P29	Annular	Fs	3	0.24	Shrubby meadow
P31	Annular	ms	4	0.15	Meadow
P14	Weathering	Fs	12	0.54	Savanna-meadow
<i>Light grey</i>					
P22	Annular	Si	36	0.44	Savanna-meadow
P23	Weathering	Fs	27	0.55	Meadow

Udoxic index:  $\text{silt}\% + 2 \times \text{clay}\%$  (Soil Survey Staff 2014)

index values correlate with the highest organic carbon contents in subsurface layers (P22 and P23) (Table 9.7). Sites with high udoxic index occur in most glacis types except annular glacis and in three of the six study areas (Atabapo, Ventuari, and Yapacana). Soils showing good correlation between greyish subsurface color, high udoxic index, and mixed meadow-savanna vegetation are P7, P8, P14, P22, and P23 (Table 9.7).

**9.3.4.2 Particle Size Distribution in Glacis Sediments: Dominance of Fine and Medium Sand**

All particle size classes show large ranges of values. The two dominant particle size classes, i.e., medium sand and fine sand, are complementary in such a way that the sums of both fit in relatively narrow ranges: 73–81% in annular glacis, and 60–70% in longitudinal glacis. The range is larger in the case of weathering glacis that are more diverse (51–75%) (Table 9.8).

To establish the ranking of sand separates, only separates with more than 15% sand were taken into consideration. The sequences of relative importance of sand separates are based on sand content differences higher than 30% (>>>), 15% (>>), and 5% (>), respectively, in relation to subsequent separates.

Fine sand and medium sand alone constitute the largest part of the sand fraction at all sites. Fine sand (0.25–0.125 mm) is the dominant sand separate at 11 out of

**Table 9.8** Particle size distribution in glacial sediments and ranking of sand separates

Profile	Depth cm	Number of layers	Very coarse sand	Coarse sand	Medium sand	Fine sand	Very fine sand	Total sand	Medium and fine sand	Ranking of sand separates (> 15% sand)
<i>Annular glacis</i>										
P29	0-50	3	2	8	39	42	6	97	81	fs = ms
P30	1-70	3	4	15	33	40	6	98	73	fs > ms
P31	0-75	4	0	11	45	33	7	96	78	ms > fs
Average			2	12	39	38	6	97	77	
Range			0-4	8-15	33-45	33-42	6-7	96-98	73-81	
<i>Longitudinal glacis</i>										
P7	0-100	2	0	4	23	40	18	85	63	fs >> ms > vfs
P8	0-50	3	0	2	20	40	25	87	60	fs >> vfs > ms
P9	0-100	2	1	2	16	54	20	93	70	fs >> vfs > ms
P13	0-50	2	7	20	27	33	10	97	60	fs > ms > cs
P98	0-130	7	3	24	44	23	3	97	67	ms >> cs = fs
Average			2	11	26	38	15	92	64	
Range			0-7	2-24	16-44	23-54	3-25	85-97	60-70	
<i>Weathering glacis (surface material reworked by colluviation or splay)</i>										
P6	3-55	3	2	6	29	46	12	95	75	fs >> ms
P14	0-80	2	2	3	27	46	12	89	73	fs >> ms
P23	0-60	3	1	2	7	45	25	80	52	fs >> vfs
P24	0-80	5	4	4	20	48	14	90	68	fs >> ms
P27	35-70	1	13	20	31	20	3	87	51	ms > fs = cs
P87	0-43	3	1	1	12	63	16	93	75	fs >>> vfs
Average			4	6	21	45	14	90	66	
Range			1-13	1-20	7-31	20-63	3-25	80-95	51-75	

14 sites and subdominant at the other sites. In general, fine sand percentages remain fairly constant with depth, while other sand separates may vary between layers. For instance, profile P24 has a range of 43–54% fine sand over five horizons (0–80 cm) (Table 9.8). Medium sand is dominant at three sites and subdominant at seven. Very fine sand occurs as subdominant or subordinate separate at five sites. Coarse sand is a subordinate separate at five sites. Overall, peneplain glacia sediments are overwhelmingly fine and medium sand regardless of the type of glacia.

The predominance of medium and fine sand in all glacia types reveals remarkable homogeneity and affinity between sites often far apart. This suggests that, in spite of differences in transportation and deposition processes between glacia types, there is a factor that contributes to the generalization of a narrow range of particle size, mainly 0.5–0.125 mm. Even when the rocks upslope the glacia are fairly coarse-grained (e.g., sandstone, quartzite, rapakivi granite, gneiss), the clastic debris generated by their weathering are substantially finer grained. For instance, profile P6, located in the proximal part of a glacia 100 m downslope of coarse-grained sandstone outcrops that originate the sediment, has 46% fine sand and 75% medium + fine sand. Profile P30 located 60 m downslope from the boundary of a granitic dome has 40% fine sand and 73% medium + fine sand. Profile P29 also on a proximal glacia has 42% fine sand and 81% medium + fine sand. Profile P31 on a distal glacia has 33% fine sand and 78% medium + fine sand (Table 9.8). The similarity of these particle size patterns whatever the distance from the origin of the sediments and the transport length (proximal or distal) indicates that sand grains are fragile in the oligotrophic wet meadow environment and are fragmented to an endproduct size of fine and medium sand. Very fine sand and silt are mostly low proportion at all sites.

#### 9.3.4.3 Particle Size Patterns and Glacia Formation

The general pattern regardless of glacia type is that of sand concentration in two dominant separates of medium and fine sand, with subordinate proportions of coarse and very fine sand.

Annular glacia are more homogeneous than the other glacia types. Medium and fine sand sums up nearly 80% of the total sand fraction, with similar sand proportions in both separates and relatively narrow ranges of variation. Annular glacia are mostly colluvial glacia. Colluviation produces a well-sorted, bi-modal particle size distribution pattern, similar to that of overflow in alluvial sediments.

Longitudinal glacia sediments are less sorted than annular glacia deposits. Usually, particles are distributed over three separates (tri-modal pattern) with dominant fine sand and lesser proportions of medium sand and very fine sand. Some sites show a shift toward coarse sand. Particle ranges are large reflecting heterogeneity within sites and between sites. Splay is the most common depositional process in longitudinal glacia.

Weathering glacia can be in annular or longitudinal landscape position, but particle size distribution of the material is influenced by the fragmentation of the bedrock at shallow to moderate depth. They show a strong concentration of fine sand and smaller proportions of medium and very fine sand, with large ranges of particle variation. Heterogeneity reflects the large spectrum of particle sizes in weathering

rocks, especially granitic ones (Fig. 9.4b). Weathered products are reworked on the glacis surface by colluvial or splay processes causing similarity with pure depositional glacis.

Figure 9.4c is based on assembling all individual profile layers per glacis type. It highlights the dominance of fine sand and medium sand in glacis deposits. Large variability values show the heterogeneity of longitudinal and weathering glacis sediments as compared to the more homogeneous annular glacis deposits. There is some similarity between longitudinal and weathering glacis sediments because sands covering the weathering bedrocks are usually a mixture of weathered clastics and splay sands from upslope.

#### **9.3.4.4 Differences Between Peneplain Glacis Sediments and Alluvial Plain Sediments**

Sand distribution in alluvial plain landscape is more complex than that in peneplain landscape. In peneplain, the dominant relationship between glacis and meadow vegetation results in a greater uniformity of the geophysical conditions that contribute to controlling the vegetation cover. The alluvial plain meadow environment is more diverse, with particle sizes stretching from coarse to medium and fine sand.

Absent or weak granulometric stratification is a distinctive glacis feature. This differentiates glacis from alluvial plain sediments, especially splay sediments, in which the effect of shifting river deposition, with reworking of sand, causes stratified layers separated by lithological discontinuities. Glacis is geomorphically a more stable environment than alluvial plains for not being exposed to repeated river or stream disruptions. The same process operates over time with only slight variations. This may also explain why glacis soils tend to be rather greyish than white:

- Colluvial sediments of annular glacis forming around granitic hillocks bear some resemblance with alluvial sediments in overflow mantles. In both sediment types, sand concentrates in two codominant separates, i.e., medium and fine sand. This convergence of depositional facies can be considered fortuitous as colluviation and overflow are two different processes, but lead to similar particle sorting. Colluvial profiles tend to be less stratified, and more homogeneous over depth than overflow mantle profiles.
- Peneplain glacis soils are better drained than alluvial plain soils. Although glacis occupy in general the highest positions in the lowland context, soils remain moist from the surface except in the Ventuari valley where surface layers of Typic Quartzipsamments dry up to 15–25 cm depth during the lower rainfall period (January–March).
- The occurrence of fairly well-sorted sediments in the 0.5–0.125 cm particle size range at some places raises the hypothesis of eolian reworking of alluvial deposits. However, there is no geomorphic field evidence of current or past wind activity on peneplain terrain surfaces except eolian blanket sediments covering glacis in the Camani area. Usually, glacis heads are directly connected with rock outcrops and sediments are poor in very fine sand and silt.

## 9.4 Valley Sediments: River Levees and Terraces (Pasimoni and Siapa Valleys)

Overall rivers and major streams have unobtrusive levees because generalized overbank flow does not deposit selectively the coarser sediments in the immediate margin of the waterways but expands the deposition over larger adjacent areas forming overflow or splay mantles. River-shaped landscape was found only in the southern part of the study region, in the lower Pasimoni and Siapa watersheds. This sector has fluvial geomorphic features that are not present elsewhere in the study region. The most common geomorphs are meander lobes, flattened inactive levees, and large undifferentiated terrace benches. Commonly river levees expand laterally into mantles, under meadows as well as coating vegetation. Soils are well to moderately well drained, as the regional water level in the Pasimoni area has been lowered through floodplain incision. A remarkable feature is that all these river-related geomorphs show similar particle size distribution patterns. Features of the fluvial landscape of rivers Pasimoni and Siapa are described in Chap. 6 (see Sect. 6.8). Figures 6.14 and 6.15, show topographic and geomorphic features of the Pasimoni valley.

### 9.4.1 Riverbank Overflow Levee

*Profile P105* (Oxyaquic Quartzipsamment, 125 m a.s.l.) is located on the right bank of river Siapa, downstream the confluence with river Manipitare (Table 6.7). The site is a convex crescent-shaped terrain form, the configuration of which simulates a floodplain meander lobe (point bar). It dominates an abandoned infilled channel by 1–1.5 m elevation (P106, Psammaquent with a shallow organic toplayer, colonized by *Lagenocarpus*). Vegetation is shrubby savanna with a mixture of grass (e.g., *Axonopus* sp., *Mesosetum* sp.) and meadow species (e.g., *Bulbostylis* sp., *Eriocaulaceae*). Upper layers (0–31 cm) are grey, while the lower layers are white. Groundwater is at 90 cm depth as controlled by the nearby abandoned channel. Overall sand content is 92%, with 5% silt, and 3% clay. The profile is homogeneous with similar particle size distribution pattern in the upper 90 cm and low standard deviation values for all separates. There is a strong dominance of fine sand (49%) followed by medium sand (22%), with a background matrix of other particle sizes, that reflects a relatively well-sorted overflow sediment. Below the lithological discontinuity at 90 cm depth, the material is unsorted splay sediment. This levee has been built up by periodic overflow aggradation above the splay substratum.

### 9.4.2 Terrace Overflow Levee

*Profile P108* (Udoxic Quartzipsamment, 125 m a.s.l.) occupies a levee position on the right side of river Pasimoni (Table 6.7) (Fig. 9.5a, b). The site is an elongated flattened bank with 1% lateral slope to a poorly drained depression 1–1.5 m lower



(P107, Hydric Haplohemist, with organic horizons over white sand substratum; an important source of humic acids to the groundwater) (Fig. 9.5d, e). Vegetation is shrubby savanna. Soil color changes with depth: brown to pinkish grey (0–35 cm), white (35–100 cm), and brown to very pale brown without organic carbon increase (100–150 cm). The white layer is very compact (densipan). Average sand content is 86%, with 11% silt and 3% clay. The profile is homogeneous with similar particle size distribution pattern in the upper 100 cm. Fine sand is dominant (36%) followed by medium sand (24%) with a background matrix of other particle sizes, reflecting moderately well-sorted overflow sediment (Fig. 9.5c). This levee has been built up by periodic overflow aggradation over splay substratum. The levee of P108 and the depression of P107 form together a fluvial geomorphology association built up on white sands previously brought by river Pasimoni, with later geomorphic differentiation and accumulation of organic matter in the depression.

Profiles P105 (former section) and P108 are remarkably similar in terms of particle size composition and distribution with depth; this similarity reflects a regional trend in riverbank overflow sediment facies over basal splay material.

### 9.4.3 Terrace Overflow Mantle

*Profile P109* (Arenic Alorthod, 125 m a.s.l.) is located on a large bench-like terrace covered by shrubby savanna at the confluence of river Pasimoni and a tributary stream, about 3 km east of the river. Particle size pattern is fairly homogeneous over the whole depth (1–140 cm), with slight variations in particle separates among layers but without significant lithological discontinuities. Fine sand (42%) and medium sand (30%) are the two dominant separates with a background matrix of other particle sizes. In all layers the sequence is fine > medium > coarse sand, showing that the overflow process with similar flow energy has been operating over the entire deposition time (Fig. 9.6a).

*Profile P104* (Udoxic Quartzipsamment, 125 m a.s.l.) is located on a large terrace south of river Siapa, close to the confluence with river Casiquiare, under caatinga forest. Particle size pattern is homogeneous over depth (12–150 cm) (Table 6.7). Fine sand (34%) and medium sand (29%) are codominant within a particle background ranging from coarse sand to clay (Fig. 9.6b).

Profiles P109 and P104 belong to different soil classes (Alorthod and Quartzipsamment) and have developed under different kinds of vegetation cover (shrubby savanna and caatinga) from a material of remarkably similar depositional facies although in two watersheds 50 km apart (Pasimoni and Siapa) (Table 6.7) (Fig. 9.6c).

### 9.4.4 Discussion and Conclusion

Profiles described in the Pasimoni and Siapa valleys vary in geomorphic position, vegetation cover, and taxonomic classification. However, they are remarkably

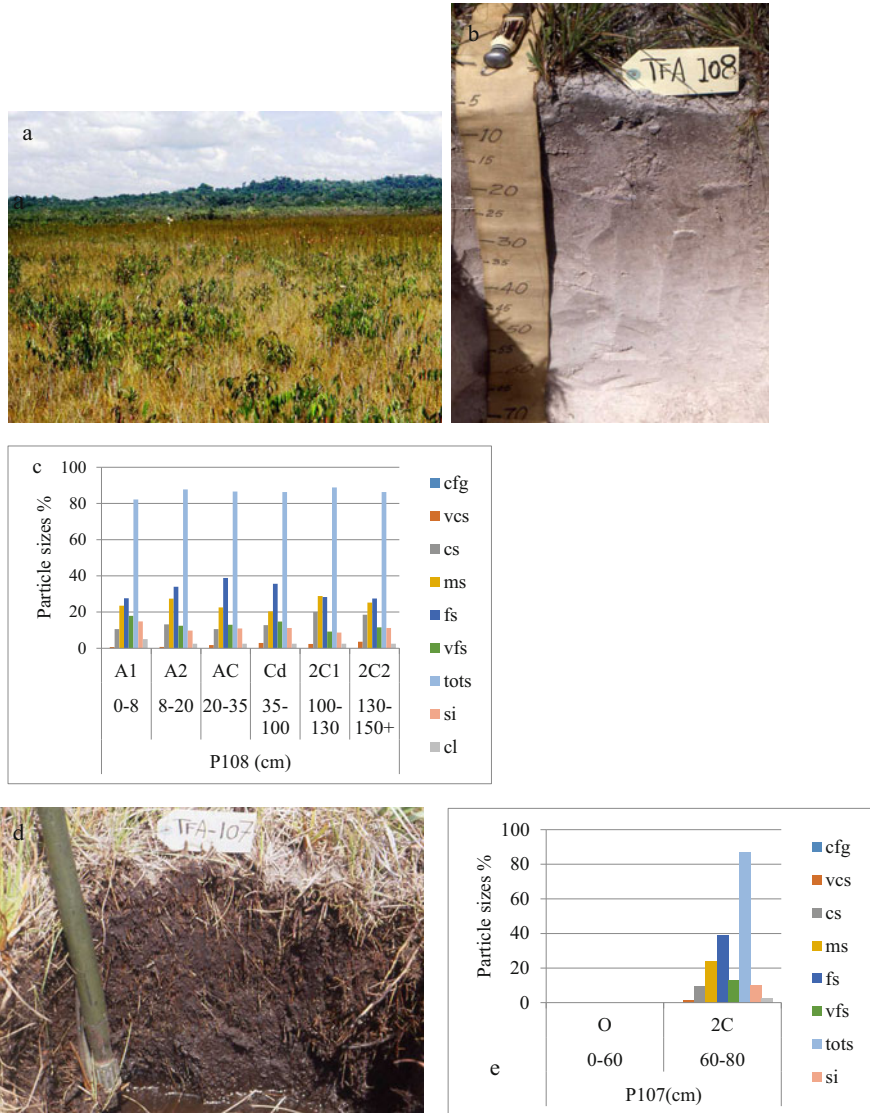


**Fig. 9.5** Low terrace of Pasimoni river: (a) levee covered by shrubby meadow in the foreground; the brownish colored area in the middle of the picture corresponds to a poorly drained depression, originally a backswamp (P107 Hydric Haplohemist in figure d); (b) well-drained levee soil-sediment at P108 (Udoxic Quartzipsamment); 1% OC in the dark grey topsoil; (c) moderately sorted levee sediment with a large particle size spectrum but dominance of fine and medium sand. (d) Profile P107: Hydric Haplohemist; poorly drained soil in a backswamp depression associated with the levee on the low terrace of river Pasimoni shown in figure (a) (P108); (e) histic horizon overlying a white-sand layer at 60 cm depth; groundwater at 40 cm

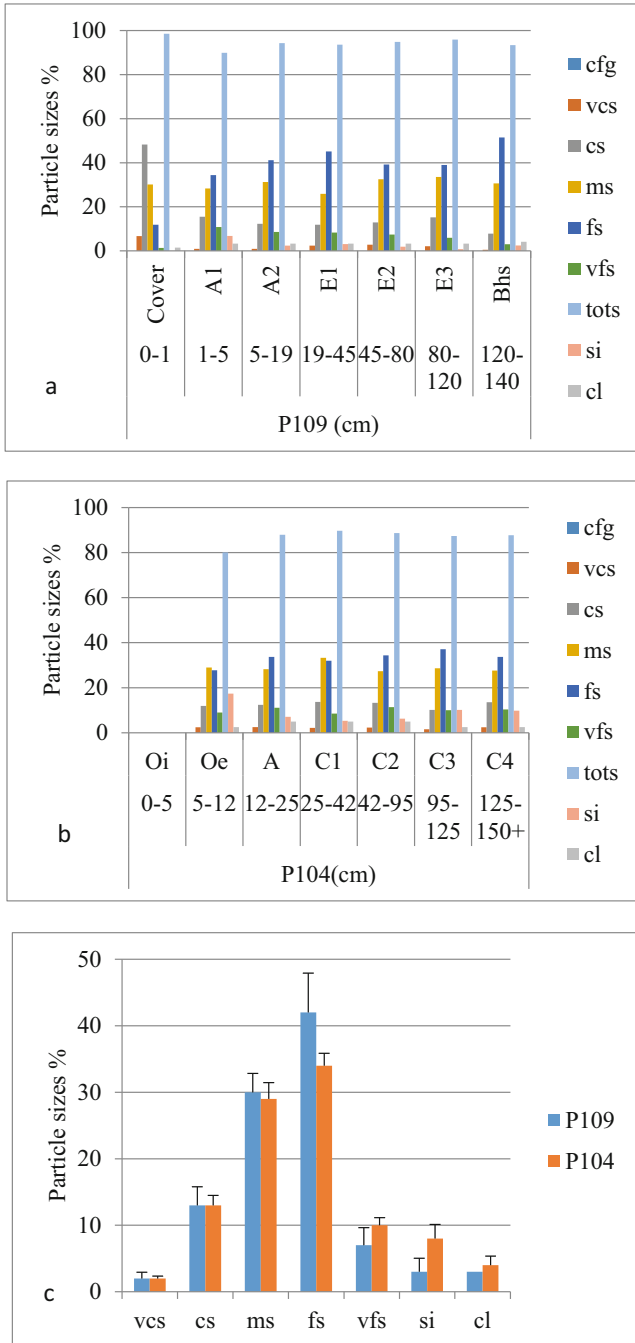


**Fig. 9.6** (a, b) Overflow mantle sediments on river terrace: P109 (Arenic Alorthod) in the Pasimoni valley and P104 (Udoxic Quartzipsammit) in the Siapa valley show similar depositional facies with dominance of fine and medium sand. (c) Similarity of well-sorted overflow sediment pattern with dominance of fine and medium sand (>60% together) between two observation points

similar in particle size distribution pattern that repeats in space between distant locations (Fig. 9.5c). They belong to a common depositional facies.

Relevant characteristics of the profiles occupying geomorphic riverine positions are summarized in Table 9.9. Soil classes include four Quartzipsamments, two Spodosols, and one Ultisol. Although they have formed originally from sandy sediments, these soils are somewhat different from pure white sands typical of the alluvial plains. Top layers are pinkish grey, light grey, or pale brown; subsurface and subsoil layers are white or light grey; spodic horizons are very dark brown or dark reddish brown. In spite of being taxonomically different, the seven selected soils share a similar particle size pattern characterized by a strong dominance of fine and medium sand together with subordinate separate distribution over all particle size classes (Table 9.10).

Total sand varies from 86 to 96%. Medium and fine sands constitute the largest part of the sand fraction (68% on average). Fine sand is the dominant separate (39% on average). The soils have an udoxic index (i.e., silt + 2× clay) substantially higher than that of pure white sands in overflow and splay deposits of the lowland alluvial plains. This may contribute to lower the moisture stress in surface layers during dry spells.

This kind of deposits reflects thus a process of core sediment sorting accompanied by a large spectrum of sedimentological impurities (udoxic index >5%). Particle sorting is incomplete as deposition traps some sediment in suspension (very fine sand, silt, and clay) and some bottom load sediment (very coarse and coarse sand). This may result from generalized overbank flow over large, flattened levees.

The proximity of the Pasimoni-Siapa fluvial lowlands to the upper watersheds of the rivers in the mountain hinterland may explain why the overflow sediments in this area have a larger spectrum of particle size classes than that of the typical overflow mantles of reworked sands in the large alluvial plains.

The seven profiles in Fig. 9.7a constitute a fairly homogeneous set of observation points with low standard deviation values in the various particle size classes (Fig. 9.7b). It shows that mixed overflow sediments repeat in distant fluvial deposits, allowing for the spatialization of point data. It is a common depositional facies in the southern riverine landscape. Soils so much different as Spodosols, Ultisols, and Quartzipsamments have developed under various types of vegetation cover from the same kind of sediment, possibly in different time spans (see discussion on Spodosols in Chap. 10). This kind of sediment departs from typical levee with coarse sand and convex shape and from typical overflow mantle that is usually better sorted (Fig. 9.7c).

---

←  
**Fig. 9.6** (continued) 50 km apart (P109, 94% sand, sand separate averages of 6 layers at 1–140 cm depth; P104, 88% sand, sand separate averages of 5 layers at 12–150 cm depth)

**Table 9.9** Selected profiles on river-related geomorphic positions in the Pasimoni-Siapa lower watersheds and some other fluvial areas

Profile	Soil class	Geoform	Study area	Texture	Udoxic index	Color moist	Vegetation
P104	Udoxic Quartzipsamment	Terrace	Pasimoni	Fine sand	16	Very dark grey/grey/light grey	Caatinga
P108	Udoxic Quartzipsamment	Levee/terrace	Pasimoni	Fine sand	15	Brown/white/very pale brown	Shrubby meadow
P105	Oxyaquic Quartzipsamment	Meander lobe	Pasimoni	Fine sand/coarse sand	11	Grey/white	Shrubby meadow
P131	Plinthic Quartzipsamment	River levee	Ventuari	Fine sand/medium sand	23	Pale brown/white/strong brown	Meadow-savanna
P109	Arenic Alorthod	Levee/terrace	Pasimoni	Fine sand	9	Brown/white/reddish brown	Shrubby savanna
P103	Oxyaquic Alorthod	Meander lobe	Pasimoni	Fine sand/medium sand	10	Pinkish grey/white/very dark brown	Shrubby meadow
P56	Grossarenic Kandiodult	Alluvial flat	Yapacana	Fine sand	6	Pinkish grey/pale brown/ light grey	Meadow

Udoxic index: silt%+2× clay% (Soil Survey Staff 2014)

**Table 9.10** Particle size distributions and ranking of sand separates of selected profiles on river-related geomorphic positions in the Pasimoni-Siapa lower watersheds and some other fluvial areas (see Table 9.9)

Profile	Depth cm	Number of layers	Very coarse sand	Coarse sand	Medium sand	Fine sand	Very fine sand	Total sand	Silt	Clay	Ranking of sand separates (>10% sand)
P56	7-110	5	2	11	31	44	8	96	2	2	fs > ms > cs
P103	1-44	4	2	14	33	36	8	93	4	3	fs ≥ ms > cs
P104	12-150	5	2	13	29	34	10	88	8	4	fs > ms > cs
P105	1-90	5	2	8	22	49	11	92	5	3	fs > > ms > vfs
P108	8-100	3	2	12	24	36	13	87	11	2	fs > ms > vfs = cs
P109	1-140	6	2	13	30	42	7	94	3	3	fs > ms > cs
P131	14-130	5	2	14	33	30	7	86	5	9	ms ≥ fs
Average			2	12	29	39	9	91	5	4	
Range			2	8-14	22-33	30-49	7-13	86-96	2-11	2-9	

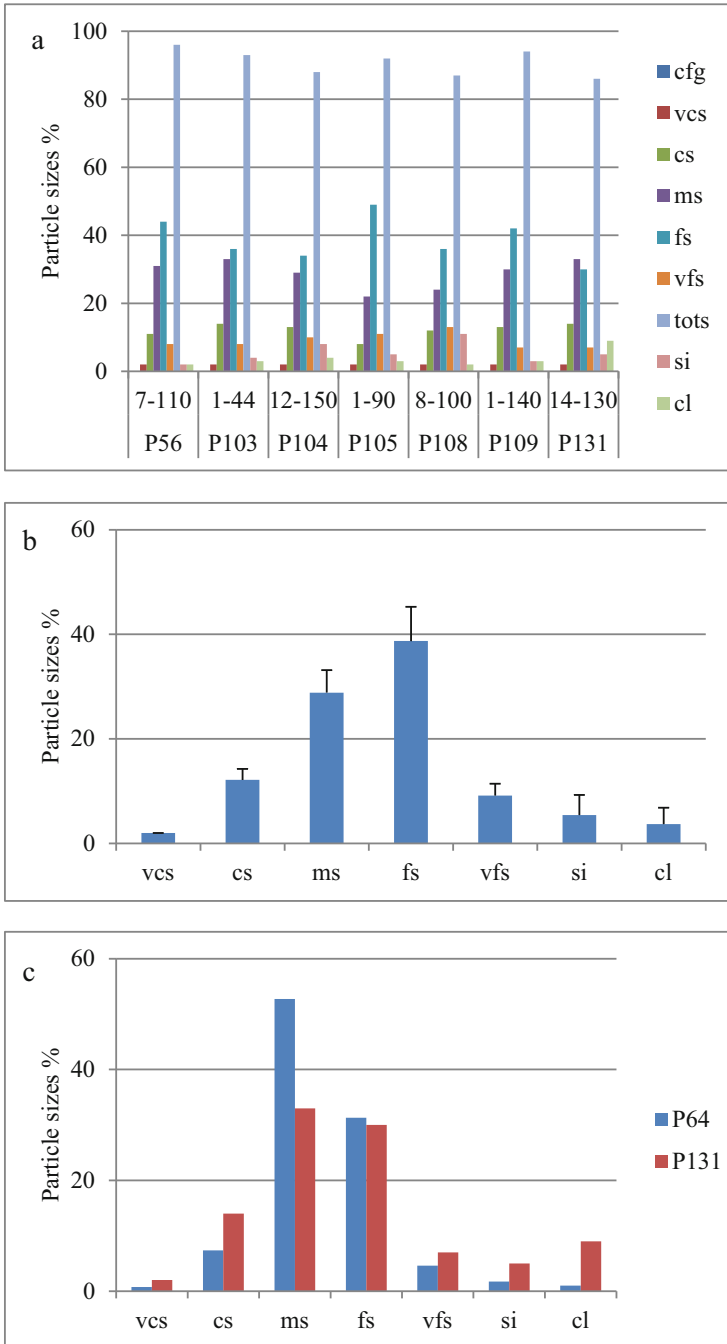


**Fig. 9.7** (a) Comparison of selected profiles showing similar particle size distribution patterns with two dominant separates (fine and medium sand) within a background matrix of other particle sizes; averages of whole profiles over indicated depths; (b) average particle size classes of the seven profiles shown in (a) (33 layers); (c) comparison between pure overflow mantle in alluvial plain (well sorted) at P64 and mixed overflow sediment on river levee (moderately sorted) at P131



## 9.5 Wind-Blown Sand Deposits

The global view of the study region on Google Map shows a mosaic of light-colored, unwooded islands in a dominant woodland-forest cover throughout the Orinoco-Rio Negro lowlands. On Google image at small scale (i.e., 1:2,500,000), can be observed a concentration of white patches aligned in a NE-SW diagonal strip (corridor) from NE of San Juan de Manapiare to San Fernando de Atabapo and Maroa in the SW along the border between Colombia and Venezuela, thus paralleling the trajectory of the trade winds. This might be a simple coincidence and cannot be taken as evidence of eolian activity. In fact, the soil survey of the whole region carried out by MARNR-ORSTOM (1986) has not identified eolian sand deposits.

However, there is evidence of eolian activity on sand bars in river channels. Nordin and Perez-Hernandez (1989) describe dunes that form from recycled wind-blown sand in the Orinoco river channel and lower reaches of tributaries. During average low flows, alluvial banks along the rivers are exposed to deflation and short-distance transport of sand. Dunes formed in river channels are ephemeral but those built up on side banks persist. The dunes have formed on the leeward side of river Atabapo in front of the junction with *caño* Caname. Dunes are fed by trade-wind deflation on sand bars in the river bed at low water levels.

Eolian activity in meadow environment can take place during and especially at the end of the low rainfall season. Discontinuous rainfall in January–March and temperatures up to 65 °C at 1 cm depth below bare soil (O. Huber, personnel communication) cause surface sand layers to dry up allowing local deflation and drifting of white sands and their accumulation at short distances. Sites in the area of “caño” Caname (e.g., P65 and P85) were dry to 60 cm depth by the end of March. Past signs of eolian activity may have been obliterated by rainfall erosion in areas with scarce vegetation cover or have not been detected under forest cover.

Field visits allowed identifying a set of geofoms that can be interpreted as of eolian origin on the basis of shape and sediment facies. They include dune-like mounds, eolian blankets on glacia, and eolian sheets in drowned depressions.

### 9.5.1 Dune-Like Mounds

A few sites among the visited places show evidence of recent short-distance sand translocation and accumulation, mainly in the Atabapo area. Isolated dune-like mounds were observed in the “caño” Caname watershed, a tributary of river Atabapo. The mounds are elongated, slightly oval, convex, about 200 m long, and 100 m wide. They dominate the surrounding flat terrain surface by 2–3 m elevation at most, with a lateral slope of 5–10% and sharp basal boundaries. Vegetation cover is scarce, including mainly herbs and sometimes small clusters of shrubs. At one site, five such mounds were aligned NE-SW. Dune-like mounds can occur close to rivers and streams, but usually, they are found at some distance.

### 9.5.1.1 Isolated Mounds

*Profile P65* (Typic Quartzipsamment, 100 m a.s.l.) is located on an isolated dune-like mound south of middle *caño* Caname (Plate 9.11a, b). The convex mound has a sharp contact, without transition, with the neighboring unit (P66), indicating that the mound is superposed on a pre-existing terrain. Vegetation is open scrub with shrubs being interspersed by bare white sand patches (Plate 9.11a). The mound surface is covered by a recent loose sandy layer a few centimeters thick, with many rounded, dull sand grains. This surface layer buries a thin crust of charcoal and partially burned twigs, followed by an 8–10 cm thick, dark grey sandy A horizon, with few roots and pieces of charcoal. The profile is essentially a sequence of C layers with 95–100% sand (Plate 9.11b, c). On a 100% sand basis, 73% is coarse sand (2–0.5 mm) and 21% is medium sand (0.5–0.25 mm), indicating short distance deflation and accumulation through saltation, by reworking sand from surface layers of the surroundings and/or from stream bed at low water stage in January–March. In the middle and lower parts of the profile, cross-stratifications are underlined by darker oblique strips and buried roots. Moist color is grey to light grey (10YR6/1–7/1) and dry color is light grey to white (10YR7/1–8/1). The material is slightly stratified with small variations of sand separates (Plate 9.11b). A few sand grains are rounded and have dull surface. All horizons, down to 125 cm depth, contain small lenses of charcoal fragments and buried roots, reflecting accretion by periodic sand deposition events. Loose sand at the surface indicates that the accretion is still active. By the end of the short dry season in March, the soil was fully dry to 60 cm depth and nearly dry in the following layers. Herbaceous plants were water-stressed and wilting. This is the driest soil observed in the short low rainfall season in the whole study region.

The mound of P65 lies atop a flat terrain where profile P66 is located at a 200 m distance. P66 is a stratified Typic Quartzipsamment composed of several layers of unsorted splay material and with groundwater at 114 cm depth (see Sect. 9.2.3.1; Fig. 9.1). The bottom layer of the dune profile (125–160 cm) corresponds to the terrain surface buried under the wind-blow sand and correlates with the topsoil of the terrain surface surrounding the dune-mound (Plate 9.11).

### 9.5.1.2 Clusters of Mounds

Clusters of dune-like mounds occur on alluvial flats bordering stream floodplains. Mounds aligned NE-SW were identified in the middle *caño* Caname, halfway between river Atabapo and river Orinoco. The mounds are elongated, 100 m wide, clearly convex, shrubby, dominating the surrounding terrain surface by about 1 m. *Profile P85* (Udoxic Quartzipsamment, 100 m a.s.l.) is a representative site (Plate 9.11e). The profile is stratified, showing changes in sand particle sizes between layers and irregular variations of organic carbon with depth. Several small layers include horizontally lying fossil roots (at 8 cm, 32–37 cm, and 48–53 cm depth). The material is fully white and very loose, contrasting with the cohesion and sometimes compactness of the sand layers in alluvial sediments. Groundwater is at 160 cm.

Stratification is significant, including three surface layers (0–20 cm) with dominant coarse and medium sand, three subsurface layers (20–70 cm) with coarse sand

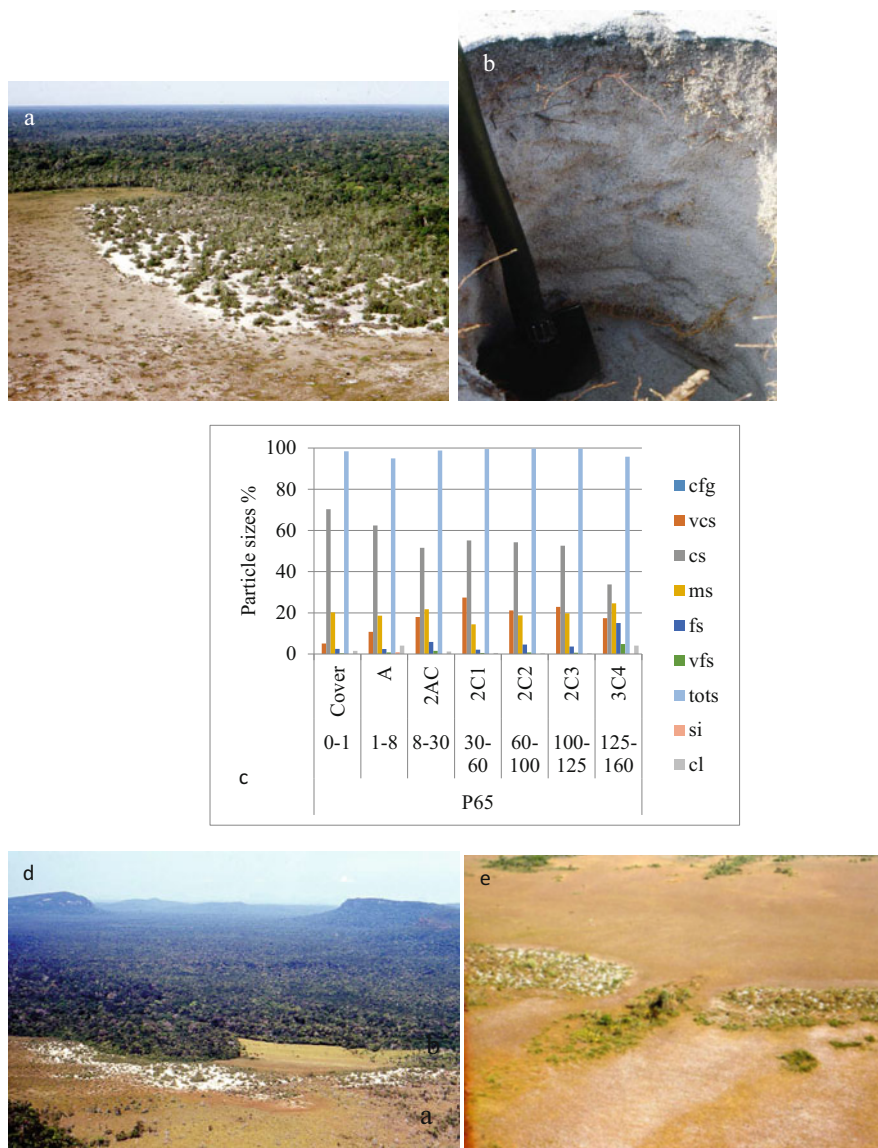


**Plate 9.11** Dune-like mound in the caño Caname watershed: (a) sharp contact between the wind-blown white-sand mound (scrub) and the underlying alluvial flat (meadow); (b) profile P65 (Typic Quartzipsamment) showing cross-stratifications that result from periodic accretion of coarse sand from short distance; (c) profile P65: Typic Quartzipsamment, weakly stratified coarse sand fed by sand drifting from short distance. (d) Dune-like mound in the caño Caname watershed. Clusters of dune-like mound on the edge of an alluvial plain flat in contact with a stream floodplain, west of La Esmeralda; excavated anticline in the background (Orinoco valley); (e) alluvial plain flat in the caño Caname watershed (site of profile P85)

dominant, and three subsoil layers (70–160 cm) with poorly sorted sand separates. The upper section of the profile (0–70 cm) has 89% average sand, while the lower section has 99%. The former together with a change in particle size distribution shows a major lithological discontinuity at 70 cm depth that may correspond with the top of the alluvial terrain surface buried under the dune. Profile P86 is an Oxyaquic Quartzipsamment, on an alluvial flat 300 m apart from the dune mound of P85 (see Fig. 7.6 in Chap. 7). Groundwater is at 75 cm depth that correlates with groundwater depth under the mound at 160 cm. The similarity between the two unsorted splay patterns highlights the spatial relationship between burying and buried sediments.

Profile P85 (Table 6.6) has been built up by stepwise cumulation of sediments, with interruptions in sand accumulation as highlighted by the occurrence of small layers with buried roots and variation of organic carbon with depth. This is in contrast with the more homogeneous sand accretion at site P65 (isolated mound). The presence of about 10% fines could reflect a somewhat longer transport distance as compared to the local drifting at site P65.

### 9.5.2 Eolian Blankets on Glacis

North-west of San Juan de Manapiare, at the northern edge of the study region, a narrow mountain gap between the Guanay range to the west and the Yutajé range to the east is the divide between the watershed of the Suapare river draining to the north and that of the Manapiare river draining to the south (see Plate 6.1d in Chap. 6). Monoclinical reliefs, mainly Roraima sandstone hogbacks, flank the mountain ranges and gently sloping glacis have developed at the foot slopes of these structural reliefs. In the valley of “caño” Camani, a tributary of river Ventuari, glacis soils show remarkably high fine sand, very fine sand, and silt contents.

*Profile P33* (Udoxic Quartzipsamment, 150 m a.s.l.) is located east of “caño” Camani on a glacis (0.5–1% slope) lying at the foot of a piedmont belonging to the backslope of Cerro Morrocoy, a sandstone hogback, at the border of a large tectonic depression with structural geoforms open toward south-east (Fig. 9.8a). The glacis surface shows suffusion pans and discontinuous rills under open Caraipa forest. The soil is greyish loamy sand. Except for the surface layer (0–10 cm), particle size distribution is homogeneous over depth, with fine sand clearly dominant in the two lower layers (27–70 cm). Average fine sand, very fine sand, and silt sum up 93% of the sediment (47% + 32% + 14%, respectively). Global fine sand (0.25–0.05 mm) is 97% on 100% sand basis, the highest rate detected in the whole region. There are only traces of very coarse and coarse sand (Fig. 9.8b).

*Profile P32* (Udoxic Quartzipsamment, 140 m a.s.l.) is located west of “caño” Camani on a glacis lying at the foot of the front slope of Cerro Morrocoy hogback. The glacis terrain is very gently sloping (0.5–1%) toward a riparian palm tree forest (morichal) that shows a dense pattern of channels 30–50 cm deep and 10–40 cm large. The glacis is covered by a moderately dense shrubby meadow. There are only traces of organic matter in the soil (0.02% OC). Suffusion pans and discontinuous rills are frequent. The soil is pinkish grey loamy sand, formed from pinkish Roraima

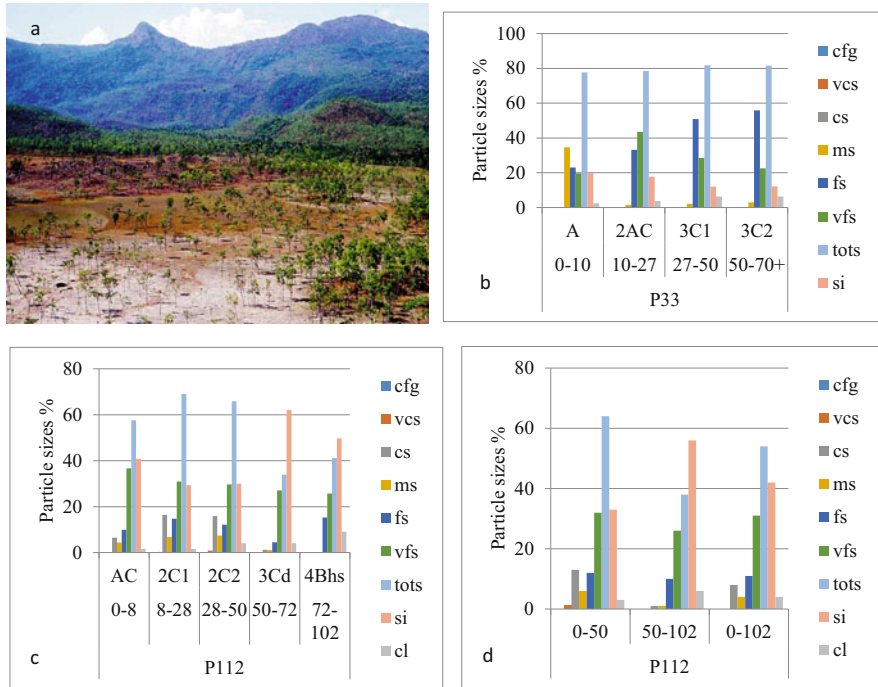


**Fig. 9.8** (a, b) Profile P33: Udoxic Quartzipsamment on an eolian blanket sediment covering a partially burned (white area) piedmont glacia; greyish soil with the dominance of fine and very fine sand (79% on average), the highest combined rate detected in the study region; backslope of Cerro Morrocoy in the background. (c) Profile P112: Oxyaquic Alorthod on an eolian sheet in a drowned depression in the watershed of caño Pimichín; high silt content (42%) and very fine sand plus silt content (73%); (d) shift from silt dominance in the lower part of the deposit (50–102 cm) to sand dominance in the upper part (0–50 cm) corresponding to two consecutive episodes of eolian activity

sandstone. Particle size distribution is homogeneous over depth. Fine sand is the dominant sand separate. Average fine sand, very fine sand, and silt sum up 88% of the sediment (51% + 24% + 13%, respectively). There is no clay and only traces of very coarse and coarse sand (<1%).

There are no specific terrain features evidencing past eolian activity, but the strong concentration of fine sand, very fine sand, and silt (0.25–0.002 mm) lies in the range of wind competence for particle selection and transport at medium distance. This suggests that the sand has been transported by wind from the north, possibly through the Guanay pass, and deposited as eolian blankets and preserved in sheltered positions on both sides of Cerro Morrocoy acting as a natural barrier. This might also explain northern influence from the Llanos in the vegetation composition, with a large proportion of grass species, south of the Guanay gap. Intermountain valleys favor the entrapment of airborne fine sand and silt particles as signaled also by Latrubesse and Nelson (2001) for similar settings in the area of Boa Vista, eastern part of the Brazilian state Roraima.

### 9.5.3 Eolian Sheets in Drowned Depressions

Evidence of wind-blown sand accumulation in the form of dune-like mounds was found mainly in the large interfluvium between “caño” Caname to the north and “caño” Pimichin to the south along the course of river Atabapo. Associated with these punctual sand deposits, large silt-blanketed areas were detected. Drifting eolian particles settled down selectively as coarse sand mounds and fine-grained sheets.

#### 9.5.3.1 Eolian Sheet Under Shrubby Meadow

*Profile P112* (Oxyaquic Alorthod, 120 m a.s.l.) is located in the headwater area of “caño” Pimichin. Terrain is a slightly concave lowland flat with 30 cm high meadow vegetation (30–40% cover) and small scattered shrubs (1–1.5 m high) with *Archythaeta angustifolia* and *Terminalia yapacana*. The profile is composed of two pinkish white surface layers (0–28 cm), a moderately densified white layer containing a perched water table (28–50 cm), a very pale brown, very compact dry densipan layer that supports the perched water table (50–72 cm), and a brown incipient spodic horizon with dark organic matter lamellae 5–6 mm thick (72–102 cm) (Fig. 9.8c). The sediment as a whole is 54% sand, 42% silt, and 4% clay (Table 6.6). Very fine sand and silt dominate in all layers. The profile is stratified with variations of total sand, very fine sand, and silt. Below a shallow cover material, two layers show fairly similar particle size distribution patterns with 30% very fine sand and 30% silt (8–50 cm). The densipan layer (50–72 cm) has 62% silt and 27% very fine sand, while the spodic horizon has 50% and 26%, respectively. Coarse, medium, and fine sands that are present in the upper layers (0–50 cm) are scarce in the lower layers (50–102 cm). Stratification favors the depositional hypothesis over the weathering hypothesis, and high silt content supports eolian origin rather than alluvial.

The compactness of the densipan (50–72 cm) is caused by the clogging of macropores by silt particles and possibly dissolved silica. Part of the silt fraction may have formed in situ through the fragmentation of sand grains.

Most probably, the incipient spodic horizon (0.62% OC) does not result from organic matter illuviation; it appears may be enriched in organic substances from groundwater. The former discards the possibility that the spodic horizon might have formed under caatinga, subsequently degraded and replaced by meadow vegetation.

On average (0–102 cm), the soil has one of the highest silt contents (42%) and very fine sand plus silt contents (73%) of the whole study region. A significant lithological discontinuity takes place at 50 cm depth where total sand drops from 66% to 34% and silt increases from 30% to 62% (Fig. 9.8d). The sum of very fine sand and silt is 65% in the upper part of the profile (0–50 cm) while it is 82% in the lower part (50–102 cm). This well-sorted silty material suggests eolian sheet deposition in a flat, poorly drained terrain surface where wind-driven particles may have been trapped by environmental moisture and herbaceous cover. The profile records two consecutive episodes of eolian activity (Fig. 9.8c, d). The presence of coarse sand (16%) in the upper layers (8–50 cm) could indicate the advection of local



surface sand by the time of sediment deposition. This site lies south of the *caño* Caname area where dune-like mounds were found.

The terrain surface is crossed by a labyrinthine pattern of branching channels 20–30 cm wide and 5–7 cm deep, and discontinuous forming small closed patterns that cannot be attributed to surface drainage rills. Frequent closed rounded and oval pans and closed channels are caused by suffusion. The absence of external surface drainage and the milky stain of the perched water table indicate that these labyrinthine shallow channels most likely result from terrain subsidence along lines of quartz grain dissolution in a drowned landscape area (see Sect. 10.4 in Chap. 10).

### 9.5.3.2 Eolian Sheet Under Caatinga

Eolian sheets are sediment patches that blanket discontinuously the lowland alluvial substratum. *Profile P113* (Histic Humaquept) lies at the edge where an eolian sheet cover overlaps underlying alluvial sediments. P113 is located in the same watershed of “caño” Pimichin as P112, 300 m apart, in a 15 cm deep erosion channel under caatinga forest. The soil starts at the bottom of the channel with a mat of horizontally lying roots (mainly 0.2–1 cm and some 5–6 cm thick) with mycorrhizae, including leaf fragments and little mineral material. The root mat is 7 cm thick in the channel and 22 cm on the terrain surface. The following horizon (7–35 cm) is still root mat but mixed with decomposed organic matter and mineral material. These organic horizons lie on a light grey sand layer that contains a large spectrum of particle sizes (35–50 cm).

The profile shows a significant lithological discontinuity at 35 cm depth between two materials that are contrasting in terms of particle size distribution, organic matter content, and soil reaction. The eolian cover is a well-sorted deposit with 71% silt, while the underlying alluvium is unsorted splay sediment with 73% sand (Table 9.11). The silt content of the eolian sheet is by far the largest found in the study region. Groundwater remains high during the low rainfall season (February–March), at 35 cm under the channel and 50 cm under the terrain surface. This shows that silty wind-driven particles have deposited preferentially in drowned depressions. The eolian event is not recent as caatinga vegetation has had time to colonize the area. This is in contrast with the shrubby meadow vegetation at site P112 which may be a degradation stage of the original caatinga cover as silty soils are more attractive for slash-and-burn farming than white sands. Erosion channels are shallow here as compared to other caatinga areas, and this may be attributed to the low-lying position in the landscape of the drowned area. They are covered with thick litter under caatinga and colonized by forbs (e.g., *Brocchinia* sp.) in contiguous

**Table 9.11** Contrast of soil properties between the burying eolian sheet and the buried alluvial sediment at site P113

Depth cm	Depositional material	Sand%	Silt%	pH	OC%
7–35	Eolian cover sheet	25	71	3.7	13.3
35–50	Buried alluvial sediment	73	4	5.1	0.25



bana. Thus, channels are not eroding today and may have incised at lower base levels.

#### 9.5.4 Discussion

The absence of dunes in the central part of the Amazon basin together with other criteria, in particular pollen data, has been used by Colinvaux et al. (2000) to refute the hypothesis of arid periods during the Quaternary. This view disregards the occurrence of dune fields in the Rio Branco basin and in the Rio Negro basin. A clearly NE-SW-oriented topographic and drainage pattern was recognized from remote sensing images in the region of Boa Vista in the upper catchment of Rio Branco, on the northern Brazilian margin of the Amazon basin (Carneiro Filho and Zinck 1994). The orientation of the landscape patterns, parallel to the dominant wind direction, and the sandy textures of the soil mantle suggest an eolian origin of the cover formation as an obliterated dune field. Because present climatic conditions with 1660 mm yearly rainfall do not favor significant wind-driven morphodynamics, the sand cover formation and the associated savanna vegetation may be relics of drier conditions in the Quaternary history of the region, possibly going back to the late Pleistocene (Carneiro Filho and Zinck 1994; Latrubesse and Nelson 2001).

Similarly, eolian sands forming long chains of linear dunes up to 10–35 m high were identified bordering the Rio Negro and some tributaries in the northern Amazon basin (Carneiro Filho et al. 2002). Dunes are now fixed by vegetation varying from low forest (campinaranas) to herbaceous cover (campinas) under 2500 mm annual rainfall. Using thermoluminescence (TL), the authors obtained dune formation ages spanning the period 32,000–8000 years BP and encompassing several events of eolian activity from the Late Pleniglacial to Early Holocene. Final dune stabilization took place after 7800 years BP, possibly followed by a more humid climate favoring forest development. These findings suggest the occurrence of relatively dry climatic conditions for dune construction in the Rio Negro basin and indicate that climate fluctuations should be considered on local to regional scales.

There is some coincidence between the period of dune stabilization in the Rio Negro basin (after 7800 years BP) and the dates of peat inception on table-mountain summits (tepui) in the Venezuelan Guayana Highlands (mainly 1500–2500 m a.s.l.). Peat initiation  $^{14}\text{C}$  dates go back to 6000 years BP in the eastern highlands (Schubert and Fritz 1985; Schubert et al. 1994), 7500 years BP in the western highlands (Zinck et al. 2011), and 10,630 years BP at one site in the Chimantá massif, eastern highlands (Nogué et al. 2009). The western highlands form the direct mountain periphery of our study lowlands and are the closest to the Rio Negro watershed. The oldest organic material dated in these highlands, on a sandstone meseta in the Marahuaka massif (ca 2800 m a.s.l.), is 7490 years BP (8400 calBP). The current mean annual rainfall for the overall highland area is 3250 mm (Huber and García 2011). Before peat started forming, climatic conditions at the onset of the Holocene must have been much drier and the tepui summits were most probably bare rock. Peat formation during the Holocene was neither continuous nor linear. In some

places, peat accumulation was interrupted by depositional hiatuses, some of which might have been induced by climate forcing and others by truncation through sliding or cutting by creek migration. A significant depositional gap occurred between ca. 5200 and 3600 years BP which suggests that peat areas could have considerably shrunk in this period because of decreasing moisture or more frequent dry spells (Zinck 2011).

It is unlikely that climate change from dry to moist with peat initiation at tepui summits at the onset of the Holocene would not have paralleled climate change in the surrounding lowlands, with possible fluctuations even during the Holocene as shown by peat depositional gaps. A decrease in yearly rainfall and/or longer dry seasons can have caused a lowering of the groundwater level, keeping dry the upper white sand layers for longer periods, and causing caatinga forest to be degraded and replaced by bana and meadow. Thus, smaller climatic fluctuations could induce edaphic drought with significant influence on the vegetation cover.

---

## 9.6 General Conclusion

The geographic coverage of this work shows that pale to white sands can occur in a variety of settings in meadow environment. This advocates in favor of a multisource hypothesis of sand production and spatial (re)distribution. Primary sands resulting from erosion in highlands and uplands, from rock weathering in the lowlands, and from lateral soil transformation along hillslopes are reworked and redistributed mainly by water and, to a much lesser extent, by wind (see Chap. 8). It is uncommon to find weathering profiles at the surface in the flat meadow lowlands, as the weathering front of the bedrock is generally buried under cover sands.

“White sands” is a generic term referring to sand expanses that occur in various parts of the Amazon basin. Many sand covers are indeed white sands but there are also greyish, pinkish grey, and pale brown sands included in the same concept. Sands of diverse colors are colonized by a variety of vegetation types including forests, woodlands, scrublands, and meadows. This chapter is concerned with sandy sediments under meadow vegetation varying from pure herbaceous to mixed shrubby covers. Sites on sandy materials were described in the field. Site observations and laboratory data were analyzed from a sedimentological point of view.

The variety of geomorphic settings and sedimentological processes that characterizes sand covers in meadow environment is summarized in Fig. 9.9. Twenty-five profiles were selected, each comprising several layers (2–9) distributed over variable depths (50–160 cm). Sand percentages were recalculated on 100% sand basis. The original five sand separates were generalized into three sand classes including coarse sand (2–0.5 mm), medium sand (0.5–0.25 mm), and fine sand (0.25–0.05 mm). The figure displays the generalized sand composition of the six main geofoms supporting different types of meadow vegetation in plain and peneplain landscapes, i.e., (1) splay mantle in alluvial plain, (2) overflow mantle in alluvial plain, (3) annular glacia in peneplain, (4) longitudinal glacia in peneplain,

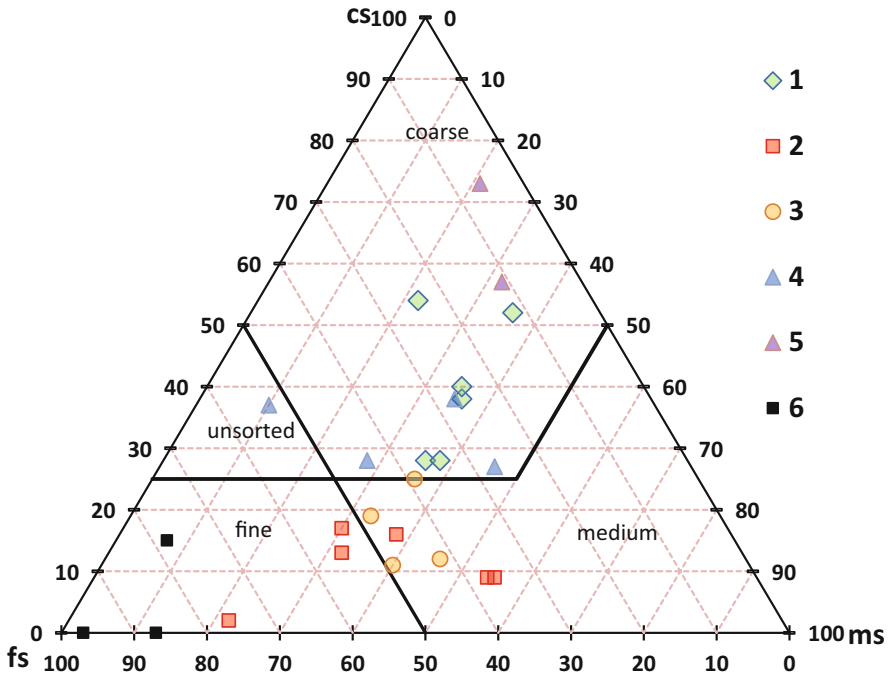


**Fig. 9.9** Variation of sand facies in geoforms bearing depositional sand covers under meadow vegetation (from herbaceous to shrubby) in plain and peneplain landscapes: (1) splay mantle in alluvial plain, (2) overflow mantle in alluvial plain, (3) annular glacia in peneplain, (4) longitudinal glacia in peneplain, (5) dune-like mound, and (6) eolian blanket

(5) dune-like mound, and (6) eolian blanket. Splay sediments in alluvial plains classify as coarse sand in the proximity of medium sand, while overflow sediments classify as medium to fine sand. A similar distinction occurs in peneplain landscape, with annular glacia formed by colluviation classifying as medium to fine sand and longitudinal glacia formed by splay as coarse sand. Eolian deposits are far apart in the diagram with dune-like mounds classifying as coarse sand and blankets as fine sand.

Meadow vegetation *sensu lato* has been established mainly on two lowland landscape types, i.e., alluvial plains and peneplains. In alluvial plains, sand deposits are ubiquitous, from river and stream proximities to large interfluvies between watercourses. Sand deposition takes place on river and stream banks through overflow at high water levels. Resulting riverine levees are more conspicuous along streams (*caños*) than along rivers because river overflows tend to spread over large interfluvie areas. A particular feature of sand deposition is found in confluence areas between waterways. At simultaneous high waters, smaller streams cannot join larger rivers and discharge water and sediments in the junction area forming confluence fans. River-shaped landscape was found in the southern part of the study region, in the Pasimoni and Siapa watersheds. This sector has fluvial

geomorphic features that are not present elsewhere in the study region. The most common geoforms are meander lobes, flattened inactive levees, and large undifferentiated terrace benches.

Alluvial plain interfluvies between waterways are flats where two main depositional processes, namely overflow and splay, contribute to forming sand mantles. Overflow generates well-sorted sediment facies based on two dominant sand separates of medium and fine sand that together concentrate about 80% of the deposits. In contrast, splay generates an unsorted sediment facies with sand distributed almost equally over several codominant separates (three to four) and a shift toward coarse sand. Disordered particle size distribution patterns, for instance, the sequence of medium>coarse>fine>very coarse sand are frequent. It is unlikely that such sequences of highly stratified splay layers would be pedogenic albic material resulting from podzolization.

Regardless of the type of facies, alluvial sediment sequences are usually stratified and interrupted by lithological discontinuities. This reveals geomorphic instability and frequent sediment reworking by river shifting and bank overflow, in contrast with homogeneous soil mantles resulting from deep in situ weathering. Standard deviation values show that layering is more heterogeneous in splay than in overflow. These two dominant depositional patterns coexist or are intermingled in the sandfields. Low density of observation points did not allow mapping their spatial distribution.

Boundary and transitional situations show vertical and horizontal shifts of depositional facies. Superposition and juxtaposition of different kinds of sediments are frequent. For instance, basal splay layers can appear overtopped by overflow layers. Both sediment bodies are usually separated by a clear lithological discontinuity showing that the sequence results from two consecutive depositional events and not from fining-upward of the deposition. At full bank regime, river flow tends to break through the levees and discharge coarse-grained sediments into marginal depressions. This results in associations of crevasse splay fans, segments of interrupted levees, and overflow/splay mantles. Admixture of bedrock-weathered saprolite with alluvial sediments results in materials showing a large, unsorted spectrum of particle sizes.

The peneplain landscape consists typically of hills, glacis, and drainage swales. Glacis are the landscape elements where meadow cover and sand substrate occur associated. Annular and longitudinal glacis are distinguished on the basis of their configuration. Annular glacis surround individual hills or small hill clusters as ring-shaped sloping terrains. The particle size pattern is well sorted with two codominant separates, i.e., medium and fine sand, resulting from colluviation. Longitudinal glacis develop along the front of hill ranges as broad, elongated, inclined terrains, formed by the coalescence of smaller glacis or fans. The particle size pattern is usually poorly sorted, with three dominant separates including coarse, medium, and fine sand, resulting from splay process.

Bedrock underlies all types of glacis but often at depths such that the weathering products are not recognizable in the sand covers. However, at some places, in annular as well as longitudinal positions, the weathering front is close enough to

the terrain surface so that rock fragments and saprolite are mixed with surface materials. Weathered clastics are reworked and distributed on the surface by colluviation or splay.

Evidence of past to recent eolian activity was identified especially in the Atabapo area. Coarse sand accumulation in dune-like mounds results from short-distance transport of reworked alluvial sediments or drifted river-bar sands. Associated with these punctual sand deposits, large eolian silty sheets were detected in drowned depressions with silt content up to 70%, by far the largest registered in the study region. Very fine grained deposits were also found blanketing glacia in a leeward position of an important mountain wind gap between northern and southern regional basins, with fine sand content above 90%, the highest recorded in the whole region.

Sclerophyllous caatinga forest and bana scrubland as well as meadow vegetation are established on the same alluvial, in general stratified substratum that overlies the igneous-metamorphic basement in-between residual peneplain reliefs. There is spatial continuity of the regional sand cover under the various vegetation types. The maximum extent of the sand cover may be assumed to coincide with the combined geographic distribution of caatinga, bana, and meadow vegetation.

The ranking of the dominant sand separates shows a frequency sequence of medium sand > coarse sand > fine sand, with each of these being alternatively codominant. Thus, splay sediments are overwhelmingly coarse to fine sand domain resulting from moderately high energy flow. Abundance of coarse and very coarse sand (36% together) in alluvial plain splays suggests new sand input in the alluvial lowlands coming from the basin periphery.

White sand is the main substratum sediment in alluvial plains whether these are active or stabilized under vegetation cover varying from meadow to woodland. However, sand cover is not a uniform mantle. Sand distribution in alluvial plains is complex, much more than that in peneplain landscape. Complexity of the alluvial landscape is related with the following factors:

- Discontinuous spatial distribution of white-sand areas and patches within a matrix of residual peneplain reliefs, in correlation with similar spatial patterns of the meadow areas in a matrix of wooden vegetation types
- Diversity of depositional situations controlled by two main processes, splay and overflow and their spatial variations and intergradation
- Frequency of boundary situations because of the adjacency or superposition of different depositional facies and the co-occurrence of depositional and weathering materials
- Importance of stratification and lithological discontinuities in transported materials revealing geomorphic instability and frequency of sediment reworking by river shifting and bank overflow, in contrast with homogeneous soil mantles resulting from deep in situ bedrock weathering
- Influx of silty deposits in the dominantly sandy lowland environment
- Limited evidence of current eolian activity but a possible larger extent of eolian geoforms in the past, obliterated by the present fluvial reworking of the sand covers

There are slight differences in particle size patterns between the three types of glacia. In annular glacia, colluviation tends to be the main transport and depositional process causing particle sorting that is often reflected in codominance of two sand separates (i.e., medium and fine sand). In longitudinal glacia, the prevalence of splay in sediment distribution results in less sorting, with often three dominant sand separates (i.e., coarse, medium, and fine sand). Substratum weathering causes generally a larger spectrum of particle separates in the cover sand including very fine sand, silt, and clay.

Typic Quartzipsamments dominate in well to moderately well drained conditions, while Oxyaquic Quartzipsamments are frequent in imperfectly to poorly drained conditions with groundwater within 1 m depth during the rainy season. The occurrence of mottles is rare as reworked sand sediments are mostly free of iron hydroxides. Dominant textures are coarse, medium, and fine sand. Shrubby meadow is the most common vegetation cover.

---

## References

- Ab'Sáber AN (2000) The natural organization of Brazilian inter- and subtropical landscapes. *Revista do Instituto Geológico de São Paulo* 21(1/2):57–70
- Carneiro Filho A, Zinck JA (1994) Mapping paleo-aeolian sand cover formations in the northern Amazon basin from TM images. *ITC J* 1994- 3:270–282
- Carneiro Filho A, Schwartz D, Tatumi SH, Rosique T (2002) Amazonian paleodunes provide evidence for drier climate phases during the Late Pleistocene-Holocene. *Quat Res* 58:205–209
- Colinvaux PA, De Oliveira PE, Bush MB (2000) Amazonian and neotropical plant communities on glacial time-scales: the failure of the aridity and refuge hypotheses. *Quat Sci Rev* 19:141–169
- Huber O, García P (2011) The Venezuelan Guayana region and the study areas: geo-ecological characteristics. In: Zinck JA, Huber O (eds) *Peatlands of the Western Guayana Highlands, Venezuela*. Ecological studies 217. Springer, Heidelberg, pp 29–89
- Latruesse EM, Nelson BW (2001) Evidence for Late Quaternary aeolian activity in the Roraima-Guyana Region. *Catena* 43:63–80
- MARNR-ORSTOM (1986) Atlas del inventario de tierras del Territorio Federal Amazonas (Venezuela). Dirección de Cartografía Nacional, MARNR, Caracas
- Meade RH (1994) Suspended sediments of the modern Amazon and Orinoco rivers. *Quat Int* 21: 29–39
- Meade RH (2007) Transcontinental moving and storage: the Orinoco and Amazon rivers transfer the Andes to the Atlantic. In: Gupta A (ed) *Large rivers: geomorphology and management*. Wiley, New York, pp 45–63
- Mendoza V (2005) *Geología de Venezuela: Escudo de Guayana, Andes Venezolanos y Sistema Montañoso del Caribe*. Ciudad Bolívar, Universidad de Oriente
- Nogué S, Rull V, Montoya E, Huber O, Vegas-Vilarrúbia T (2009) Paleocology of the Guayana Highlands (northern South America): Holocene pollen record from the Eruoda-tepui, in the Chimantá massif. *Palaeogeogr Palaeoclimatol Palaeoecol* 281:165–173
- Nordin CF, Perez-Hernandez D (1989) Sand waves, bars, and wind-blown sands of the Rio Orinoco, Venezuela and Colombia. US Geological Survey, Water Supply Paper 2326-A, Denver, 74pp
- Rossetti DF, Zani H, Cremon EH (2014) Fossil megafans evidenced by remote sensing in the Amazonian wetlands. *Zeitschrift für Geomorphologie* 58(2):145–161
- Rossetti DF, Moulatlet GM, Tuomisto H, Gribel R, Toledo PM, Valeriano MM, Ruokolainen K, Cohen MCL, Cordeiro CLO, Rennó CD, Coelho LS, Ferreira CAC (2019) White-sand

- vegetation in an Amazonian lowland under the perspective of young geological history. *Anais da Academia Brasileira de Ciências* 91(4):e20181337. <https://doi.org/10.1590/0001-3765201920181337>
- Schnütgen A, Bremer H (1985) Die Entstehung von Decksanden im oberen Rio Negro-Gebiet. *Z Geomorph NF Suppl-Bd* 56:55–67
- Schubert C, Fritz P (1985) Radiocarbon ages of peat, Guayana Highlands (Venezuela). Some paleoclimatic implications. *Naturwissenschaften* 72:427–429
- Schubert C, Fritz P, Aravena R (1994) Late Quaternary paleoenvironmental studies in the Gran Sabana (Venezuelan Guayana Shield). *Quat Int* 21:81–90
- Soil Survey Staff (2014) *Keys to soil taxonomy*, 12th edn. USDA, Washington, DC
- Zinck JA (2011) Synthesis: the peatscape of the Guayana Highlands. In: Zinck JA, Huber O (eds) *Peatlands of the Western Guayana Highlands, Venezuela*. Ecological studies 217. Springer, Heidelberg, pp 247–259
- Zinck JA, García P, van der Plicht J (2011) Tepui peatlands: age record and environmental changes. In: Zinck JA, Huber O (eds) *Peatlands of the Western Guayana Highlands, Venezuela*. Ecological studies 217. Springer, Heidelberg, pp 189–236





# Features and Trends of Meadow Landscape Evolution 10

J. A. Zinck and P. García Montero

---

## 10.1 Introduction

This chapter focuses on the evolution of the physical landscape in the meadow environment as it can be inferred from geomorphic and pedologic features and their relationships. It is based on data collected mainly from meadow areas and additionally from some ecotone fringes between meadow and caatinga–bana vegetation. The scope is limited in depth and space as it refers only to cover materials (to about 2 m depth) and areas with meadow and shrubby meadow vegetation. Because of its non-protective vegetation cover, meadow environment is exposed to geomorphic activity and thus able to show recent and sub-recent geopedologic changes. In contrast, forest and scrubland areas (caatinga and bana) are relatively stable from geomorphic point of view as terrain is protected by wooded cover and, in the case of caatinga, by thick root mat.

Meadow environment has monotonous, nearly level topography, interrupted by hill and rock outcrops in plain and penepain landscapes. Therefore, the appreciation of landscape evolution is not based on spectacular relief modifications. Meadow landscape evolution is subtle, but features and trends can be inferred from field observations supported by routine laboratory data.

Four types of features were selected that may help highlighting processes and trends of evolution in the physical landscape. Some are surface features (e.g., microrelief); others are subsurface features (e.g., stratifications). They include the following types of evidence:

---

J. A. Zinck (✉)

Faculty of Geo-Information Science and Earth Observation (ITC), University of Twente, Enschede, The Netherlands

P. G. Montero

Caracas, Venezuela

- Stratifications in white sand sediments and soils, with an emphasis on lithological discontinuities, used as markers of sedimentological changes and proxies of landscape evolution.
- Ecotone dynamics taking place in contact areas between forest (caatinga) and scrubland (bana) areas and meadow environment.
- Formation of reticular microrelief resulting from incision of erosion channels and suffusion depressions.
- Paleogeographic significance of the occurrence of Spodosols in current meadow areas.

---

## **10.2 Stratifications and Lithological Discontinuities in White-Sand Sediments and Soils: Signatures of Changes in the Meadow Environment**

Stratifications in white sand covers can be of geogenic or pedogenic origin. Geogenic stratifications result from discontinuous sedimentation. Depositional interruptions can be caused by the migration of the sand transportation channels from one to another place, i.e., shifting streams. Subsequently, deposited layers can be exposed to erosion before being covered by new sediments, often of different sedimentary facies. Geogenic stratifications are relevant indicators that record changes in the sedimentation process and environmental conditions. Pedogenic stratifications result from the differentiation of the parent material into horizons under the action of soil forming processes. In the particular context of white sands, pedogenesis is inhibited and stratifications result mainly from illuviation of organic matter. In the following set of examples, different kinds of stratification pattern occurring in the study region are described and interpreted to infer features of landscape evolution in the meadow environment.

### **10.2.1 Stratifications of Geogenic Origin**

Stratifications in sediments and other kinds of geogenic layering reveal sequences of events that have led to the upbuilding of a deposit (Arnold 1968). Stratifications can be contrasting enough to constitute ruptures in the depositional process and form lithological discontinuities between consecutive layers. Lithological discontinuities are significant changes in particle size distribution or mineralogy that represent differences in lithology within a soil (Soil Survey Staff 2014). In sedimentary areas, lithological discontinuities can reflect depositional hiatuses following repeated river migrations or changes in the nature of the depositional process, for instance from overflow to splay or vice versa. Contrasting sand sizes, for instance, result from differences in energy at the time of deposition by water or wind (Soil Survey Staff 2014). As sands are frequently reworked during flooding events, sand covers are polygenic with vertical, lateral, and longer-distance spatial variations. These variations are recorded as stratifications in the sedimentation archives. The

identification of layering and lithological discontinuities helps understand landscape evolution in the white-sand alluvial plains.

Sediment stratifications are frequent in alluvial plains and much less in peneplains. Colluviation that is a relevant process of glacia formation and transformation in peneplains usually does not cause strong depositional changes. In contrast, avulsion that mainly controls the formation and transformation of low-gradient alluvial flats commonly causes significant changes in the depositional column. Sequences of contrasting layers form especially in the meadow environment that is open to sediment accumulation and removal by shifting rivers and streams. Large parts of the sand covers result from fluvial reworking of sandy materials that originated in other lowland places. This is frequent in areas of river confluences. Simultaneous high water levels among tributaries during the rainy season result in flooding with generalized overflows or local splay fans.

Terrain surface instability influences vegetation colonization and establishment. Changing geomorphic dynamics may favor plant dispersal but also imposes meadow plants to repeatedly adapt to unstable surface conditions. This constraint may result in lowering plant diversity while favoring endemism. Under forest (caatinga) and scrubland (bana), the avulsion process is obstructed by the vegetation cover, although riparian forests may be locally affected by periodic overbank flows. If contrasting geogenic stratifications are detected in sediments under current forest cover, it may reflect a change of vegetation type from earlier meadow to present forest.

Stratifications are mainly caused by changes in particle size distribution of the sand fraction between consecutive depositional layers. Additionally, white-sand sediments may contain heavy, weathering-resistant minerals showing contrasting contents with depth. For instance, in Spodosols (Alaquods) of the eastern Colombian Amazon (Mitú area, Vaupés Department), zircon content was found to be high (>50% of the heavy minerals) in A and E horizons but low (<10%) in spodic horizons (Malagón Castro 1995; Pulido Roa and Malagón Castro 1996). Such abrupt mineralogical change allows inferring a lithological discontinuity between the upper and lower parts of the soil and suggests that the Spodosol may be in fact a duplex soil, with sand cover and underlying spodic horizon possibly unrelated.

Another kind of contrast among white-sand layers is caused by the incorporation of small amounts of organic matter during the stepwise aggradation of the sediment, resulting in irregular variations of organic carbon with depth. Such variations can be caused by organic matter mixed with the sediments, for instance sediments coming from the erosion of caatinga areas. Buried A horizons were not found in white-sand layer sequences because depositional surfaces supposedly did not stabilize long enough for dense vegetation cover to establish before the following sedimentation event. Aligned charcoal fragments can represent a stratification feature in sediment. In our area, macroscopic fragments were found at different depths (e.g., 12–125 cm) in sandy layers (e.g., P26, P65 in Table 6.6, and P99 in Table 6.2, Chap. 6). Dark sand lenses and band strips were identified at a few places, frequently together with charcoal fragments and horizontally lying buried roots indicating lithological discontinuity rather than incipient podsolization.

By masking relevant variations in particle size composition, total sand is insufficient to detect lithological discontinuities and reveals little about the

sedimentological history of a deposit. All layers of the sediment may have 99–100% sand but different sand separates that indicate changes in sedimentation flow energy. Sand separates allow (1) inferring the degree of flow energy and the kind of process controlling the nature of a sediment by the time of its deposition (for instance, distinction between eolian, alluvial, and colluvial, between overflow and splay, and between degrees of sorting from poor to well) and (2) identifying contrasting sand sizes among layers with similar total sand but variations in sand separates that indicate stratifications and lithological discontinuities.

Stratifications identified in the field and corroborated through particle size analysis are signatures of changes in the history of the sediment and the concomitantly evolving landscape. Hereafter, a few examples are described.

### 10.2.1.1 Stratified Sediment Under Meadow with Lithological Discontinuities

*Profile P21* is an example of a stratified sediment that shows sand separate percentages varying with depth. The soil sediment is an Oxyaquic Quartzipsamment located on a meadow alluvial flat in the middle Guayapo watershed (Sipapo area, Table 6.2). Four layers were separated in the field on the basis of sensed differences in sand grain sizes. All layers are 99% sand (98.6–99.3%), thus apparently a very homogeneous sediment throughout. However, sand particle size distribution changes clearly with depth (Fig. 10.1a). In the first layer (2–20 cm), below a covering of loose runoff sand in transit, medium sand is dominant at nearly 60%. In the second layer (20–50 cm), sand is poorly sorted, with very coarse, coarse, and medium sand showing fairly similar proportions. In the third layer (50–90 cm), sand is better sorted and there is a shift toward finer sand, with medium and fine sand codominant (about 40% each). The fourth layer (90+ cm) shows a sand distribution spectrum similar to that of the second layer. The four strata have similar total sand but contrasting sand separates.

Sand grain sorting varies from well to poor to moderate to poor consecutively with depth. This reflects energy variations of the water flow during the accumulation of the sediment. Layers 1 and 3 are overflow deposits with medium and fine sand dominant, resulting from lower energy flow and good sorting. In contrast, layers 2 and 4 are splay deposits with very coarse, coarse, and medium sand codominant, resulting from higher energy flow and poor sorting. The strata sequence is evidence of four consecutive depositional episodes with changing flow energy and degree of sand selection in a cyclic pattern based on the alternation of two different sedimentary processes, i.e., overflow and splay.

Profile P21 is a layered depositional profile, not a pedogenic one. White-sand layers are not albic E horizons, just C material. Organic carbon contents in the four consecutive layers are 0.13–0.0–0.06–0.53%, respectively. The increase of organic carbon in the lower layer is due to enrichment of organic substances by brownish groundwater at 90 cm depth. Spodic features can be expected to occur in depth (i.e., giant podzols), but they are unlikely to be related to the current organic-matter-poor meadow environment. Similarly to P21, many soils in the meadow lowlands owe

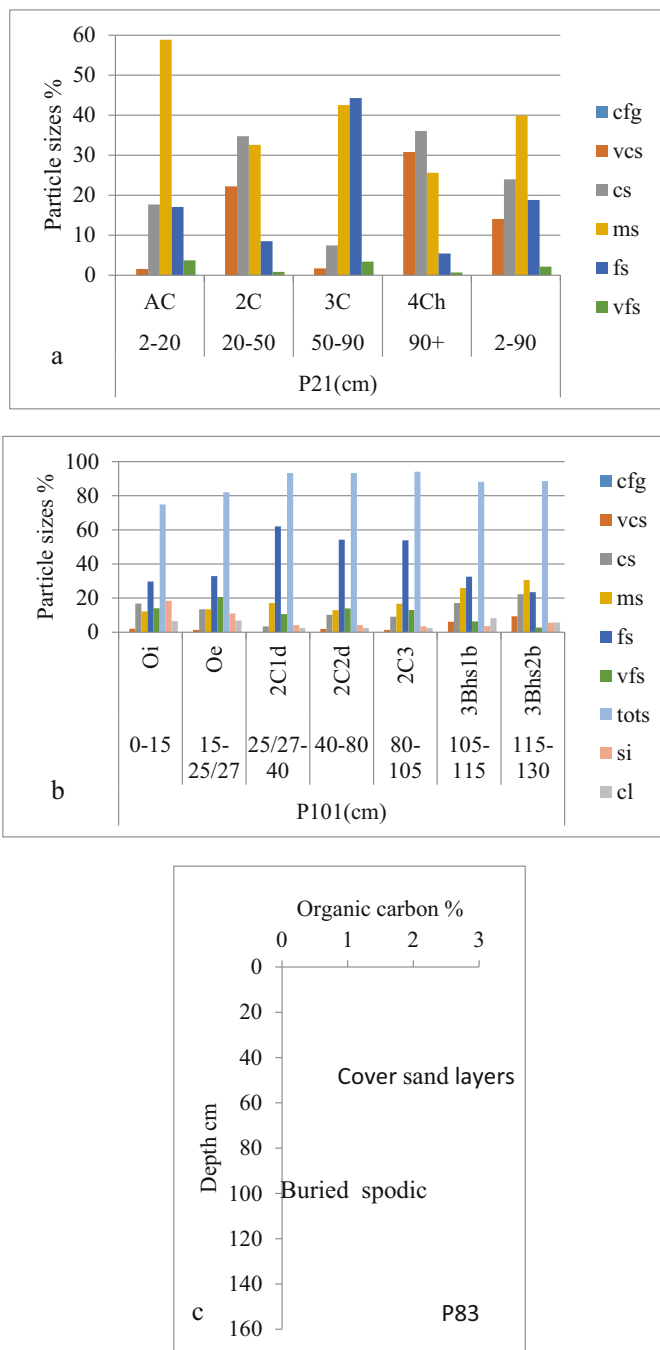


**Fig. 10.1** (a) Profile P21: Oxyaquic Quartzipsamment developed on stratified white-sand deposit showing changes of particle size pattern with depth in alternating layers: overflow sediment in AC and 3C and splay sediment in 2C and 4Ch. (b) Profile P101: Arenic Alorthod developed in stratified overflow fine sand sediment (25–105 cm) under caatinga forest, with cover sand burying truncated

more to sedimentological history than to pedogenic development. For this reason, they belong mainly to the Quartzipsamment class.

### 10.2.1.2 Duplex Profiles Under Caatinga and Shrubby Meadow: Stratified Sand Cover Burying Spodic Horizon

A few sites under caatinga vegetation were visited. In general, profiles are stratified similarly to meadow profiles and often composed of two contrasting sediment-soil bodies that are not genetically related (i.e., duplex profiles). *Profile P101* (Pasimoni area, Table 6.7) is an Arenic Alorthod located on a low terrace in the Siapa watershed in the southern part of the study region. It is composed of three sections showing contrasted particle size distributions (Fig. 10.1b). The surface layers (2–25 cm) that correspond to the root mat of the caatinga forest have developed in an unsorted splay deposit with fairly more silt (11–18%) and clay (7%) than the underlying C layers. This is followed by a sequence of three layers (25–105 cm) with a similar pattern of particle size distribution and a clear dominance of fine sand (50–60%) that indicates highly selected overflow sediment. The lower section (105–130 cm) is a poorly sorted mixture of coarse, medium, and fine sand reflecting a splay mantle deposit in which a spodic horizon has formed. The profile is stratified with two lithological discontinuities at 25 cm and 105 cm depth, respectively.

The textural organization of the profile suggests that the spodic horizon is most probably the remnant of a truncated Spodosol buried under more recent sediments. Accordingly, the site would have undergone significant changes over time. First, a Spodosol has formed most likely under caatinga, the usual forest cover with which Spodosols are associated in this region. Truncation of the Spodosol and the subsequent deposition of stratified layers burying the spodic horizon require an open vegetation cover to take place, most likely meadow or shrubby meadow. This was followed by a return to the current caatinga cover.

Similar situations of truncated Spodosols, buried under more recent stratified white-sand sediments, were found in the Guayapo watershed (*Profiles P82 and P83*; Sipapo area, Tables 6.2 and 10.3). Current vegetation is shrubby meadow that allows sedimentation to proceed and prevents caatinga forest to re-install. In other cases of buried spodic horizons (e.g., *Profile P20*; Sipapo area, Tables 6.2 and 10.3), sedimentation has stopped and vegetation has evolved to the stage of bana scrubland. Sand layers above the lithological discontinuity that makes boundary with the fossilized spodic horizon show often irregular variations of organic carbon with depth, as for instance in the case of *Profile P83* above the spodic horizon at 90 cm depth (Fig. 10.1c). Such sand covers have fluventic character, suggesting cumulative deposition by river overflow, and are thus unconformable with the underlying spodic horizon.

---

**Fig. 10.1** (continued) spodic horizons formed in splay sand substratum. (c) Profile P83: irregular variation of organic carbon in a sequence of sand layers that bury a spodic horizon at 90 cm depth, remnant of a truncated Spodosol (Typic Durorthod)

### 10.2.1.3 Duplex Profiles Under Meadow: Contrasting Sand Cover Burying Saprolite Residuum

White sands derived from bedrock weathering under meadow vegetation occur in the peneplain landscape, for instance at the footslope of crystalline domes. In contrast, mineral materials directly derived from in situ weathering of bedrock are unusual to detect in meadow plains, as the terrain surface is covered by reworked sandy sediments. In general, the sand cover masks the saprolite residuum in place, resulting in the superposition of two different materials. *Profiles P81, P87, and P128* (Tables 6.5 and 6.6 in Chap. 6) are examples of duplex profile with upper layers of depositional origin and deeper layers resulting from weathering of the bedrock.

*Profile P128* is an Oxyaquic Quartzipsamment covered by dense shrubby meadow west of Serranía Cariche, on the left bank of river Orinoco. The profile is uniformly pinkish white sand. In contrast, particle size distribution changes abruptly at 44 cm depth. Although total sand is unvarying with depth (>97% in all layers), the upper layers (1–44 cm) are dominantly fine and medium sand, while the lower layers (44–100 cm) are dominantly very coarse and coarse sand. Lower layers contain feldspar fragments coming from the weathering of coarse-grained rapakivi granite with feldspar phenocrysts (outcroppings in stream channels). Thus, the profile is a composite one with a strong lithological discontinuity at 44 cm depth between well-sorted overflow sediment and fossilized saprolite of weathering crystalline substratum (see also *Profile P81* in Chap. 9, Sect. 9.2.5.4; Fig. 9.2a).

Profile P128 is an example where total sand content of the full profile would mask the lithological discontinuity that underlines the contrasting change in particle size distribution at 44 cm depth and conceal the presence of two different materials. Detailed analysis of the profile reveals the superposition of two layer sets showing opposite patterns of particle size distribution. Fine and medium sand dominate at 1–44 cm depth, while very coarse and coarse sand dominate at 44–100 cm depth (Fig. 9.2b, c; Sect. 9.2.5.4; Chap. 9).

### 10.2.1.4 Stratified Splay Mantle with Turbulent Flow Layer

Splay mantle is together with overflow mantle the most common white-sand cover type in meadow plains. Usually, splay sediments are poorly sorted, in any case much less sorted than overflow sediments. They are transported by high energy flows during heavy floods and laid down as crevasse splays or torrential overbank splays. They include often unselected strata where all sand separates are present in similar percentages, indicating disordered and irregular turbulent flow and deposition. Sometimes, dominant splay layers alternate with overflow inclusions creating heterogeneous sediment sequences.

*Profile P66* in the Atabapo area (Table 6.6) is a Typical Quartzipsamment located on a flat terrain under shrubby meadow, south of the middle “caño” Caname. The whole profile is splay sediment, with more than 98% sand in all layers, but upper (0–33 cm), middle (33–63 cm), and lower (63–130 cm) parts show varying associations of sand separates and different splay facies. This is reflected by two lithological discontinuities at 33 and 63 cm depth, respectively. The intermediate layer between the breaks (33–63 cm) is outstanding in that it shows a fully



undifferentiated particle size distribution and disordered depositional pattern, including 12% fine quartz gravel (2–4 mm). This implies variations in flow energy between consecutive splay events, resulting in a heterogeneous, strongly differentiated sand deposit.

### 10.2.1.5 Stratifications in Piedmont Sediments

Sediments deposited at the foot of upland and highland reliefs, especially at the foot of tepui plateaus, are usually stratified. A major lithological discontinuity separates the gravelly stony base sediment from overlying sandy layers. The skeletal substratum results from torrential accumulation of coarse fragments that form the basal layers of the piedmont fan-glacis and reflect intensive geomorphogenic activity with erosion in the upland areas, possibly in pre-Holocene drier periods. The sandy cover layers have deposited during more recent times, possibly after peat formation inception at tepui summits and vegetation development along tepui slopes (see Chap. 8, Sect. 8.4.3).

## 10.2.2 Stratifications of Pedogenic Origin

Stratifications in soil material result from horizon formation controlled by pedogenic processes and soil forming factors. White sands because of their quartzose nature inhibit soil development. For this reason, Quartzipsamments are the most common soil class in the lowland white sands under meadow vegetation. More evolved soils on white sands are Spodosols that are usually associated with caatinga forest and, secondarily, with bana scrubland. Spodosols or remnants thereof were also found in the meadow environment, but they seem to be unrelated to the current herbaceous cover. Two kinds of pedogenic stratifications were identified in white sands that indicate interruption of soil formation and change of environmental conditions. These features are (1) double spodic horizons in some Spodosols and (2) densic layers in some Quartzipsamments and Udorthents.

### 10.2.2.1 Dual Spodic Horizons

*Profile P84* is a Durihumod located south-east of the lower Guasacavi river in the Atabapo area (Table 6.6). Terrain is flat, covered by shrubby meadow with dense herbaceous layer, scattered shrubs, and small open patches. *Profile P84* has the thickest spodic horizon (80–170+ cm) with the highest amount of organic carbon (2.7–5.7%) among all Spodosols and spodic materials found in the study region under meadow vegetation. The spodic horizon is bimodal with two peaks of illuvial organic matter accumulation: one peak of 4.7–5.7% OC at 90–120 cm (younger) and another peak of 5.3–5.5% OC at 150–170 cm (older), separated by a low of 2.9–3.1% OC at 120–150 cm (Fig. 10.2a). Peak layers are moderately indurated and sustain perched water tables, while the intermediate layer is soft. This indicates variation in podsolization intensity over time. If the intensity of podsolization is controlled by the degree of moisture in the soil, then the two maxima would correlate with abundant rainfall periods separated by a drier episode. Such a strongly

developed, polygenic spodic horizon is unlikely to have formed under the present meadow vegetation with poor organic matter production and is most probably an inheritance of earlier conditions under caatinga cover. The thickness of the spodic horizon in P84 is comparable to equally thick spodic horizons dated as from the beginning of the Holocene in eastern Colombian Amazonas (Mitú area, Vaupés Department) (Malagón Castro 1995; Pulido Roa and Malagón Castro 1996). Podsolization at P84 may have started early in the Holocene under forest cover to develop the thick spodic horizon but with intensity variation controlled by soil moisture. More recently, forest cover has been degraded into meadow vegetation with which the formation of the Spodosol is unrelated.

The stratigraphic column of P84 is rather homogeneous throughout, with systematic dominance of medium sand (60% on average) accompanied by variable proportions of fine sand (Fig. 10.2b). The irregular occurrence of about 10% silt in albic as well as spodic horizons causes slight textural stratifications. However, there is no significant lithological discontinuity at the top of the spodic horizon at 80 cm depth to consider the hypothesis of a duplex soil with cover sand burying the spodic horizon. There are no irregular variations of organic carbon in the upper horizons (0–80 cm) as in the case of *Profile P83* (Fig. 10.1c).

#### 10.2.2.2 Densic Layers (Densipan)

The occurrence of a densipan layer is a contrasting feature that causes lithological discontinuity with the overlying and underlying rather loose white-sand sediments. Some profiles show double densipans such as *Profile P77* in the Yapakana area (Table 6.5) at 39–65 cm and 115–145 cm depth, generating several lithological discontinuities in the depositional sequence. The characteristics of densipans are described in Chap. 7, Sect. 7.2.4.

---

### 10.3 Contact Areas: Ecotone Dynamics

The question can be raised whether meadow vegetation is the pioneer stage of an evolutionary sequence leading to bana scrubland and caatinga forest or, the other way around, the final stage of wooded vegetation degradation. Contact areas at the edge of distinct vegetation types are often sensitive places of contrasting environmental dynamics and ongoing changes in terms of regression or progression. In the lowland mosaic of wooded and herbaceous areas, contact spaces between enclaved meadow patches and surrounding forest matrix may be able to reveal features and processes of landscape evolution. Hereafter, a few ecotone situations between caatinga, bana, and meadow are analyzed.

Current geodynamics (i.e., erosion and deposition) takes place mainly in the meadow environment as the wooded areas are fairly protected and stabilized by the vegetation cover. However, there is evidence that vegetation distribution has changed during the Holocene, in particular under the effect of frequent and widespread fires induced by climate change and/or human disturbance (Sanford et al. 1985; Saldarriaga and West 1986; Cordeiro et al. 2008). Sandy areas now covered by

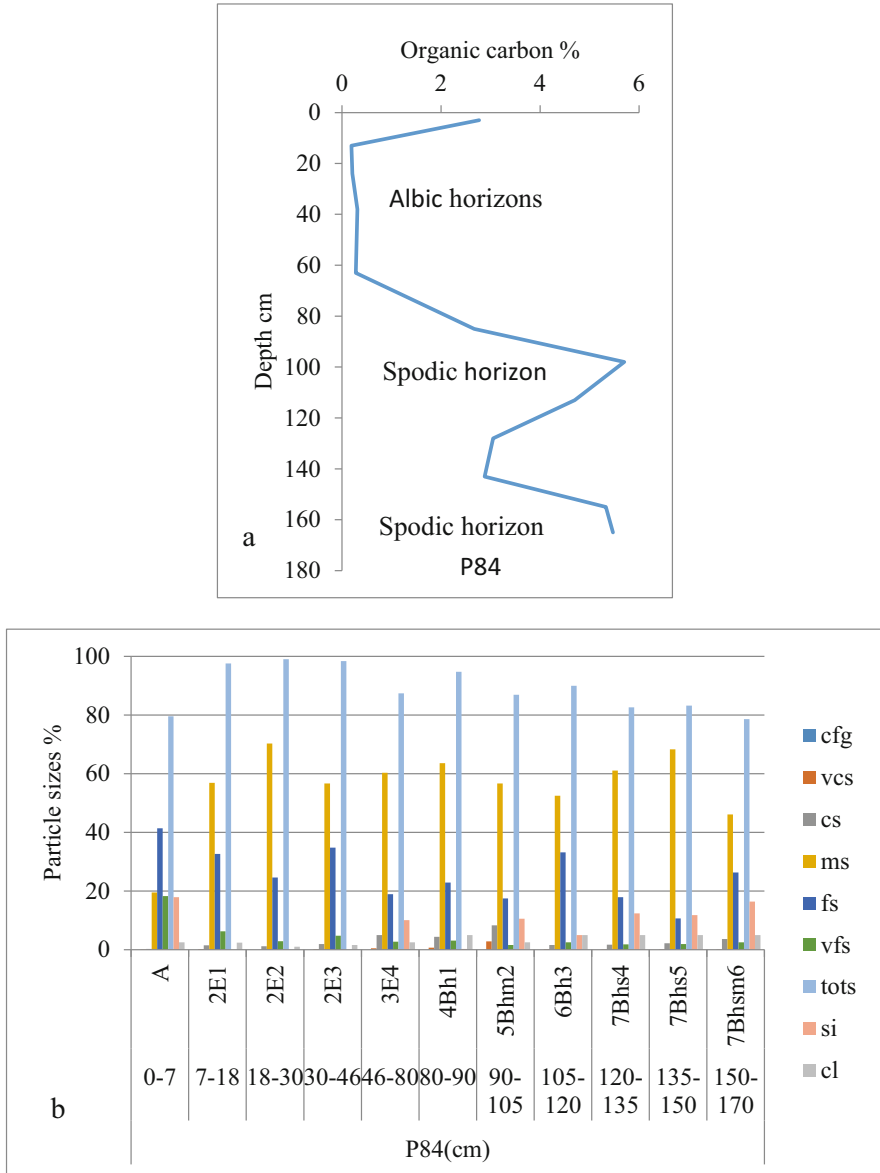


**Fig. 10.2** (a) Profile P84: bimodal spodic horizon complex in a Durihumod located in the Atabapo area. (b) Profile P84: Durihumod; stratigraphically homogeneous Spodosol with medium sand dominant in all layers, evidencing overflow deposition; thick spodic complex (80–170 cm) showing two indurated spodic horizons at 90–105 cm and 150–170 cm depth

caatinga or bana have a sedimentary history, possibly similar to the current meadow areas, except for forests and woodlands on soils developed from different kinds of weathered bedrock (“terra-firme” forests).

### **10.3.1 Association Caatinga-Bana-Meadow on Sandy Alluvial Sediment**

Caatinga forest, bana scrub, and herbaceous meadow occur often associated at relatively short distances from each other in ecotone landscapes. An example is taken from an area about 11 km east of San Carlos de Rio Negro along the road to Solano on the Casiquiare river (120 m a.s.l., 01°56'N–66°57'W).

The sand cover, concentrating in three sand separates with medium sand being dominant, is a moderately sorted splay sediment. Thus, soils and their associated vegetation types have developed from the same alluvial material after deposition stopped. Post-depositional evolution has caused some differentiation of the terrain surface. Under caatinga, the terrain is about 35 cm higher than the terrain under the neighboring bana; the difference corresponds approximately to the thickness of the organic topsoil built up by caatinga development above the mineral substratum. The meadow terrain is about 20 cm lower than the bana terrain; the difference results from truncation of the original depositional surface by shifting rills that start as individual drainage channels in the bana. The present meadow vegetation may thus be somewhat different from the original one that first colonized the depositional surface.

How did the colonization of the depositional surface start and differentiate? It can be assumed that herbaceous meadow vegetation pioneered the plant cover, followed by the development of wooded vegetation, in a progressive colonization process. In contrast, it can be supposed that the present meadow cover may have developed at the expense of bana vegetation upon or concomitantly with ongoing truncation of the bana surface.

In conclusion, three types of plant formation have developed on the same depositional surface at relatively short distance. That poses the question of what is the history of plant establishment and what are the mechanisms that control the vegetation dynamics (regressive or progressive) in contact fringes.

### **10.3.2 Contact Bana-Meadow in Alluvial Plain**

The sites are located about 10 km south of the middle Guayapo watershed (100 m a.s.l., 04°10'N–67°23'W). They illustrate a contact area between bana scrubland and low-cover open meadow. In the background stands a mixed caatinga forest on soil consisting of a thick root mat overlying white-sand substratum (Fig. 10.3a, b)

The bana terrain is incised by an interlaced pattern of channels 10–20 cm deep. Inter-channel islands are 1–10 m<sup>2</sup> large and account for half the surface area (Fig. 10.3c). They are covered by shrubs and small trees (2–4 m high). Woody

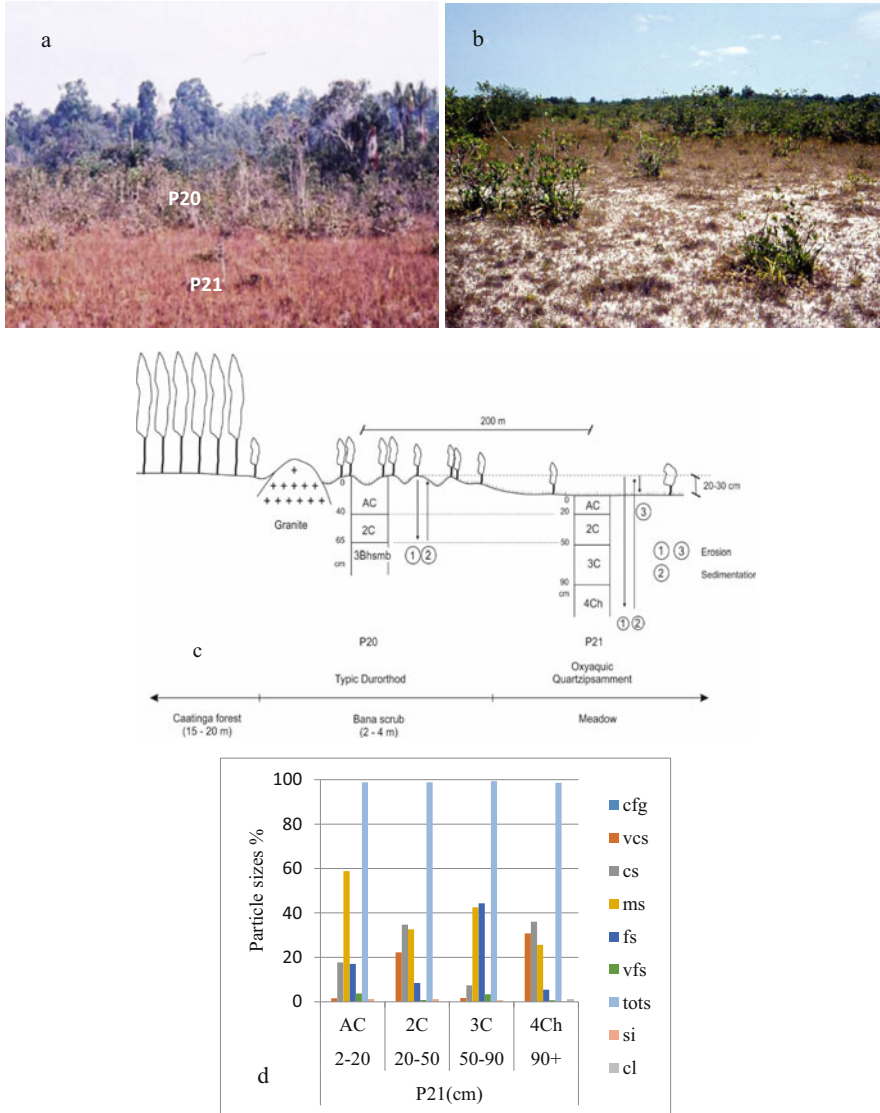


**Fig. 10.3** (a) Alluvial plain landscape in the middle Guayapo watershed (100 m a.s.l.); ecotone area with meadow in the foreground, bana in the center, and mixed caatinga in the background; P20 and P21 are soil profiles; (b) Contact fringe between bana scrub and shrubby meadow close to San Antonio in the Yapacana area: sand removed from degrading bana is spread by sheet wash over the adjacent meadow surface; (c) Cross section along the ecotone bana-meadow shown in the picture of Fig. 10.3a. (d) Profile P21: Oxyaquic Quartzipsamment developed in alternating overflow and splay sediments under meadow vegetation

clusters are surrounded by bare white-sand rims and patches with few herbs and forbs (e.g., species of Bromeliaceae, *Bulbostylis*, and *Xyris*). Tree stem feet and the borders of the woody islands show evidence of truncation by overland flow. Some granite heads about 1–2 m high outcrop at the terrain surface, showing exfoliation and granular disaggregation.

Next to the bana area extends a slightly lower (ca 20 cm) white-sand terrain surface. Vegetation is open meadow with isolated *Bulbostylis* and *Xyris* clusters. Some termite mounds (20–40 cm high) are scattered among the scarce herbaceous vegetation. *Profile P21* (Oxyaquic Quartzipsamment) (Fig. 10.1a) is 200 m distant from P20 in the bana area. Although total sand is 99% all along the profile, dominant sand separates vary among the consecutive layers: medium sand (2–20 cm); very coarse, coarse, and medium sand (20–50 cm); medium and fine sand (50–90 cm); and very coarse, coarse, and medium sand (90+). The last layer repeats the pattern of the second one (Fig. 10.3d). The profile shows an alternation of well-sorted overflow sediments and poorly sorted splay sediments (see also analysis of lithological discontinuities in Sect. 10.2). There are only traces of organic matter in the profile down to 90 cm depth where a dark sandy layer with 0.53% organic carbon appears, thus not enough to qualify for a spodic horizon. Sand is coated and loosely impregnated by organic substances brought by black groundwater (at 90 cm) flowing from neighboring caatinga and bana.

Profiles P20 and P21 have different surface and deep layers. However, the 2C layers in both profiles have similar sand separate patterns with coarse and medium sand dominant (37% and 33% in P20, and 35% and 33% in P21, respectively), together with some very coarse and fine sand. Thus, these two layers are comparable and show sedimentological spatial continuity between both sites (Fig. 10.3c). Landscape evolution can be hypothesized as follows. The original terrain has been eroded. At site P20 soil truncation was blocked by the indurated Bsm horizon, while sediment removal went deeper at site P21. Subsequently, both sites were covered again by sediments. Thus, bana and meadow are established on fairly similar depositional material. The meadow surface is a terrain level incised in the bana surface.

The bana-meadow contact area is a dynamic fringe where transfer of sand takes place. In bare patches at the bana edge (P20), medium sand is sieved off the top of the surface layer (0–5 cm) by selective runoff, leaving a residuum of very coarse and coarse sand. Removed medium sand is found back in the upper layer (2–20 cm) of P21 in the adjacent meadow where sand accretion retards the A horizon development (weak AC layer with 0.13% OC).

The bana scrubland is most likely a degradation phase of the original caatinga, present in the landscape background, possibly caused by fire and now severely affected by runoff and rill erosion. The rill pattern that incises the bana terrain changes into sheet wash in the meadow terrain. Erosion in the bana creates open patches for meadow vegetation to expand. Typical meadow species of the genera *Schoenocephalium*, *Bulbostylis*, and *Xyris* tend to invade the bana and colonize the bare white-sand patches surrounding the woody clusters. This mixed vegetation might reflect a “meadowization” process of the bana cover (Fig. 10.3b).

### 10.3.3 Contact Caatinga-Meadow in Alluvial Plain: Woody Cover in Regression

The selected contact area between mixed caatinga and shrubby meadow is located 30 km west of Serrania El Tigre in the upper watershed of “caño Yagua,” Yapacana area (130 m a.s.l., 03°51'N–66°27'W), in a basin position filled by splay sediments. Silt is an important component in these unsorted deposits (silty sands; see Chap. 9, Sect. 9.2.5.3), in contrast with the usual pure white-sand cover. Four profiles were described, two under caatinga and two in meadow (Fig. 10.4a).

The caatinga forest is 15–20 m tall. The terrain surface is incised by a network of interconnected channels with vertical walls, 40–60 cm deep and 1–1.5 m wide. Trees concentrate on inter-channel terrain heads, while only forbs grow at the bottom of the channels (Fig. 10.4b)

*Profile P60* (Entic Humudept) (Table 6.5, Chap. 6) is located on an inter-channel surface (Fig. 10.4b, c). The topsoil is a dense mat of interlaced horizontal and vertical roots (0.2–0.7 cm thick, some up to 1.5 cm), constituting 50–60% of the horizon mass (Table 6.5, Chap. 6). The mineral material is sand and silt poorly mixed with humified organic matter. *Profile P59* (Udoxic Quartzipsamment) (Table 6.5, Chap. 6) is located at the bottom of a channel 50 cm apart from P60 that is on the terrain surface (Fig. 10.4b, d). *Profile P58* (Udoxic Quartzipsamment, 130 m a.s.l) (Table 6.5, Chap. 6) is located 200 m apart from profile couple P59–P60 in a shrubby meadow (40–50% cover, with *Terminalia*, a.o.) that extends in front of the caatinga forest (Fig. 10.4b). The caatinga terrain is about 75–80 cm higher than the meadow area; both are connected by a very gentle slope (0.5%). Concave, often confined, basin positions similar to that of P58 are frequent in the lowlands. For instance, the watershed of caño Yagua between Serrania El Tigre to the east, Cerro Yapacana to the west, river Orinoco to the south, and river Ventuari to the north is a depressed, delta-like alluvial plain that stores water and sediments. The levees of the Orinoco and Ventuari in their confluence triangle slow down water evacuation during the rainy season.

The caatinga forest is characterized by a dense layer of fine roots under the litter layer, growing within a deposit of incompletely decomposed organic matter (Klinge et al. 1977). The fine roots are mostly associated with vesiculo-arbuscular mycorrhizal fungi (VAM) (Moyersoen 1993), a symbiosis essential for efficient capture of nutrients released during litter decomposition and transported in rain and throughfall water (Stark and Jordan 1978). Nutrients in the underlying white sand are very scarce (traces of phosphorus and potassium; 0.15–0.27% OC). The original substrate was a fairly leached, white-sand surface similar to the bare sand patches common in the meadow environment. How much time did it take for the evolution process to build up the necessary successions leading from herbaceous pioneer cover living on a tiny ochric epipedon to the caatinga forest that has built a dense root mat and its own organic horizon? Wildfire or slash and burn of the caatinga, with fire inevitably killing the root mat, would result after a few years of cultivation in exposing again the white-sand substratum to runoff.



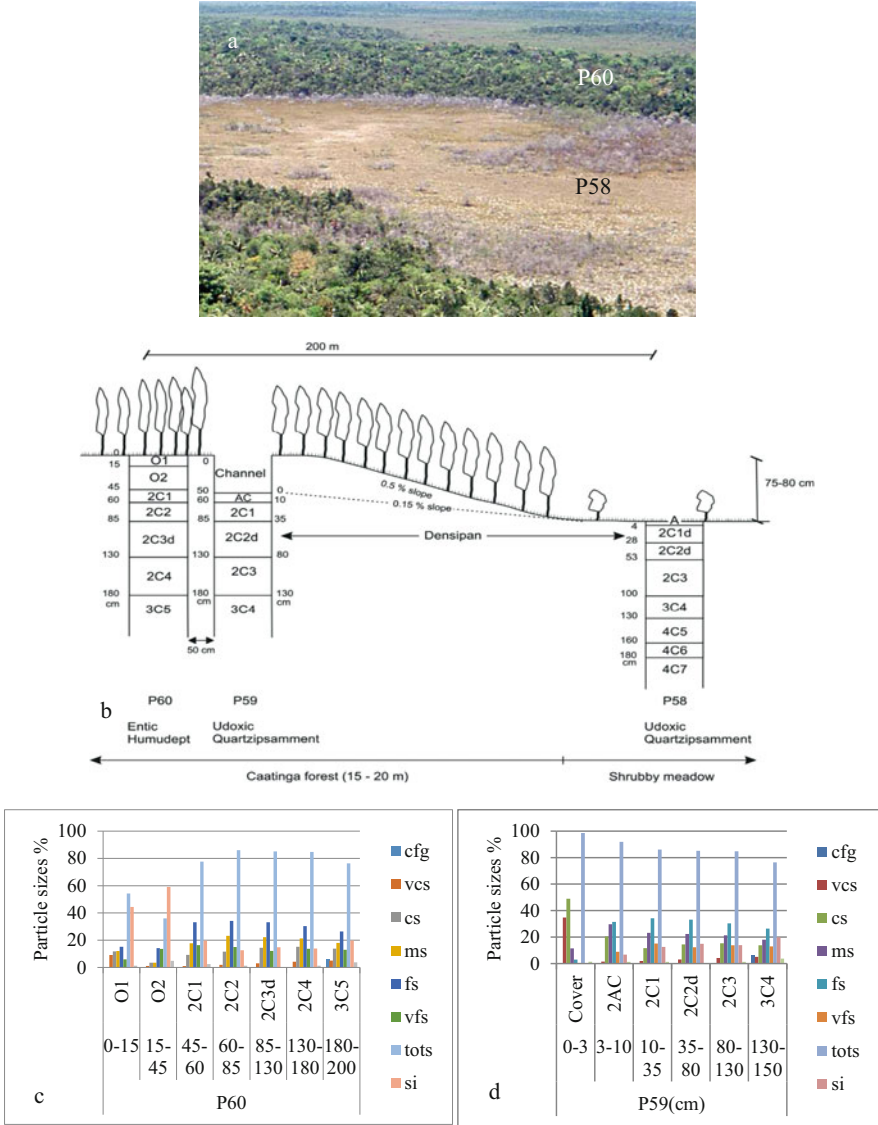


**Fig. 10.4** (a) Alluvial plain landscape in the upper watershed of caño Yagua (130 m a.s.l.); ecotone area between mixed caatinga and shrubby meadow; P58 and P60 are soil profiles. (b) Cross section along the ecotone caatinga-meadow shown in the picture of figure 10.4a. (c) Profile P60: Entic Humudept developed in unsorted sediment (45–200 cm) contrasting with the high silt content in the O horizons; profile is on the inter-channel surface under caatinga shown in figure 10.4b. (d) Profile P59: Udoxic Quartzipsamment developed in unsorted sediment; the profile is at the bottom of the channel under caatinga shown in figure 10.4b

The sediment on which caatinga forest has developed (P59 and P60) and that is exposed in the meadow (P58) has regional extent. At a distance of 10 km north of P58 site, *Profile P61* (Udoxic Quartzipsamment), located on a shrubby meadow between channels 20–30 cm deep and 20–40 cm large, often enlarging into suffusion pans (1–2 m), shows similar depositional facies in the lower layers buried by an unconformable surface deposit (0–40 cm). Particle size distribution figures are fairly similar to those of the mineral layers of P58-P59-P60 (Fig. 10.4d). However, profile P61 lacks the densipan layers that constitute a significant correlative feature in P58-P59-P60. In the meadow profile P58, densipan layers are at 4–53 cm depth. This corresponds approximately to the unconformable surface deposit (0–40 cm) in P61. The layer at 25–40 cm depth with 100% sand and prominent dominance of one sand separate (50% medium sand) reflects a depositional event of strong energy that may have erased the densipan layers.

Profile P61 lies several kilometers apart from P58 on the same extensive meadow surface. This example shows that meadows that are often confined between residual peneplain reliefs and sometimes restricted to small enclaves surrounded by woody vegetation also occur over larger surface areas. Enlarged meadow terrains were found in all study areas, especially in the Ventuari and Atabapo areas. This can have an influence on meadow plant distribution over larger, continuous spatial units with more cover uniformity and less floristic variations, in contrast with the more common small island meadows that may show differences in species associations among them at shorter distance.

The mineral layers of the selected profiles have similar patterns of unsorted sediment, slightly stratified, with a large particle size spectrum including all classes but spanning mainly from coarse sand to silt, with a relative dominance of fine and medium sand that attenuates with depth. Properties such as particle size distribution, pH, and organic carbon in mineral layers show similar values in all soils (Table 10.1). Compact, densified reference layers with similar thickness are present in caatinga and meadow soils. When considering 75 cm elevation difference between P60 and P58, the densipan layers happen to occur in both profiles at similar depths in relation to the original terrain surface (Fig. 10.5). The difference of terrain elevation between the present meadow site and the original caatinga surface corresponds to the loss of 45 cm root mat and about 30 cm mineral layer of the caatinga soil. Thus, both profiles significantly correlate.

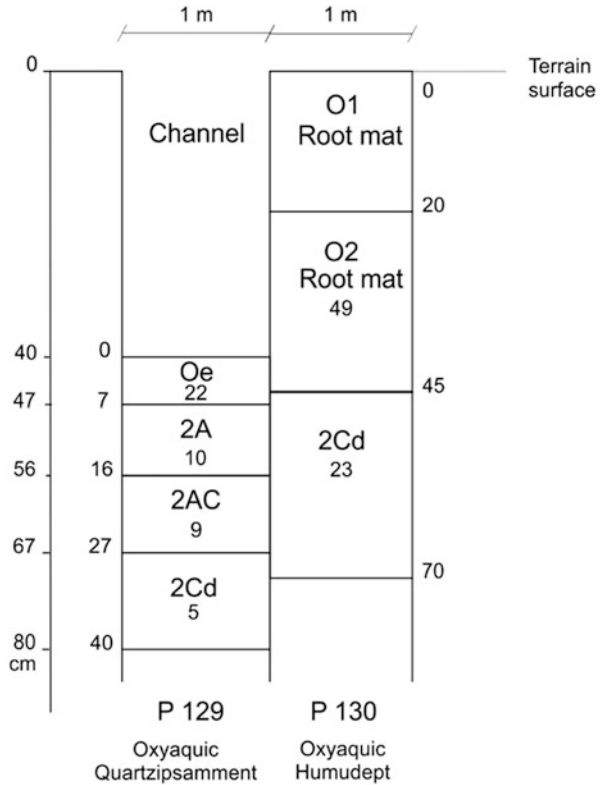
The profiles belong to the same original sediment mantle that has undergone different evolution in terms of surface geodynamics and vegetation cover. Both caatinga and meadow vegetation are resting on the same white-sand deposit. Meadow vegetation lives within the top mineral layer, while caatinga vegetation lives atop this layer. Assuming a hypothetical progressive evolution taking place after the sand mantle deposition, the vegetation cover would have shifted from pioneer meadow to intermediate bana to final caatinga. The current sclerophyllous forest would have built up an authigenic ecosystem based on symbiotic root mat formation and nutrient cycling that are both mostly independent of the mineral substratum.

**Table 10.1** Similarity of selected property values between neighboring caatinga and meadow soils

Profile	Sand %	Silt %	Clay %	pH	OC %	Densipan thickness cm	Densipan depth cm	Densipan corrected depth cm
P60-P59 caatinga	82	16	2	5.5 (5–6.1)	0.21 (0.15–0.27)	45	85–130	–
P58 meadow	82	15	3	5.5 (5–6)	0.23 (0.11–0.4)	49	4–53	79–128
P61 meadow	76	20	4	5.8 (5.4–6.1)	0.12 (0.02–0.2)	–	–	–

Average property values in mineral layers (P60: 45–120 cm; P58: 4–205 cm; P61: 40–150 cm). Densipan depth in P58 corrected on the basis of 75 cm elevation difference between caatinga terrain and meadow terrain

**Fig. 10.5** Soil differentiation between a full profile (P130) and an adjacent profile (P129) under incised channel in caatinga forest (west of Cerro Cariche)



Nowadays, the caatinga fringe seems to be relatively stable from geomorphic point of view. The terrain is incised by channels that are seemingly not erosive today as there is no deposit at the channel outlets into the contiguous meadow area. In the present conditions, channels evacuate rainwater from the caatinga but without enlarging or deepening. They may have formed in some earlier period morphogenically more active than today, possibly with a drier climate causing the lowering of the regional base level (see Sect. 10.4). The meadow surface possibly formed during the same period following some kind of disturbance of the caatinga forest, for instance natural or human-induced fire, as charcoal fragments was found in profile P60 (at 45+ cm depth). Resulting vegetation degradation and lower cover density would have exposed the caatinga terrain surface to truncation by coalescing channels and sheet wash during heavy rainfalls.

The spatial continuity of the reference densipan layer from caatinga to meadow indicates that both vegetation types are established on the same depositional material. The difference of elevation (75–80 cm) between caatinga and meadow terrains corresponds to the thickness of sediment lost as estimated by comparing the depth to the densipan layer at sites P60 (2C3d at 85 cm) and P58 (2C1d at 4 cm) (Fig. 10.4b). Thus, the meadow terrain is an erosional terrain incised in the original depositional

surface with a net loss of ca 80 cm sediment. This feature correlates with channel incision in the caatinga terrain. Current erosion in meadow by runoff and rills consists mainly of reworking surface sand.

The regressive evolution from caatinga to meadow looks like being the reversal of the original evolution sequence from meadow to caatinga. Locally, downgrading of the meadow surface is likely to stabilize when rill erosion and inter-rill sheet wash reach the top of the densipan layer, able to slow down further truncation. However, the trend in this area points to spatial extension of meadow surfaces at the expense of caatinga and bana. Nowadays, at regional scale, large caatinga–bana expanses, particularly flammable during the dry season, are decimated by the current increase of rampant wildfires.

This example shows that sediments with similar depositional facies extend over larger areas or may repeat at different places apart from each other. The main sediment body in all profiles shows a similar sand separate sequence with fine sand > medium sand > coarse sand  $\geq$  very fine sand + 10–20% silt. Surface layers may change at short distance as they reflect local reworking geodynamics with alternation of deposition and truncation.

### 10.3.4 Contact Caatinga-Meadow on Peneplain Glacis: Woody Cover in Building

In spite of the general impression provided by point observations and reconnaissance flights that indicate that caatinga and bana are in regression, possibly boosted by more frequent fires, there are also situations that can be interpreted as caatinga expansion. Such a situation is illustrated by profiles P27 and P28 located in the watershed of river Temi belonging to the Atabapo area (100 m a.s.l., 02°57'N–67°29'W) (Table 6.6, Chap. 6).

*Profile P28* is a Typic Quartzipsamment on a glacis surface (1–1.5%) covered by dense caatinga forest 15–20 m high. The material is splay white sand. The top Oe horizon of variable thickness (0–5/10 cm) is a mixture of decomposed leaves (15% OC) and dense root mat of fine and medium roots (2–5 mm), with fine earth having pH 3.5. This shallow organic horizon is mainly unconnected with the underlying sandy splay sediment (96–100% sand).

The trees have light grey, tall, straight, thin stems typical of caatinga forest. The height and density of the forest contrast with the poorly developed soil substrate. The thick, intricate root mat usually found under caatinga forest is missing here. Instead, an incipient root network is in formation with pH two units lower than that of the underlying mineral layers. This soil–vegetation association is in a pioneer stage of establishment. The young forest seems to build its own soil support atop and independent from the nutrient-depleted white sand. This case could be regarded as an example of recent caatinga establishment and expansion.

At short distance from P28 (100 m) on the same glacis surface lies *Profile P27*, a Typic Udorthent covered by a mixture of savanna and meadow species. The material is splay white sand similar to the sediment at P28 but with an important silt

component in the second layer that improves water holding capacity. Values of pH are 5–6. Why did caatinga not develop on this adjacent site providing slightly better soil conditions? Caatinga may have been present at this place but disappeared upon being degraded by fire.

It is difficult to fully ascertain from point observations the variety of changes that may take place along contact fringes between woody and herbaceous areas. However, some conclusions can be drawn from the analyzed sites. The caatinga fringe seems to be relatively stable today from geomorphic point of view but has been an active erosion front in some past time when the present meadow terrain was incised in the original depositional surface at the expense of the caatinga forest. The current erosional meadow surface as well as the channels crossing the caatinga terrain seems to be an inheritance of an earlier period when the regional base level was lower than today.

The contact area between bana and meadow is active from geomorphic and botanical points of view. The bana fringe is exposed to degradation by runoff and rill erosion that create bare white-sand patches, especially after repeated fire events. Typical meadow species tend to invade the bana and colonize the bare patches surrounding the woody clusters. This mixed vegetation might reflect a process of “meadowization” of the bana cover.

One example shows a tall caatinga forest growing on a contrasting poorly developed soil substrate. It suggests that caatinga can colonize relatively fast a meadow surface by building its own soil support on nutrient-depleted white sands.

---

## **10.4 Microrelief: Surface Features Caused by Erosion and Suffusion**

### **10.4.1 Microrelief in the Amazonian Lowlands**

Microrelief caused by surface drainage and erosion incision, including rills and channels, is a widespread feature in the Amazonian lowlands, with variations according to landscape, relief form, material, rainfall, and vegetation cover. In contrast, microforms resulting from chemical erosion and internal drainage are less frequent (i.e., dissolution of quartz grains and percolation of the silica solute through the soil). Firstly, reference is made here to the information provided by the soil survey of the Venezuelan Amazon territory carried out by MARNR-ORSTOM (1986). Subsequently, we report the results of our own field observations in the meadow environment.

The descriptive legend of the soil atlas of the Venezuelan Amazon territory reports the occurrence of erosional microforms per map units and shows their positions along landscape transects. Information presented in this section is summarized from the soil atlas descriptive legend. Two types of microform are reported to occur in the lowlands: channels (“zuros”) and mini-depressions (“minicubetas”).

Channels are incisions with vertical walls and flat bottoms, 50–100 cm deep, and several decimeters wide. They occur under various types of vegetation cover, principally in forest with different kinds of trees ( tall rainforest trees, thin-stem sclerophyllous trees, trees with stilt roots, and palms), secondarily in evergreen scrubland, and only occasionally in dense or open meadow. Channels were identified in a variety of landscapes and substrata including (1) sandy materials principally in erosional plains and secondarily in erosional-weathering peneplains and alluvial plains, (2) ferrallitic saprolites with lateral pedodynamics in weathering plains and peneplains, (3) depleted saprolites with vertical pedodynamics in weathering plains, and (4) silty and clayey materials in weathering plains and alluvial plains. Channels are most frequent in white sands of erosional plains, in particular in four types of environment including drowned areas, semi-endorheic areas, accumulation areas, and splay areas. Large concentrations of map units with channels occur in the areas of Santa Barbara-Chamuchina, Maroa-Casiquiare, and San Carlos de Rio Negro.

A common feature among most of the map units with channels is poor drainage. Terrains are inundated a large part of the year and most of the soils have aquic regime. In erosional-weathering peneplains, erosional plains, and alluvial plains, channels have developed almost exclusively in sandy materials under forest, scrubland, and meadow vegetation, in Psammaquents, Quartzipsamments, Tropaquepts, and Tropaquods, and in soils with histic features such as Troposapristis, Tropohemists, and Tropofibrists.

Mini-depressions are small pans a few square meters large, with vertical walls and flat bottoms. They have been identified mainly in weathering material from crystal-line rocks. They occur under forest cover in piedmont, erosional-weathering peneplain and weathering plain, in various soil types including Tropaquepts, Paleudults, Haplorthox, and Placaquods.

From the above information derived from the soil atlas legend, it can be concluded that microrelief caused by surface drainage and erosion is ubiquitous throughout the lowlands. Channels occur in any kind of low-lying landscape, vegetation cover, soil type, textural class, and substratum material. They are, however, more frequent in sandy material under forest cover and uncommon in sandy meadow environment. Overall, it seems that channel formation is not controlled by a specific set of environmental factors, such as an exclusive kind of material. The fact that channels have formed in a variety of conditions advocates for a more general factor that might have led to channel incision. One such a factor could be a slight tectonic uplift in the regional context, but no evidence has been reported. A sustained dry period during the Holocene may have contributed to lowering the base level in rivers and streams with regressive effect causing the incision of channels in the interfluves to connect the surface drainage with deepening river beds. This hypothesis is substantiated further in this section on the basis of site analysis.

Our field observations in the meadow environment and fringes thereof reveal a variety of microforms, including rills, channels, and pans that exhibit sometimes picturesque reticular patterns of microtopography. Some are erosion microforms caused by surface drainage, while others are suffusion microforms related to internal drainage.



### 10.4.2 Erosion Microrelief in the Meadow Environment and Contact Fringes

Rills (locally called “surco”) are shallow erosional incisions that are distributed over the meadow terrain surface in approximately parallel pattern, sometimes also in ramified and interlaced network. Straight rills are more common on peneplain glacis, while reticular rills are more frequent on alluvial plain flats. They are tens to hundreds of meter long, 10–30 cm deep, 10–50 cm wide, with vertical walls and flat bottoms. The longitudinal pattern shows often succession of enlargements and narrows. The bottom is usually covered by a few centimeters of coarse sand and films or crusts of black algae (Plate 10.1a, b).

They are relevant agents of glacis truncation upslope and burial downslope (Plate 10.1c, d). Rills develop in sands that may be provided by (1) weathering of the crystalline rocks (gneiss, granite) or sedimentary siliceous rocks (sandstone, quartzite) that constitute the substratum of the glacis or (2) the deposition of colluvium coming from the weathering of the rocky domes upslope. Radial rill patterns develop at the foot of the domes. As rills migrate over the terrain surface, alternation of truncation and burial spots can be observed around plants. However, rill incision is usually more intensive in the distal part of the glacis, following laminar runoff in the apical part. Rill reticula densify at the edge of the glacis in contact with palm swales that form the local drainage network. In these moister areas, small hips of earthworm castings are frequent. In general, vegetation is open meadow with a few shrubs. Rills are an essential agent of glacis surface evolution. Shifting incision of rills causes glacis truncation that feeds the slightly lower-lying alluvial flats. Rill patterns are repeatedly modified at heavy rainfall events.

Rills are less frequent in the level alluvial plains (<0.5% slope). They develop often in contact areas between caatinga or bana terrains and adjacent, slightly lower meadow surfaces (see contact bana-meadow in Sect. 10.3.2). Plate 10.1a, b shows a dense network of shallow (5–10 cm deep) interconnected reticular rills that cross the surface of an alluvial meadow flat. In dense rill networks, inter-rill cells covered by herbaceous tussocks have a few square meters extent, and roughly oval, elliptic, or irregular configuration.

Deep channels are frequent under wooded cover (caatinga, bana) and rather uncommon in meadows. In forest and scrubland, channels form ramified interlacements enclosing inter-channel islands that are remnants of the original terrain surface where trees and shrubs concentrate. The incision of channels fragments the forest area and is likely to contribute to the degradation of the forest vegetation (caatinga) into scrubland (bana). Channels are frequent in ecotone areas between terrain surfaces of different elevation (a few decimeters) and vegetation cover: for instance, the fringe between a higher caatinga/bana surface and a lower meadow surface, or between the distal part of a glacis and an adjacent palm swale (see Sect. 10.3.3, Fig. 10.4b). In this kind of contact areas, the bottom of the channels under caatinga/bana connects topographically with the neighboring meadow terrain surface. The difference of elevation between the caatinga surface and the meadow surface corresponds approximately to the thickness of material removed by erosion

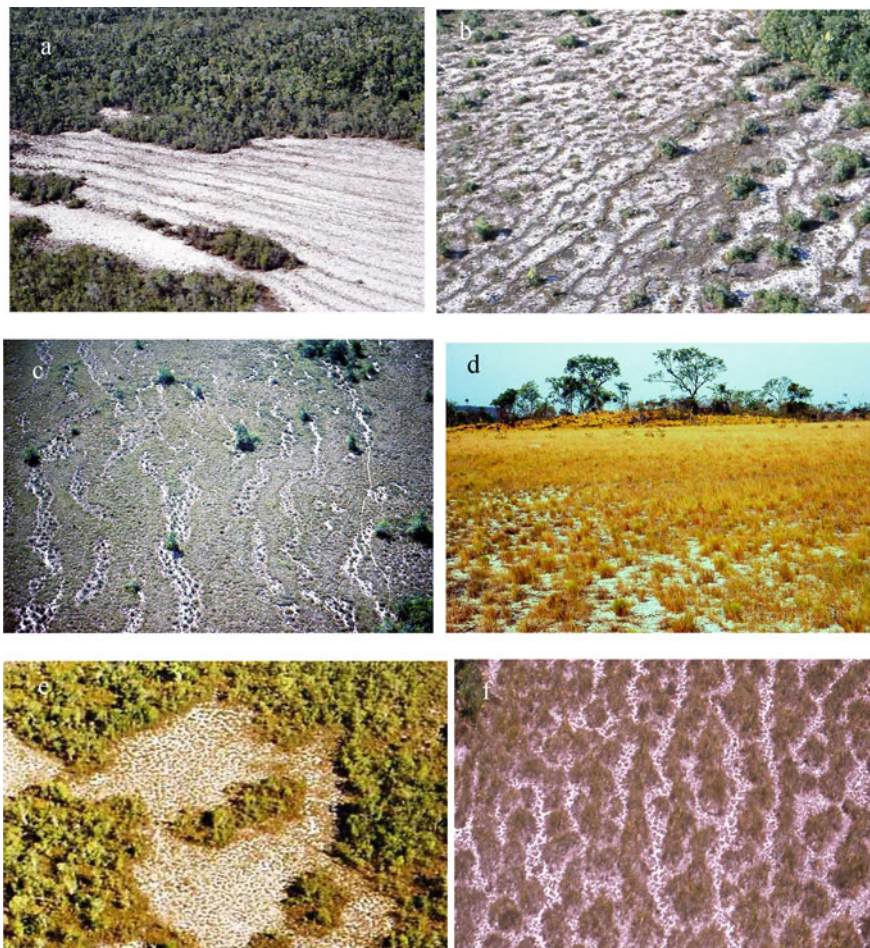


**Plate 10.1** (a) Rills in formation after the meadow vegetation has been burned and burned residues partly washed away by runoff, on a glaciais at the foot of a wooded crystalline hill. (b) Stabilized rill network on a peneplain glaciais in front of a low hill (wooded vegetation in the upper right corner). (c) Rill enlargement in the proximal part of a peneplain glaciais gradually eats away the surface layer and remobilizes colluvium. (d) Shallow colluvial sheet formed by rill coalescence that partly buries the mixed savanna-meadow vegetation in the distal part of a peneplain glaciais (Carmelitas-Yagua, Yapaçana area). (e) Reticular rill network crossing an alluvial meadow flat enclaved in wooded vegetation; (f) close-up of the reticular pattern with rills fragmenting the meadow cover into clumps of tussocks

from the caatinga terrain, mainly the root mat and sometimes the upper layer of the sand substratum. The deepest channels (up to 100 cm) were found in the confluence area between rivers Ventuari and Marueta.

In the dense reticular drainage network under caatinga, soils in channel and at the contiguous terrain surface are directly interfaced. One would expect that

homologous layers at both sites, from channel bottom downwards, would present similar features at close distance. In fact, striking contrasts in some properties were observed. An example is provided by profiles P129 and P130 located west of Serranía Cariche, close to Cariche village, on the left bank of river Orinoco (120 m a.s.l., 02°57'N–66°23'W) described in Chap. 7, Sect. 7.2.4 (Fig. 10.5; Table 6.5). The caatinga forest 10–15 m high with shrubby understory is crossed by entrenched channels, 35–40 cm deep and 50–100 cm wide. Trees assemble on inter-channel areas that form elongated islands with lobulated vertical walls. P129 is at the bottom of a 40 cm deep, stabilized channel, while P130 is at the terrain surface. They form a couple of profiles 30 cm apart.

Channel incision at profile P129 has removed the largest part of the original organic topsoil as compared to P130. Although the two profiles are only 30 cm distant from each other, the mineral layers do not match, especially concerning the silt content and the depth at which the densipan starts (Fig. 10.5). Particle size distribution of the original white-sand sediment is unlikely to change at such short horizontal distance. It seems as if the two profiles have undergone different evolution. At P130 site, the densic layer occurs at 45 cm from the soil surface, immediately beneath the root mat. At P129 site, the densic layer occurs at 27 cm under the channel bottom (i.e., 67 cm from the soil surface) beneath a shallow organic horizon and non-compact mineral layers. Thus, the horizon sequences differ at both sites and the depths at which the densic layers start do not correlate spatially. It suggests that the 2Cd layer at P129 has formed after channel incision and that this incision is therefore not recent.

The most important feature is the difference in silt content between the two profiles (Fig. 10.5). Silt is much higher in P130, especially in the O2 horizon (49%). It is hypothesized that this could result from fragmentation of sand grains upon alveolization in extremely acid organic environment (pH 3.9–4.5). Therefore, the incision of the channel network under caatinga can be assumed to be relatively old, certainly not actual. Spatial extrapolation of the differential pedogenic evolution between P129 and P130 would suggest that soil pattern under caatinga is a complex mosaic (see also in Sect. 10.3.3, profile P60 with 44–59% silt in the root mat and less than 20% in the underlying mineral layers).

The caatinga area lies in the proximity of a shrubby meadow where *Profile P128* is located, an Oxyaquic Quartzipsamment developed in overflow sediment that fossilizes weathering crystalline bedrock, with black groundwater at 57 cm depth without evidence of podsolization (see Chap. 9, Sect. 9.2.5.4). P128 is about 300 m distant from the channel profile P129. The meadow terrain is ca 40 cm lower than the caatinga terrain. That elevation difference corresponds to the thickness of the root mat under caatinga. The surface layer (0–44 cm) of P128 and the combined mineral layers beneath the channel bottom (7–40 cm) at P129 have similar particle size distribution (Table 10.2). They correlate spatially taking into account 40 cm elevation difference. Thus, they belong to the same depositional surface. The bottom of the channels under caatinga connects topographically with the terrain surface of the meadow.

**Table 10.2** Profiles P128 and P129 showing similar particle size distribution in mineral layers (data calculated on 100% sand basis)

Profile	Depth beneath terrain surface cm	Depth beneath erosion channel cm	Coarse sand 2-0.5 mm	Medium sand 0.5-0.25 mm	Fine sand 0.25-0.05 mm	Depth to groundwater cm	Vegetation
P128	0-44	-	12	33	55	57	Shrubby meadow
P129	47-80	7-40	18	34	48	29/69	Caatinga channel



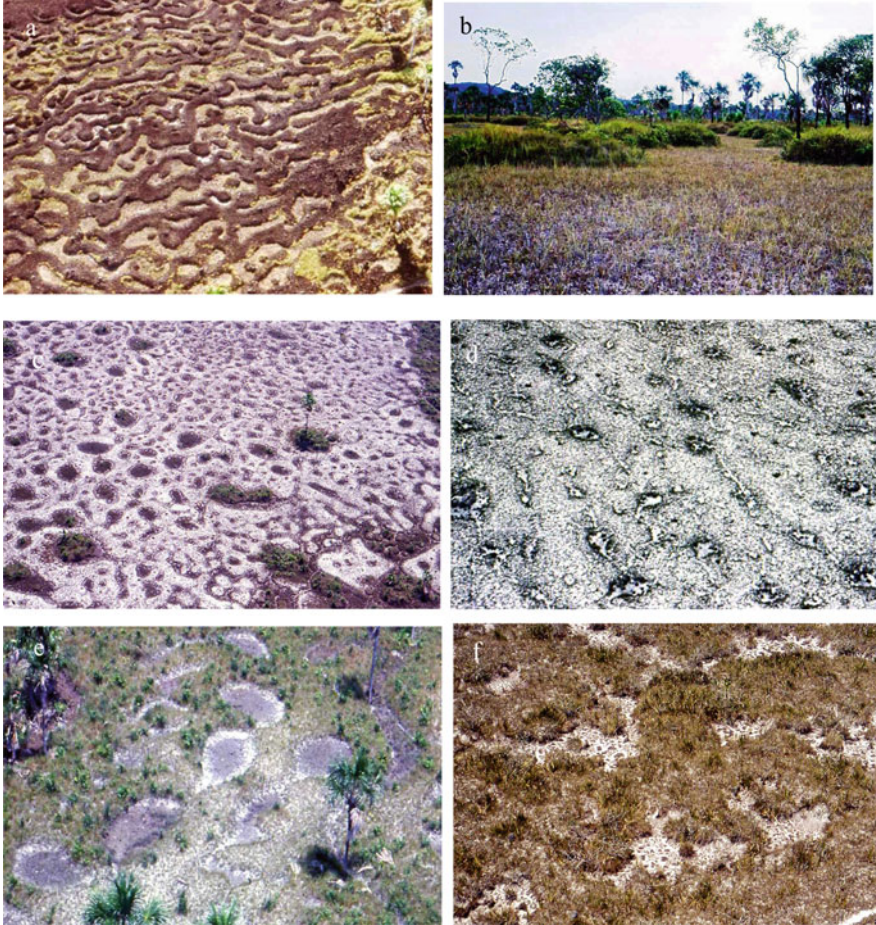


**Plate 10.2** (a) Labyrinthine entangling of convoluted terrain benches and incised flat-bottom channels in the middle Ventuari watershed; some channels discharge into the neighboring palm swale (to the right of the picture); others are closed and enlarge as suffusion pans. (b) Interlacement between benches and mounds, remnants of an earlier terrain surface, and flat-bottom channels; difference of elevation is about 1 m. (c) Field of suffusion pans and depressions of variable shapes and sizes on a stabilized sand mantle; burned terrain surface. (d) Suffusion pans in formation interconnected by overflow rills; burned terrain surface. (e) Disk-like suffusion pans on a sand cover surrounded by palm trees. (f) Suffusion cluster of irregular pans evolving into elongated depressions with fragmented algal skins in dense meadow cover

Extreme interlacements of channels and benches remnant of the original terrain surface result in labyrinthine microtopographic patterns that simulate the convoluted geometry of ornamental parterres in baroque gardens (Plate 10.2a, b). The vegetation cover is a mixture of low shrubs and herbs. This type of channel network occurs mostly in the lowest positions within white-sand terrains, especially in endorheic drowned plains. Such areas are inundated during the rainy season, receiving runoff

from the surrounding slightly higher geofoms in addition to rainwater and possibly also storing water reflux from stream confluence areas. Because of the closed basin topography only part of the stored water is discharged to streams or palm swales when the water level drops during the short lower rainfall period (January–March). A large part of the water remains in the depressions, evaporates, or seeps into the permeable sand ground. Underground diffusion, including suffusion, may play an important role and explain why some channels are not interconnected and enlarge into pans. Labyrinthine microrelief is intermediate between erosional and suffusion channel systems. The channels do not deepen today and seem to be related to a past lower regional drainage base level. Labyrinthine channel patterns (Plate 10.2a) are frequent in the upper watershed of caño Yagua, east of Cerro Yapacana.

Similar intricate channel networks called “tatucos” have been described in other regions of Venezuela, in particular in the western Llanos plains and south of Maracaibo Lake under forest as well as in deforested areas (Stagno and Steegmayer 1972). Reticular networks of natural drainage channels called “zurales” have also been described under savanna in the eastern Llanos of Colombia (Goosen 1971). In both cases, the reticular erosion channels have developed in loamy to clayey alluvial sediments, thus not in sandy cover materials as is the case in the meadow lowlands.

Dubroeuq and Volkoff (1998), in their study of the soil mantles in the Rio Negro watershed, proposed an explanation for the formation of the channel microrelief. The authors consider that landscape evolution in podzolic sand plains results from a series of soil transformation processes and sustain that dissolution and micro-fragmentation of quartz grains cause thinning and lowering of the sand cover. This would result in relief inversion so that a terrain originally slightly convex becomes a depression by the end of the landscape evolution. Rainwater and runoff from the surrounding higher terrains concentrate then in such depressions. The evacuation of excess water causes the incision of channels and the formation of reticular microrelief as the final evolution phase of podzolic sand plains.

As channel microrelief is not restricted to podzolic sand plains, a broader formation hypothesis is needed to account for the occurrence of erosion channels in a variety of lowland landscapes and very diverse soil materials as reported by the soil atlas of the Amazon Territory (MARNR-ORSTOM 1986). Our field observations show that channels in caatinga and bana are mostly not erosive today, as there is no evidence of sediment discharge at channel mouths in contact areas between wooded terrain and adjacent meadow terrain. In caatinga, channel floors are usually covered by a thick litter layer showing that there is no strong flushing effect when rainwater is evacuated. A few herbs and forbs colonize some channels. In bana scrubland, populations of *Brocchinia* sp. frequently occupy the channel bottom. These features suggest that channel incision is no longer an active process and may go back to earlier environmental conditions. The root mat and, sometimes, an underlying compact densic sand layer in which channels are incised help maintain channel walls fairly vertical. Currently, channels evacuate excess rainwater from caatinga and bana but little sediment. Their development in a variety of forest, soil, and material types may be related to an earlier change in environmental conditions, such as a drier period causing the lowering of the fluvial base level.

Dropping of the water level in rivers and streams would have a regressive effect on the regional surface drainage systems leading to the incision of channels in the interfluves to secure connection with a lower base level.

Dry phases that occurred in the second half of the Holocene have been related to climate fluctuations causing sea-level changes (Fairbridge 1976). During dry periods, total precipitation is lower but rainfall storms are heavier and have higher erosive power. Burned forest terrains are then exposed to the incision of rills and channels between the rhizospheres (i.e., root mat in caatinga forest) of individual trees to the depth of the usually compact white-sand substratum. Incisional erosion results in creating reticular drainage networks in headwater interfluves that correlate with increased gradient in rivers and streams and lowering of the regional base level. In present conditions, the base level seems to have risen as large riverbeds (e.g., river Atabapo) are plugged with white sands that form bars and islands, sometimes covered by vegetation.

### 10.4.3 Suffusion Microrelief in the Meadow Environment

Microforms caused by suffusion differ from erosional microrelief for being shallow, closed units. Usually, there is no evidence of surface removal of material. Suffusion depressions can occur as individual pans of various shapes from rounded to ovate to elongate. Often depressions form reticulated networks whose configuration can vary from fairly linear to ramified to labyrinthine. Suffusion features can occur scattered or form dense associations of diverse microforms (Plate 10.2c–f). In spite of shape differences, they have in common to be closed-end, shallow (usually 10–20 cm, exceptionally 40 cm deep), and up to a few square meters large, with vertical rims, flat bottoms, and floors covered by a few centimeters of coarse sand, skins of black algae, and sparse herbs. The terrain surfaces in which the depressions are incised are flat, without visible open exorheic drainage network. However, incipient pans are often interrelated by overflow rills as they are not large and deep enough to store all the rainwater (Plate 10.2c–f). Depressions are water-filled during the rainy season, but the surrounding terrain surface is often not flooded. Rainwater is resorbed by evaporation and internal drainage (Plate 10.2f).

#### 10.4.3.1 Pans

The soil survey of the Venezuelan Amazon territory reports the occurrence of small pans (called “tina” or “minicubeta”) in saprolitic material, but not in sand cover (MARNR-ORSTOM 1986). However, our field observations show the presence of pans in sandy meadow areas in association with non-erosive shallow channels in reticular pattern.

Pans are closed micro-depressions up to a few square meters large and 20–40 cm deep. They have variable shapes (rounded, ovate, star-shaped), vertical walls, and flat bottoms (Plate 10.2c–f). Sometimes, the depressions are elongated, 50–100 cm long and 15–30 cm wide. The floor of the pans is usually composed of sand coarser than the substratum sand and covered by black algae. The combination of closed



configuration, vertical walls, and flat bottoms suggests that suffusion is the most likely process of pan formation.

The following example compares two profiles, one at the bottom of a pan and the other at the terrain surface close to the pan. The profile couple is located 30 km west of Serrania El Tigre in the upper watershed of caño Yagua (130 m a.s.l., 03°51'N–66°27'W), in a basin position filled with unsorted silty sand layers under shrubby meadow. It is on the same depositional surface as profiles P58-P59-P60-P61 (see Sect. 10.3.3).

*Profile P62* (Udoxic Quartzipsamment) (Table 6.5, Chap. 6) is at the bottom of a pan. The pan is an egg-shaped depression with irregular border and lobulated extensions, vertical wall, and flat bottom. It is 25–30 cm deep, 1–2 m wide, and 8–10 m<sup>2</sup> large. At the bottom, are small Eriocaulaceae (4–5 cm high) and skins of black algae. The pan profile P62 is 5 m apart from *Profile P61* (Table 6.5, Chap. 6) that starts from the terrain surface. The hollow of the pan (25–30 cm deep) corresponds approximately to the thickness of the two surface layers (0–25 cm) of P61. Subsurface and subsoil layers have similar particle size patterns in both profiles. There is no evidence of external drainage and removal of material through surface runoff from the pan. This suggests that the depression results from loss of material dragged into depth by internal water percolation. The very coarse and coarse sand lining the bottom of the depression may be the residuum left by selective suffusion. Such suffusion pans are frequent in silty white sands of alluvial flats.

Elongated depressions are 10–20 cm deep, several meters long, with a succession of enlargements (up to 100 cm) and constrictions (40–50 cm), resulting in chains of interconnected small depressions (Plate 10.2f). Walls are vertical and the boundary with the flat surrounding terrain is sharp. Although several depressions may be interconnected, they do not form an open surface drainage system. Together, they can constitute one-fourth to one-third of the whole terrain surface. During the rainy season, depressions are water-filled, while the surrounding terrain surface is saturated but not flooded. There is no observable water flow in the depressions. During the short low rainfall period, as groundwater is sucked by the dropping of the water level in the rivers, water in the depressions is evacuated by deep percolation in addition to some loss by evaporation. Suffusion seems to be the controlling process. Percolating water drags along silt particles in depth, possibly together with dissolved silica, clogging the macro-pores of the sandy matrix. This causes densification of the sand mantle. The resulting densipan is difficult to auger or excavate with spade.

Such elongated channels-depressions are common in the upper watershed of “caño Yagua,” west of Serrania El Tigre. A pair of profiles was described in a shrubby meadow covering a flat white-sand terrain (130 m a.s.l., 03°52'N–66°26'W) (Plate 10.3a–c).

*Profile P16* (Udoxic Quartzipsamment) (Table 6.5, Chap. 6) is at the bottom of a 15 cm deep depression. Below a few centimeters of loose sand, the material is unsorted sandy loam to loamy sand (5–60 cm). Fine sand is dominant (38%), accompanied by medium sand (18%), very fine sand (16%), and silt (18%). Such unsorted, well-graded particle size distribution, resulting possibly from fragmentation of quartz grains, causes the clogging of the sand matrix, decreases macro-

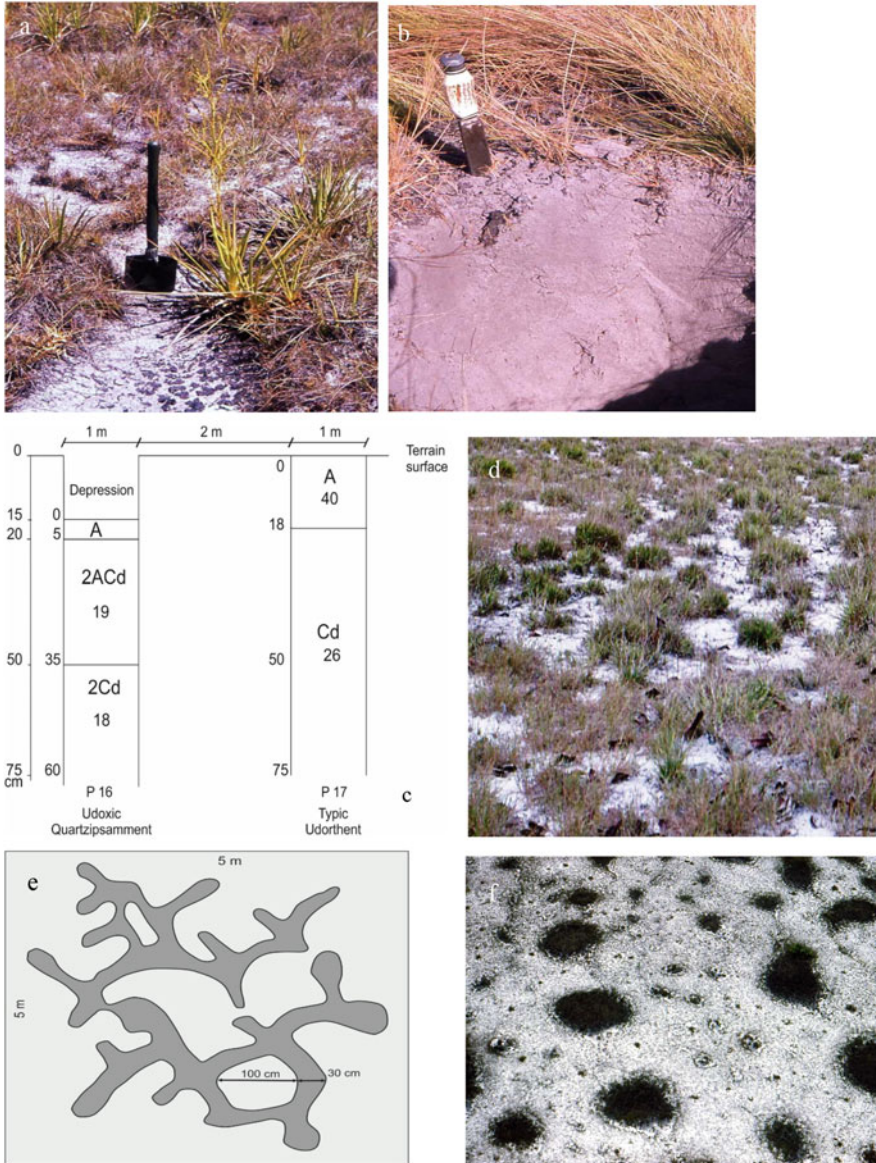


**Plate 10.3** Adjacent soils under shrubby meadow: (a) Place of P16 at the bottom of a suffusion depression showing enlargement and narrowing; (b) profile P17 on the terrain surface; the darker surface horizon of P17 (0.56% OC) is missing at P16; (c) comparison of profile P16 at the bottom of the suffusion depression and profile P17 at the terrain surface as shown in a; silt % beneath the horizon identifiers; (d) interconnected shallow pans forming a labyrinthine network in the center of the picture; isolated pans in the foreground; flakes of algal crust; (e) labyrinthine suffusion depression network close to site P112; (f) burned herbaceous vegetation established at the bottom of suffusion pans; vegetation decreases the effectiveness of the suffusion process

porosity, and results in a very compact, dense material difficult to penetrate with spade even when moist. *Profile P17* (Typic Udorthent) (Table 6.5, Chap. 6) is 2 m apart on the terrain surface surrounding the depression of P16. Similarly, fine sand (32%), very fine sand (23%), and silt (26%) dominate, contributing to create a compact fabric and dense layer. In contrast, the surface layer (0–18 cm) differs for having higher amount of silt (40%). This layer corresponds to the volume of material missing in the depression of P16. The loss of substance from the original surface layer may have been caused by quartz dissolution and suffusion to the groundwater resulting in subsidence and formation of the depression.

Densely ramified depressions form labyrinthine networks (Plate 10.3d). They occur usually in level to slightly concave, drowned areas. Although many elongated bended depressions are often interconnected, the networks they form are closed. Plate 10.3e shows such a closed network of branched channels forming a labyrinthine pattern. There is no external surface drainage. Rainwater either evaporates or percolates through the soil. Micro-channels are 20–30 cm wide and 5–10 cm deep. Usually, a few herbs (e.g., *Drosera*) grow on the floor, mainly covered by brownish alga skins. Advanced evolution and densification of the labyrinthine network reduce the original terrain surface to small islands where meadow vegetation concentrates, while the largest part of the area is white sand with few herbs and forbs.

The absence of external surface drainage and the milky aspect of the perched water table indicate that labyrinthine shallow channels most likely result from terrain subsiding along convoluted lines where quartz grains dissolve in a drowned landscape unit. The silica solute percolates, possibly together with the translocation of fine quartz grains (i.e., very fine sand and silt). The eluviation of silica and fine grains creates voids in the surface layer, followed by subsidence and formation of pans and reticules.

#### 10.4.3.2 Suffusion Depression Formation

Chemical and mechanical processes may combine effects to cause the loss of surface materials through suffusion (i.e., seepage) including (1) the dissolution of quartz grains in extremely acidic environment and percolation of the solution to the groundwater (milky aspect) and (2) the fragmentation of quartz grains upon alveolization to smaller size particles that may be entrained in depth within the dropping groundwater in January–March. The formation of alveoles in sand grains, reported by several authors (Schnütgen and Bremer 1985; Dubroeuq and Volkoff 1998), is a main cause of sand grain weakening and partition (see Chap. 8, Sect. 8.4.1). Selective erosion through vertical extraction of dissolved silica and fine-grained particles (i.e., very fine sand and silt) causes surface subsidence and the formation of pans, their deepening, and horizontal enlargement. In initial stage, suffusion can be traced through the occurrence of small piping holes at the terrain surface, isolated or aligned. Larger holes are usually 20–30 cm deep and less than a fourth of square meter large. Soils and sediments in areas with suffusion depressions have usually one or more compact, densic sand layers (densipan), restricting root penetration and fairly impermeable to water percolation. The establishment of vegetation at the bottom of the depressions slows down the suffusion process (Plate 10.3f).

Comparable microforms may have different origins. In Amazonas, climate with sustained rainfall (2500–3500 mm/year) favors suffusion, in contrast to other processes of pan formation in less humid environment. De Dapper (1991), for instance, describes pan microforms in sandy mantle under steppic grassland on the plateaus of Kolwezi in the south of Shaba (Zaire). Pans, locally called “menas,” are closed, small, shallow depressions with subvertical micro-walls, 2–10 m long, 3–5 m wide, and 15–30 cm deep. “Menas” are elongated and ramified and occur in dense pattern with long axes running parallel. De Dapper considers that the formation of the depressions cannot be caused by solution mechanisms because no collapse structures were found in the sand layers. According to the author, the formation of the “menas” results from the transformation of rills into closed depressions upon clogging of the incisions at fairly regular intervals by the liquefaction of sand at rill walls and/or upon clogging of the rills by sediments eroded from the interfluves.

---

## 10.5 White Sands and Podzolization: Spodosols as Markers of Soil-Landscape Evolution

The presence of Spodosols (i.e., Podzols) has been reported from various places in the Amazonian lowlands at large (Klinge 1965; MARNR-ORSTOM 1986; Dubroeuq and Blancaneaux 1987; Bravard and Righi 1989, 1990; Malagón Castro 1995; Pulido Roa and Malagón Castro 1996; Dubroeuq and Volkoff 1998; Schargel et al. 2000, 2001; Horbe et al. 2004; Do Nascimento et al. 2004; Schargel and Marvez 2009; Quesada et al. 2010, 2011; Medina and Cuevas 2011; IGAC 2014a, b; Mendonça et al. 2014; Adeney et al. 2016; i.a.). They are usually associated with caatinga forest and bana scrubland. However, Spodosols were also found under other kinds of forest, mainly rainforest on low hillslopes and gently undulating plains in the area of San Carlos de Rio Negro and Maroa-Yavita (Schargel et al. 2000, 2001; Schargel and Marvez 2009). In contrast, there is little information about the occurrence of Spodosols under herbaceous vegetation (savanna, meadow) in the Amazon basin in general and in particular in the middle Orinoco and upper Rio Negro lowlands in Venezuela. For instance, Mendonça et al. (2014) studying a campinarana forest-shrub-grassland gradient in the Viruá National Park, northern Brazil, found Oxyaquic Quartzipsamments under grassy-woody and sparsely vegetated sites with low organic matter content, while all soils under forest and arboreous campinarana showed well-developed spodic horizons or spodic features.

Are white sands the cause or consequence of podzolization? Are white sands related at all to podzolization or are they sediments? If white sands result from podzolization process through, for instance, fluctuating groundwater or just rainfall drainage percolating freely through the sand, it would mean that materials originally not white have been bleached to form pedogenic albic horizons in Spodosols. Pinkish sediments enter the lowlands from weathering of Roraima sandstone/quartzite in hummocky peneplain outcrops, upland hills, and highland mesetas. These weathering products turn white upon short colluvial transport distance. The weathering of crystalline bedrocks at the periphery of hills and rocky domes in

penneplains generates directly white sands. Thus, podzolization is not the only process that produces white sands in the lowlands (see Chap. 8). In contrast, existing white sands can promote podzolization as long as there is a source of organic substances in the topsoil that can be translocated to form spodic horizons in depth. The scanty meadow vegetation, even when shrubby, contributes little organic matter. It is unusual to observe dark streaks in white sand that could indicate vertical mobilization of organic substances. This leads to the hypothesis that spodic horizons found under current meadow vegetation might not be in equilibrium with the meadow environment and could have formed under forest cover, especially caatinga that is the type of vegetation usually associated with Spodosols. Spodic features found under current meadow vegetation would then be inherited remnants of a former forested landscape. This would raise the issue about what has caused the degradation of the forest cover: human activities or natural events?

The conventional perception of Spodosol as a monogenic soil body may be reconsidered when the sedimentological context of Spodosols in the Amazon lowlands is taken into account. Often spodic horizons are overlaid by stratified white-sand layers that seem genetically unrelated to the spodic subsoil. These C layers are new sand layers deposited by shifting rivers and/or reworked sands having albic feature inherited from E horizons that have been eroded elsewhere in the lowlands, presumably in the caatinga environment where Spodosols used to form.

The former point of view has an influence on Spodosol classification. In Chap. 7, a dual classification of the Spodosols found under meadow cover is discussed (Sect. 7.3.5). If spodic horizons are considered as buried remnants of truncated Spodosols, then many of these soils are duplex soils classifying as Thapto-spodic Quartzipsamments. Spodosols were also classified as one-soil body, disregarding the lithological discontinuities between the sand layers covering the spodic horizons. Hereafter, pedotaxa are labeled according to this conventional way of classifying the Spodosols occurring in meadow vegetation for the sake of comparison with the pedotaxa reported in the literature to occur under forest cover. Horizon designations, however, are adjusted to allow keeping track of the history of the profiles.

Spodosols tend to form in low-lying concave drowned areas with sand infilling and high, sustained, or fluctuating water table. This is the case of subsidence areas lying in front of uplifted ranges, such as the Sipapo-Guayapo lowland watersheds in front of the Cuao-Sipapo massif. It is also the case of the low-lying areas drained by the regional water collector axis Atabapo-Orinoco and Guainía-Rio Negro. In contrast, in the southernmost part of the study region, specifically in the Pasimoni-Siapa fluvial system, Spodosols occur on terraces that are slightly higher than the surrounding poorly drained floodplain bottom of the lowlands. Sand is provided by weathering of the substratum in the lowlands and rock weathering in the upper catchment areas of the rivers.

Thus, in a variety of situations found in the regional context, Spodosol formation under meadow vegetation may be questioned. Spodosols do not seem to be in equilibrium with the meadow environment and therefore soil and current vegetation may not be genetically related. Hereafter, a few situations are analyzed to highlight the possible disconnection between spodic horizon and vegetation cover. The



presence of stratifications and lithological discontinuities in the white sands covering spodic horizons helps distinguish between layered cover sands and E horizons and provide a different view on the formation of Spodosols in the meadow environment.

### 10.5.1 Spodic Feature Related to Lateral Flow of Black Groundwater

Rivers and streams in the meadow environment carry acidic (pH 4.5–4.8) blackwater loaded with dissolved organic substances and iron hydroxides. The meadow biotope contributes little to blackwater because of limited organic matter production. However, the groundwater in meadow white sands is frequently dark reddish brown to black, especially in the proximity of caatinga covered areas. Thus, dark groundwater is most probably originated by the drainage of the caatinga soils and penetrates the surrounding lower-lying meadow areas. This causes deeper layers in the meadow white sands to be enriched in organic substances and iron hydroxides through lateral black groundwater flow, resulting in a sort of groundwater podzolization. The influence of lateral water flow carrying dissolved organic matter bound with Al in the formation of hydromorphic podzols via lateral podzolization has been documented in the Amazon basin (Klinge 1965; Dubroeuq and Volkoff 1998; Quesada et al. 2011; Mendonça et al. 2014) and elsewhere (Driessen et al. 2001).

*Profile P63* is located 20 km east of Carmelitas and 5 km south of the Ventuari river, in the eastern Yapacana area (P63 Oxyaquic Haplorthod, 110 m a.s.l., 04°09' N–66°29' W, in Table 6.5, Chap. 6). The site is a flat low-lying flooded terrain covered by meadow vegetation, mainly Xyridaceae and Eriocaulaceae, typical of seasonally inundated meadow, with shrubby clusters. Sand grains in the dark layers are coated with organic substances and assembled in loose agglomerates. Average particle contents are 98% sand, 0.5% silt, and 1.5% clay. As a whole, the stratified profile suggests splay deposit filling a depression. The upper part of the profile (0–40 cm) corresponds to a more recent sand cover that contains charcoal fragments, few roots, and little organic matter in the surface layer (0.4% OC). It is unlikely that the dark horizons in depth have resulted from eluviation of the surface layers poor in organic carbon and free of iron. As the two spodic horizons are not indurated, thus lacking mechanical resistance, the eventuality of profile truncation can be discarded and therefore the horizons are not buried under the overlying sand layers. It is hypothesized that the organic matter in 3Bh (1% OC) and in 3Bhs (1.5% OC) has penetrated in the sandy subsoil by lateral flow of black groundwater coming from surrounding slightly higher caatinga areas.

*Profile P112* (Table 6.6 in Chap. 6; Tables 7.5 and 7.11 in Chap. 7) is another example with weak spodic horizon that may be related to the lateral flow of brownish organic-loaded groundwater. The profile is described in Chap. 9, Sect. 9.5.3.1, as sample of an eolian silt sheet sediment. P112 (Oxyaquic Alorthod, 120 m a.s.l., 03° 01' N–67°33' W) is located in the upper watershed of caño Pimichín in a shrubby meadow surrounded by dense bana vegetation.

It is unlikely that the incipient spodic horizon (0.62% OC) results from organic matter illuviation, as the average organic carbon content in the overlying layers is as

low as 0.08%, and the densipan layer above the spodic is fairly impermeable. The spodic horizon may be enriched in organic substances by the groundwater flowing from a slightly higher lying bana terrain.

### 10.5.2 White Sands Covering Truncated Spodosols

A poorly drained regional depression centered on the axis of river Guayapo lies in the east-west interfluvium between river Sipapo in the north and river Orinoco in the south, at the foot of the Cua-Sipapo massif. The highlands are the headwater areas of several blackwater rivers (e.g., Autana, Sipapo, and Guayapo) that carry sand from the weathering of the Roraima sandstone mesetas to the lowlands. Spodosols were identified in this environment. It is unlikely that the current shrubby meadow vegetation with usually less than 50% cover density generates enough organic matter to form spodic horizons in depth. Meadow vegetation (herbs, forbs, and small shrubs) has limited organic matter production and consumes most of it in respiration and tissue maintenance, leaving little to percolate into depth. In general, the A horizon has less than 0.2% organic carbon, while the spodic horizon has as much or more than 2%. The layers between the A and the spodic horizons are white sand in which organic matter streaks are uncommon but horizontally lying fossil roots are frequent.

*Profile P82* (Oxyaquic Haplorthod, 110 m a.s.l., 04°17'N–67°17'W) and *Profile P83* (Typic Durorthod, 110 m a.s.l., 04°14'N–67°30'W) in Sipapo area (Table 6.2) are located respectively north and south of river Guayapo, about 40 km apart, both on alluvial plain flats under shrubby meadow (<50% cover). These profiles show remarkably similar features at relatively similar depth (ca 1 m). In both soils, the white sand C layer (3C4 in P82 and 5C4 in P83) lying directly above the spodic horizon contains about 10% fine gravel, 97% sand, and little fines, while the spodic horizon has no gravel, 87% sand, and 13% silt+clay (Table 10.3). This contrast points to a lithological discontinuity between the C layer and the spodic horizon and suggests truncation and subsequent burying of the original Spodosol.

In spite of the above similarities, profiles P82 and P83 show two different modalities leading to the formation of stratified sand cover. This shows that the build-up of the sand cover fossilizing the truncated Spodosol took place in stepwise aggradation by consecutive flows of variable energy generating unsorted splay

**Table 10.3** Selected properties of C layers and spodic horizons in three soils of the Sipapo area

Profiles	Layers	Depth cm	Gravel %	Sand %	Silt + Clay %	OC %	pH
P82	C layer	95–115	10	97.2	2.8	0.03	6.1
	Spodic Bhs	115–135	0	86.5	13.5	1.3	4.4
P83	C layer	73–90	10	96.5	3.5	0.58	4.5
	Spodic Bhs	90–95	0	87.4	12.6	2.49	4.0
P20	C layer	40–60/65	5	99.2	0.8	0	5.8
	Spodic Bhs	60/65–75	0	80.9	19.1	2.97	4.5



materials. Organic carbon content is low in the A horizons (0.56% in A1, 0.17% in A2 and A3) and very low in the C layers (0.03–0.07%) (Table 10.3). This type of deposit results from reworking and remobilizing sediments from pure white-sand covers already existing in the meadow environment.

The above features lead to the conclusion that the original Spodosols have been truncated to the level of the spodic horizon that has resisted erosion for being fairly indurated. Subsequently, new sand layers have been deposited on top of the spodic horizon. Thus, the spodic horizon is a buried fossil soil material, remnant of an earlier terrain surface. It is improbable that Spodosols form in quartzose white-sand sediment under meadow and under low-density shrubby meadow which are both poor in organic matter production. In the Amazon lowlands, Spodosols develop usually under caatinga forest. The buried paleo-spodic horizons may thus be related to a former caatinga cover that has been degraded into shrubby meadow or replaced by pure meadow, for instance upon natural or human-made repeated fire.

### 10.5.3 Bimodal Spodosol Developed in White Sand of Eolian Origin

Eolian deposits were identified in the Atabapo area as dune-like mounds with coarse sand blown at short distance from surrounding surface layers or from river beds at low water level. In the same area there are also flat terrain sediments with significant dominance of medium sand (50–60%) and fine sand (20–30%). These well-sorted sand mantles are most likely formed by sand winnowed from north-east through medium-to-large distance transport. Profile P84 has developed on such an eolian sediment.

*Profile P84* is located 3 km south-east of the lower Guasacavi river in the Atabapo area (Durihumod, 90 m a.s.l., 03°08'N–67°30'W) (Table 6.6 in Chap. 6). Terrain is flat, covered by shrubby meadow with dense herbaceous layer (80%), dispersed shrubs, and small open patches. Typical species include *Brocchinia prismatica*, *Guacamaya superba*, and *Schoenocephalium* sp.

Surface layers are light gray, subsurface layers are white, and the subsoil is a sequence of very dark brown Bh (80–120 cm) and Bhs (120–150 cm) horizons, and dark reddish brown Bhs horizons (150–170 cm). Two moderately indurated layers, slightly moist, sustain perched water tables at 80–90 cm and 135–150 cm depth, while deep groundwater appears at 160 cm.

Total sand is about 80–100% of the sediment. This is a stratified profile of well-sorted depositional layers with on average 59% medium sand and 24% fine sand. It indicates that the same strongly selective process has been acting during the build-up of the sediment either by fluvial overflow or by eolian deposition. Although layers show variations in particle size composition, there is no clear-cut lithological discontinuity in the profile. The same depositional material extends over the whole depth, and the spodic horizon is unlikely to be a buried one.

At 80 cm depth occurs a sharp break: organic carbon increases tenfold (from 0.28 to 2.67%) and at the same time pH drops two units (from 5.8 to 3.7). Below this threshold, pH remains fairly constant (3.4–3.7). In contrast, organic carbon content

varies with depth. Two moderately indurated layers have the highest organic carbon values (5.70% at 90–105 cm, and 5.42% at 150–170 cm), while the layers with perched water table overlying the indurated horizons have the lowest values (2.67% at 80–90 cm, and 2.88% at 135–150 cm). The two maxima of organic carbon concentration are separated by a minimum (2.97% at 120–150 cm), reflecting variation in podzolization intensity. Thus, the thick spodic horizon (80–170 cm) is polygenic.

### 10.5.3.1 Soil Formation

It may be a matter of debate whether the stratified sediment was fully settled when the podzolization process started or whether sedimentation and podzolization were contemporaneous. The later hypothesis is unlikely because continuous deposition would not allow the formation of a topsoil horizon able to provide enough organic substances to be translocated into the spodic horizon. It has to be admitted that podzolization started after sedimentation stopped. It can also be argued whether the current shrubby meadow vegetation is able to provide enough organic matter to feed such a massif spodic horizon with relatively high organic carbon content, similar to the values usually found in Spodosols under caatinga forest.

P84 is a multi-layered sediment with repeated strata having slightly different granulometric composition but similar depositional facies. Stratification shows that the sediment does not result from a single depositional event but from a sequence of similar sedimentary episodes with intermediate interruptions. The thickness of the sediment (almost 2 m) showing these features indicates the permanence of the same geomorphic process for a prolonged time span. The predominance of medium and fine sand (83%) plus about 10–15% silt from 46 cm downward favors the hypothesis of eolian origin and long-distance selective transport. This is different from local reworking of coarse sand that builds up dune-like mounds in the same Atabapo area. Long-distance mobilization of sand and silt particles requires upwind areas with sparse vegetation cover allowing sustained deflation to form downwind non-dunar sand sheets. This in turn suggests drier conditions (i.e., lower annual rainfall and/or longer dry spells) than the current ones at regional scale for some time in the Holocene or earlier.

The examination of the spodic horizon contributes relevant information to this issue. Profile P84 has the thickest spodic horizon (80–170+ cm) with the highest amount of organic carbon (2.7–5.7%) among all Spodosols and spodic materials found under meadow vegetation in the study region. The spodic horizon is bimodal with two peaks of illuvial organic matter accumulation: one peak of 5.2% OC at 90–120 cm (younger) and another peak of 5.4% OC at 150–170 cm (older), separated by a low of 3% OC at 120–150 cm. This indicates variation in podzolization intensity over time. Such a polygenic spodic horizon cannot have formed under the present meadow vegetation with poor organic matter production and is most probably an inheritance of earlier conditions under caatinga cover.

Schargel and Marvez (2009) have reported organic carbon values of similar magnitude from Spodosols in the same Atabapo area under forest cover, mainly caatinga but also rainforest. From a collection of spodic horizons described in the

surroundings of Maroa and Yavita, close to the area where P84 is located, the average value of organic carbon is 2.9% with a range of 1.2–5.7%. Similarly, a representative Spodosol (P-2/AR-15, Alaquods) under forest described in the Mitú area, lower Vaupés river watershed, in the eastern Colombian Amazon, provides an organic carbon value of 4.1%, averaged from six 5-cm thick layers with organic carbon ranging from 2.0 to 6.1% (Malagón Castro 1995; Pulido Roa and Malagón Castro 1996). The spodic horizon of P84 under meadow has an average organic carbon of 4.3%, including all six layers in a range of 2.7–5.7%. Values of pH are 3.4–3.7, lying at the low end of the regional values. Horizon thickness, high organic carbon content, and layer induration suggest strong, possibly old podzolization under forest cover.

### 10.5.3.2 Landscape Evolution

Profile P84 contributes to reconstructing the history of the surrounding landscape. Briefly, eolian sediments have settled during drier conditions, before vegetation colonization started in this particular area at the beginning of the Holocene. Vegetation cover development in the lowlands could be contemporaneous with the inception of peat formation on the western Guayana highland mesetas about 7500 years BP (8400 calBP) (Zinck et al. 2011). In the Mitú area, eastern Colombian Amazon, a Bhm horizon at 90–101 cm depth, belonging to an Alaquod (AR-20), was dated 7400 years BP. This is the oldest spodic material dated in the regional context (Malagón Castro 1995; Pulido Roa and Malagón Castro 1996). Similarly at site P84, podzolization may have started early in the Holocene under forest cover to develop the 90-cm thick spodic horizon but with intensity variation. More recently forest cover has been degraded into meadow vegetation to which the formation of the Spodosol is unrelated.

Profile P84 shows that a full Spodosol profile, probably formed under forest, can remain preserved in a low-lying position today under meadow cover. Podzolization has not obliterated the original stratifications of the sedimentary material from albic to spodic horizons. The albic layers (7–80 cm) that underlie the shallow A horizon (2.8% OC) are not of pedogenic origin, but function as geogenic filters that allow organic substances and Fe-Al hydroxides to percolate and illuviate into depth. Albic layers are poor in organic carbon (0.2–0.3% OC) but show dark vertical streaks (2–4 mm large). The sand in the spodic horizons is similar to that of the albic layers, but in the former pores are clogged and sand grains are coated and, in two layers, indurated by organic matter and iron oxides. Overall, white sand in current meadow environment is not a product of podzolization but depositional material.

For the sake of comparison, profile P83 (Durorthod) located in the Sipapo area about 130 km north of profile P84 (Durihumod) has also two indurated spodic horizons at depths of 95–105 cm and 150–165 cm that are similar to the depths of the two indurated horizons of P84 (90–105 cm and 150–160 cm). In both cases, intermediate spodic horizons are not indurated. Thus, the spodic induration process in these two profiles shows remarkable bimodal coincidence. This suggests that podzolization was not constant. If the intensity of podzolization is controlled by the degree of moisture in the soil, then the two maxima would correlate with abundant

rainfall periods separated by a drier period. As the bimodal spodic horizons were observed in the north (Sipapo area) as well as in the south-west (Atabapo area), this may be considered a regional climatic trend. Spodosols reveal to be good indicators of landscape evolution.

Bimodal spodic horizons may have formed throughout the Holocene. If the bimodal spodic horizon at P84 can be assumed to be old because of its thickness, thinner bimodal spodic horizons may have formed in more recent times. For instance, profile P-2/AR-15, an Alaquod under forest cover in the Mitú area, lower Vaupés watershed, in the eastern Colombian Amazon, has a multi-layered Bhm horizon at 100–130 cm depth, showing an upper peak of 6.1% OC, a lower peak of 4.3% OC, and 2% OC in an intermediate layer. The upper layer (100–110 cm) was dated 3120 years BP (Malagón Castro 1995; Pulido Roa and Malagón Castro 1996).

Cyclic spodic horizon formation in forest environment and fossilization of truncated Spodosols in current meadow environment are features that contribute to understand landscape evolution, including climatic oscillations.

#### **10.5.4 Podzolic Sand Mantle Modified by Fluvial Morphogenesis: Siapa and Pasimoni Valleys**

The southern part of the study region corresponding to the interfluvium between the Pasimoni and Siapa rivers is in many aspects different from the large alluvial plains that occupy the center of the regional lowland basin. Here, the terrain surface is formed by a sand mantle that overlies the igneous-metamorphic basement. This sand cover has been incised by the Pasimoni and Siapa rivers that have their headwaters in hilly areas to the south and join river Casiquiare in the north, east of San Carlos de Rio Negro. In their lower stretches, both rivers have created a valley morphology that crosses an undulating low hilly relief. They have built fluvial geoforms such as terraces and floodplains and, within these, levees, adjoining backswamp depressions, meander lobes (point bars), and infilled channels, among other features. Both are blackwater rivers. Pasimoni river traverses a drowned depression with many abandoned meanders.

The Pasimoni-Siapa area is a complex dual landscape where the original terrain surface has been remodeled or partially obliterated by fluvial activity that superimposed imprints on the earlier landscape. Different kinds of soil have developed on the fluvial geoforms from the same white-sand substratum. Table 10.4 shows three different soil materials that have similar particle size distributions with dominant fine sand. Profiles P108 and P109 are described in the following sections. Profile P107 is substantially different from the formers. It is located 400 m apart from river Pasimoni in a backswamp depression incised in the original terrain surface (P107 Hydric Haplohemist, 125 m a.s.l., 01°35'N–66°33'W). The buried white-sand substratum lies beneath 60 cm histic material.

Spodosols with contrasting profile morphology were identified in a variety of positions in this fluvially modified sand mantle, showing complex relationships with

**Table 10.4** Variety of soils developed from the same basal sand mantle in the Siapa-Pasimoni watershed

Profile	Depth cm	Coarse sand 2–0.5 mm	Medium sand 0.5–0.25 mm	Fine sand 0.25–0.05 mm	Total sand	Geoform	Soil class
P107	60–80	12	24	52	88	Backswamp substratum	Hydric Haplohemist
P108	0–150	16	25	45	86	Terrace levee	Udoxic Quartzipsamment
P109	1–140	15	30	49	94	Terrace levee	Arenic Alorthod

**Table 10.5** Variety of features in profiles developed on the fluvial landscape in the Siapa-Pasimoni interfluve

Profile	Landscape position	Soil class	Stratified	Spodic horizon	Vegetation cover
P100	Terrace levee	Arenic Alorthod	Yes	Buried at 122 cm	Shrubby meadow
P101	Terrace overflow	Arenic Alorthod	Yes	Buried at 105 cm	Caatinga forest
P103	Floodplain point bar	Oxyaquic Alorthod	Yes	Buried at 122 cm	Shrubby meadow
P109	Terrace levee	Arenic Alorthod	No	At 120 cm	Shrubby savanna
P104	Terrace	Udoxic Quartzipsamment	No	No	Caatinga forest
P108	Terrace levee	Udoxic Quartzipsamment	Yes	No	Shrubby meadow

vegetation and geomorphic setting. They can be used as indicators of landscape evolution.

Spodosols found in the Siapa-Pasimoni interfluve landscape are mainly Arenic Alorthods (Table 10.5). They occupy different kinds of river terrace and floodplain positions in valley morphology, in contrast with the Spodosols occurring in the large lowland alluvial plains. Overall, medium sand and fine sand are the dominant separates in stratified layers, with fine sand largely outstanding in some layers (e.g., 54–62% at 25–105 cm depth in P101). There is no straightforward correlation between Spodosol and vegetation type in the areas sampled. Spodosols were found under meadow, savanna, and caatinga cover. In contrast, there is a caatinga site without Spodosol. Several spodic horizons seem to be remnants of truncated Spodosols that have formed on an earlier surface under caatinga and have been subsequently buried by new sediments in the meadow environment. A remarkable feature is the occurrence of spodic horizons at similar depths (ca 120 cm) at sites distant by several tens of kilometers from each other. These spodic horizons are possibly related to a regional sand substratum that has undergone podzolization in the past under forest vegetation, before the more recent river incision and sediment cover.

### 10.5.5 Spodosols and Meadow Landscape Evolution

Relationships between geomorphic landscape position, kind of Spodosol, history of sand deposition, and type of vegetation are diverse and complex. This section focuses on the paleogeographic significance of the occurrence of Spodosols in the current meadow environment. Spodosols are used here as markers to understand the evolution of the meadow lowlands. Overall, the relationship between sand cover and spodic features in the study region allows highlighting two major geomorphic events of meadow landscape evolution in the Holocene, i.e., the fossilization of spodic

horizons in the alluvial plains in the center and north of the lowlands and the dissection of podzolic terrains by fluvial activity in the south.

Spodosols were found mainly in the Sipapo, Atabapo, and Pasimoni areas. In some places, white Quartzipsamments have slightly darker subsoil layers and often brownish groundwater but do not comply with the requirements of the Aquodic subgroup and are therefore classified as Oxyaquic subgroup (Soil Survey Staff 2014). Possibly some Quartzipsamments may have deep spodic horizons (i.e., giant podzols) that were not reached by field observations. Complete, not truncated, buried Spodosols, with all profile horizons preserved, are exceptions in the meadow environment (e.g., P84 under meadow and P109 under grass savanna), but have been reported to occur beneath ca 100 cm fluvial sediment in the floodplain of lower river Guainía (Schargel and Marvez 2009).

Spodosols found in the meadow environment do not seem to be in balance with the current meadow vegetation that is characterized by low cover density, low plant stature, and limited organic matter production. The association of Amazonian herbs, forbs, and shrubs does not deliver enough organic matter to feed spodic horizon. This leads to the hypothesis that the spodic horizons under current meadow vegetation may have formed under earlier caatinga cover and would thus be an inheritance thereof.

Sand layers lying above the spodic horizons are in general stratified and show one or more lithological discontinuities. This suggests that earlier Spodosols, presumably formed under caatinga or other forest types, have been truncated by shifting river dynamics to the level of the indurated spodic horizon resisting erosion. Practically, this scenario is only possible in open vegetation conditions, thus after the degradation of the wooded cover. Forest disturbance may have been caused by natural phenomena or human activities (e.g., fires). Subsequently, new sand deposits buried the spodic horizons under stratified layers reflecting frequent changes in flow energy, in particular alternating splay and overflow processes. Thus, many Spodosols found in the meadow environment are in fact duplex soils consisting of two genetically unrelated members, cover sand C layers and fossilized spodic horizons.

Sedimentological discontinuities are supported by mineralogical discontinuities. Heavy minerals of the sand fraction have been determined in Spodosols described in the Mitú area, lower Vaupés river watershed, in the eastern Colombian Amazon (Malagón Castro 1995; Pulido Roa and Malagón Castro 1996). Zircon, for instance, shows strong contrast between upper and lower soil horizons. In an Alaquod profile (P-2/AR-15), zircon is 55% (21–85%) of the heavy minerals in the A and E horizons, but only 9% (4–10%) in the Bhm horizons. Similarly, in another Alaquod (AR-16) of the same area, zircon represents 42% (41–43%) in the A and E horizons, but only 11% (9–16%) in the Bhm horizons. Change in zircon content at the interface between albic and spodic horizons is abrupt. Comparatively, zircon accounts for 60% of heavy minerals in a Quartzipsamment (P-7), a figure similar to the zircon contents in the A and E horizons of the Spodosols. The lithological discontinuity between albic and spodic horizons points to a duplex soil configuration, with sand cover and underlying spodic horizon possibly unrelated.



Some spodic horizons are bimodal. Two layers with higher organic carbon content sandwich an intermediate layer with lower content. This reflects fluctuation in the intensity of the podzolization process. If the intensity of podzolization is controlled by the degree of moisture in the soil, then two spodic maxima would correlate with abundant rainfall periods separated by a drier period. As bimodal spodic horizons were observed in the Sipapo area, in the north of the region, as well as in the Atabapo area in the south-west of the region, this can be considered as the reflection of a regional climatic trend.

Weak spodic features may form in relatively short time spans, but well-developed spodic horizons require more time. No  $^{14}\text{C}$  data are available in our study region, but comparisons can be established with dated soils described in the Mitú area, lower Vaupés river watershed, in the eastern Colombian Amazon (Malagón Castro 1995; Pulido Roa and Malagón Castro 1996). Shallow, weakly developed Bs and Bhs layers, with low organic carbon contents in two Quartzipsamments (AR-11 and AR-14), were dated 1415 years BP and 1830 years BP, respectively. Two Bhm horizons in Alaquods were also dated: one horizon at site P-2/AR-15, 30 cm thick with 2.17% OC dated 3120 years BP at 100–110 cm depth, and the second horizon at site AR-20, with 4.19% OC dated 7400 years BP at 90–101 cm depth (no horizon thickness data provided).

Profile P84 has the thickest spodic horizon (80–170+ cm) with the highest amount of organic carbon (2.7–5.7%) among all Spodosols and spodic materials found under meadow vegetation in the study region (Table 6.6, Chap. 6). The formation of such a strongly developed, indurated spodic horizon may require a time span possibly similar to the oldest horizon mentioned above (i.e., 7400 years BP). The spodic horizon of P84 has also the particularity of being bimodal that reflects a period of lower podzolization intensity between two peaks of higher intensity. Peat dating in the western Guayana highlands shows a peat formation gap between 5200 years BP and 3600 years BP (Zinck et al. 2011). Is there any correlation between these two events that both suggest lower rainfall in highlands and lowlands?

It might be interesting comparing the few carbon 14 dates available in a larger regional context. The oldest organic material dated in the western Guayana highlands in Venezuela, on a sandstone meseta in the Marahuaka massif (ca 2800 m a.s.l.), is 7490 years BP (8400 calBP) (Zinck et al. 2011). Dune fields bordering the Rio Negro and some tributaries in the northern Amazon basin in Brazil started stabilizing after 7800 years BP (Carneiro Filho et al. 2002). The oldest spodic horizon under forest cover in the river Vaupés watershed in Colombia dates to 7400 years BP (Malagón Castro 1995; Pulido Roa and Malagón Castro 1996). There is thus a singular age coincidence between unrelated geopedologic events and vegetation changes in the lowlands and highlands surrounding the basin: inception of peat formation, dune colonization by vegetation, and onset of podzolization at the Pleistocene-Holocene turn. All three processes required a change in environmental conditions from dry to moist in the regional watersheds of middle Orinoco, upper Rio Negro, and lower Vaupés. The occurrence of charcoal in the forest soils of the Upper Rio Negro region of Colombia and Venezuela indicates the presence of

frequent and widespread fires in the Amazon basin, possibly associated with extremely dry periods or human disturbances. Charcoal ranged from 3.12 to 24.76 mg/cm<sup>3</sup> in the upper 50 cm of soil and was more abundant in Oxisols and Ultisols than in other soil types. Charcoal dates range from 6260 years B.P. to the present. Several dates coincide with dry phases recorded during the Holocene. Ceramic fragments were found at several sites, and thermoluminescence analysis indicated that their ages range from 3750 to 460 years B.P. The age of charcoal and shards confirms that this region has been exposed to fire and human disturbances during the past 6000 years (Saldarriaga and West 1986). According to Sandford et al. (1985), charcoal is common in the soils of established rain forests in San Carlos de Rio Negro in the north central Amazon basin. Carbon-14 dates of soil charcoal from this region indicate that numerous fires have occurred since the mid-Holocene period. Charcoal is most common in “terra-firme” forest Oxisols and Ultisols and less common in caatinga and igapo forest soils. Climatic changes or human activities, or both, have caused rainforest fires (Sandford et al. 1985).

Enlarging the horizon of the Holocene onset, Pivel et al. (2013) show that interglacial conditions started abruptly after 8.2 k years BP with a sharp change in faunal composition and surface hydrography at the South Brazil Bight continental slope. Even if the forest cover and woodlands in the core of the Amazon basin were not significantly modified during the Quaternary (Colinvaux et al. 2000; Mendonça et al. 2014), climate fluctuations may have occurred at its periphery.

---

## 10.6 Concluding Remarks: Trends in Meadow Landscape Evolution

In this chapter, sediment, soil, vegetation, topography, surface drainage features, sediment stratifications, microrelief forms, and Spodosol distribution are used to interpret landscape evolution in the meadow lowlands.

Sand cover sediments in the meadow environment are stratified. In some cases, consecutive layers have relatively similar particle size distributions, reflecting the persistence of the same depositional process over time. However, often stratifications between contrasting sand layers are strong enough to constitute lithological discontinuities. They highlight morphogenic instability of the fluvial system as rivers and streams move laterally over their areas of influence. This has resulted in the alternance of erosion and deposition of sand sediments and changes of depositional dynamics, in particular between splay and overflow processes. Frequent channel shifting is favored by level topography and weak mechanical resistance of meadow plants against sediment erosion and deposition. Meadow is an active geomorphic environment in contrast with the more stable caatinga and bana terrains. As a result, meadow vegetation has to periodically adapt to truncation or burial of the terrain surface. This constraint may favor the more resistant plants and therefore decrease plant diversity. Shifting river dynamics hampers (re)colonization of meadow by wooded plants.

In general, meadows extend on terrain surfaces slightly lower than the surrounding caatinga–bana terrain surface. Correlation of homologous layers (e.g., densipan layers) between meadow and caatinga shows that the former is incised by about 70–100 cm in the later. However, caatinga fringes seem to be relatively stable today from a geomorphic point of view, while bana fringes are exposed to degradation by runoff and rill erosion. Resulting bare white-sand patches are increasingly colonized by meadow species, reflecting a process of “meadowization” of the bana cover.

Microrelief is a distinctive feature of the meadow environment. Microtopography is caused by the incision of rills and channels of variable dimensions and spatial configurations. Some are caused by surface drainage and erosion and others by internal drainage and suffusion. Microforms caused by suffusion are closed units with variable shapes from pans to ramified depressions; they are characteristic features in alluvial plains. Deep erosion channels (50–100 cm deep) occur mainly under wooded vegetation (caatinga, bana) and in contact fringes between the former and meadows. There is no evidence that channels incise and erode today as there is no obvious sediment discharge at channel mouths in the contact areas between forest and meadow. Erosion channels may have developed during a drier period that has led to the dropping of the regional drainage base level and lowering of the water flow in rivers and streams, causing regressive erosion in the interfluves. Thus, erosion channels seem to be surviving features that today secure surface drainage and water evacuation during rainfalls but without substantial erosion.

The relationships between Spodosols, geomorphic activity, and vegetation are complex. The fairly thick spodic horizons found in the alluvial lowlands are not in balance with the current meadow vegetation and have most probably formed under wooded vegetation. They are covered by stratified sand layers that often show irregular decrease of organic carbon with depth, a typical fluventic aggradation feature, and lithological discontinuities above truncated spodic horizons. As this kind of profile has been detected at several sites throughout the lowlands, it can be assumed that large current meadow stretches have been covered by caatinga in the past. Bimodal spodic horizons also reveal the occurrence of drier episodes intercalated between moist periods. In the southern Pasimoni-Siapa interfluve, spodic horizons were found at similar depth at sites tens of kilometers apart, reflecting a past regional podzolization period. These spodic horizons are buried by unconformable sand sediments under different kinds of vegetation from meadow to woodlands.

In brief, features and trends in the meadow environment evolution can be highlighted as follows:

- The frequency of stratifications, some of which are contrasting enough to constitute lithological discontinuities, indicates that the regional sand cover under meadow is overall of sedimentary origin, formed by discontinuous sedimentation episodes during parts of the Holocene. Stratifications in white sands are of diverse nature. They can be physical, resulting from variable or discontinuous sedimentation process. They can be biological, resulting from variations of organic carbon

with depth. They can be mineralogical, resulting from variations of heavy minerals among consecutive layers. Stratifications in white sands are mainly of sedimentary origin. They contribute thus to elucidating the history of sand deposition in the lowlands. The importance of recognizing lithological discontinuities in sedimentary areas should not be overlooked and they should not be confused with pedogenic features. They contribute to the record of past landscape dynamics.

- Wooded vegetation (caatinga, bana) in contact areas with adjacent meadows is established on stratified sand sediments similar to those underlying the meadows. There is thus spatial continuity of the sand cover under both vegetation types.
- Caatinga terrain in ecotone areas is incised by erosion channels that seem not to be functional today, as there are no deposits at their outlets into the neighboring meadow areas. Channel incision is possibly related to climatic conditions drier than the current ones resulting in a lowering of the regional drainage base level in rivers and streams. Coalescing channel networks at the exit of the caatinga terrains cause truncation of the original sedimentary surface in the meadow.
- Microrelief is a relevant terrain feature in relatively stabilized alluvial flats and peneplain glacia. Erosion rills and channels caused by rainfall runoff and closed pans and channels resulting from suffusion evidence dynamic terrain surface morphology.
- Truncated Spodosols buried under subsequent sand sediments are possibly remnants of an earlier terrain surface under caatinga existing before the regional sand cover took place. There is no evidence of podzolization in the sand cover under the current meadow vegetation.

The origin of the meadows may be a matter of discussion. Are there meadow areas that have been established on white sands and persisted without major alterations since remote times and how remote would be these times? Although white sands are a sterile substrate for plants to flourish, meadow herbs, forbs, and shrubs have colonized it. Caatinga forest and bana scrubland have developed on stratified sand sediments similar to those underlying adjacent meadows. Caatinga was able to build its own soil support in the form of root mat for nutrient conservation and cycling as the end member of a probably long-lasting succession pioneered by meadow vegetation.

In active alluvial plains, overflows from rivers and streams at high water levels spread new sand sediments over interflaves, while shifting of migrating waterways reworks earlier sand deposits, creating bare surfaces to be colonized by herbaceous formations. A feature not related to river activity is the present spatial distribution of meadows as small to large islands irregularly distributed in a woody matrix (terra-firme and caatinga forests) that seems to result from disturbances decimating the forest cover, especially through natural and/or human-made repeated fires. Slash-and-burn parcels (i.e., "conucos") in terra-firme forest are often the places from which fire escapes and spreads to adjacent caatinga vegetation, particularly inflammable during the dry season. The dating of charcoal fragments in soils under current forest cover evidences the occurrence of dry periods favoring forest fires during part

of the Holocene. Thus, meadow formation may be the starting colonization phase of either sand surfaces exposed upon forest degradation or new sand covers resulting from river overflows.

From geomorphic and sedimentological points of view, the meadow environment is the most active compartment of the lowlands. Low stature and density of the vegetation cover oppose little obstruction to stream migration and shifting sedimentation. That is where white sands are reworked by erosion and deposition every year during flooding events. The resulting instability of the terrain surface in alluvial flats, caused by alternation of aggradation and truncation, has impact on plants. The vegetation cover has to cope with changing sedimentation and re-adapt periodically to moving sands. It can be hypothesized that the most resistant plants survive and end up dominating the meadow biotope. This may result in lowering plant diversity and increasing endemism as a reflection of sedimentary history. In contrast, areas of the lowlands under forest cover are less exposed to erosion and deposition, except places degraded by fire or human-induced disturbances. However, areas today under caatinga or bana show sand stratifications and were thus built up by sedimentation before vegetation established.

The reworking of existing sands in the lowlands as well as the redistribution of incoming sands from uplands and highlands results in stratified sediments. Stratifications can be strong enough to constitute lithological discontinuities. Stratified deposits with lithological discontinuities between layers are caused by discontinuous sedimentation with changes of depositional facies. In contrast, stratified deposits without lithological discontinuities are caused by a monotonic depositional process with short interruptions allowing some vegetation development and incorporation of organic matter that is reflected by irregular variations of organic carbon with depth.

The analysis of stratifications in sediments reveals that sand covers are discontinuous and heterogeneous. Stratifications result from sequential events of sand deposition and erosion. Lithological discontinuities between contrasting sand layers are sedimentological archive features that record changes in the landscape during the depositional process. In some places, changes were abrupt, for instance from overflow to splay, with occasional inclusion of turbulent layers. In other places, sediment aggradation was more progressive allowing vegetation to establish between depositional stages, as reflected by irregular variations of organic carbon with depth. Spodosols that most likely have formed under caatinga were truncated and subsequently buried by white sands in the meadow environment. Saprolite layers belonging to weathering profiles on bedrocks have been buried by sand cover. The repetition of genetic horizons with depth such as in the case of bimodal spodic and densic layers suggests climate fluctuations between moist and dry.

Stratified sand sediments are characteristic of the meadow environment. Non-stratified sands may be more common in other environments of the Amazon basin, as for instance under forest and woodland covers established on sandy soils derived from bedrock weathering or resulting from podsolization process. For instance, Dubroeuq and Volkoff (1998) describe a large podzolic plain in the upper Rio Negro basin covered by non-stratified white sand which corresponds to

the albic horizon of giant Spodosols. Horbe et al. (2004) studying the origin of white sands in Spodosols of the Amazonas State in Brazil did not find sedimentary structures and concluded that sands have resulted from podsolization process. Similarly, Mendonça et al. (2014) do not mention the occurrence of stratifications in Spodosols developed under campinarana forest from sandy sediments of fluvial origin in the Viruá National Park, northern Brazil.

The microrelief patterns observed in Amazonian white sands are different in shapes and materials from the microforms mentioned above. Inter-channel heads are flat-topped fragments of a terrain surface incised by channels with vertical walls. Channels seem to be relict features as incision is often not functional today. They are frequent under caatinga and bana, especially in contact areas with meadow, as well as in palm swales. They are a fairly unique feature for the shape and material in which they have formed. Rill and suffusion microtopographic features in sandy soils are not reported in the literature.

Final question: where, how, and when did the meadow flora originate? Huber (2005) considers that the Guayanan biota is autochthonous based on a unique evolutionary history since early geologic times. Within this context, the broadleaved herbaceous meadows, characterized by highly specialized, non-gramineous plants, are strictly limited to the Guayana region in an environment of geo-ecological differentiations. How did/does meadow vegetation establish and develop on sterile white-sand substrate and what are the strategies to conserve scarce nutrients, easily lixiviated through the sandy matrix, remain relevant issues to be considered. Following earlier research on Guayanan flora (Maguire 1970, 1979; Steyermark 1979; Berry and Riina 2005), Huber (2006) forwards a possible explanation for the present-day pattern of herbaceous vegetation types considering that non-gramineous meadows representing ancient species pools of Guayana-centered families had evolved successful colonization strategies in occupying extremely nutrient-poor sites at all altitudinal levels.

---

## References

- Adeney JM, Christensen NL, Vicentini A, Cohn-Haft M (2016) White-sand ecosystems in Amazonia. *Biotropica* 48(1):7–23
- Arnold RW (1968) Pedological significance of lithologic discontinuities. *Trans 9th Intl Congr Soil Sci* 4:595–603
- Berry PE, Riina R (2005) Insights into the diversity of the Pantepui flora and the biogeographic complexity of the Guayana Shield. *Biologiske Skrifter* 55:145–167
- Bravard S, Righi D (1989) Geochemical differences in an Oxisol-Spodosol toposequence of Amazonia, Brazil. *Geoderma* 44:29–42
- Bravard S, Righi D (1990) Podzols in Amazonia. *Catena* 17:461–475
- Carneiro Filho A, Schwartz D, Tatumi SH, Rosique T (2002) Amazonian paleodunes provide evidence of drier climate phases during the Late Pleistocene-Holocene. *Quat Res* 58:205–209
- Colinvaux PA, De Oliveira PE, Bush MB (2000) Amazonian and neotropical plant communities on glacial time-scales: the failure of the aridity and refuge hypotheses. *Quat Sci Rev* 19:141–169

- Cordeiro RC, Turcq B, Suguio K, Oliveira da Silva A, Sifeddine A, Volkmer-Ribeiro C (2008) Holocene fires in East Amazonia (Carajás), new evidences, chronology and relation with paleoclimate. *Elsevier Global Planetary Change* 61:49–62
- De Dapper M (1991) Late Quaternary geomorphological evolution of the sand-covered plateaus near Kolwezi, Southern Shaba, Zaïre. *Bull Soc Géog de Liège* 27:157–173
- Do Nascimento NR, Bueno GT, Fritsch E, Herbillon AJ, Allard T, Melfi AJ, Astolfo R, Boucher H, Li Y (2004) Podzolisation as a deferralization process: a study of an Acrisol-Podzol sequence derived from Palaeozoic sandstones in the northern upper Amazon Basin. *Eur J Soil Sci* 55:523–538
- Driessen P, Deckers J, Spaargaren O, Nachtergaele F (2001) Lecture notes on the major soils of the world. FAO, Rome, pp 35–37
- Dubroeuq D, Blancaneaux P (1987) Les podzols du Haut Rio Negro, région de Maroa, Venezuela. Environment et relations lithologiques. In: Righi D, Chauvel A (eds) Podzols et podzolization. AFES \$ INRA, Plaisir et Paris, pp 37–52
- Dubroeuq D, Volkoff B (1998) From Oxisols to Spodosols and Histosols: evolution of the soil mantles in the Rio Negro basin (Amazonia). *Catena* 32:245–280
- Fairbridge RW (1976) Shellfish-eating preceramic Indians in coastal Brazil. *Science* 191:353–359
- Goosen D (1971) Physiography and soils of the Llanos Orientales, Colombia. International Institute for Aerial Survey and Earth Sciences (ITC), Series B, 64. Enschede, The Netherlands
- Horbe AMC, Horbe MA, Kenitiro S (2004) Tropical Spodosols in northeastern Amazonas State, Brazil. *Geoderma* 119(1-2):55–68
- Huber O (2005) Diversity of vegetation types in the Guayana Region: an overview. *Biol Skr* 55: 169–188
- Huber O (2006) Herbaceous ecosystems on the Guayana Shield: a regional overview. *J Biogeogr* 33:464–475
- IGAC (2014a) Estudio general de suelos y zonificación de tierras del Departamento de Guainía, escala 1:100,000. Instituto Geográfico Agustín Codazzi, Subdirección de Agrología, Bogotá
- IGAC (2014b) Estudio general de suelos y zonificación de tierras del Departamento de Vichada, escala 1:100,000. Instituto Geográfico Agustín Codazzi, Subdirección de Agrología, Bogotá
- Klinge H (1965) Podzol soils in the Amazon basin. *J Soil Sci* 16(1):96–103
- Klinge H, Medina E, Herrera R (1977) Studies on the ecology of amazon caatinga forest in southern Venezuela I. General features. *Acta Cient Venezuelana* 28:270–276
- Maguire B (1970) On the flora of the Guayana Highland. *Biotropica* 2:85–100
- Maguire B (1979) Guayana, region of the Roraima Sandstone Formation. In: Larsen K, Holm-Nielsen LB (eds) Tropical botany. Academic, London, pp 223–238
- Malagón Castro D (1995) Estudio genético-taxonómico de Espodosoles, Ultisoles y Oxisoles y su relación con el manejo de las tierras en el Departamento del Vaupés (Colombia). Universidad Nacional de Colombia, Bogotá, Colombia
- MARNR-ORSTOM (1986) Atlas del inventario de tierras del Territorio Federal Amazonas (Venezuela). Dirección de Cartografía Nacional, MARNR, Caracas
- Medina E, Cuevas E (2011) Complejo caatinga amazónica bosques pluviales esclerófilos sobre arenas blancas. *BioLlania edic espec* 10:241–249, UNELLEZ, Guanare, Venezuela
- Mendonça BAFD, Simas FNB, Schaefer CEGR, Fernandes Filho EI, Vale Júnior JFD, Mendonça JGFD (2014) Podzolized soils and paleoenvironmental implications of white-sand vegetation (Campinarana) in the Viruá National Park, Brazil. *Geoderma Reg* 2–3:9–20
- Moyersoen B (1993) Ectomicorizas y microrrizas vesiculo arbusculares en caatinga Amazónica del sur de Venezuela. *Scientia Guianae* 3
- Pivel MAG, Santarosa ACA, Toledo FAL, Costa KB (2013) The Holocene onset in the southwestern South Atlantic. *Palaeogeogr Palaeoclimatol Palaeoecol* 374:164–172
- Pulido Roa C, Malagón Castro D (1996) Estudio genético y taxonómico de Espodosoles, Ultisoles y Oxisoles y su relación con el manejo de las tierras. In: Aspectos ambientales para el ordenamiento territorial del Municipio de Mitú, Departamento del Vaupés. Instituto Geográfico Agustín Codazzi, Bogotá, Colombia, Tomo I:307–399



- Quesada CA, Lloyd J, Schwarz M, Patiño S, Baker TR, Czimczik C, Fyllas NM, Martinelli L, Nardoto GB, Schmerler J, Santos AJB, Hodnett MG, Herrera R, Luizão FJ, Arneith A, Lloyd G, Dezzeo N, Hilke I, Kuhlmann I, Raessler M, Brand WA, Geilmann H, Moraes Filho JO, Carvalho FP, Araujo Filho RN, Chaves JE, Cruz Junior OF, Pimentel TP, Paiva R (2010) Variations in chemical and physical properties of Amazon forest soils in relation to their genesis. *Biogeosciences* 7:1515–1541
- Quesada CA, Lloyd J, Anderson LO, Fyllas NM, Schwarz M, Czimczik CI (2011) Soils of Amazonia with particular reference to the RAINFOR sites. *Biogeosciences* 8:1415–1440
- Saldarriaga JG, West DC (1986) Holocene fires in the Northern Amazon Basin. *Quat Res* 26:358–366
- Sanford RL Jr, Saldarriaga J, Clark KE, Uhl C, Herrera R (1985) Amazon rain-forest fires. *Science* 227:53–55
- Schargel R, Marvez P (2009) Suelos. In: Aymard GA, Schargel R (eds) *Estudio de los suelos y la vegetación (estructura, composición florística y diversidad) en bosques macrotérmicos no-inundables, Estado Amazonas, Venezuela*. BioLlania edic esp 9:99–125, UNELLEZ, Guanare, Venezuela
- Schargel R, Aymard G, Berry P (2000) Características y factores formadores de Spodosoles en el sector Maroa-Yavita, Amazonia Venezolana. *Revista UNELLEZ de Ciencia y Tecnología* 18(1):85–96
- Schargel R, Marvez P, Aymard G, Basil S, Berry P (2001) Características de los suelos alrededor de San Carlos de Río Negro, Estado Amazonas, Venezuela. *BioLlania edic esp* 7:234–264, UNELLEZ, Guanare, Venezuela
- Schnütgen A, Bremer H (1985) Die Entstehung von Decksanden im oberen Rio Negro-Gebiet. *Z Geomorph NF Suppl-Bd* 56:55–67
- Soil Survey Staff (2014) *Keys to soil taxonomy*, 12th edn. USDA, Natural Resources Conservation Service, Washington, DC
- Stagno P, Steegmayer P (1972) La erosión reticular en el sur del lago de Maracaibo. *Agronomía Tropical* 22(2):99–118
- Stark NM, Jordan CF (1978) Nutrient retention by the root mat of an Amazonian rain forest. *Ecology* 59:434–437
- Steyermark JA (1979) Flora of the Guayana Highland: endemicity of the generic flora of the summits of the Venezuelan tepuis. *Taxon* 28:45–54
- Zinck JA, García P, van der Plicht J (2011) Tepui peatlands: age record and environmental changes. In: Zinck JA, Huber O (eds) *Peatlands of the Western Guayana Highlands, Venezuela*. Ecological studies 217. Springer, Heidelberg, pp 189–236



# Plant Diversity and Endemism of the White-Sand Open Vegetation in the Lowlands of the Amazonas State, Venezuela

# 11

J. R. Grande A., O. Huber, and R. Riina

## 11.1 Introduction

Terrestrial ecosystems are usually defined by the dominant vegetation type, which is established by physiognomy and floristic composition. The climate is the primary factor determining physiognomy (Holdridge 1947; Walter 1977), but substrates can set the scene for contrasting plant formations (Rajakaruna 2004), resulting in a mosaic of zonal and azonal vegetation (Walter 1985). Azonal areas are located over soils that are nutrient-depleted, contain harmful substances or experience some kind of water stress, either permanently or temporarily. As a consequence, vegetation structure and coverage tend to be less complex, while plant species endemism and trait specialization are usually higher.

A remarkable example of areas with azonal plant communities in the Neotropics are the so-called Amazonian white-sand ecosystems (Anderson 1981; Huber 1995b; Daly et al. 2016). These singular plant formations, including forest and open (non-forested) vegetation, are restricted to the lowlands of Amazonia and the Guayana Shield, with major areas in the Río Negro basin along south-eastern Colombia (Córdoba Sánchez 2014), southern Venezuela (Amazonas, Bolívar states), and north-western Brazil (IBGE 2012; Adeney et al. 2016), but they also occur scattered throughout the Amazonia, including northeastern Peru (Fine et al. 2010), northern Pará state in Brazil (Zappi et al. 2020), and smaller patches in the Guianas, and the rest of Amazonian states of Brazil (Ferreira 2009; Adeney et al. 2016).

---

J. R. Grande A. (✉)

Departamento de Botánica, Facultad de Ciencias, Campus Fuente Nueva, Granada, Spain

O. Huber

Instituto Experimental Jardín Botánico Dr. Tobías Lasser, Universidad Central de Venezuela, Caracas, Venezuela

R. Riina

Real Jardín Botánico, RJB-CSIC, Madrid, Spain

Compared to rainforests, these open habitats occupy a relatively small proportion of the Amazonian-Guayana Shield lowlands (Eva et al. 2004) and have been long recognized as areas of high plant diversity and endemism (Huber 1995b; Lleras 1997; Adeney et al. 2016).

In this chapter, we present for the first time the results of a large set of floristic surveys conducted over several decades on open white-sand vegetation in lowland areas of the state of Amazonas in southern Venezuela. The study area was divided into six major sampling areas that were named and delineated according to the river basins where sampling sites were established (white-sand areas) namely, Atabapo, Camani, Pasimoni, Sipapo, Ventuari, and lowland areas around Yapacana National Park. These plant inventories were conducted in parallel with detailed soil studies consisting of 83 profiles, including some in bare sand areas (Chap. 6; Figs. 6.1 and 6.2). However, a sampling design involving plots or transects that could be comparable across sites and subjected to quantitative floristic analyses was not implemented in our case. The approach used was to collect and record all the plant species or morphospecies identified in each of the visited sites.

The study area has climatic conditions similar to those prevalent across most of the Amazonian region. The average annual rainfall varies between 1800 and 4095 mm, with 0–2 months with less than 100 mm, and mean-annual temperature above 26 °C (MARNR and ORSTOM 1987; Espinoza et al. 2009). Overall, the surveyed sites receive more than 2000 mm of rainfall per year (Huber 2006). Soils in the study area consist of quartzose sand and loamy sand sediments, white to light gray in color, acidic, usually deep, and highly oligotrophic (Chap. 7). A more detailed description of the landscape, terrain, and soils of the six main subareas and sampled sites is given in Chaps. 6 and 7.

---

## 11.2 Botanical Exploration in the Study Area

The history of botanical exploration in the Guayana region and the lowlands of the Venezuelan Amazonas state has been described elsewhere (Huber 1995a and Appendix 3.4 in this book). The expeditions carried out by Otto Huber between 1977 and 1983 (Appendix 11.1), include the set of localities analyzed in this chapter. They represent one of largest collecting efforts in the lowlands of the Amazonas state. The availability of helicopters in most of Huber's expeditions was crucial for surveying the sites included in this study (Fig. 6.1), some of them far away from the main rivers.

---

## 11.3 Main Vegetation Types Surveyed

The soil and floristic surveys carried out in the context of this work, spanned a variety of vegetation types including Amazon caatinga forest, meadows, palm swamps, savannas, scrubs, as well as ecotone areas between meadows and savannas (Table 11.1). Localities with meadow vegetation, in all its physiognomic diversity

**Table 11.1** Summary of the main vegetation types surveyed in this study, number of field inventories and the study areas involved

Vegetation	Inventories	Study areas
Amazonian caatinga	11	Atabapo, Camani, Pasimoni, Sipapo, Yapacana
Meadow	42	Atabapo, Camani, Pasimoni, Sipapo, Ventuari, Yapacana
Meadow/savanna ecotone	10	Atabapo, Pasimoni, Sipapo, Ventuari, Yapacana
Palm swamp (morichal)	2	Ventuari
Savanna	6	Pasimoni, Sipapo, Ventuari, Yapacana
Scrubland (shrubland)	8	Atabapo, Pasimoni, Sipapo, Yapacana
Total	79	6

See Chaps. 6 and 7 for detailed soil and landscape information on each of the sites. Note: sites of bare sand sampled in the soil study are not included

and different degrees of coverage, were the main focus of the soil study accounting for 52 (42 + 10, including meadow/savanna ecotones) of the 79 field inventories spanning approximately 50 sites or localities (Table 11.1). Although the scrubland (e.g., bana) and forest vegetation (Amazon caatinga, palm swale) were not the main focus of the soil analysis (see Chap. 6) the floristic inventory covered these plant formations. Below we provide a succinct description of the main vegetation types present in the study area following the relevant literature (Huber 1995b; Riina and Huber 2003; Huber and Oliveira-Miranda 2010).

### 11.3.1 Amazon Caatinga (Rio Negro Caatinga)

This is a type of sclerophyllous evergreen forests occurring as large stands of low to medium-sized trees, mainly in the Atabapo, Guainía, and Negro river drainages on frequently flooded, oligotrophic substrates (Huber 1995b). Rio Negro caatingas typically have an open canopy, with trees with small crowns and narrow, leathery leaves. The dominant tree species belong to the families Euphorbiaceae, Fabaceae, Combretaceae, and Clusiaceae (Huber and Oliveira-Miranda 2010). The understory is of variable density, dominated by smaller individuals of Rubiaceae and Malvaceae (Huber 1995b; Huber and Oliveira-Miranda 2010).

### 11.3.2 Palm Swamp (Morichal)

Forest restricted to permanently inundated floodplains. In the study area, these forests are usually dominated by palms in the genus *Mauritia* or *Mauritiella*, mixed with trees and treelets of various sizes. Species of *Aspidosperma* (Apocynaceae) and *Ormosia* (Olacaceae) are some of the most frequent trees and treelets.

### 11.3.3 Meadow (Herbazal)

The term meadow *sensu* Huber (1995b) refers to any herbaceous vegetation type in the Guayana Shield. Meadows are classified into (1) gramineous meadows (grasslands), dominated by grasses and/or sedges, and (2) nongramineous meadows, dominated by other herbaceous plants.

Gramineous meadows are further divided into savannas and montane grasslands (not covered in this work). Savannas are dominated by C4 grasses, restricted to macrothermic lowland areas, or submesothermic lower upland environments. Lowland savanna could be affected by periodic floods. Scattered woody elements (shrubs, treelets, trees, palms, forest islands) can be present. The predominant type of lowland savanna in the Amazonas state is the nonflooded, shrub and tree savanna, however, a relatively large area of periodically flooded savannas is found in the eastern Ventuari basin (Huber 1995b). In the Venezuelan Amazonas, they occur discontinuously in the northern and central part of the state. Although dominated by grasses, the taxonomic diversity of Poaceae in these savannas is relatively low, including a few species in the genera *Axonopus*, *Echinolaena*, and *Trachypogon*.

Nongramineous-meadows are very characteristic of the Guayana Shield and include several types, differing in floristic composition and physiognomy: (1) Broad-leaved meadows, dominated by various species of Rapateaceae, are widespread in the Guayana highlands but also in some upland and lowland areas, (2) Tubiform meadows are dominated by tubiform herbs in the families Bromeliaceae or Sarraceniaceae; these only occur at mid- and higher elevations in the Guayana Shield, (3) Rosette meadows, in which dense rosette herbs of Xyridaceae and Eriocaulaceae dominate, and are also restricted to certain tepui summits, and finally, (4) fruticose meadows which have the herbaceous layer mixed with numerous short subshrubs and are common in the study area. Species in the genus *Schoenocephalium* (Rapateaceae) constitute the main herbaceous components of fruticose meadows in the lowlands of the Amazonas state. Other members of Rapateaceae frequently found include *Monotrema*, *Cephalostemon*, as well as the endemic *Guacamaya superba*, which grow together with other herbaceous plants such as Xyridaceae (*Xyris*, *Abolboda*), Eriocaulaceae (*Syngonanthus*, *Paepalanthus*, *Eriocaulon*, *Comanthera*), and Cyperaceae (*Bulbostylis*, *Rhynchospora*, *Lagenocarpus*). Although only locally abundant, Poaceae genera such as *Axonopus*, *Paspalum*, and *Trichantheicum*, and the species *Arthrostylidium berryi* and *Steyermarkochloa angustifolia* are also found in these ecosystems (Huber 1995b; Riina and Huber 2003; Judziewicz and Davidse 2008).

### 11.3.4 Shrubland (Scrub)

In the context of the Guayana Shield, a shrubland consists of a low (up to 5 m tall) woody vegetation composed of shrubs and shrub-like plants. A shrub is defined as a plant usually 0.2–5 m tall, with woody stems and twigs branching from the base or not branching at all. This includes woody and subwoody monopodial plants, mostly

unbranched, with leaves distributed along the main stem or else concentrated towards the apex. Shrublands occur often as azonal islands of vegetation, restricted to a particular type of substrate, interspersed within forest or savanna vegetation. Trees and/or patches of herbaceous vegetation may be present, however, the shrub layer constitutes the main functional unit of the ecosystem.

The shrubland vegetation found in the study sites, consist of dense, sclerophyllous plants 1–5(–8) m tall that form small islands separated by patches of bare white sand. The most frequent species are *Humiria balsamifera* (Humiriaceae), *Ilex divaricata* (Aquifoliaceae), *Heteropterys oblongifolia* (Malpighiaceae), *Emmotum floribundum* (Icacinaceae), *Pradosia schomburgkiana* (Sapotaceae), *Ormosia macrophylla* (Fabaceae), *Calliandra tsugoides* (Fabaceae), *Pagamea guianensis* (Rubiaceae), *Tepuianthus savannensis* (Thymelaeaceae), and *Simaba guianensis* (Simaroubaceae). In transition areas between shrublands and adjacent forest, high concentrations of orchids species can be found, as well as other epiphytes such as *Aechmea brevicollis* (Bromeliaceae) (Huber 1995b).

In the southern part of the study area, especially in the upper Río Negro and Guainía rivers, there is a peculiar shrubland type, more properly a scrubland, locally called *bana* (Huber 1995b). Banas occur in small patches on seasonally flooded, deep sandy soils surrounded by Amazon caatinga forests (Klinge et al. 1977; Klinge and Medina 1979; Bongers et al. 1985). A typical bana landscape consists of a 0.5–3 m tall dense woody vegetation islands on low mounds and ridges, separated from each other by shallow, temporarily inundated depressions with ephemeral herbaceous vegetation. Important genera, in the Rio Negro bana, are *Pachira* (Bombacaceae), *Pagamea*, *Retiniphyllum*, *Remijia* (Rubiaceae), *Macairea*, *Tibouchina* (Melastomataceae), *Humiria*, *Sacoglottis* (Humiriaceae), *Neea* (Nyctaginaceae), *Aldina*, *Ormosia*, and *Pithecellobium* (Fabaceae).

---

## 11.4 Species Richness and Endemicity Patterns

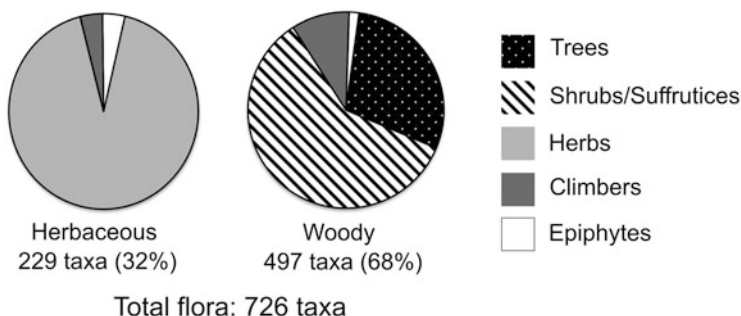
We present the first checklist of plants growing in open white-sand habitats of the Venezuelan Amazonas state. It includes all the species recorded in the surveyed sites and adjacent areas, as well as a qualitative field assessment of species relative abundance across the six study areas (Appendix 11.2, Fig. 6.1). The list was compiled using Otto Huber's collection data (Appendix 11.1) complemented with information from the Flora of the Venezuelan Guayana (Steyermark et al. 1995–2005), protologues of thereafter described species (Cuello 2003; Judziewicz and Davidse 2008; Aymard et al. 2014; Cabral et al. 2016, 2018) and direct consultation of the botanical collections housed at the Venezuelan National Herbarium (VEN).

Taxonomy and species global distributions were updated using online botanical databases such as the International Plant Name Index ([www.ipni.org](http://www.ipni.org)), Plants of the World Online (<https://powo.science.kew.org>), and TROPICOS ([www.tropicos.org](http://www.tropicos.org)). In most cases, plant classification follows Angiosperm Phylogeny Group (APG IV 2016) for Angiosperms, Christenhusz et al. (2011) for Gymnosperms, and

**Table 11.2** Taxonomic richness and endemism levels by family, genera, and species of vascular plants in the open white-sand vegetation of Amazonas, Venezuela

	Richness	N end	N local end
Species	710	365 (51.4%)	89 (12.5%)
Genera	287	4 (1.4%)	0
Families	90	0	0

N end: number of endemic taxa to the Amazonian white-sand areas of Brazil, Colombia, and Venezuela; N local end: number of endemic taxa in the narrow sense (Venezuelan white-sands, Amazonas state)

**Fig. 11.1** Main life-form components of the vascular flora from the open white-sand vegetation of the Venezuelan Amazonas state

Pteridophyte Phylogeny Group I (PPG I 2016) for ferns and allies. However, some old family names, important in previous works about the Venezuelan flora (Steyermark et al. 1995–2005; Hokche et al. 2008), were retained: Myrsinaceae (Primulaceae in APG IV), Ternstroemiaceae (Pentaphragaceae in APG IV), Turneraceae (Passifloraceae in APG IV).

Considering the relatively small area occupied by open white-sand ecosystems in the Venezuelan Amazonas state (Oliveira-Miranda et al. 2010a–c), its flora is considerably rich in herbaceous and woody plants. We recorded 710 species (726 taxa, including infraspecies, Appendix 11.2) spanning 287 genera and 90 vascular plant families. Of these, half (51%) of the species and four genera are endemic to the overall Amazonian white-sand areas across Brazil, Colombia, and Venezuela. In contrast, local endemism is relatively low, with only 12% of the recorded species restricted to the study area (Table 11.2).

More than half of the flora (68% of taxa) of the study area consists of woody elements, and the remaining 32% corresponds to herbaceous taxa (Fig. 11.1). Shrublands stand out by their floristic and physiognomic diversity across the Guayana Shield (Huber 1995b), and this pattern is confirmed in our study, where the shrubby life form, including suffrutices, constitutes the dominant one (292 taxa) among the woody elements, followed by trees (143), climbers (47) and epiphytes (8, including hemiparasites). The herbaceous component of the flora is clearly



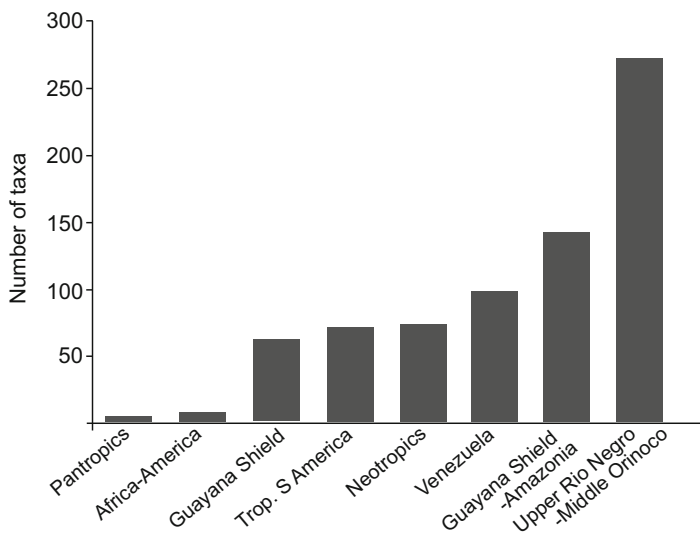


**Fig. 11.2** Number of vascular plant taxa (species and infraspecies) recorded in the open white-sand vegetation of the Venezuelan Amazonas state by geographic distribution ranges

dominated by terrestrial herbs (218, including a few aquatics) with a small number of epiphytes (9) and climbers (9).

The global distribution of this rich flora (Fig. 11.2) shows the predominance of local and regional floristic elements including specialized species restricted to white-sand areas of Brazil, Colombia, and Venezuela (Upper Río Negro-Upper Orinoco basins) and other to wider areas within the Neotropics (e.g., Guayana Shield, tropical South America). Very few species are widespread across the tropics (e.g., pantropical or amphi-Atlantic distributions) (Fig. 11.2). At the generic level, the floristic affinities are clearly dominated by tropical genera, especially those from the Neotropics, but there are also striking transoceanic disjunctions (Fig. 11.3). Amphi-Atlantic distributions, such as those found in members of Rapateaceae, Humiriaceae and Bromeliaceae, have been explained by migration through the Laurasian Arc during Paleocene (Davis et al. 2002) or long-distance dispersal during Neogene (Givnish et al. 2004; Renner 2004), but dates might be underestimated (Stevens 2001–onwards). Malayo-American disjunctions are present in a few of the genera occurring in the study area. Some of these appear to be the result of extinction of former Gondwanan lineages in Africa during drier periods (Morley 2000; Couvreur 2015). However, other explanations such as land accretion during Tertiary (Heads 2012), have been advocated within the genus *Ternstroemia* (Grande 2019). Close phylogenetic relationships of Guayana Shield-centered genera (most of them present in the study area) with Malesian and Australasian groups are shown by *Archytaea* (with *Ploiarium*, Bonnetiaceae), *Pentamerista* (with *Tetramerista*, Tetrameristaceae), and *Pakaraimaea* and *Pseudomonotes* (with Old World Dipterocarpaceae; not present in the study area) (Berry and Rogers 2005).

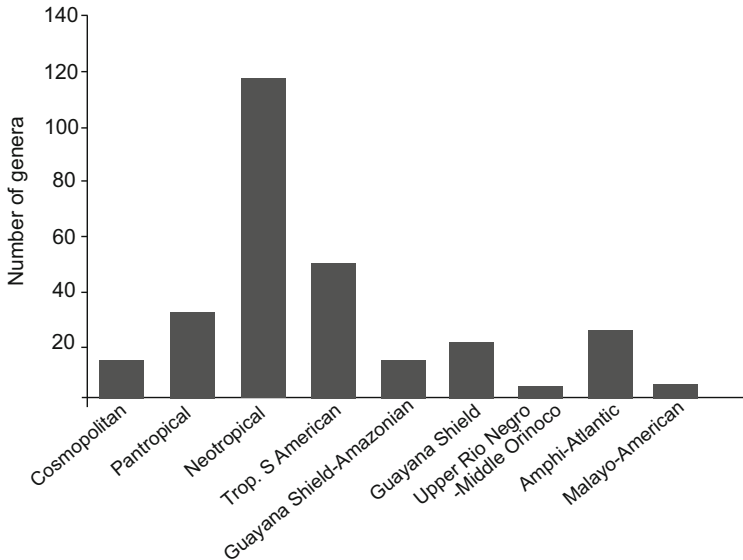


**Fig. 11.3** Floristic affinities of the flora of open-white sand areas surveyed in Amazonas, Venezuela, at the generic level

The high species richness and endemism found in the study area contrast with the relatively low diversity known in other white-sand areas in western Amazonia. Daly et al. (2016) reported 222 species in six sites of white-sand formations, including forest and non-forest vegetation, in the state of Acre in Brazil. Likewise, 221 tree species or morphospecies were inventoried in 16 plots of white-sand forest in the Peruvian Amazonia (Fine et al. 2010). However, in the latter case, levels of endemisms (50%; Fine et al. 2010) were similar to those found in our study area. Surprisingly, García-Villacorta et al. (2016) reported only 23% of endemisms in white-sand forests when looking at all available floristic data for western Amazonia (including the Guayana Shield), suggesting that the endemism of their flora has been overestimated in previous studies. A recent botanical exploration to the Cuiarí and Isana rivers, upper Río Negro basin in Colombia (Arellano-Peña et al. 2019), adjacent to our study area, reported plant species richness (726 species) similar to those found in the present study. However, the collections of Arellano-Peña et al. (2019) included, in addition to open white-sand vegetation, terra firme and flooded forests (*igapós* and *várzeas*), which were not sampled in our inventories.

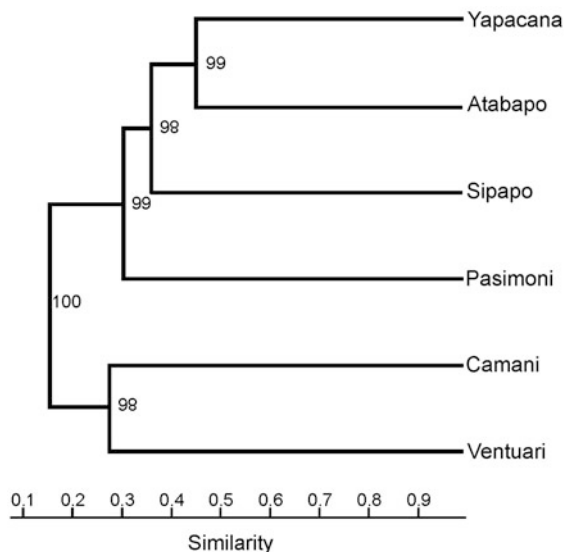
The Atabapo and Yapacana areas sampled are the richest in species of vascular plants and in endemics (Table 11.3), which is in agreement with the higher number of vegetation types present. Yapacana is also the most heterogeneous of the six areas regarding landscape and substrates, including more soil diversity and high frequency of compact sandy layers at different depths (Chaps. 6 and 7). In the other extreme, the Camani area has the lowest number of species, which is probably due to its smaller size and consequent less ecological complexity; only two vegetation types

**Table 11.3** Summary of the vascular plant species richness of the six surveyed areas in Amazonas, Venezuela

	Atabapo	Camani	Pasimoni	Sipapo	Ventuari	Yapacana
N spp	489	108	230	289	143	439
N excl	99	23	11	20	1	60
N end (%)	17 (3.5)	7 (6.5)	3 (1.3)	4 (1.4)	1 (2)	12 (2.7)

N spp: total number of species; N excl: number of species recorded only in one of the six areas, independently if they are endemic or not. N end: number of species endemic to each area

**Fig. 11.4** UPGMA dendrogram using the Jaccard index of similarity of the six surveyed areas in the Amazonas state. Similarity is based on species composition. The nodes of the dendrogram are all highly supported (97–100% bootstrap)



were present in the sampled sites (Table 11.1). Although the Pasimoni area is also small in size, it has a comparatively higher number species than Camani, which is probably due to its higher diversity in vegetation types (Table 11.1). Our floristic data reflect, at a small scale, the usual pattern of uneven distribution of organisms’ diversity across space in many areas of the world, but in our case high levels of endemism and species richness are probably enhanced by the fragmented distribution of the open white-sand vegetation patches within a matrix of Amazonian forest.

Based on similarity of floristic composition, estimated using a UPGMA (Unweighted Pair Group Method with Arithmetic Mean) cluster algorithm and the Jaccard index, the six study areas share a relatively low number of species among each other (Fig. 11.4). The most similar areas (~55% similar) are Yapacana and Atabapo, which also show the highest levels of alpha diversity and endemism (Table 11.3). These two areas together have more floristic affinities with the Sipapo and Pasimoni areas than with the cluster Camani and Ventuari (Fig. 11.4). Sampled sites in Camani and Ventuari are located further from the main, and larger, areas of white-sand of Venezuela, Colombia and Brazil (see Adeney et al. 2016), which can explain in part this marked difference in species composition with the rest of the

sampled areas. They are also relatively smaller than the rest, especially the Camani area, also with a low number of sampled sites (Fig. 6.2 in Chap. 6). The same clustering pattern of floristic similarity among areas, as shown in Fig. 11.4, was obtained when analyzing parts of the data, for example, creating subsets of data according to the plant life form (herbaceous, graminiform, or woody taxa), or using only endemic species.

The resulting pattern of similarity in species composition highlights the floristic uniqueness and the different levels of local endemism of the sampled areas of white-sand vegetation in the Venezuelan Amazonas, which is a relevant knowledge for designing environmental conservation policies and protected areas.

Patterns of species diversity across main taxonomic groups show additional insights on the flora of the white sand patches in the study area. The ten most species-rich families (> 20 species) are Melastomataceae (51), Rubiaceae (51), Fabaceae (39), Xyridaceae (35), Poaceae (30), Apocynaceae (29), Cyperaceae (28), Ochnaceae (24), Chrysobalanaceae (23), and Eriocaulaceae (21) (Fig. 11.5, Table 11.4). These families include lineages dominated by herbaceous (mostly Xyridaceae, Poaceae, Cyperaceae, Eriocaulaceae) and shrubby species. Rubiaceae, Poaceae, and Apocynaceae are the richest families both at the genus and species level. This contrasts with the Xyridaceae, with species concentrated in only two genera (*Xyris* and *Abolboda*) (Table 11.4).

Regarding groups with low diversity, more than half of the recorded families (47 out of 90) are only represented by six or fewer species, but most of them include endemic species (Fig. 11.5). Among the families with the higher proportion of endemics, lineages with predominantly herbaceous growth forms stand out (e.g., Poaceae, Cyperaceae, Eriocaulaceae, Lentibulariaceae, Polygalaceae, and Orchidaceae) (Fig. 11.5).

Differences in the pattern of species richness across families between our focal area and adjacent regions with similar azonal vegetation such as Pantepui (areas above 1500 m in the Guayana Shield; Berry and Riina 2005) are probably due to the higher topographic and climatic complexity of the Guayana Highlands (tepui slopes and summits). For example, Melastomataceae and Rubiaceae are also among the top most species-rich families present in Pantepui, but others like Orchidaceae, Asteraceae, and Bromeliaceae (extremely rich in Pantepui; Riina et al. 2019) are considerably less diverse in the lowland white-sand areas of the Venezuelan Amazonas state (Fig. 11.5, Table 11.4).

Recent floristic inventories in typical seasonal shrub and tree savannas occurring in the northwestern corner of the Venezuelan Amazonas state, along the right margin of the Orinoco river (Nozawa Furuya et al. 2019), found similar levels of taxon diversity at the family and genus levels (98 families, 286 genera), but lower species richness (563 species) in comparison with the open white-sand vegetation of our study area. In another study of savannas of eastern Amazonia in the state of Pará (Brazil), Devecchi et al. (2020) also reported similar numbers for families (92) and genera (271), but an even lower number of species (406). Besides the highest diversity and endemism of the open white-sand vegetation in our study area, there are important differences in species composition between these two types of open

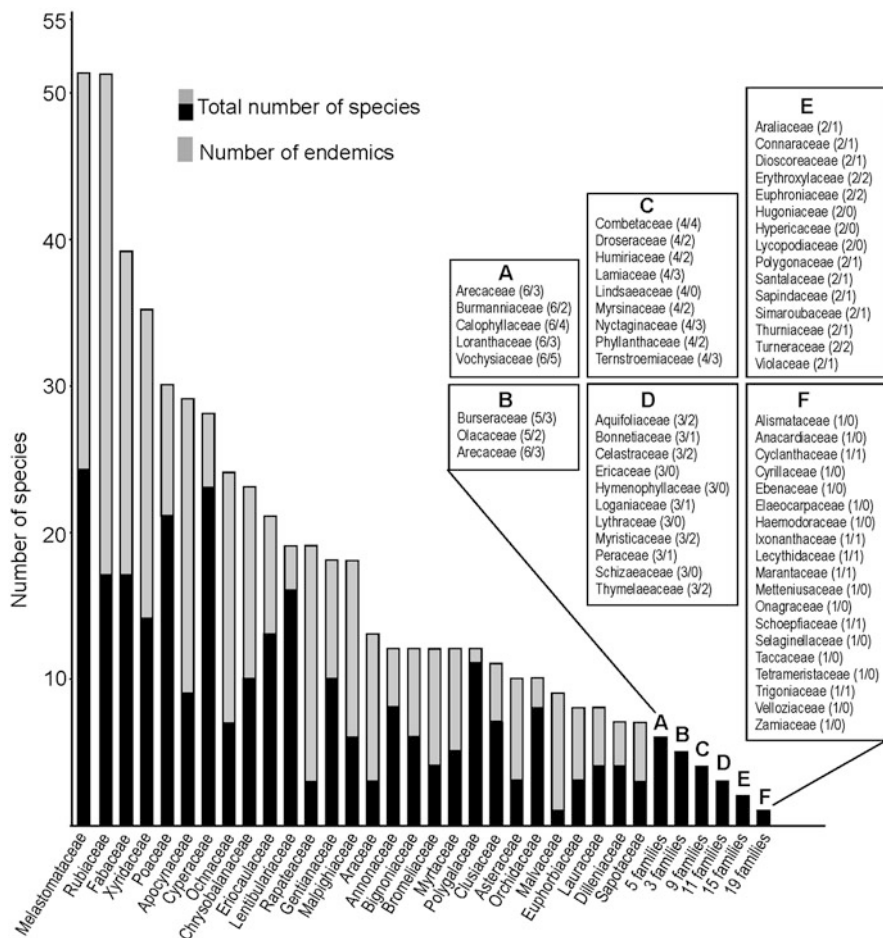


**Fig. 11.5** Total number of species for each of the 90 families of vascular plants recorded in the study area, including the number of species endemic to the Amazonian white sands in a broader sense (Brazil, Colombia, Venezuela). Bars labeled A, B, C, D, E, F, represent families with 6, 5, 4, 3, 1 species, respectively; inset boxes display these families (47) indicating their total number of species and endemics in parentheses (species/endemics)

vegetation (savannas and white-sand meadows) in the Amazonia. For example, typical savanna woody elements such as *Curatella americana*, *Bowdichia virgilioides*, and *Byrsonima crassifolia* are absent in the study area (Appendix 11.2) and in other Amazonian white-sand ecosystems with similar soil, drainage, and climatic conditions (e.g., Daly et al. 2016). Floristic differences in the herbaceous component are even larger including entire families such as Eriocaulaceae, Lentibulariaceae, Rapateaceae, and Xyridaceae, which are highly diverse in our study area (Fig. 11.5), but under-represented or almost absent in the typical savannas of the Venezuelan-Colombian Llanos or the Brazilian Cerrado (Riina et al. 2007; Nozawa Furuya et al. 2019; Flora do Brasil 2020).

**Table 11.4** List of plant families with eight or more species in the study area in Amazonas, Venezuela (see also Fig. 11.2)

Family	N gen (N end)	N spp (N end)
Melastomataceae	18	51 (27)
Rubiaceae	13 (1)	51 (34)
Fabaceae	14	39 (22)
Xyridaceae	2	35 (21)
Poaceae	14 (1)	30 (9)
Apocynaceae	17	29 (20)
Cyperaceae	6	28 (5)
Ochnaceae	7	24 (17)
Chrysobalanaceae	6	23 (13)
Eriocaulaceae	4	21 (8)
Lentibulariaceae	2	19 (3)
Rapateaceae	8 (1)	19 (16)
Gentianaceae	7 (1)	18 (8)
Malpighiaceae	7	18 (12)
Araceae	7	13 (10)
Annonaceae	5	12 (4)
Bromeliaceae	6	12 (8)
Bignoniaceae	6	12 (6)
Myrtaceae	1	12 (7)
Polygalaceae	4	12 (1)
Clusiaceae	2	11 (4)
Asteraceae	6	10 (7)
Orchidaceae	9	10 (2)
Malvaceae	3	9 (8)
Euphorbiaceae	4	8 (5)
Lauraceae	3	8 (4)

N gen: number of genera. N spp: number of species. N end: number of endemics. Endemism is relative to all the Amazonian white-sand areas of Brazil, Colombia, and Venezuela

Because of its ecological importance in Guayana Shield meadows, the family Rapateaceae stands out in the study area. It is among the 20 richest families with eight genera and 19 species (16 endemics) (Table 11.4) and their species play a significant role shaping the vegetation physiognomy and floristic composition of the broad-leaved meadows of the Amazonian white-sand areas (Huber 1995b). The monotypic genus *Guacamaya*, represented by the showy *G. superba*, is restricted to the open white-sands of Colombia and Venezuela (Berry 2005). Three out of the five species of *Schoenoecephalum* are known from open-white sand areas and the other two species, *S. schultesii* and *S. martianum*, occur in the Isibukuri area and near Araracuara (Colombia), respectively. The genera *Cephalostemon*, *Duckea*, *Rapatea*, and *Spathanthus* are also present in the study area, including *Rapatea yapacana*, which is endemic to the Yapacana area where it is also locally abundant.

Diversity patterns at the genus level show that the most species-rich group is the herbaceous genus *Xyris* (Xyridaceae) with 25 species, followed by *Utricularia* (Lentibulariaceae), *Ouratea* (Ochnaceae), *Myrcia* (Myrtaceae), *Rhynchospora*

**Table 11.5** Most species-rich genera (with five or more species) recorded in the study area

Genus	Family	N spp	V end
<i>Xyris</i> L.	Xyridaceae	25	3
<i>Utricularia</i> L.	Lentibulariaceae	16	0
<i>Ouratea</i> Aubl.	Ochnaceae	15	8
<i>Myrcia</i> DC.	Myrtaceae	12	3
<i>Rhynchospora</i> Vahl	Cyperaceae	12	0
<i>Syngonanthus</i> Ruhland	Eriocaulaceae	12	2
<i>Macrobium</i> Schreb.	Fabaceae	11	2
<i>Abolboda</i> Bonpl.	Xyridaceae	10	1
<i>Palicourea</i> Aubl.	Rubiaceae	10	2
<i>Clusia</i> L.	Clusiaceae	9	2
<i>Hirtella</i> L.	Chrysobalanaceae	9	2
<i>Pagamea</i> Aubl.	Rubiaceae	9	2
<i>Lagenocarpus</i> Nees	Cyperaceae	8	0
<i>Licania</i> Aubl.	Chrysobalanaceae	8	0
<i>Macairea</i> DC.	Melastomataceae	8	0
<i>Trichantheium</i> Zuloaga & Morrone	Poaceae	8	1
<i>Byrsonima</i> Rich. ex Kunth	Malpighiaceae	7	0
<i>Miconia</i> Ruiz & Pav.	Melastomataceae	7	0
<i>Pachira</i> Aubl.	Malvaceae	7	1
<i>Retiniphyllum</i> Bonpl.	Rubiaceae	7	0
<i>Caraipa</i> Aubl.	Calophyllaceae	6	1
<i>Comolia</i> DC.	Melastomataceae	5	0
<i>Doliocarpus</i> Rol.	Dilleniaceae	6	0
<i>Ocotea</i> Aubl.	Lauraceae	6	0
<i>Paepalanthus</i> Mart.	Eriocaulaceae	5	3
<i>Polygala</i> L.	Polygalaceae	6	0
<i>Tococa</i> Aubl.	Melastomataceae	6	0
<i>Amphilophium</i> Kunth	Bignoniaceae	5	0
<i>Burmannia</i> L.	Burmanniaceae	5	1
<i>Guatteria</i> Ruiz & Pav.	Annonaceae	5	0
<i>Paspalum</i> L.	Poaceae	5	1
<i>Remijia</i> DC.	Rubiaceae	5	1
<i>Sauvagesia</i> L.	Ochnaceae	5	0

N spp: total number of species; V end: number of endemic species to the Venezuelan white-sand areas in the Amazonas state

(Cyperaceae), *Syngonanthus* (Eriocaulaceae), *Macrobium* (Fabaceae), *Abolboda* (Xyridaceae), and *Palicourea* (Rubiaceae). Among the richest genera, *Ouratea* is the one with the highest number of endemics, whereas *Utricularia* standouts for its lack of endemics in the area (Table 11.5). Some similarities are found with the nearby higher elevation open habitats of the Guayana Highlands. For example, *Xyris* is the second genus in number of species in Pantepui, and *Myrcia* and *Palicourea* are also among the top ten most diverse genera occurring on tepui summits (Riina et al. 2019).



## 11.5 Ecological Determinants of Open White-Sand Vegetation

The origin of non-forested ecosystems in areas with higher precipitation in the tropics has been explained by (a) human disturbances, including slash and burn agriculture and anthropic fires in places with fragile soils (e.g., Budowski 1956), (b) paleoclimatic influences (e.g., Eden 1974), (c) influence of soils physico-chemical properties, and (d) climate and morphodynamic processes. In addition, the alternating periods of water saturation and drought, together with nutrient deficiency are the most limiting factors for biomass accumulation in white-sand ecosystems, and constitute strong environmental filters that promote speciation and explain endemism and floristic composition.

Studies on white-sand forest have found that shortage of nitrogen in soils of low and tall Amazon caatinga forests around San Carlos de Río Negro and La Esmeralda (Amazonas state, Venezuela) appears to determine major structural and physiognomic features, and depth of aerated soil influences plant stature (Medina and Cuevas 1989, Coomes and Grubb 1996, and Chap. 4 in this book). On the other hand, Demarchi et al. (2018), studying plots of Amazonian white-sand forests in lower Río Negro (Brazil), indicated that the variable sum of bases was directly related to species composition, but that species richness and vegetation structure were not related to soil parameters. In our case, soil characteristics do not seem determinant in shaping vegetation structure or floristic composition, since most of the study areas share more or less similar soil properties with slight variations among them (see Chaps. 6 and 7).

An additional factor in some white-sand areas is the presence of high water tables caused by delayed drainage (Klinge and Cuevas 2000), which is due to an underlying hardpan that impedes the water flow, resulting in long periods of saturation even if the area appears dry on the surface (Adeney et al. 2016). Zinck (Chaps. 6 and 7) indicated some differences in drainage pattern within and among some of the study areas, and these could have potentially a stronger effect in vegetation structure, density, and species composition than nutrient availability.

Unfortunately, detailed studies about the influence of the edaphic mantles/substrates and drainage variation on vegetation structure and patterns of species richness and composition, as those carried out in some Amazonian forests, are still lacking for open white-sand vegetation of the Guayana Shield-Amazonian region.

---

## 11.6 Conservation of Amazonian White-Sand Areas

Recolonization after clearing is supposed to be extremely slow on Amazonian white-sand habitats because of limiting factors such as nutrient paucity and excessive drainage during dry season (Prance and Schubart 1978). During the rainy season, some of these ecosystems are subject to frequent flooding, but during the dry season they are submitted to drought stress, leading to the accumulation of a considerable amounts of dry woody and herbaceous matter making them highly susceptible to fires of anthropogenic origin (Prance and Schubart 1978; Vicentini 2004; Guimarães and Bueno 2016; Delprete 2018).

Some areas of open white-sand habitats in southern Venezuela have been slowly deteriorating in the last decades (Oliveira-Miranda et al. 2010a–c). Traditionally, there have been only marginal disturbances as a result of the activities of local human populations. Most local communities live outside of the open white-sand areas, preferentially along rivers or in more mesic areas. However, in the last years mining and its associated activities have been threatening parts of these unique ecosystems (Oliveira-Miranda et al. 2010a–c; Provita 2021). Mining in Amazonas is mostly concentrated in areas around the Cerro Yapacana (Provita 2021). However, the negative effect of mining on the landscape is highly localized in comparison with activities related to agriculture and livestock (Lozada and Carrero 2017). The lower slopes of Cerro Yapacana have been the focus of gold miners since at least the 1980s (Huber 1995c; Castillo and Salas 2007). Due to the political and economic crisis in Venezuela (Lozada 2019), there has been an increase in activities such as mining, logging, and shifting cultivation in all areas of the Venezuelan Guayana with human settlements.

Five of the six surveyed areas are at least in part within the limits of special administrative units for conservation, including the Yapacana National Park, Parima-Tapirapécó National Park, the Alto Orinoco-Casiquiare Biosphere Reserve, and several sectors of the Tepuis Natural Monument. The only exception is the Atabapo area, identified here as the richest in plant species and endemism of the Venezuelan Amazonas state white-sand open ecosystems. Our study provides the basic botanical knowledge to justify the protection of the highly diverse white-sand habitats of the Atabapo basin as well as the maintenance and further expansion of the current conservation units that include parts of the remainder white-sand areas of the Amazonas state.

Future biological research in the Venezuelan Amazonas state needs to be broadened beyond species inventories to include the creation of detailed vegetation and ecological maps, and the study of the impacts of human activities on these singular and fragile ecosystems.

**Acknowledgements** We are grateful to Alfred Zinck for encouraging us to write this chapter. To the staff of the VEN and MYF herbaria for their continuous support of the floristic inventory. Financial support for fieldwork was provided by the former Comisión para el Desarrollo del Sur (CODESUR) from the Venezuelan Government. To the editors and reviewers for their valuable suggestions.

---

## Appendix 11.1

Expeditions to lowland areas of the Amazonas state in southern Venezuela organized by Otto Huber (OH) between 1977 and 1983. The term “sabana” is used here informally for any kind of open vegetation (including white-sand meadows). Some data could not be retrieved because of lack of access to Huber’s notebooks during the elaboration of this work.

Expedition	Period	Participants	Date	Locality (verbatim)	Elev (m)	Lat N	Lon W
San Juan de Manapiare	26 Jan–04 Feb 1977	O. Huber, M. Huber, G. Stieffermann	29/1/77	Cuenca de San Juan de Manapiare. Cerros en la parte N del cerro Morrococoy.	200–350	05°20'	66°10'
San Juan de Manapiare	10–19 Oct 1977	O. Huber	11/10/77	Sabana de Canaripó (margen izquierda del bajo río Ventuari).	98	04°03'47"	66°49'45"
San Juan de Manapiare			16/10/77	Cuenca del río Manapiare; sabanas al pie de los cerros septentrionales del cerro Morrococoy, en los alrededores del sitio "Pozo de la Carolina", a unos 12 km al O de San Juan de Manapiare.	150–200	05°19'	66°06'
San Juan de Manapiare			16/10/77	Cuenca del río Manapiare; sabanas al pie de los cerros septentrionales del cerro Morrococoy, en los alrededores del sitio "Pozo de la Carolina", a unos 12 km al O de San Juan de Manapiare. Sabanas sobre las colinas, con <i>Caraipa llanorum</i> y <i>Vellozia tubiflora</i> .	200–250	05°19'	66°06'
San Juan de Manapiare			17/10/77	Cuenca del río Manapiare; sabanas situadas al pie de y en los cerros al N del cerro Morrococoy, a unos 10 km al O del pueblo de San Juan de Manapiare.	150–200	05°19'	66°06'
Cerro Yapacana	14 Feb–01 Mar 1978	O. Huber, P. Schwartz, J. Cerda, S. Gorzula, J. Roze, C. W. Myers, J. Daley, S.S. Tillett	17/2/78	Cabeceras del caño Cotúa, sitio llamado "Puerto", ± 5 km al E del río Orinoco, cerca de la base O del cerro Yapacana.	100	03°40'	66°50'

Cerro Yapacana	Idem	18/2/78	Cabeceras del caño Cotúa, primera sabana entre "Puerto" y el cerro Yapacana (sabana I de Maguire et al.)	100	03°40'	66°50'
Cerro Yapacana	Idem	19/2/78	Cabeceras del caño Cotúa, sitio llamado "Puerto". Sabana arbolada en la margen derecha de la laguna. Yapacana.	100	03°40'	66°50'
Cerro Yapacana	Idem	20/2/78	Cabeceras del caño Cotúa; entre "Puerto" y la primera sabana en el camino hacia el cerro Yapacana. En la primera sabana.	100	03°40'	66°50'
Cerro Yapacana	Idem	20/2/78	Cabeceras del caño Cotúa. Segunda sabana en el camino hacia el cerro Yapacana.	100	03°40'	66°50'
Cerro Yapacana	Idem	21/2/78	Cabeceras del caño Cotúa. Tercera sabana en el camino hacia el cerro Yapacana.	100	03°40'	66°50'
Cerro Yapacana	Idem	22/2/78	Cabeceras del caño Cotúa. Vegetación arbustiva en los alrededores de la laguna al final del caño. Yapacana.	100	03°40'	66°50'
Cerro Yapacana	Idem	23/2/78	Cabeceras del caño Cotúa. Entre el bosque húmedo semi-inundado inmediatamente precedente a la tercera sabana y el bosque húmedo al pie del cerro, lado S, del cerro Yapacana. En la tercera sabana.	100	03°40'	66°50'
Cerro Yapacana	Idem	25/2/78	Cabeceras del caño Cotúa. Entre el bosque húmedo semi-inundado inmediatamente precedente a la tercera sabana y el bosque húmedo	100	03°40'	66°50'

(continued)

Expedition	Period	Participants	Date	Locality (verbatim)	Elev (m)	Lat N	Lon W
Lower Ventuari	22 May 06 Jun 1978	O. Huber, M. Hoogmoed, J. Cerda	25/5/78	al pie del cerro, lado S del cerro Yapacana. En la tercera sabana. Sabana en medio del bosque húmedo al pie del cerro, lado SO. En el campamento base, cabeceras del caño Cottúa, sitio llamado "Puerto".			
Lower Ventuari		Idem	29/5/78	Atabapo: cabeceras del caño Cottúa, sitio llamado "Puerto".			
Lower Ventuari		Idem	30/5/78	Atabapo: Canaripó.			
Lower Ventuari		Idem	31/5/78	Atabapo: Canaripó			
Lower Ventuari		Idem	3/6/78	Atabapo: Canaripó.			
Lower Ventuari		Idem	4/6/78	Atabapo: Yapacana-savannas III.			
Heli-trip I	13-28 Aug 1978	O. Huber, J. Cerda, L. Chesney	15/8/78	Atabapo: Yapacana-savannas III, II. Atures: Manapiare.			
Heli-trip I		Idem	16/8/78	Atures: Palmensavanne caño Majagua.			
Heli-trip I		Idem	19/8/78	Atures: Sabana del Oso I.			
Heli-trip I		Idem	19/8/78	Atures: Sabana del Oso II.			
Heli-trip I		Idem	19/8/78	Atures: Sabana de cerro am río Parú S von Cacurí.			

Heli-trip I	Idem	19/8/78	Atures: Laja im Wald SE von Manapiare		
Heli-trip I	Idem	20/8/78	Atures: sabanas arenosas al SO del cerro Morrocoy		
Heli-trip I	Idem	20/8/78	Atures: Sabanas Alto Guanay en Caño Santo		
Heli-trip I	Idem	20/8/78	Atures: Alto Guanay [ohne Samml.]		
Heli-trip I	Idem	20/8/78	Atures: Savanneninsel E von Yutajé [ohne Samml.]		
Heli-trip I	Idem	22/8/78	Atures: Sabana arenosa del bajo Caño Coro coro (al N del bajo Ventuari)		
Heli-trip I	Idem	22/8/78	Atures: sabana de ripio del Caño Picure		
Heli-trip I	Idem	22/8/78	Atures:		
Heli-trip I	Idem	22/8/78	Atures: frente Carmelitas (bajo Ventuari) Feuchtsavanne		
Heli-trip I	Idem	22/8/78	Atures:		
Heli-trip I	Idem	23/8/78	Atures: Frente Sta. Bárbara, al N del Orinoco		
Heli-trip I	Idem	23/8/78	Atures: sídl. des Caño Guayapo		
Heli-trip I	Idem	23/8/78	Atures: Sabana arbustiva al N de la ribera del Orinoco medio		
Heli-trip I	Idem	23/8/78	Atabapo: Sabana de Mimicio		
Heli-trip I	Idem	24/8/78	Atabapo: Sabana de San Antonio		
Heli-trip I	Idem	24/8/78	Atabapo: sabanita al S del Cerro Yapacana		
Heli-trip I	Idem	24/8/78	Atabapo: sabana margen S del Caño Yagua		
Heli-trip I	Idem	24/8/78			

(continued)

Expedition	Period	Participants	Date	Locality (verbatim)	Elev (m)	Lat N	Lon W
				Atabapo: sabana al NE de la Laguna Yagua			
Heli-trip I		Idem	25/8/78	Atabapo: Maroa, campo de aterrizaje			
Heli-trip I		Idem	25/8/78	Atabapo: sabana de Pimichín			
Heli-trip I		Idem	25/8/78	Atabapo: sabana a lo largo del río Temi			
Heli-trip I		Idem	25/8/78	Atabapo: sabana cerca de Meroy, con lajas			
Heli-trip I		Idem	25/8/78	Atabapo: sabana de Guarinuma			
Heli-trip I		Idem	26/8/78	Atabapo: sabanas al S de Carmelitas, bajo Ventuari			
Heli-trip I		Idem	26/8/78	Atabapo: sabana de calceta al SE de Carmelitas			
Caño Yagua, Yapacana área	14 Feb–01 Mar 1978	O. Huber, P. Schwartz, J. Cerda, S. Gorzula, J. Roze, C. W. Myers, J. Daley, S.S. Tillet					
Heli-trip II	17 Feb–3 Mar 1979	O. Huber, J. Cerda, A. Zinck	17/2/79	Atures: sabanas de arena blanca con <i>Panicum orinocanum</i> cerca Munduapo, al S del bajo río Sipapo			
Heli-trip II		Idem		Atures: sabana y arbustal sobre arena al N del bajo río Autana			
Heli-trip II		Idem	18/2/79	Atabapo: sabana sobre arena blanca y afloramientos cuarzosos de arenisca, a unos 20 km al NO de San Antonio	120	03°30'	66°50'



Heli-trip II	Idem	18/2/79	Atabapo: sabanas ubicadas al pie NE del cerro Cucurito, ribera SE del caño Yagua	120	03°36'	66°34'
Heli-trip II	Idem	18/2/79	Atabapo: área pantanosa abierta, seca temporalmente, a la orilla derecha (O) del alto caño Yagua	130	03°44'	66°33'
Heli-trip II	Idem	19/2/79	Atures: sabana ubicada al pie SE del cerro Moriche	120	04°43'	66°22'
Heli-trip II	Idem	19/2/79	Atures: sabana con "tatuco" (montículos irregulares, en la región de las cabeceras del caño Coro-Coro (afluente derecho del bajo Ventuari), a aprox. 20 km al SO del cerro Moriche	130	04°32'	66°25'
Heli-trip II	Idem	19/2/79	Atures: sabana sobre arena blanca a unos 10 km de la ribera N del bajo río Ventuari, aprox. Frente al caño Maraya, a unos 10 km de distancia del río Ventuari	100	04°07'	66°57'
Heli-trip II	Idem	20/2/79	Atabapo: sabana sobre colinas y planicies a ± 10 km al E del caserío de Carmelitas, en la ribera S del bajo río Ventuari	220	04°07'	66°28'
Heli-trip II	Idem	20/2/79	Atabapo: región del alto caño Yagua, al O de la serranía El Tigre	130	03°52'	66°26'
Heli-trip II	Idem	20/2/79	Atabapo: sabanas sobre arena blanca al E del caño Perro de Agua, ribera derecha E del río Orinoco, poco antes de su confluencia con el río Ventuari	100	03°47'	67°00'

(continued)

Expedition	Period	Participants	Date	Locality (verbatim)	Elev (m)	Lat N	Lon W
Heli-trip II		Idem	21/2/79	Atures: sabanas ubicadas a unos 10 km al S del medio río Guayapo	100	04°10'	67°23'
Heli-trip II		Idem	22/2/79	Atabapo: La Esmeralda. Vegetación herbácea y arbustiva sobre la fila de colinas de arenisca al SE de la misión	130–150	03°11'	65°32'
Heli-trip II		Idem	23/2/79	Atabapo: sabana abierta sobre arena blanca, ± a 1 km al E del caserío de Guarinuma	95	03°37'	67°26'
Heli-trip II		Idem	23/2/79	Casiquiare: sabana arbustiva temporalmente secada, en la ribera S del medio caño San Miguel, a unos 60–70 km al E de la desembocadura en el río Guainía	100	02°37'	67°02'
Heli-trip II		Idem	24/2/79	Casiquiare: sabanita en la ribera S del caño San Miguel, a unos 30 km al E de la desembocadura en el río Guanía	90	02°38'	67°16'
Heli-trip II		Idem	24/2/79	Casiquiare: pequeña sabanita en la ribera O del caño Pimichín, un poco al S del caserío Pimichín	110	02°50'	67°33'
Heli-trip II		Idem	24/2/79	Casiquiare: pequeña sabanita al O del medio río Temi, aprox. A unos 5 km del río	100	02°57'	67°29'
Heli-trip II		Idem	24/2/79	Casiquiare: sabana sobre arena blanca a aprox. 5 km al O del bajo río Temi	100	03°12'	67°27'
Heli-trip II		Idem	26/2/79	Atabapo: sabanita ubicada a unos 10 km al NE del cerro Moriche, en la ribera E del medio río Ventuari.	120	04°48'	66°17'

Heli-trip II	Idem	27/2/79	Atabapo: sabana sobre arena blanca a aprox. 5 km al O del bajo río Temi.	130	04°58'	66°05'
Heli-trip II	Idem	27/2/79	Atabapo: sabana sobre arena blanca a unos 22 km al S de la confluencia entre los ríos Manapiare y Ventuari.	130	04°53'	66°06'
Heli-trip II	Idem	27/2/79	Atabapo: sabana y morichal a unos 22 km al S de la confluencia entre los ríos Manapiare y Ventuari, ± 1 km al NE del sitio 252.	130	04°53'	66°06'
Heli-trip II	Idem	27/2/79	Atures: sabana sobre arena blanca en el sector occidental del valle del medio caño Camani, al SO del cerro Morrocoy.	140	05°14'	66°12'
Heli-trip II	Idem	27/2/79	Atures: sabana recién quemada sobre aren blanca-grisácea, ubicada en el sector NE del valle del alto caño Camani.	150	05°21'	66°10'
Heli-trip II	Idem	28/2/79	Atures: sabana sobre cerros al pie de la Serranía de Guanay (lado O del abra de Guanay).	260	05°44'	66°21'
Heli-trip II	Idem	28/2/79	Atures: sabana ubicada en el fondo del valle del alto caño Guanay, poco más al S del paso del abra de Guanay.	170	05°48'	66°21'
Heli-trip II	Idem	28/2/79	Atures: sabana inundable en el valle del caño Guanay, aprox. en el centro del valle, a la altura del cerro El Santo.	150	05°42'	66°18'
Heli-trip II	Idem	1/3/79	Atures: sabanita ubicada en la base de la vertiente E de la fila de cerros ubicada al O del medio río Asita.	150	05°18'	65°37'

(continued)

Expedition	Period	Participants	Date	Locality (verbatim)	Elev (m)	Lat N	Lon W
Heli-trip II		Idem	1/3/79	Atures: sabana y morichal inundable en la base de la vertiente SO de la serranía de La Coroba, cuenca media del río Parucito.	150	05°30'	65°52'
Heli-trip II		Idem	1/3/79	Atures: sabanita entre colinas bajas al NO de la laguna Maguari, cuenca alta del río Parucito.	300	05°43'	65°48'
Heli-trip II		Idem	1/3/79	Atures: sabana recién quemada a ± 1 km al O de la pista de aterrizaje de Yutajé.	150	05°37'	66°07'
Heli-trip II		Idem	2/3/79	Atabapo: sabana de El Oso, en la ribera S del alto río Ventuari.	160	04°56'	65°25'
Heli-trip II		Idem	2/3/79	Atabapo.			
Heli-trip II		Idem	2/3/79	Atabapo: sabanita ubicada en la ribera N del alto río Parú, en el sector N del cerro Parú (Asisa).	500	04°36'	65°32'
Heli-trip II		Idem	3/3/79	Atabapo: sabanas gramíneas en la planicie central del sector N del cerro Parú (Asisa).	800	04°32'	65°31'
Heli-trip II		Idem	3/3/79	Atabapo: sabanas gramíneas en la planicie central del sector N del cerro Parú (Asisa).	850	04°33'	65°28'
Heli-trip III	25 Jun–04 Jul 1979	O. Huber, J. Cerda, A. García					
Heli-trip IV	30 Sep–12 Oct 1979	O. Huber, J. Cerda					

Heli-trip V	26 Feb– 14 Mar 1980	O. Huber, J. Cerda, A. Zinck	28/2/80	Atabapo: sabanas de arena blanca a unos 10 km al N del sector NE del cerro Yapacana.	100	03°44'	66°48'
Heli-trip V		Idem	28/2/80	Atabapo: al borde del alto caño Yagua, en zona de rebalse desecada.	130	03°44'	66°33'
Heli-trip V		Idem	28/2/80	Atabapo: sabana a unos 5 km al N de la laguna Yagua, al E del cerro Yapacana.	120	03°51'	66°32'
Heli-trip V		Idem	29/2/80	Atabapo: sabanas a unos 30 km al O de la serranía El Tigre, en la región del alto caño Yagua.	130	03°51'	66°27'
Heli-trip V		Idem	29/2/80	Atabapo: sabanas a unos 10 km al N de 597, al O de la serranía El Tigre, en la región del alto caño Yagua.	130	03°51'	66°27'
Heli-trip V		Idem	29/2/80	Atabapo: sabana sobre arena blanca a uno 5 km al S del río Ventuari, aprox. a 20 km al E de Carmelitas.	110	04°09'	66°29'
Heli-trip V		Idem	1/3/80	Casiquiare: pequeña sabana a unos 10 km al W del caño Pimichín y a unos 5 km al N de Tonina en el río Guainía.	100	02°53'	67°44'
Heli-trip V		Idem	1/3/80	Casiquiare: orilla del alto caño Pimichín.	100	02°54'	67°42'
Heli-trip V		Idem	1/3/80	Atabapo: sabanas con bancos de arena alargados en la región al S del medio caño Caname.	100	03°35'	67°11'
Heli-trip V		Idem	4/3/80	Atabapo: sabanas sobre la altiplanicie del cerro Mahedi, ribera N del río Ocamo medio.	600	02°58'	64°45'

(continued)

Expedition	Period	Participants	Date	Locality (verbatim)	Elev (m)	Lat N	Lon W
Heli-trip V		Idem	4/3/80	Atabapo: sabanas sobre la altiplanicie E del cerro Mahedi, en la ribera N del río Ocamo medio.	350	02°58'	64°43'
Heli-trip V		Idem	4/3/80	Atabapo: sabanas en la región del río Ocamo medio, en la ribera N, poco más río arriba de Guabutagüey-teri.	230	03°12'	64°37'
Heli-trip V		Idem	5/3/80	Atabapo: sabana de Culebra, ribera izquierda (S) del medio río Cunucunuma.	350	03°45'	65°47'
Heli-trip V		Idem	5/3/80	Atabapo: pequeña sabana al pie SE del cerro Huachamacari, en la ribera derecha del río Cunucunuma medio.	400	03°48'	65°43'
Heli-trip V		Idem	5/3/80	Atabapo: sabana sobre arena blanca a unos 10–12 km al O de Esmeralda, en la ribera derecha (N) del río Orinoco.	130	03°11'	65°37'
Heli-trip V		Idem	7/3/80	Atabapo: sierra de Parima, sabana sobre cerros en los alrededores de una pista de aterrizaje al N de Simarawochi.	850	03°49'	64°36'
Heli-trip V		Idem	7/3/80	Atabapo: sabana a unos 10–12 km al W de Esmeralda, en la ribera derecha (N) del río Orinoco.	125	03°11'	65°37'
Heli-trip V		Idem	8/3/80	Atabapo: pequeña sabana a 15 km al N de Esmeralda, entre el río Iguapé y el pie SE del cerro Duida.	300	03°19'	65°31'
Heli-trip V		Idem	8/3/80	Atabapo: pequeña sabana a unos 5 km al S del caserío Puruname en el río Puruname bajo.	100	03°22'	65°30'

Heli-trip V		Idem	9/3/80	Atures: sabana en la ribera derecha (N) del río Guayapo medio.	110	04°17'	67°17'
Heli-trip V		Idem	9/3/80	Atures: extensas sabanas a unos 10 km al SO del río Guayapo medio.	110	04°14'	67°30'
Heli-trip V		Idem	10/3/80	Casiquiare: sabana y caatinga abierta a unos 2-3 km al SE del bajo río Guasacavi.	90	03°08'	67°30'
Heli-trip V		Idem	10/3/80	Atabapo: sabana abierta a unos 20 km al S del medio caño Caname.	100	03°33'	67°12'
Heli-trip V		Idem	10/3/80	Atabapo: sabana a unos 40 km al NO de San Antonio y a unos 10 km al O de la ribera izquierda del río Orinoco, con afloramientos rocosos de arenisca.	100	03°40'	67°00'
Heli-trip V		Idem	11/3/80	Atabapo: sabana al S de Sta. Bárbara.			
Heli-trip VI	14-29 Jul 1980	O. Huber, A. Zinck, S.S. Tillett	14/7/80	Atures: sabana ubicada a unos 4 km al O de la serranía del Cuao.	100	04°59'	67°32'
Heli-trip VI		Idem	14/7/80	Atures: vegetación arbustiva sobre banco de arena blanca a unos 20 km al NO del cerro Autana.	100	04°54'	67°36'
Heli-trip VI		Idem	14/7/80	Atures: sabana grande ubicada a unos 6 km al E del río Orinoco, frente a Isla Ratón.	90	05°06'	67°45'
Heli-trip VI		Idem	15/7/80	Atures: pequeña sabana sobre arena blanca a ± 5 km al NE de Limón de Parhueña.	70	05°54'	67°16'
Heli-trip VI		Idem	16/7/80	Atures: matorrales arbustivos extensos a unos 5 km al SE del cerro Autana y a unos 2 km al N del medio río Autana.	100	04°48'	67°26'

(continued)



Expedition	Period	Participants	Date	Locality (verbatim)	Elev (m)	Lat N	Lon W
Heli-trip VI		Idem	16/7/80	Atures: arbustal abierto sobre arena blanca sobre glacis a unos 12 km al OSO del cerro Autana	150	04°51'	67°34'
Heli-trip VI		Idem	18/7/80	Atabapo: sabana ubicada a unos 8 km al N de la laguna Yagua.	100	03°52'	66°35'
Heli-trip VI		Idem	20/7/80	Atabapo: sabana sobre arena blanca a unos 2 km al O de San Antonio del Orinoco.	120	03°27'	67°47'
Heli-trip VI		Idem	22/7/80	Atabapo: pequeña sabana ubicada a unos 2 km al S del medio río Puruname, al SE del caserío de Puruname.	100	03°20'	66°32'
Heli-trip VI		Idem	22/7/80	Atabapo: sabanita sobre arena blanca a unos 5 km al S de la laguna Yagua.	100	03°43'	66°38'
Heli-trip VI		Idem	27/7/80	Atures: sabana ubicada en la ribera izquierda (S) del río Guayapo medio.	100	04°14'	67°22'
Heli-trip VI		Idem	27/7/80	Atures: sabana ubicada a ± 2 km al N del río Guayapo medio.	100	04°16'	67°23'
Heli-trip VI		Idem	27/7/80	Atabapo: sabanita sobre arena blanca a unos 5 km al S de la laguna Yagua.	100	03°49'	66°50'
Heli-trip VI		Idem	27/7/80	Atabapo: amplias sabanas ubicadas a 1 km al N de la laguna Yagua.	100	03°50'	66°35'
Heli-trip VI		Idem	28/7/80	Atures: sabanas ubicadas a unos 4 km al N del río Sipapo medio, aprox. a unos 5 km al O del macizo del Sipapo.	120	04°36'	67°12'

San Carlos de Río Negro	15-17 Sep 1981	O. Huber, R. Herrera, H. Fölster, W. Franco	16/9/80	Río Negro: "Bana de Mary" en el KM 11 de la Pica San Carlos-Solano.	120	01°56'	67°03'
Heli-trip VII	04-19 Feb 1981	O. Huber, A. Zinck, E. Medina	6/2/81	Río Negro: pequeña sabana ubicada en la margen derecha (E) del bajo río Siapa.	125	01°57'	66°02'
Heli-trip VII		Idem	6/2/81	Río Negro: domo rocoso de gneiss granitoide ubicado aprox. 15 km al E de la punta septentrional del cerro Aracamuni.	350	01°41'	65°41'
Heli-trip VII		Idem	7/2/81	Río Negro: pequeña sabana en la ribera izquierda (S) del bajo río Siapa, poco distante de su desembocadura en el río Casiquiare.	125	02°05'	66°25'
Heli-trip VII		Idem	8/2/81	Río Negro: pequeña sabana en la margen derecha del bajo río Siapa, poco debajo de la boca del río Manipitiare.	125	02°06'	66°12'
Heli-trip VII		Idem	8/2/81	Río Negro: extensa sabana en la margen derecha del bajo río Pasimoni.	125	01°35'	66°33'
Heli-trip VII		Idem	9/2/81	Río Negro: río Pasimoni.			
Heli-trip VII		Idem	10/2/81	Río Negro: Cerro Aracamuni.	750		
Heli-trip VII		Idem	11/2/81	Casiquiare: cabeceras Caño Pimichín.			
Heli-trip VII		Idem	11/2/81	Casiquiare: S río Guasacavi.			
Heli-trip VII		Idem	13/2/81	Atabapo: Sierra Parima.	1200		

(continued)

Expedition	Period	Participants	Date	Locality (verbatim)	Elev (m)	Lat N	Lon W
Heli-trip VII		Idem	13/2/81	Atabapo: Sierra Parima, con indígenas.	1100		
Heli-trip VII		Idem	14/2/81	Río Negro: colina de arenisca Río Siapa.	600		
Heli-trip VII		Idem	14/2/81	Río Negro: Serranía Vinilla.	400		
Heli-trip VII		Idem	15/2/81	Río Negro: rebalse en el bajo río Yatúa.			
Heli-trip VII		Idem	17/2/81	Castiquare: cabeceras río San Miguel.			
Heli-trip VII		Idem	18/2/81	Atabapo: pequeñas sabanas ubicadas en la ribera izquierda del bajo río Ventuari, unos 10 km al NE de la desembocadura del caño Marueta.	110	04°18'	66°16'
Heli-trip VIII	11-17 Jun 1981	O. Huber, R. Hidalgo	12/6/81	Atabapo: helechales y formaciones secundarias en la Sierra Parima, aprox. 35 km al NNE de Parima "B", cabeceras del río Ocamo.	1150	03°03'	64°13'
Heli-trip VIII		Idem	12/6/81	Atabapo: extensa sabana sobre glacis al pie del cerro Duida, aprox. 6 km al NNO de La Esmeralda.	250	03°14'	65°34'
Heli-trip VIII		Idem	13/6/81	Río Negro: sabanas abiertas sobre altiplanicie en la Serranía del Vinilla, ± 20 km al SO de Mavaca, hacia el borde SO de la meseta.	760	02°20'	65°22'
Heli-trip VIII		Idem	13/6/81	Río Negro: sabana colinosa en el sector central de una altiplanicie en la serranía del Vinilla, aprox. 20 km al SO de Mavaca.	420	02°26'	65°20'

Heli-trip VIII	Idem	14/6/81	Atabapo: sabana en la ribera derecha del medio río Asisa, aprox. a unos 10 km al O de la serranía Asisa.	250	04°29'	65°46'
Heli-trip VIII	Idem	14/6/81	Atabapo: río Asisa.			
Heli-trip VIII	Idem	15/6/81	Atabapo: Cerro Cucurito, Caño Yagua.			
Heli-trip VIII	Idem	16/6/81	Atures: río Sipapo medio.			
Caño Puruname	O. Huber, J. Cerda, S. Gorzula, G. Medina, E. Alvarez, S. S. Tillett					
Sabana Yapacana	O. Huber, R. Kral	25 May–09 Jun 1982 8–12 Aug 1983	Atabapo: pie oeste del Cerro Yapacana, entre la laguna del Caño Cotúa y el pie del cerro	100	03°38'	66°52'

## Appendix 11.2

Checklist of taxa (species and infraspecies) of vascular plants recorded in the six open white-sand areas sampled in Amazonas state, southern Venezuela

Family	Taxon	Habit	Sip	Cam	Ven	Yap	Ata	Pas
Alismataceae	<i>Helanthium tenellum</i> (Mart. ex Schult. & Schult. f.) Britton	H				1		1
Anacardiaceae	<i>Tapirira guianensis</i> Aubl.	T		1		1	1	
Annonaceae	<i>Duguetia dimorphopetala</i> R.E. Fr.	S/S	1			1	1	
Annonaceae	<i>Duguetia venezuelana</i> R.E. Fr.	S/S				1		
Annonaceae	<i>Gutteria atabapensis</i> Aristeg. ex D.M. Johnson & N.A. Murray	S/S					1	
Annonaceae	<i>Gutteria foliosa</i> Benth.	S/S					1	
Annonaceae	<i>Gutteria punctata</i> (Aubl.) R.A. Howard	S/S					1	1
Annonaceae	<i>Gutteria maguirei</i> R.E. Fr.	S/S				1	1	
Annonaceae	<i>Gutteria maypurensis</i> Kunth	S/S			1	1		
Annonaceae	<i>Oxandra espintana</i> (Spruce ex Benth.) Baill.	S/S				1		
Annonaceae	<i>Tetrameranthus duckei</i> R.E. Fr.	T					1	1
Annonaceae	<i>Xylopia aromatica</i> (Lam.) Mart.	S/S			1			
Annonaceae	<i>Xylopia emarginata</i> Mart.	T				1		
Annonaceae	<i>Xylopia ligustrifolia</i> Dunal	T				1		
Apocynaceae	<i>Aspidosperma verruculosum</i> Müll. Arg	T	1			1		1
Apocynaceae	<i>Blepharodon glaucescens</i> (Decne.) Fontella	Cw	1					

(continued)

Family	Taxon	Habit	Sip	Cam	Ven	Yap	Ata	Pas
Apocynaceae	<i>Couma catingae</i> Ducke	T					1	
Apocynaceae	<i>Ditassa buntingii</i> (Morillo) Liede	Cw					1	
Apocynaceae	<i>Ditassa franciscoi</i> (Morillo) Liede	Cw	1					1
Apocynaceae	<i>Ditassa nigrescens</i> (E. Fourn.) W.D. Stevens	Cw						1
Apocynaceae	<i>Ditassa sobradoi</i> (Morillo) Liede	Cw					1	1
Apocynaceae	<i>Forsteronia lucida</i> Markgr.	Cw				1		1
Apocynaceae	<i>Galactophora</i> <i>crassifolia</i> (Müll. Arg.) Woodson	Cw	1	1			1	
Apocynaceae	<i>Galactophora</i> <i>pulchella</i> Woodson	Cw				1		1
Apocynaceae	<i>Galactophora</i> <i>pumila</i> Monach.	Cw	1			1	1	
Apocynaceae	<i>Himatanthus</i> <i>attenuatus</i> (Benth.) Woodson	S/S						1
Apocynaceae	<i>Himatanthus</i> <i>semilunatus</i> Markgr.	S/S				1		
Apocynaceae	<i>Lacmellea</i> <i>microcarpa</i> (Müll. Arg.) Markgr.	S/S	1		1		1	
Apocynaceae	<i>Lacmellea pygmaea</i> Monach.	S/S				1	1	
Apocynaceae	<i>Malouetia</i> <i>molongo</i> M.E. Endress	S/S					1	
Apocynaceae	<i>Mandevilla huberi</i> Morillo	Ch				1		
Apocynaceae	<i>Mandevilla</i> <i>javitensis</i> (Kunth) K. Schum.	Ch					1	1
Apocynaceae	<i>Mandevilla</i> <i>obtusifolia</i> Monach.	Ch					1	
Apocynaceae	<i>Tassadia guanchezii</i> (Morillo) Liede & Meve	Ch			1	1	1	1
Apocynaceae	<i>Tassadia stricta</i> (E. Fourn.) Liede & Rapini	Ch	1		1	1	1	1

(continued)

Family	Taxon	Habit	Sip	Cam	Ven	Yap	Ata	Pas
Apocynaceae	<i>Metastelma huberi</i> (Morillo) Liede	Ch	1		1	1	1	1
Apocynaceae	<i>Nephradenia pendula</i> Rusby	Ch	1	1	1	1		
Apocynaceae	<i>Molongum laxum</i> (Benth.) Pichon	T						1
Apocynaceae	<i>Molongum lucidum</i> (Kunth) Zarucchi	S/S					1	1
Apocynaceae	<i>Odontadenia geminata</i> Müll. Arg.	Cw				1		
Apocynaceae	<i>Odontadenia glauca</i> Woodson	Cw				1		
Apocynaceae	<i>Parahancornia surrogata</i> Zarucchi	T						1
Apocynaceae	<i>Spongiosperma oleifolium</i> (Monach.) Zarucchi	S/S				1		
Aquifoliaceae	<i>Ilex divaricata</i> Mart. ex Reissek	T	1			1	1	1
Aquifoliaceae	<i>Ilex savannarum</i> Wurdack var. <i>savannarum</i>	T				1		
Aquifoliaceae	<i>Ilex spruceana</i> Reissek	T				1	1	1
Araceae	<i>Anthurium bonplandii</i> G.S. Bunting	H				1	1	1
Araceae	<i>Anthurium guanchezii</i> G.S. Bunting	H	1					
Araceae	<i>Caladium humboldtii</i> (Raf.) Schott	H					1	
Araceae	<i>Philodendron dyscarpium</i> R.E. Schult.	H	1			1	1	
Araceae	<i>Philodendron maroae</i> G.S. Bunting	H					1	
Araceae	<i>Philodendron pimichinense</i> G.S. Bunting						1	
Araceae	<i>Philodendron remifolium</i> ssp. <i>sabulosum</i> (G.S. Bunting) G.S. Bunting						1	
Araceae	<i>Thaumatophyllum venezuelense</i> (G.S. Bunting) Sakur, Calazans & Mayo						1	1
Araceae	<i>Philonotion spruceanum</i> Schott	H	1			1	1	

(continued)



Family	Taxon	Habit	Sip	Cam	Ven	Yap	Ata	Pas
Araceae	<i>Urospatha sagittifolia</i> Schott	H				1		
Araceae	<i>Urospatha wurdackii</i> (G.S. Bunting) A. Hay	H				1	1	
Araceae	<i>Xanthosoma exiguum</i> G.S. Bunting	H					1	
Araceae	<i>Xanthosoma maroae</i> G.S. Bunting	H					1	
Araliaceae	<i>Didymopanax pimichinensis</i> (Maguire, Steyer. & Frodin) Fiaschi & G.M. Plunkett	T					1	
Araliaceae	<i>Crepinella spruceana</i> (Seem.) G.M. Plunkett, Lowry & D.A. Neill	T					1	1
Arecaceae	<i>Attalea racemosa</i> Spruce	T	1				1	
Arecaceae	<i>Bactris campestris</i> Poepp.	S/S				1	1	
Arecaceae	<i>Bactris major</i> Jacq.	S/S				1		
Arecaceae	<i>Leopoldinia pulchra</i> Mart.	T				1	1	
Arecaceae	<i>Mauritia carana</i> Wallace	T				1	1	
Arecaceae	<i>Mauritiella pumila</i> Burret	T					1	
Asteraceae	<i>Calea abelioides</i> S.F. Blake	S/S	1					
Asteraceae	<i>Calea tolimana</i> Hieron.	S/S		1	1	1		
Asteraceae	<i>Gongylolepis martiana</i> (Baker) Steyer. & Cuatrec.	S/S	1		1		1	1
Asteraceae	<i>Mikania amazonica</i> Baker	Cw					1	
Asteraceae	<i>Mikania solidinervia</i> V.M. Badillo	Cw		1				
Asteraceae	<i>Piptocoma spruceana</i> (Benth.) Pruski	T	1				1	

(continued)

Family	Taxon	Habit	Sip	Cam	Ven	Yap	Ata	Pas
Asteraceae	<i>Stenopadus campestris</i> Maguire & Wurdack	S/S	1				1	1
Asteraceae	<i>Stenopadus cucullatus</i> Maguire & Wurdack	S/S		1				
Asteraceae	<i>Unxia camphorata</i> L. f.	S/S		1		1	1	
Asteraceae	<i>Unxia suffruticosa</i> (Baker) Stuessy	S/S				1		
Bignoniaceae	<i>Amphilophium arenarium</i> (A.H. Gentry) L.G. Lohmann	Cw	1	1	1			
Bignoniaceae	<i>Amphilophium elongatum</i> (Vahl) L.G. Lohmann	Cw		1				
Bignoniaceae	<i>Amphilophium laeve</i> (Sandwith) L.G. Lohmann	Cw				1		
Bignoniaceae	<i>Amphilophium magnoliifolium</i> (Kunth) L.G. Lohmann	Cw		1			1	
Bignoniaceae	<i>Amphilophium monophyllum</i> (Sandwith) L.G. Lohmann	Cw	1			1	1	1
Bignoniaceae	<i>Fridericia nigrescens</i> (Sandwith) L.G. Lohmann	Cw	1	1	1		1	
Bignoniaceae	<i>Handroanthus barbatus</i> (E. Mey.) Mattos	T				1		
Bignoniaceae	<i>Handroanthus</i> sp. A	T				1	1	
Bignoniaceae	<i>Jacaranda ceratophora</i> (A.H. Gentry) Ragsac	T	1			1	1	
Bignoniaceae	<i>Martinella iquitosensis</i> A. Samp.	Cw						1
Bignoniaceae	<i>Martinella obovata</i> Bureau & K. Schum.	Cw				1	1	
Bignoniaceae		Cw				1	1	

(continued)

Family	Taxon	Habit	Sip	Cam	Ven	Yap	Ata	Pas
	<i>Pleonotoma exserta</i> A.H. Gentry							
Bonnetiaceae	<i>Archytaea angustifolia</i> Maguire	S/S					1	1
Bonnetiaceae	<i>Archytaea triflora</i> Mart.	S/S				1		
Bonnetiaceae	<i>Bonnetia sessilis</i> Benth.	S/S	1			1	1	1
Bromeliaceae	<i>Aechmea brevicollis</i> L.B. Sm.	Eh	1			1	1	
Bromeliaceae	<i>Aechmea contracta</i> Baker	Eh					1	
Bromeliaceae	<i>Aechmea corymbosa</i> Mez	Eh					1	
Bromeliaceae	<i>Aechmea politii</i> L.B. Sm.	Eh					1	
Bromeliaceae	<i>Brewcaria hohenbergioides</i> (L.B. Sm.) B. Holst	H	1	1				
Bromeliaceae	<i>Brewcaria reflexa</i> (L.B. Sm.) B. Holst	H	1				1	
Bromeliaceae	<i>Brocchinia hechtiioides</i> Mez	H	1					
Bromeliaceae	<i>Brocchinia prismatica</i> L.B. Sm.	H				1	1	
Bromeliaceae	<i>Navia huberiana</i> L.B. Sm., Steyerm. & H. Rob.	H				1		
Bromeliaceae	<i>Pitcairnia juncooides</i> L.B. Sm.	H	1	1	1	1	1	1
Bromeliaceae	<i>Vriesea melgueiroi</i> I. Ramírez & Carnevali	Eh	1					
Bromeliaceae	<i>Vriesea socialis</i> L.B. Sm. Ex R.E. Schult.	Eh					1	
Burmanniaceae	<i>Apteria aphylla</i> Barnhart	H				1	1	
Burmanniaceae	<i>Burmannia bicolor</i> Mart.	H		1				
Burmanniaceae	<i>Burmannia capitata</i> Mart.	H				1		
Burmanniaceae	<i>Burmannia compacta</i> Maas & H. Mass	H					1	
Burmanniaceae	<i>Burmannia dasyantha</i> Mart.	H				1		

(continued)

Family	Taxon	Habit	Sip	Cam	Ven	Yap	Ata	Pas
Burmanniaceae	<i>Burmannia polygaloides</i> Schltr.	H					1	1
Burseraceae	<i>Dacryodes glabra</i> (Steerm.) Cuatrec.	T	1			1		
Burseraceae	<i>Dacryodes microcarpa</i> Cuatrec.	T	1			1		
Burseraceae	<i>Protium carolense</i> Daly	T					1	
Burseraceae	<i>Protium heptaphyllum</i> ssp. <i>ulei</i> (Swart) Daly	T	1			1	1	
Burseraceae	<i>Protium reticulatum</i> (Engl.) Engl.	T					1	1
Celastraceae	<i>Cheiloclinium klugii</i> A.C. Sm.	Cw	1					
Celastraceae	<i>Maytenus huberi</i> Steerm.	T	1	1				
Celastraceae	<i>Maytenus insculpta</i> Steerm.	T		1				
Chrysobalanaceae	<i>Gaulettia canomensis</i> (Mart.) Sothers & Prance	T				1	1	
Chrysobalanaceae	<i>Couepia paraensis</i> ssp. <i>glaucescens</i> (Spruce ex Hook. f.) Prance	T	1			1		
Chrysobalanaceae	<i>Hirtella adderleyi</i> Prance	T	1		1	1	1	
Chrysobalanaceae	<i>Hirtella bullata</i> Benth.	T	1		1			
Chrysobalanaceae	<i>Hirtella cordifolia</i> Prance	T						1
Chrysobalanaceae	<i>Hirtella longipedicellata</i> Prance	T		1	1			
Chrysobalanaceae	<i>Hirtella paniculata</i> Sw.	T					1	
Chrysobalanaceae	<i>Hirtella pimichina</i> Lasser & Maguire	T				1	1	
Chrysobalanaceae	<i>Hirtella scabra</i> Benth.	T	1	1	1	1		
Chrysobalanaceae	<i>Hirtella subscandens</i> Spruce ex Hook. f.	T					1	
Chrysobalanaceae	<i>Hirtella ulei</i> Pilg.	T	1			1	1	
Chrysobalanaceae		T				1	1	1

(continued)

Family	Taxon	Habit	Sip	Cam	Ven	Yap	Ata	Pas
	<i>Leptobalanus apetalus</i> (E. Mey.) Sothers & Prance							
Chrysobalanaceae	<i>Licania cordata</i> Prance	T				1	1	1
Chrysobalanaceae	<i>Licania foldatsii</i> Prance	T					1	
Chrysobalanaceae	<i>Licania hypoleuca</i> Benth.	T					1	1
Chrysobalanaceae	<i>Hymenopus intrapetiolaris</i> (Spreng. ex Hook. f.) Sothers & Prance	T	1			1	1	
Chrysobalanaceae	<i>Licania lanceolata</i> Prance	T	1			1	1	
Chrysobalanaceae	<i>Licania mollis</i> Benth.	T				1		
Chrysobalanaceae	<i>Licania orbicularis</i> Spruce ex Hook. f.	T					1	1
Chrysobalanaceae	<i>Leptobalanus parvifolius</i> (Huber) Sothers & Prance	T				1	1	
Chrysobalanaceae	<i>Licania savannarum</i> Prance	T				1	1	1
Chrysobalanaceae	<i>Licania steyermarkii</i> Maguire	T						1
Chrysobalanaceae	<i>Leptobalanus wurdackii</i> (Prance) Sothers & Prance	T		1			1	1
Calophyllaceae	<i>Caraipa caespitosa</i> F.N. Cabral	T					1	
Calophyllaceae	<i>Caraipa grandifolia</i> Mart.	T				1	1	1
Calophyllaceae	<i>Caraipa llanorum</i> Cuatrec. ssp. <i>llanorum</i>	T	1	1	1	1	1	1
Calophyllaceae	<i>Caraipa llanorum</i> ssp. <i>cordifolia</i> Kubitzki	T		1	1	1		
Calophyllaceae	<i>Caraipa longipedicellata</i> Steyerm.	T				1	1	
Calophyllaceae	<i>Caraipa savannarum</i> Kubitzki	T				1		1

(continued)

Family	Taxon	Habit	Sip	Cam	Ven	Yap	Ata	Pas
Calophyllaceae	<i>Caraipa acutata</i> F.N. Cabral	S/S					1	
Clusiaceae	<i>Clusia columnaris</i> Engl.	T	1	1	1	1	1	
Clusiaceae	<i>Clusia gratula</i> Maguire	T					1	1
Clusiaceae	<i>Clusia lopezii</i> Maguire	T				1	1	1
Clusiaceae	<i>Clusia opaca</i> Maguire	T				1	1	
Clusiaceae	<i>Clusia palmicida</i> Rich. ex Planch. & Triana	T	1			1	1	
Clusiaceae	<i>Clusia renggerioides</i> Planch. & Triana	T				1		1
Clusiaceae	<i>Clusia spathulaefolia</i> Engl.	T				1	1	
Clusiaceae	<i>Clusia troncosii</i> Maguire	T	1	1		1		
Clusiaceae	<i>Clusia viscida</i> Engl.	T		1			1	
Clusiaceae	<i>Tovomita stergiosii</i> Cuello	T	1			1		1
Clusiaceae	<i>Tovomita eggersii</i> Vesque	T				1	1	
Combretaceae	<i>Terminalia crispialata</i> (Ducke) Alwan & Stace	T				1	1	1
Combretaceae	<i>Terminalia ramatuella</i> Alwan & Stace	T	1	1			1	
Combretaceae	<i>Terminalia virens</i> (Eichler) Alwan & Stace	T				1	1	
Combretaceae	<i>Terminalia yapacana</i> Maguire	T	1		1	1	1	
Connaraceae	<i>Conarus cordatus</i> L.A. Vidal, Carbonó & Forero	Cw	1		1		1	1
Connaraceae	<i>Conarus coriaceus</i> G. Schellenb.	Cw	1				1	1
Cyclanthaceae	<i>Sphaeradenia amazonica</i> Harling	H					1	
Cyperaceae	<i>Bulbostylis capillaris</i> (L.) Kunth ex C.B. Clarke	H	1			1		1

(continued)

Family	Taxon	Habit	Sip	Cam	Ven	Yap	Ata	Pas
Cyperaceae	<i>Bulbostylis junciformis</i> (Kunth) C.B. Clarke	H				1		
Cyperaceae	<i>Bulbostylis lanata</i> (Kunth) Lindm.	H	1	1	1	1	1	
Cyperaceae	<i>Bulbostylis schomburgkiana</i> (Steud.) M.T. Strong	H				1	1	
Cyperaceae	<i>Calyptracarya monocephala</i> Steud.	H				1	1	
Cyperaceae	<i>Diplacrum capitatum</i> Boeckeler	H				1		
Cyperaceae	<i>Lagenocarpus amazonicus</i> (C.B. Clarke) H. Pfeiff.	H	1	1		1	1	1
Cyperaceae	<i>Lagenocarpus celiae</i> T. Koyama & Maguire	H	1		1	1	1	1
Cyperaceae	<i>Lagenocarpus eriopodus</i> T. Koyama & Maguire	H				1		
Cyperaceae	<i>Lagenocarpus guianensis</i> Nees ssp. <i>guianensis</i>	H				1	1	1
Cyperaceae	<i>Lagenocarpus pendulus</i> T. Koyama	H					1	
Cyperaceae	<i>Lagenocarpus rigidus</i> Nees	H		1		1	1	
Cyperaceae	<i>Lagenocarpus sabanensis</i> Gilly	H	1		1	1	1	1
Cyperaceae	<i>Lagenocarpus verticillatus</i> (Spreng.) T. Koyama & Maguire	H	1			1	1	1
Cyperaceae	<i>Rhynchospora albida</i> Boeckeler	H				1	1	
Cyperaceae	<i>Rhynchospora barbata</i> Kunth	H		1	1	1		
Cyperaceae	<i>Rhynchospora bolivarana</i> Steerm.	H					1	
Cyperaceae		H				1	1	1

(continued)



Family	Taxon	Habit	Sip	Cam	Ven	Yap	Ata	Pas
	<i>Rhynchospora capitata</i> Roem. & Schult.							
Cyperaceae	<i>Rhynchospora dentinix</i> C.B. Clarke	H	1	1	1		1	
Cyperaceae	<i>Rhynchospora duckei</i> R. Gross	H					1	1
Cyperaceae	<i>Rhynchospora filiformis</i> Vahl	H		1		1	1	
Cyperaceae	<i>Rhynchospora globosa</i> (Kunth) Roem. & Schult.	H				1		
Cyperaceae	<i>Rhynchospora longibracteata</i> Boeckeler	H				1	1	
Cyperaceae	<i>Rhynchospora maguireana</i> T. Koyama	H	1			1	1	
Cyperaceae	<i>Rhynchospora puber</i> (Vahl) Boeckeler	H				1	1	
Cyperaceae	<i>Rhynchospora tenuis</i> Link	H		1		1	1	1
Cyperaceae	<i>Scleria amazonica</i> Camelb., M.T. Strong & Goetgh.	H	1			1	1	
Cyperaceae	<i>Scleria cyperina</i> Kunth	H				1		
Cyrillaceae	<i>Cyrilla racemiflora</i> L.	S/S				1	1	
Dilleniaceae	<i>Davilla nitida</i> (Vahl) Kubitzki	Cw			1	1	1	
Dilleniaceae	<i>Doliocarpus areolatus</i> Kubitzki	Cw			1		1	
Dilleniaceae	<i>Doliocarpus dentatus</i> ssp. <i>undulatus</i> (Eichler) Kubitzki	Cw	1		1	1		
Dilleniaceae	<i>Doliocarpus leiophyllus</i> Kubitzki	Cw	1			1	1	
Dilleniaceae	<i>Doliocarpus paucinervis</i> Kubitzki	Cw				1	1	
Dilleniaceae		Cw				1	1	

(continued)

Family	Taxon	Habit	Sip	Cam	Ven	Yap	Ata	Pas
	<i>Doliocarpus savannarum</i> Sandwith							
Dilleniaceae	<i>Doliocarpus spraguei</i> Cheesman	Cw			1	1		
Dioscoreaceae	<i>Dioscorea cuspidata</i> Humb. & Bonpl. ex Willd.	Ch					1	
Dioscoreaceae	<i>Dioscorea fodinarum</i> Kunth	Ch				1	1	
Droseraceae	<i>Drosera biflora</i> Willd. ex Roem. & Schult.	H	1			1	1	1
Droseraceae	<i>Drosera cayennensis</i> Sagot	H	1					
Droseraceae	<i>Drosera esmeraldae</i> (Steyerm.) Maguire & Wurdack	H	1	1		1	1	
Droseraceae	<i>Drosera sessilifolia</i> A. St.-Hil.	H	1					
Ebenaceae	<i>Lissocarpa benthamii</i> Gürke	T	1			1	1	1
Elaeocarpaceae	<i>Sloanea floribunda</i> Spruce ex Benth.	T					1	1
Ericaceae	<i>Agarista duckei</i> (Huber) Judd	S/S				1		
Ericaceae	<i>Bejaria sprucei</i> Meisn.	S/S					1	
Ericaceae	<i>Vaccinium puberulum</i> Klotzsch ex Meisn. var. <i>puberulum</i>	S/S	1					
Eriocaulaceae	<i>Eriocaulon humboldtii</i> Kunth	H		1		1		
Eriocaulaceae	<i>Eriocaulon tenuifolium</i> Klotzsch ex Körn.	H	1		1	1	1	
Eriocaulaceae	<i>Paepalanthus aristatus</i> Moldenke	H				1	1	
Eriocaulaceae	<i>Paepalanthus fasciculatus</i> Kunth	H					1	
Eriocaulaceae	<i>Paepalanthus chiquitensis</i> Herzog	H				1		
Eriocaulaceae	<i>Paepalanthus polytrichoides</i> Kunth	H	1			1		
Eriocaulaceae		H	1		1	1		

(continued)

Family	Taxon	Habit	Sip	Cam	Ven	Yap	Ata	Pas
	<i>Paepalanthus yapacanensis</i> var. <i>hirsutus</i> (Moldenke) Hensold							
Eriocaulaceae	<i>Paepalanthus yapacanensis</i> (Moldenke) Hensold var. <i>yapacanensis</i>	H	1			1		1
Eriocaulaceae	<i>Syngonanthus acephalus</i> Hensold	H					1	
Eriocaulaceae	<i>Syngonanthus amapensis</i> Moldenke	H			1	1		
Eriocaulaceae	<i>Syngonanthus biformis</i> Gleason	H	1	1				
Eriocaulaceae	<i>Syngonanthus caulescens</i> Ruhland	H		1		1		
Eriocaulaceae	<i>Syngonanthus cowanii</i> Moldenke	H	1			1	1	1
Eriocaulaceae	<i>Syngonanthus humboldtii</i> Ruhland	H		1	1	1		
Eriocaulaceae	<i>Syngonanthus longipes</i> Gleason	H			1	1		1
Eriocaulaceae	<i>Syngonanthus nitens</i> Ruhland	H	1		1	1	1	
Eriocaulaceae	<i>Syngonanthus ottohuberi</i> Hensold	H				1		
Eriocaulaceae	<i>Comanthera reflexa</i> (Gleason) L.R. Parra & Giul.	H	1		1	1	1	1
Eriocaulaceae	<i>Syngonanthus setifolius</i> Hensold	H				1	1	
Eriocaulaceae	<i>Syngonanthus tenuis</i> var. <i>bulbifer</i> (Huber) Hensold	H	1				1	
Eriocaulaceae	<i>Syngonanthus tenuis</i> Ruhland var. <i>tenuis</i>	H	1			1	1	
Eriocaulaceae	<i>Syngonanthus williamsii</i> (Moldenke) Hensold	H				1	1	
Eriocaulaceae	<i>Comanthera xeranthemoides</i> (Bong.) L.R. Parra & Giul.	H	1			1	1	
Erythroxylaceae		T	1			1		

(continued)

Family	Taxon	Habit	Sip	Cam	Ven	Yap	Ata	Pas
	<i>Erythroxylum guanchezii</i> Plowman							
Erythroxylaceae	<i>Erythroxylum hypoleucum</i> Plowman	T					1	
Euphorbiaceae	<i>Alchornea discolor</i> Poepp. & Endl.	T				1		
Euphorbiaceae	<i>Croton scutatus</i> P.E. Berry	S/S	1			1	1	1
Euphorbiaceae	<i>Croton spiraeifolius</i> Jabl.	S/S	1			1	1	
Euphorbiaceae	<i>Croton trinitatis</i> Millsp.	S/S					1	
Euphorbiaceae	<i>Mabea frutescens</i> Jabl.	Cw				1	1	
Euphorbiaceae	<i>Mabea linearifolia</i> Jabl.	Cw				1		
Euphorbiaceae	<i>Maprounea amazonica</i> Esser	S/S	1				1	
Euphorbiaceae	<i>Maprounea guianensis</i> Aubl.	S/S				1		
Euphorbiaceae	<i>Euphronia acuminatissima</i> Steerm.	S/S	1		1	1	1	
Euphorbiaceae	<i>Euphronia hirtelloides</i> Mart. & Zucc.	S/S	1			1	1	1
Fabaceae	<i>Chamaecrista desvauxii</i> (Collad.) Killip	S/S	1		1	1	1	
Fabaceae	<i>Chamaecrista orenocensis</i> (Spruce ex Benth.) H.S. Irwin & Barneby	S/S		1	1	1		
Fabaceae	<i>Chamaecrista ramosa</i> (Vogel) H.S. Irwin & Barneby	S/S	1	1	1	1		
Fabaceae	<i>Dimorphandra cuprea</i> Sprague & Sandwith	S/S	1				1	1
Fabaceae	<i>Dimorphandra macrostachya</i> ssp. <i>glabrifolia</i> (Ducke) M.F. Silva	S/S				1		
Fabaceae	<i>Dimorphandra polyandra</i> Benoist	S/S				1	1	1

(continued)

Family	Taxon	Habit	Sip	Cam	Ven	Yap	Ata	Pas
Fabaceae	<i>Dimorphandra unijuga</i> Tul.	S/S	1			1	1	1
Fabaceae	<i>Heterostemon mimosoides</i> Desf. var. <i>mimosoides</i>	S/S				1	1	
Fabaceae	<i>Macrolobium angustifolium</i> (Benth.) R.S. Cowan	S/S					1	
Fabaceae	<i>Macrolobium anomalum</i> R.S. Cowan	S/S		1				
Fabaceae	<i>Macrolobium canaliculatum</i> Spruce ex Mart. var. <i>canaliculatum</i>	S/S					1	
Fabaceae	<i>Macrolobium discolor</i> Benth.	S/S	1		1	1	1	
Fabaceae	<i>Macrolobium limbatum</i> Spruce ex Benth.	S/S					1	1
Fabaceae	<i>Macrolobium longipes</i> R.S. Cowan	S/S					1	1
Fabaceae	<i>Macrolobium punctatum</i> Spruce ex Benth.	S/S	1				1	1
Fabaceae	<i>Macrolobium rubrum</i> R.S. Cowan	S/S	1				1	
Fabaceae	<i>Macrolobium savannarum</i> R.S. Cowan	S/S				1	1	
Fabaceae	<i>Macrolobium schinifolium</i> R.S. Cowan	S/S				1	1	
Fabaceae	<i>Macrolobium suaveolens</i> Spruce ex Benth. var. <i>suaveolens</i>	S/S				1	1	
Fabaceae	<i>Aldina heterophylla</i> Spruce ex Benth.	T	1					
Fabaceae	<i>Aldina kunhardtiana</i> R.S. Cowan	T	1				1	
Fabaceae	<i>Aldina latifolia</i> var. <i>latifolia</i> R.S. Cowan	T	1				1	
Fabaceae		T				1	1	1

(continued)

Family	Taxon	Habit	Sip	Cam	Ven	Yap	Ata	Pas
	<i>Aldina macrophylla</i> Spruce ex Benth.							
Fabaceae	<i>Andira trifoliolata</i> Ducke	T					1	1
Fabaceae	<i>Andira</i> sp. A	T					1	
Fabaceae	<i>Clitoria coriacea</i> Schery	S/S	1			1		1
Fabaceae	<i>Clitoria guianensis</i> (Aubl.) Benth.	S/S		1				
Fabaceae	<i>Dioclea</i> <i>steyermarii</i> R.H. Maxwell	Cw		1				
Fabaceae	<i>Ormosia coccinea</i> Jacks.	Cw	1	1	1	1	1	
Fabaceae	<i>Ormosia</i> <i>macrophylla</i> Benth.	Cw	1			1	1	1
Fabaceae	<i>Ormosia nobilis</i> Tul.	Cw					1	
Fabaceae	<i>Swartzia floribunda</i> Spruce	T					1	
Fabaceae	<i>Taralea cordata</i> var. <i>rigida</i> (Schery) H.C. Lima	T				1	1	
Fabaceae	<i>Calliandra</i> <i>tsugoides</i> R.S. Cowan	S/S				1	1	
Fabaceae	<i>Calliandra</i> <i>vaupesiana</i> var. <i>oligandra</i> Barneby	S/S	1		1		1	
Fabaceae	<i>Macrosamanea</i> <i>discolor</i> Britton & Rose ex Britton & Killip	T	1			1	1	1
Fabaceae	<i>Macrosamanea</i> <i>simabifolia</i> (Spruce ex Benth.) Pittier	T				1	1	1
Fabaceae	<i>Parkia barnebyana</i> H.C. Hopkins	T					1	
Fabaceae	<i>Parkia discolor</i> Spruce ex Benth.	T				1		1
Gentianaceae	<i>Adenolisianthus</i> <i>arboreus</i> Gilg.	S/S	1				1	
Gentianaceae	<i>Chelonanthus</i> <i>alatus</i> (Aubl.) Pulle	S/S		1	1	1	1	
Gentianaceae	<i>Chelonanthus</i> <i>grandiflorus</i> (Aubl.) Hassl.	S/S	1				1	
Gentianaceae		S/S	1			1	1	

(continued)

Family	Taxon	Habit	Sip	Cam	Ven	Yap	Ata	Pas
	<i>Coutoubea minor</i> Kunth							
Gentianaceae	<i>Coutoubea ramosa</i> Aubl.	S/S		1		1		
Gentianaceae	<i>Coutoubea reflexa</i> Benth.	S/S	1				1	
Gentianaceae	<i>Coutoubea spicata</i> Aubl.	S/S			1		1	
Gentianaceae	<i>Curtia conferta</i> Knobl.	S/S	1			1	1	1
Gentianaceae	<i>Curtia obtusifolia</i> Knobl.	S/S	1			1	1	
Gentianaceae	<i>Curtia tenuifolia</i> Knobl.	S/S	1	1	1	1		
Gentianaceae	<i>Irlbachia nemorosa</i> (Willd. ex Roem. & Schult.) Merr.	S/S	1				1	
Gentianaceae	<i>Irlbachia plantaginifolia</i> Maguire	S/S					1	1
Gentianaceae	<i>Irlbachia pratensis</i> (Kunth) L. Cobb. & Maas	S/S	1			1	1	1
Gentianaceae	<i>Irlbachia pumila</i> (Benth.) Maguire	S/S				1	1	1
Gentianaceae	<i>Potalia elegans</i> Struwe & V.A. Albert	S/S	1			1	1	1
Gentianaceae	<i>Potalia maguireorum</i> Struwe & V.A. Albert	S/S						1
Gentianaceae	<i>Potalia resinifera</i> Mart.	S/S				1	1	1
Gentianaceae	<i>Voyria aphylla</i> (Jacq.) Pers.	H					1	
Haemodoraceae	<i>Schiekia orinocensis</i> Meisn. ssp. <i>orinocensis</i>	H		1	1	1	1	1
Hugoniaceae	<i>Hebepetalum humirifolium</i> (Planch.) Benth. & Hook. f. ex B.D. Jacks.	T				1	1	
Hugoniaceae	<i>Roucheria calophylla</i> Planch.	T				1		

(continued)



Family	Taxon	Habit	Sip	Cam	Ven	Yap	Ata	Pas
Humiriaceae	<i>Humiria balsamifera</i> Aubl.	T	1	1	1	1	1	1
Humiriaceae	<i>Humiria balsamifera</i> Aubl. var. <i>balsamifera</i>	T	1					1
Humiriaceae	<i>Humiria balsamifera</i> var. <i>floribunda</i> (Mart.) Cuatrec.	T	1		1		1	
Humiriaceae	<i>Humiria balsamifera</i> var. <i>guianensis</i> (Benth.) Cuatrec.	T	1				1	
Humiriaceae	<i>Humiria balsamifera</i> var. <i>laurina</i> (Urb.) Cuatrec.	T	1					1
Humiriaceae	<i>Humiria balsamifera</i> var. <i>savannarum</i> (Gleason) Cuatrec.	T		1	1	1		1
Humiriaceae	<i>Humiria balsamifera</i> var. <i>subsessilis</i> (Urb.) Cuatrec.	T	1					1
Humiriaceae	<i>Humiria fruticosa</i> Cuatrec.	T				1		
Humiriaceae	<i>Humiria wurdackii</i> Cuatrec.	T	1			1	1	
Humiriaceae	<i>Sacoglottis guianensis</i> Benth.	T	1					1
Hymenophyllaceae	<i>Trichomanes crispum</i> L.	H	1			1	1	1
Hymenophyllaceae	<i>Trichomanes hostmannianum</i> (Klotzsch) Kuntze	H	1			1	1	
Hymenophyllaceae	<i>Trichomanes humboldtii</i> (Bosch) Lellinger	H				1	1	
Hypericaceae	<i>Vismia japurensis</i> Reichardt	T				1	1	
Hypericaceae	<i>Vismia schultesii</i> N. Robson	T						1
Ixonanthaceae	<i>Ochthocosmus multiflorus</i> Ducke	S/S	1					
Ixonanthaceae	<i>Ochthocosmus multiflorus</i> var.	S/S				1		

(continued)

Family	Taxon	Habit	Sip	Cam	Ven	Yap	Ata	Pas
	<i>angustifolius</i> Steerm. & Luteyn							
Ixonanthaceae	<i>Ochthocosmus</i> <i>multiflorus</i> var. <i>canaripoensis</i> Steerm. & Luteyn	S/S			1	1		
Ixonanthaceae	<i>Ochthocosmus</i> <i>multiflorus</i> Ducke var. <i>multiflorus</i>	S/S					1	
Lamiaceae	<i>Aegiphila hoehnei</i> var. <i>venezuelensis</i> Moldenke	S/S					1	1
Lamiaceae	<i>Hyptis dilatata</i> Benth.	S/S		1	1		1	
Lamiaceae	<i>Hyptis huberi</i> Harley	S/S		1				
Lamiaceae	<i>Vitex sprucei</i> Briq.	T					1	
Lauraceae	<i>Cassytha filiformis</i> L.	H				1	1	
Lauraceae	<i>Endlicheria</i> <i>macrophylla</i> (Meisn.) Mez	T				1		
Lauraceae	<i>Ocotea aciphylla</i> (Nees & Mart.) Mez	T				1		
Lauraceae	<i>Ocotea debilis</i> Mez	T					1	
Lauraceae	<i>Ocotea</i> <i>esmeraldana</i> Moldenke ex Gleason	T	1	1	1	1	1	1
Lauraceae	<i>Ocotea gracilis</i> (Meisn.) Mez	T					1	
Lauraceae	<i>Ocotea myriantha</i> (Meisn.) Mez	T				1	1	1
Lauraceae	<i>Ocotea tomentosa</i> van der Werff	T					1	
Lecythidaceae	<i>Eschweilera</i> <i>tenuifolia</i> Miers	T	1			1	1	1
Lentibulariaceae	<i>Genlisea pygmaea</i> A. St.-Hil.	H		1				
Lentibulariaceae	<i>Genlisea repens</i> Benth.	H	1				1	
Lentibulariaceae	<i>Genlisea</i> <i>sanariapoana</i> Steerm.	H	1	1				
Lentibulariaceae	<i>Utricularia</i> <i>amethystina</i> Salzm.	H	1			1	1	

(continued)

Family	Taxon	Habit	Sip	Cam	Ven	Yap	Ata	Pas
	ex A. St.-Hil. & Girard							
Lentibulariaceae	<i>Utricularia chiribiquitensis</i> A. Fernández	H			1	1		
Lentibulariaceae	<i>Utricularia cucullata</i> A. St.-Hil. & Girard	H	1		1			
Lentibulariaceae	<i>Utricularia fimbriata</i> Kunth	H		1	1	1		
Lentibulariaceae	<i>Utricularia foliosa</i> L.	H				1		
Lentibulariaceae	<i>Utricularia guyanensis</i> A. DC.	H				1		
Lentibulariaceae	<i>Utricularia hispida</i> Lam.	H		1		1		
Lentibulariaceae	<i>Utricularia longeciliata</i> A. DC.	H	1		1	1	1	1
Lentibulariaceae	<i>Utricularia myriocista</i> A. St.-Hil. & Girard	H		1				
Lentibulariaceae	<i>Utricularia nana</i> A. St.-Hil. & Girard	H	1					
Lentibulariaceae	<i>Utricularia nervosa</i> Weber ex Benj.	H			1	1		
Lentibulariaceae	<i>Utricularia sandwithii</i> P. Taylor	H				1		
Lentibulariaceae	<i>Utricularia simulans</i> Pilg.	H		1	1			
Lentibulariaceae	<i>Utricularia subulata</i> L.	H	1	1	1	1	1	1
Lentibulariaceae	<i>Utricularia tenuissima</i> Tutin	H		1			1	
Lentibulariaceae	<i>Utricularia viscosa</i> Spruce ex Oliv.	H				1		
Lindsaeaceae	<i>Lindsaea javitensis</i> Humb. & Bonpl. ex Willd.	H				1	1	1
Lindsaeaceae	<i>Lindsaea rigidiuscula</i> Lindm.	H				1	1	1
Lindsaeaceae	<i>Lindsaea schomburgkii</i> Klotzsch	H				1	1	1
Lindsaeaceae	<i>Lindsaea stricta</i> (Sw.) Dryand.	H	1			1	1	1
Loganiaceae	<i>Antonia ovata</i> Pohl	S/S					1	
Loganiaceae	<i>Bonyunia aquatica</i> Ducke	S/S	1		1	1	1	

(continued)

Family	Taxon	Habit	Sip	Cam	Ven	Yap	Ata	Pas
Loganiaceae	<i>Spigelia gracilis</i> A. DC.	H	1		1	1	1	
Loranthaceae	<i>Passovia bisexualis</i> (Rizzini) Kuijt	Ew				1		
Loranthaceae	<i>Phthirusa</i> <i>guyanensis</i> Eichler	Ew	1			1		
Loranthaceae	<i>Passovia</i> <i>pedunculata</i> (Jacq.) Kuijt	Ew	1			1		
Loranthaceae	<i>Phthirusa</i> <i>stenophylla</i> Eichler	Ew				1	1	
Loranthaceae	<i>Psittacanthus</i> <i>clusifolius</i> Eichler	Ew					1	
Loranthaceae	<i>Psittacanthus</i> <i>julianus</i> Rizzini	Ew	1			1		1
Lycopodiaceae	<i>Lycopodiella</i> <i>contexta</i> (Mart.) Holub	H					1	
Lycopodiaceae	<i>Pseudolycopodiella</i> <i>meridionalis</i> (Underw. & F.E. Lloyd) Holub	H	1			1		1
Lythraceae	<i>Cuphea annulata</i> Koehne	S/S					1	
Lythraceae	<i>Cuphea</i> <i>antisiphilitica</i> var. <i>acutifolia</i> Benth.	S/S		1				
Lythraceae	<i>Cuphea</i> <i>antisiphilitica</i> Kunth	S/S		1				
Lythraceae	<i>Cuphea odonellii</i> Lourteig	S/S	1		1	1		
Malpighiaceae	<i>Blepharandra</i> <i>angustifolia</i> (Kunth) W.R. Andersson	S/S				1	1	1
Malpighiaceae	<i>Blepharandra</i> <i>heteropetala</i> W.R. Andersson	S/S	1				1	
Malpighiaceae	<i>Byrsonima</i> <i>chrysophylla</i> W.R. Andersson	S/S	1		1	1		
Malpighiaceae	<i>Byrsonima</i> <i>coniophylla</i> A. Juss.	S/S	1			1	1	1
Malpighiaceae	<i>Byrsonima cuprea</i> Griseb.	S/S			1	1	1	1
Malpighiaceae	<i>Byrsonima</i> <i>laevis</i> Nied.	S/S		1			1	
Malpighiaceae		S/S	1	1	1	1	1	

(continued)

Family	Taxon	Habit	Sip	Cam	Ven	Yap	Ata	Pas
	<i>Byrsonima luetzelburgii</i> Steyerem.							
Malpighiaceae	<i>Byrsonima punctulata</i> W.R. Anderson	T	1				1	
Malpighiaceae	<i>Byrsonima wurdackii</i> W.R. Andersson	T				1	1	
Malpighiaceae	<i>Glandonia williamsii</i> Steyerem.	S/S	1			1		1
Malpighiaceae	<i>Heteropterys atabapensis</i> W.R. Anderson	S/S	1		1	1	1	
Malpighiaceae	<i>Heteropterys macradena</i> (DC.) W.R. Anderson	Cw		1				
Malpighiaceae	<i>Heteropterys nervosa</i> A. Juss.	Cw				1	1	1
Malpighiaceae	<i>Heteropterys oblongifolia</i> Gleason	S/S	1		1	1	1	1
Malpighiaceae	<i>Hiraea celiانا</i> W.R. Andersson	Cw	1					
Malpighiaceae	<i>Mezia huberi</i> W.R. Andersson	S/S		1				
Malpighiaceae	<i>Tetrapteryx gracilis</i> W.R. Andersson	S/S	1			1	1	1
Malpighiaceae	<i>Tetrapteryx styloptera</i> A. Juss.	Cw					1	
Malvaceae	<i>Catostemma sancarlosianum</i> Steyerem.	S/S					1	
Malvaceae	<i>Mollia speciosa</i> Mart.	T	1			1	1	1
Malvaceae	<i>Pachira amazonica</i> (A. Robyns) W.S. Alverson	S/S				1	1	1
Malvaceae	<i>Pachira coriacea</i> (Mart. & Zucc.) W.S. Alverson	S/S	1	1		1		
Malvaceae	<i>Pachira faroensis</i> (Ducke) W.S. Alverson	S/S					1	
Malvaceae	<i>Pachira gracilis</i> (A. Robyns) W.S. Alverson ssp. <i>gracilis</i>	T	1		1	1	1	1

(continued)

Family	Taxon	Habit	Sip	Cam	Ven	Yap	Ata	Pas
Malvaceae	<i>Pachira humilis</i> Decne.	S/S			1	1	1	
Malvaceae	<i>Pachira sordida</i> (R.E. Schult.) W.S. Alverson	T	1			1	1	
Malvaceae	<i>Pachira yapacanae</i> Steyserm. ex W.S. Alverson	T				1		
Marantaceae	<i>Goepertia acuminata</i> (Steyserm.) Borchs. & S. Suárez	H					1	1
Melastomataceae	<i>Acanthella sprucei</i> Hook. f.	S/S	1					
Melastomataceae	<i>Aciotis polystachya</i> (Bonpl.) Triana	H					1	
Melastomataceae	<i>Noterophila nana</i> (Ule) Kriebel & M.J. Rocha	H		1				
Melastomataceae	<i>Adelobotrys barbatus</i> Triana	S/S				1	1	
Melastomataceae	<i>Adelobotrys fruticosus</i> Wurdack	S/S				1	1	1
Melastomataceae	<i>Bellucia grossularioides</i> (L.) Triana	S/S					1	
Melastomataceae	<i>Bellucia huberi</i> (Wurdack) S.S. Renner	S/S		1			1	
Melastomataceae	<i>Clidemia novemnervia</i> (DC.) Triana	S/S		1			1	
Melastomataceae	<i>Clidemia sericea</i> D. Don	S/S		1		1		
Melastomataceae	<i>Comolia leptophylla</i> (Bonpl.) Naudin	S/S	1	1	1	1		
Melastomataceae	<i>Comolia microphylla</i> Benth.	S/S	1					1
Melastomataceae	<i>Comolia nummularioides</i> (Bonpl.) Naudin	S/S	1			1		
Melastomataceae	<i>Comolia prostrata</i> Wurdack	S/S					1	
Melastomataceae	<i>Comolia villosa</i> Triana	S/S				1		
Melastomataceae	<i>Desmoscelis villosa</i> (Aubl.) Naudin	S/S					1	

(continued)

Family	Taxon	Habit	Sip	Cam	Ven	Yap	Ata	Pas
Melastomataceae	<i>Henriettea granulata</i> Berg ex Triana	S/S				1	1	1
Melastomataceae	<i>Henriettea horridula</i> Pilg.	S/S				1		
Melastomataceae	<i>Henriettea martusii</i> (DC.) Naud.	S/S					1	
Melastomataceae	<i>Macairea axilliflora</i> Wurdack	S/S				1	1	1
Melastomataceae	<i>Macairea lanata</i> Gleason	S/S	1				1	
Melastomataceae	<i>Macairea lasiophylla</i> (Benth.) Wurdack	S/S				1		
Melastomataceae	<i>Macairea maroana</i> Wurdack	S/S					1	
Melastomataceae	<i>Macairea rufescens</i> DC.	S/S					1	
Melastomataceae	<i>Macairea spruceana</i> Berg ex Triana	S/S					1	1
Melastomataceae	<i>Macairea stylosa</i> Triana	S/S				1	1	1
Melastomataceae	<i>Macairea thyrsoflora</i> DC.	S/S	1	1	1	1	1	
Melastomataceae	<i>Meriania urceolata</i> Triana	S/S	1		1	1		
Melastomataceae	<i>Miconia alborufescens</i> Naudin	S/S	1					
Melastomataceae	<i>Miconia biglomerata</i> DC.	S/S				1	1	
Melastomataceae	<i>Miconia campestris</i> Triana	S/S			1	1	1	
Melastomataceae	<i>Miconia ciliata</i> (Rich.) DC.	S/S	1	1	1	1		1
Melastomataceae	<i>Miconia eugenioides</i> Triana	S/S	1			1	1	1
Melastomataceae	<i>Miconia maroana</i> Wurdack	S/S					1	
Melastomataceae	<i>Miconia wittii</i> Ule	S/S	1			1	1	1
Melastomataceae	<i>Mouriri subumbellata</i> Triana	S/S			1	1	1	
Melastomataceae	<i>Mouriri unciithec</i> Morley & Wurdack	S/S				1	1	

(continued)



Family	Taxon	Habit	Sip	Cam	Ven	Yap	Ata	Pas
Melastomataceae	<i>Pachyloma huberioides</i> Triana	S/S			1	1	1	1
Melastomataceae	<i>Pachyloma pusillum</i> Wurdack	S/S				1		
Melastomataceae	<i>Pachyloma setosum</i> Wurdack	S/S	1			1	1	
Melastomataceae	<i>Rhynchanthera grandiflora</i> DC.	S/S		1	1	1		
Melastomataceae	<i>Siphanthera cowanii</i> Wurdack	S/S			1	1	1	
Melastomataceae	<i>Siphanthera fasciculata</i> (Gleason) Almeda & O.R. Rob.	S/S	1			1	1	
Melastomataceae	<i>Tibouchina aspera</i> Aubl. var. <i>aspera</i>	S/S	1	1		1	1	
Melastomataceae	<i>Tibouchina spruceana</i> Cogn.	S/S	1			1		
Melastomataceae	<i>Tibouchina striphnocalyx</i> (DC.) Pittier	S/S	1			1	1	1
Melastomataceae	<i>Tococa ciliata</i> Triana	S/S				1	1	1
Melastomataceae	<i>Tococa hirta</i> Berg ex Triana	S/S					1	
Melastomataceae	<i>Tococa macrophysca</i> Spruce ex Triana	S/S	1			1	1	
Melastomataceae	<i>Tococa macrosperma</i> Mart.	S/S	1			1	1	
Melastomataceae	<i>Tococa nitens</i> Triana	S/S	1		1	1	1	
Melastomataceae	<i>Tococa rotundifolia</i> (Triana) Wurdack	S/S				1	1	
Metteniusaceae	<i>Emmotum floribundum</i> R.A. Howard	T	1			1	1	1
Myristicaceae	<i>Compsonoura debilis</i> Warb.	T	1	1		1	1	1
Myristicaceae	<i>Irianthera obovata</i> Ducke	T				1	1	1
Myristicaceae	<i>Virola pavonis</i> (A. DC.) A.C. Sm.	T	1			1	1	1
Myrtaceae	<i>Myrcia crebra</i> (McVaugh) A.R. Lourenço & E. Lucas	S/S					1	

(continued)

Family	Taxon	Habit	Sip	Cam	Ven	Yap	Ata	Pas
Myrtaceae	<i>Myrcia neoforsteri</i> A.R. Lourenço & E. Lucas	S/S					1	
Myrtaceae	<i>Myrcia convexivenia</i> (B. Holst) E. Lucas & C.E. Wilson	S/S					1	1
Myrtaceae	<i>Myrcia mcvaughii</i> (B. Holst) E. Lucas & C.E. Wilson	S/S					1	1
Myrtaceae	<i>Myrcia suborbicularis</i> (McVaugh) E. Lucas & C.E. Wilson	S/S	1			1	1	
Myrtaceae	<i>Myrcia ventuarensis</i> (B. Holst) E. Lucas & C.E. Wilson	S/S		1	1			
Myrtaceae	<i>Myrcia clusiifolia</i> (Kunth) DC.	S/S	1			1		1
Myrtaceae	<i>Myrcia dichasialis</i> McVaugh	S/S				1		
Myrtaceae	<i>Myrcia grandis</i> McVaugh	S/S				1	1	1
Myrtaceae	<i>Myrcia guianensis</i> DC.	S/S					1	
Myrtaceae	<i>Myrcia revolutifolia</i> McVaugh	S/S	1					1
Myrtaceae	<i>Myrcia</i> sp. A	S/S					1	1
Nyctaginaceae	<i>Guapira sancarlosiana</i> Steyerm.	S/S					1	
Nyctaginaceae	<i>Neea clarkii</i> Steyerm.	S/S				1	1	
Nyctaginaceae	<i>Neea obovata</i> Spruce ex Heimerl	S/S	1		1	1	1	1
Nyctaginaceae	<i>Neea robusta</i> Steyerm.	S/S				1	1	1
Ochnaceae	<i>Blastemanthus gemmiflorus</i> ssp. <i>sprucei</i> (Tiegh.) Sastre	S/S	1			1	1	
Ochnaceae	<i>Froesia tricarpa</i> Pires	S/S					1	
Ochnaceae	<i>Ouratea aquatica</i> Engl.	S/S	1		1	1	1	1
Ochnaceae	<i>Ouratea brevicalyx</i> Maguire & Steyerm.	S/S			1		1	

(continued)

Family	Taxon	Habit	Sip	Cam	Ven	Yap	Ata	Pas
Ochnaceae	<i>Ouratea clarkii</i> Sastre	S/S					1	
Ochnaceae	<i>Ouratea diminuta</i> Maguire & Steyerf.	S/S	1				1	
Ochnaceae	<i>Ouratea evoluta</i> Maguire & Steyerf.	S/S				1	1	
Ochnaceae	<i>Ouratea heterobracteata</i> Sastre	S/S					1	
Ochnaceae	<i>Ouratea huberi</i> Maguire & Steyerf.	S/S			1	1		
Ochnaceae	<i>Ouratea longistyla</i> Maguire & Steyerf.	S/S						1
Ochnaceae	<i>Ouratea papillata</i> Maguire & Steyerf.	S/S				1		1
Ochnaceae	<i>Ouratea polyantha</i> Engl.	S/S	1	1		1		
Ochnaceae	<i>Ouratea roraimae</i> Engl.	S/S			1	1		1
Ochnaceae	<i>Ouratea spruceana</i> Engl.	S/S	1		1	1	1	1
Ochnaceae	<i>Ouratea steyermarkii</i> Sastre	S/S	1			1	1	
Ochnaceae	<i>Ouratea thyrsoides</i> Engl.	S/S		1	1	1	1	1
Ochnaceae	<i>Ouratea yapacana</i> Sastre	S/S				1		
Ochnaceae	<i>Quiina tinifolia</i> Planch. & Triana	S/S					1	
Ochnaceae	<i>Sauvagesia erecta</i> L.	S/S	1			1	1	1
Ochnaceae	<i>Sauvagesia linearifolia</i> ssp. <i>venezuelensis</i> Maguire & Wurdack	S/S	1		1	1	1	1
Ochnaceae	<i>Sauvagesia nudicaulis</i> Maguire & Wurdack	S/S	1		1	1	1	1
Ochnaceae	<i>Sauvagesia ramosa</i> (Gleason) Sastre	S/S	1			1		
Ochnaceae	<i>Sauvagesia tenella</i> Lam.	S/S		1				
Ochnaceae	<i>Wallacea insignis</i> Spruce ex Benth. & Hook. f.	S/S				1	1	1
Olacaceae		S/S				1	1	

(continued)

Family	Taxon	Habit	Sip	Cam	Ven	Yap	Ata	Pas
	<i>Aptandra liriosmoides</i> Spruce ex Miers							
Olacaceae	<i>Cathedra acuminata</i> Miers	S/S	1			1		
Olacaceae	<i>Chanochiton angustifolium</i> Sleumer	S/S	1	1	1	1		
Olacaceae	<i>Chanochiton loranthoides</i> Benth.	S/S				1	1	
Olacaceae	<i>Dulacia redmondii</i> Steyerf.	S/S	1		1	1	1	
Onagraceae	<i>Ludwigia rigida</i> (Miq.) Sandwith	S/S		1				
Orchidaceae	<i>Cleistes rosea</i> Lindl.	H	1		1	1		1
Orchidaceae	<i>Cleistes tenuis</i> Schltr.	H	1				1	1
Orchidaceae	<i>Duckeella pauciflora</i> Garay	H	1		1	1	1	1
Orchidaceae	<i>Epistephium parviflorum</i> Lindl.	H		1	1	1	1	
Orchidaceae	<i>Eriopsis biloba</i> Lindl.	H	1				1	
Orchidaceae	<i>Koellensteinia hyacinthoides</i> Schltr.	H	1			1	1	
Orchidaceae	<i>Octomeria gemmula</i> Carnevali & I. Ramírez	H	1				1	
Orchidaceae	<i>Orleansia yauaperyensis</i> Barb. Rodr.	H	1					
Orchidaceae	<i>Otostylis brachystalix</i> (Rchb. f.) Schltr.	H		1		1		
Orchidaceae	<i>Sobralia liliastrum</i> Lindl.	H	1			1	1	1
Passifloraceae	<i>Turnera argentea</i> Arbo	S/S				1		
Passifloraceae	<i>Turnera steyermarkii</i> Arbo	S/S				1	1	
Peraceae	<i>Pera bicolor</i> (Klotzsch) Müll. Arg.	T				1	1	
Peraceae		T				1	1	

(continued)

Family	Taxon	Habit	Sip	Cam	Ven	Yap	Ata	Pas
	<i>Pera citriodora</i> Baill.							
Peraceae	<i>Pera glabrata</i> (Schott) Poepp. ex Baill.	T				1	1	
Phyllanthaceae	<i>Amanoa almerindae</i> Leal	T	1				1	
Phyllanthaceae	<i>Amanoa glaucophylla</i> Müll. Arg.	T	1				1	
Phyllanthaceae	<i>Phyllanthus atabapoensis</i> Jabl.	S/S	1			1	1	1
Phyllanthaceae	<i>Phyllanthus myrsinites</i> Kunth	S/S	1			1	1	1
Poaceae	<i>Andropogon leucostachyus</i> Kunth	H	1	1				1
Poaceae	<i>Andropogon virgatus</i> Ham.	H		1		1	1	
Poaceae	<i>Arthrostylidium berryi</i> Judz. & Davidse	H	1			1	1	1
Poaceae	<i>Axonopus casiquirensis</i> Davidse	H				1	1	1
Poaceae	<i>Axonopus fissifolius</i> (Raddi) Kuhlman.	H						1
Poaceae	<i>Axonopus schultesii</i> G.A. Black	H				1	1	1
Poaceae	<i>Anthaenantia lanata</i> (Kunth) Benth.	H		1			1	
Poaceae	<i>Cyphonanthus discrepans</i> (Döll) Zuloaga & Morrone	H	1				1	
Poaceae	<i>Mesosetum chlorostachyum</i> Chase	H					1	
Poaceae	<i>Mesosetum filifolium</i> F.T. Hubb.	H			1	1	1	
Poaceae	<i>Mesosetum rottboellioides</i> Hitchc.	H	1		1	1	1	1
Poaceae	<i>Otachyrium grandiflorum</i> Send. & Soderstr.	H				1	1	
Poaceae	<i>Panicum rudgei</i> Roem. & Schult.	H	1	1	1	1		1
Poaceae		H	1			1	1	1

(continued)

Family	Taxon	Habit	Sip	Cam	Ven	Yap	Ata	Pas
	<i>Rugoloa pilosa</i> (Sw.) Zuloaga							
Poaceae	<i>Trichantheicum cyanescens</i> (Nees ex Trin.) Zuloaga & Morrone	H	1	1	1	1		1
Poaceae	<i>Trichantheicum granuliferum</i> (Kunth) Zuloaga & Morrone	H	1		1	1		1
Poaceae	<i>Trichantheicum micranthum</i> (Kunth) Zuloaga & Morrone	H	1		1	1	1	1
Poaceae	<i>Trichantheicum nervosum</i> (Lam.) Zuloaga & Morrone	H	1					
Poaceae	<i>Trichantheicum orinocanum</i> (Luces) Zuloaga & Morrone	H	1	1	1	1	1	1
Poaceae	<i>Trichantheicum parvifolium</i> (Lam.) Zuloaga & Morrone	H					1	
Poaceae	<i>Trichantheicum petrense</i> (Swallen) Zuloaga & Morrone	H	1			1		
Poaceae	<i>Trichantheicum yavitaense</i> (Swallen) Zuloaga & Morrone	H					1	1
Poaceae	<i>Paspalum atabapense</i> Davidse & Zuloaga	H				1		
Poaceae	<i>Paspalum carinatum</i> Humb. & Bonpl. ex Flügge	H	1			1		1
Poaceae	<i>Paspalum lanciflorum</i> Trin.	H	1	1	1		1	1
Poaceae	<i>Paspalum pulchellum</i> Kunth	H	1	1	1			1
Poaceae	<i>Paspalum tillettii</i> Davidse & Zuloaga	H				1	1	1
Poaceae	<i>Rhytachne guianensis</i> (Hitchc.) Clayton	H				1		
Poaceae	<i>Steyermarkochloa angustifolia</i> (Spreng.) Judz.	H	1			1	1	
Poaceae		H				1	1	

(continued)

Family	Taxon	Habit	Sip	Cam	Ven	Yap	Ata	Pas
	<i>Trachypogon spicatus</i> (L. f.) Kuntze							
Polygalaceae	<i>Bredemeyera divaricata</i> (DC.) J.F.B. Pastore	Cw	1				1	1
Polygalaceae	<i>Bredemeyera densiflora</i> A.W. Benn.	Cw				1	1	
Polygalaceae	<i>Moutabea guianensis</i> Aubl.	S/S	1		1	1	1	1
Polygalaceae	<i>Polygala adenophora</i> DC.	S/S	1	1	1	1	1	
Polygalaceae	<i>Polygala appressa</i> Benth.	S/S	1			1	1	1
Polygalaceae	<i>Polygala savannarum</i> Chodat	S/S			1	1		
Polygalaceae	<i>Polygala spruceana</i> A.W. Benn.	S/S		1	1			
Polygalaceae	<i>Polygala subtilis</i> Kunth	S/S		1	1			
Polygalaceae	<i>Polygala trichosperma</i> Jacq.	S/S	1	1	1			
Polygalaceae	<i>Securidaca coriacea</i> Bonpl. ex Steud.	Cw		1	1	1		
Polygalaceae	<i>Securidaca retusa</i> Benth.	Cw					1	
Polygalaceae	<i>Securidaca savannarum</i> Chodat	Cw				1		
Polygonaceae	<i>Coccoloba excelsa</i> Benth.	S/S					1	
Polygonaceae	<i>Coccoloba wurdackii</i> R.A. Howard	S/S					1	
Primulaceae	<i>Cybianthus deltatus</i> Pipoly	S/S	1			1	1	
Primulaceae	<i>Cybianthus fulvopulverulentus</i> (Mez) G. Agostini	S/S	1	1	1	1		1
Primulaceae	<i>Cybianthus reticulatus</i> (Benth. ex Miq.) G. Agostini	S/S				1	1	1
Primulaceae	<i>Cybianthus spicatus</i> (Kunth) G. Agostini	S/S	1		1	1	1	1

(continued)



Family	Taxon	Habit	Sip	Cam	Ven	Yap	Ata	Pas
Rapateaceae	<i>Cephalostemon affinis</i> Körn.	H	1		1	1	1	
Rapateaceae	<i>Cephalostemon microglochis</i> Sandwith	H		1				
Rapateaceae	<i>Duckea cyperaceoidea</i> (Ducke) Maguire	H					1	1
Rapateaceae	<i>Duckea flava</i> (Link) Maguire	H	1		1	1	1	1
Rapateaceae	<i>Duckea junciformis</i> Maguire	H					1	
Rapateaceae	<i>Duckea squarrosa</i> (Willd. ex Link) Maguire	H				1	1	1
Rapateaceae	<i>Guacamaya superba</i> Maguire	H					1	
Rapateaceae	<i>Monotrema aemulans</i> Körn.	H	1			1	1	1
Rapateaceae	<i>Monotrema x affine</i> Maguire	H				1	1	
Rapateaceae	<i>Monotrema bracteatum</i> Maguire ssp. <i>bracteatum</i>	H				1		
Rapateaceae	<i>Monotrema bracteatum</i> ssp. <i>major</i> Maguire	H					1	
Rapateaceae	<i>Monotrema xyridoides</i> Gleason	H	1	1	1	1	1	
Rapateaceae	<i>Rapatea circasiana</i> García-Barr. & L.E. Mora	H	1				1	
Rapateaceae	<i>Rapatea longipes</i> Spruce ex Körn.	H					1	
Rapateaceae	<i>Rapatea spruceana</i> Körn.	H	1			1	1	1
Rapateaceae	<i>Rapatea yapacana</i> Maguire	H				1		
Rapateaceae	<i>Saxofridericia inermis</i> Ducke	H					1	1
Rapateaceae	<i>Schoenocephalum cucullatum</i> Maguire	H	1		1	1	1	1
Rapateaceae	<i>Schoenocephalum teretifolium</i> Maguire	H	1				1	1
Rapateaceae		H				1		1

(continued)

Family	Taxon	Habit	Sip	Cam	Ven	Yap	Ata	Pas
	<i>Spathanthus bicolor</i> Ducke							
Rubiaceae	<i>Spermacoce capitata</i> Ruiz & Pav.	S/S	1	1	1			
Rubiaceae	<i>Spermacoce intricata</i> (Steerm.) Govaerts	S/S	1				1	
Rubiaceae	<i>Spermacoce macrocephala</i> (Standl. & Steerm.) Govaerts	S/S				1	1	1
Rubiaceae	<i>Spermacoce wurdackii</i> (Steerm.) Govaerts	S/S					1	
Rubiaceae	<i>Dendrosipanea revoluta</i> Steerm.	S/S				1		1
Rubiaceae	<i>Dendrosipanea spigelioides</i> Ducke	S/S					1	
Rubiaceae	<i>Henriquezia nitida</i> Spruce ex Benth. var. <i>nitida</i>	S/S				1	1	
Rubiaceae	<i>Mitracarpus frigidus</i> var. <i>orinocensis</i> Steerm.	S/S	1				1	
Rubiaceae	<i>Pagamea anisophylla</i> Standl. & Steerm.	S/S	1	1	1	1	1	
Rubiaceae	<i>Pagamea capitata</i> ssp. <i>conferta</i> (Standl.) Steerm.	S/S	1					
Rubiaceae	<i>Pagamea coriacea</i> Benth.	S/S	1	1	1	1	1	1
Rubiaceae	<i>Pagamea guianensis</i> Aubl.	S/S			1	1	1	1
Rubiaceae	<i>Pagamea hirsuta</i> Spruce ex Benth.	S/S				1	1	1
Rubiaceae	<i>Pagamea plicata</i> Spruce ex Benth.	S/S	1			1	1	1
Rubiaceae	<i>Pagamea plicatiformis</i> Steerm.	S/S				1	1	
Rubiaceae	<i>Pagamea thyrsoflora</i> Spruce	S/S	1				1	1
Rubiaceae	<i>Pagamea velutina</i> Steerm.	S/S	1					

(continued)

Family	Taxon	Habit	Sip	Cam	Ven	Yap	Ata	Pas
Rubiaceae	<i>Palicourea foldatsii</i> Steerm.	S/S	1				1	1
Rubiaceae	<i>Palicourea grandiflora</i> Standl.	S/S					1	
Rubiaceae	<i>Palicourea huberi</i> Steerm.	S/S				1		
Rubiaceae	<i>Palicourea lancigera</i> (Standl.) Steerm.	S/S				1	1	
Rubiaceae	<i>Perama dichotoma</i> Poepp. & Endl.	S/S	1			1		
Rubiaceae	<i>Perama galioides</i> Poir.	S/S	1		1	1		
Rubiaceae	<i>Perama plantaginea</i> (Kunth) K. Schum.	S/S	1			1	1	1
Rubiaceae	<i>Platycarpum negrense</i> var. <i>glaucum</i> G.K. Rogers	T					1	
Rubiaceae	<i>Platycarpum orinocense</i> Bonpl.	T					1	
Rubiaceae	<i>Platycarpum schultesii</i> var. <i>zarucchii</i> G.K. Rogers	T			1	1	1	
Rubiaceae	<i>Palicourea adderleyi</i> (Steerm.) Borhidi	S/S					1	
Rubiaceae	<i>Palicourea blakei</i> (Standl. & Steerm.) Borhidi	S/S				1	1	
Rubiaceae	<i>Palicourea cardiomorpha</i> (C.M. Taylor & A. Pool) Delprete & J.H. Kirkbr.	S/S		1	1	1		
Rubiaceae	<i>Palicourea humboldtiana</i> (Cham.) Delprete & J.H. Kirkbr.	S/S				1	1	
Rubiaceae	<i>Palicourea spadicea</i> (Pittier) Borhidi	S/S	1			1	1	
Rubiaceae	<i>Palicourea vareschii</i> (Steerm.) Borhidi	S/S				1		1
Rubiaceae		S/S				1		

(continued)

Family	Taxon	Habit	Sip	Cam	Ven	Yap	Ata	Pas
	<i>Psychotria yapacanensis</i> Steyerem.							
Rubiaceae	<i>Remijia argentea</i> Steyerem.	S/S			1	1	1	
Rubiaceae	<i>Remijia hispida</i> Spruce	S/S	1			1	1	1
Rubiaceae	<i>Remijia longifolia</i> Benth. & Standl.	S/S	1			1	1	1
Rubiaceae	<i>Remijia morilloi</i> Steyerem.	S/S	1				1	
Rubiaceae	<i>Remijia wurdackii</i> Steyerem.	S/S	1				1	
Rubiaceae	<i>Retiniphyllum concolor</i> (Spruce ex Benth.) Müll. Arg.	S/S	1			1	1	1
Rubiaceae	<i>Retiniphyllum discolor</i> Müll. Arg.	S/S			1			
Rubiaceae	<i>Retiniphyllum pauciflorum</i> Kunth ex K. Krause	S/S	1				1	
Rubiaceae	<i>Retiniphyllum pilosum</i> Müll. Arg.	S/S					1	1
Rubiaceae	<i>Retiniphyllum schomburgkii</i> Müll. Arg.	S/S	1	1		1	1	
Rubiaceae	<i>Retiniphyllum secundiflorum</i> Bonpl.	S/S				1	1	1
Rubiaceae	<i>Retiniphyllum truncatum</i> Müll. Arg.	S/S					1	
Rubiaceae	<i>Sabicea morillorum</i> Steyerem.	S/S					1	
Rubiaceae	<i>Sabicea tillettii</i> Steyerem.	S/S					1	
Rubiaceae	<i>Sipaneopsis foldatsii</i> Steyerem.	S/S	1			1	1	
Rubiaceae	<i>Sipaneopsis maguirei</i> Steyerem.	S/S	1		1	1	1	
Rubiaceae	<i>Sipaneopsis pacimonensis</i> Steyerem.	S/S						1
Salicaceae	<i>Piparea multiflora</i> C.F. Gaertn.	S/S				1		
Salicaceae		S/S				1		

(continued)

Family	Taxon	Habit	Sip	Cam	Ven	Yap	Ata	Pas
	<i>Casearia sylvestris</i> var. <i>lingua</i> (Cambess.) Eichler							
Salicaceae	<i>Euceraea nitida</i> Mart.	S/S	1			1		
Salicaceae	<i>Irenodendron coriaceum</i> (Spruce ex Benth.) M.H. Alford & Dement	S/S	1			1	1	
Salicaceae	<i>Ryania spruceana</i> Monach.	S/S	1				1	
Santalaceae	<i>Phoradendron microstachyum</i> Kuijt	Ew			1			
Santalaceae	<i>Phoradendron platycaulon</i> Eichler	Ew				1	1	
Sapindaceae	<i>Matayba atropurpurea</i> Radlk.	S/S					1	
Sapindaceae	<i>Matayba opaca</i> Radlk.	S/S	1		1		1	1
Sapotaceae	<i>Ecclinusa atabapoensis</i> (Aubrév.) T.D. Penn.	T	1			1	1	
Sapotaceae	<i>Ecclinusa orinocoensis</i> Aubrév.	T				1		
Sapotaceae	<i>Elaeoluma schomburgkiana</i> Baill.	T	1				1	1
Sapotaceae	<i>Manilkara bidentata</i> ssp. <i>surinamensis</i> (Miq.) T.D. Penn.	T	1					
Sapotaceae	<i>Micropholis humboldtiana</i> (Roem. & Schult.) T.D. Penn.	T				1		1
Sapotaceae	<i>Pouteria pimichinensis</i> T.D. Penn.	T					1	1
Sapotaceae	<i>Pradosia schomburgkiana</i> (A. DC.) Cronquist	T	1			1	1	
Schoepfiaceae	<i>Schoepfia clarkii</i> Steyerm.	S/S					1	
Selaginellaceae		H			1	1	1	

(continued)

Family	Taxon	Habit	Sip	Cam	Ven	Yap	Ata	Pas
	<i>Selaginella coarctata</i> Spring							
Schizaeaceae	<i>Actinostachys pennula</i> Hook.	H	1			1		1
Schizaeaceae	<i>Actinostachys subtrijuga</i> C. Presl	H					1	1
Schizaeaceae	<i>Schizaea incurvata</i> Schkuhr	H				1	1	1
Simaroubaceae	<i>Simaba guianensis</i> ssp. <i>huberi</i> Franceschin. & W.W. Thomas	S/S	1		1	1	1	
Simaroubaceae	<i>Simaba monophylla</i> (Oliv.) Cronquist	S/S	1					
Taccaceae	<i>Tacca parkeri</i> Seem.	H	1		1		1	1
Ternstroemiaceae	<i>Ternstroemia campincola</i> B.M. Boom	S/S	1			1	1	1
Ternstroemiaceae	<i>Ternstroemia oleifolia</i> Wawra	S/S					1	
Ternstroemiaceae	<i>Ternstroemia pungens</i> Gleason	S/S	1					1
Ternstroemiaceae	<i>Ternstroemia</i> sp. A	S/S					1	
Tetrameristaceae	<i>Pentamerista neotropica</i> Maguire	S/S				1	1	1
Thurniaceae	<i>Thurnia polycephala</i> Schnee	H	1			1	1	
Thurniaceae	<i>Thurnia sphaerocephala</i> (Rudge) Hook. f.	H	1				1	1
Thymelaeaceae	<i>Lasiadenia ottohuberi</i> Plowman & Nevling	S/S				1	1	
Thymelaeaceae	<i>Lasiadenia rupestris</i> Benth.	S/S	1			1	1	
Thymelaeaceae	<i>Tepuianthus savannensis</i> Maguire & Steyerm.	S/S	1		1	1		1
Trigoniaceae	<i>Trigonia spruceana</i> Benth. ex Warm.	S/S			1		1	1
Velloziaceae	<i>Vellozia tubiflora</i> Kunth	H				1		
Violaceae	<i>Paypayrola arenacea</i> Aymard & G.A. Romero	S/S					1	
Violaceae	<i>Rinorea sprucei</i> Kuntze	S/S	1				1	1

(continued)

Family	Taxon	Habit	Sip	Cam	Ven	Yap	Ata	Pas
Vochysiaceae	<i>Qualea wurdackii</i> Marc.-Berti	T	1		1	1		
Vochysiaceae	<i>Ruizterania esmeraldae</i> (Standl.) Marc.- Berti	T	1			1	1	
Vochysiaceae	<i>Ruizterania obtusata</i> ssp. <i>multivenosa</i> Marc.- Berti	T					1	1
Vochysiaceae	<i>Ruizterania retusa</i> (Spruce ex Warm.) Marc.-Berti	T				1	1	1
Vochysiaceae	<i>Vochysia angustifolia</i> Ducke	T				1	1	1
Vochysiaceae	<i>Vochysia catingae</i> Ducke	T				1	1	
Xyridaceae	<i>Abolboda acaulis</i> Maguire	H				1	1	
Xyridaceae	<i>Abolboda acicularis</i> Idrobo & L.B. Sm.	H	1			1	1	
Xyridaceae	<i>Abolboda americana</i> (Aubl.) Lanj.	H	1			1	1	
Xyridaceae	<i>Abolboda bella</i> Maguire	H				1		
Xyridaceae	<i>Abolboda ebractata</i> Maguire & Wurdack var. <i>ebracteata</i>	H				1		
Xyridaceae	<i>Abolboda ebractata</i> var. <i>brevifolia</i> Maguire	H			1	1		
Xyridaceae	<i>Abolboda grandis</i> Griseb.	H					1	
Xyridaceae	<i>Abolboda killipii</i> Lasser	H	1			1	1	
Xyridaceae	<i>Abolboda linearifolia</i> Maguire	H			1	1	1	1
Xyridaceae	<i>Abolboda macrostachya</i> Spruce ex Malme var. <i>macrostachya</i>	H	1	1	1	1	1	1
Xyridaceae	<i>Abolboda sprucei</i> Malme	H					1	
Xyridaceae	<i>Xyris arachnoidea</i> Maguire & L.B. Sm.	H				1	1	
Xyridaceae		H	1			1	1	1

(continued)



Family	Taxon	Habit	Sip	Cam	Ven	Yap	Ata	Pas
	<i>Xyris cryptantha</i> Maguire & L.B. Sm.							
Xyridaceae	<i>Xyris esmeraldae</i> Steierm.	H	1			1	1	
Xyridaceae	<i>Xyris fallax</i> Malme	H	1				1	
Xyridaceae	<i>Xyris frequens</i> Maguire & L.B. Sm.	H				1	1	
Xyridaceae	<i>Xyris globosa</i> L.A. Nilsson	H			1	1	1	
Xyridaceae	<i>Xyris guianensis</i> Steud.	H	1			1	1	1
Xyridaceae	<i>Xyris huberi</i> Kral & L.B. Sm.	H				1	1	
Xyridaceae	<i>Xyris involucrata</i> Nees	H	1			1	1	1
Xyridaceae	<i>Xyris jupicai</i> Rich.	H	1			1	1	1
Xyridaceae	<i>Xyris</i> <i>lomatophylla</i> Mart.	H	1		1	1	1	
Xyridaceae	<i>Xyris oblata</i> Kral & L.B. Sm.	H					1	
Xyridaceae	<i>Xyris oxylepis</i> Idrobo & L.B. Sm.	H	1	1	1	1	1	
Xyridaceae	<i>Xyris paraensis</i> Poepp. ex Kunth	H	1		1	1	1	
Xyridaceae	<i>Xyris rubrolimbata</i> Heimerl	H					1	
Xyridaceae	<i>Xyris savanensis</i> Miq.	H		1		1	1	
Xyridaceae	<i>Xyris</i> <i>spathacea</i> Lanj.	H	1			1		
Xyridaceae	<i>Xyris spruceana</i> Malme	H					1	
Xyridaceae	<i>Xyris stenostachya</i> Steierm.	H	1	1	1	1		
Xyridaceae	<i>Xyris subglabrata</i> Malme	H	1		1	1	1	
Xyridaceae	<i>Xyris subuniflora</i> Malme	H					1	1
Xyridaceae	<i>Xyris surinamensis</i> A. Spreng.	H			1			1
Xyridaceae	<i>Xyris teinosperma</i> Idrobo & L.B. Sm.	H				1	1	
Xyridaceae	<i>Xyris uleana</i> Malme	H	1	1	1	1	1	1
Xyridaceae	<i>Xyris wurdackii</i> Maguire & L.B. Sm. ssp. <i>wurdackii</i>	H					1	
Zamiaceae		S/S	1					1

(continued)

Family	Taxon	Habit	Sip	Cam	Ven	Yap	Ata	Pas
	<i>Zamia lecointei</i> Ducke							

Presence of each taxon in a study area is indicated with a number. Values indicate the approximate relative abundance in a given area (1 = scarce, 2 = common, 3 = abundant). Sip: Sipapo; Cam: Camani; Ven: Ventuari; Yap: Yapakana; Ata: Atabapo; Pas: PasimoniFor habits: T = tree, S/S = shrubs/suffrutices, H = herbs, Ch = herbaceous climbers, Cw = woody climbers, Eh = herbaceous epiphytes, Ew = woody epiphytes (cf. Fig. 11.1)

## References

- Adeney JM, Christensen NL, Vicentini A, Cohn-Haft M (2016) White-sand ecosystems in Amazonia. *Biotropica* 48:7–23
- Anderson AB (1981) White-sand vegetation of Brazilian Amazonia. *Biotropica* 13:199–210
- APG [Angiosperm Phylogeny Group] (2016) An update of the Angiosperm Phylogeny Group classification for the orders and families of flowering plants: APG IV. *Bot J Linnean Soc* 181: 1–20
- Arellano-Peña H, Bernal-Gutiérrez G, Calero-Cayopare A, Castro-L F, Lozano A, Bernal-Linares DS, Méndez-R C, Aymard G (2019) The first botanical exploration to the upper Cuiarí (Cuyarí) and Isana rivers, upper Río Negro basin, Guainía department, Colombia. *Harv Pap Bot* 24:83–102
- Aymard G, Campbell LM, Romero-González GA (2014) *Paypayrola arenacea* (Violaceae), a new species with an unusual life-form from a white sand savanna in the Amazon river basin of Venezuela. *Harv Pap Bot* 19:175–183
- Berry PE (2005) Rapateaceae. In: Berry PE, Holst B, Yatskievych K (eds) *Flora of Venezuelan Guayana*, vol 9. Missouri Botanical Garden Press, St Louis, pp 413–472
- Berry PE, Riina R (2005) Insights into the diversity of the Pantepui flora and the biogeographic complexity of the Guayana Shield. *Biologiske Skrifter* 55:145–167
- Berry PE, Rogers ZS (2005) Tepuianthaceae. In: Berry PE, Holst B, Yatskievych K (eds) *Flora of Venezuelan Guayana*, vol 9. Missouri Botanical Garden Press, St Louis, pp 297–299
- Bongers F, Engelen D, Klinge H (1985) Phytomass structure of natural plant communities on Spodosols in southern Venezuela: the bana woodland. *Vegetatio* 63:13–34
- Budowski G (1956) Tropical savannas, a sequence of forest falling and repeated burning. *Turrialba* 6:23–33
- Cabral FN, Bittrich V, Amaral MCE (2016) Four new species of *Caraiipa* (Calophyllaceae) from the Amazon basin and the Guiana Shield. *Phytotaxa* 286:245–255
- Cabral FN, Bittrich V, Amaral MCE (2018) Five new species of *Caraiipa* (Calophyllaceae) from the Venezuelan Guayana. *Syst Bot* 43:240–249
- Castillo R, Salas V (2007) Estado de Conservación del Parque Nacional Yapacana. Reporte Especial. In: *BioParques: Asociación Civil para la Conservación de los Parques Nacionales*. Programa Observadores de Parques. [www.bioparques.org](http://www.bioparques.org) / [www.parkswatch.org](http://www.parkswatch.org)
- Christenhusz MJM, Reveal JL, Farjon A, Gardner MF, Mill RR, Chase MW (2011) A new classification and linear sequence of extant gymnosperms. *Phytotaxa* 19:55–70
- Coomes DA, Grubb PJ (1996) Amazonian caatinga and related communities at La Esmeralda, Venezuela: forest structure, physiognomy and floristics, and control by soil factors. *Vegetatio* 122:167–191
- Córdoba Sánchez MP (2014) Análisis de la Riqueza Vegetal y Patrones Fitogeográficos para la Región del Escudo Guayanés Colombiano. Universidad Nacional de Colombia, Facultad de Ciencias, Departamento de Biología, Doctorado en Ciencias (Línea de Biodiversidad y Conservación), Bogotá

- Couvreur TLP (2015) Odd man out: why are there fewer plant species in African rain forests? *Plant Syst Evol* 301:1299–1313
- Cuello NL (2003) A new species of *Tovomita* (Clusiaceae) from Amazonian Venezuela and Peru. *Novon* 13:34–36
- Daly DC, Silveira M, Medeiros H, Castro W, Obermüller FA (2016) The white-sand vegetation of Acre, Brazil. *Biotropica* 48:81–89
- Davis CC, Bell CD, Mathews S, Donoghue MJ (2002) Laurasian migration explains Gondwanan disjunctions: evidence from Malpighiaceae. *Proc Natl Acad Sci USA* 99:6833–6837
- Delprete PG (2018) Two new species of the tribe Sipaneeae (Rubiaceae) from white-sand areas of Brazilian and Colombian Amazon. *Phytotaxa* 382:125–135
- Demarchi LO, Scudeller VV, Moura LC, Dias-Terceiro RG, Lopes A, Wittmann FK, Piedade MTF (2018) Floristic composition, structure and soil-vegetation relations in three white-sand soil patches in central Amazonia. *Acta Amazonica* 48:46–56
- Devecchi M, Lovo J, Moro M, Andrino C, Barbosa-Silva R, Viana P, Giulietti AM, Antar G, Watanabe M, Zappi D (2020) Beyond forests in the Amazon: biogeography and floristic relationships of the Amazonian savannas. *Bot J Linnean Soc* 20:1–26
- Eden MJ (1974) Palaeoclimatic influences and the development of savanna in Southern Venezuela. *J Biogeogr* 1:95–109
- Espinoza JC, Ronchail J, Guyot JL, Cochonneau G, Naziano F, Lavado W, de Oliveira E, Pombosa R, Vauchel P (2009) Spatio-temporal rainfall variability in the Amazon basin countries (Brazil, Peru, Bolivia, Colombia, and Ecuador). *Int J Climatol* 29:1574–1594
- Eva HD, Belward AS, De Miranda EE, Di Bella CM, Gond V, Huber O, Jones S, Sgrenzaroli M, Fritz S (2004) A land cover map of South America. *Global Change Biol* 10:731–744
- Ferreira CAC (2009) Análise comparativa de vegetação lenhosa do ecossistema campina na Amazônia Brasileira. PhD Dissertation, Instituto Nacional de Pesquisas da Amazônia, Manaus
- Fine PV, García-Villacorta R, Pitman NCA, Mesones I, Kembel SW (2010) A floristic study of the white-sand forests of Peru. *Ann Mo Bot Gard* 97:283–305
- Flora do Brasil (2020) Jardim Botânico do Rio de Janeiro. Available at <http://floradobrasil.jbrj.gov.br/>. Accessed on 17 Jan 2022
- García-Villacorta R, Dexter KG, Pennington T (2016) Amazonian white-sand forests show strong floristic links with surrounding oligotrophic habitats and the Guiana shield. *Biotropica* 48:47–57
- Givnish TJ, Millam KC, Evans TM, Hall JC, Pires JC, Berry PE, Systsma KJ (2004) Ancient vicariance or recent long-distance dispersal? Inferences about phylogeny and south American–African disjunctions in Rapateaceae and Bromeliaceae based on *ndhF* sequence data. *Int J Plant Sci* 165(4 Suppl):S35–S54
- Grande AJR (2019) Estudio sistemático del género *Ternstroemia* Mutis ex L.f. (Ternstroemiaceae) para el área del Escudo Guayanés (Brasil, Colombia, Guayana Francesa, Guyana, Surinam y Venezuela). PhD Dissertation, Facultad de Ciencias, Universidad Central de Venezuela, Caracas
- Guimarães FS, Bueno GT (2016) As campinas e campinaranas amazônicas. *Caderno de Geografia* 26:113–133
- Heads M (2012) Biogeography of the Hawaiian islands, the global context. In: Heads M (ed) *Molecular panbiogeography of the tropics*. University of California Press, Berkeley
- Hokche O, Berry PE, Huber O (2008) Nuevo Catálogo de la Flora Vasculare de Venezuela. In: Fundación Instituto Botánico de Venezuela “Dr. Tobías Lasser”, Caracas
- Holdridge LR (1947) Determination of world plant formations from simple climatic data. *Science* 105:267–268
- Huber O (1995a) History of botanical exploration. In: Berry PE, Holst B, Yatskievych K (eds) *Flora of Venezuelan Guayana*, vol 1. Timber Press, Portland, OR, pp 63–95
- Huber O (1995b) Vegetation. In: Berry PE, Holst B, Yatskievych K (eds) *Flora of Venezuelan Guayana*, vol 1. Timber Press, Portland, OR, pp 97–160

- Huber O (1995c) Conservation of the Venezuelan Guayana. In: Berry PE, Holst B, Yatskiyevych K (eds) Flora of Venezuelan Guayana, vol 1. Timber Press, Portland, OR, pp 193–218
- Huber O (2006) Herbaceous ecosystems on the Guayana Shield, a regional overview. *J Biogeogr* 33:464–475
- Huber O, Oliveira-Miranda MA (2010) Representación de las formaciones vegetales de Venezuela. In: Rodríguez JP, Rojas-Suárez F, Giraldo HD (eds) Libro Rojo de los Ecosistemas Terrestres de Venezuela, Provita, Shell Venezuela, Lenovo (Venezuela). Caracas, Venezuela, pp 43–53
- IBGE (2012) Manual técnico da vegetação brasileira: Sistema fitogeográfico, inventário das formações florestais e campestres, técnicas e manejo de coleções botânicas, procedimentos para mapeamentos. Instituto Brasileiro de Geografia e Estatística (IBGE), Manuais Técnicos de Geociências
- Judziewicz EJ, Davidse G (2008) *Arthrostylidium berryi* (Poaceae, Bambusoideae, Bambuseae, Arthrostylidiinae), a new species from white sand shrublands in Venezuela and Colombia. *Novon* 18:361–365
- Klinge H, Cuevas E (2000) Bana: una comunidad leñosa sobre arenas blancas en el Alto Río Negro, Venezuela. *Scientia Guianae* 11:37–49
- Klinge H, Medina E (1979) Río Negro caatingas and campinas, Amazonas States of Venezuela and Brazil. In: Goodall DW (ed) Ecosystems of the world, Specht RL (ed) 9A: Heathlands and related shrublands. Elsevier, Amsterdam, pp 483–488
- Klinge H, Medina E, Herrera R (1977) Studies on the ecology of the Amazon Caatinga forest in southern Venezuela 1. General features. *Acta Científica Venezolana* 28:270–276
- Lleras E (1997) Upper Río Negro region (Brazil, Colombia, Venezuela). In: Davies SD, Heywood VH, Herrera-MacBryde O, Villa-Lobos J, Hamilton AC (eds) Centres of plant biodiversity. Volume 3: The Americas. World Wildlife Fund for Nature & The World Conservation Union, Cambridge, pp 333–337
- Lozada JR (2019) The Orinoco Mining Arc: a historical perspective. *Gold Bull* 52:153–163
- Lozada JR, Carrero YA (2017) Estimación de las áreas deforestadas por minería y su relación con la gestión ambiental en la Guayana Venezolana. *Revista Forestal Venezolana* 61:59–77
- MARNR, ORSTOM (1987) Atlas del Inventario de Tierras del Territorio Federal Amazonas. MARNR, DGSIIA, Caracas
- Medina E, Cuevas E (1989) Patterns of nutrient accumulation and release in Amazonian forests of the upper Río Negro basin. In: Proctor J (ed) Mineral nutrients in tropical forest and savanna ecosystems. Blackwell, Oxford, pp 217–240
- Morley RJ (2000) Origin and evolution of tropical rain forests. Wiley, New York
- Nozawa Furuya S, Castillo-Suárez A, Huber O (2019) Catálogo y análisis florístico de las sabanas en el sector Puerto Ayacucho del estado Amazonas, Guayana venezolana. *Acta Botanica Venezuelica* 42:31–113
- Oliveira-Miranda MA, Huber O, Rodríguez JP, Rojas-Suárez F, De Oliveira-Miranda R, Zambrano-Martínez S (2010a) Arbustales siempreverdes per se. In: Rodríguez JP, Rojas-Suárez R, Giraldo Hernández D (eds) Libro Rojo de los Ecosistemas Terrestres de Venezuela, Provita, Shell Venezuela, Lenovo (Venezuela). Caracas, Venezuela, pp 171–175
- Oliveira-Miranda MA, Huber O, Rodríguez JP, Rojas-Suárez F, De Oliveira-Miranda R, Zambrano-Martínez S (2010b) Arbustales ribereños. In: Rodríguez JP, Rojas-Suárez R, Giraldo Hernández D (eds) Libro Rojo de los Ecosistemas Terrestres de Venezuela. Provita, Shell Venezuela, Lenovo (Venezuela). Caracas, Venezuela, pp 184–187
- Oliveira-Miranda MA, Huber O, Rodríguez JP, Rojas-Suárez F, De Oliveira-Miranda R, Zambrano-Martínez S (2010c) Arbustales ribereños. In: Rodríguez JP, Rojas-Suárez R, Giraldo Hernández D (eds) Libro Rojo de los Ecosistemas Terrestres de Venezuela, Provita, Shell Venezuela, Lenovo (Venezuela). Caracas, Venezuela, pp 216–219
- PPG I [The Pteridophyte Phylogeny Group] (2016) A community-derived classification for extant lycophytes and ferns. *J Syst Evol* 54:563–603

- Prance GT, Schubart HOR (1978) Notes on the vegetation of Amazonia I. A preliminary note on the origin of the open white sand campinas of the lower R o Negro. *Brittonia* 30:60–63
- Provita (2021) Cobertura y uso del suelo en la Amazon a venezolana A o 2000. Geoportall Provita. <https://geoportall.provita.org.ve/>. Accessed 9 Oct 2021
- Rajakaruna N (2004) The edaphic factor in the origin of plant species. *Int Geol Rev* 46:471–478
- Renner S (2004) Plant dispersal across the tropical Atlantic by wind and sea currents. *Int J Plant Sci* 165(4 Suppl):S35–S54
- Riina R, Huber O (2003) Ecosistemas exclusivos de la Guayana. In: Aguilera MM, Az ocar A, Gonz alez JE (eds) Biodiversidad en Venezuela, vol 2. Fundaci n Polar, Ministerio de Ciencia y Tecnolog a, Fondo Nacional de Ciencia, Tecnolog a e Innovaci n (FONACIT), Caracas, pp 828–861
- Riina R, Duno R, Aymard G, Fern andez A, Huber O (2007) Diversidad flor stica de los Llanos de Venezuela. In: Duno R, Aymard G, Huber O (eds) Cat logo Anotado e Ilustrado de la flora vascular de los Llanos de Venezuela. Fundaci n Polar-Fundaci n Instituto Bot nico de Venezuela, Caracas, Venezuela, pp 107–123
- Riina R, Berry PE, Huber O, Michelangeli FA (2019) Pantepui plant diversity and biogeography. In: Rull V, Vegas-Vilarr bia T, Huber O, Se ariz J (eds) Biodiversity of Pantepui: The Pristine “Lost World” of the Neotropical Guiana Highlands. Academic, Cambridge, pp 121–147
- Stevens PF (2001–onwards) Angiosperm phylogeny website. Version 14, July 2017 [and more or less continuously updated since]. Available at: [www.mobot.org/MOBOT/research/APweb/](http://www.mobot.org/MOBOT/research/APweb/)
- Steyermark JA, Berry PA, Holst BK (1995–2005) Flora of the Venezuelan Guayana, 9 volumes. Missouri Botanical Garden Press and Timber Press, St. Louis and Portland
- Vicentini A (2004) Vegeta o ao longo de um gradiente ed fico no Parque do Ja . In: Borges SH, Iwanaga S, Durigan CC, Pinheiro MR (eds) Janelas para a biodiversidade no Parque Nacional do Ja : uma estrat gia para o estudo da biodiversidade na Amaz nia. Funda o Vit ria Amaz nica (FVA)/WWF/IBAMA, Manaus, pp 117–143
- Walter H (1977) Vegetationszonen und Klima. Uni-Taschenb cher, no. 14. 309 pp. Verlag Eugen Ulmer, Stuttgart
- Walter H (1985) Vegetation of the earth and ecological systems of the geobiosphere, 3rd edn. Springer, Berlin
- Zappi DC, Andrino CO, Barbosa-Silva RG (2020) Lista preliminar de especies bot nicas coletadas nos Campos do Ariramba,  bidos, Floresta Estadual do Trombetas, Par . Instituto Tecnol gico VALE, Produ o T cnica ITV DS N012/2020. <https://doi.org/10.29223/PROD.TEC.ITV.DS.12.Zappi>



# Ecophysiological Features of the Lowland meadow's Species within the Upper Rio Negro and Orinoco Basins

# 12

E. Medina

## 12.1 Introduction

Meadow is not a technical botanical or ecological concept but is commonly used in temperate latitudes and high mountain tropical areas to describe “an ecosystem type composed of one or more plant communities dominated by herbaceous species. It supports plants that use surface water and/or shallow ground water (generally at depths of less than one meter)” [https://www.fs.usda.gov/Internet/FSE\\_DOCUMENTS/stelprdb5397692.pdf](https://www.fs.usda.gov/Internet/FSE_DOCUMENTS/stelprdb5397692.pdf)

In this study, meadow vegetation includes herbaceous plant communities dominated, in terms of biomass, by non-gramineous species that typically live on flood-prone, lowland, white sands substrates throughout the upper Rio Negro and Orinoco basins. They consist mainly of broadleaved herbaceous species belonging to highly specialized monocot families such as Rapateaceae, Bromeliaceae, Xyridaceae, Eriocaulaceae, and narrow-leaved herbs of the Cyperaceae and Poaceae. Among dicots the Melastomataceae, Rubiaceae, and Fabaceae are well represented with numerous sclerophyllous forbs, and subshrubby species. The occurrence of carnivore species from Lentibulariaceae and Droseraceae is also a common trait of the Amazonian meadows (Fig. 12.1).

Meadows contrast to lowland tropical grasslands (savanna) that are dominated by drought-tolerant gramineous herbs (Poaceae and Cyperaceae) (Huber 2006).

The environmental conditions under which meadow ecosystems thrive within the study areas in Amazonas state of Venezuela might be broadly defined as follows:

1. Rainfall: higher than 100 mm per month, with seasonal variation in number of dry days (daily rainfall < daily evapotranspiration).

---

E. Medina (✉)

Centro de Ecología, Instituto Venezolano de Investigaciones Científicas, Caracas, Venezuela

International Institute of Tropical Forestry, USDA Forest Service, San Juan, Puerto Rico



**Fig. 12.1** Herbaceous vegetation (meadow) located at the western margin of the Ekeweni creek tributary of the caño San Miguel (2°44'12" N; 66°47'48" W; 100 m abs), dominated by monocot broadleaved families (Bromeliaceae, Orchidaceae, Rapateaceae, Xyridaceae), only one Poaceae species, the C3 *Steyermarkochloa angustifolia*. (Photo and description courtesy of Gustavo Romero-González, Oakes Ames Orchid Herbarium, Harvard University Herbaria, Cambridge, Massachusetts 02138, U.S.A)

2. Soils: sandy, with very low water retention capacity, resulting in frequent oscillations between water potentials near zero in saturated soils, and short periods of water stress after one or more rainless days. Soils are a poor source of mineral plant nutrients, and their supply depends on the steady renovation by water flowing through the system. The processes of nutrient uptake, recycling, and release from biomass resembles a kind of hydroponic system, in which the actual nutrient concentrations in the soil solution are well below the level of saturation of the root nutrient uptake mechanisms.

The sampling method employed in the present study for vegetation analysis could not be processed in quantitative terms due to varying number of sampling sites within the selected areas (See Chaps. 6 and 11 for study area descriptions). The effort was directed to obtain a plant species list as complete as possible from each site. The sampling included several vegetation types on white sands, from forests to shrublands and herbaceous communities, and the ecotones within them (species checklist in Chap. 11).



## 12.2 The Botanical Composition of Amazonian Meadows

For a more accurate analysis of meadow vegetation *sensu stricto*, I selected from the species checklist of the white-sand sites (Appendix 11.1, Chap. 11) those that could be classified as herbaceous or subshrubby. Species habit information was obtained mainly from Bernal et al. (2020). The total number of species selected amounts to 227, from which 76 belong to 12 dicot families and 151 belong to 11 monocot families (Table 12.1).

Among the dicots the dominant families are well known for thriving in wet, acid, and nutrient-poor habitats: Lentibulariaceae with 19 species (17 within the genus *Utricularia*), and Gentianaceae with 6 genera and 15 species. Other well-represented families occurring in similar habitats are the Burmanniaceae, Droseraceae, and Ochnaceae. Herbaceous Melastomataceae species were found in all study sites with seven species distributed within six genera. The other six families also occur preferentially in wet to flooded soils but are not restricted in their distribution to white-sand areas.

By contrast, the monocots are represented by 11 families and 151 species. From this group, 5 families stand out all belonging to the order Poales: Xyridaceae (2 genera and 36 species), Poaceae (14 genera and 30 species), Cyperaceae (6 genera, and 28 species), Eriocaulaceae (4 genera and 23 species), and Rapateaceae (8 genera and 20 species).

The ratio of monocot/dicot species ranges from 2.6–2.9 in the Pasimoni, Atabapo, Yapacana areas, to 1–1.5 in the Camani, Ventuari areas, suggesting large differences in community structure and composition.

---

## 12.3 Physiological Traits Related to Nutrient Deficiency, Flooding Tolerance, and Drought

### 12.3.1 Dicots Families

Lentibulariaceae species thrive in wet, acid habitats; individuals grow on sandy or peaty, very nutrient poor, frequently water-logged soils, seldom fully covered by water (Stevens 2001 onwards, Raynai-Roques and Jeremie 2005). The two recorded genera (*Genlisea* and *Utricularia*) contain species with modified leaves that function as traps for small aquatic organisms. Such traps may constitute a significant source of N and P in the dystrophic white-sand soils. These plants are carnivores capable of capturing small crustaceans, copepoda, cladocerans, and several other groups. *Utricularia* species constitute the largest group of plant carnivores (Poppinga et al. 2016).

The Gentianaceae is represented by six genera (*Adenolisianthus*, *Chelonanthus*, *Coutubea*, *Curtia*, *Irlbachia*, *Voyria*) that are commonly found growing in dystrophic soils in Amazonian lowlands and on sandstone mountains in the Guayana shield (Struwe et al. 2008). The micoheterotroph, achlorophyllous genus *Voyria* is represented by a widespread species in the neotropics, *V. aphylla* (Imhof 1999).

**Table 12.1** Number of genera and species per family in each study area. Names of the study areas indicated by the first three letters (Sipapo, Camani, Ventuari, Yapacana, Atabapo, Pasimoni)

Family	Order	N° Genera	N° Species	Sip	Cam	Study areas			Yap	Ata	Pas
						Vent	Vent	Vent			
Lentibulariaceae	Lamiales	2	19	7	8	7	7	11	5	2	
Gentianaceae	Gentianales	7	15	9	3	3	3	8	13	4	
Melastomataceae	Myrtales	6	7	2	2	3	3	8	8	2	
Burmanniaceae	Dioscoreales	2	6		1			3	3	1	
Polygalaceae	Fabales	1	6	3	4	5	5	3	2	1	
Droseraceae	Caryophyllales	1	4	4	1			2	2	1	
Fabaceae	Fabales	2	4	3	3	3	3	4	1	1	
Lythraceae	Myrtales	1	4	1	2	1	1	1	1		
Ochnaceae	Malpighiales	1	4	3	1	2	2	3	2	2	
Rubiaceae	Gentianales	1	4	2	1	1	1	1	3	1	
Lamiaceae	Lamiales	1	2	2	1			1			
Loganiaceae	Gentianales	1	1		1			1	1	1	
<b>Total Dicots</b>	<b>13</b>	<b>26</b>	<b>76</b>	<b>36</b>	<b>28</b>	<b>25</b>	<b>25</b>	<b>46</b>	<b>41</b>	<b>16</b>	
Xyridaceae	Poales	2	36	17	5	12	12	27	30	9	
Poaceae	Poales	14	30	16	8	9	9	20	19	17	
Cyperaceae	Poales	6	28	9	7	5	5	24	21	9	
Eriocaulaceae	Poales	4	23	11	4	6	6	19	12	4	
Rapateaceae	Poales	8	20	8	2	3	3	12	16	9	
Bromeliaceae	Poales	5	8	5	2	1	1	3	4	1	
Thurniaceae	Poales	1	2	2				1	2	1	
Alismataceae	Alismatales	1	1					1		1	
Haemodoraceae	Commelinales	1	1		1	1	1	1	1	1	
Marantaceae	Zingiberales	1	1						1	1	
Velloziaceae	Pandanales	1	1					1			
<b>Total Monocots</b>	<b>5</b>	<b>44</b>	<b>151</b>	<b>68</b>	<b>29</b>	<b>37</b>	<b>37</b>	<b>109</b>	<b>106</b>	<b>53</b>	

The family Burmanniaceae contains several mycoheterotrophic species, represented in the study areas only by *Apteria aphylla*, whereas the *Burmannia* species recorded are photosynthetically independent, and probably forming mycorrhizal symbiosis. The species recorded from the study areas occur in wet places (oligotrophic sandy meadows), growing together with various grasses and sedges, and with species of *Xyris*, *Utricularia*, *Curtia*, and several Eriocaulaceae (Maas et al. 1986).

Four *Drosera* species were recorded in the Sipapo area, and none in the Ventuari area. All *Drosera* species have leaves with glandular hairs secreting sticky mucilage, acids, and proteolytic enzymes. These leaves act as semi-passive traps for small insects that are digested slowly by the secretion of leaf hairs. They are a good example of “insectivorous” plants that obtain N and P from insect prey complementing these very scarce elements supplied from the substrates on which they grow (Stevens 2001).

The six species of *Polygala* are commonly found in wet lowlands in northern South America. I found no reference in the literature to ecophysiological traits of plants associated with nutrient-poor white-sands in these species.

The Ochnaceae are represented by only one genus, *Sauvagesia*, common in white-sand vegetation throughout the Amazon basin, I found no special studies on adaptations to nutrient-poor soils.

The Melastomataceae in general are well-known Al accumulators (Jansen et al. 2002) mostly within the ligneous species. They are represented by six genera (*Aciotis*, *Desmoscelis*, *Noterophila* = *Acisanthera*, *Pachyloma*, *Rynchanthera*, and *Siphanthera*) and seven herbaceous or subshrubby species, all from wet soils. Herbaceous and subshrub species of the genera *Pterolepis* and *Desmocelis* and *Rhychanthera*, growing on wet, acid soils, have been shown to be also strong Al accumulators (Renner 1990; Olivares et al. 2013).

No special reference was found on the association of the species from the other five dicot families with wet and acid soils.

Although no studies on biomass of meadow ecosystems of the Amazonian lowlands were found, the contribution of the dicot total aboveground biomass is probably small compared to the contribution of the monocot species.

### 12.3.2 Monocots Families

The Xyridaceae within the study areas occur in meadows that are seasonally or permanently wet or moist, always on sandy substrates (Campbell 2004). The family is represented by the genera *Xyris* (25 species) and *Abolboda* (11 species). Dense root hairs and a multilayered exodermis are present in many Xyridaceae (Campbell 2004), a trait that may be associated with efficient nutrient capture and uptake in nutrient-poor environments (Lambers et al. 2015). The family apparently is not mycorrhizal in nature (Stevens 2001).

The Poaceae are represented in the study area by 30 species distributed within 11 genera. The species differ in photosynthetic types (Osborne et al. 2014). Twelve

C<sub>3</sub> species from wet, or partially shaded habitats of the study area were distributed among five genera (*Trichantheicum* being the most common), typical from wet habitats or partially shaded habitats. Eighteen species within nine genera were identified as typical C<sub>4</sub> grasses. These species belong to genera mostly associated with savanna grasslands (*Axonopus*, *Trachypogon*, *Andropogon*, *Mesosetum*, *Anthraenanthia*, *Paspalum*), ecosystems differing from meadows by their seasonal drought stress and relatively higher nutrient availability and highly mobile Al. The Poaceae form mycorrhizal symbiosis under natural conditions and savanna species appear to be strongly dependent on mycorrhizal symbiosis for P procurement (Toro 2003; Brundrett 2017).

The Cyperaceae are represented by 6 genera and 28 species, that can be separated by photosynthetic types. The genera *Lagenocarpus*, *Scleria*, *Calyptrocharya*, and *Diplacrum* have only C<sub>3</sub> species. Of the 12 species of *Rhynchospora* 6 are C<sub>3</sub>, and 6 are C<sub>4</sub>, whereas the four *Bulbostylis* species are typical C<sub>4</sub> occurring most frequently in seasonally dry savanna grasslands (Bruhl and Wilson 2007). Cyperaceae species appear predominantly to be non-mycorrhizal and have several root traits that qualify them as efficient scavengers of nutrients, particularly P, in strongly oligotrophic environments (Stevens 2001; Lambers and Teste 2013). Those traits include dense proliferation of root hairs and development of dauciform roots (Muthukumar et al. 2004). Physiological studies indicate that dauciform roots in Cyperaceae are an adaptation for nutrient scavenging in severely nutrient-poor soils, and do not form mycorrhizal symbiosis (Miller 2005; Shane et al. 2006).

The Eriocaulaceae are well represented in the study area, particularly by species of the genera *Paepalanthus* (6) and *Syngonanthus* (13). There are a few ecophysiological studies on species of Eriocaulaceae, confirming their occurrence in extremely nutrient-poor and wet environments. Root cortex is aerenchymatous in several species (Stevens 2001), a trait counteracting hypoxia in saturated soils. A temperate species of *Eriocaulon* has a high fraction of its dry weight in the roots and takes up most of its inorganic C through its roots (Raven et al. 1988). Mycorrhizal symbiosis has been shown to occur naturally in a few species of this family (Raven et al. 1988; Pagano and Scotti 2009). Considering the huge altitudinal distribution range of this family within the Amazonas- Guayana regions, and its occurrence in habitats differing in hydrological regimes, it would be worthwhile to conduct an isotopic study (C, and N) to elucidate photosynthetic and nutritional patterns.

Rapateaceae is a family with 17 genera from which 8 were recorded in the study area. There are no ecophysiological studies in the literature on any species of this family, except one paper on the natural abundance of <sup>13</sup>C showing the predominance of C<sub>3</sub> photosynthesis and signs of weak CAM in species of *Kunhardtia*, *Marahuacaea*, *Saxofridericia*, and *Stegolepis* (Crayn et al. 2001). In their study on *Guacamaya superba* Fernández-Lucero et al. (2016) hypothesize that possible adaptations to the oligotrophic habitats in which Rapateaceae occur, are traits such as abundant mucilage, idioblasts containing a tannin-like substance, leaf fibers, presence of epidermal silica, formation of telmata, and vesicular-arbuscular mycorrhizal fungi.

From the Bromeliaceae only eight terrestrial species were included as components of meadows, distributed within the genera *Brewcaria*, *Brocchinia*, *Navia*, *Pitcairnia*, and *Vriesea*. These genera are certainly of the C<sub>3</sub> photosynthetic type (Crayn et al. 2015). No specific studies on mycorrhizal associations were found, but terrestrial bromeliads have been shown to form symbiotic associations depending on the presence of mycorrhizal fungi in the soil (Grippa et al. 2007; Leroy et al. 2021).

The remaining monocot families in Table 12.1 are scarcely represented and are not discussed further.

### 12.3.3 Similarity of Species Composition among Study Areas

I selected characteristic families to conduct a botanical similarity analysis among the study areas. To that end the actual number of species per family was expressed as % of the total amount of species recorded at each site (Table 12.2). The relative predominance of monocot species is clear ranging from 70–75% in the southern sites (Yapacana, Atabapo, and Pasimoni) to 51–58 in the northern sites (Camani and Ventuari), suggesting again clear floristic separation among the study areas. The monocots are the predominant group of plants in terms of species proportion. Among them, the families most probably accounting for the largest proportion of biomass per unit area in the meadows sampled are the Bromeliaceae, Cyperaceae, Eriocaulaceae, Poaceae, Rapateaceae, and Xyridaceae.

I selected the first six families of the dicots and monocots groups of plants, containing 76% and 96% of each group, respectively, and used the standardized values to run a cluster analysis. The result shows that the Pasimoni and Sipapo areas are well separated in agreement with their contrasting latitudinal locations (Fig. 12.2). The graph identifies Camani-Ventuari and Yacapana-Atabapo as separate units with higher similarity in botanical composition. This botanical separation agrees with the clustering analysis conducted in Chap. 11 based on common species using the full data set. The Pasimoni site stands out due to its large proportion of Poaceae, whereas the Camani site is characterized by its lower proportions of Xyridaceae and Eriocaulaceae (Table 12.2). It should be observed that the proportion of Xyridaceae is lower than the proportion of Poaceae only in the Camani and Pasimoni sites.

---

## 12.4 Concluding Remarks

The semi-quantitative analysis of meadow vegetation in six areas of the upper Río Negro and Orinoco basins in Venezuela revealed differences in floristic composition associated to their latitudinal location. These differences cannot be related in a simple fashion to pedological factors, as soil texture and physicochemical properties are quite similar in the study areas (see Chap. 6). Grouping of the northerner Sipapo-Camani-Ventuari areas in opposition to the southerner Yapacana-Atabapo-Pasimoni

**Table 12.2** Standardized species composition per family and sites

Family	Total	Sip	Cam	Ven	Yap	Ata	Pas
<b>Dicots</b>							
Lentibulariaceae	8	7	14	11	7	3	3
Gentianaceae	7	9	5	5	5	9	6
Melastomataceae	3	2	4	5	5	5	3
Burmanniaceae	3		2		2	2	1
Polygalaceae	3	3	7	8	2	1	1
Droseraceae	2	4	2		1	1	1
Fabaceae	2	3	5	5	3	1	1
Lythraceae	2	1	4	2	1	1	0
Ochnaceae	2	3	2	3	2	1	3
Rubiaceae	2	2	2	2	1	2	1
Lamiaceae	1		4	2		1	
Loganiaceae		1		2	1	1	
<b>Monocots</b>							
Xyridaceae	16	16	9	19	17	20	13
Poaceae	13	15	14	14	13	13	24
Cyperaceae	12	9	12	8	15	14	13
Eriocaulaceae	10	11	7	9	12	8	6
Rapateaceae	9	8	4	5	8	11	13
Bromeliaceae	3	5	4	2	2	3	1
Thurniaceae	1	2			1	1	1
Alismataceae				1		1	
Haemodoraceae	2	2	1	1	1		
Marantaceae					1	1	
Velloziaceae				1			
<b>Sum Dicots</b>	33	34	49	42	29	28	21
<b>Sum Monocots</b>	65	65	51	58	70	71	75
<b>(Xyridaceae + Eriocaulaceae + Rapateaceae)/(Poaceae + Cyperaceae)</b>							
	1.4	1.4	0.7	1.5	1.3	1.5	0.8

The numbers in each cell represent the % contribution of the species by each family. Included values only  $\geq 1\%$

areas suggests that reduction of rainfall seasonality along the N-S axis may be one of the proximal causes, as it may be related to: (a) recurrence of soil saturation and reduction of dry days' periods and (b) maintenance of nutrient supply through the continuous underground flow of soil water.

The revised literature shows little information related to the physiology in general, and the nutrient relations of the dominant families in white-sand meadows in the upper Rio Negro and Orinoco basins. At the ecosystem level there is scattered information on species composition and mycorrhizal symbiosis, but virtually nothing could be found regarding their structure, quantitative species composition, biomass distribution, and productivity.

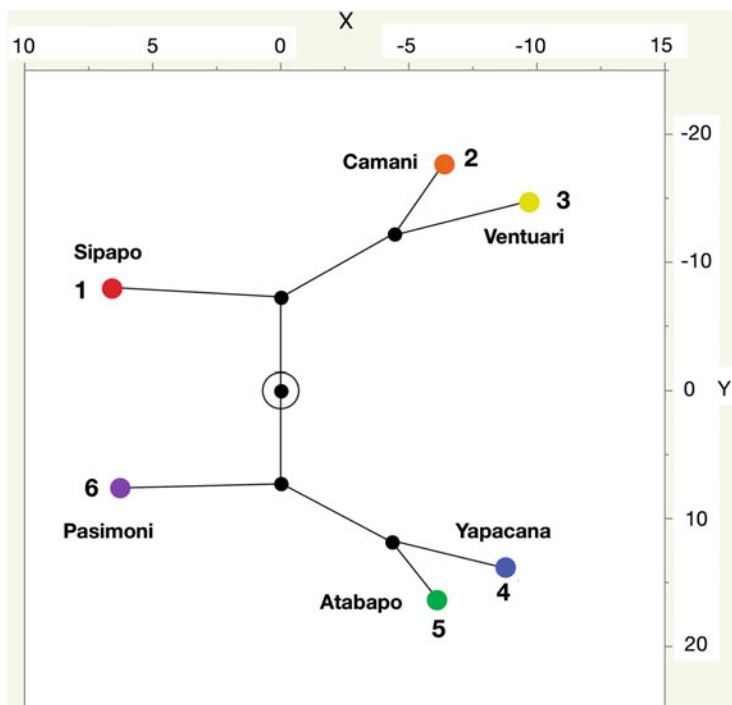


**Fig. 12.2** Clustering of study areas (Ward method) based on the normalized family abundance of species (Lentibulariaceae, Gentianaceae, Melastomataceae, Burmanniaceae, Polygalaceae, Droseraceae, Cyperaceae, Poaceae, Rapateaceae, Eriocaulaceae, Xyridaceae, Bromeliaceae) ( $N^\circ$  of species per family/ $N^\circ$  of herbaceous species at each site)

The importance of those studies cannot be overstated because (a) there are still many white-sand areas unexplored in the upper Río Negro and Orinoco basins, (b) the rate of meadow disturbance due to land use change (forestry, agriculture, mining) is rapidly increasing, (c) experimental studies are needed to elucidate the nutrient uptake mechanisms allowing adequate nutrient supply to plants on white-sand substrates. Support of existing field stations in Brazil, Colombia, Peru, and Venezuela is recommended to facilitate field and experimental studies.

**Acknowledgments** Gerardo Aymard, Ariel Lugo, José Grande and Ricarda Riina provided useful comments to the first version of this paper.

## References

- Bernal R, Gradstein SR & Celis M (eds.). 2020. Catálogo de Plantas y Líquenes de Colombia. v1.1. Universidad Nacional de Colombia. Dataset/Checklist. <https://doi.org/10.15472/7avdh>
- Bruhl JJ, Wilson KL (2007) Towards a comprehensive survey of C3 and C4 photosynthetic pathways in Cyperaceae. *Aliso* 23:99–148



- Brundrett MC (2017) Global diversity and importance of mycorrhizal and nonmycorrhizal plants. In: Tedersoo L (ed) *Biogeography of mycorrhizal Symbiosis*. Springer, Switzerland, pp 533–566. [*Ecological Studies* 230]
- Campbell LM (2004) Anatomy and systematics of Xyridaceae with special reference to *Aratitoyopea*. Ph.D. Dissertation. City University of New York
- Crayn DM, Smith JAC, Winter K (2001) Carbon-isotope ratios and photosynthetic pathways in the neotropical family Rapateaceae. *Plant Biol* 3(5):569–576
- Crayn DM, Winter K, Schulte K, JAC S (2015) Photosynthetic pathways in Bromeliaceae: phylogenetic and ecological significance of CAM and C3 based on carbon isotope ratios for 1893 species. *Bot J Linn Soc* 178:169–221
- Fernández-Lucero M, Santiago Madriñán S, Campbell LM (2016) Morphology and anatomy of *Guacamaya superba* (Rapateaceae) and Schoenocephalieae with notes on the natural history of the flor de Infrida. *Harv Pap Bot* 21:105–123
- Grippa CR, Hoeltgebaum MP, Stürmer SL (2007) Occurrence of arbuscular mycorrhizal fungi in bromeliad species from the tropical Atlantic Forest biome in Brazil. *Mycorrhiza* 17:235–240
- Huber O (2006) Herbaceous ecosystems on the Guayana shield, a regional overview. *J Biogeogr* 33(3):464–475
- Imhof S (1999) Root morphology, anatomy and mycotrophy of the achlorophyllous *Voyria aphylla* (Jacq.) Pers. (Gentianaceae). *Mycorrhiza* (1999) 9:33–39
- Jansen S, Watanabe T, Smets E (2002) Aluminium accumulation in leaves of 127 species in Melastomataceae, with comments on the order Myrtales. *Ann Bot* 90(1):53–64. <https://doi.org/10.1093/aob/mcf142>
- Lambers H, Teste FP (2013) Interactions between arbuscular mycorrhizal and non-mycorrhizal plants: do non-mycorrhizal species at both extremes of nutrient availability play the same game? *Plant, Cell and Environment* 36:1911–1915
- Lambers H, Martinoia E, Renton M (2015) Plant adaptations to severely phosphorus-impooverished soils. *Curr Opin Plant Biol* 25:23–31
- Leroy C, Maes AQ, Louisanna E, Schimann H, Séjalon-Delmas N (2021) Taxonomic, phylogenetic and functional diversity of root-associated fungi in bromeliads: effects of host identity, life forms and nutritional modes. *New Phytol* 231:1195–1209
- Maas PJM, Maas-Van De Kamer, Van Benthem HJ, Snelders HCM, Rübsamen T (1986) Burmanniaceae [Monograph 42] *Flora Neotropica*, Vol. 40/42, Saprophytes Pro Parte, pp. 1–189
- Miller RM (2005) The nonmycorrhizal root – a strategy for survival in nutrient-impooverished soils. *New Phytol* 165:655–658
- Muthukumar T, Udaiyan K, Shanmughavel P (2004) Mycorrhiza in sedges—an overview. *Mycorrhiza* 14:65–77. <https://doi.org/10.1007/s00572-004-0296-3>. REVIEW
- Olivares E, Benítez M, Peña E, Colonnello G (2013) Aluminium accumulation and nutrients in *Pterolepis glomerata*, *Desmoscelis villosa*, and *Rhynchanthera grandiflora* in palm swamp communities. *Botany* 91:202–208. <https://doi.org/10.1139/cjb-2012-0228>
- Osborne CP, Salomaa A, Kluver TA, Visser V, Kellogg EA, Morrone O, Vorontsova MS, Clayton WD, Simpson DA (2014) A global database of C4 photosynthesis in grasses. *New Phytol* 204:441–446
- Pagano MC, Scotti MR (2009) A survey of the arbuscular mycorrhiza occurrence in *Paepalanthus bromelioides* and *Bulbostylis* sp. in rupestrian fields, Brazil. *Micologia Aplicada International* 21(1):1–10
- Poppinga S, Weisskopf C, Westermeier AS, Masselter T, Speck T (2016) Fastest predators in the plant kingdom: functional morphology and biomechanics of suction traps found in the largest genus of carnivorous plants. *AoB PLANTS* 8:plv140. <https://doi.org/10.1093/aobpla/plv140>
- Raven JA, Handley LL, Macfarlane JJ, Mcinroy S, Mckenzie L, Richards JH, Samuelsson N (1988) The role of CO<sub>2</sub> uptake by roots and CAM in acquisition of inorganic carbon by plants of the isoetid life-form: a review with new data on *Eriocaulon decangulare* L. *New Phytol* 108:125–148

- Raynai-Roques A, Jeremie J (2005) Biologic diversity in the genus *Utricularia* (Lentibulariaceae). *Acta Bot Gallica* 152(2):177–186
- Renner SS (1990) A revision of *Rhynchanthera* (Melastomataceae). *Nord J Bot* 9:601–630
- Shane MS, Cawthray GR, Cramer MD, Kuo J, Lambers H (2006) Specialized 'dauciform' roots of Cyperaceae are structurally distinct, but functionally analogous with 'cluster' roots. *Plant Cell Environ* 29(10):1989–1999
- Stevens, P. F. (2001 Onwards). Angiosperm phylogeny website. Version 14, July 2017 <http://www.mobot.org/MOBOT/research/APweb/>
- Struwe S, Nilsson S, Albert VA (2008) *Roraimaea* (Gentianaceae: heliceae)—a new gentian genus from white sand Campinas and Cerro de la Neblina of Brazil and Venezuela. *Harv Pap Bot* 13: 35–45
- Toro M (2003) Micorrizas arbusculares en ecosistemas de sabana. *Venesuelos* 11(1–2):54–66

---

**Part III**  
**Synthesis**



J. A. Zinck, E. Medina, and P. García Montero

## 13.1 Introduction

White-sand ecosystems are characterized by distinctive vegetation covers ranging from purely herbaceous (meadows) to closed forests (caatingas), growing on the most infertile tropical soils widely scattered in the Amazon region. They are examples of habitat specialization, relatively low biodiversity and prominent endemism. The contemporary landscape, soilscape, drainage network, phytogeography, species diversity and endemism are unquestionable signals of ancient processes that contributed to their evolution and current status within the Amazon region. White-sand ecosystems have expanded and contracted over centuries, influencing the spatial arrangement of plants and animal life. River deposits and geological changes in the Pleistocene helped create unique life conditions in white-sand habitats. Contemporary white-sand areas in the Amazon region are assumed to be relict or ancestral areas of earlier widespread habitats now covered by more recent sediments coming mainly from the Andean orogeny. Despite their generally lower species richness compared to other Amazonian ecosystems, WSE present a distinctive assembly of species, where dominance is a relevant attribute.

Studies on Amazonian lowland ecosystems have concentrated so far on forests, while herbaceous and shrubby vegetation types have attracted less attention and

---

J. A. Zinck

Faculty of Geo-Information Science and Earth Observation (ITC), University of Twente, Enschede, The Netherlands

E. Medina (✉)

International Institute of Tropical Forestry, USDA Forest Service, San Juan, Puerto Rico

Centro de Ecología, Instituto Venezolano de Investigaciones Científicas, Caracas, Venezuela

P. G. Montero

Private Activity, Soil Survey and Environmental Planning, Caracas, Venezuela

remain still poorly documented. However, herbaceous vegetation islands embedded within forest or scrubland matrices occur throughout the Amazon region at large.

The first section of this book provided a review and update on the current knowledge of forests and shrublands on white-sand substrates. The second section focused on the meadow environment, that is, those environments with predominant herbaceous or herbaceous-shrubby types of vegetation, in the Amazonas state of Venezuela. In the following text, we highlight some of the most relevant findings.

---

### 13.2 Forested and Shrublands Peinobiomes

The forests in the upper Rio Negro (north-western Amazon) and adjacent south-western Orinoco basins, were subjected to a phytosociological analysis based on both floristic composition and species relative dominance. The descriptive nature of this phytosociological study is justified considering the state of baseline knowledge on the northern and north-western Amazonian ecosystems.

The region harbors unique plant communities that thrive under wet climatic conditions on oligotrophic soils, drained by mostly black, white, or clear water rivers. The floristic composition and classification of the vegetation types were determined using a two-way indicator species procedure (TWINSPAN). This analysis defined the phytosociological class *Eperuo leucanthae* - *Eperuetea purpureae*, composed of two orders, a) the *Heveo guianensis* - *Eperuetalia purpureae* (with six distinct forest associations), and b) the *Virolo elongatae* - *Brosimetalia utiles* with a large group of undefined forests associations. The first order includes the forests that grow on sandy, acidic, and extremely leached soil substrate, which include two typical upper Rio Negro associations, the Amazon caatinga forests (*Micrandro elatae* - *Micrandretum sprucei* and *Oenocarpedo batauae* - *Eperuetum purpureae*). Within the second order, the Alliance *Goupio glabrae* - *Minquartiion guianensis* includes forests drained by white and clear waters, growing on clay soils.

The Amazon caatinga is dominated by sclerophyllous species, tolerant to pulses of short-term hypoxia during flooding, and water stress after spells of dry days. Dominant vegetation is characterized by high leaf mass/area ratios, and low concentrations of N and P. Despite consistently positive soil  $\delta^{15}\text{N}$  values, leaves show strongly negative values, probably associated with the widespread occurrence of mycorrhizal symbiosis, and the extreme N deficiency in white-sand soils. Amazon caatinga species have relatively long leaf lifespans (>1 year), and low maximum rates of photosynthesis. Endomycorrhizal species are common, while ectomycorrhizal species are restricted to a relatively small number of genera, belonging mostly to Fabaceae, Nyctaginaceae, and Polygonaceae.

### 13.3 The Meadow Environment

Meadow refers to herbaceous plant communities thriving on lowland white-sands. Meadow vegetation is dominated by broadleaved herbaceous species belonging to highly specialized families such as Rapateaceae, Bromeliaceae, Xyridaceae, Eriocaulaceae, and Cyperaceae, in contrast to grassland (i.e., savanna) that consists mainly of graminaceous herbs (Poaceae).

The study region encompasses the lowlands lying between the Orinoco and the Rio Negro rivers to the west and the borders of the Guayana highlands to the east, approximately between 5°N and 2°N. It was divided into six study areas showing the presence of meadow islands within forest matrices, selected in major river watersheds, having distinctive physiographic and drainage features, and previous botanical information.

An inventory of the meadow vegetation and the sand substrate was carried out to establish relationships between geomorphic landscapes and soils as a basis to identify physiognomic and floristic variations of meadow vegetation. The study areas were labeled after the name of the main river draining each area or a relevant relief feature, including from north to south: Sipapo, Camani, Ventuari, Yapacana, Atabapo, and Pasimoni.

Study areas were described in terms of terrain features, main soil types, and variety of vegetation cover. Meadow vegetation including pure herbaceous meadow, shrubby meadow, and mixed meadow-savanna, occurs mainly in two landscape types: (1) alluvial flats formed by river and stream deposition in plain landscape, and (2) slightly sloping glaciais formed by colluviation in peneplain landscape. Soils derive from quartzose sand and loamy sand sediments, are white to light gray when dry, acidic, nutrient-poor, and have limited water-holding capacity.

Meadow areas are fragmented, discontinuously interspersed on residual peneplain reliefs. Sand is the substratum material in all meadow areas. However, there is a differentiation in particle size classes according to landscape type: coarse sand dominates in alluvial plain flats, while fine sand is more frequent in peneplain glaciais.

The psammic peinobiome of meadow vegetation is comparable to a hydroponic system with very limited nutrient supply from rainfall, surface runoff, and groundwater. Whether Quartzipsamments or Spodosols, differences in soil types are possibly of little relevance generating variations in vegetation growth and cover density. Deep quartzose sand is a substrate extremely low in plant nutrients, without influence on the shallow-rooted meadow vegetation. Forbs, herbs, and shrubs live mainly in the upper soil layer and commonly do not explore more than 50 cm depth.

#### 13.3.1 Remote Sensing Analysis of Vegetation Cover

Microwave remote sensing was applied to identify herbaceous formations on white-sands in the surrounding forest matrix in the six selected study areas. A white-sand land cover map was obtained using a synergistic integration of Global

PALSAR-2 and SENTINEL-1 products with the LANDSAT-based Normalized Difference Vegetation Index (NDVI).

An interpretation key was developed combining an improved Expectation-Maximization (EM) algorithm classification with post-classification refinement (Bayesian Information Criterion) as well as the integration of contextual spatial information and high-resolution imagery (Google Earth and Bing images). The Normalized Difference Vegetation Index was applied in the EM classification to test all data sets and select the most accurate thematic product for mapping white-sand covers at regional scale. Special attention was given to the mapping of herbaceous formations (meadows) and flooded vegetation.

Three factors appeared to be significant when determining the variations in the backscattering coefficient for the environmental setting: (1) vegetation type (texture and structure), (2) surface aspect or soil/vegetation conditions (tone, roughness), and (3) surface water/flooded vegetation.

The backscattering intensity changes with these parameters produced a range of image brightness variations, expressed as changes in the pixel gray levels or color of the images analyzed. The supervised classification differentiated forest (closed to open), inundated forest, dry or flooded open white-sand scrublands, shrubby meadows, shrubby, or herbaceous cover flooded regularly, mosaics of plant communities, sparse vegetation, bare rocky areas, and sandbanks/sandridges.

The approach of combining two different microwave sensors revealed to be effective as an orbital sensor that can acquire multi-frequency and multi-polarization data. The implementation of integrated image classification (L- and C-band with NDVI data) allowed grouping spectral combinations of classes, being an operative way for mapping complex units. The results showed information not only on the canopy structure but also on the vegetation's greenness. Five out of 14 distinguished land cover classes show the highest potential of having Amazonian meadow species, including herbs, forbs, and shrubs. NDVI ranges of land cover types in different years indicated land cover changes.

Information was gathered via interpretation of satellite images and field observation and sampling. Landscape features were identified using DEM modelling and terrain algorithms. The DEM improved the terrain analysis resolution detail because it allowed an accurate determination of drainage slopes and location of channels and ridges, among other parameters.

Several terrain algorithms were used to describe terrain features. Geomorphic landscape units were distinguished based on elevation ranges (hypsometric slicing algorithm), using an iteration procedure to obtain the best fits from several trials of elevation ranges. Expert knowledge and contour lines were used for demarcating the unit extents. Two slope classes were selected to distinguish between flat to nearly level areas (<1%) in alluvial plains and gently sloping areas (1–5%) in peneplain and piedmont landscapes.



### 13.3.2 The Soilscape: Soil Classes, Distribution, and Properties

Meadow vegetation varies from meadow proper, in which typical herbs and forbs dominate, to shrubby meadow and open scrub. The substrate of this variety of cover types is quartzose white-sand, essentially of sedimentary origin, in alluvial plain flats and peneplain glacis.

Quartzipsamments are the dominant soils under meadow vegetation *sensu lato*. A feature common to all soils is the high content of whitish quartzose sand that has very limited water-holding capacity. The regional soil moisture regime as influenced by climatic conditions is udic in the northern part of the region and perudic in the southern part, together with widespread aquic regime soils in poorly drained low-lying alluvial flats. Most of the soils have a weak ochric epipedon with low organic matter content overlying white-sand C layers. A particularity in some meadow soils is the presence of compact densic sand layers that restrain root penetration and water movement.

The geographic distribution of the main soil classes is landscape related. Typical Quartzipsamments occur mainly on well-drained geomorphic positions including peneplain glacis, splay and overflow alluvial plains, and dune-like mounds.

Although Spodosols are usually associated with caatinga-bana vegetation, they were also found in current meadow environment with which they do not seem to bear genetic relationship. They are duplex soils, constituted by an upper tier of stratified sand cover with lithological discontinuities and a lower tier corresponding to the remnant of truncated Spodosol.

Whatever the taxonomic class, all soils have very low water-holding capacity and nutrient availability. They provide similarly limited life-supporting conditions for plants to establish and grow. With their extreme level of nutrient deficiency and bleached sandy textures, meadow soils typify appropriately the environment of a psammic peinobiome.

### 13.3.3 The Sandscape: Depositional Processes, Sand Distribution, Sediment Characteristics

The most striking sandscapes are those that are practically bare or have very scattered vegetation. The largest open white-sand areas result commonly from vegetation cover degradation by yearly repeated and expanding fires; others result from new sand deposition by shifting rivers and streams.

Some sands are authigenic, having formed in situ in the lowlands by deep vertical weathering of the crystalline substratum or through lateral, oblique transformation.

Others are allogenic, having formed in the surrounding highlands and uplands by physical-chemical disintegration of the Roraima sandstone-quartzite shield cover or by weathering of the crystalline shield basement rocks, and subsequently imported to the lowlands by surface and karstic underground water flows.

Lowland sand covers are essentially reworked sands distributed over the low-lying areas by alluvial, colluvial, and/or eolian activity. It is uncommon to

find deep weathering profiles at the terrain surface in the flat meadow lowlands, as the weathering front of the bedrock substratum is generally buried under cover sands.

A sedimentological approach was implemented to identify the variety of (white) sand covers in meadow environment, using three main criteria: (1) stratifications and lithological discontinuities in the sand covers to understand the sedimentological history and evolution of the landscape; (2) particle size distribution patterns to determine the main depositional facies of the area and unravel features of Holocene sedimentation; and (3) truncation or fossilization of soil profiles to reveal the history of soil formation.

Meadow vegetation *sensu lato* has established mainly on two lowland landscape types, i.e., alluvial plains and peneplains. In alluvial plains, sand deposits are ubiquitous, from river and stream proximities to large interfluves between watercourses. Alluvial plain interfluves are flats where two main depositional processes, namely overflow and splay, contribute to forming sand mantles.

Overflow generates a well-sorted sediment facies based on two dominant sand separates of medium and fine sand that together concentrate about 80% of the deposits. By contrast, splay generates an unsorted sediment facies with sand distributed almost equally over several codominant separates (three to four) and a shift towards coarse sand. These two dominant depositional patterns coexist or are intermingled in the sandscape.

Meadow vegetation and contiguous sclerophyllous formations (caatinga, bana) were found to be established on the same alluvial, in general stratified substratum that overlies the igneous-metamorphic basement in-between residual peneplain reliefs. There is spatial continuity of the regional sand cover under the various vegetation types. The maximum extent of the sand cover may be assumed to coincide with the combined geographic distribution of caatinga, bana, and meadow vegetation.

### 13.3.4 Trends in Meadow Landscape Evolution

Meadow environment is exposed to geomorphic activity and thus able to show recent and sub-recent geopedologic changes. By contrast, forest and scrubland areas (caatinga and bana) are relatively stable from geomorphic point of view as terrain is protected by wooded cover. Because of its nearly level topography, meadow environment does not show spectacular relief modifications. However, some surface and subsurface features highlight processes and trends of evolution in the physical meadow landscape. They are stratifications in white-sand sediments and soils, ecotone dynamics between adjacent forested and herbaceous areas, formation of reticular microrelief, and occurrence of Spodosols in current meadow areas.

The frequency of stratifications indicates that the regional sand cover under meadow is overall of sedimentary origin, formed by discontinuous sedimentation episodes during parts of the Holocene. Frequent channel shifting is favored by level

topography and weak mechanical resistance of meadow plants against sediment erosion and deposition. Meadow is an active geomorphic environment in contrast with the more stable caatinga and bana terrains. As a result, meadow vegetation must periodically adapt to truncation or burial of the terrain surface. This constraint may favor the more resistant plants and therefore decrease plant diversity. Shifting river dynamics hampers (re)colonization of meadow by wooded plants.

Wooded vegetation (caatinga, bana) in contact areas with adjacent meadows are established on stratified sand sediments similar to those underlying the meadows. There is thus spatial continuity of the sand cover under both vegetation types. Caatinga fringes seem to be relatively stable today from geomorphic point of view, while bana fringes are exposed to degradation by runoff and rill erosion. Resulting bare white-sand patches are increasingly colonized by meadow species, reflecting a process of “meadowisation” of the bana cover.

Caatinga terrain in ecotone areas is incised by erosion channels possibly related to climatic conditions drier than the current ones. Erosion channels seem to be surviving features that secure today surface drainage and water evacuation during rainfalls but without substantial erosion.

Microrelief is a distinctive feature of meadow environment caused by the incision of rills and channels, and suffusion depressions. The thick spodic horizons found in the alluvial lowlands are not in balance with the current meadow vegetation. They are covered by stratified sand layers that often show irregular decrease of organic carbon with depth, a typical fluventic aggradation feature, and lithological discontinuities above truncated spodic horizons. As this kind of profiles has been detected at several sites throughout the lowlands, it can be assumed that large current meadow stretches have been covered by caatinga in the past.

Meadows may result from variable circumstances. In active alluvial plains, overflows from rivers and streams at high water levels spread new sand sediments over interfluves, creating bare surfaces to be colonized by herbaceous vegetation. There are also meadows irregularly distributed in woody matrix, resulting from natural and/or human-made disturbances decimating the forest cover. Thus, meadow formation may be the starting colonization phase of either sand surfaces exposed upon forest degradation or new sand covers resulting from river overflows.

---

### **13.4 Diversity and Endemicity of White-Sand Vegetation**

Open (non-forested) white-sand ecosystems are restricted to the lowlands of Amazonia and the Guayana Shield, with major extents in the Río Negro basin along south-eastern Colombia, southern Venezuela (Amazonas, Bolívar states), and north-western Brazil, Peru, and smaller patches in the Guianas.

Their flora in the Venezuelan Amazonas state is considerably rich in herbaceous and woody species. In the six study areas, 710 species were recorded distributed in 287 genera and 90 vascular plant families. Half of the species and four genera are endemic to the overall Amazonian white-sand areas across Brazil, Colombia, and Venezuela. In contrast, local endemism is relatively low (12%). Approximately 68%

of the taxa are woody and 32% are herbaceous. Shrubs, including suffrutices, constitute the dominant life form (292 taxa), followed by trees (143), climbers (47) and epiphytes (8, including hemiparasites). The herbaceous component is dominated by terrestrial herbs (218, including a few aquatics) with a small number of epiphytes (9) and climbers (9). The high species richness and endemism found in the study area contrast with the relatively low diversity reported for other white-sand areas in western Amazonia.

Among the study sites Yapacana and Atabapo have the highest levels of alpha diversity and endemism and are the most similar (Jaccard index). They also show more floristic affinities with the Sipapo and Pasimoni areas than with the cluster Camani and Ventuari. This similarity pattern in species composition highlights the floristic heterogeneity of local endemism of white-sand vegetation in the Venezuelan Amazonas. The high levels of endemism and species richness are probably related to the fragmented distribution of the open white-sand vegetation patches within a forest matrix.

The ten most species-rich families (>20 species) are Melastomataceae (51), Rubiaceae (51), Fabaceae (39), Xyridaceae (35), Poaceae (30), Apocynaceae (29), Cyperaceae (28), Ochnaceae (24), Chrysobalanaceae (23), and Eriocaulaceae (21). Among the families with the higher proportion of endemics, lineages with predominantly herbaceous growth forms stand out (e.g., Poaceae, Cyperaceae, Eriocaulaceae, Lentibulariaceae, Polygalaceae, and Orchidaceae).

The alternating periods of water saturation and drought, together with nutrient deficiency, are the most limiting factors for biomass accumulation in white-sand ecosystems and constitute strong environmental filters that promote speciation and explain endemism and floristic composition. However, species richness and vegetation structure in the study areas were not related to soil parameters, since they share similar soils.

---

### **13.5 Ecophysiological Features of Lowland Meadows Species within Upper Rio Negro and Orinoco River Basins**

Herbaceous meadows are dominated, in terms of biomass, by non-gramineous species thriving in flood-prone, lowland, white-sandy substrates throughout the upper Rio Negro and Orinoco basins. They are broadleaved herbaceous species belonging to highly specialized families (Rapateaceae, Bromeliaceae, Xyridaceae, Eriocaulaceae), and narrow-leaved herbs of the Cyperaceae and Poaceae. Meadows contrast to lowland tropical grasslands (i.e., savanna) that are dominated by drought tolerant of grasses and sedges (Poaceae and Cyperaceae).

The total number of strict meadow species is 214, from which 63 belong to 6 dicot families, and 151 belong to 11 monocot families. Among the dicots, the dominant families were: Lentibulariaceae, Gentianaceae, and Polygalaceae. Among the monocots five families stand out, Xyridaceae, Poaceae, Cyperaceae, Eriocaulaceae, and Rapateaceae. Species within these families have morpho-physiological traits that promote tolerance to the white-sand environmental conditions: (1) alternation of

short periods of soil water saturation and water stress, and (2) low availability of all plant nutrients. Examples of those traits are development of sclerophyllous leaves, fibrous and dense roots systems, and highly specialized cluster and dauciform roots. Most species within the Cyperaceae and Poaceae have the C3 photosynthetic pathway. A few C4 species were also identified, that are probably associated with meadow-savanna ecotones.

Based on cluster analysis of percentual herbaceous species composition, the Pasimoni (southernmost) and Sipapo (northernmost) areas are clearly separated from each other, and the Pasimoni area appears more related to the cluster Atabapo and Yacapana, whereas the Sipapo area is more similar to the contiguous cluster of Camani and Ventuari.

There is very little information on the ecophysiology of nutrient relationships of the dominant families in white-sand meadows in the upper Rio Negro and Orinoco basins. At the ecosystem level, there is scattered information on species composition and mycorrhizal symbiosis, but virtually nothing could be found regarding their structure, quantitative species composition, biomass distribution, and productivity.